UC San Diego

Title
Increasing the Efficiency and Utility of Bifunctional Alkene Isomerization Catalysts

Permalink
https://escholarship.org/uc/item/9pg4s93z

Author
Paulson, Erik Richard

Publication Date
2018

UNIVERSITY OF CALIFORNIA SAN DIEGO
SAN DIEGO STATE UNIVERSITY

Increasing the Efficiency and Utility of Bifunctional Alkene Isomerization Catalysts

A dissertation submitted in partial satisfaction of the
requirements for the degree Doctor of Philosophy

in

Chemistry

by

Erik Richard Paulson

Committee in charge:

University of California San Diego

Professor Simpson Joseph
Professor Joseph O'Connor

San Diego State University

Professor Douglas Grotjahn, Chair
Professor Temesgen Garoma
Professor Byron Purse

2018

The Dissertation of Erik Richard Paulson is approved, and it is acceptable in quality and form for publication on microfilm and electronically:

_____

_____

_____

_____

_____

Chair

University of California San Diego

San Diego State University

2018

iii

DEDICATION

To Aurea and Violet, for being my inspiration and my foundation.

TABLE OF CONTENTS

LIST OF FIGURES

LIST OF TABLES

ACKNOWLEDGEMENTS

My journey in graduate school began in 2011, when I quit my job as a high school teacher in Burbank, CA, and came to San Diego to gain a deeper understanding of chemistry. I was not yet sure of the next step in the journey, but I enjoyed learning enough to take the plunge towards earning a Ph.D., and I still enjoy it today.

The first person I would like to thank is Professor Douglas Grotjahn for being my mentor and guide throughout this whole process. We went through a lot of interesting transitions in the lab (even just with funding: we were well-funded when I joined, then went through a couple of lean years, and now we're back!), but you stayed steady the whole time. You gave me direction with my research, but you also gave me the freedom to explore my thoughts and hypotheses. Perhaps I hit too many dead-ends, but we also ended up learning things that make for a rich and interesting story, so thank you so much for that.

I would also like to acknowledge Professor Andrew Cooksy, who advised me in computational chemistry and enriched my rudimentary kinetic work. You always had an open and patient ear, even though the projects we were working on were well outside of my comfort zone. And Professor Dave Pullman, who painstakingly helped build our gas collection apparatus, your expertise and knowledge were invaluable to the process.

In the time I have spent in the lab, I have worked with, learned from, trained, and had a good time with so many people, I will not even attempt to name everyone. But I must acknowledge the people in the phosphine subgroup that struggled with me to make phosphines proud. First and foremost, I have to thank my two graduate student mentors, Casey Larsen and Gulin Erdogan. When I had joined the lab, it had been years since I had done any real chemistry (if you don't count performing demos and setting up experiments for high school kids!). Conversely, Casey and Gulin

were very experienced, having almost completed their Ph.D. journey. Despite the fact that they were both working on their thesis, they took the time to train me and answer my annoying questions and keep me from blowing myself up (I mean this in the literal sense, Gulin, with the dilithioferrocene in the antechamber!). Their work and their training provided the foundation for my entire Ph.D. studies. The many other talented graduate/postgraduate students in the phosphine subgroup: Dave Catrone, Melinda Pope, Hai Tran, Farhana Barmare, Thomas Cao (half-in, half on the dark side), Braden Silva, Dan Sattler and Iris Landman, and undergraduate students Michael Tran, Hanne Henriksen, and Kiersten Sukert. I would like to give special thanks to the undergraduates who worked under my direction: Annaliese Dang, Vy Le, Patrick Brklycica, Rafael Tavares De Sa, and Esteban Delgado, all of whom (except Rafael) worked on a project that is near and dear to my heart. Regardless of the ultimate outcome of the project, I want you all to know that I appreciate the trust you put in me, and I hope you have all learned something from me.

I would also like to especially thank the lab mates that I have spent the most time with, and let them know how they impacted my life. Dave Marelius, when I first came into the lab, you and Evan's hood was pretty close to my desk, so I got to be a passive observer to many of your conversations and crazy workups. I didn't say very much that first year. But by the time you left, we became good friends, and I always enjoy seeing that twinkle in your eye when you talk about something you are passionate about, and we both happen to be passionate about a lot of the same things and have the same views on life. Jayneil Kamdar, I first hated your whistling, when I was trying to focus on my UCSD classes, but I ultimately ended up loving our whistle battles/ballads. We have a very similar sense of humor. Let's go get some cawf. Braden Silva, I love your passion for chemistry. It may even surpass mine. You are always down to talk and exchange ideas, and I expect big things from you in life. Aaron Nash, you are like a study in contradictions. You're

xxiv

stubborn, yet compassionate, fiery yet level-headed, eccentric yet responsible. I enjoy our conversations, and I am always trying to figure you out even as you are trying to understand others. Dan Sattler, I have enjoyed our adventures, and will always try to procure the totality of them.

Outside of the lab, I want to thank each and every member of my family. My dad, for raising me and for being the pioneer for doing research in our family. I might not have developed an interest in science if you had not been doing it first. My mom, for also raising me, and always believing in me and encouraging me to do my best. To Lorien and Evan (and Jen, Kyle, and Emily), for being supportive and giving me opportunities to blow off some steam. To game nights! (that sometimes lead to game mornings!)

I would also like to thank my good friends outside of the lab, for providing distractions and interesting conversations. Particularly, I would like to thank Dan Novakovich, for being my best friend, always being there for me, and always providing interesting and fresh perspectives on life, and Matt Dickerson, who can chat on the phone with me, and before you know it, an hour has gone by. Where did the time go?

I have saved the most important for last. Aurea, my wife, my rock, the love of my life. We have known each other for eighteen years, have been together for ten, and have been married for five. We were together before I went to graduate school, and you encouraged me to switch careers and apply. You have supported me throughout the entire graduate school process, as long as it has been, and have been extraordinarily patient with me. I know it is a trait that most companions would not be able to handle, and it is one of the many ways you are a special woman and I am lucky to have you. Best of all, you have given me the best gift I could have ever asked for. You brought our sweet daughter Violet into this world. It has certainly not been easy raising her with

you working part-time, and me trying to write my thesis, but I would not exchange it for anything. I love you, and will for all time.

The contents of chapter 1 are similar to the material published in the following encyclopedia article: Paulson, E.R., Grotjahn, D.B. "Isomerization and Hydrogenation of Alkenes". *Encyclopedia of Inorganic and Bioinorganic Chemistry*, Published 15 December 2017. This article was an update to the version published in 2006 in the *Encyclopedia of Inorganic Chemistry* by Dr. Fred Jardine, so thank you to Dr. Jardine for his original contribution.

Chapter 2 contains material that is similar to the material published in the following manuscript: Larsen, C.E., Paulson, E.R.,[†] Erdogan, G.,[†] Grotjahn, D.B. "A Facile, Convenient, and Green Route to (*E*)-Propenylbenzene Flavors and Fragrances by Alkene Isomerization". *Synlett*, **2015**, 26(17), 2462. ([†]co-2nd authors)

The contents of Chapter 3 are similar to a portion of the material submitted for publication in the following manuscript: Paulson, E.R., Moore, C.E., Rheingold, A.L., Grotjahn, D.B. "Dynamic π-Bonding of Imidazolyl Substituent in a Formally 16-electron Cp*Ru(κ^2P,N) Catalyst Allows Dramatic Rate Increases in (E)-Selective Monoisomerization of Alkenes" *ACS Catalysis*, Submitted.

The contents of Chapter 4 contain material from the following two publications: 1) Paulson, E.R., Moore, C.E., Rheingold, A.L., Grotjahn, D.B. "Dynamic π-Bonding of Imidazolyl Substituent in a Formally 16-electron Cp*Ru(κ^2P,N) Catalyst Allows Dramatic Rate Increases in (E)-Selective Monoisomerization of Alkenes" *ACS Catalysis*, Under Review. 2) Paulson, E.R., Delgado III, E., Cooksy, A.L., Grotjahn, D.B. "Catalyst vs. Substrate Control of Monoselectivity in Bifunctional Ruthenium Alkene Isomerization", *Organic Process Research and Development* **2018**, Accepted.

VITA

2004   Bachelor of Science, University of California, Riverside

2006   Teaching Credential (Chemistry, Physics, Geoscience), University of California, Riverside

2006-2011   High School Teacher, Burbank, CA

2011-2018   Teaching Assistant, San Diego State University

2011-2018   Graduate Researcher, San Diego State University

2012-2018   Ph.D., University of California San Diego and San Diego State University

Publications

1. Erik R. Paulson, Douglas B. Grotjahn, "Isomerization and Hydrogenation of Alkenes" Encyclopedia of Inorganic and Bioinorganic Chemistry" Published December 15, 2017.

2. Iris R. Landman, Erik R. Paulson, Arnold L. Rheingold, Douglas B. Grotjahn, and Gadi Rothenberg, "Designing bifunctional alkene isomerization catalysts using predictive modeling" Catal. Sci. Technol. 2017, 7, 4842-4851.

3. Casey R. Larsen, Erik R. Paulson[‡], Gulin Erdogan[‡], Douglas B. Grotjahn, "A Facile, Convenient, and Green Route to (E)-Propenylbenzene Flavors and Fragrances by Alkene Isomerization", Synlett 2015, 26, 2462-2466. [‡]Authors contributed equally

Patents

1. Douglas Grotjahn, Casey Larsen, Gulin Erdogan, Erik Paulson "Terminal alkene monoisomerization catalysts and methods" Patent No. 9708236. Granted July 18, 2017

Submitted Publications

1. Paulson, Erik R., Moore, Curtis E., Rheingold, Arnold L., Grotjahn, Douglas B. ""Dynamic π-Bonding of Imidazolyl Substituent in a Formally 16-electron Cp*Ru(κ^2P,N) Catalyst Allows Dramatic Rate Increases in (E)-Selective Monoisomerization of Alkenes" *ACS Catalysis*, Under Review.

2. Paulson, Erik R., Delgado III, Cooksy, Andrew L., Grotjahn, Douglas B., "Catalyst vs. Substrate Control of Monoselectivity in Bifunctional Ruthenium Alkene Isomerization", *Organic Process Research and Development* **2018**, Accepted.

Presentations

Oral:

1. Erik Paulson, Douglas B. Grotjahn, "Ruthenium Monoisomerization Catalyst: Studies in Selectivity" Student Research Symposium, San Diego State, University, San Diego, California, March 3, 2017

2. Erik Paulson, Douglas B. Grotjahn, Curtis E. Moore, Arnold L. Rheingold, "A Highly Selective and Efficient Coordinatively Unsaturated Ruthenium Monoisomerization Catalyst" Student Research Symposium, San Diego State University, San Diego, California, March 4, 2016

3. Erik Paulson, Douglas B. Grotjahn, Curtis E. Moore, Arnold L. Rheingold, "Synthesis, Characterization and Reactivity of a Coordinatively Unsaturated Ruthenium Monoisomerization Catalyst" Fall 2015 SoCal Organometallics Meeting, Riverside California, December 5, 2015

4. Erik Paulson, Douglas B. Grotjahn, Curtis E. Moore, Arnold L. Rheingold, "Synthesis, Characterization and Reactivity of a Coordinatively Unsaturated Ruthenium

Monoisomerization Catalyst" X Simposio Internacional: Investigacion Qumica en la Frontera 2015, Tijuana, Baja California, Mexico, November 2015

Poster:

1. "Substrate versus Catalyst Control of Alkene Isomerization" Erik Paulson, Douglas B. Grotjahn, Poster Presentation, 27th Biennial Organic Reactions Catalysis Society Conference, San Diego, California, April 8th – 12th, 2018

2. "Selective Migration of Double Bonds with a 16-Electron Ruthenium Catalyst" Erik Paulson, Douglas B. Grotjahn, Curtis E. Moore, Arnold L. Rheingold, Poster Presentation, ACS Scientist of the Year Dinner, San Diego, California, April 28th, 2017

3. "Controlled Monoisomerization of 1-Alkenes by a 16-Electron Ruthenium Monoisomerization Catalyst" Erik Paulson, Douglas B. Grotjahn, Curtis E. Moore, Arnold L. Rheingold, Poster Presentation, 253rd ACS National Meeting and Exposition, San Francisco, California, April 2nd–6th, 2017

4. "Highly Active and (E)-Selective Bifunctional 16-Electron Ruthenium Monoisomerization Catalyst" (2)* Erik Paulson, Douglas B. Grotjahn, Curtis E. Moore, Arnold L. Rheingold, Poster Presentation, 39th Annual Gordon Research Conference, Salve Regina University, Newport, Rhode Island, July 10-15th, 2016 *Different poster, same title

5. "Highly Active and (E)-Selective Bifunctional 16-Electron Ruthenium Monoisomerization Catalyst" (2)* Erik Paulson, Douglas B. Grotjahn, Curtis E. Moore, Arnold L. Rheingold, Poster Presentation, 11th Annual Gordon Research Seminar, Salve Regina University, Newport, Rhode Island, July 9-10th, 2016 *Different poster, same title

6. "Highly Active and (E)-Selective Bifunctional 16-Electron Ruthenium Monoisomerization Catalyst" (1) Erik Paulson, Douglas B. Grotjahn, Curtis E. Moore, Arnold L. Rheingold, Poster Presentation, 75th San Diego ACS Anniversary Symposium, San Diego, California, April 6th, 2016

7. "Highly Active and (E)-Selective Bifunctional 16-Electron Ruthenium Monoisomerization Catalyst" (1) Erik Paulson, Douglas B. Grotjahn, Curtis E. Moore, Arnold L. Rheingold, Poster Presentation, ARCS Scientist of the Year Dinner, San Diego, California, April 1st, 2016

8. "Highly Active and (E)-Selective Bifunctional 16-Electron Ruthenium Monoisomerization Catalyst" (1) Erik Paulson, Douglas B. Grotjahn, Curtis E. Moore, Arnold L. Rheingold, Poster Presentation, 251st ACS National Meeting and Exposition, San Diego, California, March 13th-17th, 2016

9. "Increasing the Activity of a Bifunctional Ruthenium Monoisomerization Catalyst" Erik Paulson, Douglas B. Grotjahn, Poster Presentation, 248th ACS National Meeting and Exposition, San Francisco, California, August 10th-14th, 2014

10. "Iron- and Ruthenium-Based Bifunctional Catalysts: Synthesis and Catalytic Activity" Erik Paulson, Douglas B. Grotjahn, Poster Presentation, 25th Biennial Organic Reactions Catalysis Society Conference, Tuscon, Arizona, March 2nd-6th, 2014

11. "Iron- and Ruthenium-Based Bifunctional Catalysts: Synthesis and Catalytic Activity" Erik Paulson, Douglas B. Grotjahn, Poster Presentation, IX International Symposium: Chemistry in the Border Region, Tijuana, Mexico, November 2013

<u>Other Author</u>

xxx

1. "Origin of Selectivity in CpRu Catalyst for Alkene Isomerization" Thomas Chi Cao, Erik Paulson, Andrew L. Cooksy, Douglas B. Grotjahn, Poster Presentation, 27th Biennial Organic Reactions Catalysis Society Conference, San Diego, California, April 8th – 12th, 2018

2. "Toward (Z)-Selective Alkene Isomerization Catalysts and Potential Anti-Cancer Agents" Poster Presentation, 254th ACS National Meeting and Exposition, Washington, D.C., August 20th – 24th, 2017

3. "Synthesis and Electrochemistry of Ruthenium-2,2'-Bipyridine-6,6'-Dicarboxylate Catalysts Using Different Phosphorus Ligands" Poster Presentation, Sima Yazdani, Jayneil M. Kamdar, Erik R. Paulson, Arnold L. Rheingold, Douglas B. Grotjahn, 253rd ACS National Meeting and Exposition, San Francisco, California, April 2nd–6th, 2017

4. "Effect of Cyclopentadienyl Ligands on Alkene Isomerization Catalysts", Patrick Brklycica, Erik Paulson, Douglas Grotjahn, Poster Presentation, 251st ACS National Meeting and Exposition, San Diego, California, March 13th-17th, 2016

5. "Effect of Electron-Deficient, Fluorinated Phosphines on the Catalytic Properties of Bifunctional Catalysts" Farhana Barmare, Erik Paulson, Hai Tran, Douglas Grotjahn, Poster Presentation, 251st ACS National Meeting and Exposition, San Diego, California, March 13th-17th, 2016

ABSTRACT OF THE DISSERTATION

Increasing the Efficiency and Utility of Bifunctional Alkene Isomerization Catalysts

by

Erik Richard Paulson

Doctor of Philosophy in Chemistry

University of California San Diego, 2018
San Diego State University, 2018

Professor Douglas Grotjahn, Chair

While classical alkene transformations have been known since the 1800s, the last 10-20 years have seen a renewed interest in providing transition metal catalysts to expand the diversity of alkene reaction partners. One important goal is selective isomerization of alkenes, to produce unique isomeric compounds that expand the scope of other synthetic transformations. In the past 11 years, the Grotjahn group has been at the forefront of the development of highly (*E*)-selective alkene isomerization catalysts; one that began with the discovery of the efficient catalyst **1.1** and continued with the development of more positionally selective catalyst **1.2** (& **1.2a**). Catalyst **1.1** is currently sold commercially by Strem Chemicals, and has been used in a number of tandem and sequential processes to produce high-value compounds.

This dissertation details applications and modifications of existing Grotjahn catalysts (cyclopentadienyl)[2-(di-i-propylphosphino)-4-(t-butyl)-1-methyl-1H-imidazole]acetonitrile ruthenium(II) hexafluorophosphate (**1.1**) and (pentamethylcyclopentadienyl)[2-(di-i-propylphosphino)-4-(t-butyl)-1-methyl-1H-imidazole]acetonitrile ruthenium(II) hexafluorophosphate (**1.2**), along with its bisacetonitrile analogue **1.2a**. The major goal that drives the direction of the dissertation include increasing the efficiency of **1.2** + **1.2a** by developing a new version of the catalyst (discussed in chapters 3 and 4) that allows for dramatically increased reaction rates, and observation of the interactions of alkenes with this catalyst to understand more about the origins of selectivity and efficiency of this new catalyst. Other goals include determining the degree of the difference in selectivity between the new catalyst and existing Grotjahn catalysts, and increasing the scope of use of existing catalyst **1.1**.

Chapter 1

Transition-Metal Catalyzed Alkene Isomerization: Perspective and Progress

1.1 Introduction

The importance and presence of alkenes in commercial and industrial products is almost without parallel in the realm of organic chemical materials. Ethylene, principally synthesized by the cracking of higher alkanes, is produced on a larger scale than any other organic compound, with global demand of more than 157 million tons in 2015.[1] Oligomerization of ethylene can produce larger terminal alkenes, such as 1-butene, 1-hexene, and 1- octene,[2] which can be used directly in plastic and polymer as is, or converted into a number of other compounds through a host of chemical processes. The transformation most commonly associated with alkene isomerization is double-bond migration,[3] without skeletal isomerization involving or facilitated by the alkene moiety.

The flavor and fragrance sector is a rapidly growing industry, with a market of over $16 billion[4] annually. Certain fragrances can be transformed via isomerization to distinctly different fragrances, traditionally performed by strong bases and high temperatures.[5] As such an important process, it is not surprising that transition metal-catalyzed alkene isomerization is a process that has been studied for more than 70 years.

Among the longest-studied homogeneous transition-metal catalytic processes, double-bond migration has often been considered as an unwanted side reaction in other processes. Over the last fifteen years, however, the field of catalyzed double-bond migration has rapidly

developed to become a mild and atom-economical tool in diversifying the synthetic routes toward both natural and unnatural products. A notable example is the late-stage conversion of an allyl group to a propenyl group via isomerization followed by metathesis and hydrogenation in the total synthesis of (-)tuberostemonine by Wipf and Spencer (Figure 1.1), in which other methods proved incompatible with existing functional groups in the molecule.[6] Two notable areas of recent progress in the field of alkene isomerization are regio- and stereoselective isomerization, and either tandem or sequential isomerization/functionalization, ideally forming a single product made in high yield, which is a prerequisite for effective synthesis.
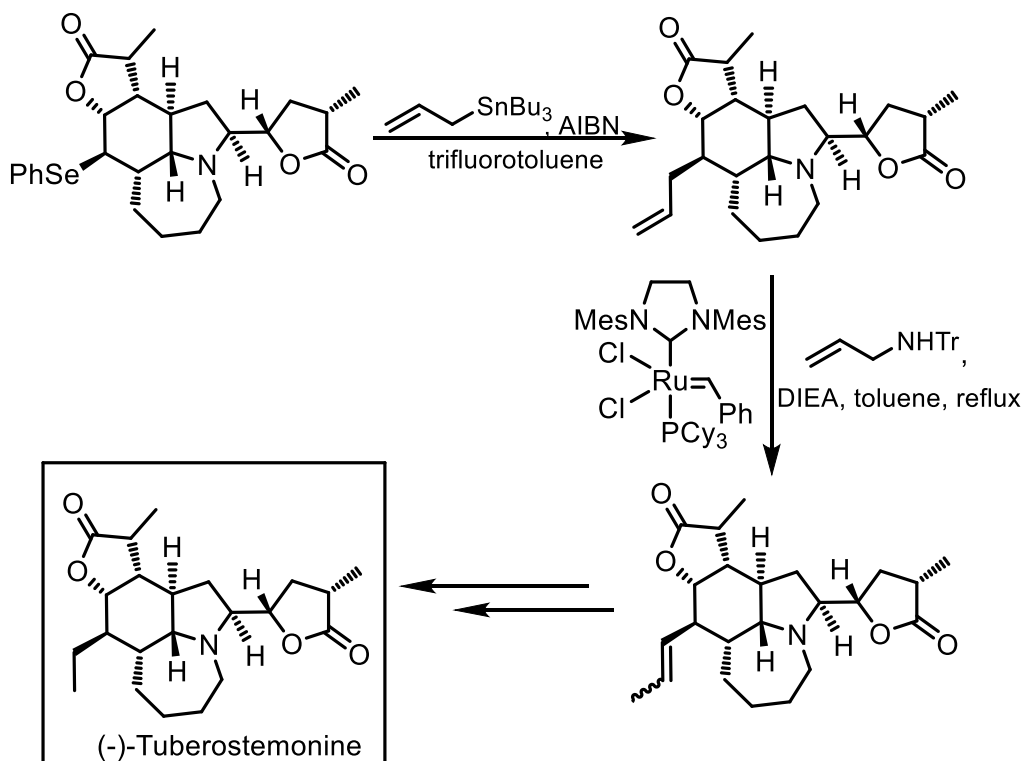
Figure 1.1. Alkene isomerization in the total synthesis of (-)-tuberostemonine

1.2 Mechanisms of double-bond migration

A double-bond migration requires the rearrangement of four electrons and a hydrogen atom, and transition metal catalysts can differ in the way in which the electrons and atoms move. The two principal transition-metal catalyzed mechanisms by which double-bond migration occur are illustrated for the case of 1-alkene in Figure 1.2. In the π-allylic mechanism, the alkene interacts with a transition metal and undergoes a formal oxidative addition of an allylic C-H bond to form an η^3-allyl hydrido complex. The hydride is then transferred back to the opposite end of the η^3-allyl to complete a 1,3-hydride shift. In the second, more common mechanism, a hydrido complex reacts with an alkene to form an alkyl complex. The alkyl complex then reverts to an isomeric alkene and the hydrido complex by undergoing a β-hydride elimination reaction.[7]
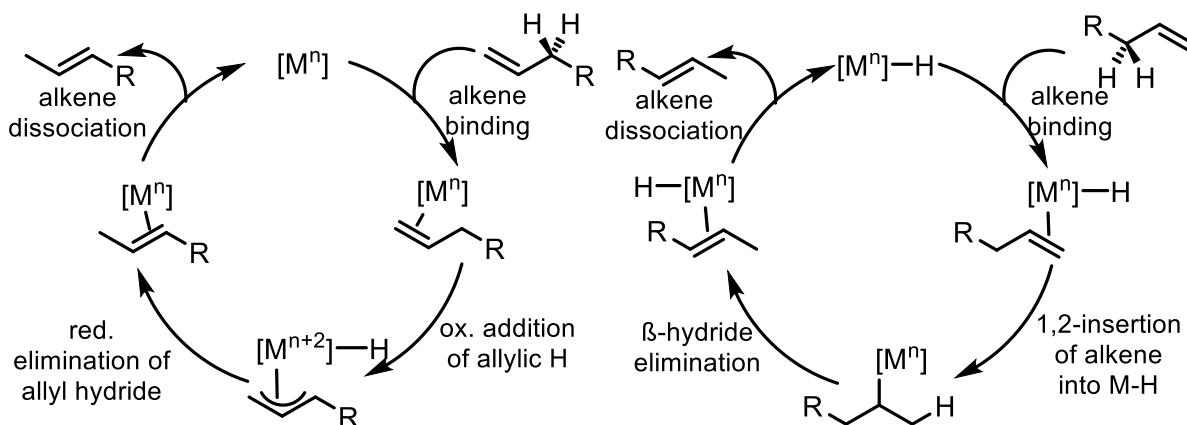
Figure 1.2. Left: the π-allyl mechanism; right: the σ-alkyl mechanism.

In double-bond migration reactions that operate by the σ-alkyl mechanism, monohydrido transition metal complexes tend to be the most active catalysts. The relatively long lifetimes of alkyl complexes in these systems allows them to undergo β-hydride abstraction reactions before they can react with the other reagents present.[8] Insertion of a 1-alkene into the metal hydride can either form a 1-alkyl or 2-alkyl complex. The 1-alkyl complex can either react with other

reagents or revert to the original alkene and hydrido complex via a β-hydride elimination. If the insertion of the 1-alkene into the hydride forms a 2-alkyl complex, thermodynamically it is more favorable that the 2-alkyl complex will lead to the 2-alkene than revert to the 1-alkene by competing β-hydride elimination reactions. Classic complexes that follow this pathway are $HCo(CO)_4$,[9] $[HNi(PPh_3)_3]^+$[10], and $HRuCl(PPh_3)_3$[11]

Isomerization by the π-allyl mechanism begins with a complex that does not initially contain a hydride. The 1-alkene binds to the metal, which acidifies the allylic C-H bond(s). An allylic proton is subsequently transferred to either an external base or the metal itself (a formal oxidative addition, forming a metal hydride), and the anionic allyl ligand either binds to the metal in an η^1- or η^3- fashion. The allyl ligand can then be protonated at the 3-carbon, reforming the 1-alkene, or at the 1-carbon, forming the 2-alkene.[12] Some classic catalysts that have been shown to operate by this pathway are $Fe(CO)_5$[9], and $ClRh(PPh_3)_3$[13].

Isomerization in the absence of a hydrido complex or added hydrogen can often be incorrectly assigned an η^3-allylic mechanism. This facile assignment overlooks the possibility of hydrido complexes being formed from reactions with alcohols or other solvents or reagents during the reaction. Several isomerizations brought about by $[RhCl(PPh_3)_3]$ fall into this category. Hydrolysis of added $SnCl_2 \cdot 2H_2O$ forms HCl, which adds to the catalyst forming the pentacoordinate monohydride $[RhHCl_2(PPh_3)_2]$, which can bring about the isomerization of polyunsaturated carboxylic acids and their esters.[14] The isomerization can be inhibited by the addition of lithium carbonate, which, by removing the HCl formed, prevents the formation of the hydrido complex. Another way in which hydrido complexes can be formed in situ is by orthometalation[15]. It has been demonstrated that $[RuCl_2(PPh_3)_3]$ is particularly susceptible to orthometalation, leading to hydrido complex $[RuHCl\{(2-C_6H_4)PPh_2\}$ $(PPh_3)_2]$ that may well

catalyze the many isomerizations brought about by [RuCl$_2$(PPh$_3$)$_3$], which is a more active catalyst than many other transition metal complexes in the isomerization of allyl groups. It usually isomerizes allyl groups to (*E*)-prop-2-enyl substituents, but allyl 2,6-dimethylphenyl ether forms mainly the (*Z*)-product (Figure 1.3)[16].
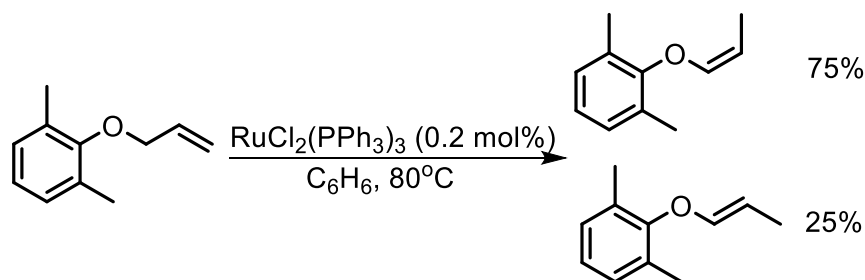
Figure 1.3. Isomerization of allyl ethers with RuCl$_2$(PPh$_3$)$_3$

A general way to distinguish which mechanism is operating for a given migration reaction is to isotopically label either the hydride complex or the substrate with deuterium. If an isomerization of a 1-alkene is carried out using a deuteride complex under the σ-alkyl mechanism (Figure 1.4), and the insertion gives a 1-alkyl, there is a 50% chance of isotopic exchange for the hydrogens on the 2-carbon occurring upon reversion to the 1-alkene. On the other hand, if a 2-alkyl is formed, β-hydride elimination can either reform the 1-alkene or give the 2-alkene, both of which could have deuterium incorporation at the 1-carbon. The same 50:50 ratio of deuterated:nondeuterated 2-carbon will be obtained if starting with a 2-deuterio-1-alkene and a hydride complex. For the π-allyl mechanism, since the complex does not contain a hydride, the deuterium can either exist on the substrate, or be introduced during the allyl intermediate stage. 3,3-dideuteroprop-1-en-3-ol is the ideal substrate to test for the allylic mechanism (Figure 1.5).[17] If one of the deuterium atoms is removed from the 3-carbon via the allylic mechanism and then transferred to the 1-carbon, 1,3-dideuteroprop-2-en-3-ol is formed, which quickly tautomerizes to the aldehyde. Once the aldehyde is formed, no further reversible isomerization

5

will occur, so there will be one deuterium at each of the 1- and 3-carbons, and none at the 2-carbon. If the isomerization proceeds through the alkyl mechanism, there will be some deuterium incorporation at the 2-position.
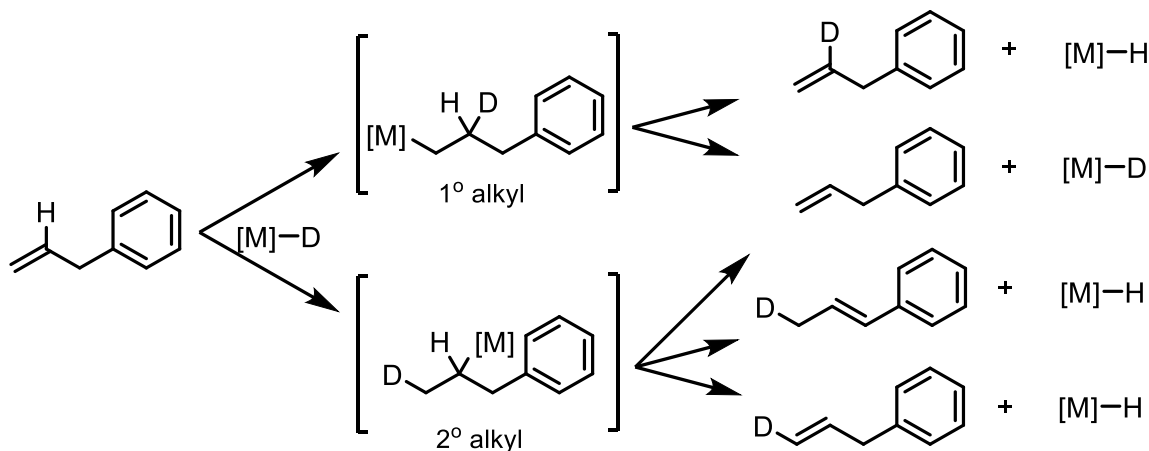
Figure 1.4. Deuterium labelling of complex - alkyl mechanism
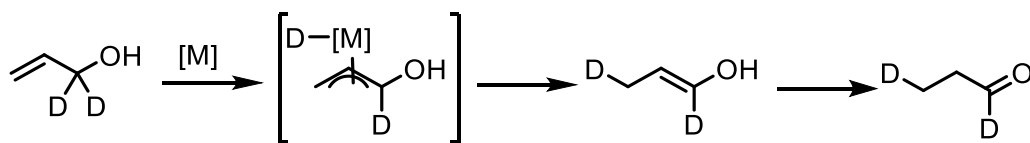
Figure 1.5. Deuterium labelling of substrate - allyl mechanism

Another common way to probe the mechanism is through a crossover experiment: two different alkene substrates (one deuterated, one not) are mixed together, and subjected to an isomerization catalyst. Presumably, exchange of deuterium from the deuterated substrate to the non-deuterated substrate occurs in a more facile manner, via a deuterido complex, in an alkyl isomerization. Deuterium incorporation on the initially non-deuterated substrate therefore can indicate the occurrence of the alkyl mechanism.[12] A specific example of this is the use of 3,3-dideutero-3-(4-methylphenyl)-1-propene and another non-deuterated phenyl propene, such as 3-phenyl-1-propene (Figure 1.6).[18] The challenge is to ensure that deuterium exchange is not

6

occurring with the solvent. Using a CpRu(imidazolylphosphine) catalyst developed in our group (and discussed further in Chapters 2 and 4), facile deuteration of alkene substrates can be accomplished using a mixture of acetone and D_2O.[19] H/D exchange is proposed to occur upon protonation of the pendant imidazole during the formation of the allyl species, and provide crucial evidence of the allyl mechanism, since deuteration only occurs at the 1- and 3-carbons on substrates that cannot undergo positional isomerization, such as propene and diallyl ether.
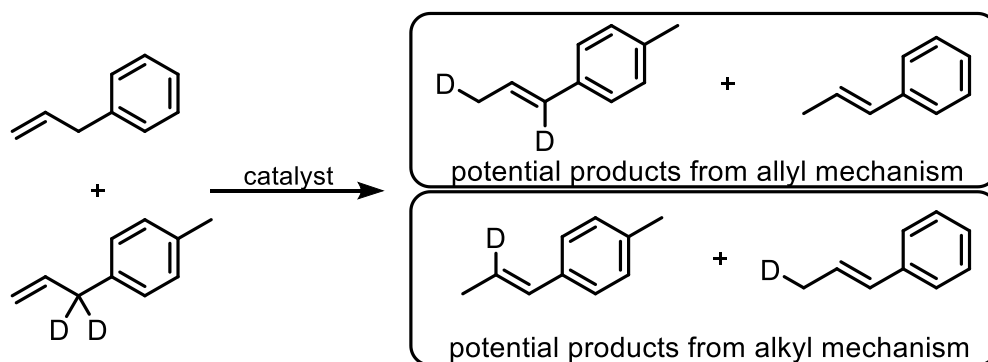
Figure 1.6. Crossover experiment to determine isomerization mechanism

Another unambiguous demonstration of the η^3-π-allylic mechanism occurs in the [RuCl$_2$(PPh$_3$)$_3$] catalyzed isomerization of a dihydropyridazine derivative (Figure 1.7). Both polyhydrido ruthenium complexes and [RuHCl(PPh$_3$)$_3$] were inferior catalysts for the reaction, and the addition of ethanol to the reaction mixture reduced the yield by a factor of 25. All these observations lead to the conclusion that hydrido complexes, and by implication the β-hydride mechanism, were not involved.[20]
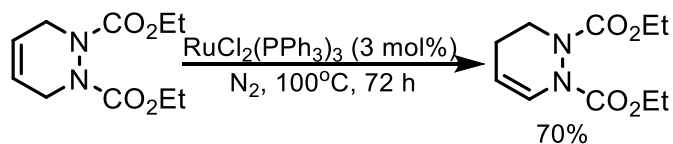
Figure 1.7. Dihydropyrazine isomerization

Alkene isomerization is somewhat unusual in the realm of organic reactions, because the potential exists, depending on the substrate, for the reaction to repeat itself. That is, regardless of which mechanism is in operation, under conditions where reactions are reversible, the potential to migrate more than one position down a chain or around a ring (given the presence of allylic protons) exists. As a result, in the absence of a clear thermodynamic preference for one product, catalytic double-bond migrations often result in mixtures of positional and geometrical isomers that can be troublesome to separate. If the goal of a synthetic chemist is to produce a single isomeric product in high yield, they must be cognizant of the thermodynamic stability of the various potential isomers that can be formed in the isomerization process.

Isomerization reactions should therefore be divided into two classes. One class involves the transformation of a more stable isomer to a quasi-equilibrium mixture of isomers, with the goal of placing the alkene in a more reactive position for further functionalization that consumes alkene, in what are often referred to as tandem isomerization/functionalization reactions. Another class is the conversion of less thermodynamically stable isomers to more stable isomers, the most ubiquitous being the isomerization of terminal alkenes to internal alkenes. A third group, related to both of the other two classes, is sequential isomerization/functionalization reactions. Sequential isomerization/functionalization reactions can be either one-pot or the intermediate could be isolated between steps. However, a requirement of sequential isomerization/functionalization, since it is stepwise, is that the isomerization step must be thermodynamically favorable for the first intermediate to be in high yield. Therefore, sequential isomerization/functionalization is more of an extension of the second class of isomerization reactions (thermodynamically favorable migrations), and therefore will not be a major focus of this chapter. Both classes offer different challenges in terms of development of catalysts that can

assist in selective transformations. General features of catalysts used in tandem isomerization/functionalization reactions are high efficiency of isomerization (generally, because the isomerization occurs prior to the functionalization, the isomerization catalytic cycle should be faster than the functionalization), and compatibility with other catalysts (if a dual-catalyst system is used in the tandem process). Catalysts used for thermodynamically favorable migrations should ideally also be efficient, but functional group tolerance and kinetic control are important features. This introduction will overview a number of examples of developments in each of these classes of isomerization reactions, and will highlight and put into perspective the contributions provided by catalysts **1.1** and **1.2** + **1.2a**, developed in the Grotjahn group (Figure 1.8). The investigations that the dissertation author have performed on catalyst **1.1** will be discussed in chapter 2, and the development of a more efficient alternative for **1.2** + **1.2a** (catalyst **3.14**) will be discussed in chapters 3 and 4.
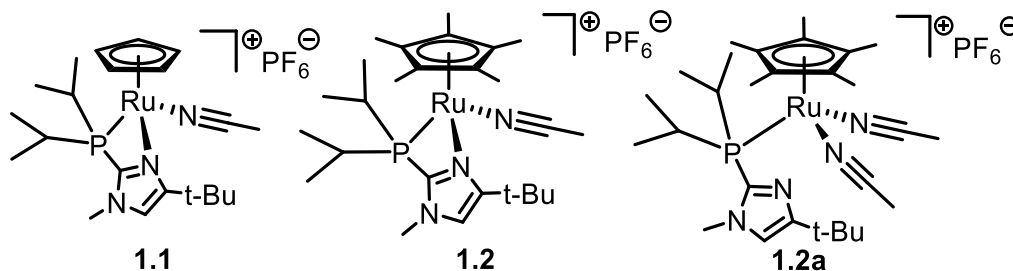
Figure 1.8. Catalysts previously developed in the Grotjahn group

1.3 Tandem isomerization/functionalization reactions

Alkenes are one of the most versatile groups for functionalization in organic synthesis, and many of these functionalizations can be mediated or aided by transition-metal catalysis. Catalyst systems that incorporate an isomerization of an alkene prior to the functionalization step are generally called tandem isomerization/functionalization reactions. These tandem reactions can involve either one or two catalysts, and typically involve isomerization of the alkene to a

more reactive or accessible position. The more reactive position may require an internal alkene, and often, the more sterically accessible position is the terminal alkene (which, in turn, can make it more reactive with an external reagent or another catalyst). This section will discuss important one-pot isomerization/functionalization reactions, with a bias towards single catalysts that can perform both the isomerization and the functionalization, and dual-catalyst systems that perform the isomerization and the functionalization in parallel, which is also known as orthogonal tandem catalysis.

1.3.1 Tandem isomerization/hydroformylation

One of the most common and widely developed tandem isomerization/functionalization processes in homogeneous transition metal catalysis is isomerization/hydroformylation. Hydroformylation, known as the oxo process in industry, is formally an addition of a C-H bond of formaldehyde across a double bond. In practice, however, the process is achieved through application of syngas, which is a mixture of CO and H_2 gas. Although the exact mechanistic steps can differ between catalysts, typically an alkene inserts into a metal-hydride bond to form an alkyl ligand. The alkyl then migrates into metal-CO bond, forming an acyl ligand, which then undergoes reductive elimination with another hydride ligand to form the aldehyde. The identity of the alkyl ligand that migrates into the metal-CO bond will determine the position of the aldehyde in the product. Carbonylation of a secondary alkyl leads to a branched aldehyde, whereas carbonylation of a primary alkyl leads to a linear aldehyde product. If a linear aldehyde is desired, a terminal alkene is generally used, since in the absence of alkene isomerization, only terminal alkenes can form primary alkyls. However, since the first step in the mechanism is the same as the first step in the σ-alkyl isomerization mechanism (insertion of the alkene into the metal-hydride bond to form the alkyl), a subsequent β-hydride elimination can lead to alkene

isomerization. If the isomerization is much faster than the hydroformylation, even alkene mixtures can form terminal alkene that undergoes hydroformylation to form the linear aldehyde (Figure 1.9). Sterically demanding ligands and acid or hydride additives have been found to favor the formation of linear aldehydes in this manner.
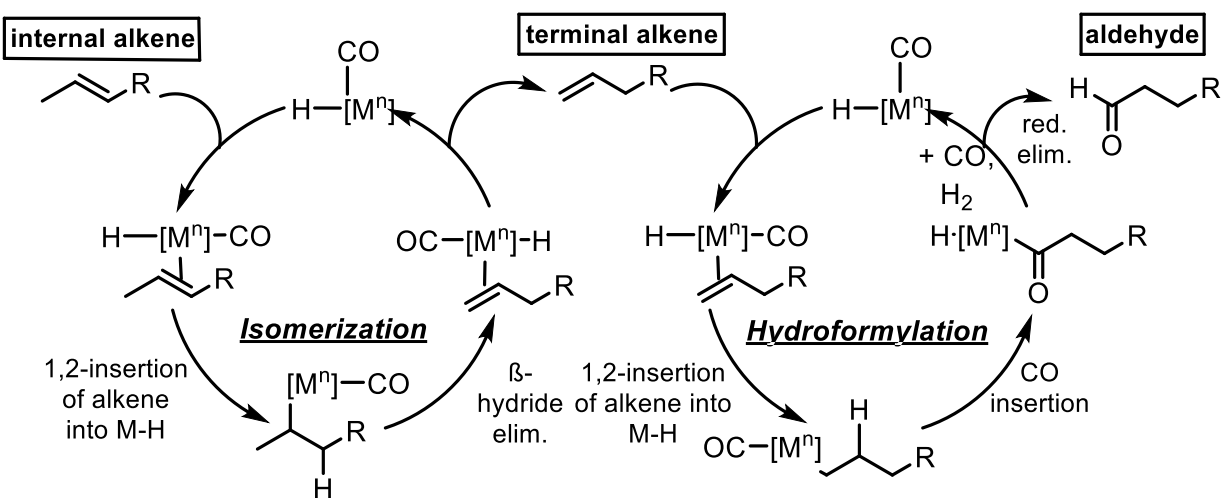
Figure 1.9. Tandem isomerization-hydroformylation catalytic cycles

Recently, a rhodium(I)catalyst ([Rh(cod)$_2$]BF$_4$) with the addition of IPHOS was able to catalyze the tandem isomerization/hydroformylation, and reductive amination of internal olefins to terminal amines in a one-pot process (Figure 1.10) with 88% conversion and 68% terminal amine selectivity in the case of piperidine.[21]

11
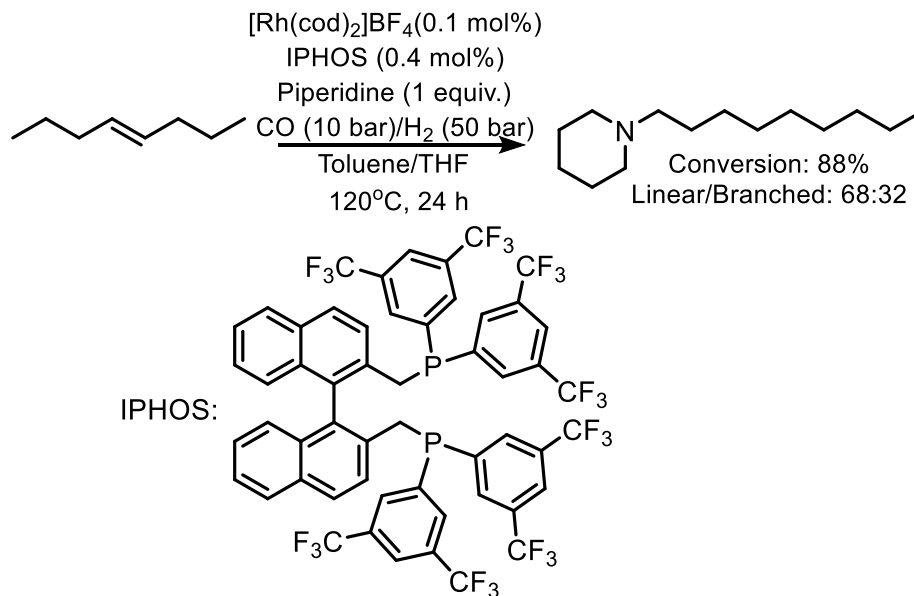
Figure 1.10. Tandem isomerization/hydroformylation/reductive amination

1.3.2 Tandem isomerization/hydroboration

Hydroborations of terminal alkenes can occur without the use of a catalyst with the use of boranes such as BH_3, catecholborane, and 9-BBN; internal alkenes can also be hydroborated, and hydroboration generally proceeds with *anti*-Markovnikov selectivity. Hydroboration of internal alkenes can often be sluggish, however, and transition-metal catalysts have been developed that can promote the isomerization of internal alkenes to terminal alkenes before the hydroboration step. Pinacolborane is an ideal borane source for the catalyzed tandem isomerization/hydroboration for two reasons: 1) The borane is not effective at hydroboration in the absence of a transition-metal catalyst or Lewis acid, and 2) upon oxidative addition of the pinacolborane to the metal, it will undergo rapid insertion/β-hydride elimination steps until it reaches a 1° alkyl, at which time a reductive elimination occurs to form the terminal alkylborane. Several metal complexes have been shown to promote the reaction, such as [RhCl(C$_2$H$_4$)$_2$], [Ir(cod)Cl]$_2$ with (bisdiphenylphosphino)-methane or –ethane, a bis(imino)pyridine cobalt complex, or a *N*-phosphinoamidinate cobalt complex. Notably, the bis(imino)pyridine complex

12

is quite active even with a hindered disubstituted alkene (2,5-dimethyl-3-hexene), producing the terminal alkylboronic ester with 75% yield (Figure 1.11). [21]
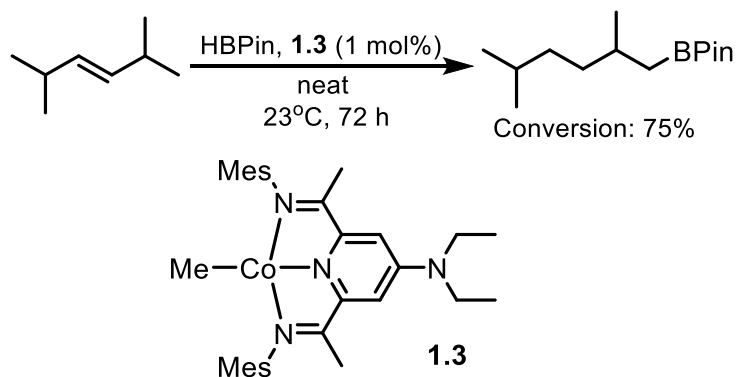
Figure 1.11. Tandem isomerization/hydroboration of 2,5-dimethyl-3-hexene

1.3.3 Tandem isomerization/hydrozirconation

Although not catalytic, Schwartz's reagent (Cp$_2$Zr(H)Cl) is a transition metal complex that effects the isomerization of internal alkenes to terminal alkylzirconocenes, and therefore bears mentioning here. While not the only metal complex that can achieve this migration, Schwartz's reagent is quite selective for forming the terminal alkylzirconocene, and can isomerize over a long chain (>10 bonds). The alkylzirconocene can be used directly or transmetallated for use as a nucleophile. One of the drawbacks of the chemistry is the difficulty reacting with trisubstituted alkenes.[21]

1.3.4 Tandem isomerization/metathesis

In most of the above-mentioned tandem isomerization/functionalization reactions, the goal of the isomerization is to bring the alkene to the terminal position, where it will perform the functionalization step. Alkene metathesis, which is an exchange of substituents of two different double bonds, can change the length of a carbon chain as well as the substituents attached to it. The combination of isomerization and metathesis, if properly tuned, can modulate both the

13

length of a carbon chain and the position of a double bond in that carbon chain, providing a valuable tool for diversity of synthetic products. Of the two main catalyst systems for alkene metathesis, Grubbs' ruthenium-based catalyst and Schrock's tungsten system, metathesis using Grubbs 1st and 2nd generation catalysts are indeed found to catalyze the isomerization of various substrates prior to or during metathesis.[22] Often, isomerization is considered to be an unwanted side product during metathesis. Mechanistic studies have shown the isomerization to be due to a ruthenium hydride species that is a decomposition product of the metathesis catalyst. Isomerization can then be inhibited by the addition of hydride scavengers such as benzoquinone. On the other hand, when subsequent isomerization of the product is desired, tandem metathesis/isomerization is accomplished by inducing catalyst decomposition to a ruthenium hydride species after metathesis. The reverse reaction, an isomerization followed by metathesis, is more challenging with the catalyst decomposition method, because as the effectiveness of the isomerization increases due to greater catalyst decomposition, the efficiency of the metathesis decreases. As a result, a tandem isomerization/metathesis process is hard to control with the single catalyst.

However, dual catalyst systems are being developed for selective isomerization/metathesis. Isomerization/metathesis on (*E*)-3-hexene produced (Z)-5-decene with 59% chain-length selectivity and a 7:93 *E*:*Z* ratio. The two catalysts used are orthogonal and compatible with each other in that the Grotjahn isomerization catalyst (**1.1**) only acts on (*E*)-alkenes, and the Schrock metathesis catalyst only reacts with terminal or (*Z*)-alkenes. The Schrock catalyst therefore does not metathesize the internal (*E*)-alkenes, waiting for some terminal alkene to form. Conversely, **1.1** does not isomerize the (*Z*)-configured final product.[21] Another fascinating example of orthogonal tandem isomerization/metathesis is performed by

14

Gooβen, in which kairomones 3-ethylphenol and 3-propylphenol (tsetse fly attractants) are synthesized from cashew nut extracts. While the previous example used metathesis as a way to lengthen the molecule, the goal of metathesis here is to make the alkene chain shorter. The key step involves the conversion of 3-(8-nonenyl)phenol to a mixture of 3-(1-ethenyl)phenol and 3-(1-propenyl)phenol by isomerization and metathesis with ethylene. The process is performed by a one-pot dual-catalyst system, $[(PtBu_3)PdBr]_2$ for isomerization and Hoveyda catalyst for metathesis. Although the isomerization / metathesis could be done sequentially, the dual process succeeds in dynamically shortening the length of the chain as it is being isomerized. While mixtures of the two products could be obtained, the mixture could be selectively converted to one or the other by purging of the reaction atmosphere with either ethylene or 2-butene.[23]

1.3.5 Other tandem isomerization/bond formations

A number of other interesting transformations occur upon isomerization of unconjugated enones to their α,β-unsaturated carbonyl counterparts. The conjugated carbonyl can act as a classic Michael acceptor to a waiting nucleophile, as seen by Dierker in the conjugate additions of pyrrolidine and a phenyl group from BPh_4^- to alkenyl esters using Rh(acac)(cod) and BIPHEPHOS[24]. The opposite reactivity can be seen by Ryu with $RuHCl(CO)(PPh_3)_3$, whereby isomerization to the enone or other carbonyl moiety generates an enolate which can react with electrophiles such as aryl aldehydes[25].

Isomerization can also be triggered by a Heck reaction using a suitable palladium source. Several groups report the isomerization of an alkene to the carbonyl when coupling aryl or alkenyl groups to alkenyl alcohols using $Pd(dba)_2$ and base, or $Pd_2(dba)_3/Pd(CH_3CN)_2(OTs)_2$ with the PyrOx ligand.[21]

1.4 Thermodynamically favorable migrations

Alkene thermodynamic stability can be generally related to the number and identity of substituents on the alkene. In the absence of conjugating or heteroatom substituents, monosubstituted, or terminal alkenes, are less stable than di-, tri- or tetrasubstituted alkenes. Alkenes conjugated to heteroatoms or π-systems are generally significantly more stable that their nonconjugated isomers. When less stable (i.e. less-substituted and / or nonconjugated) alkenes are subjected to isomerization catalysts, the overall effect is isomerization to a more stable isomer or a mixture of comparably stable isomers. If a single isomer is desired in high yield, that isomer must be either considerably more stable than others, allowing it to dominate upon reaching equilibrium, or a kinetic preference for that isomer must be established that causes it to form faster and / or more slowly evolve to other isomers, dominating the reaction mixture at some stage of the isomerization.

1.4.1 O-allyl and N-allyl isomerization

While the isomerization of linear 1-alkenes to internal disubstituted alkenes is thermodynamically favorable, the added stabilization is found by introducing the alkene into conjugation with a heteroatom or other π-system provides an added thermodynamic driving force. The double-bond migration of allyl ethers and amines to form *O-* and *N*-(1-propenyl) compounds has been established in organic synthesis as a method of protection and deprotection of –OH and -NH groups. While the mechanism for double-bond migration occurs through one of the two mechanisms mentioned above, the behavior of the catalytic system can be influenced by potential pre-coordination of the oxygen or nitrogen atom to the metal prior to isomerization. Pertici postulated that the simultaneous coordination of the oxygen atom, as well as the η^3-allyl group, to the metal explains the high *Z*-stereoselectivity for *Z* complexes operating through the π-

allyl mechanism.[26] Golborn, in his study of the isomerization of allyl ethers with PdCl$_2$(CH$_3$CN)$_2$, illustrates the advantage of *O*-chelation in competing catalytic cycles, suggesting the (*Z*)-isomer forms faster because of the ability to form the *O*-allyl chelate (Scheme 1.12). The addition of phosphines to [RuCl$_2$(COD)]$_x$ induces isomerization that is richer in *E*-isomers, and the selectivity can be influenced by the bulkiness of added phosphines.[16]
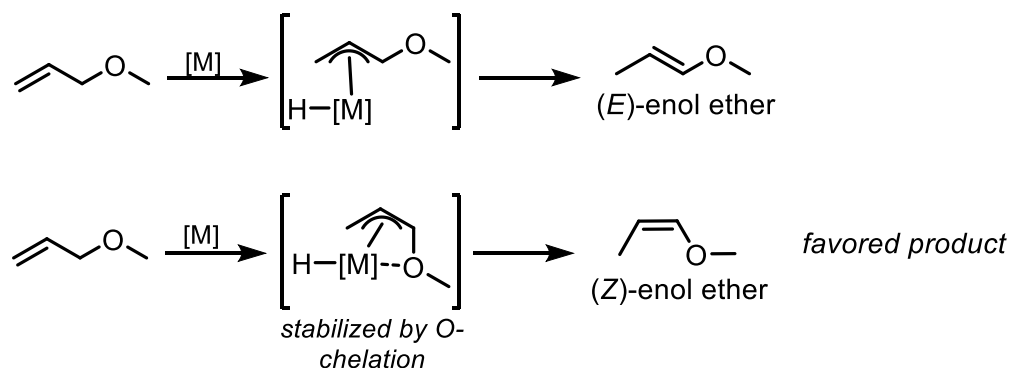
Figure 1.12. O-chelation assisting formation of (*Z*)-enol ethers

O-chelation becomes a less important factor in the isomerization of *O*-allyl substrates with weaker donor properties, such as allyl carboxylates (allyl esters). Selectivity is often lower as a result. Allyl esters have the added challenge of oxidative addition of the C-O bond to form stable (allyl)(carboxylato) complexes, although Gooβen obtained high yields of enol esters with the [(PtBu$_3$)PdBr]$_2$ dimer, such as 97% 1-propenyl acetate (*E:Z* ratio: 1:2) from allyl acetate.[27]

N-allyl isomerization can also be achieved by many of the classical isomerization catalysts, with rhodium being the most common metal used, such as the isomerization of *N,N*-dimethyl-*N*-allylamine with RhH(CO)(PPh$_3$)$_3$ (1 mol%, 80 °C, 2 h, 100:0 *E:Z* ratio). From most allylamine isomerizations, the *E:Z* enamine product ratio is exceedingly high, likely owing to the strong *N*-coordination. If the nitrogen is not tertiary, however, the enamine quickly tautomerizes to the imine, and stereochemical information is lost. *N*-allylamide isomerization produces a

mixture of *E*:*Z* isomers, with neither dominating,[28] unless the *E*-selective catalyst **1.1** (Figure 1.8) is used, in which case >99:1 selectivity is achieved through catalyst control.[29]

1.4.2 Allylic alcohol isomerization

The isomerization of allylic alcohols deserves special recognition for the sheer number of catalysts capable of performing the reaction, including ones that enantioselectively establish a chiral center in the process. Typically, the metal catalyst moves the alkene function of the allylic alcohol over one position, as in the case of *O*-allyl substrates, to an enol. However, an important difference from *O*-allyl substrate isomerization is that the enol can tautomerize, with or without the aid of the metal, to form a ketone or aldehyde. A carbonyl is generally the more stable tautomer; exceptions arise when the enol is involved in significant conjugation to stabilize it. The conversion of alkene to carbonyl is fundamentally an intramolecular redox process, with the C-C double bond formally undergoing a reduction, while the alcohol is becoming oxidized to a carbonyl.

One of the earliest catalysts to be used for allylic alcohol isomerization was $Fe(CO)_5$. When studying $(1,3\text{-butadiene})Fe(CO)_3$ complexes, upon exposure to water, some 2-butanone would form. It was postulated that one of the double bonds is hydrated to form the allylic alcohol, and subsequently isomerized to obtain the ketone. Other iron carbonyls like $Fe_2(CO)_9$ and $Fe_3(CO)_{12}$ are more efficient, and can isomerize allylic, homoallylic and even more remote alkenyl alcohols (up to 8 bonds), as well as trisubstituted allylic alcohols, although catalyst loadings are quite high (10 – 30%).

$RhCl_3$ and $Rh_2(SO_4)_3$ have shown to be competent catalysts for the transformation as well, and perform better under biphasic conditions, since the allylic alcohol substrates can be

soluble in water with the catalyst, but the ketone or aldehyde products have better solubility in the organic phase. As expected, as the length of the chain on the allylic alcohol increases, the turnover frequency for the biphasic system decreases. Bisphosphines such as dppe also increase the activity. Interestingly, Tani *et al.* were able to observe by NMR, using small amounts of [(bisphosphine)Rh(solvent)$_2$]ClO$_4$ (0.5 mol %) the enol intermediate of various allylic alcohol isomerizations (Figure 1.13).[30] The lifetime of the enol intermediate depends on both the length and substituents of the bisphosphine linker: the wider and more bulky the bisphosphine, the faster the tautomerization occurs, suggesting at least for that particular catalyst system tautomerization is aided by the catalyst. The stereochemistry of the enol formed is also very important, with Z-enols tautomerizing much more slowly (Tables 1.1 and 1.2).
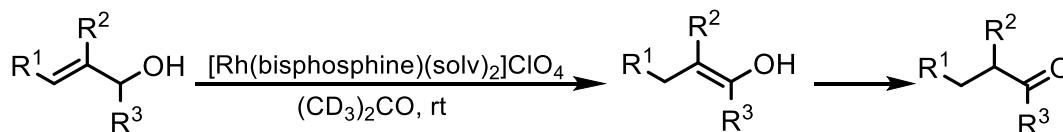
Figure 1.13. Rhodium bisphosphine catalyzed allylic alcohol isomerization (see Tables 1.1 and 1.2 for effect of bisphosphine linker and R-groups on allylic alcohol)

Table 1.1. Effect of bisphosphine length and substituent on rate of keto/enol tautomerization with [Rh(bisphosphine(solv)$_2$]ClO$_4$[30]

diphosphine	time^a (min)	enol (%)	ketone (%)
Ph$_2$P(CH$_2$)$_2$PPh$_2$ (dppe)	14	89	11
Cy$_2$P(CH$_2$)$_2$PCy$_2$ (dcype)	<5	0	100
Ph$_2$P(CH$_2$)$_3$PPh$_2$ (dppp)	45	0	100
Ph$_2$P(CH$_2$)$_4$PPh$_2$ (dppb)	19	25	75
BINAP	21	80.4	19.6

^{a} Time required to convert 98% allyl alcohol to product

Table 1.2. Effect of substituents on allylic alcohol on time to produce enol and time to tautomerize to ketone[30]

R^1	R^2	R^3	enol production time[a]	enol tautomerization time[b]
H	H	H	14 min	(Z): 120 min, (E): 40 min
H	H	Me	9 min	(Z): 180 min, (E): 50 min
H	H	Ph	124 min	(Z): 5.5 h
Ph	H	H	167 min	(Z): ~8 h, (E): ~6h

[a] Time required to convert 98% allyl alcohol to product
[b] Time required to convert 98% enol into carbonyl

RuCl$_3$, on the other hand, is a poor catalyst for allylic alcohol isomerization, but the dicationic Ru(H$_2$O)$_6$(tos)$_2$ performs quite well in water with 3-buten-2-ol, as does RuCl$_2$(PPh$_3$)$_3$. The Trost group tested a large range of allylic alcohol substrates with CpRu(PPh$_3$)$_2$Cl and (Ind)Ru(PPh$_3$)$_2$Cl with Et$_3$NHPF$_6$, showing reasonable activity and good yields for a number of non-hindered secondary allylic alcohols. The selectivity in terms of relative rates of isomerization for allylic alcohols over non-allylic alcohols and remote alkenes stands out.[17]

1.4.3 Alkenes in conjugated C-C pi systems

Double-bond migration also occurs in dienes. Again, the isomerization gives rise to more stable products usually containing conjugated double bonds. Possibly one of the most simple reactions is the (Z) → (E) conversion of penta-1,3-diene by [Fe(CO)$_5$],[31] or the isomerization of cyclohexa-1,4-diene to cyclohexa-1,3-diene by [RuCl(PPh$_3$)$_3$]. Occasionally, examples of deconjugation are seen, such as the isomerization of cycloocta-1,3-diene (the most stable isomer), to a chelated cycloocta-1,5-diene complex (Figure 1.14) using RhCl$_3$·3H$_2$O. The deconjugation reaction is stoichiometric, however, because the chelation of the 1,5-diene to rhodium provides the necessary stabilization to drive the reaction forward. Since no intermediate

cycloocta-1,4-diene can be observed in the reaction, it was presumed to proceed via an η^3-intermediate.[32]
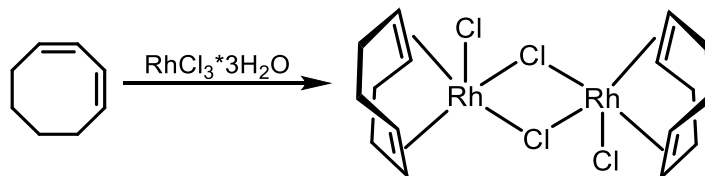
Figure 1.14. Isomerization of 1,3-octadiene to coordinated 1,5-octadiene

The stabilization afforded by converting allylbenzenes into their conjugated phenylpropenoids results in a more facile isomerization than with non-aryl alkenes. Moreover, enhanced acidity from two unsaturated substituents enables the use of mild bases such as sodium and potassium hydroxide, sometimes at relatively high temperatures. A few notable examples are the isomerization of 2-allyl-6-methoxy-4-methylphenol in refluxing methanol to produce the phenylpropenoid with an excellent 95% yield in 10 hours in the synthesis of (+)-herbertenediol, and the solventless isomerization of 2-allyl-6-methylaniline over solid potassium hydroxide at 300 °C. Other bases, such as sodium *tert*-butoxide and *n*-butyllithium, have also been used. Despite the success that simple bases have had, transition-metal catalyzed isomerization of allylbenzenes is a superior choice for faster reaction times, lower temperatures, greater *E/Z* selectivity, and for substrates that contain base-sensitive functionalities.[18]

A number of palladium complexes have been used for allylbenzene isomerizations, including PdCl$_2$(MeCN)$_2$, Pd(PPh$_3$)$_2$Cl$_2$, PdCl$_2$(PhCN)$_2$, PdCl$_2$, Pd$_2$(dba)$_2$, and Pd(OAc)$_2$. Once again, PdCl$_2$(MeCN)$_2$ is the most often used palladium catalyst for intentional isomerization, with reactions typically run at reflux in dichloromethane or toluene, from 7-24 hours, ~10% catalyst, and yields often >90% and *E/Z* ratios >90:10. Often, isomerization is observed in spite of the presence of additives intended for cross-coupling, such as aryl halides, excess phosphines,

and bases. However, there have been examples of sequential isomerization/coupling reactions using palladium, which will be discussed in the next section.
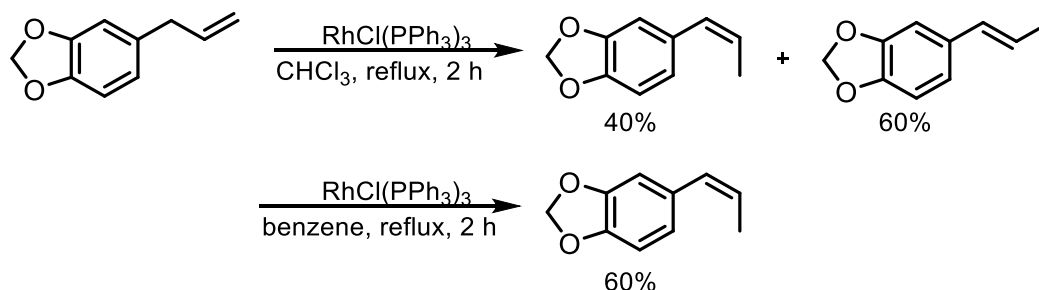
Figure 1.15. Isomerization of safrole to isomers of isosafrole with RhCl(PPh$_3$)$_3$

Rhodium catalysts are also used for isomerization of allylbenzenes, with simple RhCl$_3$ in alcoholic solvent being the most common choice. There is some evidence that a rhodium hydride species is the active catalyst for the isomerization with RhCl$_3$, either generated from the alcohol solvent, or from molecular hydrogen, as a low pressure of hydrogen increases the rate of isomerization. Rao showed that Wilkinson's catalyst ((PPh$_3$)$_3$RhCl) proved to be a competent catalyst for the isomerization of safrole. An interesting note is that in refluxing chloroform, after 2 hours, a mixture of *cis* (40%) and *trans* (60%) isosafrole was obtained, but in refluxing benzene under the same time period, only *cis*-isosafrole was present, with 60% conversion (Figure 1.15). Baba showed with the [Rh(OH)(cod)]$_2$ dimer in 1,4-dioxane that a range of allylbenzenes could be isomerized; importantly, the rhodium-hydride complex could be generated in situ from an interaction between the cod ligand and the hydroxide ligands, without any external hydrogen source (Figure 1.16). Many of the catalyst examples above suggest the alkyl mechanism is in operation, but a supported cyclopentadienyl rhodium(III) chloride system capable of isomerizing allylbenzene is able to be quenched completely by addition of triethylamine, suggesting that the π-allyl mechanism may be in operation for that particular system (since the base can reverse the oxidative addition of allyl hydride). Rhodium catalysts

have also shown promise in tandem isomerization/hydroformylation of allyl benzenes, which will also be discussed later.[18]
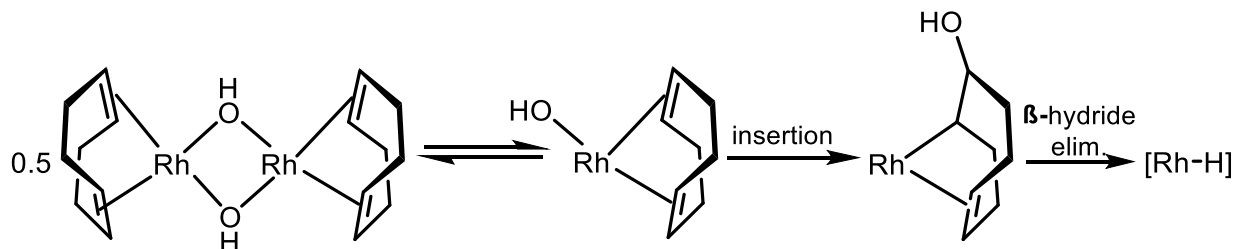
Figure 1.16. Formation of active Rh hydride species from [Rh(cod)OH]$_2$ dimer

Ruthenium is quite commonly used in the isomerization of allyl benzenes, with advantages including often high conversions with good to excellent E:Z selectivity. The simple complexes RuCl$_3$*3H$_2$O, RuCl$_2$(PPh$_3$)$_3$ and Ru(acac)$_3$ have been proven to be effective for allyl benzene isomerizations, the former used by Castonguay and Brassard on an allyl anthroquinone skeleton (Figure 1.17) in the total synthesis of ($\pm$)-averulin and ($\pm$)-bipolarin. The result is significant because the authors reported that this skeleton was resistant to isomerization with other common metal catalyst systems for isomerization. Ruthenium hydride complexes such as HClRu(PPh$_3$)$_3$ and RuClH(CO)(PPh$_3$)$_3$ have also been effective, with the later used in several syntheses of natural products. In addition, Grubbs' second-generation metathesis catalysts have been reported to decompose to a ruthenium hydride species, which has shown to be active for isomerization.[18]
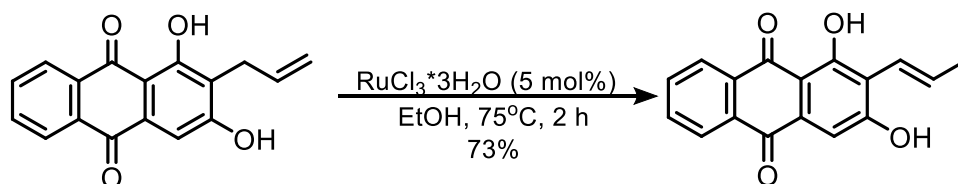
Figure 1.17. Isomerization of 2-allyl-1,3-dihydroxyanthraquinone with RuCl$_3$*3H$_2$O

Much work has been put into developing 'greener' methods for isomerization using polymer-supported ruthenium catalysts, or performing isomerizations in neat allyl benzene substrate. Sulfonated phosphine derivatives of $RuCl_2(PPh_3)_3$, among other rhodium and iridium phosphine complexes, can be immobilized in SiO_2-sol gel matrices and subjected to allylbenzene; the ruthenium derivative performed most efficiently. Crochet and Cadierno developed complexes **1.4** and **1.5** (Figure 1.18) capable of performing isomerizations of estragole (paraallyl anisole) and eugenol (4-allyl-2-methoxyphenol) in polar solvents including water (0.2 – 1.0 mol%, 80°C).[18] The cationic complex **1.1** (Figure 1.8), also isomerizes various allyl benzene substrates with high efficiency, both in organic solvents and without solvent. In a particular example of a 'green' method of isomerization, we showed that polymer-supported analogue of **1.1**, when encased in a polyethylene mesh bag was shown to be capable of repeated cycles of isomerization in distilled neat eugenol without loss of activity for up to 10 cycles.[33] This application of **1.1** will be discussed further in chapter 2.
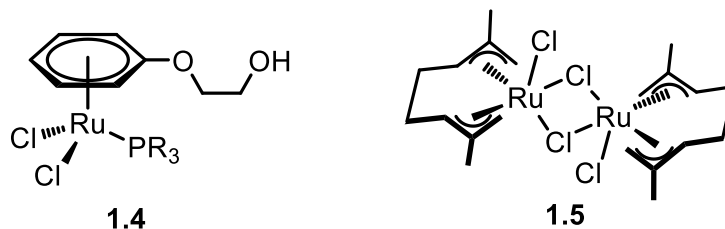
Figure 1.18. Water-soluble complexes for allyl benzene isomerization

1.4.4. Long-range isomerizations

Long-range isomerization can be defined as isomerization over more than two bonds. Several isomerization catalysts will isomerize longer-chain alkenes to mixtures of isomers that contain some amount of three or more bond migrations, for example 1-octene to (*E*)-4-octene. Two challenges are apparent: first, mixtures of isomers are often undesirable, and more isomers

of comparable stability are possible the longer the chain. The second challenge is the speed of the isomerization; slow catalysts will not perform the number of double-bond migrations necessary to complete the transformation in a reasonable amount of time. The solution to the first challenge is the substrate: usage of a substrate that has a thermodynamic sink at one position (often at the opposite end) of the chain from the alkene is required to prohibit reversibility once the double bond reaches it. An aromatic ring or a carbonyl π-system can conjugate with the alkene, or an alcohol can become an enol and then a more stable carbonyl, as in allylic alcohol isomerization. The second challenge involves the catalyst. Although numerous catalysts can efficiently isomerize allylic and short-chain alkenes, rarer are those that have been shown to be sufficiently active enough to catalyze the long-range isomerization of alkenes. In 2000, Mori noted that $RuHCl(CO)(PPh_3)_3$ could be used to deconjugate α,β-unsaturated esters and amides, and showed that the alkene would conjugate to an unsaturated moiety or an ether up to four bonds away (Figure 1.19).[34] Mori's work is significant because it shows that the process can be initiated from deconjugation of the more stable conjugated ester to temporarily produce the less stable unconjugated ester. In 2007, our group showed the impressive activity of **1.1**, isomerizing a terminal alkene 30 positions to form the enol and subsequent ketone.[35] In 2012, Kochi used (1,10-phenanthroline)Pd(Me)(Cl) to migrate a terminal alkene up to eight positions via "chain-walking" mechanism, where the alkyl-Pd then undergoes an intramolecular insertion with another alkene to form a five-membered ring.[36] Mazet, in 2014, catalyzed the isomerization of citronellal derivatives with dcype(1,2-bis(dicyclohexylphosphino)ethane)Pd(Me)Cl (**1.6**, in figure 1.19), converting a trisubstituted alkene to a carbonyl over eight positions past a congested tertiary carbon, and a 10 carbon isomerization of both terminal and phenyl-conjugated, disubstituted alkene to an α,β-unsaturated phenyl ether.[37] In 2016, Mazet extended the range of

25

isomerization to over 30 positions with a bulkier 1,2-bis-(di-*tert*-butylphosphino)ethane complex (**1.7**).[38]
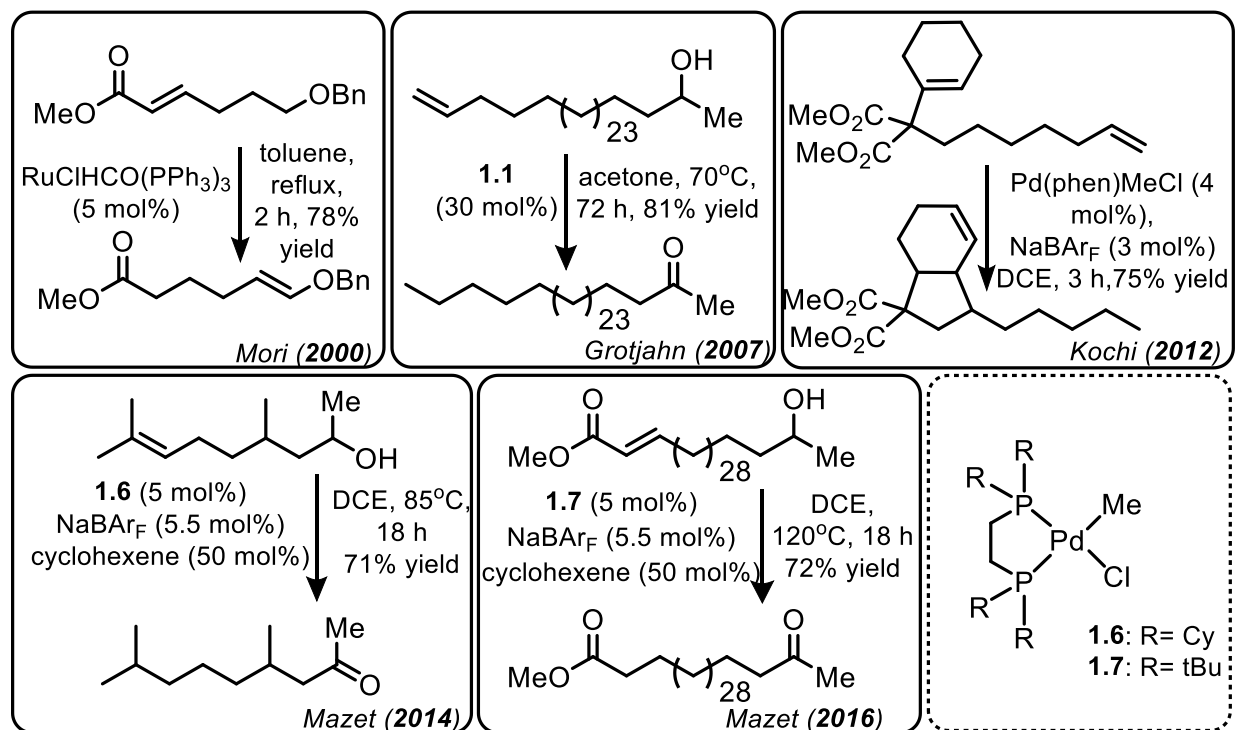
Figure 1.19. Notable long range alkene isomerizations

1.4.5. Controlled isomerization of linear unfunctionalized alkenes

For a number of examples above, catalyst and substrate control of selectivity for a given substrate is largely limited to geometrical (E/Z) isomerism, as opposed to positional isomers. The reason is largely a thermodynamic one: one positional isomer will dominate if it possesses a higher degree of stability (i.e. highly substituted, conjugated to a π-system, etc). If several isomers are of similar thermodynamic stability, such as in the case of linear internal alkenes, a mixture of isomers will be obtained under conditions of thermodynamic control. For example, the equilibrium product distribution of the five isomers of heptene (Figure 1.20) calculated from enthalpies of formation by D'Souza closely matched the experimental product distribution after

26

isomerization of 1-heptene with $RhCl_3 \bullet nH_2O$ (~1 mol%) + $BH_3 \bullet THF$ (10 mol%) for 24 hours (Table I.3)[39].
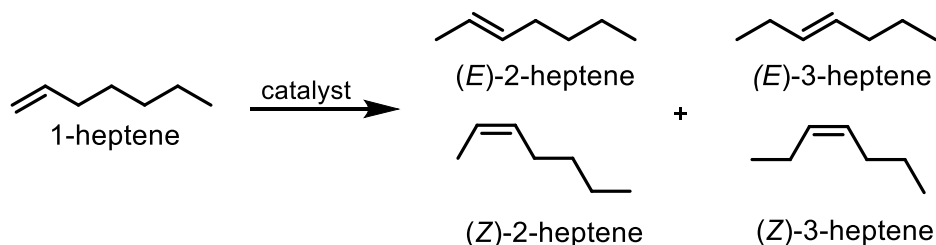
Figure 1.20. Double-bond isomers of heptene

Table 1.3. Calculated and experimental distribution of heptene isomers using $RhCl_3$ + BH_3 as catalyst[39]

Heptene isomer	ΔH_f (kcal/mol)	Calculated %	Experimental %
1-heptene	-23.35	0.427	0.728
cis-2-heptene	-25.31	11.743	12.724
trans-2-heptene	-26.15	48.525	43.254
cis-3-heptene	-25.00	6.939	7.262
trans-3-heptene	-25.91	32.366	36.032

A large number of classical double-bond migration catalysts give similar equilibrium mixtures upon isomerization of linear alkenes. Catalysts that can achieve positional or cis-trans selectivity for linear alkenes must therefore rely on kinetic control, where the transition state leading to the desired product is considerably more stabilized than the transition states leading to other products. For the case of 1-alkene reactants, positionally selective isomerization catalysts presumably have an advantage in that a 2-alkene must be formed before isomerizing to the 3-alkene, but often overisomerization occurs as rapidly as the first isomerization.

Indeed, prior to the last ten years, the best reported catalyst for monoisomerization of 1-alkenes was $Ru(CO)_3(PPh_3)_2$; in the early stages of isomerization of 1-hexene using

Ru(CO)$_3$(PPh$_3$)$_2$ (0.5 mol%, 3 h, 40 °C), one obtained 80% 2-hexene (*E/Z* ratio: 2:1), along with 16% 3-hexene.[40] Since 2008, a select number of catalyst systems[41] (e.g., Ru$_3$(CO)$_{12}$, Fe$_3$(CO)$_{12}$ with added 3N KOH, a Cr(NCN) pincer complex, Fe(acac)$_3$ activated by PhMgBr, and a bulky bis-carbene Ir pincer complex activated by NaOtBu) have improved selectivity, reporting yields of 2-alkenes from 92->99%, with *E:Z* ratios ranging from 2:1 to 6:1. Notably, using the bulky bis-carbene Ir pincer complex activated by NaOtBu, there was no significant increase in the amount of 3-octene after 24 hours.

Stereochemical (*E/Z*) control of linear alkene formation from 1-alkenes is also challenging, but can be important for synthesis. The expected product ratio of trans-2-heptene to cis-2-heptene calculated from the percentages in Table 1.3 is around 4.1 to 1, which is similar to the product *E/Z* ratios produced by catalysts referenced in the previous paragraph. In contrast, a few catalysts can achieve high selectivity for either *E*- or *Z*- isomers of linear alkenes. Two systems that have been identified as highly *E*-selective are a cobalt-carbene complex activated with a silyl Grignard reagent (88:1 *E/Z* selectivity in forming 2-tetradecene) by Oshima[42] (**1.8**, Figure 1.21), and the cyclopentadienyl ruthenium complex with a bifunctional imidazolyl phosphine from our group[35] (**1.1**, Figure 1.21) (>99:1 *E:Z* selectivity across a broad spectrum of substrates). There is evidence for both systems that indicate they operate by a π-allyl mechanism; more detailed mechanistic and computational studies on the mechanism of **1.1** will be discussed in chapter 2, because the one published computational study does not address *E/Z* selectivity.[43] Two other systems capable of not only *E*-selective but also monoselective isomerization of 1-alkenes to (*E*)-2-alkenes are **1.2** (Figure 1.22, (**1.2a** not shown)[41] from our group and **1.9**.[44] Discussion of **1.2** (+ **1.2a**) will be discussed largely in chapters 3 and 4, although reactivity studies are performed using the nitrile-free catalyst introduced in that chapter.
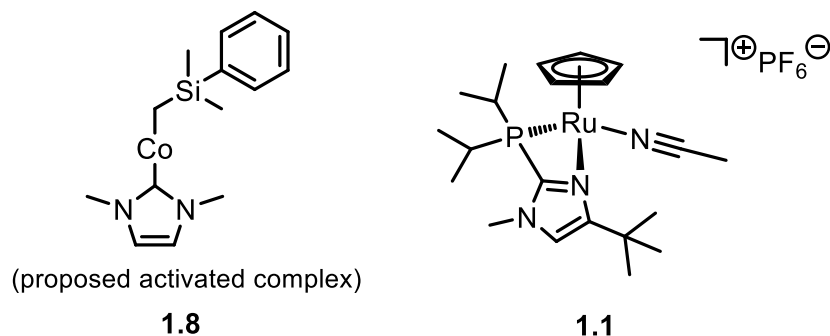
Figure 1.21. (*E*)-selective isomerization catalysts
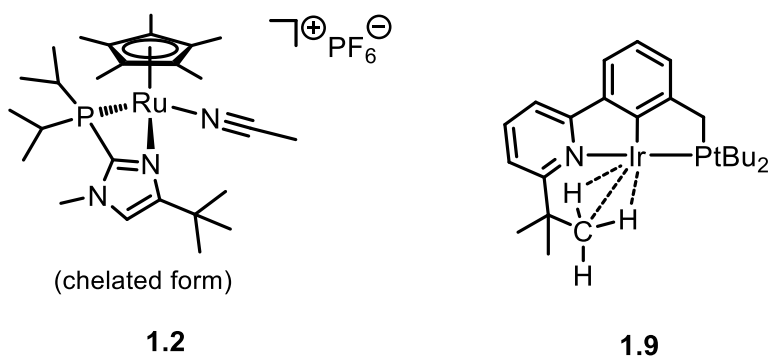
Figure 1.22. (*E*)- and monoselective isomerization catalysts

Catalyzed isomerization of 1-alkenes to (*Z*)-2-alkenes remains underdeveloped, although two catalyst systems in particular, developed in the last few years, are *Z*-selective: a Co- or Ni(dppp)(PPh$_2$H) complex by Hilt (Figure 1.23, **1.10**)[45-46] and a diketiminate cobalt alkyl complex developed by Weix and Holland (Figure 1.22, **1.11**).[47] The cobalt analogue of **1.10** typically attains ~80% conversions and 80:20 *Z:E* ratios (5-10 mol%, 24 hr, rt), although selectivity is completely reversed when using conjugatable substrates. Functional groups that are tolerated with **1.10** include esters, silyl/phenyl/alkyl ethers, silyl groups, boronate esters, and bromides. Catalyst **1.11**, on the other hand, uses lower catalyst loadings (0.5 – 1 mol%), but functional groups tested are limited to phenyl and silyl substituents, and *Z:E* selectivity appears to erode before conversion is complete. Despite their individual challenges, however, both **1.10** and **1.11** are rare in that they select for the less thermodynamically favorable geometrical isomer,

the *Z* isomer. Both systems appear to operate by the σ-alkyl mechanism, in which presumably the first step is hydride insertion into the alkene to form the 2-alkyl. When the 2-alkyl is formed, carbon 1 by definition will be facing away from the metal. Sufficient steric bulk of the ligands on the metal center can force carbon 4 to rotate away as well, leading to *Z*-selectivity.
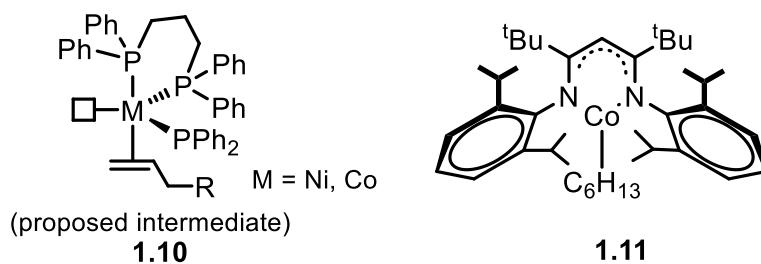
Figure 1.23. (*Z*)- and monoselective isomerization catalysts

A wide range of factors can dictate selectivity and reactivity for alkene isomerization catalysts: catalyst stability, solvent, type of mechanism (alkyl or allyl), sterics and electronics of both the catalyst and the substrate, potential chelating groups on the substrate, and, in the case of tandem reactions, the nature of the other catalyst (its selectivity, efficiency). What is clear is that advances in the development of alkene isomerization catalysts and their application to the production of important compounds is still occurring. The contribution of the Grotjahn group to this process is to continue to discover catalysts that are selective and efficient in order to generate alkenes with high yield and purity.

The contents of chapter 1 are similar to the material published in the following encyclopedia article: Paulson, E.R., Grotjahn, D.B. "Isomerization and Hydrogenation of Alkenes". *Encyclopedia of Inorganic and Bioinorganic Chemistry*, Published 15 December 2017. This article was an extensive update to the version published in 2006 in the *Encyclopedia of Inorganic Chemistry* by Dr. Fred Jardine, whom I thank for his original contribution.

1.5. References

1.   Plotkin, J. *Beyond the Ethylene Steam Cracker - American Chemical Society*. [online] American Chemical Society. **2016**. [Accessed 8 Dec. 2018].
 Available at: https://www.acs.org/content/acs/en/pressroom/cutting-edge-chemistry/beyond-the-ethylene-steam-cracker.html

2.   Al-Jarallah, A. M.; Anabtawi, J. A.; Siddiqui, M. A. B.; Aitani, A. M.; Al-Sa'doun, A. W., Ethylene dimerization and oligomerization to 1-butene and linear a-olefins: A review of catalytic systems and processes. *Catal. Today* **1992**, *14*, 1.

3.   H.M. Colquhoun, J. H., D.J. Thompson, M.V. Twigg, *New Pathways for Organic Synthesis: Practical Applications of Transition Metals*. Plenum Press: New York and London, 1984.

4.   Fahlbusch, K. G.; Hammerschmidt, F. J.; Panten, J.; Pickenhagen, W.; Schatkowski, D.; Bauer, K.; Garbe, D.; Surburg, H., Flavors and fragrances. In *Ullmann's Encyclopedia of Industrial Chemistry*, Wiley-VCH: Weinheim, Germany, 2003.

5.   Scarso, A.; Colladon, M.; Sgarbossa, P.; Santo, C.; Michelin, R. A.; Strukel, G., Highly Active and Selective Platinum(II)-Catalyzed Isomerization of Allylbenzenes: Efficient Access to (*E*)-Anethole and Other Fragrances via Unusual Agostic Intermediates. *Organometallics* **2010**, *29*, 1487.

6.   Wipf, P.; Spencer, S., Asymmetric Total Syntheses of Tuberostemonine, Didehydrotuberostemonine, and 13-Epituberostemonine. *J. Am. Chem. Soc.* **2005**, *127*, 225.

7.   Wang, X.; Woo, L. K., Isomerization of olefin carboxylic esters catalyzed by nickel and palladium compounds. *J. Mol. Catal. A: Chem.* **1998**, *130*, 171.

8.   Larionov, E.; Li, H.; Mazet, C., Well-defined transition metal hydrides in catalytic isomerizations. *Chem. Commun.* **2014**, *50*, 9816.

9.   Baudry, D.; Ephritikhine, M.; Felkin, H., Isomerisation of allyl ethers catalysed by the cationic iridium complex [Ir(cyclo-octa-1,5-diene)(PMePh$_2$)$_2$]PF$_6$. A highly stereoselective route to trans-propenyl ethers. *J. Chem. Soc., Chem. Comm.* **1978**, 694.

10.   Yamamoto, Y., Miyairi, T., Ohmura, T. Miyaura, N., Synthesis of Chiral Esters of (*E*)-3-(Silyloxy)-2-propenylboronic Acid via the Iridium-Catalyzed Isomerization of the Double Bond. *J. Org. Chem.* **1999**, *64*, 296.

11.   Ohmura, T., Shirai, Y., Yamamoto, Y., Miyaura, N., A stereoselective isomerization of allyl silyl ethers to (*E*)- or (*Z*)-silyl enol ethers using cationic iridium complexes. *Chem. Commun.* **1998**, 1337.

12.   Crabtree, R. H., *The organometallic chemistry of the transition metals*. Third Edition; John Wiley & Sons, Inc.: New York, Chichester, Weinheim, Brisbane, Singapore, Toronto, 2001.

13.   Hanessian, S., Giroux, S., Larsson, A., Efficient Allyl to Propenyl Isomerization in Functionally Diverse Compounds with a Thermally Modified Grubbs Second-Generation Catalyst. *Org. Lett.* **2006**, *8*, 5481.

14.   Consorti, C. S.; Aydos, G. L. P.; Ebeling, G.; Dupont, J., Multiphase catalytic isomerisation of linoleic acid by transition metal complexes in ionic liquids. *Appl. Catal., A: General* **2009**, *371*, 114.

15.   Hudson, B.; Webster, D. E.; Wells, P. B., Homogeneous catalysis of olefin isomerization. Part I. Reactions of *trans*-[^{2}H$_2$]ethylene catalysed by complexes of cobalt, ruthenium, rhodium and palladium. *J. Chem. Soc., Dalton Trans.* **1972**, 1204.

16.   Kuznik, N.; Krompiec, S., Transition metal complexes as catalysts of double-bond migration in O-allyl systems. *Coord. Chem. Rev.* **2007**, *251*, 222.

17.   Uma, R.; Crevisy, C.; Gree, R., Transposition of allylic alcohols into carbonyl compounds mediated by transition metal complexes. *Chem. Rev.* **2003**, *103*, 27.

18.   Hassam, M., Taher, A., Arnott, G.E., Green, I.R., van Otterlo, W.A.L., Isomerization of Allylbenzenes. *Chem. Rev.* **2015**, *115*, 5462.

19.   Erdogan, G.; Grotjahn, D. B., Mild and Selective Deuteration and Isomerization of Alkenes by a Bifunctional Catalyst and Deuterium Oxide. *J. Am. Chem. Soc.* **2009**, *131*, 10354.

20.   Menchi, G.; Matteoli, U.; Serivanti, A.; Paganelli, S.; Botteghi, C., Homogeneous isomerization of 1,2-dicarbethoxy-1,2,3,6-tetrahydropyridazine by ruthenium complexes. *J. Organometal. Chem.* **1988**, *354*, 215.

21.   Vasseur, A.; Bruffaerts, J.; Marek, I., Remote functionalization through alkene isomerization. *Nat. Chem.* **2016**, *8*, 209.

22.   Arisawa, M.; Terada, Y.; Takahashi, K.; Nakagawa, M.; Nishida, A., Non-metathesis reactions of ruthenium carbene catalysts and their application to the synthesis of nitrogen-containing heterocycles. *Chem. Rec.* **2007**, *7*, 238.

23.   Baader, S.; Podsiadly, P. E.; Cole-Hamilton, D. J.; Gooben, L. J., Synthesis of tsetse fly attractants from a cashew nut shell extract by isomerising metathesis. *Green Chem.* **2014**, *16*, 4885.

24.   Ohlmann, D. M.; Gooßen, L. J.; Dierker, M., Regioselective synthesis of ß-aryl- and ß-amino-substituted aliphatic esters by rhodium-catalyzed tandem double-bond migration/conjugate addition. *Chem. Eur. J.* **2011**, *17*, 9508.

25.   Fukuyama, T.; Doi, T.; Minamino, S.; Omura, S.; Ryu, I., Ruthenium hydride catalyzed regioselective addition of aldehydes to enones to give 1,3-diketones. *Angew. Chem. Int. Ed.* **2007**, *46*, 5559.

26.   Pertici, P.; Malanga, A.; Guintoli, G.; Vitulli, G.; Martra, G., The (η^6-naphthalene)(η^4-cycloocta-1, 5-diene)ruthenium(0) complex as precursor for homogeneous and heterogeneous catalysts in the isomerization of allyl ethers and allyl acetals to vinyl derivatives. *Gazz. Chim. Ital.* **1996**, *126*, 587.

27.   Mamone, P.; Grunberg, M.; Fromm, A.; Khan, B. A.; Gooben, L. J., [Pd(μ-Br)(P^{t}Bu$_3$)]$_2$ as a highly active isomerization catalyst: Synthesis of enol esters from allylic esters. *Org. Lett.* **2012**, *14*, 3716.

28.   Krompiec, S.; Krompiec, M.; Penczek, R.; Ignasiak, H., Double bond migration in N-allylic systems catalyzed by transition metal complexes. *Coord. Chem. Rev.* **2008**, *252*, 1819.

29.   Larsen, C. R.; Grotjahn, D. B., Stereoselective Alkene Isomerization over One Position. *J. Am. Chem. Soc.* **2012**, *134*, 10357.

30.   Tani, K., Asymmetric isomerization of allylic compounds and the mechanism. *Pure Appl. Chem.* **1985**, *57*, 1845.

31.   Emerson, G. F., Mahler, J.E., Kochlar, R., Petit, R., Organo-iron complexes. IV. Reactions of substituted dienes with iron pentacarbonyl. *J. Org. Chem.* **1964**, *29*, 3620.

32.   Reinhardt, R. E., Lasky, J.S., The isomerization of 1,3-cyclooctadiene to 1,5-cyclooctadiene via the rhodium(I) π-complex. *J. Am. Chem. Soc.* **1964**, *86*, 2516.

33.   Larsen, C. R., Paulson, E.R., Erdogan, G., Grotjahn, D.B., A Facile, Convenient, and Green Route to (*E*)-Propenylbenzene Flavors and Fragrances by Alkene Isomerization. *Synlett* **2015**, *26*, 2462.

34.   Wakamatsu, H.; Nishida, M.; Adachi, N.; Mori, M., Isomerization Reaction of Olefin Using RuClH(CO)(PPh$_3$)$_3$. *J. Org. Chem.* **2000**, *65*, 3966.

35.   Grotjahn, D. B.; Larsen, C. R.; Gustafson, J. L.; Nair, R.; Sharma, A., Extensive Isomerization of Alkenes Using a Bifunctional Catalyst: An Alkene Zipper. *J. Am. Chem. Soc.* **2007**, *129*, 9592.

36.   Kochi, T.; Hamasaki, T.; Aoyama, Y.; Kawasaki, J.; Kakiuchi, F., Chain-Walking Strategy for Organic Synthesis: Catalytic Cycloisomerization of 1,*n*-Dienes. *J. Am. Chem. Soc.* **2012**, *134*, 16544.

37.   Larionov, E.; Lin, L.; Guenee, L.; Mazet, C., Scope and Mechanism in Palladium-Catalyzed Isomerization of Highly Substituted Allylic, Homoallylic, and Alkenyl Alcohols. *J. Am. Chem. Soc.* **2014**, *136*, 16882.

38.   Lin, L.; Romano, C.; Mazet, C., Palladium-Catalyzed Long-Range Deconjugative Isomerization ofHighly Substituted α,β-Unsaturated Carbonyl Compounds. *J. Am. Chem. Soc.* **2016**, *138*, 10344.

39.   Morrill, T. C.; D'Souza, C. A., Efficient Hydride-Assisted Isomerization of Alkenes via Rhodium Catalysis. *Organometallics* **2003**, *22*, 1626.

40.   Krompeic, S.; Suwinski, J.; Grobelny, J., Highly active ruthenium catalyst for double bond migration. *Pol. J. Chem.* **1996**, *70*, 813.

41.   Larsen, C. R.; Erdogan, G.; Grotjahn, D. B., General Catalyst Control of the Monoisomerization of 1-Alkenes to *trans*-2-Alkenes. *J. Am. Chem. Soc.* **2014**, *136*, 1226.

42.   T. Kobayashi, H. Y., K. Oshima, Cobalt-Catalyzed Isomerization of 1-Alkenes to (E)-2-Alkenes with Dimethylphenylsilylmethylmagnesium Chloride and Its Application to the Stereoselective Synthesis of (E)-Alkenylsilanes. *Chem. - Asian J.* **2009**, *4*, 1078.

43.   Tao, J.; Sun, F.; Feng, T., Mechanism of alkene isomerization by bifunctional ruthenium catalyst: A theoretical study. *J. Organometal. Chem.* **2012**, *698*, 1.

44.   Wang, Y.; Qin, C.; Jia, X.; Leng, X.; Huang, Z., An agostic iridium pincer complex as a highly efficient and selective catalyst for monoisomerization of 1-alkenes to *trans*-2-alkenes. *Angew. Chem. Int. Ed.* **2017**, *56*, 1614.

45.   Schmidt, A.; Nodling, A. R.; Hilt, G., An Alternative Mechanism for the Cobalt-Catalyzed Isomerization of Terminal Alkenes to (Z)-2-Alkenes. *Angew. Chem. Int. Ed.* **2015**, *54*, 801.

46.   Weber, F.; Schmidt, A.; Rose, P.; Fischer, M.; Burghaus, O.; Hilt, G., Double-Bond Isomerization: Highly Reactive Nickel Catalyst Applied in the Synthesis of the Pheromone (9Z, 12Z)-Tetradeca-9-12-dienyl Acetate. *Org. Lett.* **2015**, *17*, 2952.

47.   Chen, C.; Dugan, T. R.; Brennessel, W. W.; Weix, D. J.; Holland, P. L., Z-Selective Alkene Isomerization by High-Spin Cobalt(II) Complexes. *J. Am. Chem. Soc.* **2014**, *136*, 945.

Chapter 2

The Unique Reactivity and Applications of Catalyst 1.1

2.1. Introduction

This Chapter starts with a detailed overview of the development and applications of catalyst **1.1** and its polymer-supported analogues **PS-1.1** and **PSL-1.1**. Chapter 2 continues with the specific application of **1.1** and its analogues to the isomerization of allylbenzenes to phenylpropenes used as flavors and fragrances.
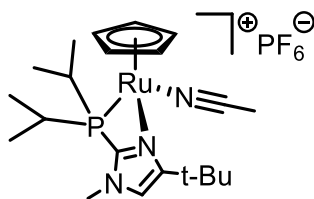
1.1

Figure 2.1. Catalyst **1.1** developed in the Grotjahn group

Although several transition-metal catalyst systems have been developed to provide general control over positional and/or geometric selectivity during the isomerization of alkenes, catalyst **1.1** (Figure 2.1), developed in our group and published in 2007 has shown unparalleled selectivity in the production of (*E*)-alkenes with high kinetic control, and is robust and functional-group tolerant enough to reach a thermodynamic equilibrium; in one outstanding example, an alkene migration occurred over 30 bonds to reach a thermodynamic sink (a ketone). Another advantage that **1.1** has is functional group tolerance toward ethers, amides, and alcohols.[1]
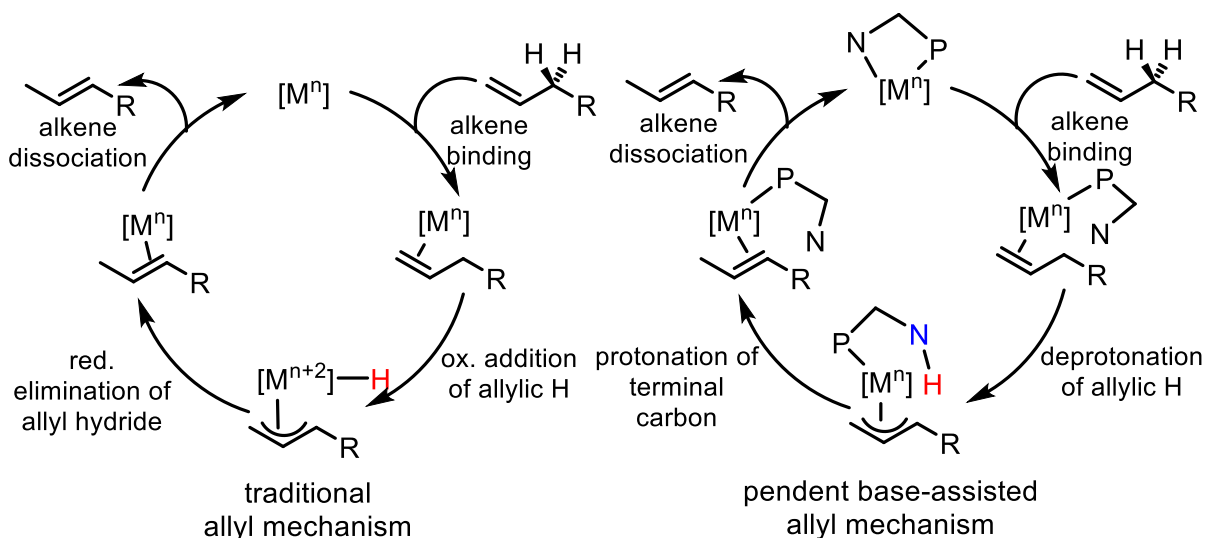
Figure 2.2. The catalytic cycles for the traditional allyl mechanism (left) and pendent base-assisted allyl mechanism (right)

Our group's working hypothesis is that the nitrogen acts as a pendent base during catalysis, transferring a proton in a 1,3-shift via an allyl intermediate, similar to the π-allyl mechanism detailed in Chapter 1 and Figure 2.2. The base is thought to both assist in the deprotonation of the allylic proton (as a more effective base than the metal), as well as facilitate the migration of the proton. This mechanism is supported by a computational paper by Tao et. al.[2] that explores a few mechanistic routes with and without assistance from the pendent base; the pendent base-assisted mechanism was found to be the lowest energy route. Tao's study did not involve any experimental verification, and also did not address *E/Z* selectivity. Because of the high efficiency of the process, identifying intermediates in the catalytic cycle has been challenging, but a number of experiments have shown some support for the pendent base hypothesis.
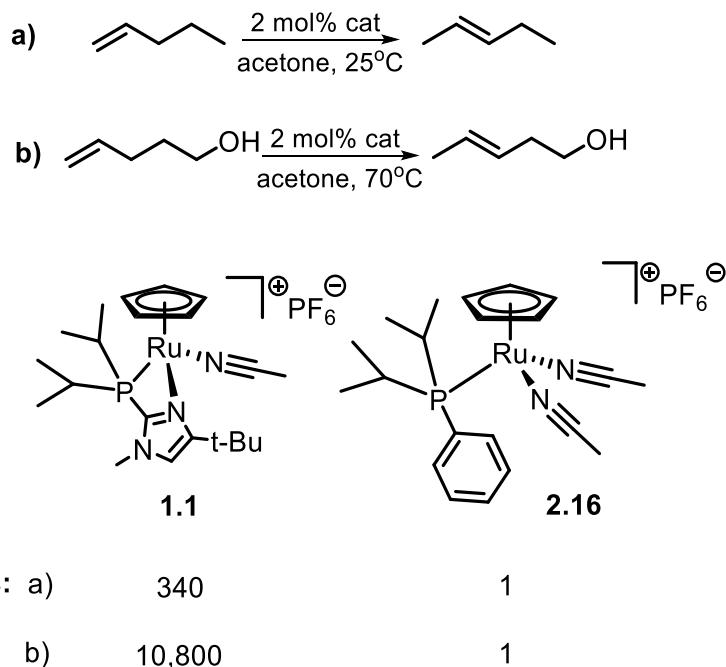
Figure 2.3. Comparison of rates of isomerization with catalyst **1.1**, containing a heterocyclic imidazole, and **2.16**, lacking a heterocyclic group (adapted from ref. [3]).

Comparison of **1.1** to [CpRu(iPr$_2$PPh)(CH$_3$CN)$_2$]PF$_6$ (**2.16**, Figure 2.3) shows a dramatic rate increase when switching the phenyl group of the iPr$_2$PPh ligand to the heterocyclic 1-methyl-4-tert-butyl imidazole.[3] It should be also noted that concurrent with the change to the heterocycle, the chelation of the heterocycle removes a nitrile ligand. The extra nitrile ligand in **2.16** could be part of the reason for its lower rate during isomerization, but the imidazole behaving as a pendent base could also play a role. In 2014, we published a much more conclusive version of this experiment in which Gulin Erdogan showed that one equivalent of each of the phosphine ligands in **1.1** and **2.16** to Cp*Ru(NCCH$_3$)$_3$PF$_6$ generated **1.2a** + CH$_3$CN and **2.17** + CH$_3$CN. Both complexes feature a monodentate phosphine ligand and two bound nitrile ligands, as well as one free phosphine ligand.
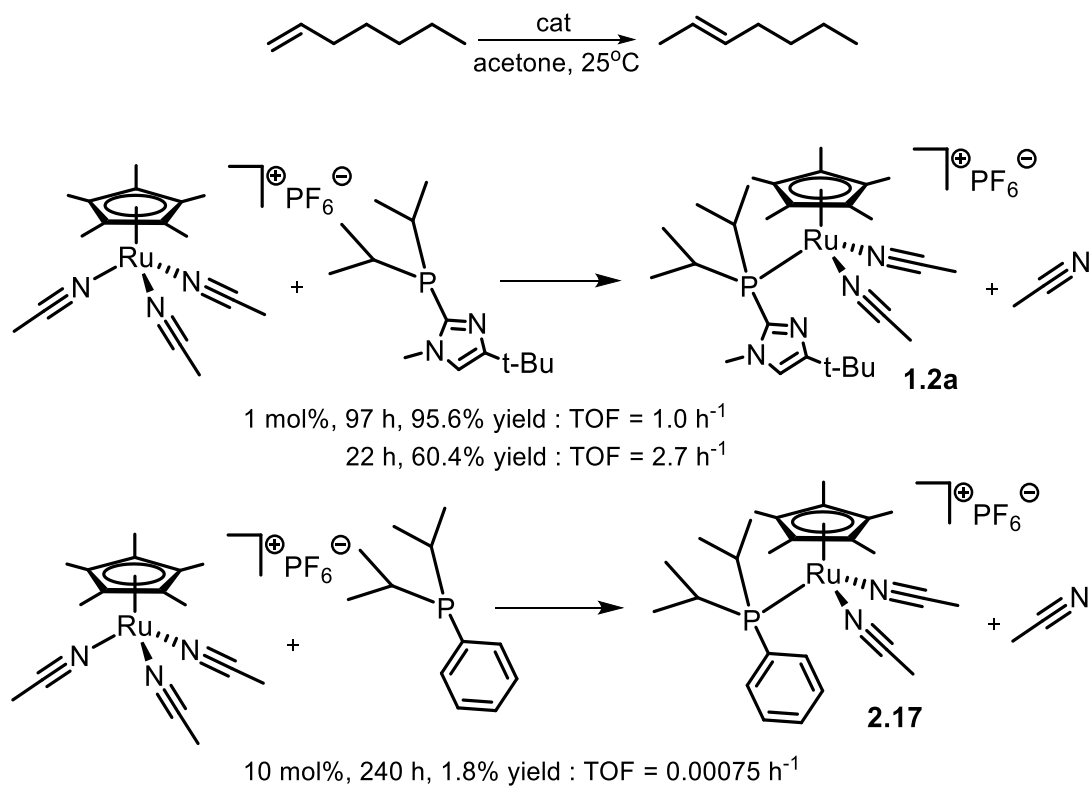
Figure 2.4. Comparison of rates of isomerization with catalyst **1.2a** + CH₃CN and catalyst **2.17** + CH₃CN
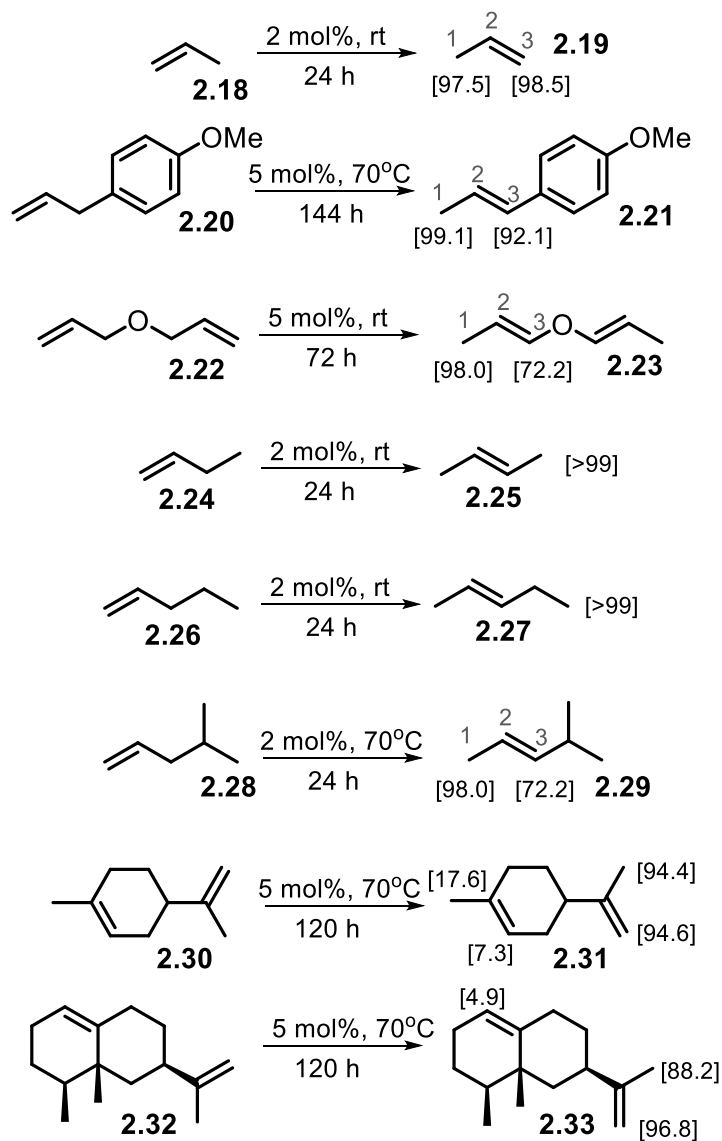
Figure 2.5. Deuteration of alkene substrates with D_2O in the presence of **1.1**. (Adapted from ref. [4]). Enough D_2O added so 20 D for each exchangeable H. rt: room temperature. % deuterium incorporation in brackets.

Evidence that isomerization with **1.1** proceeds through an allyl mechanism presents itself during the facile incorporation of deuterium into alkene substrates using D_2O. With 2 – 5 mol% loading of **1.1** and reaction times of 24 to 144 h, several substrates undergo complete deuterium exchange with all accessible protons. In the allylic mechanism, since the exchangeable proton undergoes a 1,3-shift, deuteration will only occur on protons that are allylic to one of the isomers of the alkene. In the isomerization of butene and pentene, all protons are allylic to one of the two

isomers (i.e. 1-butene (**2.24**) and (*E*)-2-butene(**2.25**)). On the other hand, substrates such as propene (**2.18**), 4-allylanisole (**2.20**), diallylether (**2.22**), and 4-methyl-1-pentene (**2.28**) would be restricted to exchanging protons between the 1- and 3-carbons in an allyl mechanism. As expected, complete incorporation of deuterium occurs with butene and pentene, whereas no incorporation of deuterium on the 2-carbon is observed during deuteration of the 1- and 3-carbons of isomerized products propene (**2.19**), (*E*)-anethole (**2.21**), (*E,E*)-dipropenylether (**2.23**), and 4-methyl-(*E*)-2-pentene (**2.29**) (Figure 2.5)[4]. An item of note is that both the 1- and 3-carbons become mostly deuterated in all isomers with disubstituted alkenes, suggesting that the reversibility of the isomerization is facile as well. In the proposed pendent base-assisted mechanism, the H/D exchange with D_2O would likely occur when the proton is located on the imidazole nitrogen. That being said, H/D exchange has been shown to occur with ruthenium-hydride species during isomerization in the presence of D_2O,[5] so the facile deuteration also is not definitive evidence of the pendent base directly assisting in proton transfer, although the fact that propene was *only* deuterated at the *terminal* carbons, even after >30 days, means that if any deuteration occurs via insertion of propene into a Ru-D bond, the regioselectivity of the insertion must be very high. The Tao et al. mechanism suggests that a transient Ru^+(PN)-H(D) species is rapidly converted to more stable Ru(PNH$^+$)(eta-3 allyl) species.. More definitive results relating to the role of the pendent heterocycle have been underway. Our group, led by Thomas Cao, is currently undertaking a combined computational and experimental investigation of the isomerization mechanism to elucidate the origin of the efficiency and (*E*)-selectivity of catalyst **1.1**.
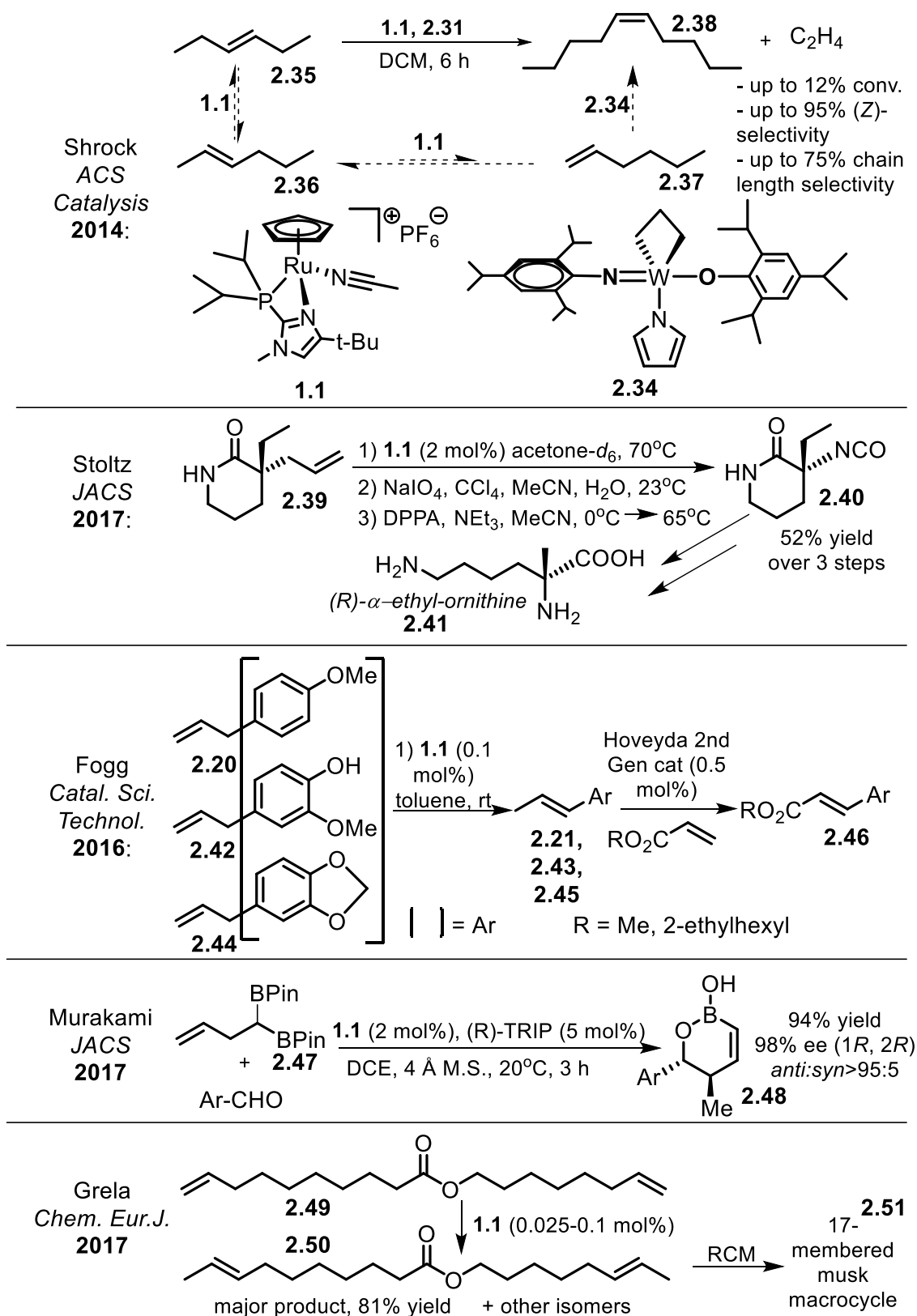
Figure 2.6. Examples of utility of **1.1** in sequential isomerization/functionalization reactions

Because of its versatility, **1.1** has been found to be a very effective partner with other catalysts in sequential and tandem processes to produce a number of high-value compounds. Some examples include the synthesis of (*Z*)-5-decene (**2.35**) from (*E*)-3-hexene (**2.32**) in a tandem isomerization-metathesis (ISOMET) collaboration with Prof. Richard Schrock,[6] an isomerization-oxidation sequence by Stoltz's group to synthesize unnatural amino acids such as (R)-alpha-ethyl-ornithine (**2.41**),[7] sequential isomerization-metathesis processes by the Fogg and Grela groups (to produce cinnamate and ferulate esters of the general form **2.46**[8] and musk macrocycles like **2.51**,[9] respectively), and an isomerization-allylation sequence by Murakami to produce *anti*-1,2-oxaborinan-3-enes (**2.48**) from aldehydes and 1,1-di(boryl)alk-3-enes (**2.47**).[10] These catalyst systems mentioned take advantage of several different features of **1.1**. The cinnamate syntheses outlined by Fogg's group and the isomerization/oxidation process by Stoltz's group exploit the high efficiency of catalyst **1.1**. The isomerization/oxidation process also utilizes the ruthenium metal in **1.1** in the second step, which upon oxidation by $NaIO_4$, becomes the oxidant. The isomerization/allylation sequence by Murakami's group and the Schrock groups' ISOMET strategy both take advantage of the propensity of **1.1** for producing (*E*)-isomers, in the former case by influencing final product selectivity, and in the latter case by ensuring no intermediate (*Z*)-isomers are present prior to metathesis. The isomerization/ring-closing metathesis system outlined by Grela et al uses very low concentrations of **1.1** to selectively monoisomerize two long alkene chains in **2.49** to produce **2.50**, which is then subjected to RCM to create the macrocycle **2.51**.

2.2. Flavors and Fragrances

Another direct and important application of catalyst **1.1**, explored in our group, is in the area of flavors and fragrances. Allylbenzenes and their internal conjugated analogues the

phenylpropenoids (Figure 2.7) are major constituents in many essential oils. Often, the scents exhibited by the unconjugated allylbenzene isomer are markedly different than the internal conjugated propenylbenzene compounds. Former Ph.D. students Gulin Erdogan[4, 11] and Casey Larsen[12] previously had shown that allylbenzene substrates 4-allylanisole (estragole, **2.20**) and eugenol (**2.42**) were amenable to catalysis and produced (*E*)-anethole and (*E*)-isoeugenol, respectively, in good yield using both the homogeneous catalyst **1.1** and polystyrene-supported catalyst analogues **PS-1.1** and **PSL-1.1** developed by Gulin Erdogan and published in 2014. To highlight this application and show the catalysts' versatility, in 2015 we set out to investigate the isomerization of several allylbenzene substrates used in flavors and fragrances with **1.1**, **PS-1.1**, and **PSL-1.1**. Isomerizations of allylbenzene substrates listed in Figure 2.7 were carried out by Casey and Gulin in acetone solution and are summarized in Table 2.2 below.
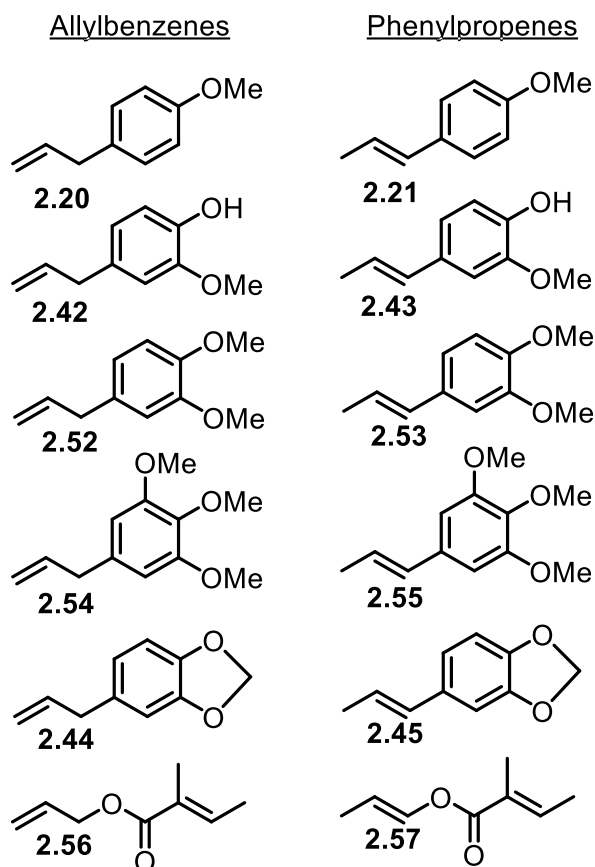
Figure 2.7. Allylbenzene and propenylbenzene compounds as flavors and fragrances

Table 2.1. Isomerization of allylbenzenes to propenylbenzene flavors and fragrances[a]

Entry	Substrate	Product	Catalyst	Mol %	Time (min)	Yield (%)
1			**1.1**	0.05	40	99
2	**2.20**	**2.21**		0.1	10	100
3			**PS-1.1**	2	20	95
4			**PSL-1.1**	2	20	91
5			**1.1**	0.05	20	100
6	**2.42**	**2.43**		0.1	10	100
7			**PS-1.1**	1	45	96
8			**PSL-1.1**	1	60	94 [2.9][b]
9			**1.1**	0.1	15	100
10	**2.52**	**2.53**	**PS-1.1**[c]	1.1	85	97 [1.8][b]
11			**PSL-1.1**[c]	1.1	220	91 [2.4][b]
12			**1.1**	0.1	20	98
13	**2.54**	**2.55**	**PS-1.1**[c]	1	130	95 [4.9][b]
14			**PSL-1.1**[c]	1.1	115	96 [3.4][b]
15			**1.1**	0.6	10	98
16	**2.44**[d]	**2.45**	**PS-1.1**[c]	1.9	90	98
17			**PSL-1.1**[c]	2	75	96 [2.7][b]
18	**2.56**	**2.57**	**1**	0.9	300	96 [2.9][b]

[a]Substrate (0.50 mmol), acetone-d6 solvent, RT, NMR yield. In cases where NMR yield (est. 1% uncertainty) was measured as slightly above 100, the yield is given as 100. No starting material detectable, unless otherwise specified. [b]The amount of starting material remaining (%) is in brackets; when left longer, reactions did proceed further, but for comparative data, ~95% yield time points are given here. [c] 70°C. [d]>90% safrole in sassafras oil.

Yields of the conjugated (E)-propenylbenzenes for all products with all three catalysts are >90% by NMR spectroscopic analysis. In all cases, catalyst loadings for **1.1** of less than 1 mol%, and as little as 0.05 mol%, yet the desired products exceeded 95% in under two hours. Polymer-supported analogues **PS-1.1** and **PSL-1.1** required a higher catalyst loading (1-2%), but produced yields of (E)-propenylbenzenes >95% in most cases, in generally less than two hours.
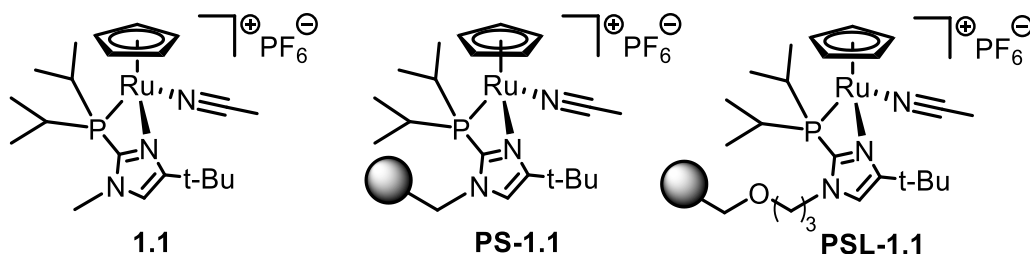
Figure 2.8. Catalyst **1.1** and polymer-supported analogues **PS-1.1** and **PSL-1.1**

I attempted to extend the success of the three catalysts in acetone solution towards reactions in neat substrate, as the elimination of solvent would provide a less wasteful process for the production of propenylbenzene products. We also wanted to know if isolations of isomerized product would be possible in high yield on a larger scale. To make the process more attractive to the synthetic chemist, an effort was made to run the reaction outside the glovebox, in a simple flask sealed with a septum rather than attached to a Schlenk line. This way, the synthetic chemist would simply need a nitrogen or argon tank to complete the reaction. The substrate flask was loaded with substrate and initially deoxygenated by bubbling with nitrogen, then lowered into a room-temperature water bath to maintain the reaction close to room temperature. Catalyst, while weighed inside of the glovebox, was brought out in a sealed vial (which could be an ampoule as purchased). Both caps were removed, the catalyst was dumped in, and the system quickly purged with nitrogen afterwards. The reaction was monitored by taking out small aliquots and checking by NMR for completion, which was achieved in 45 min for **2.21** and 20 min for **2.43** using 0.1 mol% of **1.1**.

After distillation to remove the product from the catalyst, products **2.20** and **2.40** were obtained in high yield (**2.21**: 4.65 g, 93.0% yield; **2.43**: 15.76 g, 95.9% yield). Most notably, no corresponding (*Z*)-isomer was detected with an estimated detection limit of 0.1% for **2.21**. With **2.43**, 0.4% of (*Z*)-isomer was found, which may be attributed to active catalyst still working at the higher temperatures required for distillation.
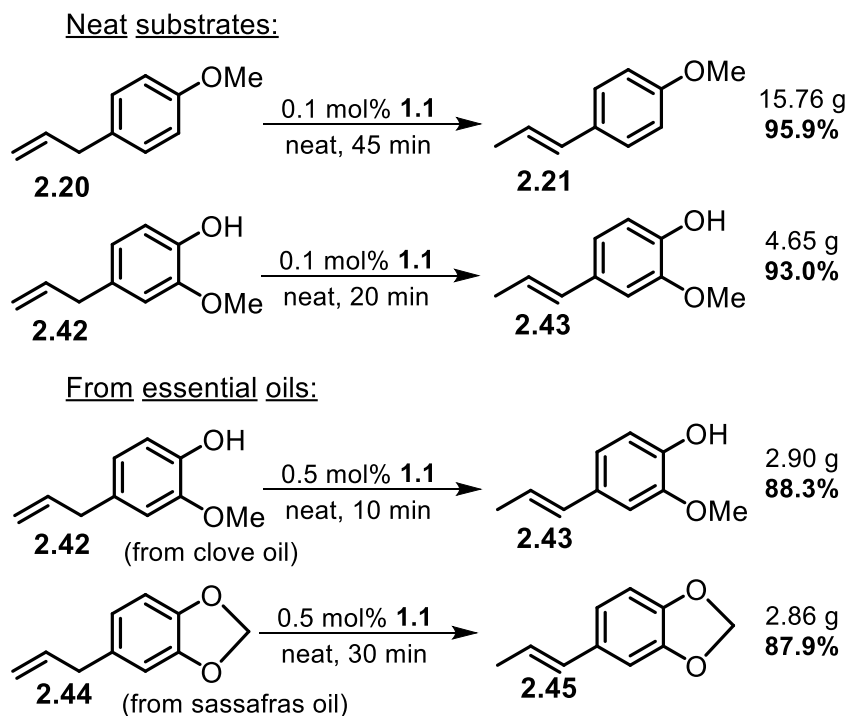
Figure 2.9. Isomerization of neat fragrance substrates and essential oils with **1.1**

While **2.20** and **2.42** isomerize efficiently and with high yield and selectivity in the presence of **1.1** without solvent, the samples of **2.20** and **2.42** used for these reactions were essentially pure substrate. A common source of these allylbenzene substrates is in essential oils, which can be of variable purity. The listed purity for sassafras oil sold by Sigma-Aldrich is >90% safrole (**2.44**), along with arsenic, cadmium, mercury, and lead as listed minor impurities, while major impurities likely consist of various organic compounds extracted from the plant material. The impurities present in essential oil samples have the potential to interfere with and possibly deactivate the catalyst. Nevertheless, when using slightly higher catalyst loadings of 0.5 mol%, the safrole in sassafras oil and the eugenol in clove oil were completely consumed and isomerized to (*E*)-isosafrole (**2.45**) and (*E*)-isoeugenol (**2.43**), in 30 min and 10 min, respectively, without prior purification. After distillation, both isomerized products were

46

obtained with high yield (**2.45**: 87.9%, **2.43**: 88.3%).   All results with neat substrates and essential oils are summarized in Figure 2.8.

Finally, in an effort to extend the aim of performing reactions in neat substrate and reduce waste, we desired to utilize the polymer-supported catalysts **PS-1.1** and **PSL-1.1**. The advantage of using the polymer-supported catalysts would (at least theoretically be) the ease of separation of catalyst from substrate, as well as the ability to re-use the catalyst. However, the removal of the polymer from the catalyst in neat conditions is much more challenging than when using solvent, because the polymer-supported catalyst is usually rinsed with solvent before repeated usage.

Table 2.2. Methods attempted for repeated isomerization of neat eugenol (**2.42**)

Method	Description	Hypothesis	Results
1: Vial with Teflon cap	Substrate is loaded into a 20-mL scintillation vial, along with **PS-** or **PSL-1.1** beads, heated at 70˚C	Can stir and heat, allowing for facile isomerization, followed by filtration	100% isomerization within 24 h, but can only recover 65-70%, whether through filtration or pipetting of product from the polymer (sticks to vial and filter
2: Syringe	Substrate and polymer are loaded into a plastic syringe fitted with a frit and a Luer lock	Filtration could be assisted by forcing product through frit; also, low surface area	Can't stir or heat; substrate only 20% isomerized in 44 h
3: Two flasks connected by a Schlenk filter adapter (Figure 2.9)	Substrate in 2-neck flask with polymer, connected via a 2-way filter adapter to a 2nd 2-neck flask	Flasks can be heated and stirred, continually switched out for fresh substrate while under nitrogen	Reaction heated at 70˚C for 24 h shows 100% completion; after switching for fresh substrate, adapter collects unisomerized substrate. Each subsequent batch is contaminated with substrate
4: Vial with polyethylene mesh bag containing polymer	**PS-1.1** or **PSL-1.1** is loaded into polyethylene mesh bag, rolled and tied with copper wire, and submerged into vial with substrate and stirbar, and capped with Teflon-lined cap	Should have all of the advantages of Method 1, along with ability to remove all polymer from reaction, which can be transferred to new vial containing fresh substrate	*Easily most preferred method*: First cycle shows similar loss of product as Method 1, due to retention in bag, but virtually no loss in subsequent cycles because bag is saturated
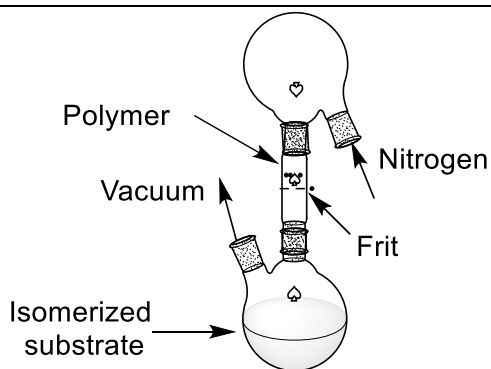
Figure 2.10. Reaction set-up for Method **3** (after filtration)

A number of methods for isomerization and separation of neat eugenol (**2.39**) were attempted including stirring **PS-1.1** and **PSL-1.1** with neat **2.42** in a vial (Method 1), reaction in a syringe with filter (Method 2), a two-flask filtration system (Method 3, setup shown in Figure 2.9), and stirring substrate in a vial containing the polymers stored in a polyethylene mesh bag (Method 4) summarized in Table 2.3. In terms of ease of set-up, efficiency of reaction, and yields after repeated cycles of isomerization, Method 4 was the clear choice for the process. Repeated isomerization runs, or cycles, were then performed, each using a mesh bag containing either **PS-1.1** or **PSL-1.1**. The results for **PS-1.1** are described in Tables 2.3 and 2.4. Pictures of the reaction vial before and after cycle III with **PS-1.1** are shown in Figure 2.10.

Table 2.3. Isomerization of eugenol (**2.42**) using **PS-1** and recycling of the catalyst

Cycle	Substrate used	Catalyst loading (mol%)	Product Isolated	Yield
I	3.2932 g	0.507	2.5095 g	76.2%
II	3.2959 g	0.507	3.2266 g	97.9%
III[a]	3.2840 g	0.508	3.2707 g	99.6%

[a]Cycle III was not complete in 24 h (see Table 2.5 for completion time).

Table 2.4. Percentages of Eugenol (**2.42**) and Isoeugenol (**2.43**) Remaining After Each Cycle

| Cycle | Time (h) | Mass (mg) | Eugenol Int. | | | Isoeugenol Int. | | | | %**2.39/2.40** |
			5.11 ppm	3.34 ppm	Units	6.36 ppm	6.12 ppm	1.90 ppm	Units	
I	24	101.9	0.88	0.80	0.42	87.38	87.42	268.5	88.1	0.5/99.5%
II	24	100.2	8.22	8.18	4.10	189.6	191.8	584.1	192.0	2.1/97.9%
III	36	100.4	3.31	3.41	1.68	100.7	100.8	301.2	100.6	1.6/98.4%

Peaks corresponding to those reported[13] for (*Z*)-isoeugenol were hard to detect because of overlap with large signals. In particular, the phenolic H gave rise to a large signal that overlapped the possible d of q centered at 5.69 ppm reported[13] for (*Z*)-isoeugenol. Therefore, the 100.4 mg sample from cycle III above in CDCl$_3$ (1 mL) was shaken with D$_2$O (246.8 mg and an additional 608.7 mg, 20.2 + 49.7 equiv), followed by separation of the CDCl$_3$ phase for analysis. The lessening the phenolic OH signal was similar to that seen for the sample described on page 45 above. Unlike the sample described on page 45 above, no peaks besides the residual, small phenolic O-H peak could be seen. Conclusion: no (*Z*)-isoeugenol was present, with an estimated detection limit of 0.1%, meaning composition of the distillate was 1.6% eugenol and 98.4% (*E*)-isoeugenol as listed in the last row of Table 2.5 above.
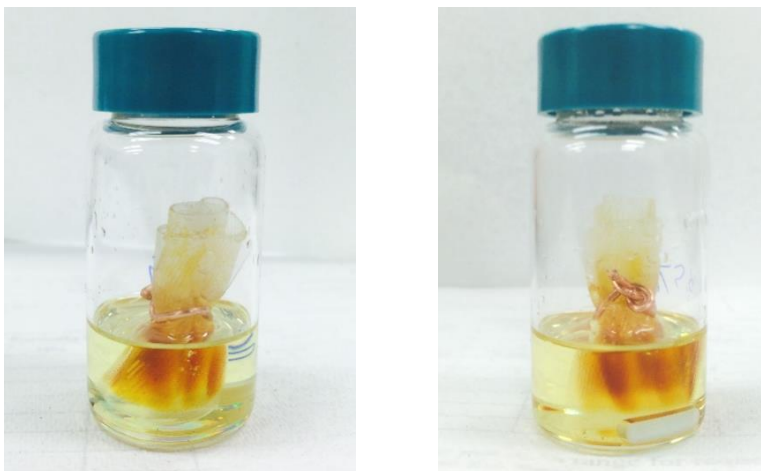
Figure 2.11. Pictures before (left) and after (right) Cycle III with **PS-1.1**

Each cycle was analyzed after heating at 70˚C for 24 hours by removing a small aliquot (~5 μL) to determine if starting material remained. If the starting material was less than 3%, the bag was removed from the vial and placed in a new vial with fresh **2.42** to begin the next cycle. The vials were then weighed to determine the amount of product remaining in the vial. For the first cycle with PS-1.1, the yield was expectedly low (76.2%) due to the mesh bag absorbing and retaining the liquid substrate/product. As much as the bag was drained and squeezed to return the product to the vial, this yield could not be improved. However, the following two cycles exhibited nearly 100% yield because the bag was saturated from the previous cycle. To determine the final ratio of **2.42** to **2.43**, a ~100 mg aliquot was removed from each vial after each cycle and subjected to NMR analysis, which indicated 2% or less **2.42** remaining for each of the three cycles with no apparent formation of (*Z*)-isomer, with estimated 0.1% uncertainty. Cycle III, however, required 36 h as opposed to 24 h for the other two cycles, indicating a small loss in activity, possibly due to catalyst deactivation.

Table 2.5. Isomerization of eugenol (**2.42**) using **PSL-1** and recycling of the catalyst

Cycle	Substrate used	Catalyst loading (mol%)	Product Isolated	Yield
I	3.2919 g	0.484	2.4039 g	73.0%
II	3.2894 g	0.485	3.2696 g	99.4%
III	3.2161 g	0.496	3.2427 g	100.8%
IV[a]	6.5709 g	0.243	6.4420 g	98.0%

[a]Cycle IV was not complete in 24 h (see Table 2.7 for completion time).

Table 2.6. Percentages of Eugenol (**2.42**) and (*E*)-Isoeugenol (**2.43**) Remaining After Each Cycle

Cycle	Time (h)	Mass (mg)	Eugenol Int.			Isoeugenol Int.				%
			5.11 ppm	3.34 ppm	Units	6.36 ppm	6.12 ppm	1.90 ppm	Units	
I	24	101.2	1.96	2.60	1.14	348.5	348.4	1063.8	350.5	0.3/99.7%
II	24	105.4	40.75	39.42	20.04	682.9	676.4	2110.3	687.6	2.8/97.2%
III	24	101.3	5.81	5.82	2.91	520.6	521.3	1604.2	525.5	0.6/99.4%
IV	65	101.0	2.65	2.71	1.33	176.7	176.0	542.2	177.8	1.5/98.5%

Results from reaction cycles using **PSL-1.1** are shown in Tables 2.5 and 2.6. A similar loss in product is seen from Cycle I with **PSL-1.1.** The remaining cycles gave 98% or greater recovery, however, and analysis of the cycles showed conversion over 97% for all cycles. Unlike the reaction cycles with **PS-1.1**, there was no apparent loss in activity during Cycle III, so a fourth cycle was attempted with double the substrate, and therefore half of the catalyst loading. Predictably, the reaction took considerably longer, showing completion at 65 h rather than 24 h for each of the previous cycles.

Table 2.7. Isomerization of eugenol (**2.42**) using **PSL-1** and recycling of the catalyst

Cycle	Substrate used	Catalyst loading (mol%)	Product Isolated	Yield
I	3.3086 g	0.385	2.3909 g	72.3%
II	3.2910 g	0.388	3.2920 g	100.0%
III	3.2908 g	0.388	3.2428 g	98.5%
IV	3.2952 g	0.387	3.2131 g	97.5%
V	3.2924 g	0.387	3.3063 g	100.4%
VI	3.2844 g	0.388	3.2062 g	97.6%
VII	3.2884 g	0.388	3.2788 g	99.7%
VIII	3.2858 g	0.388	3.2958 g	100.3%
IX	3.2878 g	0.388	3.2460 g	98.7%
X[a]	3.2911 g	0.388	3.2252 g	98.0%

[a]Cycle X was not complete in 24 h (see Table 2.9 for completion time).

Table 2.8. Percentages of Eugenol (**2.42**) and (*E*)-Isoeugenol (**2.43**) Remaining After Each Cycle

Cycle	Time (h)	Mass (mg)	Eugenol integrals 5.11 ppm	3.34 ppm	Units	Isoeugenol integrals 6.36 ppm	6.12 ppm	1.90 ppm	Units	%3/3a
I	24	101.7	2.07	1.97	1.01	354.3	356.5	1058.6	354.5	0.3/99.7
II	24	99.6	2.80	2.69	1.37	429.9	432.6	1295.6	431.5	0.3/99.7
III	24	113.2	2.56	3.70	1.57	629.0	629.5	1895.4	630.1	0.2/99.8
IV	24	109.0	9.29	9.05	4.59	540.1	545.2	1593.3	538.8	0.9/99.1
V	24	100.8	2.51	2.04	1.38	491.3	493.7	1473.5	492.1	0.3/99.7
VI	24	104.5	6.82	6.92	3.44	578.9	578.8	1742.6	579.5	0.6/99.4
VII	18	104.8	3.37	3.73	1.78	533.0	534.7	1587.9	532.3	0.3/99.7
VIII	24	102.8	14.87	13.94	7.20	476.1	476.2	1450.6	478.6	1.5/98.5
IX	24	100.2	7.55	7.67	3.81	559.2	560.4	1658.6	557.5	0.7/99.3
X	48	99.9	8.29	8.25	4.14	493.9	494.5	1499.7	496.1	0.8/99.2

While some loss of activity was apparent with both experiments with **PS-1.1** and **PSL-1.1**, the robustness of the two polymer-supported catalysts was noteworthy. The activity loss could be attributed to impurities in the substrate interacting with and deactivating the catalyst. It would reason that the more cycles the catalyst was subjected to, the more deactivation would occur. Therefore, to increase the number of cycles that the catalyst stayed active, **2.42** was distilled to enhance its purity. The purified eugenol was then subjected to cycles with catalyst **PSL-1.1**. Remarkably, using the purified substrate, no apparent loss in activity occurred <u>over nine cycles</u>, with complete conversion occurring within 24 h for each cycle. A tenth cycle completed, but required additional time than the 24 h. The results are seen in Tables 2.7 and 2.8.

2.4. Conclusion

For the isomerization of alkenes, catalyst **1.1** has shown unparalleled efficiency and (*E*)-selectivity across a broad range of substrates. Its selectivity and tolerance of other functional groups has proved it valuable in a number of tandem isomerization/functionalization reactions and production of high-value compounds such as the flavors and fragrances described in this Chapter. Explorations of catalyst **1.1** with neat fragrance substrates has extended its range of applications and highlights its versatility. Catalyst **1.1** can either be used with relatively pure substrates or used directly with unpurified essential oils. Polymer-supported analogues **PS-1.1** and **PSL-1.1** can be used in repeated cycles of isomerization using a mesh tea bag, showing little loss in activity in over ten cycles. Further studies will focus on determining the generality of the cycling of other neat substrates with the polymer-supported analogues of catalyst **1.1**.

2.5. Experimental

Data for Figure 2.8: Large Scale Isomerizations Using Catalyst 1.1 Under Neat Conditions

Estragole to (*E*)-Anethole: In a glove box, a 25 mL round bottomed flask equipped with a magnetic stir bar was added estragole (5.01 g, 0.0338 mol), capped with a rubber septum, brought out of the glove box, and partially submerged in a water bath above a stirplate. In an inert atmosphere glove box, catalyst **1.1** (21.5 mg, 0.0356 mmol, 0.1 mol%) was measured into a vial, which was capped and brought out of the glove box. The septum was removed from the reaction flask and the catalyst was quickly added, followed by bubbling nitrogen through the liquid to remove any air that had entered. Aliquots (ca. 5 μL) were removed from the reaction at 5, 10, 20, 30, and 45 minutes using a gastight syringe and analyzed by ^{1}H NMR spectroscopy for completion. Full conversion of estragole to (*E*)-anethole occurred after 45 minutes, and the product was isolated by vacuum distillation (750 mTorr 55 °C) to afford 4.65 g (93.0%) of (*E*)-anethole as a clear, colorless oil. To determine amounts of starting material remaining, 104.2 mg of the distillate was added to an NMR tube containing 0.5-0.7 mL CDCl$_3$ and analyzed by ^{1}H NMR spectroscopy at 600 MHz; percentages were calculated assuming a two-component mixture (estragole/(*E*)-anethole). Peaks used: estragole 5.12 ppm (2H), 3.34 ppm (2H); (*E*)-anethole: 6.42 ppm (1H), 6.15 ppm (1H), 1.90 ppm (3H). No peaks corresponding to those reported[13] for (*Z*)-anethole were detected; in particular, lack of any signal near 5.69 ppm is taken as evidence of less than 0.1%.

Table 2.9. Ratio of starting material to product during large scale estragole (**2.20**) to (*E*)-anethole (**2.21**) isomerization

Estragole integrals			(*E*)-anethole integrals				%**2/2a**
5.12 ppm	3.34 ppm	Units	6.36 ppm	6.12 ppm	1.90 ppm	Units	
0.21	0.21	0.11	46.61	46.84	141.87	46.91	**0.2/99.8%**

Eugenol to (*E*)-Isoeugenol: In a glove box, a 50 mL round bottomed flask equipped with a magnetic stir bar was added eugenol (16.43 g, 0.1001 mol), capped with a rubber septum, and removed from the glove box, and partially submerged in a room-temperature water bath above a stirplate. In an inert atmosphere glove box, catalyst **1.1** (60.5 mg, 0.101 mmol, 0.1 mol%) was measured into a scintillation vial, capped, and brought out of the glove box. The septum was removed from the reaction flask and the catalyst was quickly added, followed by bubbling nitrogen through the liquid to remove any air that had entered. Aliquots (ca. 5 µL) were removed from the reaction at 5, 10, and 20 minutes using a gastight syringe and analyzed by ^{1}H NMR spectroscopy for completion. Full conversion of eugenol to (*E*)-isoeugenol occurred after 20 minutes, and the product was isolated by vacuum distillation (2 torr, 98 °C) to afford 15.76 g (95.9%) of (*E*)-isoeugenol as a clear, colorless oil. To accurately determine amount of starting material remaining, 105.1 mg of the distillate was weighed out in an NMR tube containing 0.5-0.7 mL CDCl$_3$ and analyzed by ^{1}H NMR spectroscopy; percentages were calculated assuming a two-component mixture (eugenol/isoeugenol), using residual chloroform peak as internal standard. Peaks used: eugenol 5.11 ppm (2H), 3.34 ppm (2H); isoeugenol 6.36 ppm (1H), 6.12 ppm (1H), 1.90 ppm (3H).

Table 2.10. Ratio of starting material to product during large scale eugenol (**2.42**) to (*E*)-isoeugenol (**2.43**) isomerization

Eugenol integrals			Isoeugenol integrals				%3/3a
5.11 ppm	3.34 ppm	Units	6.36 ppm	6.12 ppm	1.90 ppm	Units	
5.21	5.41	2.66	602.4	603.6	1833.9	605.8	**0.4/99.6%**

Peaks corresponding to those reported[13] for (*Z*)-isoeugenol were hard to detect because of overlap with large signals. In particular, the phenolic H gave rise to a large signal that overlapped the possible d of q centered at 5.69 ppm reported[13] for (*Z*)-isoeugenol. Therefore, a 102.8 mg

sample of the distillate in CDCl$_3$ (0.8 mL) was shaken with D$_2$O (501.9 mg, 40 equiv), lessening the phenolic OH signal to the point where four downfield peaks of the eight for the d of q could be integrated as contributing 0.20 units, hence the full integral for 1H of the (Z)-isoeugenol would be 0.40 units, under conditions where the d of q at 6.07 ppm for (E)-isoeugenol was set to 100.0 units. Conclusion: 0.4% (Z)-isoeugenol was present, meaning composition of the distillate was 0.4% each eugenol and (Z)-isoeugenol, and 99.2% (E)-isoeugenol.

Data for Figure 2.8: Large Scale Isomerization Using Catalyst 1.1 of Essential Oils

Clove Oil: A 50 mL round bottomed flask equipped with a magnetic stir bar was added clove oil (3.29 g, 0.0200 mol assuming 100% eugenol), capped with a rubber septum, and purged with N$_2$ to deoxygenate oil and head space of flask. The flask was then submerged in a room-temperature water bath above a stirplate. In an inert atmosphere glove box, catalyst **1.1** (60.8 mg, 0.101 mol, 0.5 mol%) was also measured into a scintillation vial, capped, and brought out of the glove box. The septum was removed from the reaction flask and the catalyst was quickly added, followed by bubbling nitrogen through the liquid to remove any air that had entered. Aliquots (ca. 5 μL) were removed from the reaction at 5 and 10 minutes using a gastight syringe and analyzed by ^{1}H NMR spectroscopy for completion. Full conversion of clove oil to (E)-isoeugenol occurred after 10 minutes, and the product was isolated by vacuum distillation (750 mTorr, 67 ^{o}C) to afford 2.90 g (88.3%) of (E)-isoeugenol as a clear, colorless oil. To accurately determine amount of starting material remaining, 102.1 mg of the distillate was weighed out in an NMR tube containing 0.5-0.7 mL CDCl$_3$ and analyzed by ^{1}H NMR spectroscopy; percentages were calculated assuming a two-component mixture (eugenol/isoeugenol). Peaks used: eugenol 5.11 ppm (2H), 3.34 ppm (2H); isoeugenol 6.36 ppm (1H), 6.12 ppm (1H), 1.90 ppm (3H).

Table 2.11. Ratio of starting material to product during large scale isomerization of clove oil

Eugenol integrals			Isoeugenol intergrals				%**2.39/2.40**
5.11 ppm	3.34 ppm	Units	6.36 ppm	6.12 ppm	1.90 ppm	Units	
7.11	5.15	3.07	503.6	506.2	1516.0	505.0	0.6/99.4%

Sassafras Oil: A 25 mL round bottomed flask equipped with a magnetic stir bar was added clove oil (3.26 g, 0.0201 mol assuming 100% safrole), capped with a rubber septum, and purged with N_2 to deoxygenate oil and head space of flask. The flask was then partially submerged in a room-temperature water bath above a stirplate. In an inert atmosphere glove box, catalyst **1.1** (60.6 mg, 0.100 mol, 0.5 mol%) was measured into a scintillation vial, capped, and brought out of the glove box. The septum was removed from the reaction flask and the catalyst was quickly added, followed by bubbling nitrogen through the liquid to remove any air that had entered. Aliquots (ca. 5 μL) were removed from the reaction at 5, 10, 20, and 30 minutes using a gastight syringe and analyzed by ^{1}H NMR spectroscopy for completion. Full conversion of sassafras oil to (*E*)-isosafrole occurred after 30 minutes, and the product was isolated by vacuum distillation (750 mTorr, 60 °C) to afford 2.86 g (87.9%) of (*E*)-isosafrole as a clear, colorless oil. To accurately determine amount of starting material remaining, 102.1 mg of the distillate was weighed out in an NMR tube containing 0.5-0.7 mL $CDCl_3$ and analyzed by ^{1}H NMR spectroscopy; percentages were calculated assuming a two-component mixture (safrole/isosafrole). Peaks used: safrole 5.11 ppm (2H), 3.36 ppm (2H); isosafrole 6.39 ppm (1H), 6.13 ppm (1H), 1.92 ppm (3H)

Table 2.12. Ratio of starting material to product during large scale isomerization of sassafras oil

Safrole integrals			Isosafrole integrals				%**2.41/2.42**
5.11 ppm	3.36 ppm	Units	6.39 ppm	6.13 ppm	1.92 ppm	Units	
10.34	9.46	4.95	565.9	555.9	1800.3	574.0	0.9/99.1%

Neat Large Scale Isomerization and Recycling Using Heterogeneous Catalysts PS-1.1 and PSL-1.1

Procedure for experiment in Tables 2.4 and 2.5 - Eugenol to (*E*)-isoeugenol using **PS-1.1:** Inside the glovebox, in a small polyethylene mesh bag, **PS-1.1** (149.1 mg, 0.102 mmol) was weighed out, and the bag rolled up and secured with copper wire (see photos below for more detail). Eugenol **2.42** for cycle I was weighed out in a scintillation vial equipped with a magnetic stir bar and fitted with a Teflon lined cap. The bag was lowered into the vial, becoming partially submerged into the liquid substrate, where some substrate is absorbed via capillary action into the porous bag. The capped vial was removed from the glove box and submerged into an oil bath (70 °C). After 24 hours, the vial was transferred into the glove box and an aliquot (ca. 5 μL) was removed and analyzed by ^{1}H NMR spectroscopy. Upon completion, eugenol for cycle II was weighed out into a scintillation vial equipped with magnetic stir bar where the polyethylene bag containing the **PS-1.1** catalyst was transferred from the first vial into the second vial. Each subsequent cycle were performed as described. After completion of the cycles, the vials containing the isomerized product were weighed to determine yield. To accurately determine amount of starting material remaining, larger aliquots (~100 mg) were weighed out in an NMR tube containing 0.5-0.7 mL CDCl$_3$ and were analyzed by ^{1}H NMR spectroscopy; percentages were calculated assuming a two-component mixture (eugenol/isoeugenol). Peaks used: eugenol 5.11 ppm (2H), 3.34 ppm (2H); isoeugenol 6.36 ppm (1H), 6.12 ppm (1H), 1.90 ppm (3H).

Eugenol to (*E*)-isoeugenol using **PSL-1.1:** Inside the glovebox, in a small polyethylene mesh bag, **PSL-1.1** (150.1 mg, 0.0971 mmol) was weighed out, and the bag rolled up and secured with copper wire (see photos below for more detail). Eugenol **2.42** for cycle I was weighed out in a scintillation vial equipped with a magnetic stir bar and fitted with a Teflon lined cap. The bag was lowered into the vial, becoming partially submerged into the liquid substrate,

where some substrate is absorbed via capillary action into the porous bag. The capped vial was removed from the glove box and submerged into an oil bath (70 °C). After 24 hours, the vial was transferred into the glove box and an aliquot (ca. 5 μL) was removed and analyzed by ^{1}H NMR spectroscopy. Upon completion, eugenol for cycle II was weighed out into a scintillation vial equipped with magnetic stir bar where the polyethylene bag containing the **PSL-1.1** catalyst was transferred from the first vial into the second vial. Each subsequent cycle were performed as described, except for cycle IV, which was checked by ^{1}H NMR as described above after 24 h, 48 h, and 65 h; NMR spectroscopy showed 85% conversion to isoeugenol after 24 h, 97.5% after 48 h, and no detectable eugenol after 65 h After completion of the cycles, the vials containing the isomerized product were weighed to determine yield. To accurately determine amount of starting material remaining, larger aliquots (~100 mg) were weighed out in an NMR tube containing 0.5-0.7 mL CDCl$_3$ and were analyzed by ^{1}H NMR spectroscopy; percentages were calculated assuming a two-component mixture (eugenol/isoeugenol). Peaks used: eugenol 5.11 ppm (2H), 3.34 ppm (2H); isoeugenol 6.36 ppm (1H), 6.12 ppm (1H), 1.90 ppm (3H).

Eugenol to (*E*)-isoeugenol using PSL-1.1: Inside the glovebox, in a small polyethylene mesh bag, **PSL-1.1** (120.1 mg, 0.07767 mmol) was weighed out, and the bag rolled up and secured with copper wire. Freshly distilled eugenol **2.42** for cycle I was weighed out in a scintillation vial equipped with a magnetic stir bar and fitted with a Teflon lined cap. The bag was lowered into the vial, becoming partially submerged into the liquid substrate, where some substrate is absorbed via capillary action into the porous bag. The capped vial was removed from the glove box and submerged into an oil bath (70 °C). After 24 hours, the vial was transferred into the glove box and an aliquot (ca. 5 μL) was removed and analyzed by ^{1}H NMR spectroscopy. Upon completion, eugenol for cycle II was weighed out into a scintillation vial

equipped with magnetic stir bar where the polyethylene bag containing the **PSL-1.1** catalyst was transferred from the first vial into the second vial. Each subsequent cycle were performed as described, except for cycle VII, which was checked by ^{1}H NMR spectroscopy after 18 h and determined to be complete, and for cycle X, which was checked by ^{1}H NMR spectroscopy as described above after 24 h and 48 h, ^{1}H NMR spectroscopy showed 85% conversion to isoeugenol after 24 h and no detectable eugenol after 48 h. After completion of the cycles, the vials containing the isomerized product were weighed to determine yield. To determine amount of starting material remaining, larger aliquots (~100 mg) were weighed out in an NMR tube containing 0.5-0.7 mL CDCl$_3$ and analyzed by ^{1}H NMR spectroscopy; percentages were calculated assuming a two-component mixture (eugenol/isoeugenol). Peaks used: eugenol 5.11 ppm (2H), 3.34 ppm (2H); isoeugenol 6.36 ppm (1H), 6.12 ppm (1H), 1.90 ppm (3H).

Chapter 2 contains material similar to the material published in the manuscript: Larsen, C.E., Paulson, E.R.,[†] Erdogan, G.,[†] Grotjahn, D.B. "A Facile, Convenient, and Green Route to (*E*)-Propenylbenzene Flavors and Fragrances by Alkene Isomerization". *Synlett*, **2015**, 26, 2462. ([†]co-2nd authors)

2.6. References

1.   Grotjahn, D. B.; Larsen, C. R.; Gustafson, J. L.; Nair, R.; Sharma, A., Extensive Isomerization of Alkenes Using a Bifunctional Catalyst: An Alkene Zipper. *J. Am. Chem. Soc.* **2007**, *129*, 9592.

2.   Tao, J.; Sun, F.; Fang, T., Mechanism of alkene isomerization by bifunctional ruthenium catalyst: A theoretical study. *J. Organometal. Chem.* **2012**, *698*, 1.

3.   Grotjahn, D. B., Structures, mechanisms, and results in bifunctional catalysis and related species involving proton transfer. *Top. Catal.* **2010**, *53*, 1009.

4.   Erdogan, G.; Grotjahn, D. B., Mild and Selective Deuteration and Isomerization of Alkenes by a Bifunctional Catalyst and Deuterium Oxide. *J. Am. Chem. Soc.* **2009**, *131*, 10354.

5.   Tse, S. K. S.; Xue, P.; Lin, Z.; Jia, G., Hydrogen/Deuterium Exchange Reactions of Olefins with Deuterium Oxide Mediated by the Carbonylchlorohydridotris(triphenylphosphine)ruthenium(II) Complex. *Adv. Synth. Catal.* **2010**, *352*, 1512.

6.   Dobereiner, G. E.; Erdogan, G.; Larsen, C. R.; Grotjahn, D. B.; Schrock, R. R., A One-Pot Tandem Olefin Isomerization/Metathesis-Coupling (ISOMET) Reaction. *ACS Catal.* **2014**, *4*, 3069.

7.   Liniger, M.; Liu, Y.; Stoltz, B. M., Sequential Ruthenium Catalysis for Olefin Isomerization and Oxidation: Application to the Synthesis of Unusual Amino Acids. *J. Am. Chem. Soc.* **2017**, *139*, 13944.

8.   Higman, C. S.; de Araujo, M. P.; Fogg, D. E., Tandem catalysis versus one-pot catalysis: ensuring process orthogonality in the transformation of essential-oil phenylpropenoids into high-value products via olefin isomerization– metathesis. *Catal. Sci. Technol.* **2016**, *6*, 2077.

9.   Sytniczuk, A.; Forcher, G.; Grotjahn, D. B.; Grela, K., Sequential Alkene Isomerization and Ring-Closing Metathesis in Production of Macrocyclic Musks from Biomass. *Chem. Eur. J.* **2018**, *24*, 10403.

10.   Miura, T.; Nakahashi, J.; Zhou, W.; Shiratori, Y.; Stewart, S. G.; Murakami, M., Enantioselective Synthesis of *anti*-1,2-Oxaborinan-3-enes from Aldehydes and 1,1-Di(boryl)alk-3-enes Using Ruthenium and Chiral Phosphoric Acid Catalysts. *J. Am. Chem. Soc.* **2017**, *139*, 10903.

11.   Erdogan, G.; Grotjahn, D. B., Supported Imidazolylphosphine Catalysts for Highly (E)-Selective Alkene Isomerization. *Org. Lett.* **2014**, *16*, 2818.

12.   Larsen, C. R.; Grotjahn, D. B., Stereoselective Alkene Isomerization over One Position. *J. Am. Chem. Soc.* **2012**, *134*, 10357.

13.   Sharma, S. K.; Srivastava, V. K.; Jasra, R. V., Selective double bond isomerization of allyl phenyl ethers catalyzed by ruthenium metal complexes. *J. Mol. Catal. A: Chem.* **2006**, *245*.

Chapter 3

Synthesis and Characterization of Nitrile-Free Pentamethylcyclopentadienylruthenium Phosphine Complexes for Alkene Isomerization

3.1 Introduction

While there are a number of catalysts that can achieve selective isomerization for compounds containing specific functional groups such as allylic alcohols,[1-2] ethers[3] and amines,[4] few isomerization catalysts exist that can exhibit regio- and/or stereoselectivity in a general fashion for substrates that do not contain branching or other steric factors that could inhibit repeated isomerizations down a chain. There has been a significant improvement in the controlled positional isomerization of 1-alkenes to 2-alkenes in the last 20 years, but most of these catalysts give (*E*)-2 and (*Z*)-2 product in close to thermodynamic ratio of about 4:1 for linear unbranched alkenes.[5]

The challenge is more acute when attempting to control **both** positional **and** *E*/*Z* selectivity. Three recent catalysts that are positional- and (*Z*)-selective are from the Holland and Hilt groups. Holland was able to obtain 61% 2-octene and *E*/*Z* ratio of 1:7.2 with a cobalt(II)diketiminate alkyl complex (5 mol%, 80 °C, 12 h).[6] The complex acted on linear alkene substrates, but showed signs of deactivation with certain substrates (silyl, dienes) and would not tolerate protic or C=O functionality. Hilt had significant success with a catalyst system that employed Ph_2PH, Zn, ZnI_2 and either $NiCl_2(dppp)$[7] or $CoBr_2(dpppBuEt)$.[8] Hilt's nickel system (10 mol% Ni, -60 °C, 6 h) gave 72% 2-decene with an *E*/*Z* ratio of 28:72, although selectivity eroded at higher temperatures. The cobalt system (5-10 mol%, rt, 1-24 h) gave 95% 2-hexadecene with a *E*/*Z* ratio of 15:85.
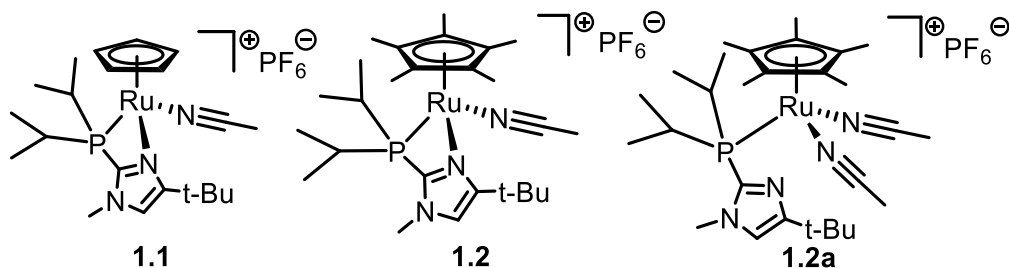
Figure 3.1. Existing alkene isomerization catalysts from the Grotjahn group

At present, two recent catalysts achieve high positional and (*E*)-selectivities. In 2014 we disclosed the Cp* analogue of the zipper catalyst **1.1**[9] (**1.2** + **1.2a**, Figure 3.1), which can selectively achieve >95% yields of (*E*)-2-alkenes, with no detectable (*Z*)-isomers by ^{1}H NMR spectroscopy and GC and little (<3%) overisomerization, all with reasonably low loadings and mild conditions (1 mol%, 40 °C, 48 h) (Table **3.1**). After we started the work reported here, in 2017 Wang et al reported an iridium pincer complex that generally furnishes 90-95% (*E*)-2 alkenes with 20-50:1 *E/Z* selectivity, also with low loadings and temperatures, though we note the authors purified alkene substrates by distillation from LiAlH₄.[10]
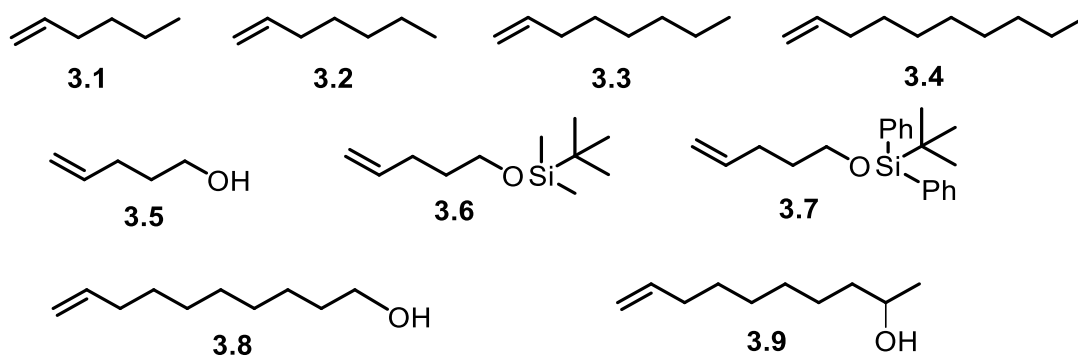
Figure 3.2. Substrates studied for comparison between isomerization catalysts including **1.1** and **1.2** + **1.2a**

Table **3.1**. Comparison of catalysts **1.1** and **1.2** + **1.2a** and other reference catalysts in isomerization of various substrates (complied primarily from ref. [11] and [9])

Entry	Alkene	Catalyst	Mol %	Time	Temp (C°)	1-alkene (%)	(E)-2-alkene (%)	(E)-3-alkene (%)	(Z)-2-alkene (%)
1	3.1	1.2 + 1.2a		48 h	40	2.3	95.5	2.1	<0.5
2		1.1	1	2 h	rt	1.6	75.5	24.2	<0.5
3		1.2 + 1.2a		48 h	40	2.5	95.6	2.9	<0.5
4		1.1		4 h	rt	0.9	51.9	45.2	<0.5
5		RhCl$_3$/BH$_3^a$				0.7	43.3	36.0	12.7
	3.2	calc w/out (Z)^b				0.5	59.7	39.8	0
6		Cp*Ru(ACN)$_3^{+c}$	2	66 h		81.8	8.5	4.2	2.0
7		Cp*Ru(ACN)$_2$La$^{+c,d}$	4	72 h		97.9	0.7	<0.5	<0.5
8		Cp*Ru(ACN)$_2$Lb$^{+c,e}$	4	72 h		99.0	0.2	<0.5	<0.5
9		1.2 + 1.2a		48 h		2.7	95.7	2.4	<0.5
10	3.3	(1.2 + 1.2a) + ACN	1	97 h	40	2.7	94.7	2.7	<0.5
11		1.2a + ACN		97 h		4.5	95.6	1.8	<0.5
12	3.4	1.2 + 1.2a	2	48 h		2.6	95.8	2.2	<0.5
13	3.5	1.2 + 1.2a	1	24 h		2.7	94.4	0	<0.5
14		1.1	2	2 h	70	0	0	0	0^g
15	3.6	1.2 + 1.2a	1	48 h	40	4.7	95.1	0	<0.5
17		1.1	5	4 h	70	0	0	0	0^h
18	3.7	1.2 + 1.2a	2^f	48 h	40	5.0	90.3	1.0	<0.5
19	3.8	1.2 + 1.2a	1	5 h	70	4.2	95.1	2.1	<0.5
20		1.1	5	7 h		0	0	0	<0.5
21	3.9	1.2 + 1.2a	1	46 h	40	2.2	97.7	Trace	<0.5
22		1.1	5	4 h	70	0	0	0	<0.5

^{a}Values from ref. [12]. ^{b}Entry 5 calculated out of 100% if (Z)-isomers are excluded. ^{c}With PF$_6^-$ anion. ^{d}La: iPr$_3$P. ^{e}iPr$_2$PPh. ^{f} 2 mol% **1.2** + **1.2a** + 6 mol% extra phosphine ligand. ^{g}Isomer not listed: 100% pentanal. ^{h}Isomer not listed: 91.7% enol ether.

We conclusively showed that the imidazolyl nitrogen in **1.2a** creates a catalyst that is >3000 times faster than an analog of **1.2a** with a P(iPr)$_3$ ligand.[13] However, comparing **1.1** and **1.2**+**1.2a**, the price of high positional control by the latter is about 1000-fold reduction in rate. In the search for a more active catalyst, we considered nitrile-free complex **3.14** (Figure 3.3). Nitrile inhibition had been demonstrated by us on two occasions: (1) addition of an equivalent of CH$_3$CN to **1.2**+**1.2a** slowed the catalyst by a factor of 2; (2) addition of 1.5 – 2 equiv of CH$_3$CN slows Cp catalyst **1.1**, but not in a way that prevents isomerization of 2-alkene to 3-alkene.[13]

Hence, our hypothesis was that **3.14** would be faster than **1.2+1.2a**, because of no competition of nitrile and alkene. As described herein, **3.14** is more than 400 times faster than **1.2+1.2a** and about as fast as Cp analog **1.1**, but like **1.2+1.2a** has the ability to form (*E*)-2 alkenes in ca. 95% yields. Here we also describe the unusual ability of the ruthenium-bound imidazole ring to engage in π-bonding, thus stabilizing the formally 16-electron structure of **3.14**. Moreover, we show that it is the steric bulk of the Cp* ligand and not its greater electron donation that is responsible for slowing the further positional isomerization.

3.2. Synthesis and characterization of complexes

3.10: $R^1=R^2=CH_3, R^3=tBu$ **3.14:** $R^1=R^2=CH_3, R^3=tBu$
3.11: $R^1=CH_3, R^2=CF_3, R^3=tBu$ **3.15:** $R^1=CH_3, R^2=CF_3, R^3=tBu$
3.12: $R^1=R^2=CH_3, R^3=H$ **3.16:** $R^1=R^2=CH_3, R^3=H$
3.13: $R^1=CH_3, R^2=CF_3, R^3=H$ **3.17:** $R^1=CH_3, R^2=CF_3, R^3=H$
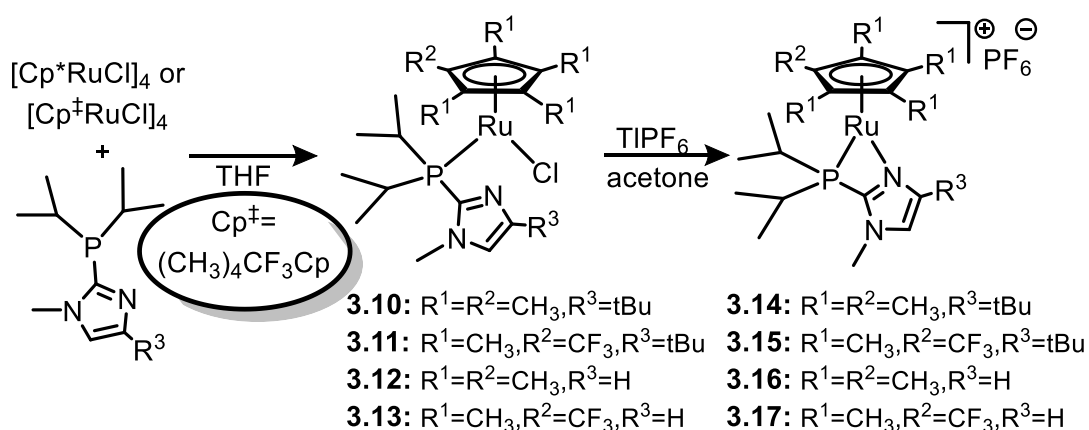
Figure 3.3. Synthesis of complexes **3.10 – 3.17**

Complex **3.10** appeared an ideal intermediate to make **3.14** (Figure 3.3). In 1988, Tilley and Chaudret independently discovered the pioneer complexes $Cp*Ru(PR_3)Cl$, where R = iPr or Cy. $Cp*Ru(L)X$ complexes have been synthesized by complexation of PR_3 with either $Cp*RuCl_4$[14] or a mixture of $Cp*RuCl_2$ dimer and Zn.[15] A striking feature of both reported complexes is their blue color both in solution and in the solid state, contrasting with yellow to orange color of 18-electron CpRu(II) species mentioned here in this article. It has been suggested

that the blue color in these and subsequent Cp*Ru(P)X complexes is the result of π-donation of a lone pair from the halide to the metal center, which stabilizes a formally 16-electron state.[16]

After Tilley's and Chaudret's initial discoveries, several 16-electron complexes of the general formula Cp*Ru(L)X could be accessed if L was a bulky phosphine ligand with the general formula $P(R^1)_2(R^2)$ where R^1 was isopropyl or cyclohexyl, and where X was either a halide[16-19] or a weakly basic oxygen-containing X-type ligand such as triflate, Ph$_3$SiO$^-$, or CF$_3$CH$_2$O$^-$.[16, 20-21] We reasoned that the Cp*RuCl fragment could therefore accommodate the (diisopropyl)(imidazolyl)phosphine ligand employed in catalysts **1.1** and **1.2**, although it was not clear whether the ligand would bind in a monodentate fashion to produce a 16-electron complex akin to Tilley and Chaudret's examples, or would chelate through the imidazole as well to produce an 18-electron complex. Since the switch of the Cp ligand in catalyst **1.1** to the bulkier and more electron-rich Cp* ligand in catalyst **1.2** + **1.2a** engendered an increase in monoselectivity, we wondered whether steric or electronic factors lead to the change. The pentamethylcyclopentadienyl (Cp*) ligand is both more electron-rich and sterically bulky than the cyclopentadienyl (Cp) ligand.[22-23] Given the distinct differences in reactivity between Cp-containing catalyst **1** (which is fast but not positionally selective) and Cp*-containing **1.2** + **1.2a** and **3.14** (which is selective for monoisomerization), we wanted to investigate whether the change in selectivity during catalysis is the result of steric or electronic influences between the metal center and the alkene. Catalytic and structural comparisons between Cp- and Cp*Ru complexes[24-30] have been undertaken employing the 1-(trifluoromethyl)-2,3,4,5-tetramethylcyclopentadienyl (Cp‡) ligand developed by Gassman,[31] reported to mimic the electronics of the Cp ligand and the sterics of the Cp ligand.[31-33] We therefore made **3.11** (and

ultimately **3.15**) with the more electron-poor tetramethyl(trifluoromethyl)cyclopentadienyl (Cp‡) ligand.

The [Cp‡RuCl]₄ tetramer was first prepared following a protocol by Evju and Mann[34] in which they speculated the tetramer had formed during the synthesis. The [Cp‡RuCl₂]₂ dimer was reduced with Zn metal in refluxing methanol, and the tetramer was isolated in 91% yield, characterized, and a crystal structure was obtained (Figure 3.4). This [Cp‡RuCl]₄ tetramer exhibits a similar solid-state structure to the [Cp*RuCl]₄ parent,[35] crystallizing as a distorted cubane in the highly unsymmetrical triclinic P-1 space group. Both tetramers exhibit an average Ru-Cl bond length of 2.52 Å.
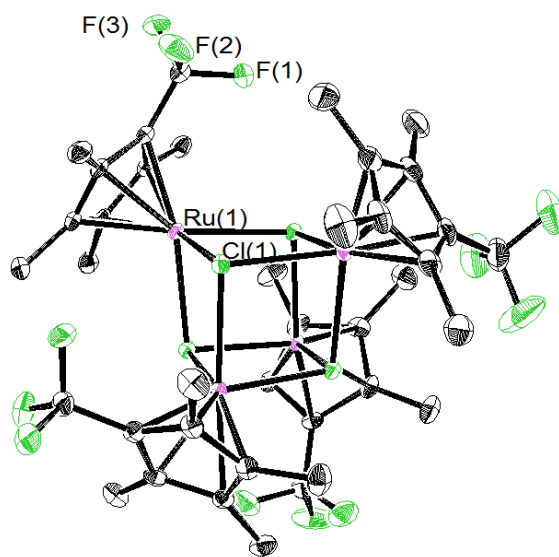
Figure 3.4. X-Ray crystal structure of [Cp‡RuCl]₄. Range of bond lengths across two molecules in unit cell (in Å): Ru-Cl: from 2.5024(6) to 2.5299(7) (out of 12 Ru-Cl bonds), Ru-Cp(centroid): from 1.725 to 1.733 (out of 8 Ru-Cp(centroid) distances).

Complexation of the requisite phosphine with [Cp*RuCl]₄ or [Cp‡RuCl]₄ occurs efficiently in solvents such as acetone and THF, with a rapid change in color of the solution from deep red to deep blue. While the blue color is reminiscent of many Cp*Ru 16-electron

complexes, NMR data for the major species (>90% by ^{31}P NMR spectroscopy) are also consistent with the formally 16-electron species $Cp^RRu(L)Cl$ (**3.10** – Cp* and **3.11** – Cp[‡]). There is some evidence of equilibrium between these monomeric species and related tetrameric species For the major species, the isopropyl group signals in the ^{1}H NMR spectra of **3.10** and **3.11** appear as a single dd, suggesting either a symmetrical static structure such as that drawn in Figure 3.3; alternatively, if solvent is bound, forming an 18-electron species, the association of solvent is weak. The ^{15}N HMBC chemical shift of the basic nitrogen of the imidazole in **3.10** (δ^{15}N -100.6 ppm) is consistent with an unchelated imidazolylphosphine,[36] as is the coupling constant for the phosphorus to the C-2 of the imidazole ($^1J_{CP}$ =51.9 Hz). Complexes **1.2** + **1.2a** can be used as comparisons for the $^1J_{CP}$ coupling constant, as both chelated (**1.2**) and unchelated (**1.2a**) forms of the complex exist. The $^1J_{CP}$ in **3.10** much more closely resembles that in **1.2a** (58.0 Hz) rather than that in **1.2** (28.6 Hz).[9] The large C-2 coupling constant for complex **3.11** (J = 43.7 Hz) also suggests a lack of chelation and hence 16-electron character.

For the minor species, the monomer-cluster equilibrium is consistent with the following spectra of **3.10** in different solvents: ~10-12 mg of **3.10** was dissolved in a J. Young NMR tube containing 0.6 mL of one of the following three solvent systems, and ^{1}H and ^{31}P NMR spectra were acquired. The signals assigned to the monomer are predominant in the most polar solvent, and the proportions are roughly equal in cyclohexane-d_{12}. Generally, in ^{31}P NMR spectra the integration for the signal assigned to the cluster matches the integration for the free phosphine. Given these data and the starting ratio of Ru:P is 1:1, we propose that the structure of the cluster is one with formula $C_{48}H_{114}Cl_4P_2Ru_4$, in which the ratio of Ru:P is 2:1, which would allow for equal proportions of complex and free phosphine.
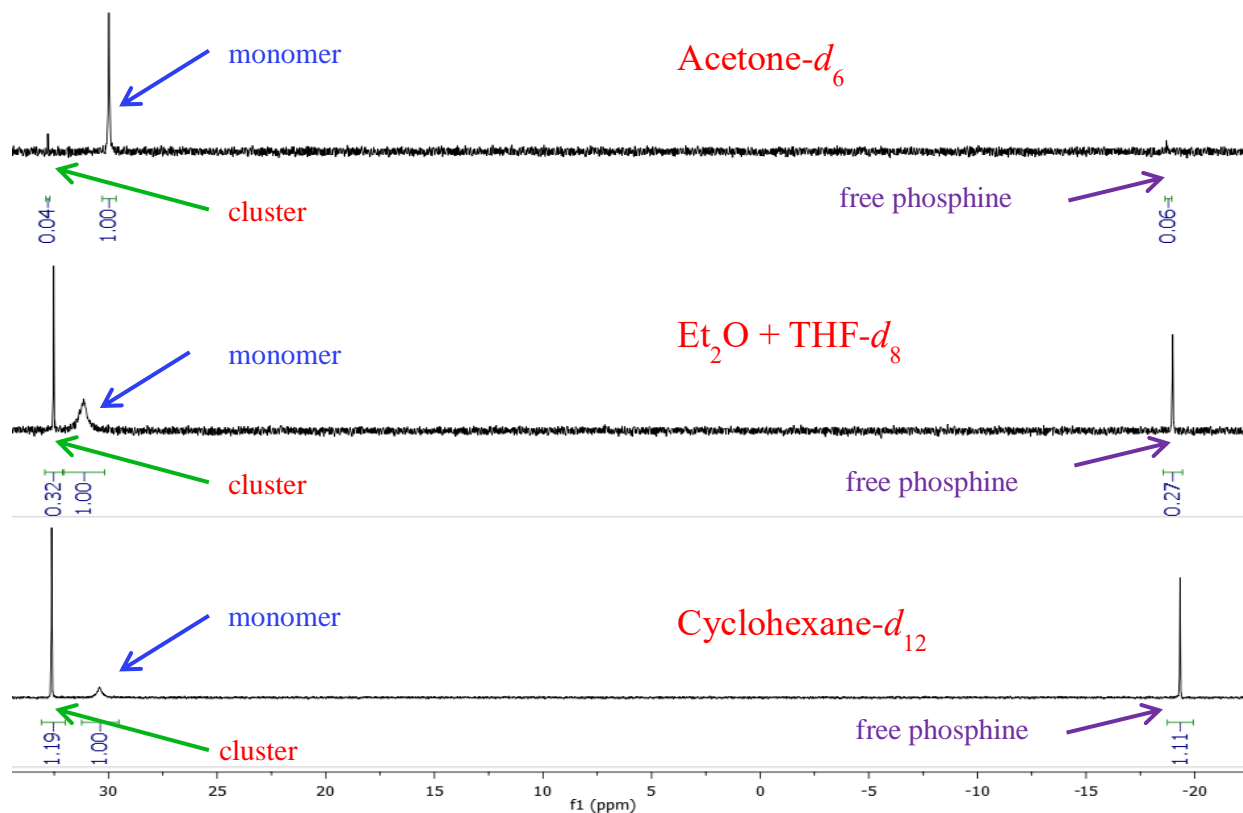
Figure 3.5. $^{31}P\{^1H\}$ NMR spectra at 202 MHz showing changes in ratios of monomer **3.10**, tetraruthenium bisphosphine (Ru₄P₂) cluster (**3.18** – see structure in Figure 3.7 below), and free phosphine in equilibrium

The following spectra were taken after addition of an extra 2 equivalents (~10 mg) of

phosphine, during which a color change from purple to blue was observed:
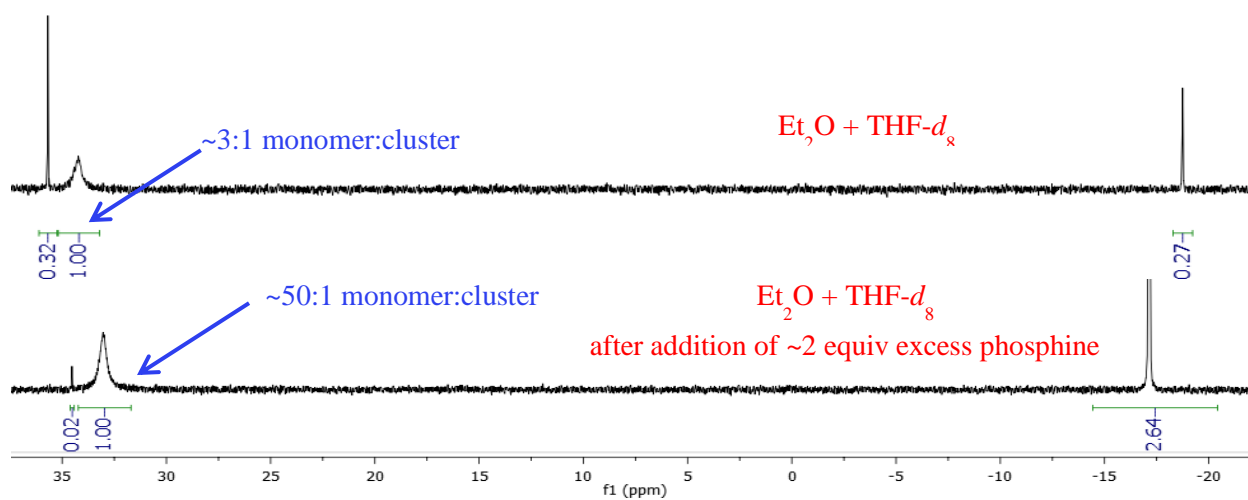
Figure 3.6. $^{31}P\{^1H\}$ NMR spectra at 202 MHz of before and after adding excess phosphine to complex mixture, shifting equilibrium towards monomer **3.10**

The spectrum after additional phosphine is added indicates a shift of the equilibrium towards the monomer. Conversely, if the reaction is set up using half as much tetramer (i.e. with a ratio of P:Ru of 2:1 instead of 4:1) in cyclohexane-d_{12}, only signals for the Ru_4P_2 cluster are seen by ^{1}H and ^{31}P NMR (see Figures 3.8 and 3.25-3.30 in experimental). The solvents that seem to favor the cluster are non-polar, which suggests a structure with a small to zero net dipole. Thus, we propose the following 'ladder-like' structure (**3.18** - Figure 3.7), which is consistent with ^{1}H NMR data in Figure 3.8, in which the signals for the two phosphine ligands are equivalent, and there are two different environments for the Cp* protons:
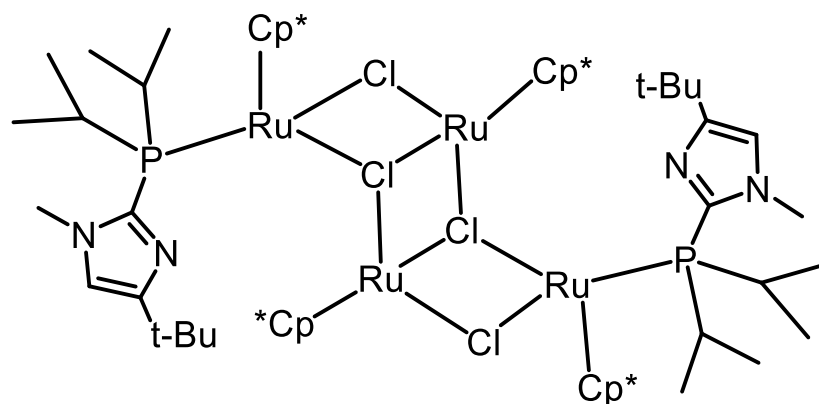
Figure 3.7. Proposed structure for Ru_4P_2 cluster **3.18**
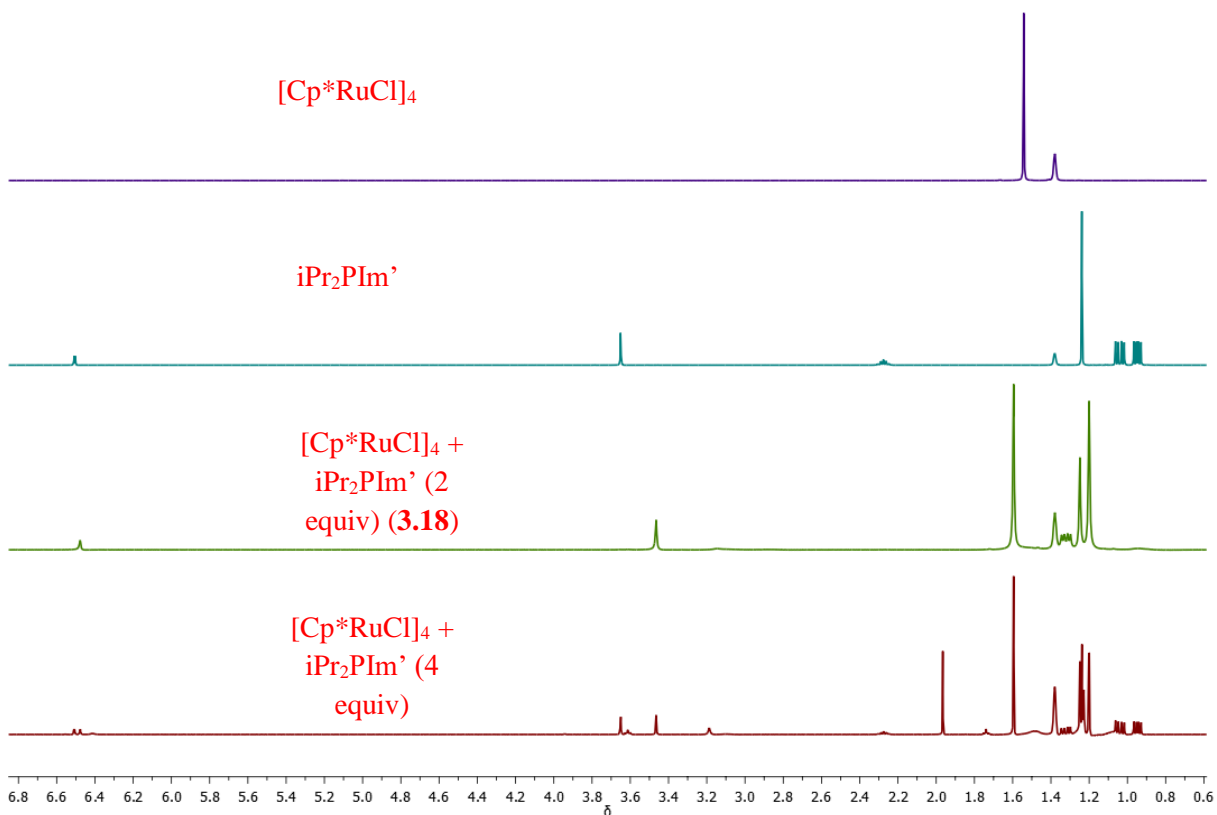
Figure 3.8. ^{1}H NMR spectra at 500 MHz of (top two) pure Ru$_4$ tetramer and pure phosphine, and results of mixing Ru$_4$ and P in 1:2 and 1:4 ratios. All samples are in cyclohexane-d_{12}
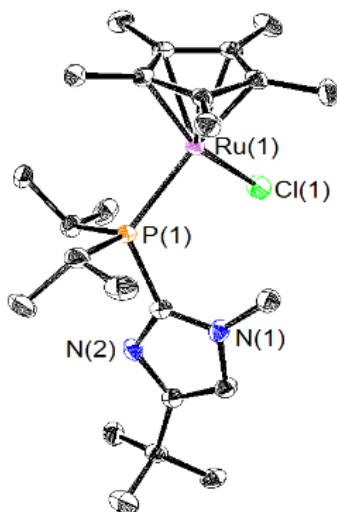
Figure 3.9. X-Ray crystal structure of complex **3.10.** Key bond lengths (Å) with values for each independent molecule in the unit cell**:** Ru-P, 2.3582(13) and 2.3699(13); Ru-Cl, 2.703(12) and 2.3591(12); Ru-Cp(centroid), 1.772 and 1.780, respectively.

Prolonged storage in cyclohexane at -40°C gave crystals of **3.10** suitable for X-ray diffraction. The crystal structure of **3.10** (Figure 3.9) shows a two-legged piano-stool structure characteristic of 16-electron Cp*Ru complexes, with P(1), Cl(1) and Ru(1) coplanar with the Cp* centroid. Consistent with the HMBC data, the basic N(2) shows no interaction with ruthenium, in contrast to other systems containing Cp*RuCl metal fragments with a P-N ligand. The P-N ligands iPr$_2$P-2-dimethylaminoindenide studied by Stradiotto[37], Ph$_2$P(CH$_2$)$_2$NMe$_2$ by Kirchner[38] and Ph$_2$P(CH$_2$)$_2$NH$_2$ by Ikariya[39-41] were shown to chelate through both the phosphorus and nitrogen to Cp*RuCl, leading to 18-electron complexes. All three published systems feature a P-C- C-N-Ru five-membered chelate. We have shown previously in an alkyne hydration catalytic system with a pyridyl-phosphine ligand that the introduction of a *tert*-butyl group adjacent to the nitrogen can greatly enhance the hemilability of the chelate.[36] We presume that the steric and angle strain combined with the strong π-donation of the halide prevents chelation from occurring in **3.10** and **3.11**.

73
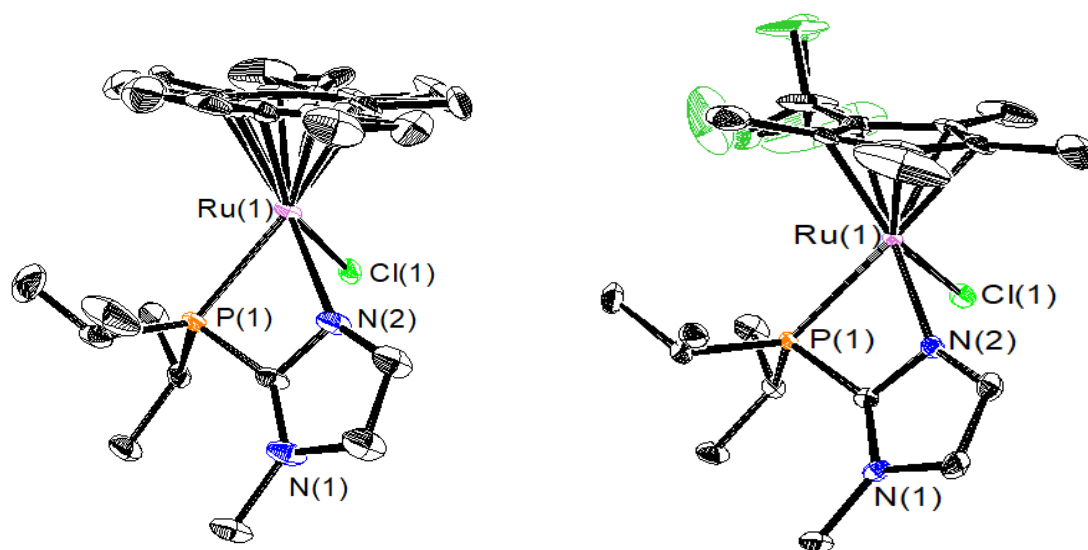
Figure 3.10. X-Ray crystal structure of complexes **3.12** and **3.13**. Key bond lengths (Å) and angles (deg)**: 3.12:** Ru-P, 2.3906(10); Ru-N, 2.203(4); Ru-Cl, 2.4713(10); Ru-Cp(centroid), 1.779; P-Ru-N, 66.94(10). **3.13**: Ru-P, 2.3925(9); Ru-N, 2.185(2); Ru-Cl, 2.4595(8); Ru-Cp(centroid), 1.780; P-Ru-N, 66.92(7).

To examine this further, complexes **3.12** and **3.13**, lacking the *tert*-butyl group, were generated from the appropriate tetramer and phosphine. Although some evidence for 16-electron species, or at least rapid hemilability of the chelate, is presented in solution (blue color for **3.12**, symmetry in ^{1}H NMR spectra for **3.12** and **3.13**), the X-ray crystal structures for **3.12** and **3.13** feature a chelated nitrogen (Figure 3.10). The chelate lengthens the Ru-Cl bond of **3.12** as compared to **3.10** (2.47 Å vs 2.36 Å), which could be ascribed to the lack of Ru-Cl multiple-bond character for **3.12**.

3.19: Cp*
3.20: Cp‡
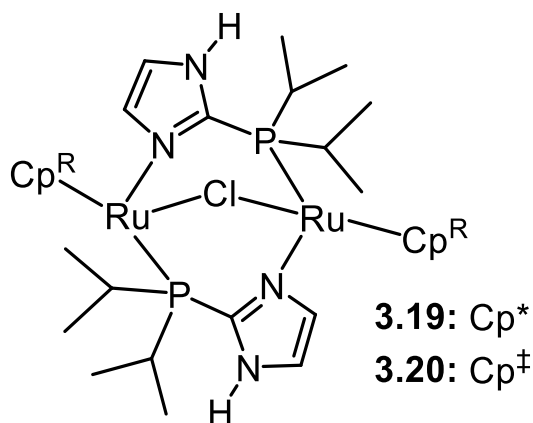
Figure 3.11. Structures of complexes **3.19** and **3.20**

Interestingly, when the methylated imidazole moiety is replaced by the protic imidazole, the expected monomers are not the major products. Instead, dinuclear complexes **3.19** and **3.20** are formed, in which two P,N ligands (and one chloro ligand) bridge two ruthenium centers, with the second chloride in the outer sphere (Figure 3.11). Complexes **3.19** and **3.20** show limited solubility in most solvents, that allowed for facile growth of crystals. Significantly, when TlPF$_6$ is added to **3.19**, only the outer-sphere chloride is exchanged, showing the robustness of the bridging chloride.
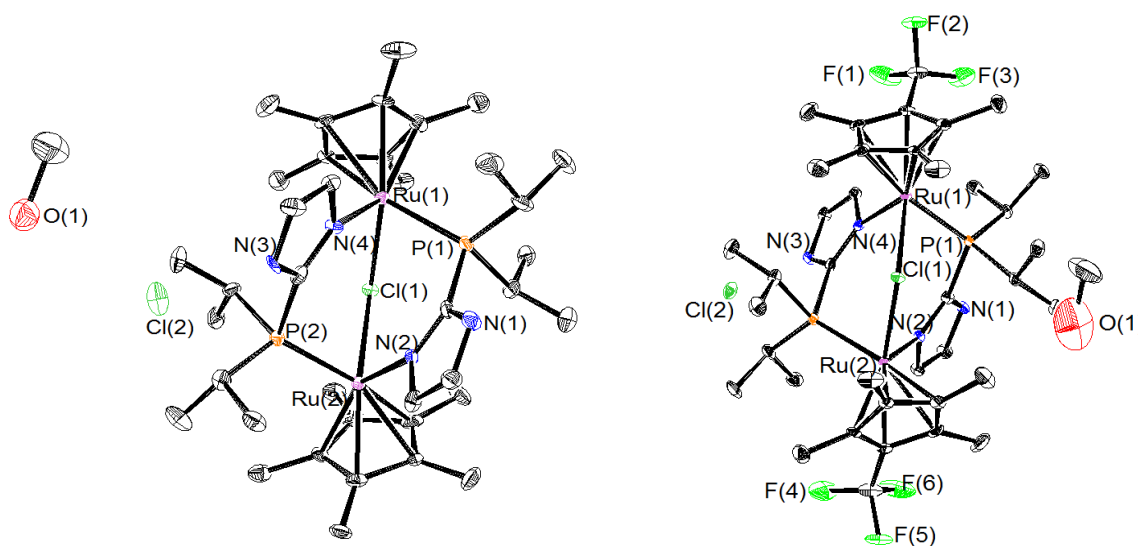
Figure 3.12. Crystal structures of **3.19** and **3.20**.
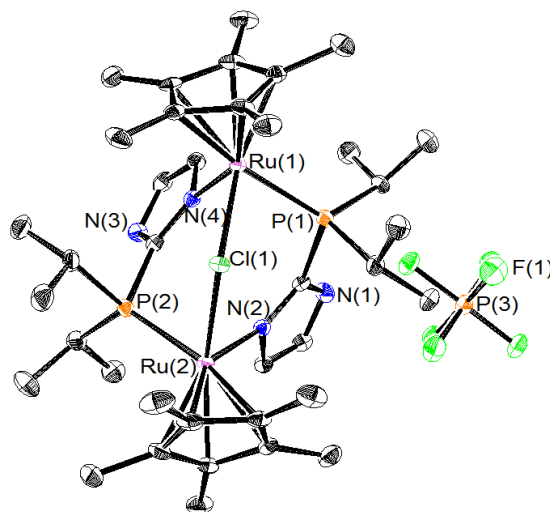
Figure 3.13. Crystal structure of **3.19** after addition of TlPF$_6$

The mixture containing complex **3.10** was tested for isomerization under similar conditions as **1.2** + **1.2a**, but was found to be a very poor catalyst (<1 turnover in 1 week!). There could be a few reasons for the sluggish catalysis: either the halide is too strong of a π-donor, thereby inhibiting binding of the alkene to the metal center, or the anionic character of the halide disfavors binding of the alkene or formation of a formally anionic allyl ligand during catalysis. To overcome the halide inhibition, the mixture containing **3.10** was subjected to several different halide abstraction salts; TlPF$_6$ appeared to be an ideal choice for clean and complete removal of the chloride to make a cationic complex (**3.14**) in acetone, which was obtained in 98.2% yield; **3.11** was cleanly ionized with TlPF$_6$ in the same fashion to obtain complex **3.15** in 94 % yield.

Table 3.2. $^1J_{C-P}$ (Hz) and ^{13}C and ^{15}N chemical shifts (ppm)

Complex	Im-C1		N(2)	N(1)
	^{13}C chemical shift	J	^{15}N chemical shift	^{15}N chemical shift
1.2	142.5	58.0	n.d.	n.d.
1.2a	148.3	28.5	n.d	n.d.
3.10[a,b]	141.9	51.9	-100.6	-213.1
3.11	146.0	43.7	-136.2	-213.7
3.12[c]	146.5	34.7	n.d.	n.d.
3.13[c]	152.5	24.1	-164.3	-210.2
3.14[a,c]	152.0	19.3	-147.0	-203.1
3.15[a,c]	151.9	21.7	-155.7	-204.5
3.16	152.6	22.1	-158.3	-203.7
3.17	152.3	25.2	-168.8	-205.1

Data for **1.2** and **1.2a** are from literature. [13] [a]16-electron in crystal structure. [b]N(2) unbound to Ru in crystal structure. [c]N(2) bound to Ru in crystal structure. n.d.: not determined.

We expected that upon ionization and halide ligand loss from **3.10**, the cationic complex would bind the imidazole nitrogen as well as another solvent molecule to produce an 18-electron complex due to the removal of the π-stabilizing chloride ligand. A significant upfield shift of the ^{15}N HMBC resonance for the basic imidazole nitrogen (δ_N = -147.0 ppm) occurs, which brings it within the range for *P,N*-chelated imidazolyl phosphine ligands.[36] However, the ^1H NMR

spectrum shows sharp peaks for all resonances, with one septet of doublets (2H) for the isopropyl C-H protons and two dd (each 6H) for the isopropyl-CH_3 protons, suggesting planar symmetry[16] or fast reversible binding of solvent molecules to the metal center.[42] However, no broadening of the ^1H signals occurred, nor did we observe new signals (for either bound acetone or desymmetrization of the phosphine ligand) consistent with binding of acetone upon cooling the solution to -30 °C. Surprisingly, the color of the solution upon ionization remains deep blue; UV-vis spectroscopy shows a large broad absorption centered around 572 nm (ε= 748 L/mol*cm). The combination of spectroscopic data point to the persistence of a 16-electron complex, despite the removal of the halide ligand. The blue color remains upon removal of solvent, and the intensely blue powder is stable for months under air-free conditions. Solutions of **3.14** can be made with undried acetone, which can maintain their color and activity for a few days.
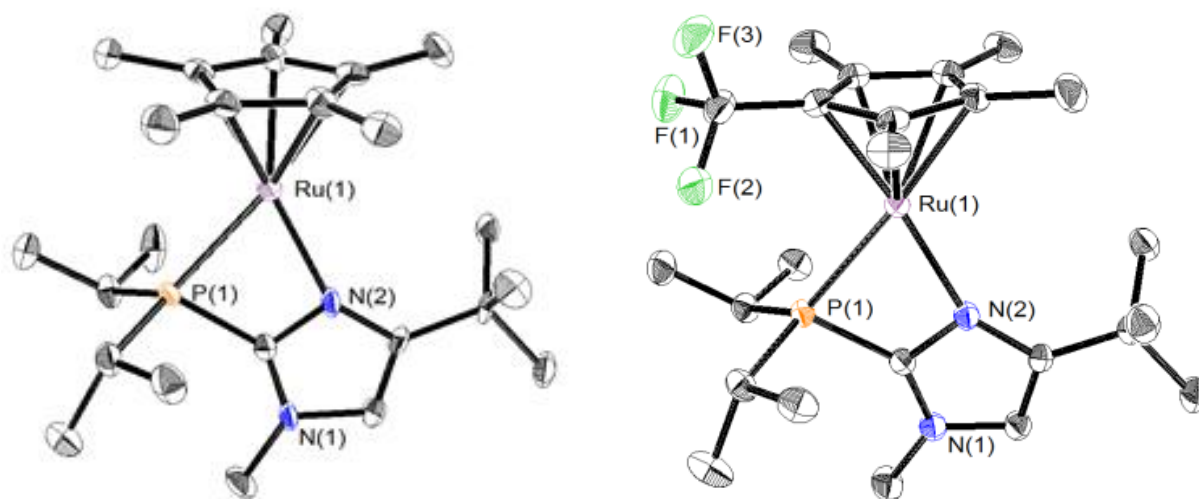
Figure 3.14. X-Ray crystal structures of the cations in complexes **3.14** and **3.15** (PF_6^- anions omitted). Key bond lengths (Å) and angles (deg) with values for each independent molecule in the unit cell: **3.14** (one molecule in unit cell): Ru-P, 2.386(2); Ru-N, 2.242(10); Ru-Cp(centroid), 1.773; N-Ru-P, 68.3(2). **3.15** (two molecules in unit cell): Ru-P, 2.3905(6) and 2.3930 (6); Ru-N, 2.1501(18) and 2.1599 (18); Ru-Cp(centroid), 1.775 and 1.773; N-Ru-P, 69.00(5) and 68.92(5), respectively.

Crystals suitable for X-ray diffraction of **3.14** and **3.15** were grown by vapor diffusion of diethyl ether into acetone (Figure 3.14). In the solid state, complexes **3.14** and **3.15**, like **3.10**, feature coplanarity of P(1), N(2), Ru (1) and the Cp centroid. No solvent molecules are coordinated and there are no C-H bonds close enough to the metal center to participate in agostic interactions, with the closest M----H interaction being between one of the methyl groups of an isopropyl with M—H distances 3.0 Å for **3.14** and 3.1 Å for **3.15.**

Crystal structures of both **3.14** and **3.15** show a cationic, formally 16-electron species. A comparison of the structures reveals similarities: the Ru-P bond distance is essentially identical (2.386(2) Å for **3.14**, 2.3905(6) Å for **3.15**), as is the distance from the metal center to the Cp centroid (1.773 Å for **3.14**, 1.775 Å for **3.15**) both well within the margin of error. However, the Ru-N distance in **3.15** (2.1501(18) Å) is almost 0.1 Å shorter than that in **3.14** (2.242(10) Å). This is perhaps a consequence of the nitrogen being directly trans to the carbon containing the –CF$_3$ group, at least in the solid state.

Cp*Ru(P-P)$^+$ and Cp*Ru(N-N)$^{+/0}$ [43-45] 16-electron complexes have been well-studied. In the absence of coordinating solvent molecules, agostic C-H bonds or even trace amounts of dinitrogen are known to lead to 18-electron complexes[46], so to make mono- and bidentate cationic Cp*Ru(PP) complexes, ionizations are performed fluorobenzene under argon[19c, 25] Related 16-electron N-N chelates appear to be more stable due to stronger σ-donation.

Although Cp- and Cp*Ru(P-N) systems have been shown by Stradiotto, Ikariya and our group to be effective catalysts for alkyne hydration, alkene hydrosilylation,[47] alkene isomerization,[9, 11, 36, 40, 48-49] and hydrogenation of ketones, epoxides,[39] imides,[50] esters and carboxamides,[51] well-defined, formally unsaturated Cp*Ru(P-N) complexes are quite rare; several reported in the literature exhibit characteristics of 16-electron species but cannot be

isolated because of chemical instability. Stradiotto observed that upon abstraction of the halide from the Cp*Ru(iPr$_2$P-2-dimethylaminoindenide)Cl complex, either oxidative addition of one of the methyl C-H bonds or arene complexation occurred, although a 16-electron intermediate was suggested.[37, 47, 52] Similarly, Kirchner observed oxidative addition of a methyl C-H bond.[38] These transformations could be facilitated by the removal of the stabilizing π-donation afforded by the chloride ligand. The closest comparison structurally to **3.14** is a pair of complexes from Stradiotto, Cp*Ru(tBu$_2$P-N-amidinate) complexes[53] that contain chelating anionic phosphine-amido ligands. To the best of our knowledge, **3.14** is the first reported example of a fully characterized, cationic Cp*Ru(P-N) 16-electron complex, and **3.15** is the first reported 16-electron Cp‡Ru phosphine complex of any kind.
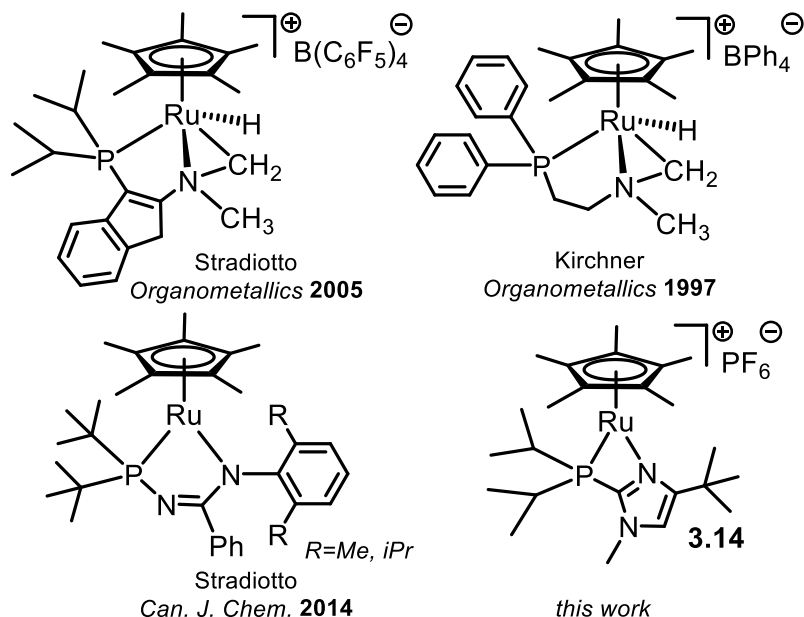
Figure 3.15. Structurally characterized Cp*Ru(PN) complexes lacking an additional X-type ligand

3.3. Bonding and stability in 16e⁻ complexes 3.14 and 3.15

The use of **3.14** is a major upgrade in efficiency over **1.2** and **1.2a**, which will be discussed further in Chapter 4. The major increase in activity of catalyst **3.14** over **1.2** + **1.2a**

clearly results from an open coordination site and the lack of the nitrile ligand that competes with the alkene. An intriguing question arises as to why the catalyst is stable enough to be isolable in the solid state and in weakly binding solvents such as acetone and THF, yet reactive enough to efficiently isomerize terminal alkenes. To probe this question, a computational study was undertaken to analyze the orbitals involved in stabilization of the 16-electron species. The WB97XD functional with an SDD basis set with effective core potential for ruthenium, and the cc-pVDZ basis set for all other atoms after benchmarking with experimental data for Ru-N and Ru-P bond distances, NMR and UV-vis (see Tables 3.9-3.17 in Experimental Section for details).

An analysis of the relevant molecular orbitals with π-symmetry between the ruthenium and chloride in complex **3.10** reveals four MOs with π-bonding character (HOMO-9, HOMO-8, HOMO-7 and HOMO-5) and three MOs that are antibonding (HOMO-2, HOMO-1, and HOMO) with respect to the two atoms, resulting in one 'leftover' π-bond. The LUMO is also antibonding with π-symmetry with respect to ruthenium and chloride. A similar bonding scenario can be seen when we subjected Tilley and Chaudret's Cp*Ru(iPr$_3$P)Cl complex to the same computational analysis (see Table 3.24), and is consistent with other analyses of Cp*Ru(PR$_3$)X systems.
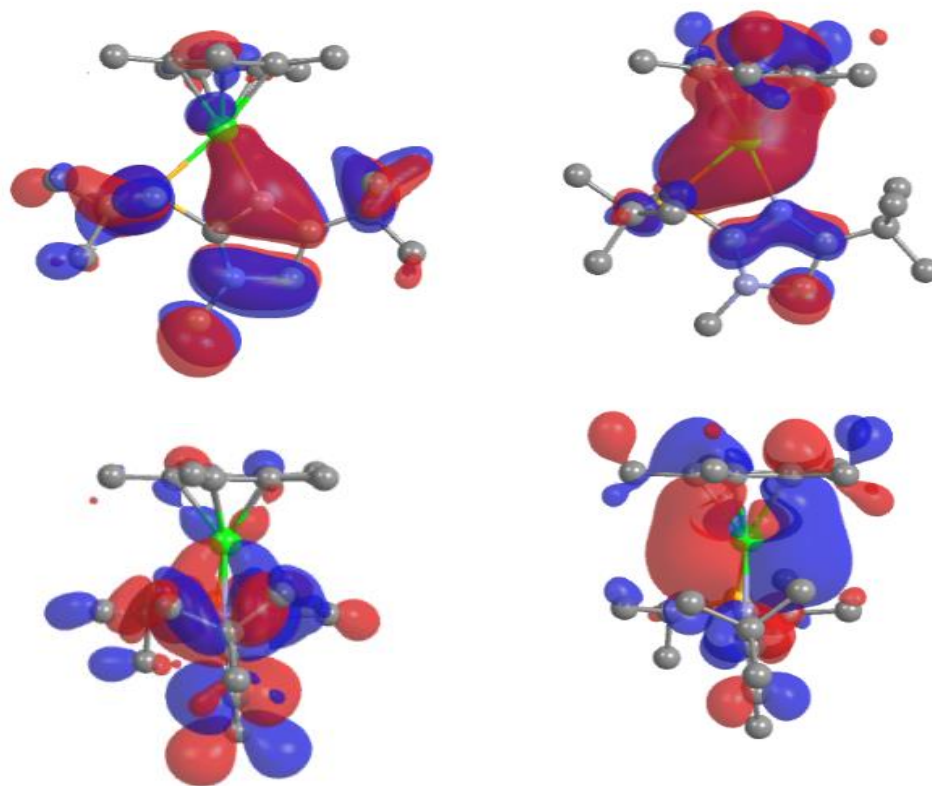
Figure 3.16. Computed molecular orbitals for complex **3.14**. Top Left: HOMO – 8 (face view). Bottom left: HOMO – 8 (edge view). Top right: LUMO (face view). Bottom right: LUMO (edge view).

Upon abstraction of the halide from **3.10** and **3.11** to form complexes **3.14** and **3.15** respectively, crystal structure and NMR data are consistent with a 5-legged piano stool complex with planar symmetry, similar to **3.10** and other formally 16-electron complexes. The computed molecular orbitals for complexes **3.14** and **3.15** indicate a similar π-stabilizing interaction. For complex **3.14**, the HOMO-8 represents a π-bonding interaction between the coordinated basic nitrogen and the two neighboring carbons of the imidazole and the metal center (Figure 3.16). This bonding MO resembles a filled molecular orbital on the free ligand and a large majority of its contribution and can therefore be assigned as a ligand-to-metal π-donation. For complex **3.15**, the HOMO-9 is a similar π-type bonding orbital, albeit with the electron density shifted from the C4 carbon towards the phosphorus. The π-donation shown from the imidazole provides the metal

with the missing two electrons from the formal 16-electron assignment to generate an electronically saturated complex in a similar fashion to the Cp*Ru(PR$_3$)X (where X = Cl, Br, I, OR, NR),[14, 19, 41, 59] but differs in that the donation originates from a π system on the imidazole rather than a lone pair on an anionic X atom. While π-donation is not needed to generate a 16-electron cationic Cp*Ru species, as seen with Cp*Ru(P-P)$^+$ and Cp*Ru(N-N)$^+$ complexes, the competent π-donating ability of imidazole[60-61] likely leads to a higher level of stability for **3.14** and **3.15**. It should be noted that the bulk of the *tert*-butyl group on the *N*-methyl-4-*tert*-butylimidazole moiety also contributes to the persistent 16-electron nature of **3.14** and **3.15** in solution. Complexes **3.16** and **3.17**, formed by ionization of **3.12** and **3.13**, respectively, lack the *tert*-butyl group. Although the ^{1}H NMR spectra at room temperature of **3.16** and **3.17** also are consistent with symmetrical structures, the solutions lack the characteristic blue color that is prevalent in the 16-electron Cp*Ru complexes, hence we conclude that **3.16** and **3.17** undergo rapid reversible binding of solvent. Whether the difference in behavior is due to steric or electronic properties of the *tert*-butyl group is not clear.

The LUMO of complexes **3.14** and **3.15**, on the other hand, is antibonding with respect to the ruthenium and the π-system of the imidazole, much like in complex **3.10**. The LUMO resides mostly on the ruthenium, suggesting that if an incoming ligand binds to the metal and its electrons populate the LUMO, the π-bonding interaction could be severed to establish a coordinatively saturated complex that retains its 18-electron count. The flat and diffuse shape of the LUMO appears to be ideal to accommodate the π-orbital of an alkene, as opposed to a lone pair on a solvent molecule. Evidence of the alkene-metal LUMO interaction for catalyst **3.10** can be seen in the spectrophotometric changes that occur upon addition of terminal alkenes such as 1-hexene to solutions of the catalyst, which will also be discussed in Chapter 4.

3.4. Conclusion
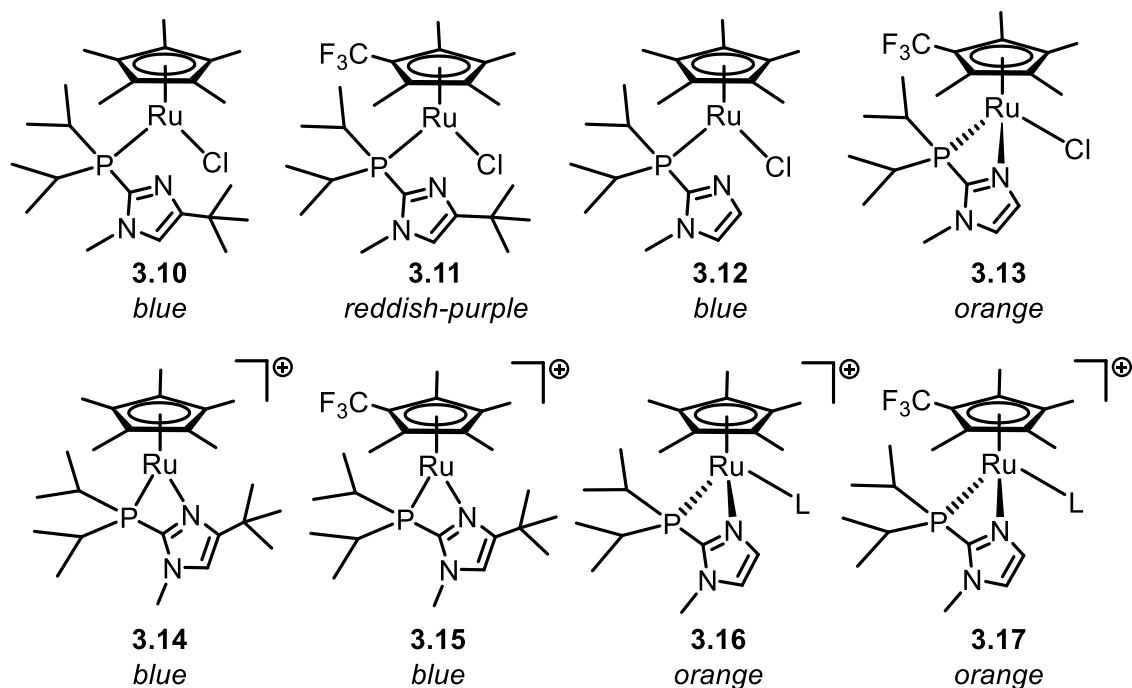
Figure 3.17. Proposed structures and observed colors of complexes **3.10 – 3.17** in solution (acetone-d_6 for complexes **3.10 – 3.12** and **3.14**, or dry THF-d_8 for all complexes). L = solvent (acetone, THF or water)

A series of monomeric complexes **3.10 – 3.17** were generated in an effort to develop a more efficient (*E*)-selective monoisomerization catalyst and to understand the bonding characteristics of the imidazole ligand. While rapid exchange of solvent and/or lability of the chelate introduce fluxionality in the coordination environment for some complexes, Figure 3.17 depicts likely the most relevant structure in solution for complexes **3.10 – 3.17**. A common way to determine the bonding environment around the metal in Cp- or Cp*Ru(P-N) complexes, including **1.2** and **1.2a**, is by the appearance of the NMR signals for the P-N ligand. For example, with any iPr$_2$P(imidazolyl) ligand, if the nitrogen is unchelated, the symmetry of the resulting complex (whether 16e- with one ligand or 18e- with two equivalent ligands) places both isopropyl groups in identical environments. This leads to only two CH(CH_3)$_2$ signals (note: the

methyls are diastereotopic even in the free ligand). If the nitrogen is chelated and another ligand (like chloride or solvent) is present, the isopropyl groups become diastereotopic and four $CH(CH_3)_2$ signals can be seen. This analysis provides for simple distinction of the **1.2** and the **1.2a** complexes. However, turning to the species in Figure 3.17, only with complex **3.13** is there even broadening of signals that would indicate an unsymmetrical complex. While color is often not a reliable indicator of bonding in organometallic complexes, a large number of reported 16-electron Cp*RuL$_1$L$_2$ complexes[14-19, 21, 43-44, 46, 53-58] (L$_1$: P, N; L$_2$: P, N, O, Cl, Br, I), most with solid-state structures confirming their unsaturated nature, have been described as showing a blue or purple color in solution and the solid state. Holding true to this trend, crystals of complexes **3.10**, **3.14** and **3.15** were blue and exhibited coordinative unsaturation in their crystal structures. In solution, **3.10**, **3.14**, and **3.15** are blue, as is **3.12**. In the solid state, however, **3.12** is orange, and its crystal structure shows a chelated nitrogen and a coordinatively saturated complex. Presuming **3.12** is coordinatively unsaturated in solution would imply that perhaps dipole interactions with the basic nitrogen of the imidazole with solvent prevent the nitrogen from chelating in solution, but once those stabilizing interactions are removed, the nitrogen readily chelates in the solid state; crystal packing forces may also be partly responsible.

Although purple was referenced in several of the reports listed above as a characteristic color of unsaturated complexes, the reddish-purple color of **3.11** is somewhat ambiguous. Two other NMR indicators can lend some insight into the bonding process, however: ^{15}N chemical shift, and the $^1J_{P-C}$ coupling constant between the phosphorus and the C-2 carbon of the imidazole. Baseline values for both chelated and non-chelated complexes using both measurements are clear. In the non-chelated case, we can look to complex **3.10**, whose ^{15}N chemical shift is equal to that of free imidazole (~-100.6 ppm – referenced to CH_3NO_2), and

whose $^1J_{\text{P-C}}$ value is 51.7 Hz. For the chelated case, we can look at **3.13** (whose four signals for

CH(CH_3)$_2$ protons in ^{1}H NMR spectra acquired at low temperatures suggest asymmetry and

chelation despite the presence of the chloride ligand), as well as the ionized complexes **3.14** –

3.17. For this group of complexes, ^{15}N values range from -147 to -168 ppm, and $^1J_{\text{P-C}}$ values

range from 19.3 – 25.3 Hz. It should be noted that values for **3.13** are not the highest or lowest

for either of these measurements, suggesting a reasonably strong chelation for **3.13**. In the case

of the more ambiguous **3.11**, its ^{15}N chemical shift value of -136.2 ppm is inbetween the values

for chelates **3.11** and **3.13** - **3.17**. However, its $^1J_{\text{P-C}}$ value of 43.7 Hz is much closer to that of the

unchelated **3.10** than that of the other chelated complexes, which is why its structure is indicated

in Figure **3.17** as having an unchelated ligand. A more accurate description would likely be one

of fast, reversible chelation.

In summary, complexes **3.10** – **3.17** all show some characteristic signs of coordinative

unsaturation. Five complexes show relatively persistent 16-electron character (**3.10**, **3.11**, **3.12**,

3.14, and **3.15**) in solution, with three (**3.10**, **3.14**, and **3.15**) exhibiting coordinative unsaturation

in the solid state as evidenced by crystal structures. The consequences of coordinative

unsaturation, particularly with **3.14** and **3.15**, when applied to alkene substrates, will be

discussed further in Chapter 4.

3.5. Experimental

Reactions were performed under dry nitrogen, using a combination of Schlenk line and glovebox techniques. Tetrahydrofuran and diethyl ether were purchased from Fisher Chemicals and either refluxed over Na/benzophenone or passed through a plug containing basic alumina in the procedure described below to remove peroxides/water. Acetone, methanol, ethyl acetate and absolute ethanol were purchased from Fisher Chemicals, and acetone-d_6, THF-d_8, dmso-d_6, and cyclohexane-d_{12} were received from Cambridge Isotope Labs. All solvents were deoxygenated prior to use by bubbling nitrogen gas through the liquid. NMR tube reactions were performed in resealable J. Young NMR tubes. Syntheses of [Cp‡RuCl$_2$]$_2$[34] and [Cp*RuCl]$_4$[59-60] were carried out as reported in the literature.

Unless otherwise specified, NMR data were measured at 25°C; 'room temperature' typically refers to temperatures between 22-25°C. Characterization of complexes were performed on Varian and Bruker spectrometers: a 600 MHz Bruker Avance III HD Spectrometer with a Bruker Triple-Resonance TXI PFG probe (600 MHz refers to 599.250 MHz for ^{1}H and 150.68 MHz for ^{13}C), a 500-MHz Varian INOVA with either an AutoX ^{1}H/X PFG Broadband probe or an inverse-dectection ^{1}H/^{13}C-^{15}N Penta probe (500 MHz for ^{1}H = 499.940 MHz and ^{13}C = 125.718 MHz), a 400-MHz Varian NMR-S Spectrometer with an AutoX ^{1}H/X PFG Broadband probe (^{1}H =399.763 MHz and ^{13}C = 100.525 MHz). Unless otherwise specified, NMR time points for isomerization reactions were performed on the 500-MHz Varian INOVA, 16 scans, with a 15 degree pulse width and 10 second delay between scans.

^{1}H and ^{13}C NMR chemical shifts are reported in ppm, referenced to solvent resonances for characterization (acetone-d_5 - ^{1}H NMR: δ 2.05 ppm, ^{13}C : δ 29.92 ppm, THF-d_7 – ^{1}H NMR: δ 1.72 ppm, ^{13}C : δ 25.31 ppm, dmso-d_5 – ^{1}H NMR: δ 2.50 ppm, ^{13}C: δ 29.84 ppm, cyclohexane-

d_{11} – ^{1}H NMR: δ 1.38 ppm, ^{13}C: δ 26.43 ppm), and tetrakis(trimethylsilylmethane) as an internal standard for isomerization (^{1}H NMR: δ 0.264 ppm in acetone-d_6). Coupling constants J are given in Hz. Chemical shifts for ^{15}N are reported on a scale with CH_3NO_2 = 0 ppm. In order to maintain a consistent scale, ^{15}N shifts measured on Bruker 600 were adjusted by subtraction of 380.55 ppm from the measured chemical shift, determined by 1D and 2D HMBC as chemical shift of CH_3NO_2 in a 90% CH_3NO_2 / 10% CD_3NO_2 solution.
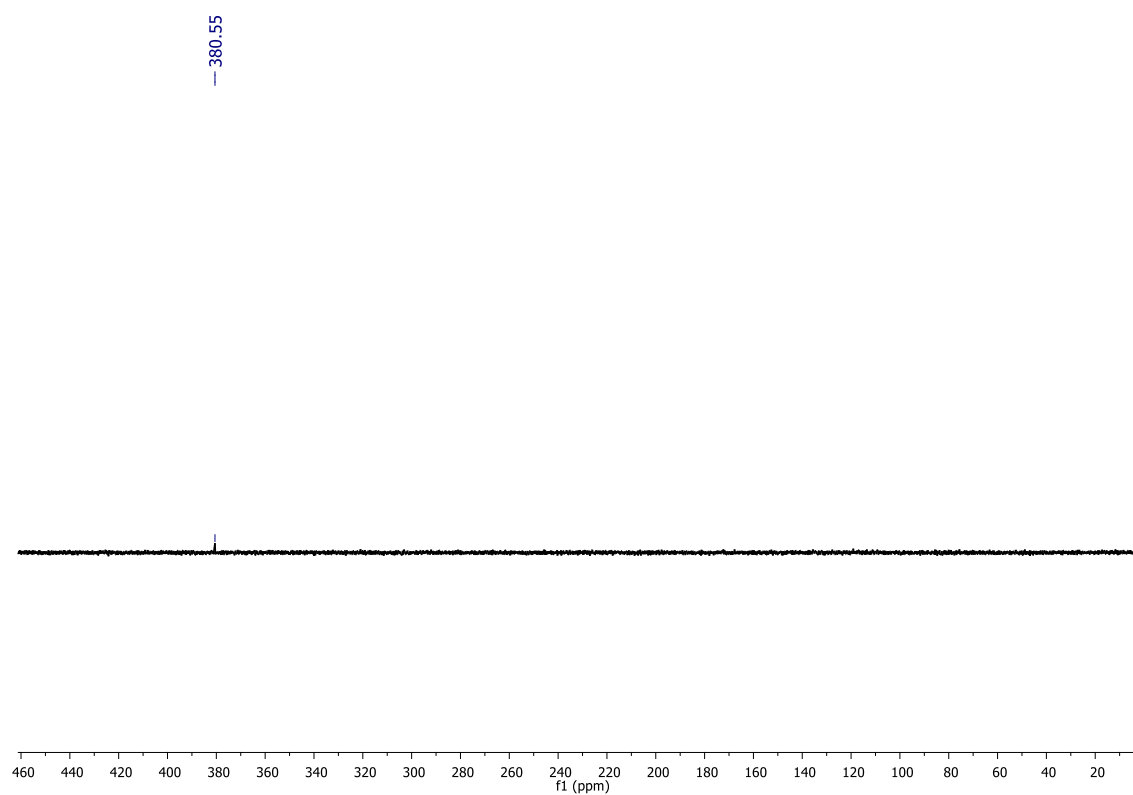
Figure 3.18. ^{15}N 1D NMR spectrum of CH_3NO_2 on Bruker 600 MHz NMR
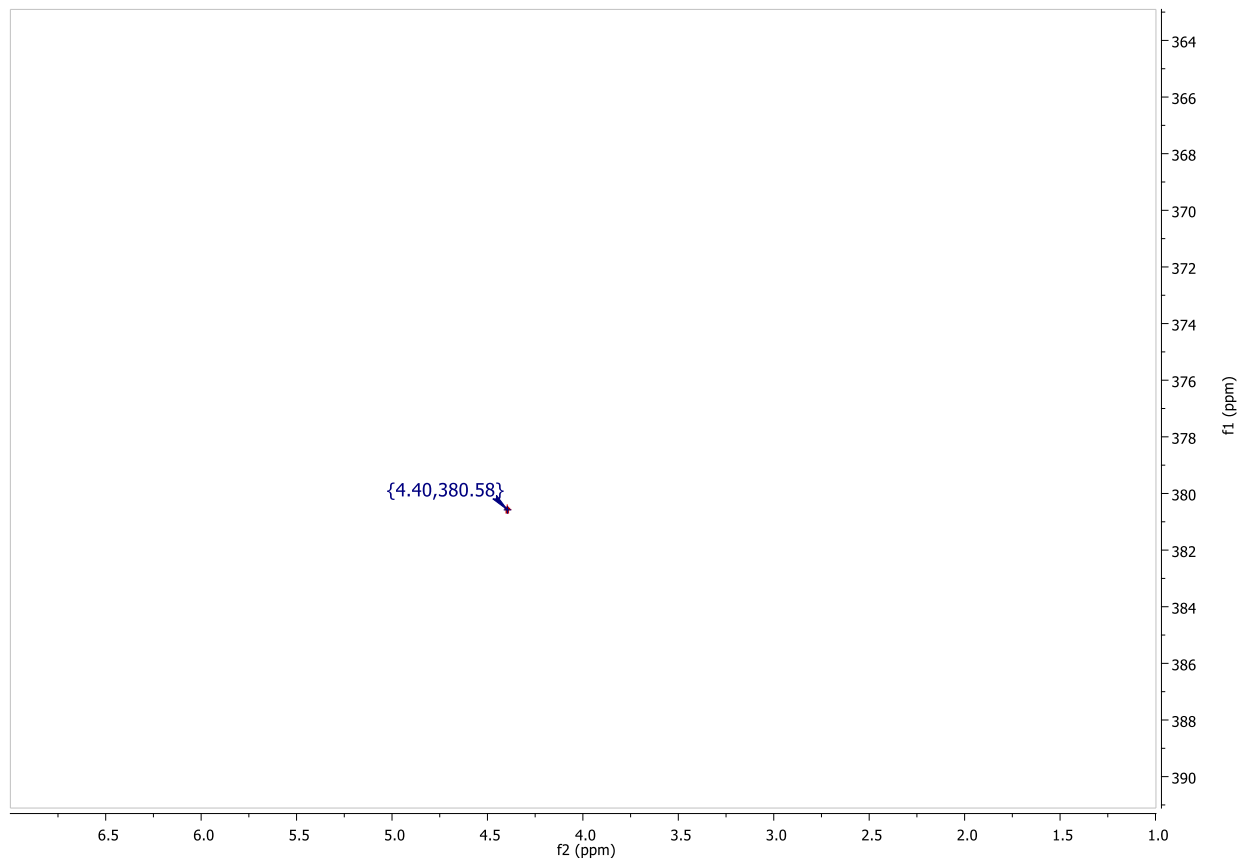
Figure 3.19. ^{1}H - ^{15}N HMBC 2D NMR spectrum of CH_3NO_2 on Bruker 600 NMR

Elemental analyses were performed at NuMega Laboratories (San Diego). X-Ray analysis of single crystals were performed by Arnold Rheingold and Curtis Moore at the University of California, San Diego.

Preparation and characterization of [Cp‡RuCl]₄, 3.10 – 3.17

Synthesis of [Cp‡RuCl]₄ tetramer

In a 100 mL round-bottom flask equipped with stirbar, [Cp‡RuCl₂]₂ (400.8 mg, 0.5548 mmol) and Zn powder (110.8 mg, 1.69 mmol) were weighed out, and deoxygenated methanol (15 mL) was added. The solution turned a deep green. The flask was attached to a reflux

condenser under positive N_2 pressure and was refluxed for 1 hour. During the reflux, the solution changed color from deep green to red, and an orange-red precipitate began forming on the sides of the flask. The flask containing the reaction mixture was transferred to the glovebox, where it was filtered and the precipitate washed with deoxygenated methanol (15 mL). The precipitate on the filter was then extracted through the filter using deoxygenated THF (50 mL). The volatiles were then removed in vacuo, leaving a cakey residue that was broken up, yielding a fine orange-red powder (348.2 mg, 0.2672 mmol, 91.0% yield). ^{1}H NMR (500 MHz, THF-d_8, 25°C): 1.70 ppm (broad s, 24H), 1.65 (broad s, 24 H). ^{13}C {^{1}H} NMR (125 Hz, THF-d_8, 25°C): 131.45 ppm (q, $J = 270.3$), 75.03 (s), 73.30 (s), 56.98 (q, $J = 35.8$), 10.05 (s), 9.58 (s). ^{19}F NMR (470 MHz, THF-d_8, 25°C) -50.53 ppm (s). Elemental Analysis: Calculated for $C_{40}H_{48}Cl_4F_{12}Ru_4$ (1302.86 g/mol): C: 41.79, H: 5.71, N: 4.06. Found: C: 41.30, H: 5.72, N: 3.69. Crystals suitable for X-ray diffraction were grown by dissolving [Cp‡RuCl]$_4$ in methanol and allowing the methanol to evaporate out of the solution into ethyl acetate.
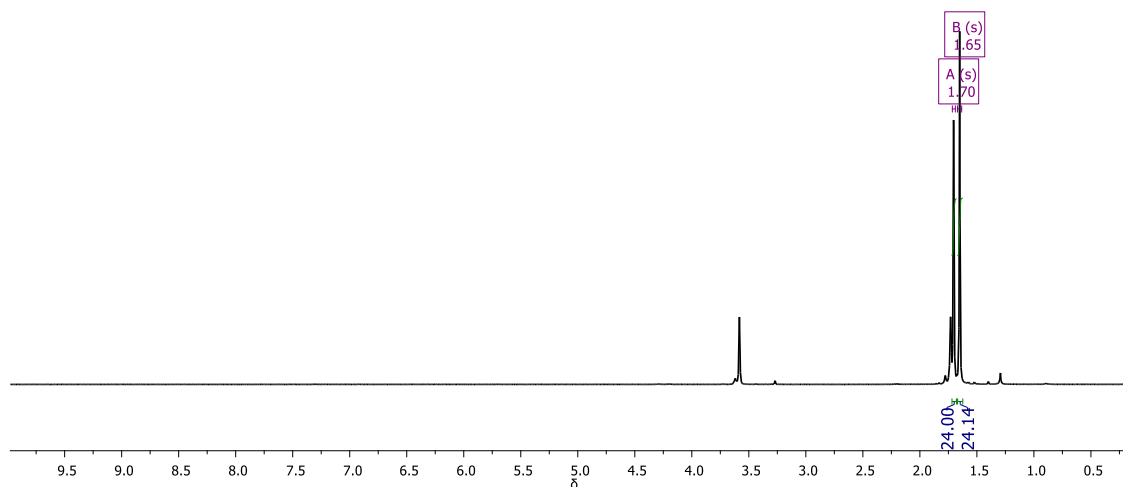
Figure 3.20. ^{1}H NMR spectrum at 500 MHz of [Cp‡RuCl]$_4$ in THF-d_8
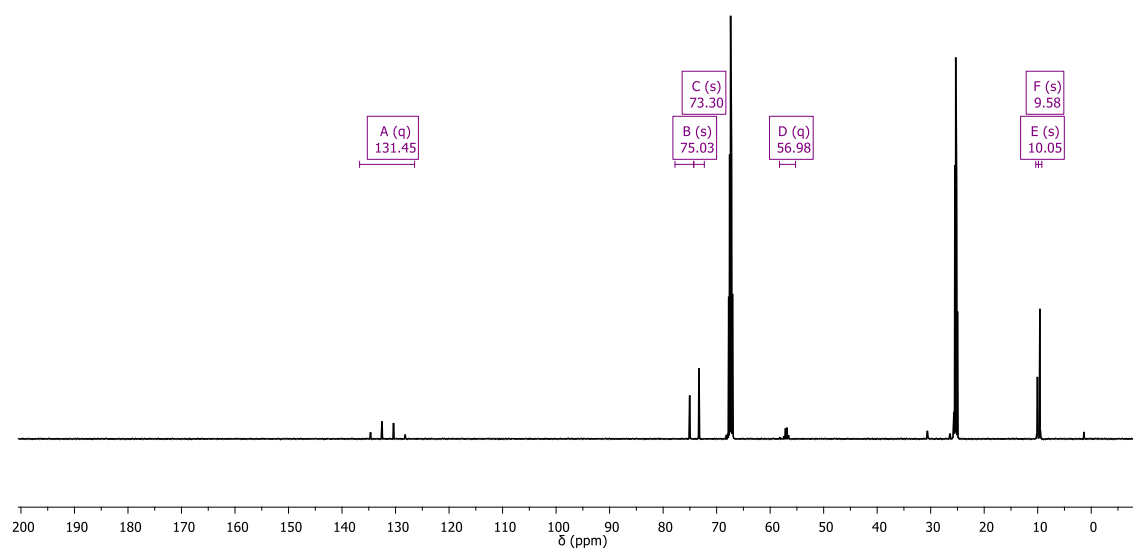
Figure 3.21. $^{13}\text{C}\{^1\text{H}\}$ NMR spectrum at 125.7 MHz of $[\text{Cp}^{\ddagger}\text{RuCl}]_4$ in THF-d_8

Synthesis of complex 3.10: reaction of iPr$_2$PIm' with [Cp*RuCl]$_4$

In a 100 mL round-bottom flask equipped with a stirbar inside the glovebox, [Cp*RuCl]$_4$ (542.1 mg, 0.4983 mmol) was weighed out, and dry deoxygenated THF (7 mL) was added, forming a reddish solution. In a scintillation vial, iPr$_2$PIm' (507.0 mg, 1.993 mmol) was weighed out and dry deoxygenated THF (3 mL) was added. The phosphine solution was then added dropwise to the solution of the tetramer over the course of 5 min. During the addition, the color of the solution changed from red to purple, then to blue. The vial was rinsed with THF (3 x 1 mL), and the rinses were added to the reaction mixture. The solution was left to stir for 16 h. The solvent was then removed in vacuo, forming a blue residue, to which deoxygenated acetone (5 mL) was added. The acetone was removed and the process was repeated (2 x 5 mL acetone), leaving a blue microcrystalline powder (1.046 g, 1.988 mmol, 99.7% yield). During multiple attempts at preparation of a sample for elemental analysis, the blue powder transformed to

90

brown/black, potentially from oxidation. Elemental analysis was performed on the black sample, and results are as follows. Calculated for $C_{24}H_{42}ClN_2PRu$ (526.17 g/mol) (pure): C: 54.78, H: 8.06, N: 5.32. Calculated for one added O (oxide) per Ru-P unit, $C_{24}H_{42}ClN_2PORu$ (542.17 g/mol): C: 53.20, H: 7.82, N: 5.17. Found: C: 53.14, H: 7.31, N: 5.07. Crystals suitable for X-ray diffraction were grown by prolonged storage of a concentrated solution of cyclohexane-d_{12} at -40°C.

NMR data suggest that three species exist in solution: a major complex, a minor complex, and free phosphine, as evidenced by the three imidazole-H signals in ^{1}H NMR in acetone-d_6 (6.95 ppm (d, $J = 1.8$), 6.84 (s) – free phosphine, 6.75 (s) – major signal), and three signals in ^{31}P NMR (32.9 ppm, 30.5 ppm – major signal, and -18.5 ppm – free phosphine signal). Integrations of ^{1}H and ^{31}P signals indicate a ratio of <u>4</u> (likely a phosphine-deficient Ru_4P_2 cluster – **3.18**): <u>6</u> (free phosphine): <u>100</u> (major species - monomer), although the ratio changes depending on solvent polarity and amount of phosphine (see Figures 3.5 – 3.8, and 3.25 – 3.30 below). Variations of in ^{1}H, ^{31}P, and ^{15}N NMR chemical shifts for the major species are small across solvents, and the overall appearance of the spectra are similar; data for both are presented below. Major species: ^{1}H NMR (400 MHz, acetone-d_6): 6.75 ppm (s, 1H), 3.34 (s, 3H), 3.04-3.15 (m, 2H), 1.49 (s, 15H), 1.29 (dd, $J = 14.0, 7.0$), 1.23 (s, 9H), 1.08 (dd, $J = 14.4, 7.1$). ^{1}H NMR (500 MHz, THF-d_8, 30°C): 6.67 (s, 1H), 3.22 (s, 3H), 3.03-3.10 (m, 2H), 1.52 (s, 15H), 1.29 (dd, $J = 15.2, 7.7, 6H$), 1.23 (s, 9H), 1.03 ppm (dd, $J = 13.7, 6.3, 6H$). ^{31}P{^{1}H} NMR (202.38 MHz, acetone-d_6, -20 °C): 30.2 ppm (s). ^{31}P{^{1}H} NMR (202.38 MHz, THF-d_8, 25 °C): 30.5 ppm (s). ^{13}C{^{1}H} (101 Hz, acetone-d_6, 25°C): 151.7, 141.5 (d, $J = 51.9$), 117.4, 76.3, 35.7, 31.4, 29.6 , 25.0 (d, $J = 21.9$), 19.4, 18.6, 10.0 (d, $J = 16.7$. ^{13}C{^{1}H} (125 Hz, THF-d_8, 25°C): 153.1 (d, $J = 6.4$), 141.9 (d, $J = 50.0$), 118.6, 77.1, 37.1, 32.6, 30.8, 26.2 (d, $J = 22.7$), 20.3, 19.7, 11.2. The

^{15}N chemical shifts for the complex were obtained by ^{1}H-^{15}N HMBC on a sample in acetone-d_6 at 25°C and on a sample in THF-d_8 at 30 °C. ^{15}N{^{1}H} (60.7 MHz, acetone-d_6, 25 °C): -102.4 ppm (basic N), -214.1 (non-basic N). ^{15}N{^{1}H} (50.7 MHz, THF-d_8, 30 °C): -100.6 ppm (basic N), -213.1 (non-basic N). On the basis of previously reported data for imidazolyl and pyridylphosphine complexes (e.g., *Dalton Trans.* **2008**, 6497; *J. Am. Chem. Soc.* **2008**, *130*, 20), the chemical shift values of -102.4 ppm and -100.6 ppm for the nonmethylated nitrogen are consistent with **3.10** (Figure 3.24), with neither coordination of N nor significant hydrogen bonding to it.
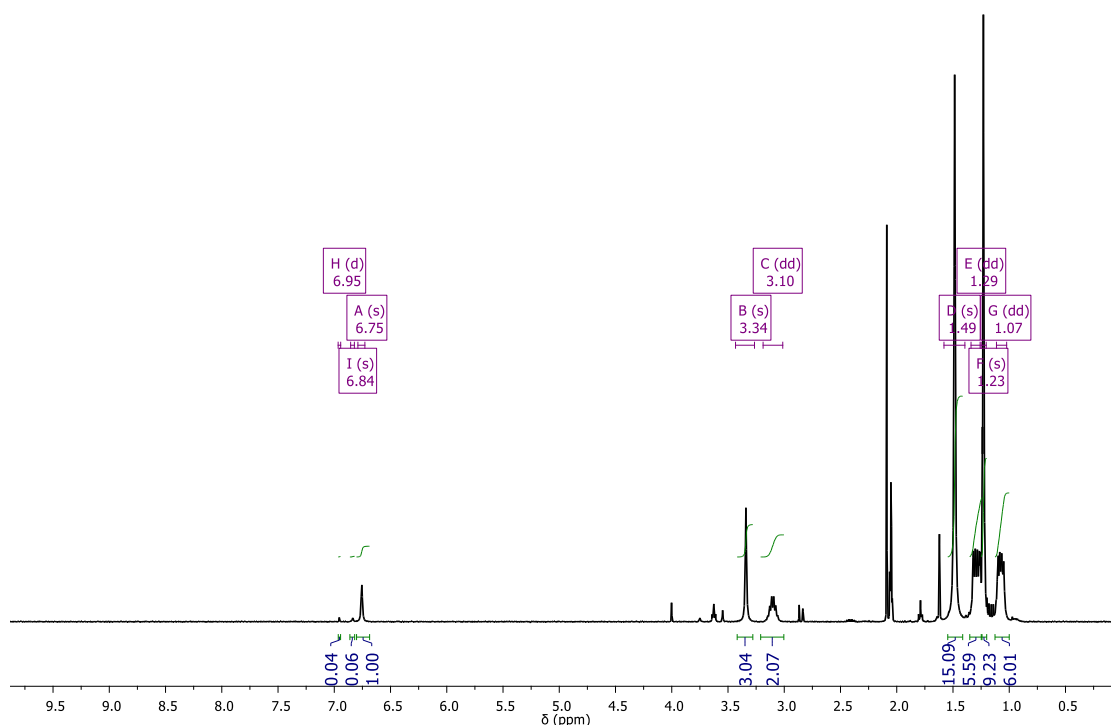
Figure 3.22. ^{1}H NMR spectrum at 500 MHz of complex **3.10** in acetone-d_6
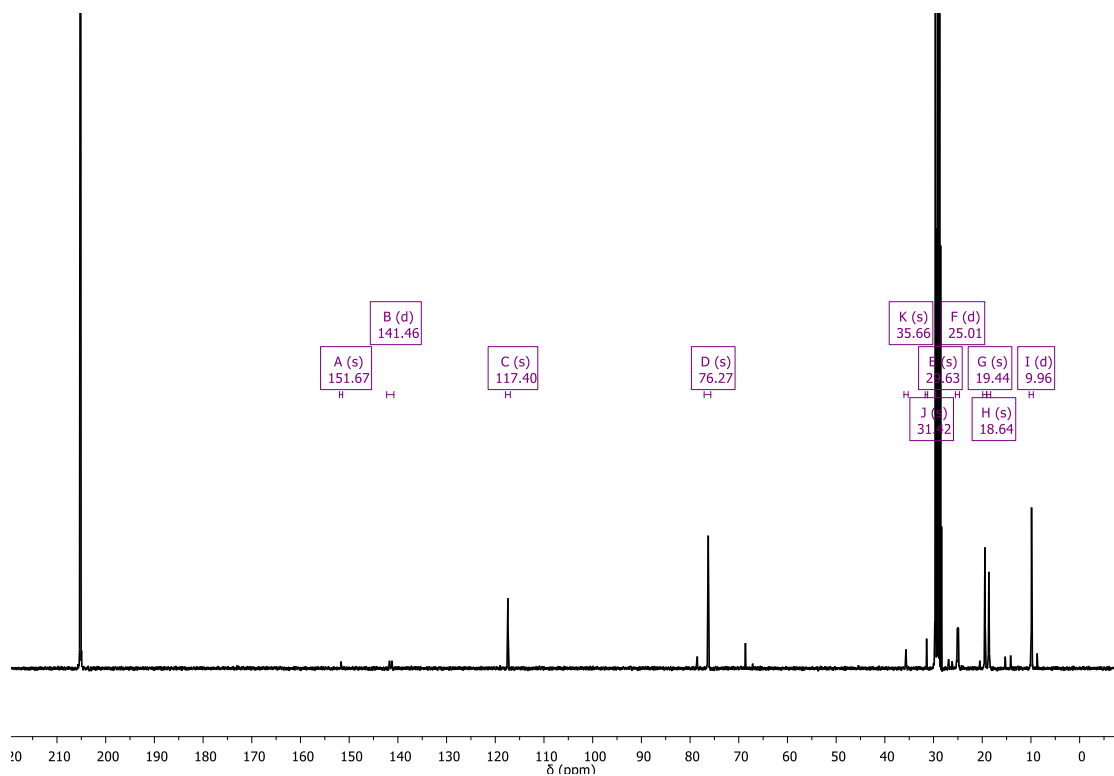
Figure 3.23. $^{13}C\{^1H\}$ NMR spectrum at 101 MHz of complex **3.10** in acetone-d_6
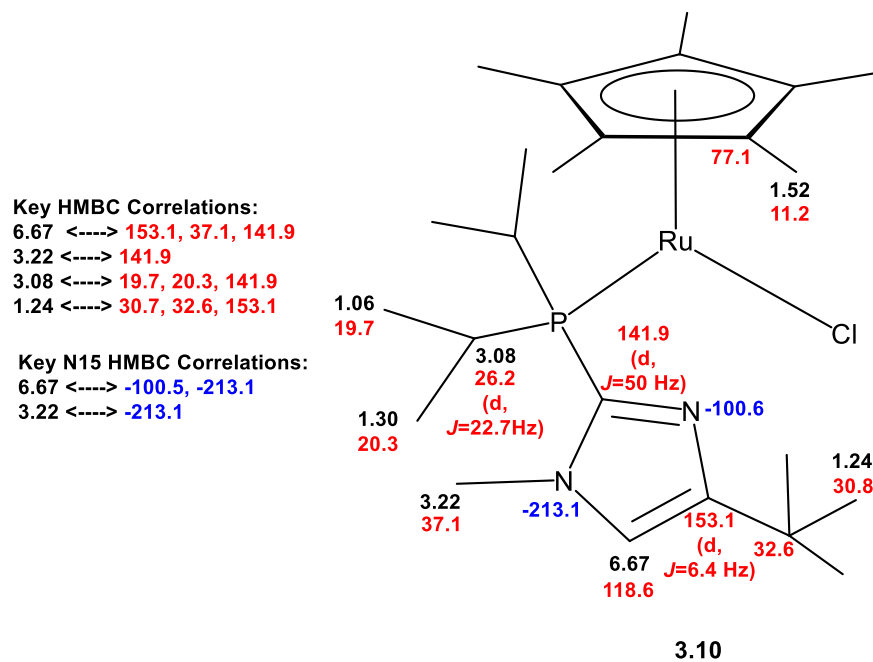
Figure 3.24. Selected NMR data for complex **3.10**
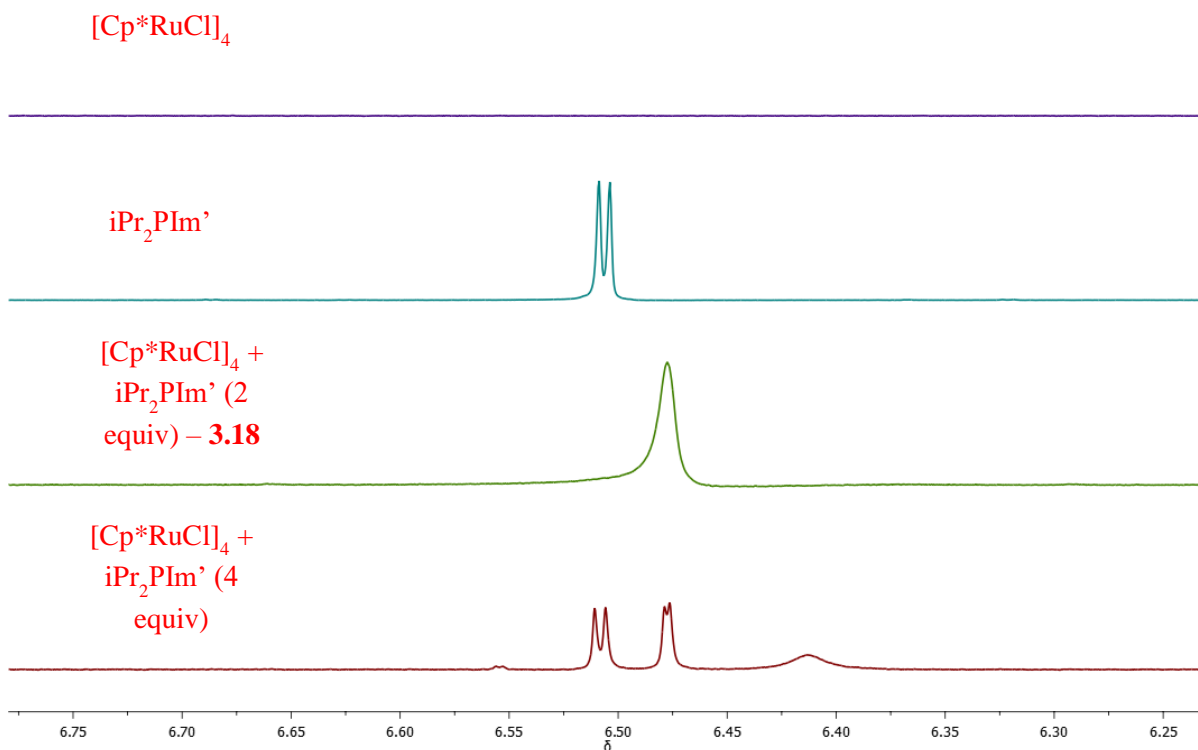
Figure 3.25. 6.8 to 6.2 ppm region of ^{1}H NMR spectra from Figure 3.8
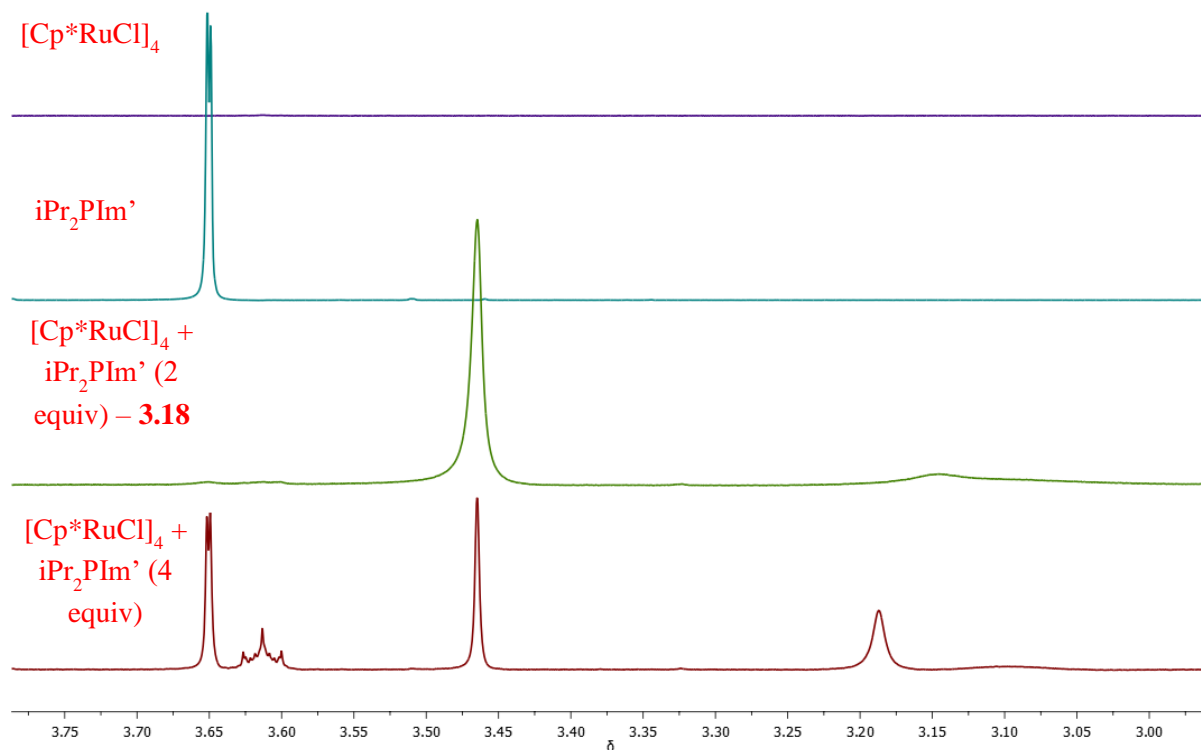
Figure 3.26. 3.8 to 2.9 ppm region of ^{1}H NMR spectra from Figure 3.8
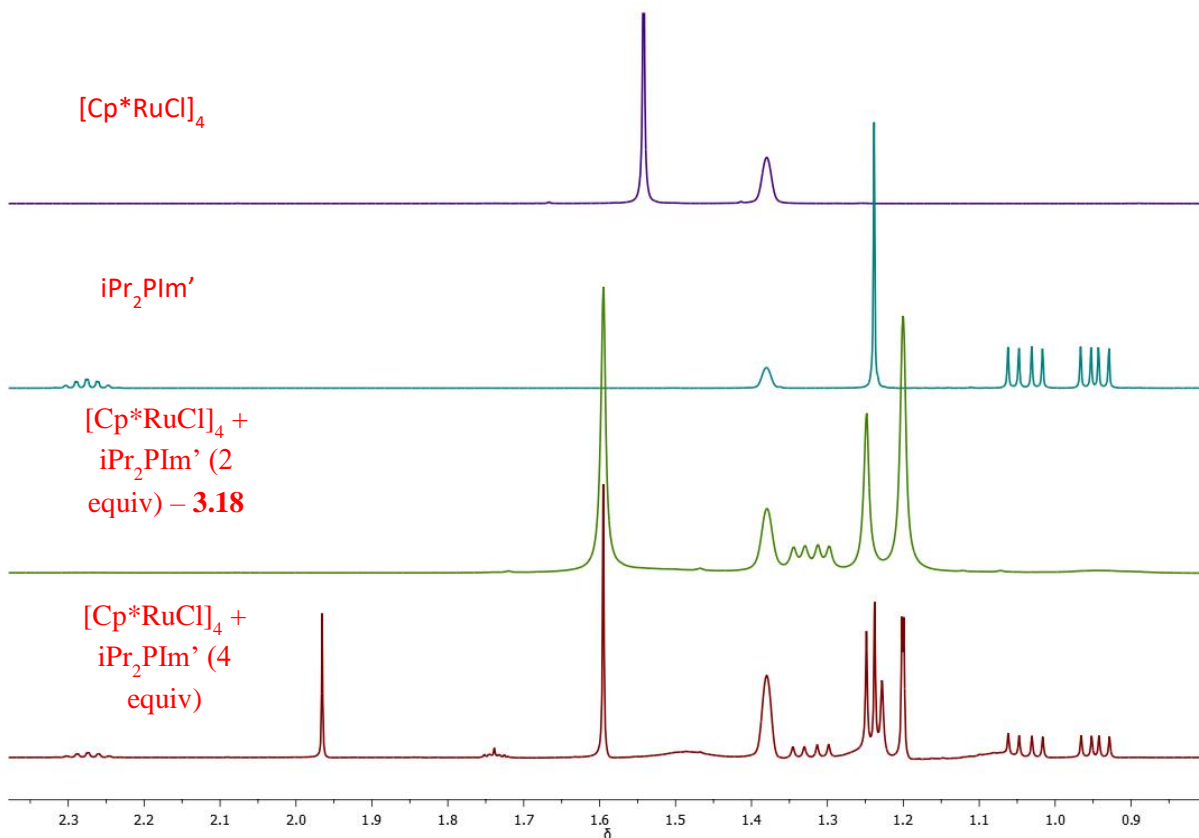
Figure 3.27. 2.4 to 0.8 ppm region of ^{1}H NMR spectra from Figure 3.8
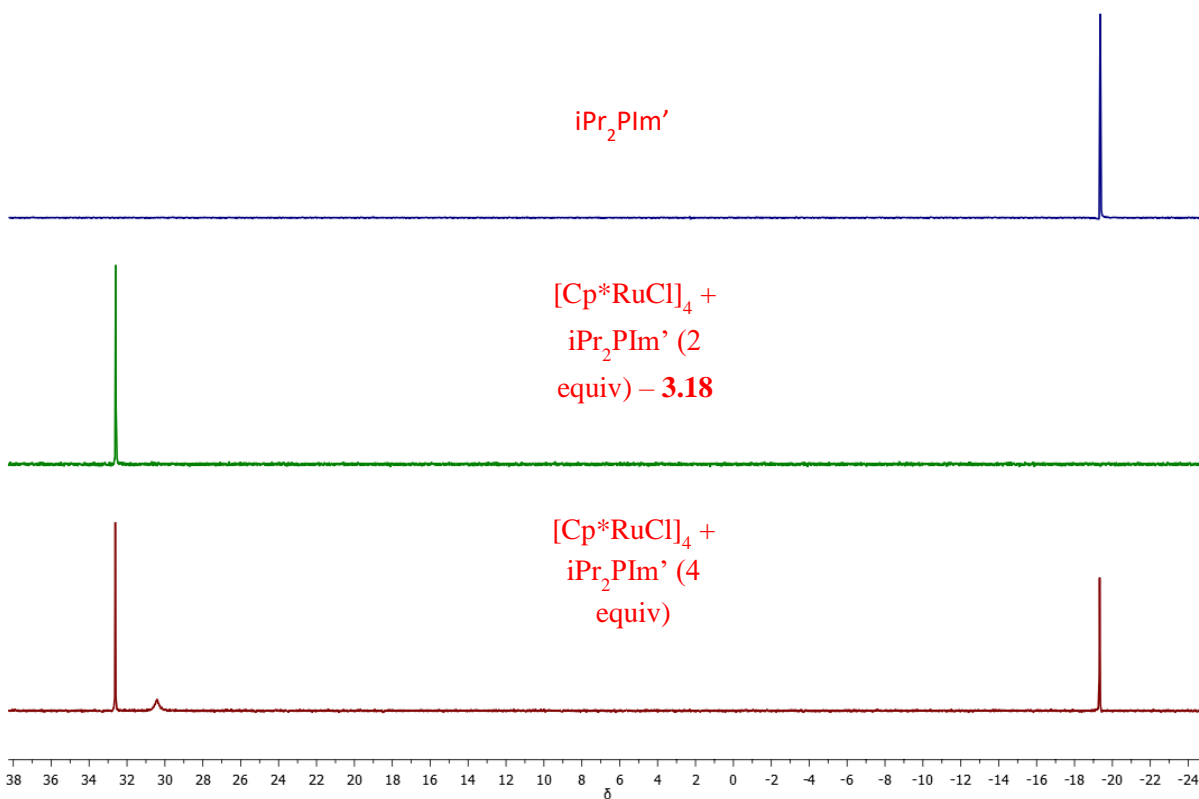
Figure 3.28. 2.4 to 0.8 ppm region of ^{1}H NMR spectra from Figure 3.8
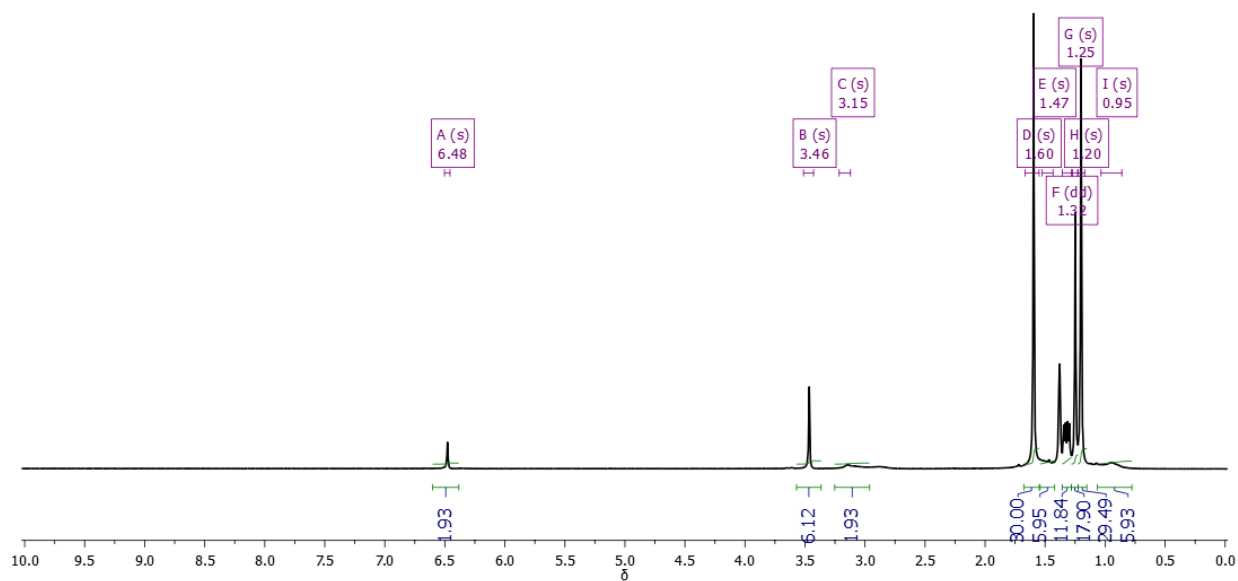
Figure 3.29. ^{1}H NMR at 500 MHz of Ru$_4$P$_2$ cluster (**3.18**) in cyclohexane-d_{12}

\
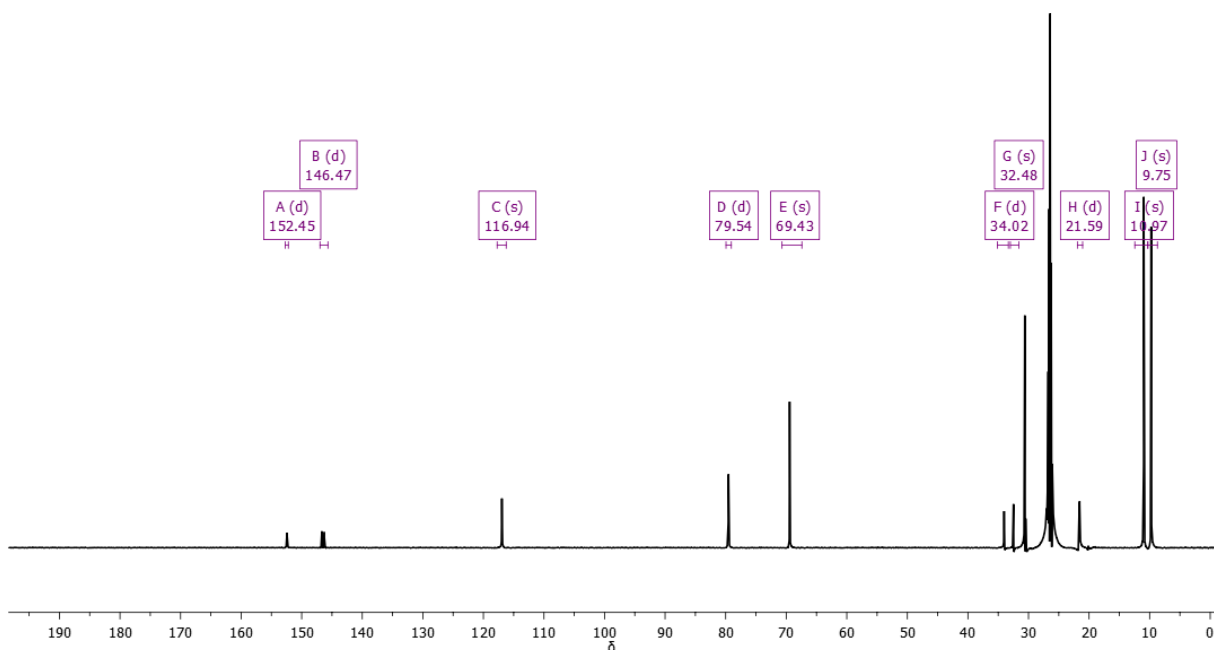
Figure 3.30. ^{13}C {^1H} NMR at 125.7 MHz of Ru$_4$P$_2$ cluster (**3.18**) in cyclohexane-d_{12}

Synthesis of complex 3.11: reaction of iPr$_2$PIm' with [Cp‡RuCl]$_4$

In a scintillation vial containing a stirbar inside the glovebox, [Cp‡RuCl]$_4$ tetramer (51.8 mg, 0.0398 mmol) was weighed out, and dry deoxygenated THF (2 mL) was added, forming a light reddish brown suspension. In a separate scintillation vial, the phosphine (42.5 mg, 0.167 mmol) was weighed out and dissolved in THF (3 mL), forming a colorless solution. The phosphine solution was then pipetted dropwise into the stirred solution of the tetramer. During the addition, the color of the reaction mixture changed to reddish purple. The phosphine solution vial was rinsed with additional THF (3 x 0.5 mL) and transferred to the reaction vial, and the solution was left to stir for 16 h. The solvent was then removed in vacuo, forming a reddish

purple sticky residue, to which deoxygenated acetone (5 mL) was added. The acetone was removed and the process was repeated (2 x 5 mL acetone), leaving a reddish purple residue (229.5 mg, 0.4362 mmol, 94.8% yield). The mixture contains three species, with the major one comprising ~80%, believed to be the monomeric Cp‡Ru(iPr$_2$PIm')Cl (**3.11**). ^{1}H NMR (500 MHz, acetone-d_6): 6.78 (s, 1H), 3.53 (s, 3H), 3.08 (dsept, J = 14.4, 7.1, 2H), 1.79 (s, 6H), 1.70 (s, 6H), 1.35 (dd, J = 15.7, 7.1, 6H), 1.29 (s, 9H), 1.21 (dd, J = 14.8, 7.1, 6H). ^{13}C {^{1}H} NMR (101 MHz, acetone-d_6): 151.2 (d, J = 11.3), 145.1 (d, J = 43.7), 130.2 (q, J = 269.8), 117.9 (s), 80.27 (d, J = 94.8), 61.6 (d, J = 35.2), 34.8 (s), 29.7 (s), 29.5 (s), 24.2 (d, J = 20.0), 19.14 (s), 19.0 (d, J = 4.3), 11.4 (s), 9.4 (s). ^{31}P {^{1}H} NMR (202.4 MHz, acetone-d_6): 28.9 ppm (s). ^{19}F NMR (470.4 MHz, acetone-$\underline{d}_6$): -52.3 ppm (s).
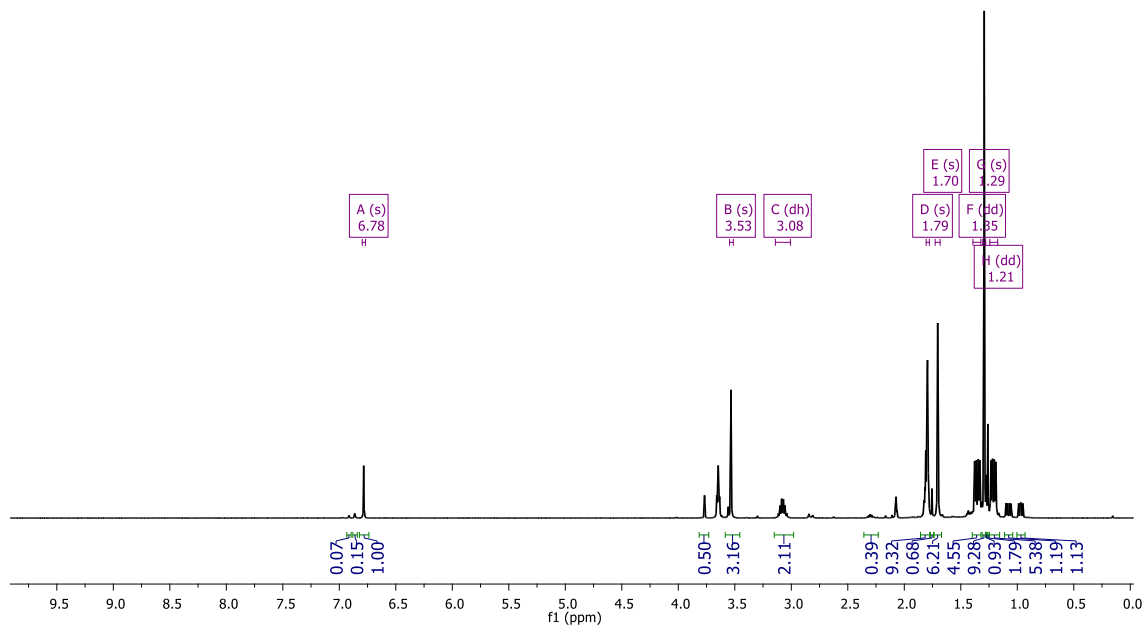
Figure 3.31. ^{1}H NMR spectrum at 500 MHz of complex **3.11** in acetone-d_6
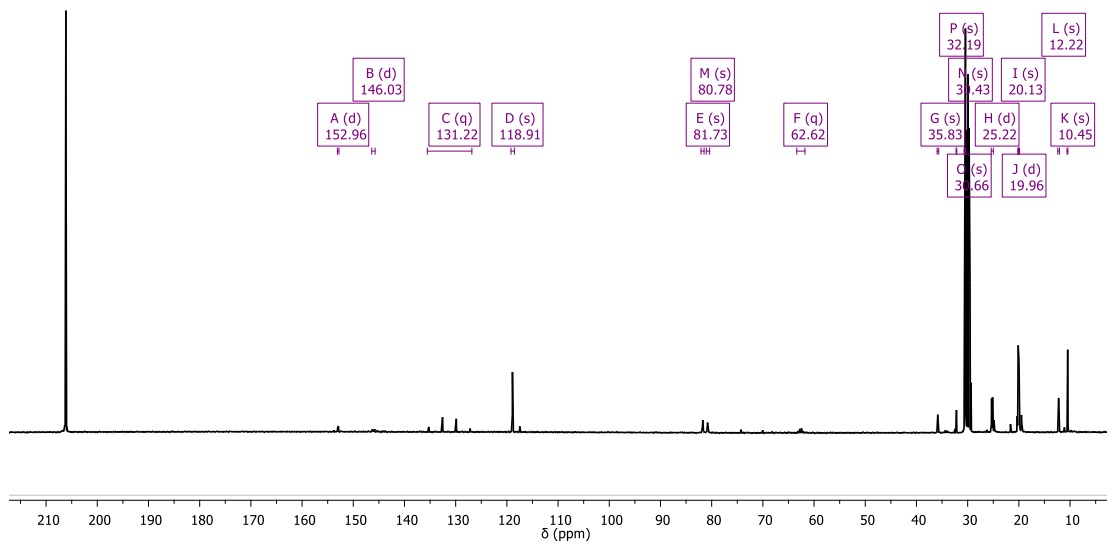
Figure 3.32. $^{13}C\{^1H\}$ NMR spectrum at 101 MHz of complex **3.11** in acetone-d_6
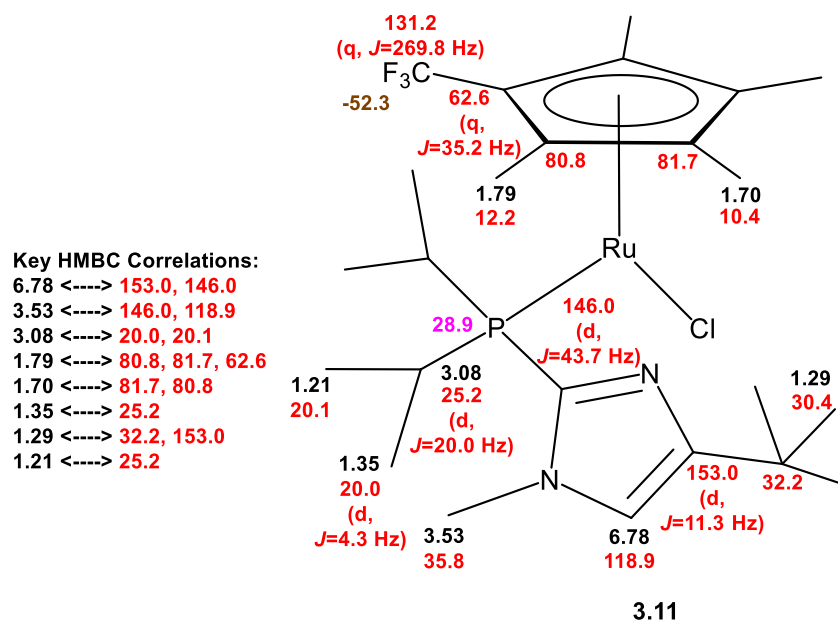
Figure 3.33. Selected NMR data for complex **3.11**

Synthesis of complex 3.14: ionization of Cp*RuCl[iPr₂PIm']

100

In a scintillation vial equipped with stir bar, complex **3.10** (114.0 mg, 0.2167 mmol) was dissolved in acetone (2 mL), forming a dark blue solution. In a separate scintillation vial, TlPF$_6$ (75.8 mg, 0.217 mmol) was weighed out, and acetone (2 mL) was added, forming a clear colorless solution. The TlPF$_6$ solution was then pipetted into the solution containing complex **3.10**. A white precipitate formed immediately, and the solution remained dark blue. The solution was then stirred for 1 h, then filtered through a fine frit into a 100 mL round-bottom flask, and the vial was then rinsed with more acetone (3 x 1 mL), which was also passed through the fritted filter. The solvent from the flask was then removed in vacuo. Upon removal of ~90% solvent, the solution briefly became brown, then became a cakey blue residue upon removal of all of the solvent. The sides of the flask were scraped down, and the flask was put back under vacuum to ensure dryness. Yield: 135.2 mg (98.2%). ^{1}H NMR (500 MHz, acetone-d_6): 7.28 (s, 1H), 3.75 (s, 3H), 3.01 (m, 2H), 1.73 (d, J = 1.6, 15H), 1.60 (s, 9H), 1.37 (dd, J = 18.8, 7.0, 6H), 1.10 ppm (dd, J = 15.9, 7.0, 6H). ^{13}C {^{1}H} NMR (125.7 MHz, acetone-d_6): 154.7 (d, J =12.2, 1H), 152.0 (d, J = 19.3, 1H), 123.0, 78.2 (d, J = 2.5 Hz), 35.2, 32.5, 30.2, 24.0 (d, J, 19.8), 20.1, 19.8 (d, J = 8.1) 12.3 ppm. ^{31}P {^{1}H} NMR (202.4 MHz, acetone-d_6): 24.6 ppm (s), -144.3 ppm (hept, J = 707.4 Hz) (PF$_6$). ^{15}N NMR (determined from ^{1}H-^{15}N HMBC): -151.6 (basic N), -206.4 ppm (non-basic N). Elemental analysis: Calculated for C$_{24}$H$_{42}$PN$_2$F$_6$Ru (mol. wt 635.69 g/mol): C: 45.34, H: 6.67, N: 4.41. Calculated with 0.5 equivalent H$_2$O: C: 44.71, H: 6.74, N: 4.35. Calculated with 1 equivalent H$_2$O: C: 44.09, H: 6.80, N: 4.29. Found: C: 44.77, H: 6.82, N: 3.91. Crystals suitable for X-ray diffraction were grown by vapor diffusion of dry deoxygenated diethyl ether into a concentrated solution of **3.14** in dry deoxygenated acetone.
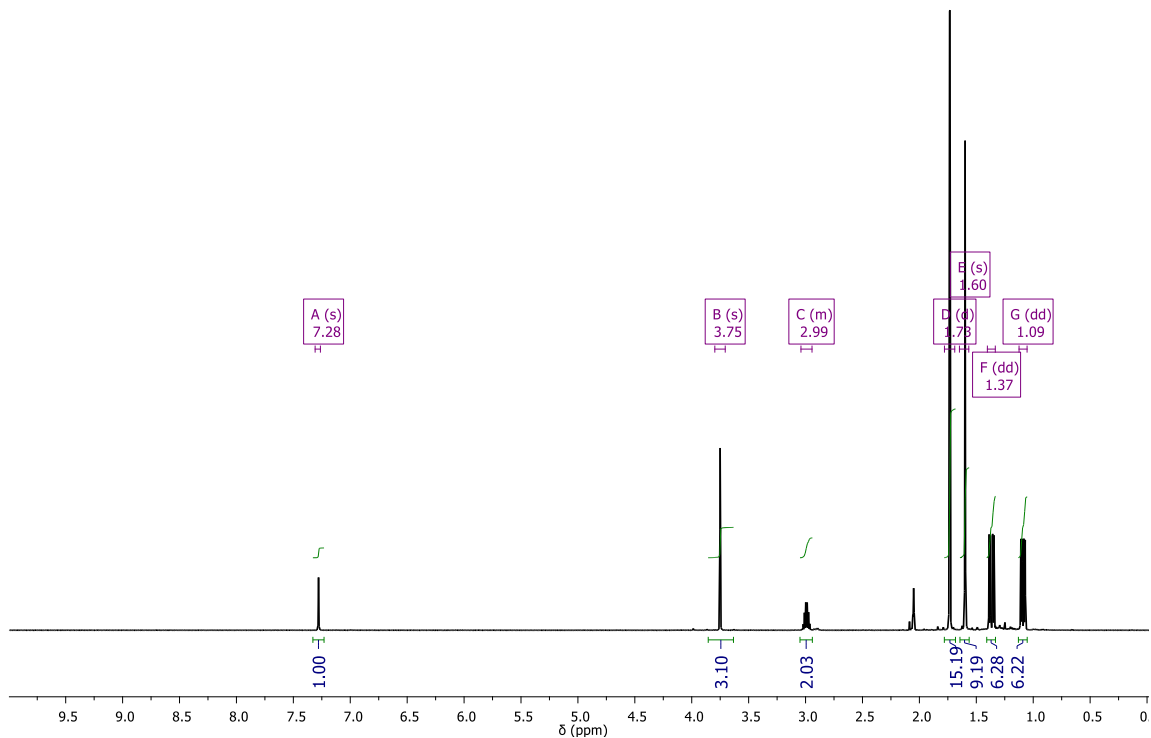
Figure 3.34. ^1H NMR spectrum at 500 MHz of complex **3.14** in acetone-d_6
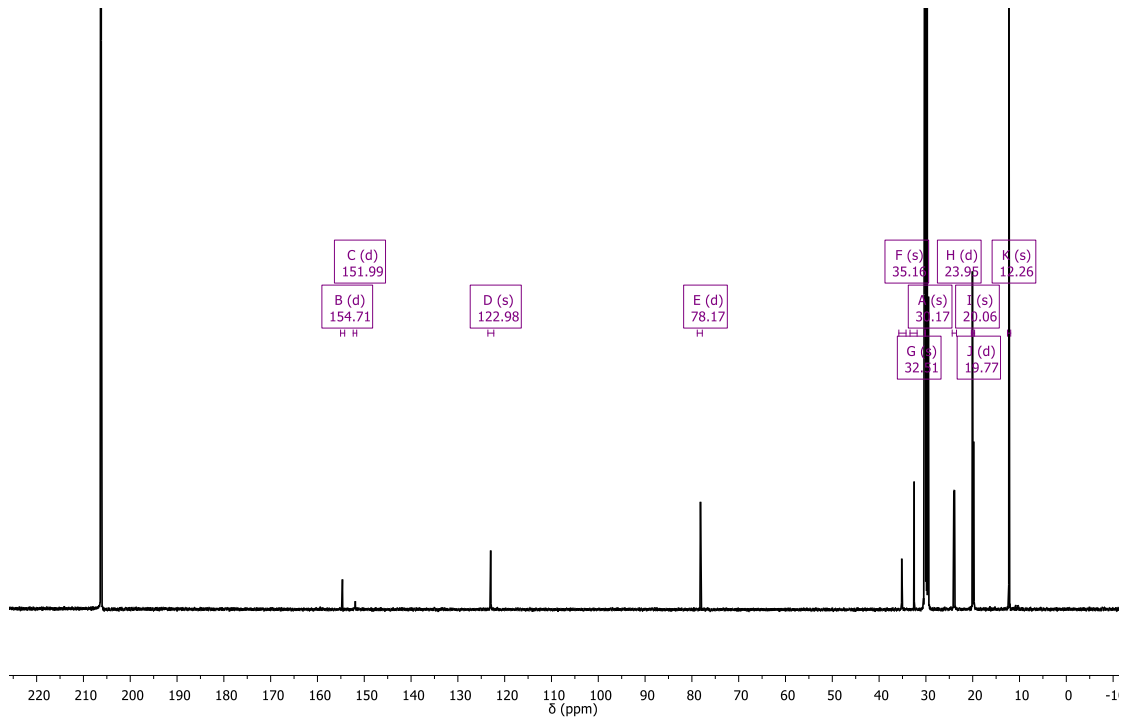
Figure 3.35. $^{13}C\{^1H\}$ NMR spectrum at 125.7 MHz of complex **3.14** in acetone-d_6
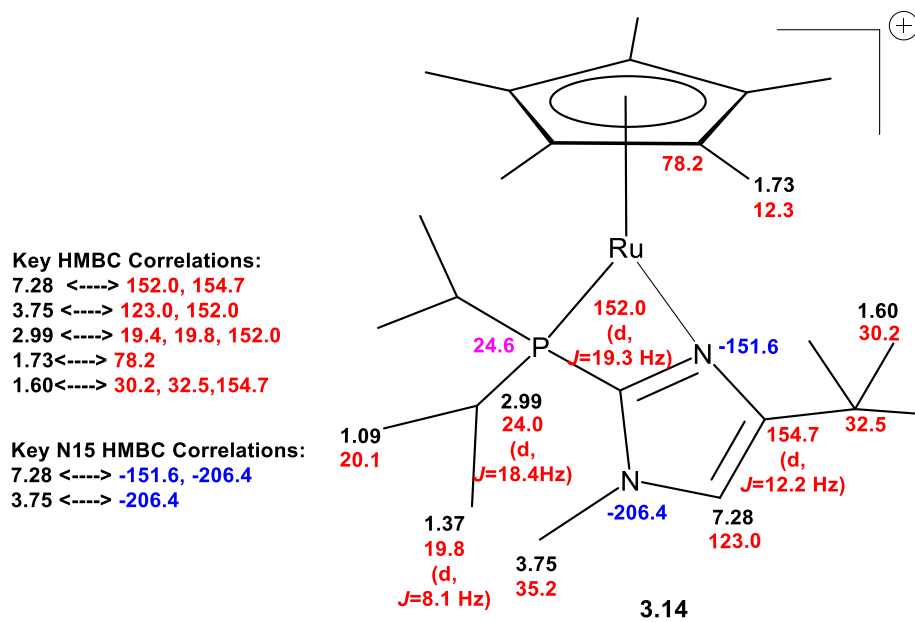
Figure 3.36. Selected NMR data for complex **3.14**

Alternative ionization testing – synthesis of 3.14
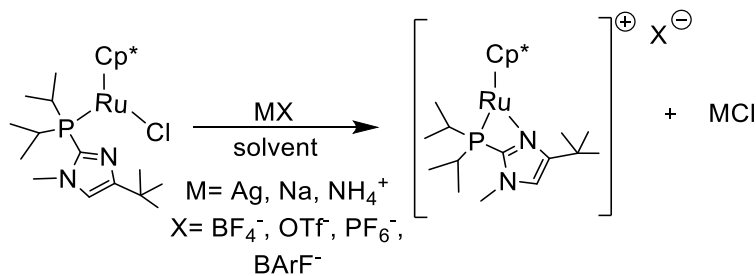
Figure 3.37. Exploring alternative ionization of complex **3.10**

All ionization reactions were performed in resealable J. Young NMR tubes or scintillation vials; separate solutions of complex mixture and ionizing reagent were made and the ionizing reagent solution was added to complex mixture dropwise. ^{1}H and ^{31}P NMR spectra were obtained after 30 min.

Isomerization testing was performed in a resealable J. Young NMR tube. 42.1 mg (0.500 mmol) of 1-hexene (purified prior to reaction by running through alumina plug to remove peroxides) and a few crystals of internal standard were added to the J. Young NMR tube, along with 0.5 mL acetone-d_6. An initial spectrum was obtained. A solution containing the ionized complex mixture (approximately 0.5 mL) was added to the J. Young NMR tube, and spectra were obtained at various times to monitor formation of internal isomers. Hexene peaks were referenced against the internal standard (10.0 arbitrary units).

Table 3.3. Ionizing reagent screening - NMR results (underlined shifts are for unionized complex **3.10**)

Entry	Ionizing Reagent	Solvent	Distinguishing Peaks		Comments/Isomerization Results
			^{1}H (ppm)	^{31}P (ppm)	
1	B(C$_6$F$_5$)$_3$	THF-d_8	6.73 (s, 0.3H), <u>6.67 (bs, 1H)</u>, 4.00 (s, 0.3H), 3.96 (s, 0.3H), 3.72 (s, 0.8H), 3.52 (s, 0.8H), <u>3.22 (bs, 3H)</u>, <u>3.08 (bm, 2H)</u>, 1.61 (s, 5H), <u>1.52 (s, 18H)</u>, <u>1.30 (dd, 6H)</u>, 1.25-1.23-1.21 (3 separate singlets, total of 20H), <u>1.04 (dd, 6H)</u>, 0.96 (dd, 2H)	<u>30.3</u> (major) 32.9	Seems like 2 species; major one (75%/25%) matches unionized complex
2	AgBF$_4$	Acetone-d_6	12.7 (vbs), 11.5 (vbs), 7.77 (s), 4.33 (s), 4.20 (bm), 3.00 (bs), 2.75 (sextet), 1.56 (s), 1.42 (s), 1.31 (dd),1.13 (dd), -0.8 (vbs)	53.3	Reasonably clean spectrum; other than small very broad peaks at 11.5, 12.7 and -0.8 ppm, major species was one clean set of peaks **5% isomerization of 1-hexene with 2 mol% mixture after 48 h at 40°C**
3	AgBF$_4$	THF-d_8	10.9 (bs, 0.15H), 9.30 (s, 0.5H), 8.38 (bs, 0.4H), 7.58 (s, 1H), 4.22 (s, 3H), 4.18 (s, 0.3H), 2.80 (sep, 2H), (Cp-CH$_3$ obscured by 1.73 solvent peak), 1.41 (s, 9H), 1.28 (dd, 6H), 1.06 (dd, 6H), -1.83 (bs, 5H)	52.3	Other than few small peaks, major species also one clean set of peaks **No isomerization of 1-hexene with 2 mol% mixture after 48 h at 40°C**
4	NaBF$_4$	Acetone-d_6	<u>6.74 (s, 1H), 3.26 (s, 3H), 3.07 (m, 2H), 1.51 (s, 15H), 1.30 (dd, 6H), 1.16 (s, 9H), 1.01 (dd, 6H)</u>	<u>30.1</u>	No major changes

*Underlined indicates chemical shifts similar to shifts of the starting complex

Table 3.3 cont.

5	NaOTf	Acetone-d_6	<u>6.74 (s, 1H), 3.26 (s, 3H), 3.08 (m, 2H), 1.54 (s, 15H), 1.30 (dd, 6H), 1.23 (s, 9H) 1.04 (dd, 6H)</u>	<u>30.1</u>	No major changes
6	AgOTf	Acetone-d_6	7.73 (s, 1H – integration reference), 7.64 (s, 0.7H), 7.49 (s, 0.8H), 7.28 (bs, 0.6H), 4.33 (bs, 3H), 4.15 (s, 2H), 4.02 (bs, 0.9H), 3.79 (m, 2H), 3.59 (s, 3H), 3.34 (m, 1.6H), 3.18 (m, 1H), 3.00 (m, 1.4H), (several peaks from 1.1 to 1.8)	24.6 50.7 53.3	3 major species **No isomerization of 1-hexene after 3 h with 2 mol% mixture at rt**
7	AgPF$_6$	Acetone-d_6	13.4 (vbs), 8.98 (s), 7.49 (s), 4.04 (s), -5.92 (bs)	24.7	Initially, very broad peaks throughout entire spectrum; after 2 days, peaks sharpened except for peaks at 13.4 ppm and -5.92 ppm (integrations minor compared to others); **no isomerization of 1-hexene after 3 hours rt with 2 mol% complex**
8	AgPF$_6$	THF-d_8	10.6-11.4 (bs), 8.4-9.4 (bs), 7.54 (s), 7.35 (bs), 4.02 (s), 3.13 (bs), -2.8 ppm (bs)	25.0, 50.0	Very broad peaks, persisted after 2 days; **isomerization of 1-hexene slow (50% E-2 hexene after 3 hours rt with 2 mol% complex)**
9	NaBAr'$_4$	Acetone-d_6	<u>6.75 (s), 3.27 (s), 3.07 (m)</u>	<u>30.1</u>	No significant changes in NMR in major species, increases in integration of minor species relative to major species; solution turned purple. **Little isomerization of 1-hexene (16%) after 6 days rt with 2 mol % complex) – essentially same rate as unionized chloro complex**
10	NaBAr'$_4$	THF-d_8	<u>6.67 (s), 3.23 (s), 3.07 (m)</u>	32.1, 34.7	Very little changes in ^{1}H NMR spectrum, but slight downfield shift in ^{31}P NMR spectrum

*Underlined indicates chemical shifts similar to shifts of the starting complex

Table 3.3 cont.

11	NH$_4$PF$_6$	Acetone-d_6	*30 min after addition*: 7.6-8.0 (vbm), 4.25 (bs), 3.2-3.4 (bs), 3.0-3.2 (bs) *2 days 40°C*: 8.96 (s), 7.48 (s), 4.04 (s), 3.76 (bs), 3.21 (bs)	*30 min:* Possible broadness @ ~30 and 70 *2 days:* No distinguishable peaks	Solution turned dark brown, broad peaks, **no isomerization of 1-hexene after 6 days rt with 2 mol% complex**
12	NH$_4$PF$_6$	THF-d_8	6.68 (bs), 3.27 (s), 3.08 (m)	32.4, 34.7	No major changes in ^{1}H NMR except slight broadening of peaks; slight downfield shift in ^{31}P NMR. No color change
13	NH$_4$PF$_6$	1,4-dioxane	6.65 (s) (other peaks obscured by solvent)	30.5 (s) (major), 32.9 (s), 48.0 (s)	Major species unchanged; no color change
14	NH$_4$PF$_6$	Et$_2$O/H$_2$O	(NMR taken in acetone-d_6): 6.76 (bs), 3.2-3.4 (bs), 3.07 (m)	30.1 (s) (major), 32.9 (s), 48.1 (s)	2-phase reaction: NH$_4$PF$_6$ (aq) was added to Et$_2$O solution of unionized complex mixture. Ether layer remained blue, aqueous clear. Layers were separated and ether removed in vacuo, and all residue was dissolved in acetone-d_6 for NMR

*Underlined indicates chemical shifts similar to shifts of the starting complex

Studies of the reactivity of 3.14 with other phosphines

Remarkably, a second mole of phosphine does not bind to **3.14**:
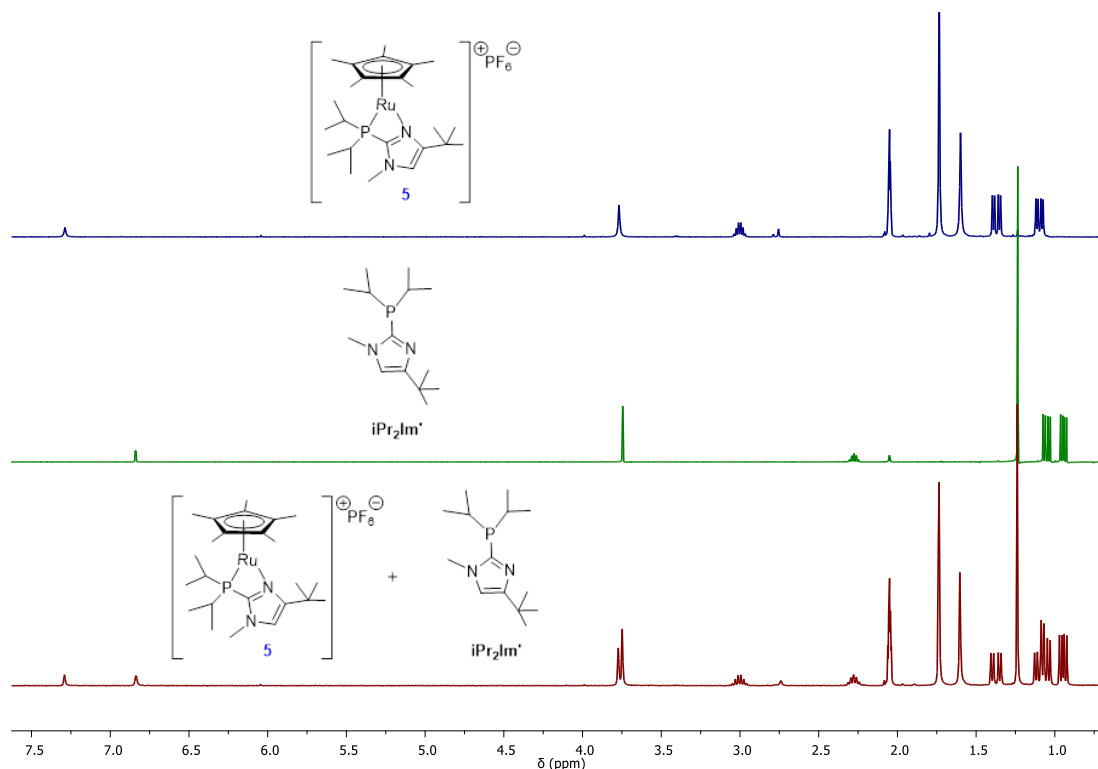
Figure 3.38. ^{1}H NMR spectra (acetone-d_6, 500 MHz) showing lack of reaction after addition of one equivalent iPr$_2$PIm' to complex 5

Synthesis of complex 3.15: ionization of Cp‡RuCl[iPr$_2$PIm']

In a resealable J. Young tube, complex **3.11** (94.0 mg, 0.162 mmol) was dissolved in acetone-d_6 (0.7 mL), and TlPF$_6$ (56.5 mg, 0.162 mmol) was added to the J. Young NMR tube and rinsed down with additional acetone-d_6 (0.1 mL). An white precipitate formed immediately, and the solution went from blue to dark brown. An NMR spectrum was acquired, and the solution was filtered through a fine frit into a 100 mL round-bottom flask, and the J. Young NMR tube was washed with 3 x 0.3 mL acetone. The solvent was then removed in vacuo. Upon removal of solvent, the cakey residue became blue. The sides of the flask were scraped down, and the flask was put back under vacuum to remove all solvent. Yield: 105.3 mg (94.3%). ^{1}H NMR (500 MHz, dry THF-d_8): 7.40 (s, 1H), 3.71 (s, 3H), 2.97-3.00 (overlapping d of septet, J = 7.4, 7.1, 2H), 1.79 (d, J = 1.5, 6H), 1.77 (bs, 6H), 1.62 (s, 9H), 1.31 (dd, J = 19.4, 7.1, 6H), 1.09

ppm (dd, J = 16.9, 7.1, 6H). ^{13}C NMR (125.7 MHz, THF-d_8): 154.8 (d, J = 10.9, 1H), 151.9 (d, J = 21.7), 130.0 (q, J = 269.8), 124.7 (s), 85.1 (d, J = 4.7), 75.7 (s), 65.4 (q, J = 35.9), 35.4 (s), 32.6 (s), 30.2 (s), 24.3 (s), 19.8 (s), 19.4 (d, J = 7.2). ^{31}P {^{1}H} NMR (202.7 MHz, dry THF-d_8): 23.2 ppm (s), -144.3 ppm (hept, J = 707.9 Hz) (PF$_6$). ^{19}F (470 MHz, dry THF-d_8): -52.7 ppm (s), -73.5 ppm (d, J = 710.1 Hz) (PF$_6$) Elemental analysis: Calculated for $C_{24}H_{39}P_2N_2F_9$ (mol. wt: 689.66 g/mol): C: 41.79%, H: 5.71%, N: 4.06%. Found: C: 41.30%, H: 5.72%, N: 3.69%. Crystals suitable for X-ray diffraction were grown by vapor diffusion of dry deoxygenated diethyl ether into a concentrated solution of **3.15** in dry deoxygenated THF-d_8.
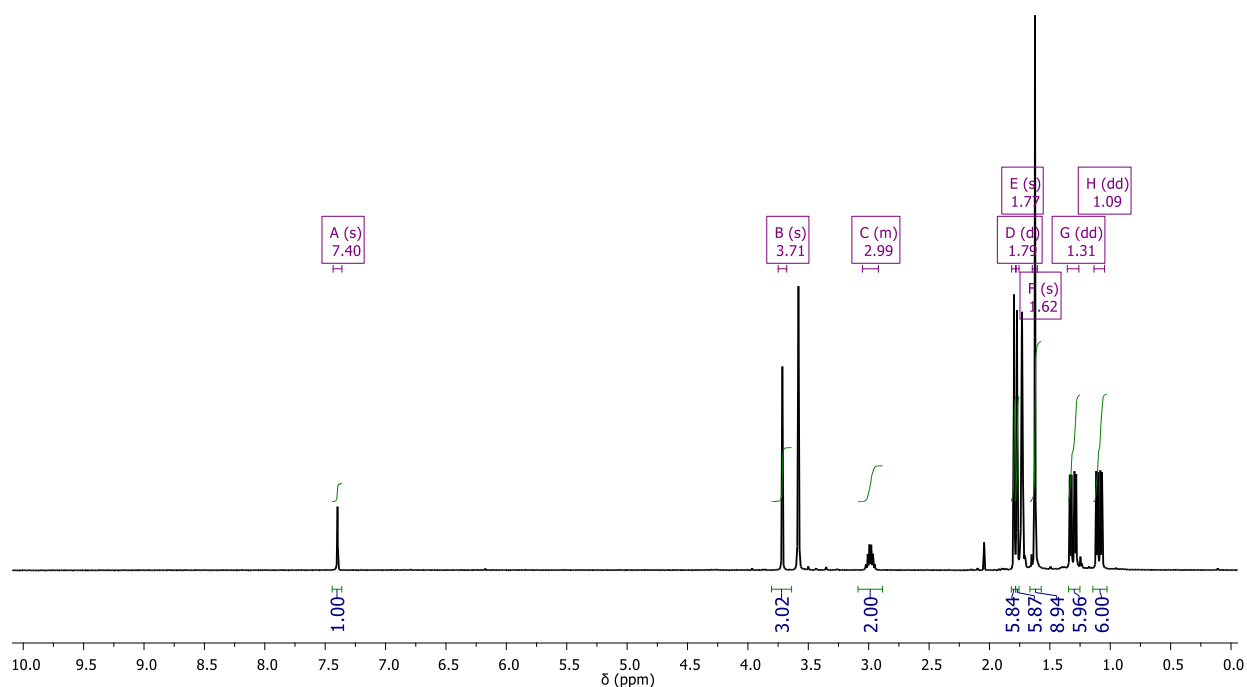
Figure 3.39. ^{1}H NMR spectrum at 500 MHz of complex **3.15** in dry THF-d_8
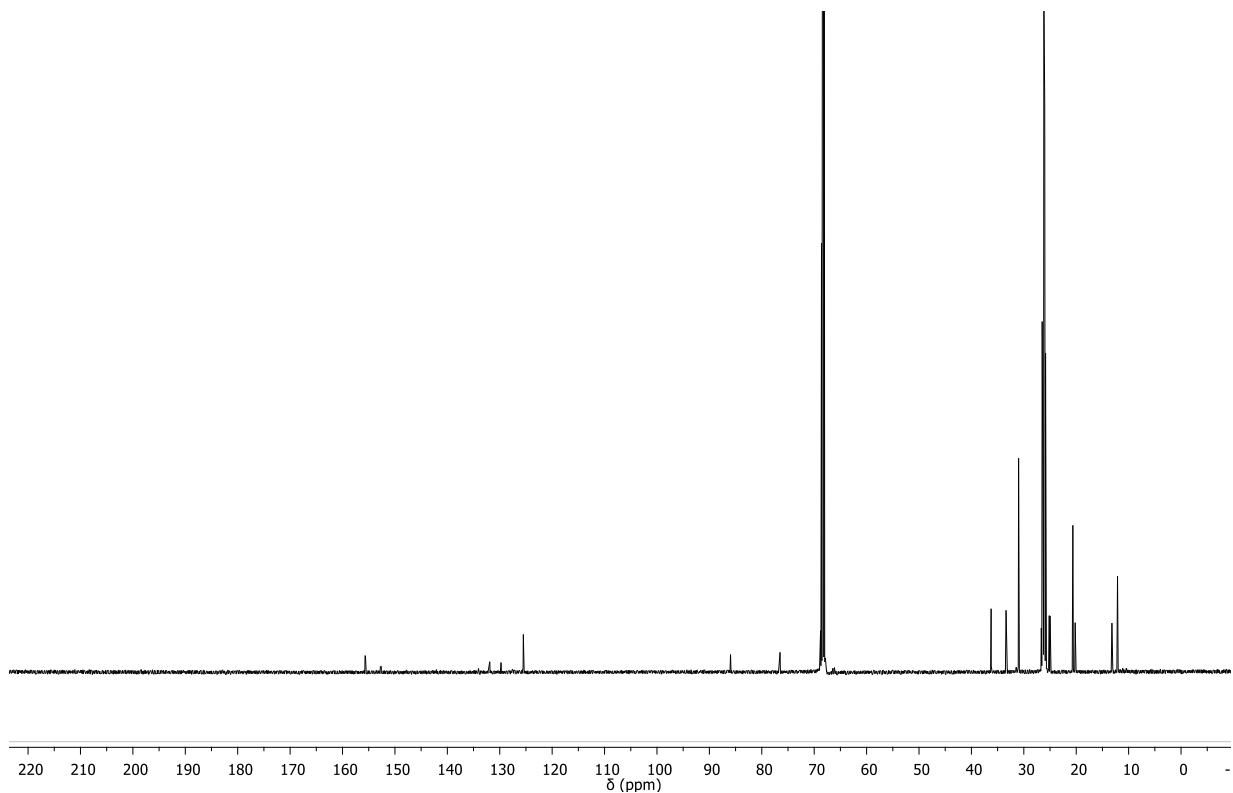
Figure 3.40. $^{13}C\{^1H\}$ NMR spectrum at 125.7 MHz of complex **3.15** in dry THF-d_8
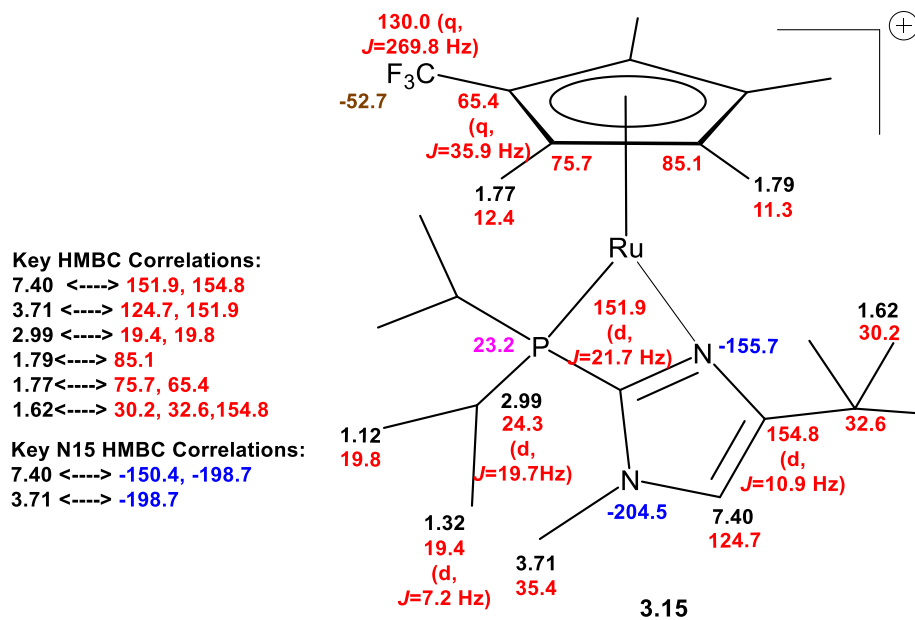
Figure 3.41. Selected NMR data for complex **3.15**

Synthesis of complex 3.12: reaction of iPr₂P(N-CH₃-Im) with Cp*RuCl₄

In a resealable J. Young NMR tube, the phosphine (28.7 mg, 0.145 mmol) was weighed out, and deoxygenated acetone-d_6 (0.2 mL) was added, forming a clear, colorless solution. To the same J. Young NMR tube, [Cp*RuCl]₄ (39.2 mg, 0.0360 mmol) was added, followed by an additional deoxygenated acetone-d_6 (0.3 mL). The solution was initially light blue, with significant amounts of insoluble orange-red precursor. After sonication and mixing, the precipitate disappeared within 20 min, and the solution was dark blue. Solution was quantitatively transferred to a 20-mL scintillation vial using additional acetone (0.5 mL), and the solvent was removed in vacuo. Upon complete removal of solvent, the resulting precipitate turned bright orange. The cakey residue was scraped off of the sides of the vial, and put back under vacuum to remove all solvent. Yield 70.0 mg (70.5% yield). ^{1}H NMR (500 MHz, acetone-d_6): 7.04 (broad s, 1H), 7.00 (broad s, 1H), 3.46 (broad s, 3H), 3.01 (m, 2H), 1.61 (s, 15H), 1.36 (dd, J= 15.5, 7.1, 6H), 1.04 (dd, J= 14.8, 7.0, 6H). ^{13}C NMR (125.7 MHz, acetone-d_6): 146.5 MHz (d, J = 34.7), 129.5 (d, J = 10.8), 124.9 (s), 77.3 (d, J = 2.6), 36.5 (d, J = 2.7), 24.8 (d, J = 19.3), 20.0 (d, J = 5.5), 19.8 (d, J = 2.8), 11.6 ppm (s). ^{31}P NMR (202.38 MHz, acetone-d_6): 32.3 ppm. Elemental analysis: Calculated for $C_{20}H_{34}ClN_2PRu$ (469.98 g/mol): C: 51.08%, H: 7.09% N: 6.14%. Found: C: 50.69%, H: 7.17%, N: 5.77%. Crystals suitable for X-ray diffraction were grown by placing a small vial containing a concentrated acetone solution of **3.12** in a larger vial containing dioxane and allowing the acetone to diffuse out of the vial, thereby concentrating it.
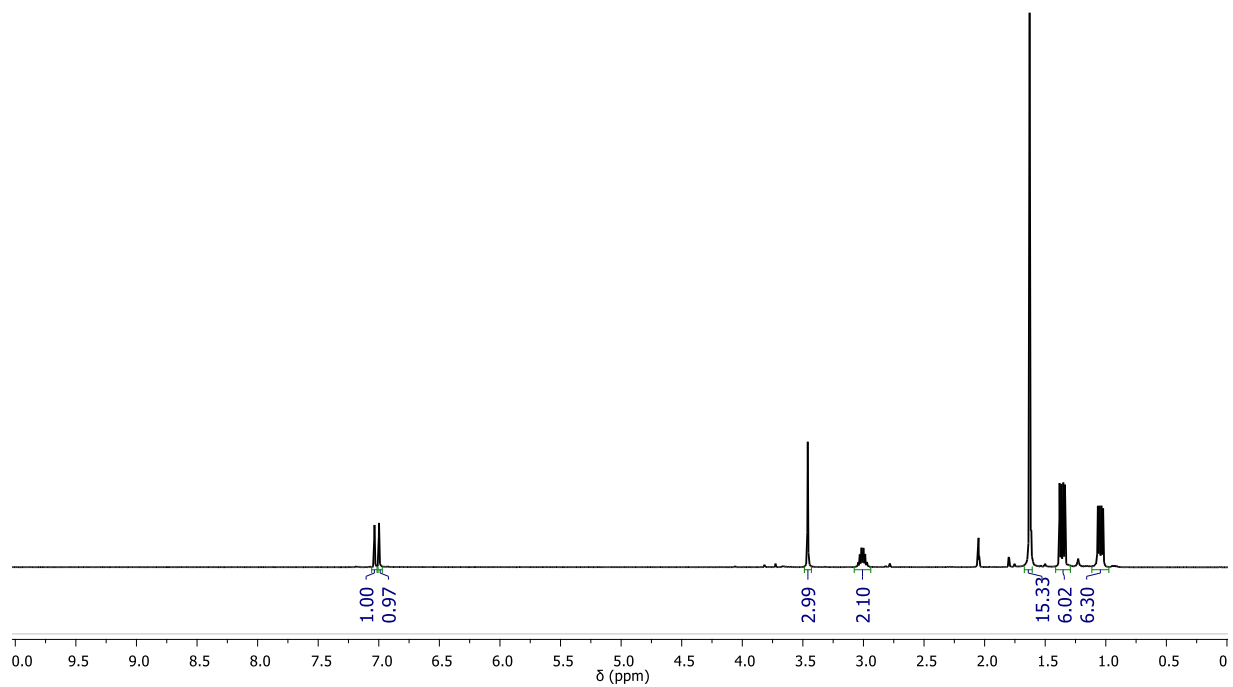
Figure 3.42. ^{1}H NMR spectrum at 500 MHz of complex **3.12** in acetone-d_6
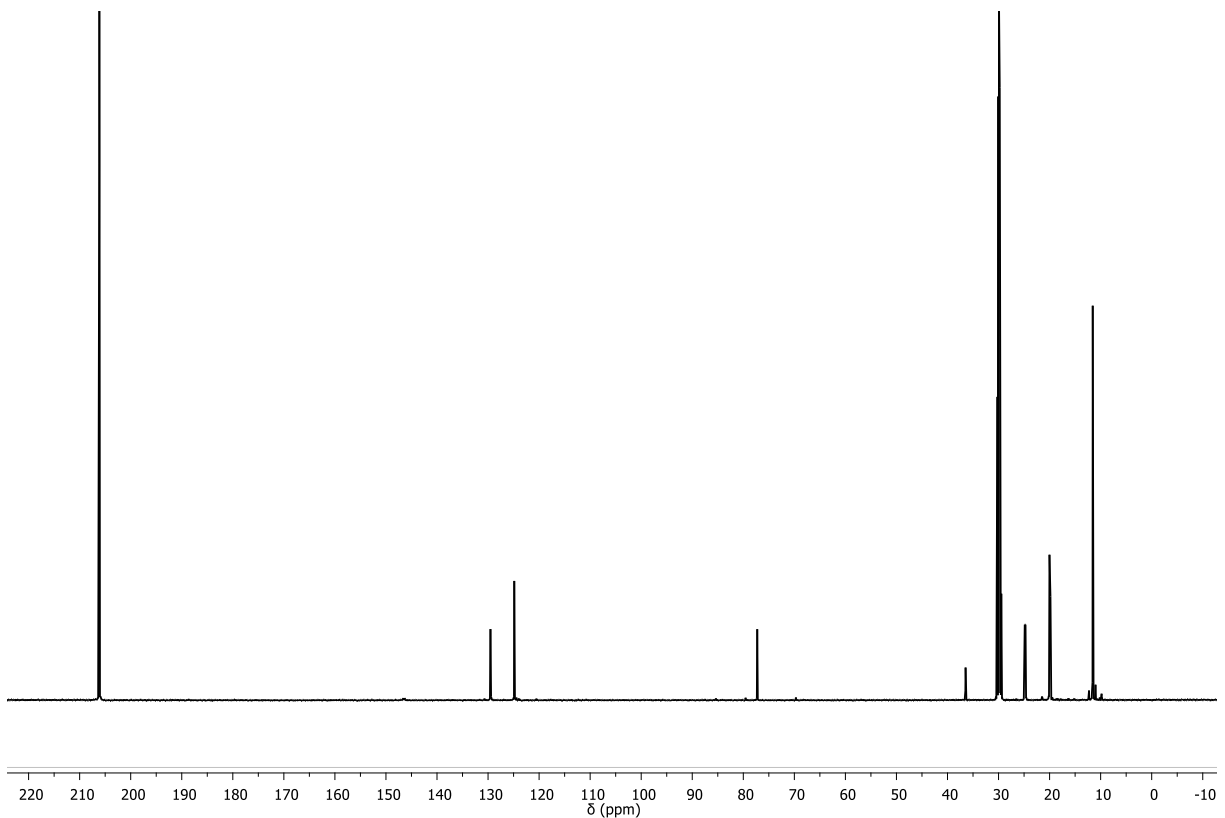
Figure 3.43. $^{13}C\{^1H\}$ NMR spectrum at 125.7 MHz of complex **3.12** in acetone-d_6

Key HMBC Correlations:
7.04 <----> 146.5, 129.4
3.46 <----> 146.5, 124.9
3.01 <----> 19.8, 20.3, 146.5
1.63 <----> 77.3
1.36 <----> 24.8
1.04 <----> 24.8

Key N15 HMBC Correlations:
6.67 <----> -100.5, -213.1
3.22 <----> -213.1

3.12
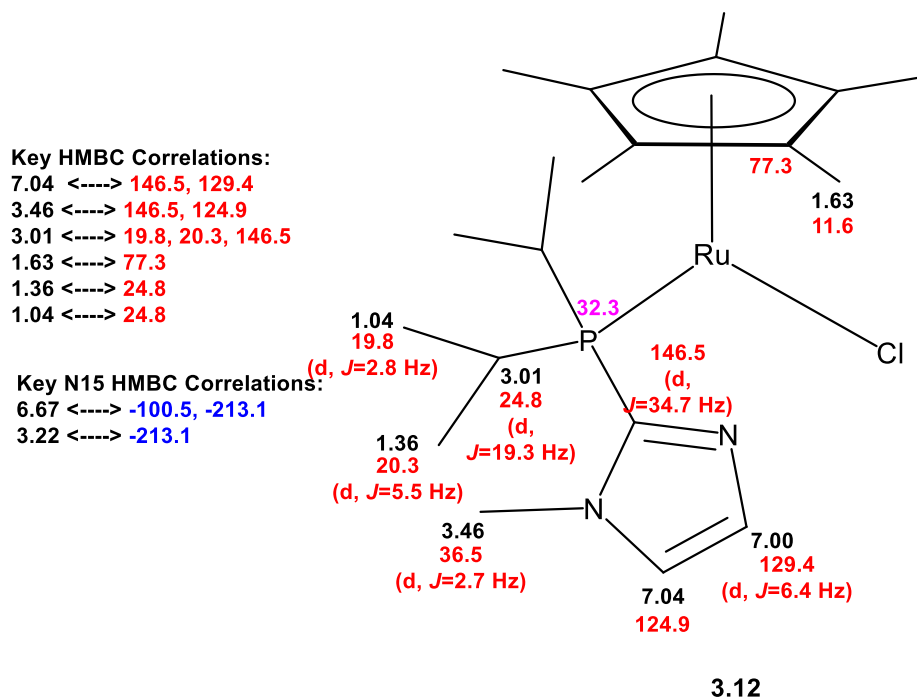
Figure 3.44. Selected NMR data for complex **3.12**

113

Synthesis of complex 3.13: reaction of iPr$_2$P(N-CH$_3$ Im) with Cp‡RuCl$_4$

In a resealable J. Young tube, the phosphine (21.8 mg, 0.110 mmol) was weighed out, and deoxygenated acetone-d_6 (0.5 mL) was added. [Cp‡RuCl]$_4$ (36.4 mg, 0.0279 mmol) was weighed in the same tube, and additional acetone-d_6 (0.5 mL) was added, forming a bright orange solution with some undissolved precursor. The J. Young tube was placed in an oil bath for 16 h, during which time the solution became homogeneous. The solution was then transferred to a vial, and the solvent was removed in vacuo, leaving a bright orange precipitate.   Yield: 56.6 mg (98.2% yield). ^{1}H NMR spectra taken at 25 ˚C and -40 ˚C show an increase in number of signals for the Cp and iPr-CH$_3$ at low temperatures, likely due to a desymmetrization of the complex due to restricted rotation of the Cp and iPr groups (see Figure 3.46): ^{1}H NMR (500 MHz, acetone-d_6): 7.11 ppm (s, 1H), 7.08 (s, 1H), 3.76 (s, 3H), 2.94 (m, 2H), 1.89 (broad s, 6H), 1.80 (broad s, 6H), 1.43 (dd, J= 14.4, 7.1, 6H), 1.10 (very broad m, 6H). ^{1}H NMR (500 MHz, acetone-d_6, -40°C): 7.18 ppm (s, 1H), 7.12 (s, 1H), 3.77 (s, 2H), 2.91 (m, 2H), 1.89 (s, 3H), 1.83 (d, J = 2.1, 6H), 1.69 (d, J = 1.2, 3H), 1.46-1.28 (three overlapping dd, 9H), 0.92 (dd, J = 15.6, 7.1, 6H), 1.22 (dd, J = 15.8, 6.9, 6H), 0.83 (dd, J = 9.1, 7.7, 6H). ^{13}C {^{1}H} NMR (125.7 MHz, acetone-d_6): 152.5 (d, J = 24.5), 131.3 (d, J = 268.9), 129.2 (d, J = 15.8), 125.6 (d, J = 2.0), 80.2 (bm), 62.3 (q, J = 34.1), 34.9 (s), 23.5 (d, J = 14.1), 19.7 (s), 12.5 (s), 10.9 ppm (s).^{31}P {^{1}H} NMR (202.4 MHz, acetone-d_6): 32.5 ppm. ^{19}F NMR (470.4 MHz, acetone-d_6): -51.5 ppm (s). Note: 'Power' phase correction applied to ^{13}C NMR.
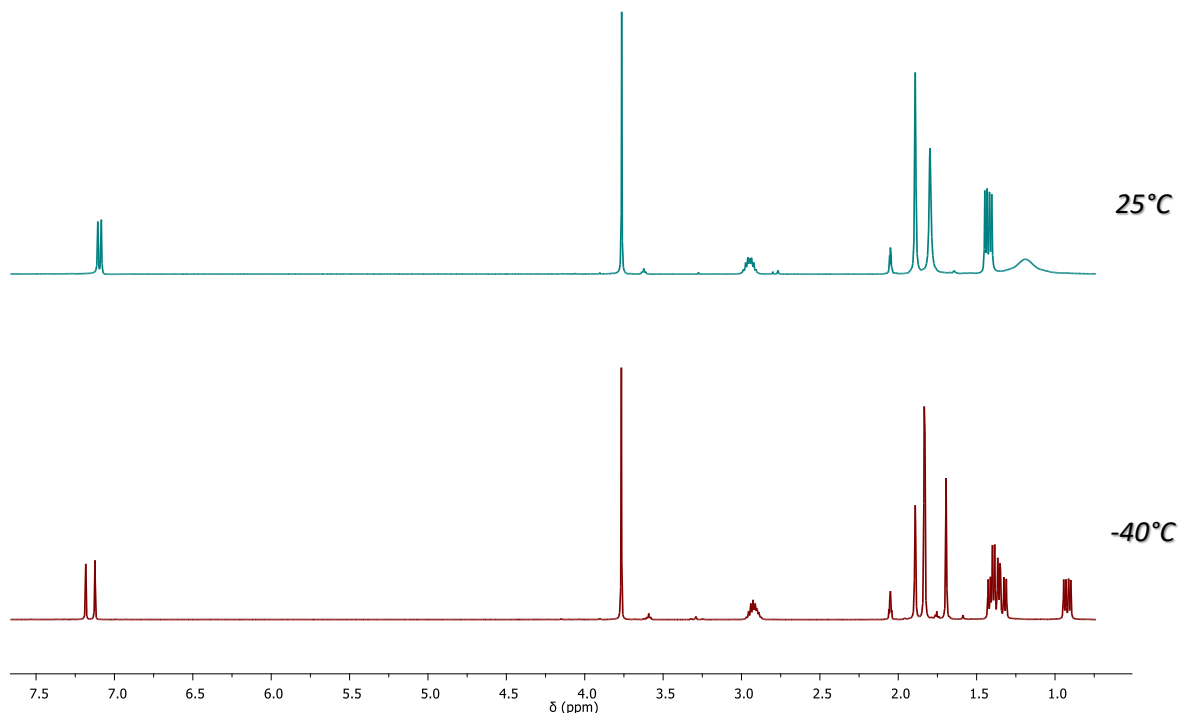
Figure 3.45. Variable temperature ^{1}H NMR spectra at 500 MHz of complex **3.13** in acetone-d_6
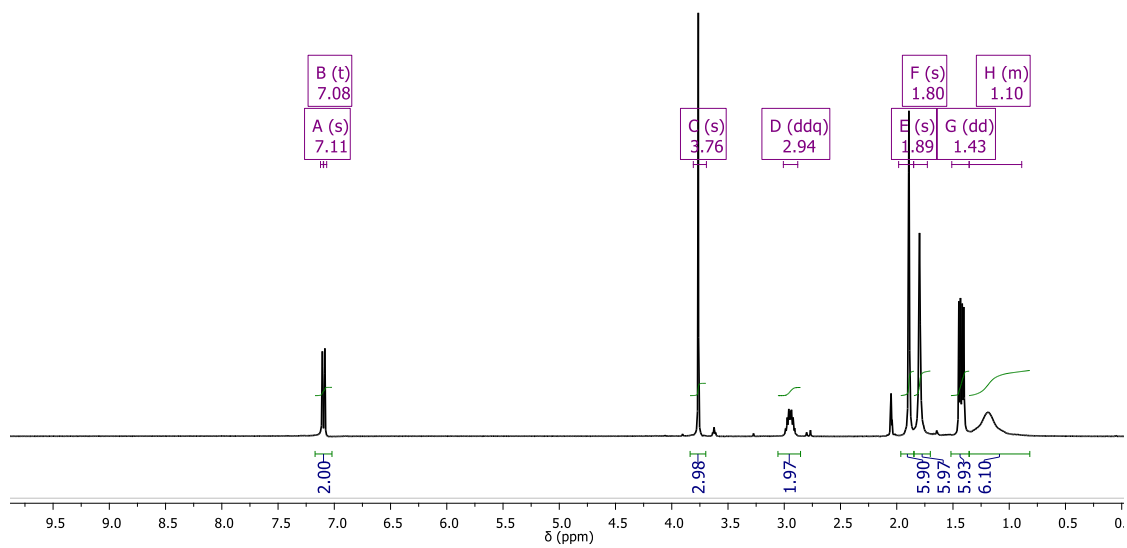
Figure 3.46. ^{1}H NMR spectrum at 500 MHz of complex **3.13** in acetone-d_6 at 25 ˚C

115
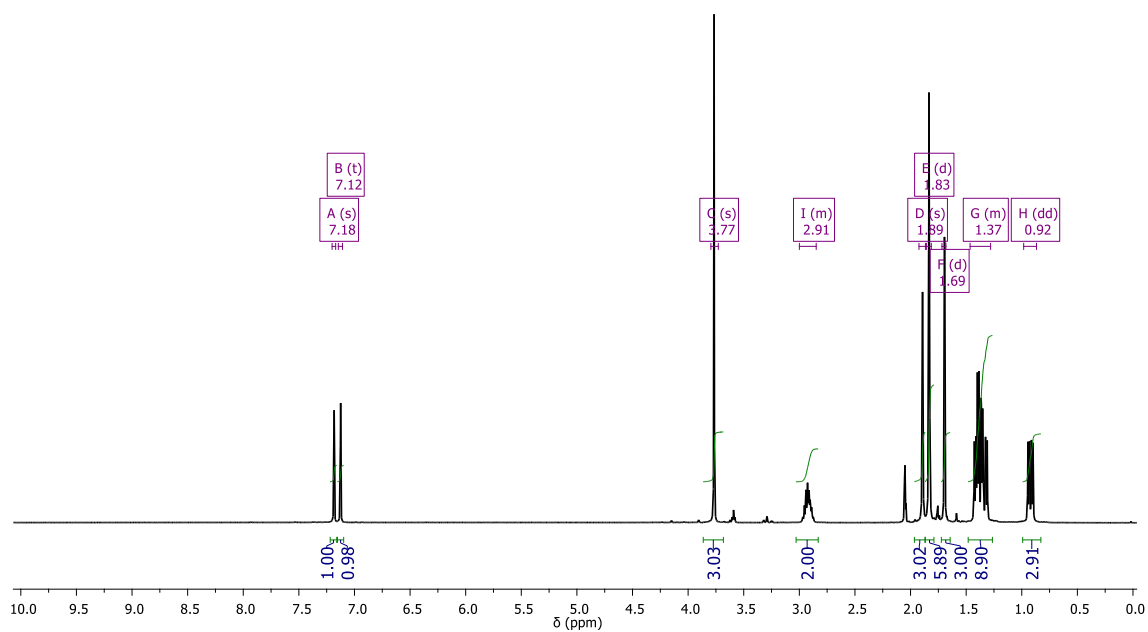
Figure 3.47. ^{1}H NMR spectrum at 500 MHz of complex **3.13** in acetone-d_6 at -40 ˚C
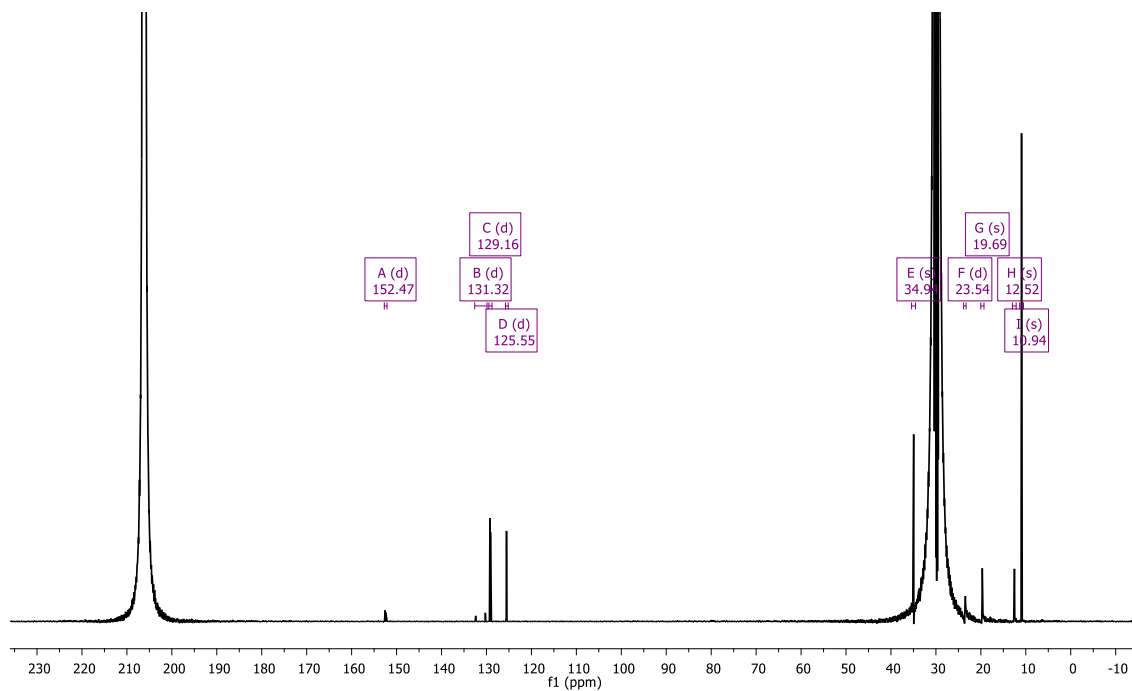
Figure 3.48. ^{13}C{^{1}H} NMR spectrum of complex **3.13** in acetone-d_6

116
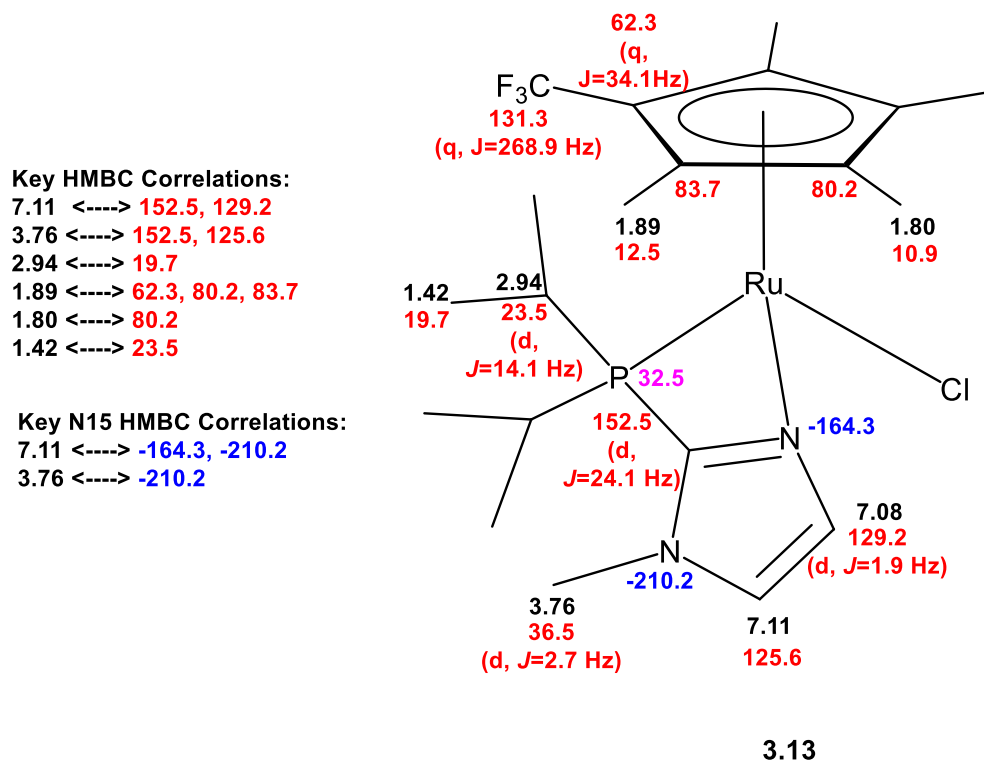
Figure 3.49. Selected NMR data for complex **3.13** at 25 ˚C

Synthesis of complex 3.16: ionization of Cp*Ru(iPr₂P(N-CH₃)ImCl

In a resealable J. Young NMR tube containing complex **7** (22.3 mg, 0.0474 mmol) and dry, deoxygenated THF-d_8 (0.5 mL), TlPF$_6$ (16.6 mg, 0.0474 mmol) was added, followed by additional dry THF-d_8 (0.3 mL). A white precipitate immediately formed, while the solution remained orange. The solution was filtered through a fine glass frit, and the J. Young NMR tube was rinsed with additional alumina-filtered, deoxygenated THF. The solvent was removed in vacuo, leaving an orange residue. The residue was scraped off the sides of the flask and put under vacuum again, yielding an orange powder. Yield: 20.5 mg (99.5% yield). ^{1}H NMR (500 MHz, THF-d_8, 25 ºC): 7.43 ppm (s, 1H), 7.53 (s, 1H), 7.42 (s, 1H), 3.75 (s, 3H), 2.75 (m, 2H), 1.77 (s, 15H), 1.40 (bm, 6H), 1.11 (bm, 6H). ^{13}C NMR (125.7 MHz, THF-d_8, 25 ºC): 152.6 (d, J = 22.1), 130.6 (d, J = 15.6), 128.4, 78.5, 35.1, 25.8, 24.2 (d, J = 13.6), 20.2 (d, J = 4.6), 20.0 (d, J

117

= 6.2), 11.8. ^{31}P {^{1}H} NMR (202.4 MHz, THF-d_8): 31.6 ppm (s), -144.3 ppm (hept, J = 707.9 Hz) (PF$_6$).
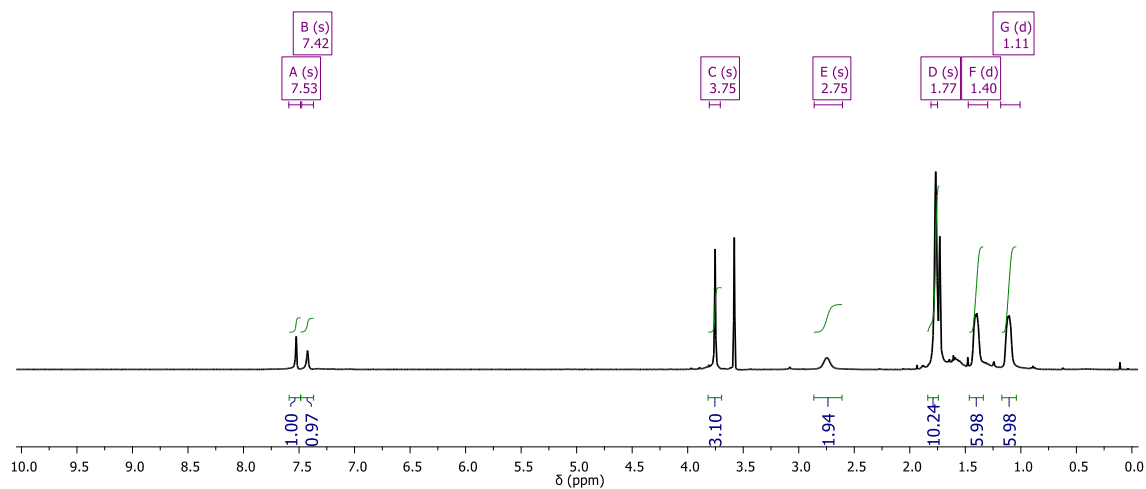
Figure 3.50. ^{1}H NMR at 500 MHz of complex **3.16** in dry THF-d_8
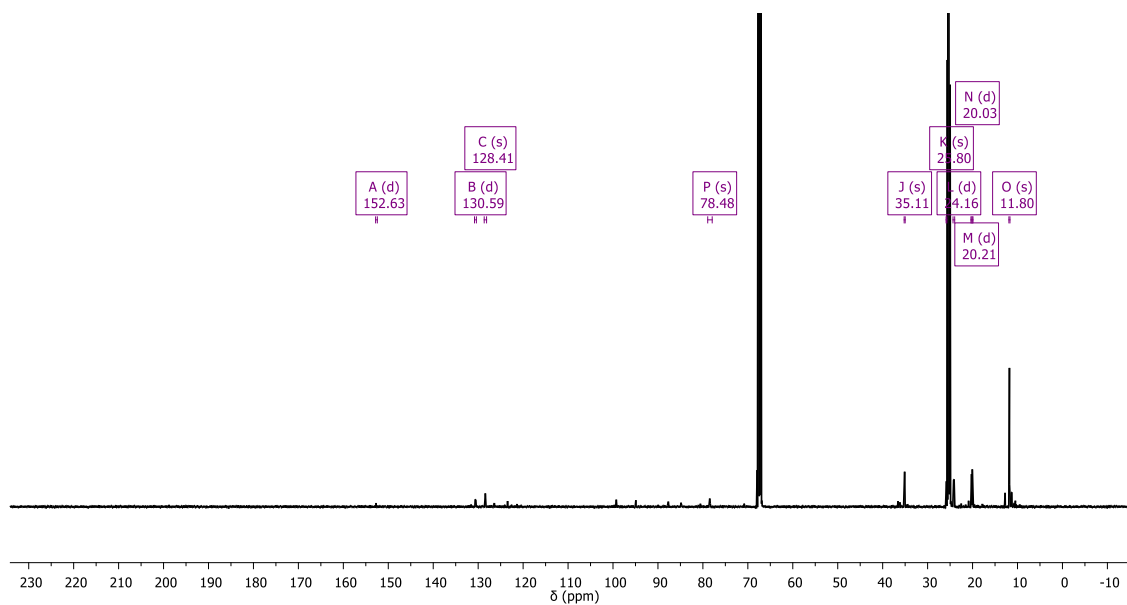
Figure 3.51. ^{13}C {^{1}H} NMR at 125.7 MHz of complex **3.16** in dry THF-d_8

118
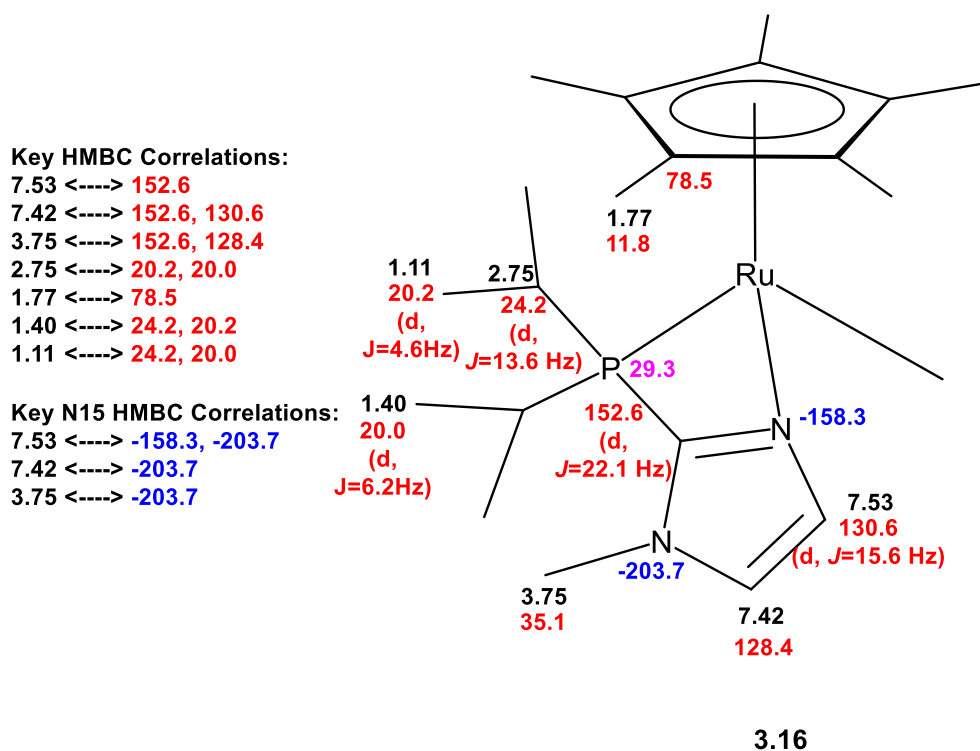
Figure 3.52. Selected NMR data for the cation of complex **3.16**

Synthesis of complex 3.17: ionization of Cp‡Ru(iPr₂P(N-CH₃)Im)Cl

To a resealable J. Young NMR tube, on a balance was added complex **3.13** (14.2 mg, 0.0271 mmol), and dry, deoxygenated THF-d_8 (0.3 mL) was added, forming an orange solution. TlPF₆ (10.5 mg, 0.0301 mmol) was then added to the J. Young NMR tube, followed by additional dry THF-d_8 (0.3 mL). A white precipitate immediately formed, while the solution remained orange. The solution was filtered through a fine glass frit, and the J. Young NMR tube was rinsed with additional alumina-filtered, deoxygenated THF. The solvent was removed in vacuo, leaving an orange residue. The residue was scraped off the sides of the flask and put under vacuum again, yielding an orange powder. Yield: 13.2 mg (99.7% yield). ^{1}H NMR (500 MHz, THF-d_8, 25 °C): 7.43 ppm (s, 1H), 7.36 (s, 1H), 3.77 (s, 3H), 2.74 (m, 2H), 1.84 (s, 6H), 1.79 (d, $J = 1.9$), 1.45 (dd, $J = 15.1$, 7.0, 6H), 1.18 (dd, $J = 17.0$, 7.3, 6H). ^{13}C NMR (125.7 MHz,

THF-d_8, 25 °C): 152.3 ppm (d, $J = 25.2$), 130.4 (q, $J = 269.2$), 129.8 (d, I= 14.7), 128.1 (s), 84.98 (s), 78.7 (s), 62.2 (q, $J = 35.2$), 35.3 (s), 23.6 (d, $J = 13.3$), 19.9 (d, $J = 6.5$), 19.8 (d, $J = 2.7$), 12.2 (s), 10.9 (s).).^{31}P {^{1}H} NMR (202.4 MHz, THF-d_8): 27.9 ppm (s), -144.3 ppm (hept, $J = 707.9$ Hz) (PF$_6$).
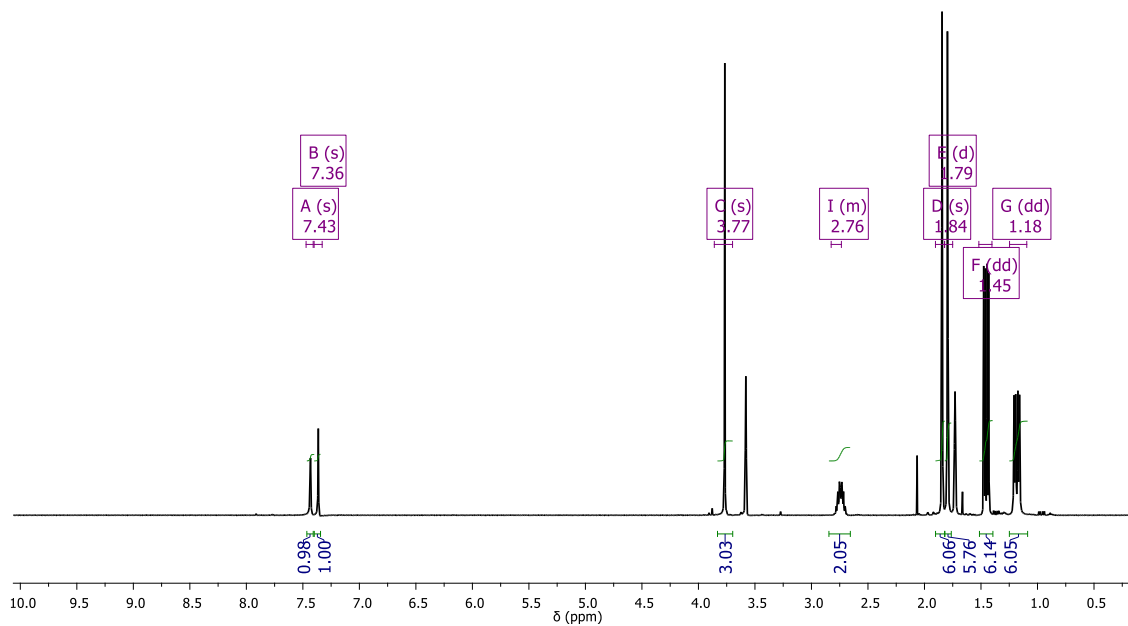
Figure 3.53. ^{1}H NMR at 500 MHz of complex **3.17** in THF-d_8
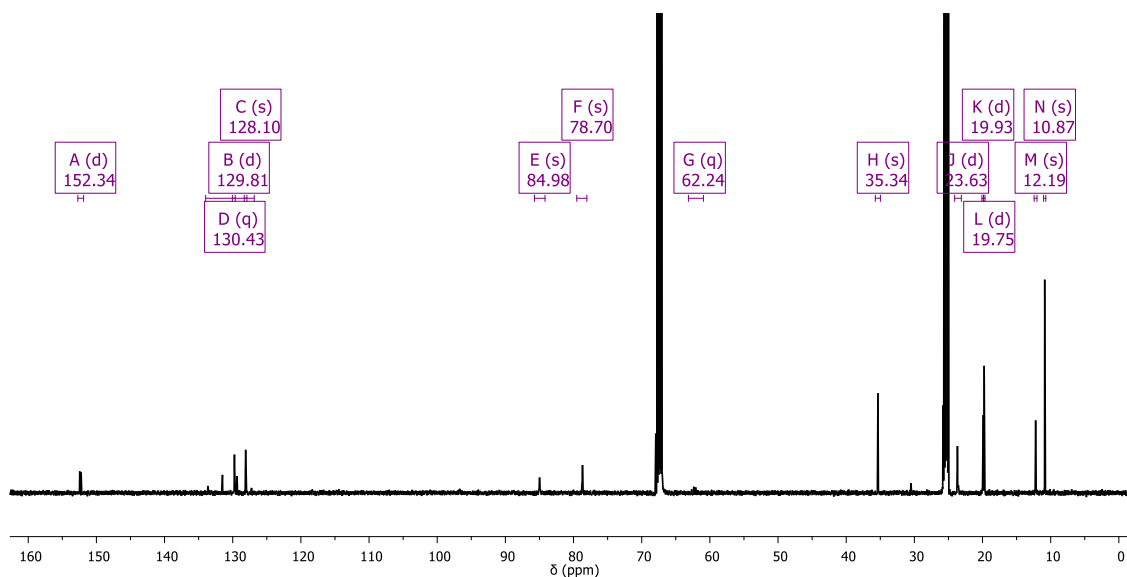
Figure 3.54. ^{13}C {^{1}H} NMR at 125.7 MHz of complex **3.17** in THF-d_8
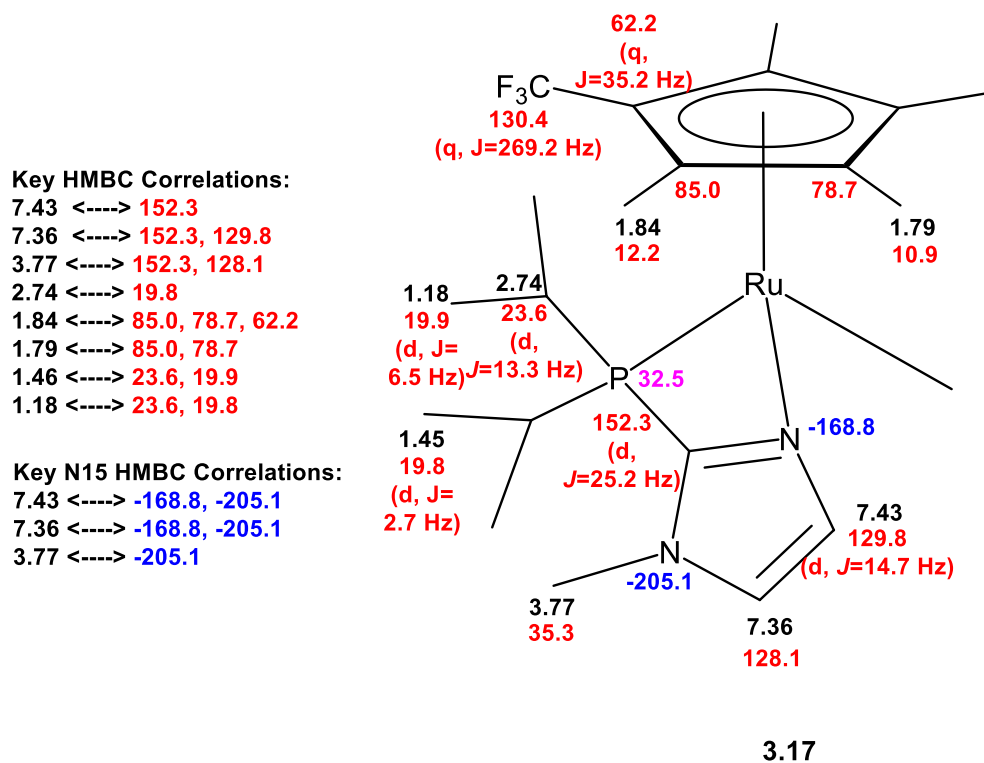
Figure 3.55. Selected NMR data for complex **3.17**

Synthesis of 3.19: complexation of iPr₂P(N-H Im) with Cp*RuCl₄

To a scintillation vial equipped with a stirbar, [Cp*RuCl]$_4$ (59.1 mg, 0.0543 mmol) was added, and dry, deoxygenated THF (2 mL) was added, forming a cloudy deep red solution. o a separate scintillation vial, the phosphine (40.1 mg, 0.218 mmol) was added and dry, deoxygenated THF (2 mL) was added. The phosphine solution was then pipetted into the precursor solution dropwise. The mixture slowly turned dark brown and produced a bright orange precipitate, which was then stirred for 12 hours then filtered through a fine frit. The precipitate was then rinsed with more dry, deoxygenated THF, and dried in vacuo. Yield 70.0 mg (70.5% yield). ^{1}H NMR (400 MHz, dmso-d_6, 25°C): 11.6 ppm (s, 2H), 6.87 (broad s, 2H), 6.83 (broad s, 2H), 2.86 (m, 2H), 2.70 (m, 2H), 1.45 (s, 30H), 1.37 (dd, J = 14.4, 7.0, 6H), 1.28 (dd, J = 17,5, 7.8, 6H), 1.22 (dd, J =15.8, 6.9, 6H), 0.83 (dd, J =9.1, 7.7, 6H). ^{13}C NMR (125.7 MHz, dmso-d_6, 25˚C): 147.9 ppm (d, J =25.4), 137.5 (s), 116.9 (s), 80.8 (d, J = 2.6), 67.0 (s), 25.6 (d, J =21.9), 25.1 (s), 24.9 (d, J =14.9), 21.7 (d, J =7.2), 19.1 (d, J =10.6), 18.5 (d, J =6.2), 16.8 (d, J =7.5), 10.2 (s). ^{31}P {^{1}H} NMR (202.38 MHz, acetone-d_6, 25ºC): 52.6 ppm. Elemental analysis: Calculated: C: 50.04%, H: 7.09% N: 6.14%. Found: C: 50.30%, H: 7.38%, N: 5.74%. Crystals suitable for X-ray diffraction were grown by placing a vial with a saturated solution of methanol containing the compound into a surrounding bath of ethyl acetate in a sealed container, and allowing the methanol to diffuse out of the vial into the bath of ethyl acetate, thereby concentrating it.
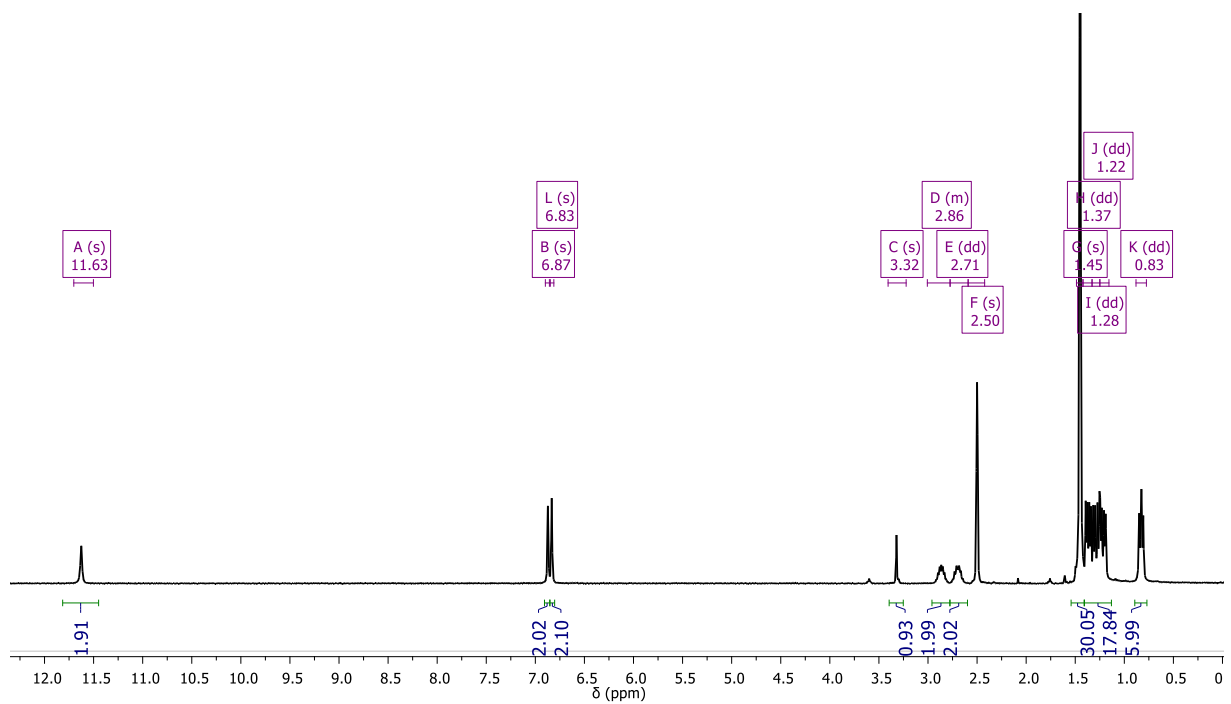
Figure 3.56. ^1H NMR at 400 MHz of complex **3.19** in dmso-d_6
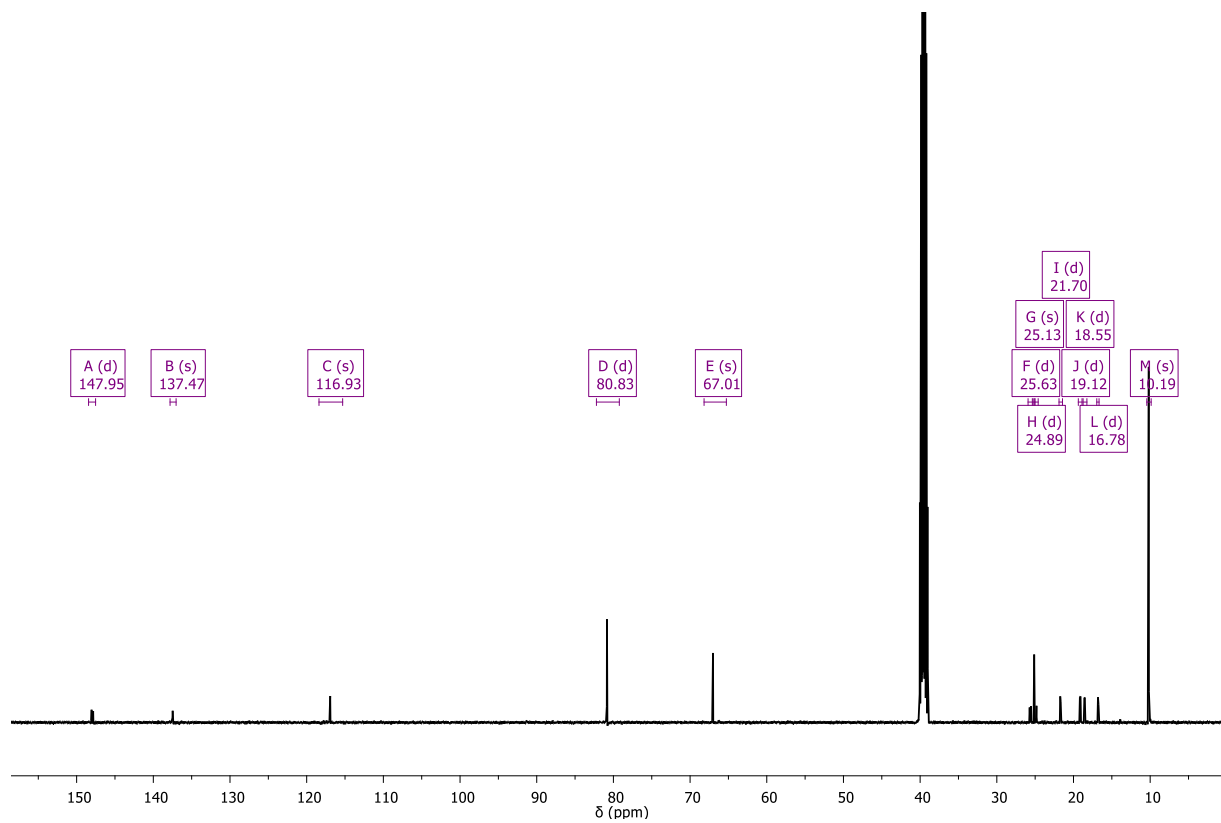
Figure 3.57. ^{13}C {^1H} NMR at 125.7 MHz of complex **3.19** in dmso-d_6

Key HMBC Correlations:
11.6 <----> 147.9, 137.5
6.87 <----> 137.5
6.83 <----> 116.9
2.86 <----> 21.7, 18.5
2.71 <----> 19.1, 16.8
1.45 <----> 80.8

Key N15 HMBC Correlations:
6.67 <----> -100.5, -213.1
3.22 <----> -213.1
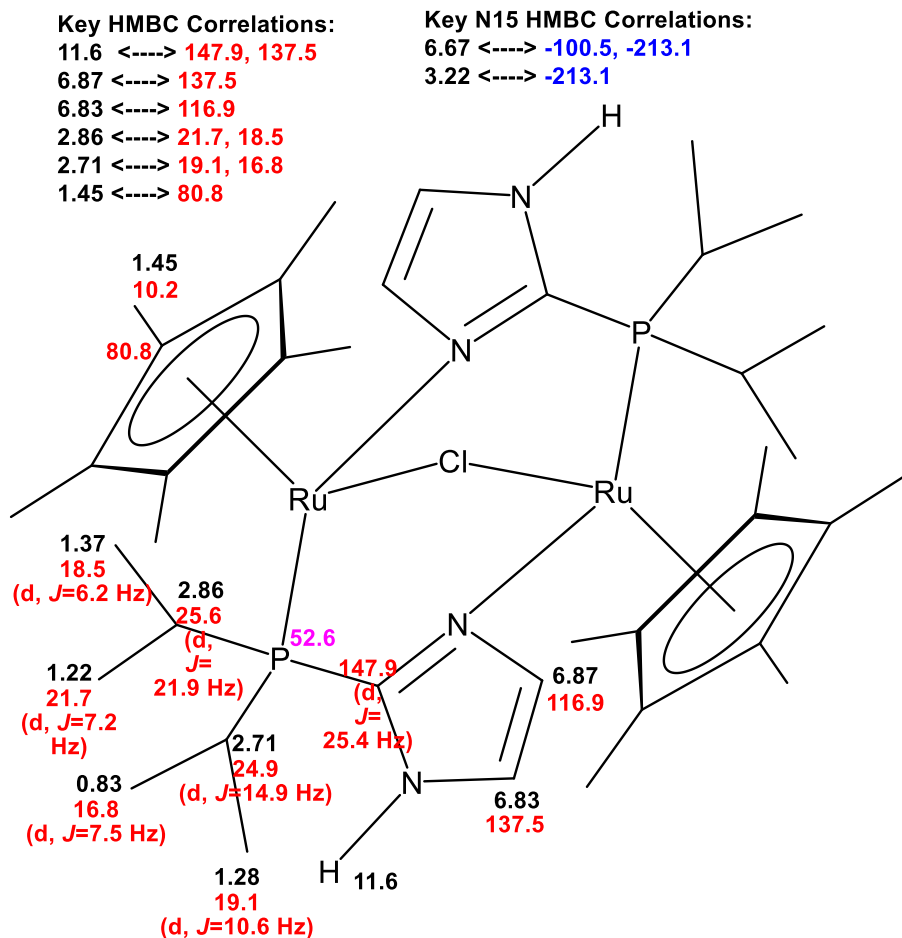
Figure 3.58. Selected NMR data for complex **3.19**

Synthesis of 3.20: complexation of iPr₂P(N-H Im) with Cp‡RuCl₄

To a scintillation vial equipped with a stirbar, [Cp‡RuCl]₄ (19.9 mg, 0.0153 mmol) was added, and dry, deoxygenated THF (2 mL) was added, forming a cloudy solution. To a separate vial, the phosphine (11.3 mg, 0.0613 mmol) was added, to which dry, deoxygenated THF (2 mL) was also added, forming a solution. The phosphine solution was then pipetted into the precursor solution dropwise. No significant color change occurred. The solution was then stirred for 16 hours then filtered through a fine frit. The precipitate was then rinsed with more dry, deoxygenated THF, and dried in vacuo. Yield 22.5 mg (72.1% yield). ^{1}H NMR (500 MHz, acetone-d_6, 25°C): 11.4 ppm (broad s, 2H), 8.00 (s, 2H), 7.47 (s, 2H), 2.81 (m, 4H), 1.85 (d, *J*

=15.8, 6H), 1.74 (d, J = 1.3, 6 H), 1.68 (s, 12H), 1.21 (m, 24H). ^{31}P {^{1}H} NMR (202.38 MHz, acetone-d_6, 25°C): 48.0 ppm. Crystals suitable for X-ray diffraction were grown by placing a vial with a saturated solution of methanol containing the compound into a surrounding bath of ethyl acetate in a sealed container, and allowing the methanol to diffuse out of the vial into the bath of ethyl acetate, thereby concentrating it.

Tables of NMR Shifts

Table 3.4. For Cp* complexes, ^{1}H NMR data (all characterization in acetone-d_6 unless otherwise noted)

Compound	Im-H 1	Im-H 2	N-Me	iPr-H	Cp*C H3	tBu	iPr-CH3 1	iPr-CH3 2
3.10 (in THF-d_8)	6.67	N/A	3.22	3.08	1.52	1.24	1.30	1.06
3.10	6.75	N/A	3.28	3.07	1.52	1.22	1.30	1.03
3.12	7.00	7.04	3.46	3.01	1.63	N/A	1.36	1.04
3.14	7.28	N/A	3.75	2.99	1.73	1.60	1.35	1.08
3.16	7.53	7.42	3.75	2.75	1.77	N/A	1.40	1.11

Table 3.5. For Cp* complexes, selected ^{13}C and ^{15}N NMR data in acetone-d_6

Compound	Im-C1	Im-C4	Im-C5	N-Me	Cp C1	Cp Me	^{15}N basic	^{15}N-CH3 nonbasic
3.10	141.9 (J = 50.0)	153.1 (J = 6.4)	118.6	37.1	77.1	11.2	-100.6	-213.1
3.12	146.5 (J = 34.7)	129.4 (J = 6.4)	124.9	36.5	77.3	11.6	n.d.	n.d.
3.14	152.0 (J = 19.3)	154.7 (J = 12.2)	123.0	35.2	78.2	12.3	-147.0	-203.1
3.16	152.6 (J = 22.1)	130.6 (J = 15.6)	128.4	35.1	78.5	11.8	-158.3	-203.7

Table 3.6. For Cp‡ complexes, ^{1}H NMR: (**3.11** and **3.13** in acetone-d_6, **3.15** and **3.17** in dry THF-d_8)

Compound	Im-H 1	Im-H 2	N-Me	iPr-H	Cp*CH$_3$	tBu	iPr-CH$_3$ 1	iPr-CH$_3$ 2
3.11	6.78	N/A	3.53	3.08	1.79, 1.70	1.29	1.35	1.21
3.13	7.11	7.08	3.76	2.94	1.89, 1.80	N/A	1.42	Broad
3.15	7.40	N/A	3.71	2.99	1.79, 1.77	1.62	1.30	1.09
3.17	7.36	7.43	3.77	2.74	1.84, 1.79	N/A	1.45	1.18

Table 3.7. For Cp‡ complexes, selected ^{13}C and ^{15}N NMR data (**3.11** and **3.13** in acetone-d_6, **3.15** and **3.17** in dry THF-d_8)

Compound	Im-C1	Im-C4	Im-C5	N-Me	Cp C1	Cp C2	Cp C3	^{15}N basic	^{15}N-CH$_3$ nonbasic
3.11	146.0 (J = 43.7)	153.0 (J = 11.3)	118.9	35.8	81.7	80.8	62.6	-122.5 (THF-d_8) -136.2 (acetone-d_6)	-213.9 (THF-d_8) -213.7 (acetone-d_6)
3.13	152.5 (J = 24.5)	129.2 (J = 10.9)	125.6	36.5	83.7	80.2	62.3	-164.3	-210.2
3.15	151.9 (J = 21.7)	154.8 (J = 10.9)	124.7	35.4	85.1	75.7	65.4	-155.7	-204.5
3.17	152.3 (J = 25.2)	129.8 (J = 14.7)	128.1	35.3	85.0	78.7	62.2	-168.8	-205.1

Table 3.8. Crystal structure data

Compound	3.10	3.14	3.15	3.12	3.13	[Cp‡RuCl]4
Formula	$C_{27}H_{49}ClN_2PRu$	$C_{24}H_{42}F_6N_2P_2Ru$	$C_{24}H_{39}F_9N_2P_2Ru$	$C_{20}H_{34}ClN_2PRu$	$C_{20}H_{31}ClF_3N_2PRu$	$C_{40}H_{48}Cl_4F_{12}Ru_4$
Formula Weight	569.17	635.60	689.58	469.98	523.96	1302.86
Crystal System	Tetragonal	Orthorhombic	Monoclinic	Monoclinic	Monoclinic	Triclinic
Space Group	$P4_1$	Pna21	P 21/c	P 21/c	P 21/c	P-1
Crystal Color	Blue	Blue	Blue	Orange	Orange	Red-orange
Unit Cell Parameters (Lengths in Å, angles in ˚)	a=13.2477 (9) b=13.2477 (9) c=32.6230 (2) α=90 β=90 γ=90	a=22.7385 (8) b=13.1551 (5) c=9.5634 (3) α=90 β=90 γ=90	a=22.5581 (7) b=12.7798 (4) c=22.1335 (7) α=90 β=113.1800(10) γ=90	a=13.3641 (6) b=15.0206 (7) c=10.9602 (6) α=90 β=93.975(2) γ=90	a=13.915(3) b=14.954(4) c=10.922(3) α=90 β=95.212(6) γ=90	a=11.6853 (6) b=20.7278 (10) c=21.1082 (10) α=114.576 (2) β=96.8470 (10) γ=99.3550 (10)
Temperature (K)	100.0	100(2)	100.0	100.0	100.0	100
Z, Z'	8,1	4,1	8, 2	4,1	4,1	4,1
Final R indices: R1(obs)	0.0312	0.0675	0.0372	0.0501	0.0384	0.0285
wR2(all)	0.0724	0.1768	0.1040	0.1120	0.0756	0.0661
GOF	1.025	1.218	1.029	1.032	1.012	1.033

Computational studies

All electronic structure calculations were carried out using the Gaussian 09 suite of programs, running on the DUGONG Joint Cluster Resource at San Diego State University, which is supported by funding from the Department of Defense DURIP Grant (W911NF-10-1-0157) and the National Science Foundation Grant (CHE-0947087). An initial benchmarking was performed to identify an acceptable level of theory with reference to experimental observations of complexes **3.10**, **3.14** and **3.15**. Geometries were first optimized at the B3LYP density functional level using the cc-pVDZ basis set for all atoms except ruthenium, which was modeled using the LANL2DZ basis set, with the crystal structures for **3.10**, **3.14** and **3.15** as the initial input geometry. Structures were then reoptimized using the CAM-B3LYP and WB97XD functionals with LANL2DZ and SDD basis sets for ruthenium. Further optimizations were performed with the polarizable continuum model with the appropriate solvent.

NMR shielding tensors were computed by the Gauge-Independent Atomic Orbital (GIAO) method, and excited-state computations were performed using the time-dependent DFT method on the optimized structures. Crystal structure (bond distances), NMR, and UV-Vis experimental data were then compared to calculated data to determine the optimum level of theory, which was determined to be the WB97XD functional with the SDD basis set for ruthenium and the cc-pVDZ basis set for all other atoms, along with the solvent correction.

A full population analysis was then computed for each of the three complexes in conjunction with the TD-DFT calculation, allowing for a qualitative analysis of the relevant molecular orbitals and transitions in the visible region.

Computational benchmarking – nitrile-free complexes

Cartesian Coordinates - Optimized geometries for benchmarking:
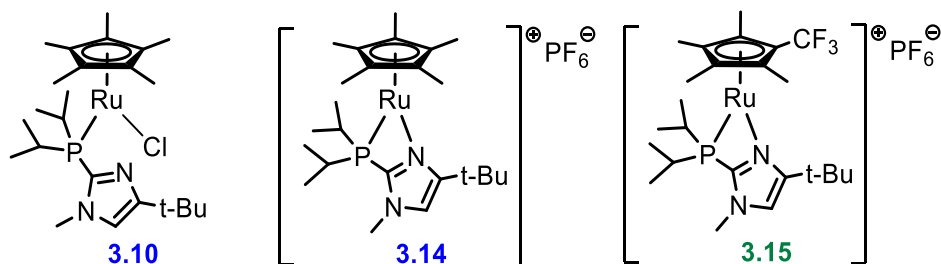
Figure 3.60. Complexes **3.10**, **3.14** and **3.15** for benchmarking

(all atoms other than Ru were optimized using the cc-pVDZ basis set; method listed first, then

basis set for Ru)

<p align="center">Cp*Ru(iPr2PIm')Cl (3.10)</p>

<u>B3LYP/LANL2DZ:</u>

Charge = 0 Multiplicity = 1

Ru	6.4128182485	6.9151391963	10.9207173774
Cl	6.1600444915	5.6672366623	12.9676852215
P	7.0151177493	4.8523780462	9.7336872562
N	4.8385002885	3.1594469142	10.6046487093
N	6.7358716695	2.0946127082	10.1341739145
C	5.2377881102	8.7470121334	11.1859678729
C	6.5200177687	8.939580275	11.7787629545
C	7.5153773163	8.7659581189	10.7315981508
C	6.8309293585	8.5491962147	9.4775715957
C	5.4236676349	8.4872723999	9.7625198245
C	3.912678138	8.8398543718	11.8806399029
H	3.1773461214	8.1485679894	11.4426523851
H	3.4989347875	9.861117279	11.7929258102
H	4.0000560573	8.6012182156	12.949312135
C	6.8042039038	9.266160847	13.2138026002

130

H	6.0411352291	8.8416830558	13.8806364953
H	6.8288886214	10.3597721978	13.3702522359
H	7.7742762069	8.8594363114	13.5335615847
C	8.9878147387	8.9850452178	10.9084761104
H	9.3468174262	8.5758039879	11.863893925
H	9.2174672442	10.0667331193	10.9045078547
H	9.5714129633	8.5224110835	10.1007592565
C	7.4701314771	8.5543961424	8.1197392086
H	8.4640591824	8.0837224349	8.12888043
H	7.6026283681	9.5911672351	7.7598643488
H	6.8572036915	8.0284822383	7.3739474046
C	4.3097599523	8.4093623283	8.7606331594
H	4.6420711525	7.9725794767	7.8091486552
H	3.9179878487	9.4195214037	8.540075562
H	3.4660186152	7.8074736945	9.1304151244
C	9.1161642363	4.1023150711	11.4970488088
H	9.0267095911	5.0394201572	12.0670655554
H	10.1498246303	3.7289189546	11.6005573274
H	8.4411682693	3.3668412942	11.9543018102
C	8.805656615	4.3098885714	10.0100355003
H	8.8757883027	3.3349435238	9.5045293496
C	9.7821154433	5.3064522471	9.3747773149
H	9.6128326107	5.4504768391	8.2961006572
H	10.8160746472	4.9428513793	9.4997158948
H	9.7140984226	6.2894568673	9.8663779655
C	5.3273785382	4.9120911691	7.4744250035
H	4.802727138	3.9773840388	7.7319243441
H	5.2127850956	5.0645654863	6.3877322307
H	4.8208538091	5.7413234886	7.9890157076
C	6.815233748	4.8277211258	7.8432628405
H	7.3025087072	5.7638908435	7.5244332599
C	7.481354725	3.6429226766	7.1317916758

H	8.5750054031	3.640559886	7.2467264085
H	7.2638581621	3.6913640098	6.0508040669
H	7.1020935516	2.6830607598	7.5146095398
C	6.145335776	3.2847612555	10.1958412246
C	5.7993475707	1.1653474181	10.5275807218
C	4.6181316771	1.8159508415	10.8207752161
H	3.652127459	1.4579011316	11.162650907
C	3.8417891475	4.1918038819	10.8511081387
H	3.7148963501	4.3549918887	11.9307323584
H	2.8860542124	3.8941431681	10.3934157227
H	4.1736267387	5.1391011956	10.4092116008
C	6.1328900501	-0.3131475616	10.5985787369
C	4.9007350402	-1.1205059719	11.0414986629
H	4.5519510168	-0.809641234	12.0398124269
H	5.1447452413	-2.1938679951	11.0930152971
H	4.0642581451	-1.0014161243	10.3332358663
C	6.5936030415	-0.7973566365	9.2068117646
H	5.7886960403	-0.683272625	8.462118767
H	6.8806501739	-1.8617988777	9.2408891862
H	7.4607302733	-0.2145545507	8.8617661273
C	7.2782892435	-0.5198991712	11.6136227517
H	8.1601356521	0.0724022483	11.3272371736
H	7.5702690429	-1.5826996098	11.6594641877
H	6.9722820996	-0.2031323602	12.6238408342

CAM-B3LYP/LANL2DZ:

Charge = 0 Multiplicity = 1

Ru	6.394026618	6.9066137578	10.9093272481
Cl	6.0626820293	5.666609996	12.93212265
P	7.0600002437	4.8611702029	9.7570893023
N	4.8418808476	3.1987030452	10.5163187962

N	6.7414573124	2.1240575973	10.1402054825
C	5.2545376182	8.7278123831	11.2530693297
C	6.576243789	8.9171471562	11.7282070946
C	7.4777695254	8.7391118546	10.6074345895
C	6.6945652921	8.5045972732	9.4281536256
C	5.3219375347	8.4435731693	9.8316971741
C	3.9997133013	8.8130970135	12.0618690816
H	3.2151054995	8.1617085703	11.6531673572
H	3.6080539733	9.8441494461	12.0668982697
H	4.174833299	8.507754348	13.1013077166
C	6.9827882811	9.2356922505	13.1311729895
H	6.2808491925	8.8046390412	13.8561844579
H	7.020399442	10.326382029	13.2900946533
H	7.9765106011	8.8275534782	13.3591947067
C	8.9559153938	8.9621637371	10.6600547885
H	9.4007339776	8.5131666568	11.5586693488
H	9.1798902547	10.042182909	10.6834312945
H	9.462956463	8.5385017927	9.7839961594
C	7.2112336733	8.474334156	8.0237114709
H	8.2174502238	8.0367305878	7.9685734493
H	7.2737163432	9.4963939193	7.6136115018
H	6.5569073059	7.894412938	7.3595503525
C	4.1310537172	8.3254957398	8.9327465416
H	4.394878364	7.8951067511	7.958523996
H	3.6909667809	9.3195314904	8.7452176137
H	3.345046238	7.6988695296	9.3772186564
C	9.0409084815	4.123566817	11.6254492586
H	8.9281385787	5.0661086866	12.1799626488
H	10.0627825922	3.7437373645	11.7870858396
H	8.335506241	3.4003570631	12.0531875919
C	8.8107656311	4.3181629351	10.1281876113
H	8.9064223021	3.3394873479	9.6371375153

133

C	9.8185633495	5.3042174757	9.5405817587
H	9.7080029741	5.4371140285	8.4539372692
H	10.8421663397	4.9421612285	9.725406185
H	9.7243936787	6.2908882222	10.0173551378
C	5.5058681045	4.940412419	7.4337554752
H	4.9516546968	4.0200621856	7.6763745939
H	5.4503404379	5.0796005501	6.3424579935
H	4.9896122667	5.784256582	7.9119409955
C	6.9644802901	4.8329937714	7.8801512328
H	7.4842620945	5.7553343882	7.5783618043
C	7.6425844806	3.6344853477	7.217405853
H	8.7274643896	3.6167174098	7.3889861879
H	7.4809648441	3.6739022539	6.1281413826
H	7.2295011529	2.6869618325	7.5924746411
C	6.160096858	3.3116431027	10.1754536648
C	5.7830691707	1.2057789084	10.4837764722
C	4.6001210158	1.8620257114	10.7185552669
H	3.6168725191	1.5093828165	11.0117305357
C	3.8520630955	4.2394882831	10.7209307061
H	3.7170291808	4.4362435967	11.7923595011
H	2.9023713805	3.931718568	10.2614518699
H	4.1916869368	5.1705803945	10.2533082135
C	6.1018321659	-0.2693320203	10.5648294064
C	4.8500912744	-1.064830596	10.9437581421
H	4.4577486147	-0.7533380725	11.9241052054
H	5.0837929408	-2.1387235806	11.0032505862
H	4.05104142	-0.9366766049	10.1969851191
C	6.6230287509	-0.7464389911	9.2012486947
H	5.8555153143	-0.6245587409	8.4211131528
H	6.903333061	-1.8109186581	9.2439040946
H	7.5068311841	-0.1652629646	8.9025713612
C	7.1909355281	-0.4832515447	11.6267596198

H	8.0846375191	0.1090777402	11.3850988567
H	7.4778323752	-1.5456071028	11.6802695638
H	6.837383632	-0.1708909743	12.6212792928

CAM-B3LYP/SDD:

Charge = 0 Multiplicity = 1

 Redundant internal coordinates found in file.

Ru	6.3968975829	6.8966474037	10.9097695446
Cl	6.0230253058	5.6703164399	12.9047351072
P	7.0615821936	4.8778758433	9.7544568773
N	4.8324294777	3.2117586083	10.4802424729
N	6.7427745638	2.1409001839	10.1521111621
C	5.264303325	8.7050219162	11.277061118
C	6.5942980681	8.8917187595	11.7328392187
C	7.4800165177	8.7176226336	10.5980555238
C	6.6789657194	8.4845053202	9.4303609033
C	5.3109407444	8.4214237468	9.8548047392
C	4.020215617	8.7852538025	12.1033099831
H	3.2416407576	8.1134112912	11.7168272531
H	3.6116454892	9.8094145872	12.0975578379
H	4.2146175849	8.4989411739	13.1445666325
C	7.0245448314	9.2028166428	13.1307233438
H	6.3157521695	8.7982735589	13.8640628242
H	7.0999900005	10.2918702957	13.2854019697
H	8.0063355036	8.7623030462	13.3505384087
C	8.9581081401	8.9478550124	10.6287410147
H	9.4173268093	8.5070468711	11.5241882765
H	9.178043692	10.0287825711	10.641342325
H	9.4552006946	8.5200658465	9.7489024058
C	7.1725559506	8.461299323	8.0172750623
H	8.184210398	8.038929767	7.9461940868

H	7.2134308571	9.483776483	7.605690511
H	6.5158478214	7.8714103801	7.3644370618
C	4.1064547294	8.3065117667	8.9731033097
H	4.3531076295	7.8661525069	7.9987742315
H	3.6718445241	9.3024023816	8.7833428243
H	3.3218504861	7.689998399	9.4339759089
C	9.0375246094	4.1401240865	11.6304391248
H	8.9448285384	5.0894654171	12.1773570163
H	10.0521924002	3.7431270979	11.7945841
H	8.3192058657	3.4338456818	12.0647659955
C	8.8098335177	4.3270937183	10.1317206984
H	8.8983457964	3.3443313543	9.6484240877
C	9.8272952312	5.2999751772	9.5387556577
H	9.7191490111	5.4274851411	8.4513164836
H	10.8469596836	4.9283199999	9.726326828
H	9.743542657	6.2903341709	10.009355488
C	5.5191055217	4.9546303214	7.4209270516
H	4.9638629874	4.0333310026	7.657354581
H	5.4709405686	5.096471049	6.3296631924
H	4.9993171271	5.7967987823	7.8977527689
C	6.9747834699	4.8463062231	7.8765907517
H	7.4984348976	5.7658959404	7.573754513
C	7.6530890429	3.6439188477	7.2206619734
H	8.7370688498	3.6235556212	7.3966744596
H	7.4961855113	3.6808894502	6.1306527092
H	7.2357969732	2.6982772392	7.5958032825
C	6.1573380581	3.3267431184	10.1659294496
C	5.7801992061	1.2217603962	10.4820752646
C	4.5905188382	1.8755971731	10.6867678736
H	3.6021903033	1.5218319468	10.9609965519
C	3.8306762638	4.2483959396	10.6423767828
H	3.608810792	4.4041130995	11.7062495392

H	2.9190700883	3.9644131365	10.0980569809
H	4.209961772	5.1949240161	10.2417219321
C	6.1020595638	-0.2515650113	10.5808580673
C	4.8456396557	-1.0483544471	10.9411144705
H	4.4330554396	-0.7306987088	11.9111137217
H	5.0815942498	-2.1209666137	11.0134037875
H	4.0610807176	-0.9285742489	10.177772329
C	6.6513958492	-0.7371153924	9.2313336802
H	5.8988267948	-0.6238205502	8.435498901
H	6.9344341243	-1.8002389346	9.28755545
H	7.5388831919	-0.1551047702	8.9454826873
C	7.1707749653	-0.4541435078	11.6654766628
H	8.0675434673	0.1386644605	11.4367326754
H	7.4592974633	-1.5152780662	11.7326460793
H	6.797029751	-0.1351659195	12.6504644117

WB97XD/LANL2DZ:

Charge = 0 Multiplicity = 1

Ru	6.4099121297	6.8724626391	10.9062669626
Cl	6.0798300174	5.6048753758	12.9210532132
P	7.06507958	4.877753203	9.727344281
N	4.8547166651	3.2355889498	10.4926148541
N	6.7573068771	2.1481220812	10.1506500545
C	5.2515005901	8.6610593555	11.2440912364
C	6.5604456777	8.8608502618	11.7549537005
C	7.4913356742	8.692650446	10.6546444952
C	6.739877315	8.4615852559	9.4508898321
C	5.3558619863	8.3896979082	9.8198600165
C	3.9729060102	8.7107514338	12.0192036909
H	3.2330767388	8.0113844067	11.6050469227
H	3.5377080059	9.7230833039	11.9854310496

H	4.1353875499	8.4356869	13.0692273371
C	6.9341762056	9.1558637364	13.1729494533
H	6.2198505232	8.7014784519	13.8717087539
H	6.9606288015	10.2430763336	13.3528874436
H	7.9247620285	8.7452317111	13.4111371523
C	8.969377023	8.9079124637	10.7508245326
H	9.3945965199	8.3879774546	11.6210372153
H	9.1915878233	9.982471374	10.8584613937
H	9.4891376051	8.5481559912	9.8534317756
C	7.2993176026	8.4208339172	8.0627739177
H	8.2788512044	7.9220809224	8.0362413621
H	7.4332632108	9.4422334387	7.6702593481
H	6.6321375561	7.8849042456	7.373739803
C	4.1828496577	8.2732557092	8.8961037465
H	4.480703764	7.9179320867	7.9012772661
H	3.7018002595	9.2569073872	8.76743125
H	3.4234499336	7.5816707684	9.2888511933
C	9.0773753087	4.1823751152	11.5577829141
H	8.9520703295	5.1317527913	12.1001095395
H	10.107607198	3.8227664143	11.7123189148
H	8.3869967139	3.4520468378	12.0001668679
C	8.823912748	4.3564479957	10.0606398726
H	8.9336936317	3.3763785843	9.5727692655
C	9.7899894568	5.3698842721	9.4472238601
H	9.6645223684	5.4796928169	8.358890832
H	10.8289768032	5.053117765	9.6295818042
H	9.6547238111	6.3582235803	9.9115448328
C	5.4486829049	4.9811617594	7.4632763645
H	4.8986709526	4.0574841189	7.7062014443
H	5.3567549964	5.1463699909	6.3780260735
H	4.9576389628	5.8166621226	7.9813220167
C	6.9209853358	4.8555278659	7.8597096196

H	7.4427774032	5.77227463	7.5440321895
C	7.5682617183	3.6454156554	7.1854378035
H	8.6575241833	3.6183980538	7.3319309359
H	7.3807695392	3.6800823053	6.1001325552
H	7.1544003482	2.7042909141	7.5786288464
C	6.17517854	3.3360454733	10.1606432532
C	5.791989564	1.2414926608	10.5046401401
C	4.6068218447	1.9037966754	10.7182149375
H	3.6209040531	1.5581238636	11.0121742362
C	3.866309853	4.284186034	10.6526164398
H	3.645628781	4.4408134795	11.716913901
H	2.9536825476	4.0146229055	10.1022935302
H	4.2601903785	5.2272541657	10.2539221289
C	6.1073444659	-0.232389221	10.6118083286
C	4.855041619	-1.0151371538	11.0210793835
H	4.4793565766	-0.6832347059	12.0020376876
H	5.0830789099	-2.0898174343	11.0945544417
H	4.0466244088	-0.8935232636	10.2824194983
C	6.6100221972	-0.7319868565	9.2472006654
H	5.8348157501	-0.608597455	8.4742800636
H	6.8794728921	-1.7993352603	9.2983574085
H	7.4973047746	-0.1630430897	8.9329991755
C	7.2096677273	-0.425811736	11.6663465679
H	8.1042192691	0.1544461636	11.397195474
H	7.4905133995	-1.488691564	11.743878716
H	6.8698631981	-0.0832047836	12.6562042165

WB97XD/SDD:

Charge = 1 Multiplicity = 1

 Redundant internal coordinates found in file.

	13.0614797269	2.4555190935	4.7008315666
Ru			

P	15.2153830281	3.265247902	4.0040026571
N	14.3215877641	4.673316114	1.5122851379
N	12.9090726954	3.7860962314	2.9613729423
C	12.2948582706	2.4345164603	6.6727814031
C	11.2279619922	1.9744430665	5.803623503
C	11.7006777787	0.8150093249	5.1312437898
C	13.0467663701	0.5285853847	5.5961605354
C	13.390921975	1.5045939846	6.5855534792
C	12.2006807522	3.6082182304	7.5951782213
H	11.6240125428	3.3399104334	8.4951973598
H	11.6923000695	4.4555953927	7.11365054
H	13.1921802893	3.9467035297	7.9235340135
C	9.8450767392	2.5446623551	5.751963121
H	9.2021848524	2.028733615	6.4829600792
H	9.3862705582	2.431386989	4.7615883623
H	9.8380613741	3.6128415768	6.004743204
C	10.948849878	-0.0333859828	4.1546582932
H	10.705238563	-1.0055238384	4.6116005105
H	11.544371506	-0.2301481105	3.2511605079
H	10.0072695614	0.4365572659	3.8455582969
C	13.8490406315	-0.6713022243	5.202140029
H	13.5645410593	-1.5398279199	5.8176585684
H	14.9251869198	-0.5028408187	5.3413729261
H	13.6784439249	-0.9392054892	4.150123463
C	14.6412189362	1.5397219664	7.4093183526
H	14.4888370658	1.0082770151	8.3617096685
H	14.9380854955	2.5707845537	7.646227167
H	15.4800043403	1.0580354039	6.8896790213
C	15.9250620696	1.2052771703	2.2888492482
H	16.7142446324	0.5955828965	1.8245815493
H	15.3420193353	1.6760841273	1.482751371
H	15.2531614546	0.5313636542	2.8428266075

C	16.5505127332	2.2391548733	3.2264967285
H	17.1968892149	2.915932334	2.6440482618
C	17.3890215239	1.5858619676	4.3284962678
H	18.1869944453	0.9753861197	3.8807417609
H	16.7685120865	0.9217300756	4.9499582489
H	17.867766549	2.3255962745	4.9872395529
C	17.1612287463	5.3613147433	4.1938523568
H	17.6283681001	6.10711435	4.8546134099
H	16.7874469212	5.9023568021	3.310675079
H	17.9525425527	4.6687252739	3.8722863461
C	16.023235272	4.6594065369	4.9329244448
H	16.4324476603	4.1470269074	5.8217802375
C	14.9465688597	5.6436315644	5.3974912508
H	15.3894433941	6.3952705709	6.0670616645
H	14.1338313687	5.1336249973	5.9356522034
H	14.5004856685	6.1761076726	4.5420881215
C	14.2040313078	3.993916693	2.6692858967
C	12.1634707302	4.3738106119	1.9613521089
C	13.0422242352	4.9189415786	1.0587536945
H	12.8677802431	5.4576470638	0.1329046338
C	15.543538987	5.0625425429	0.8297380415
H	16.4034603987	4.6575350777	1.3734773876
H	15.625298769	6.1567753214	0.7893520214
H	15.5438845126	4.6580745373	-0.1907150158
C	10.6558321091	4.3885998766	1.9644886828
C	10.1480232415	2.938415923	1.9597806194
H	10.4449240251	2.419582013	1.0353122047
H	9.0493807629	2.9186108654	2.0264838218
H	10.5613023177	2.3808064492	2.8111962532
C	10.1899350664	5.1160911123	3.2371398273
H	10.6042864095	4.6363667947	4.1346902142
H	9.0917402149	5.0992646788	3.3086126935

H	10.5168518313	6.1671879105	3.2287422007
C	10.1338380381	5.1255554704	0.7262485132
H	10.4484113568	4.6283942273	-0.2046682062
H	10.4810449827	6.1701418535	0.700632411
H	9.0343932116	5.1431689816	0.7375005649

WB97XD/SDD with acetone pcm solvent model:

Charge = 0 Multiplicity = 1

Ru	6.4149214998	6.8685131485	10.9092944585
Cl	6.0600972206	5.6181117658	12.9009413458
P	7.0496075712	4.8910262352	9.7191550331
N	4.845774403	3.2383667873	10.4901002356
N	6.7547706751	2.1601976027	10.1547267304
C	5.2565055323	8.6440029674	11.240988822
C	6.5612307878	8.8396151553	11.7690817363
C	7.5049244343	8.6781326704	10.6787924474
C	6.7671324402	8.4510380723	9.4655074605
C	5.3771474442	8.3800226057	9.8167611614
C	3.9678036562	8.688806759	12.0002651015
H	3.2403641056	7.9788568005	11.5820822911
H	3.5235962931	9.6964627044	11.9534154687
H	4.1192500237	8.4226537647	13.0541180139
C	6.921215474	9.1282913135	13.1923336271
H	6.1805953274	8.7016009886	13.8809991364
H	6.9819723496	10.2143703542	13.36940063
H	7.8929184155	8.6840775149	13.4479853618
C	8.9820811953	8.8945422057	10.7929429954
H	9.3991587017	8.368870694	11.663658591
H	9.2016369663	9.9685316602	10.9104635549
H	9.511918459	8.5427435039	9.8982443584
C	7.3450548074	8.4179255455	8.0841805743
H	8.3106462089	7.8925221037	8.0616931473

142

H	7.5122790518	9.441429068	7.7105146182
H	6.6724563363	7.9129785047	7.3773512553
C	4.2158245598	8.2730733696	8.8766532103
H	4.5249917855	7.9119070962	7.8872948158
H	3.7460985065	9.2607794403	8.7382900416
H	3.4445202672	7.5893174965	9.2598576858
C	9.0835504726	4.1996720192	11.5291479039
H	8.9822918476	5.1549615619	12.0664664358
H	10.110113224	3.82586114	11.672318748
H	8.3887031937	3.482902447	11.9863253563
C	8.8125220617	4.3679979382	10.0342192218
H	8.9139367889	3.3854352237	9.550318798
C	9.7755875472	5.3751981318	9.4059579956
H	9.6416680432	5.4780775393	8.3180879121
H	10.8151971118	5.0567437631	9.5818250935
H	9.6467865627	6.3669687751	9.8646100248
C	5.4083252363	4.974798947	7.4701490955
H	4.8730153987	4.0423298795	7.7119890221
H	5.3050582867	5.1448178861	6.3866970296
H	4.9104645731	5.8005930088	7.9966742402
C	6.8857811302	4.865175606	7.852499189
H	7.3961960896	5.7851931729	7.5284832569
C	7.5359937003	3.6586749034	7.1740154156
H	8.6272578464	3.641992252	7.3054237388
H	7.3333606476	3.688105816	6.0912972738
H	7.1358825903	2.7149518589	7.5751508991
C	6.1663012206	3.3449792042	10.1588722009
C	5.7940715157	1.2495209564	10.5112640455
C	4.6050089449	1.9059796682	10.7205337082
H	3.6205483429	1.5560184477	11.0143644168
C	3.8485370261	4.2806324411	10.6373475011
H	3.5854589447	4.4073282551	11.6960498069

H	2.9581279347	4.0255787308	10.045279949
H	4.2565697164	5.2349866432	10.2826283877
C	6.1182655122	-0.2217951275	10.6267732451
C	4.870304396	-1.0100985704	11.0386400017
H	4.4909571783	-0.6749137245	12.0170593809
H	5.1051479374	-2.0828396257	11.1187603861
H	4.0623287588	-0.8979481071	10.2980140424
C	6.6260268796	-0.7257368132	9.2656552707
H	5.8505326884	-0.6135430706	8.4913373364
H	6.9041847695	-1.7904947019	9.323816745
H	7.5089529611	-0.1515897168	8.9486535964
C	7.220232507	-0.4027049579	11.6839536014
H	8.1117224932	0.1813555674	11.4128749016
H	7.5074007059	-1.4634102667	11.7678663279
H	6.8769327152	-0.0566250007	12.6714045885

Cp*Ru(iPr2PIm')⁺ (3.14)

<u>B3LYP/LANL2DZ:</u>

Charge = 1 Multiplicity = 1

Ru	13.050001247	2.461816258	4.7582230845
P	15.2429593797	3.055127223	3.8019518804
N	14.2904261608	4.8638414911	1.5969349072
N	12.8847103241	3.9148825714	3.0342196965
C	11.7457158209	2.4706861574	6.5427072255
C	11.1671349742	1.5761794769	5.590816715
C	12.1615805128	0.5598904643	5.293104472
C	13.3174226698	0.7867922871	6.1303098654
C	13.0821388027	1.9927891387	6.8731691326
C	11.0834018548	3.6524163632	7.1809119488
H	10.7346894112	3.3866083645	8.1947004037

H	10.2104082311	3.9956167757	6.6105121179
H	11.7774592279	4.4993263784	7.2870396166
C	9.7482712241	1.5755689422	5.1065305276
H	9.1159067873	0.9905105802	5.7978838874
H	9.6519775581	1.1163958184	4.1129865525
H	9.3247000445	2.5873881232	5.051949202
C	11.9573352583	-0.6068100515	4.3773163459
H	11.4352464907	-1.422868012	4.9089583614
H	12.9118456824	-1.0109492886	4.012214042
H	11.3440453503	-0.3383715165	3.5050790746
C	14.4914875787	-0.1336880572	6.2809211467
H	14.2854807502	-0.8872365797	7.0616564315
H	15.4016259587	0.4052540332	6.5796439895
H	14.7073514329	-0.6793236727	5.3514910996
C	13.9679256193	2.5631144852	7.9392597601
H	13.7161437109	2.1222995926	8.9206864864
H	13.8504156523	3.652049668	8.033251877
H	15.0288965853	2.3483978121	7.7478146555
C	15.4437797879	1.097598785	1.7885166089
H	16.0846715466	0.453447163	1.1651580125
H	14.8325518116	1.7153841039	1.1126668543
H	14.7624392951	0.4459978285	2.3592790812
C	16.3162897643	1.9423194919	2.72568774
H	16.9579069949	2.6048583126	2.1197514133
C	17.2153869756	1.064013875	3.6094047734
H	17.8522654413	0.4293547219	2.9726297362
H	16.6166350525	0.3985052675	4.2503088872
H	17.8828292396	1.6530269911	4.2568641437
C	17.6132946568	4.7462594309	3.9670788469
H	18.2697896305	5.3034190651	4.655376595
H	17.3093361709	5.450238871	3.1762923434
H	18.2224420397	3.9522488011	3.5107935911

C	16.4038241996	4.2098376034	4.742889908
H	16.7699887178	3.5457457982	5.5474751545
C	15.6007701878	5.3475495118	5.3894894727
H	16.2494006936	5.9202682362	6.0714161049
H	14.7432228097	4.9726600799	5.9681670521
H	15.216497832	6.0480292412	4.6298345224
C	14.1822774013	4.0522009851	2.6801016051
C	12.1337146345	4.6745356373	2.148837091
C	13.0106710937	5.2614212001	1.2614372911
H	12.8349360108	5.9212417572	0.418014369
C	15.4952882472	5.2727380635	0.8826763949
H	16.3399124006	4.6523242227	1.2007779102
H	15.7256496423	6.3290785745	1.0864173495
H	15.3444308508	5.1395898166	-0.1976404456
C	10.6213082806	4.7763723221	2.1718705908
C	10.0251762687	3.3868157647	1.8553282487
H	10.3022130866	3.063157091	0.8392522153
H	8.9255352828	3.4202063356	1.9137387832
H	10.3863713005	2.6290494345	2.5643867651
C	10.1609218913	5.257145891	3.5636125448
H	10.5215683396	4.5850647297	4.3546027427
H	9.0607952708	5.2911442039	3.6095782714
H	10.5410781908	6.2689047596	3.7777619818
C	10.1430338543	5.7818000307	1.107916963
H	10.4252553166	5.4669349422	0.0904763681
H	10.5485269855	6.7903379613	1.2875487361
H	9.0453085015	5.8559682707	1.134578876

B3LYP/SDD:

Charge = 1 Multiplicity = 1

Ru	-0.40855238	-0.78162914	0.01673854

P	1.89333859	0.01875668	-0.01010908
N	1.31260848	2.97378189	-0.05484981
N	-0.30189979	1.44584079	0.00282995
C	-2.07881505	-1.89970153	0.95508895
C	-2.35536168	-1.77512472	-0.43662856
C	-1.24005654	-2.37475499	-1.16014442
C	-0.32494026	-2.94161174	-0.19901101
C	-0.80675647	-2.59651041	1.11024686
C	-2.96342166	-1.49614937	2.09531535
H	-3.43091185	-2.39151188	2.54135112
H	-3.77224921	-0.82654894	1.77637071
H	-2.39755505	-0.99298522	2.89371936
C	-3.61874207	-1.26620269	-1.06260116
H	-4.32995692	-2.09948771	-1.20259701
H	-3.43870869	-0.82582443	-2.05335231
H	-4.11667628	-0.50946425	-0.44175427
C	-1.15662827	-2.51782219	-2.64927084
H	-1.71359309	-3.41174487	-2.98306918
H	-0.11755818	-2.63126642	-2.98958013
H	-1.58990531	-1.64907263	-3.16605321
C	0.84939987	-3.82391563	-0.50517356
H	0.53572936	-4.88254067	-0.51278734
H	1.64871834	-3.72621836	0.24356210
H	1.27901615	-3.60671696	-1.49297101
C	-0.22660631	-3.04511190	2.41768383
H	-0.67077676	-4.00990777	2.72186390
H	-0.42988967	-2.32580074	3.22418395
H	0.86116278	-3.19198621	2.35609804
C	2.26159286	0.30424836	-2.78583711
H	2.94536970	0.29284782	-3.64960293
H	1.77180974	1.28985737	-2.75902018
H	1.48142696	-0.45431633	-2.95959893

C	3.04574912	0.00676093	-1.50137550
H	3.78149500	0.81197469	-1.33492761
C	3.79714455	-1.33023375	-1.58844342
H	4.49017385	-1.30823887	-2.44461910
H	3.10321471	-2.17097122	-1.74419847
H	4.39461327	-1.54245704	-0.68866844
C	4.28095160	0.68925517	1.52387794
H	4.87428122	0.42971941	2.41579617
H	4.08611321	1.77189353	1.57368627
H	4.91169081	0.48816571	0.64541456
C	2.97730455	-0.11890121	1.52910382
H	3.23348048	-1.19433578	1.52242368
C	2.14003486	0.16564298	2.78411728
H	2.72724375	-0.06969953	3.68584173
H	1.21928576	-0.43556633	2.80775324
H	1.85264915	1.22848701	2.84193593
C	1.03668190	1.64614350	-0.01108538
C	-0.90588640	2.69692903	-0.02707709
C	0.10076779	3.63760980	-0.05936869
H	0.05932779	4.72136728	-0.09152828
C	2.61310592	3.63503083	-0.09176877
H	3.39272267	2.90359055	-0.32947041
H	2.83763688	4.10070019	0.87940661
H	2.60625896	4.41123134	-0.86941813
C	-2.40235943	2.93732304	-0.06452230
C	-2.95623451	2.40088915	-1.40337080
H	-2.52656447	2.95184842	-2.25525615
H	-4.05100404	2.51898619	-1.43946579
H	-2.71922388	1.33599088	-1.53240619
C	-3.06991602	2.21535651	1.12303077
H	-2.85075393	1.13949472	1.10543853
H	-4.16258341	2.34972454	1.08396819

H	-2.71218055	2.61950126	2.08365159
C	-2.69703363	4.44588395	0.03214861
H	-2.26519947	5.00373195	-0.81418022
H	-2.31208068	4.87772566	0.96977182
H	-3.78463240	4.61259784	0.01195862

B3LYP/CEP-121G:

Ru	-0.87339800	-0.20668568	0.00768372
P	1.28436403	-1.41477341	0.04707131
N	3.10760815	0.95202049	-0.27917341
N	0.91216031	1.18788845	-0.01597277
C	-2.90582244	0.63352296	0.44803918
C	-2.85352535	0.23115330	-0.91868247
C	-2.55354366	-1.19436370	-0.96704072
C	-2.45205778	-1.67379852	0.38297014
C	-2.61541297	-0.53854340	1.26056072
C	-3.33064537	1.97052144	0.97796027
H	-4.42337628	1.98295975	1.13782987
H	-3.09076442	2.78853942	0.28534868
H	-2.86009898	2.19802318	1.94475287
C	-3.15304679	1.07621169	-2.11902737
H	-4.17658045	0.86897080	-2.47847674
H	-2.46770262	0.86187538	-2.95265880
H	-3.09407622	2.14945353	-1.89581817
C	-2.53815722	-2.02418043	-2.21538576
H	-3.56580253	-2.32001707	-2.49272449
H	-1.95575542	-2.94679131	-2.08680375
H	-2.11747575	-1.47156511	-3.06808930
C	-2.29917222	-3.10292547	0.81468447
H	-3.28932903	-3.55558553	0.99777135
H	-1.72228382	-3.19127234	1.74690672

H	-1.79873833	-3.71121987	0.04835388
C	-2.65151011	-0.57769371	2.75774953
H	-3.69507074	-0.66118603	3.11098436
H	-2.22878639	0.33559712	3.20142777
H	-2.10089293	-1.43967251	3.15924413
C	1.68324005	-1.73793697	-2.72086140
H	2.09936831	-2.33697023	-3.54670289
H	2.11714771	-0.72826226	-2.78877844
H	0.59653613	-1.65054080	-2.88107335
C	1.99305083	-2.41797243	-1.38095476
H	3.08668417	-2.45575476	-1.24187126
C	1.44754153	-3.85338265	-1.33256559
H	1.86687157	-4.43763285	-2.16713433
H	0.35065870	-3.86667399	-1.43630007
H	1.70975846	-4.37776724	-0.40097528
C	3.44202601	-2.52570384	1.65552875
H	3.68203625	-3.07579404	2.58010077
H	4.06483607	-1.61713474	1.65269977
H	3.74804278	-3.16251261	0.81204592
C	1.94757354	-2.18266654	1.63969346
H	1.37040877	-3.12429933	1.68726362
C	1.55151981	-1.31671043	2.84345522
H	1.81695998	-1.83498389	3.77862989
H	0.47113879	-1.10817407	2.86165961
H	2.08335029	-0.35099089	2.83602791
C	1.92937297	0.30056641	-0.10164018
C	1.46365774	2.45681014	-0.12274528
C	2.82349520	2.30391000	-0.29061183
H	3.61205810	3.03802676	-0.42022057
C	4.44346356	0.38858845	-0.44516461
H	4.37258686	-0.69935491	-0.54524365
H	5.07267545	0.63009770	0.42416677

H	4.90868860	0.80070998	-1.35180640
C	0.67175752	3.74721448	-0.04137094
C	-0.38443764	3.77116149	-1.16584566
H	0.09384852	3.75896865	-2.15838120
H	-0.99648939	4.68447390	-1.09481845
H	-1.05109583	2.90015244	-1.10018330
C	-0.01314731	3.82705756	1.34067857
H	-0.66904150	2.96148145	1.51069107
H	-0.62288102	4.74180765	1.41194979
H	0.73445895	3.85308565	2.14954422
C	1.61345785	4.95384178	-0.20875900
H	2.12036160	4.94316689	-1.18699306
H	2.37965071	4.98665853	0.58223649
H	1.03572080	5.88842640	-0.14670072

CAM-B3LYP/LANL2DZ:

Charge = 1 Multiplicity = 1

Ru	13.042731308	2.440261367	4.7232257483
P	15.2045911888	2.8808807697	3.6718490242
N	14.272618491	4.8139887428	1.5882534574
N	12.9222681946	4.0328763524	3.1554846053
C	11.372135012	2.224715126	6.1680427179
C	11.3623877589	1.119422614	5.2826004992
C	12.6392914924	0.437928811	5.3881399162
C	13.4185147438	1.1068139563	6.382026728
C	12.6676082037	2.2502130203	6.8192450275
C	10.2288741563	3.1345551038	6.4860619754
H	9.6473238646	2.7265669472	7.3290292375
H	9.5441735203	3.2522047195	5.6371584189
H	10.5732444276	4.1339142004	6.7822696976

C	10.2256881978	0.6500630052	4.4330423016
H	9.7880391724	-0.2639663143	4.8663007143
H	10.5532922001	0.4033649712	3.4132943976
H	9.4273725696	1.3980691712	4.363004866
C	12.980038229	-0.8425875623	4.6953382353
H	12.5708061399	-1.7009202646	5.2536737657
H	14.0649507328	-0.9894437308	4.6170357936
H	12.5571499476	-0.8803938925	3.6820582374
C	14.7403857916	0.6648032069	6.9268786867
H	14.593365247	0.0496191837	7.8294181442
H	15.3720230743	1.5172727264	7.2109835513
H	15.2977372974	0.056044966	6.2032828585
C	13.0730446831	3.2148397685	7.886090941
H	12.6579087769	2.9044722185	8.859384962
H	12.7032017385	4.228376031	7.6789072086
H	14.1640007779	3.2647481347	7.9951475643
C	15.0821749759	1.0199324533	1.5953516699
H	15.6122497098	0.3351390386	0.9166218765
H	14.512194966	1.7291298797	0.9771425948
H	14.3620077226	0.4264546289	2.1791541416
C	16.0855646612	1.7225444305	2.5091173102
H	16.7689644985	2.3285745828	1.8929416827
C	16.9174339603	0.720442497	3.3126952072
H	17.435841346	0.032911703	2.6281743922
H	16.2774116795	0.1143563659	3.9716760169
H	17.683777957	1.2067457896	3.9337479667
C	17.6534593933	4.4017697711	3.6722760856
H	18.4085209432	4.8915361035	4.3056868681
H	17.3016107254	5.1557571029	2.9521216103
H	18.164582983	3.6017514161	3.1187072893
C	16.5110190612	3.8883577903	4.5464580035
H	16.9204824302	3.1590202099	5.2672768008

C	15.8545120121	5.0216782583	5.3359396497
H	16.6081639468	5.5273715356	5.957630928
H	15.0552417679	4.6565008853	5.9964221106
H	15.4190377899	5.7768213149	4.6627357574
C	14.1732453585	4.0089659118	2.6656916962
C	12.193557634	4.9057786395	2.3703447943
C	13.033505953	5.3837557437	1.3973093219
H	12.8563044242	6.0776891936	0.5825709302
C	15.4346538859	5.0606073716	0.7500808998
H	16.2273281471	4.3512503311	1.0066933469
H	15.8056431785	6.0841601109	0.8975544204
H	15.1637631308	4.9236873896	-0.304828022
C	10.7417578575	5.2487592362	2.6052544543
C	9.9031208863	3.9650050528	2.5456035743
H	9.9545139939	3.505429763	1.5467955178
H	8.8477047107	4.1888981786	2.7626101558
H	10.2605663242	3.2287811295	3.2769451677
C	10.60861743	5.9088935219	3.9862149995
H	10.9922533642	5.2512639834	4.7775172183
H	9.5527755587	6.1306906806	4.2028013743
H	11.1696573804	6.8548646998	4.0252680254
C	10.2547008371	6.2237791565	1.5288368897
H	10.3318322894	5.7882354737	0.5210428967
H	10.821707043	7.1668297649	1.5472428946
H	9.1977711448	6.4716755612	1.7019422001

CAM-B3LYP/SDD:

Charge = 1 Multiplicity = 1

Ru	13.0511172309	2.4793639404	4.7448995134
P	15.2166721129	2.9841748308	3.7748846141
N	14.2875475326	4.8611300996	1.6359751677
N	12.892634049	3.936579743	3.0825075895

C	11.6264528938	2.443197461	6.4211517698
C	11.2293524774	1.4641509993	5.477115289
C	12.341375832	0.5479931918	5.3022518554
C	13.3888051059	0.9298741191	6.2047481998
C	12.9780998817	2.1386363438	6.8508577394
C	10.7936516159	3.5515281975	6.9811548879
H	10.4890429599	3.3040361581	8.0109223172
H	9.8804393933	3.7163336957	6.3976371214
H	11.3473104277	4.4999142081	7.0232777375
C	9.8743892095	1.2982439128	4.8668870119
H	9.2657053714	0.6190063408	5.4858958629
H	9.9295198886	0.859880066	3.8619069448
H	9.334532702	2.2500785633	4.791286669
C	12.3167297975	-0.6720432079	4.4387224001
H	11.7987019922	-1.4976816874	4.9539088885
H	13.3297093359	-1.0185738552	4.1957026933
H	11.7854419678	-0.4874293258	3.4949864146
C	14.6415119541	0.1614345035	6.4872648387
H	14.4877457069	-0.5109953508	7.3466454422
H	15.4835792589	0.8219113951	6.7343569088
H	14.9365079073	-0.4633221214	5.6344567733
C	13.7211324589	2.8658350611	7.9259214437
H	13.4405227721	2.4755068585	8.9181530575
H	13.4930852893	3.9403281307	7.9211597748
H	14.8077458492	2.7469716095	7.821461186
C	15.2593513509	1.0539217341	1.7579069401
H	15.8481886921	0.4004338851	1.0973169154
H	14.6383455292	1.7018708316	1.121876972
H	14.5842955512	0.4171057045	2.3500901771
C	16.1962377607	1.8541354592	2.6621409411
H	16.8368758461	2.4952462396	2.0356680885
C	17.0947111631	0.9401575038	3.4981249143

H	17.6748432148	0.2827392388	2.8336666471
H	16.50024638	0.2985536299	4.1647520637
H	17.8127479133	1.4995765543	4.1151167158
C	17.626853485	4.574344331	3.8697548199
H	18.3319576834	5.0920230588	4.5375237808
H	17.3105227138	5.3053515938	3.1110186941
H	18.1845331134	3.7714716159	3.3682816742
C	16.4408284348	4.0617576426	4.6850125383
H	16.8207503447	3.372036703	5.4590829635
C	15.7059519747	5.2050150648	5.3865257418
H	16.4041995406	5.7562740672	6.0332744794
H	14.8776979541	4.8403541029	6.0098385293
H	15.2927269904	5.9200666873	4.6577416946
C	14.1777322522	4.0385590061	2.6974983333
C	12.1488276847	4.7378192085	2.2342496259
C	13.0189530645	5.3093417713	1.3422764384
H	12.8436386467	5.9925509191	0.5183065243
C	15.4880708134	5.240413566	0.9087936193
H	16.2958561988	4.5409031353	1.1451996882
H	15.7995726738	6.2589436579	1.1788245972
H	15.2891090461	5.1985423447	-0.1694728239
C	10.6476144856	4.8897608064	2.2947333012
C	10.0018367812	3.5438093066	1.93088854
H	10.2471699254	3.2574898491	0.8969744414
H	8.9065361875	3.6106532201	2.0142809875
H	10.3501209566	2.7448456665	2.5977145477
C	10.2381888432	5.3142586964	3.7105199036
H	10.5942504816	4.5915922425	4.4550740239
H	9.1425506643	5.3820869714	3.7858774315
H	10.6579225262	6.2994605386	3.9648112069
C	10.1896692001	5.954617893	1.2925908
H	10.4391738159	5.6752935858	0.2577258976

H	10.6386072084	6.9357858052	1.5088409306
H	9.0976699326	6.0692722802	1.3460765822

WB97XD/LANL2DZ:

Charge = 1 Multiplicity = 1

Ru	13.0456367565	2.4501234503	4.7044469124
P	15.2329948157	3.0475959669	3.8219022558
N	14.3071139683	4.8311065973	1.600753386
N	12.9126203085	3.8964249782	3.0358634134
C	11.8017708952	2.5108451914	6.4780447081
C	11.1744686609	1.6413170122	5.5382259357
C	12.1242463318	0.5972736107	5.2263724534
C	13.2992037001	0.7815757375	6.0376115789
C	13.1190327434	1.987948924	6.7852549017
C	11.198379731	3.7209694067	7.1158775391
H	10.8889823745	3.4839834807	8.1464887295
H	10.312340016	4.0709204797	6.571991653
H	11.9180082059	4.5503954353	7.1672695723
C	9.7476817543	1.6927825324	5.0890120647
H	9.1062618964	1.1963981257	5.8348156468
H	9.6023611537	1.1739795799	4.132874032
H	9.3872181866	2.7224328169	4.9700157051
C	11.8790687178	-0.5384157343	4.2858187081
H	11.3127694935	-1.3363019567	4.7930484464
H	12.8206276523	-0.9735417175	3.9257382088
H	11.2952796394	-0.2169098941	3.4122214432
C	14.4601528474	-0.1577012991	6.133909775
H	14.2569840107	-0.9383262781	6.8841594615
H	15.377281468	0.365355164	6.4370578602
H	14.6544298874	-0.6603858207	5.1764359979
C	14.0549562417	2.5487715205	7.8091566956
H	13.8305174637	2.1258484801	8.8017422983

H	13.9611920476	3.6404338605	7.8867606613
H	15.1020419298	2.3127230365	7.5752669423
C	15.4473550393	1.0862106095	1.8813607174
H	16.0813793637	0.4180855116	1.2796797838
H	14.8423079368	1.6915348062	1.1895097622
H	14.7586390543	0.4635265194	2.4753034607
C	16.3192016875	1.9514918295	2.7929129146
H	16.9625994164	2.5992640406	2.1746566048
C	17.2086817523	1.107207795	3.710320814
H	17.8617990007	0.4617527889	3.1046989799
H	16.6011166939	0.4580469164	4.3582994535
H	17.8563896876	1.7238137304	4.3513150024
C	17.50095913	4.8016976406	4.0099145488
H	18.1189293522	5.407897768	4.6894729845
H	17.1650517537	5.4665995509	3.1997646085
H	18.1516744719	4.0270055612	3.5791885354
C	16.3146991972	4.2200075989	4.7776723703
H	16.6953104682	3.580163579	5.5937106001
C	15.4392587425	5.3140153922	5.3945890339
H	16.0317576261	5.9199355189	6.0957353311
H	14.5830058308	4.8899389512	5.9401204318
H	15.0438272745	5.9883215084	4.6178584712
C	14.1996300586	4.0294898523	2.6794328192
C	12.1632843372	4.6496872476	2.1596400517
C	13.030248411	5.230661144	1.2678679672
H	12.8493821984	5.884670997	0.4208652985
C	15.516401631	5.2188779905	0.8955287912
H	16.3395030924	4.5643982606	1.2014368456
H	15.7770251728	6.2616853316	1.1221175598
H	15.360721552	5.1098561513	-0.1849996885
C	10.6589498943	4.7219713775	2.2266285912
C	10.1021521783	3.3168964854	1.9401490045

H	10.3450560399	3.0021731211	0.9136379107
H	9.0071598035	3.3060409343	2.052684723
H	10.5312034648	2.5801038897	2.6337864476
C	10.25152199	5.1851581534	3.6339305263
H	10.6692749485	4.51582744	4.3989711152
H	9.1550330238	5.1917310402	3.7317764402
H	10.6194226706	6.2028812523	3.8356923793
C	10.1303655009	5.710734565	1.1816413928
H	10.3933465005	5.3982652297	0.1590495621
H	10.5233222317	6.7253107118	1.3505269097
H	9.0334289221	5.7639385209	1.2380139574

WB97XD/SDD:

Charge = 1 Multiplicity = 1

Ru	13.0614797269	2.4555190935	4.7008315666
P	15.2153830281	3.265247902	4.0040026571
N	14.3215877641	4.673316114	1.5122851379
N	12.9090726954	3.7860962314	2.9613729423
C	12.2948582706	2.4345164603	6.6727814031
C	11.2279619922	1.9744430665	5.803623503
C	11.7006777787	0.8150093249	5.1312437898
C	13.0467663701	0.5285853847	5.5961605354
C	13.390921975	1.5045939846	6.5855534792
C	12.2006807522	3.6082182304	7.5951782213
H	11.6240125428	3.3399104334	8.4951973598
H	11.6923000695	4.4555953927	7.11365054
H	13.1921802893	3.9467035297	7.9235340135
C	9.8450767392	2.5446623551	5.751963121
H	9.2021848524	2.028733615	6.4829600792
H	9.3862705582	2.431386989	4.7615883623
H	9.8380613741	3.6128415768	6.004743204
C	10.948849878	-0.0333859828	4.1546582932

H	10.705238563	-1.0055238384	4.6116005105
H	11.544371506	-0.2301481105	3.2511605079
H	10.0072695614	0.4365572659	3.8455582969
C	13.8490406315	-0.6713022243	5.202140029
H	13.5645410593	-1.5398279199	5.8176585684
H	14.9251869198	-0.5028408187	5.3413729261
H	13.6784439249	-0.9392054892	4.150123463
C	14.6412189362	1.5397219664	7.4093183526
H	14.4888370658	1.0082770151	8.3617096685
H	14.9380854955	2.5707845537	7.646227167
H	15.4800043403	1.0580354039	6.8896790213
C	15.9250620696	1.2052771703	2.2888492482
H	16.7142446324	0.5955828965	1.8245815493
H	15.3420193353	1.6760841273	1.482751371
H	15.2531614546	0.5313636542	2.8428266075
C	16.5505127332	2.2391548733	3.2264967285
H	17.1968892149	2.915932334	2.6440482618
C	17.3890215239	1.5858619676	4.3284962678
H	18.1869944453	0.9753861197	3.8807417609
H	16.7685120865	0.9217300756	4.9499582489
H	17.867766549	2.3255962745	4.9872395529
C	17.1612287463	5.3613147433	4.1938523568
H	17.6283681001	6.10711435	4.8546134099
H	16.7874469212	5.9023568021	3.310675079
H	17.9525425527	4.6687252739	3.8722863461
C	16.023235272	4.6594065369	4.9329244448
H	16.4324476603	4.1470269074	5.8217802375
C	14.9465688597	5.6436315644	5.3974912508
H	15.3894433941	6.3952705709	6.0670616645
H	14.1338313687	5.1336249973	5.9356522034
H	14.5004856685	6.1761076726	4.5420881215
C	14.2040313078	3.993916693	2.6692858967

C	12.1634707302	4.3738106119	1.9613521089
C	13.0422242352	4.9189415786	1.0587536945
H	12.8677802431	5.4576470638	0.1329046338
C	15.543538987	5.0625425429	0.8297380415
H	16.4034603987	4.6575350777	1.3734773876
H	15.625298769	6.1567753214	0.7893520214
H	15.5438845126	4.6580745373	-0.1907150158
C	10.6558321091	4.3885998766	1.9644886828
C	10.1480232415	2.938415923	1.9597806194
H	10.4449240251	2.419582013	1.0353122047
H	9.0493807629	2.9186108654	2.0264838218
H	10.5613023177	2.3808064492	2.8111962532
C	10.1899350664	5.1160911123	3.2371398273
H	10.6042864095	4.6363667947	4.1346902142
H	9.0917402149	5.0992646788	3.3086126935
H	10.5168518313	6.1671879105	3.2287422007
C	10.1338380381	5.1255554704	0.7262485132
H	10.4484113568	4.6283942273	-0.2046682062
H	10.4810449827	6.1701418535	0.700632411
H	9.0343932116	5.1431689816	0.7375005649

WB97XD/SDD with acetone pcm solvent model:

Charge = 1 Multiplicity = 1

Ru	13.0614797269	2.4555190935	4.7008315666
P	15.2153830281	3.265247902	4.0040026571
N	14.3215877641	4.673316114	1.5122851379
N	12.9090726954	3.7860962314	2.9613729423
C	12.2948582706	2.4345164603	6.6727814031
C	11.2279619922	1.9744430665	5.803623503
C	11.7006777787	0.8150093249	5.1312437898
C	13.0467663701	0.5285853847	5.5961605354
C	13.390921975	1.5045939846	6.5855534792

160

C	12.2006807522	3.6082182304	7.5951782213
H	11.6240125428	3.3399104334	8.4951973598
H	11.6923000695	4.4555953927	7.11365054
H	13.1921802893	3.9467035297	7.9235340135
C	9.8450767392	2.5446623551	5.751963121
H	9.2021848524	2.028733615	6.4829600792
H	9.3862705582	2.431386989	4.7615883623
H	9.8380613741	3.6128415768	6.004743204
C	10.948849878	-0.0333859828	4.1546582932
H	10.705238563	-1.0055238384	4.6116005105
H	11.544371506	-0.2301481105	3.2511605079
H	10.0072695614	0.4365572659	3.8455582969
C	13.8490406315	-0.6713022243	5.202140029
H	13.5645410593	-1.5398279199	5.8176585684
H	14.9251869198	-0.5028408187	5.3413729261
H	13.6784439249	-0.9392054892	4.150123463
C	14.6412189362	1.5397219664	7.4093183526
H	14.4888370658	1.0082770151	8.3617096685
H	14.9380854955	2.5707845537	7.646227167
H	15.4800043403	1.0580354039	6.8896790213
C	15.9250620696	1.2052771703	2.2888492482
H	16.7142446324	0.5955828965	1.8245815493
H	15.3420193353	1.6760841273	1.482751371
H	15.2531614546	0.5313636542	2.8428266075
C	16.5505127332	2.2391548733	3.2264967285
H	17.1968892149	2.915932334	2.6440482618
C	17.3890215239	1.5858619676	4.3284962678
H	18.1869944453	0.9753861197	3.8807417609
H	16.7685120865	0.9217300756	4.9499582489
H	17.867766549	2.3255962745	4.9872395529
C	17.1612287463	5.3613147433	4.1938523568
H	17.6283681001	6.10711435	4.8546134099

H	16.7874469212	5.9023568021	3.310675079
H	17.9525425527	4.6687252739	3.8722863461
C	16.023235272	4.6594065369	4.9329244448
H	16.4324476603	4.1470269074	5.8217802375
C	14.9465688597	5.6436315644	5.3974912508
H	15.3894433941	6.3952705709	6.0670616645
H	14.1338313687	5.1336249973	5.9356522034
H	14.5004856685	6.1761076726	4.5420881215
C	14.2040313078	3.993916693	2.6692858967
C	12.1634707302	4.3738106119	1.9613521089
C	13.0422242352	4.9189415786	1.0587536945
H	12.8677802431	5.4576470638	0.1329046338
C	15.543538987	5.0625425429	0.8297380415
H	16.4034603987	4.6575350777	1.3734773876
H	15.625298769	6.1567753214	0.7893520214
H	15.5438845126	4.6580745373	-0.1907150158
C	10.6558321091	4.3885998766	1.9644886828
C	10.1480232415	2.938415923	1.9597806194
H	10.4449240251	2.419582013	1.0353122047
H	9.0493807629	2.9186108654	2.0264838218
H	10.5613023177	2.3808064492	2.8111962532
C	10.1899350664	5.1160911123	3.2371398273
H	10.6042864095	4.6363667947	4.1346902142
H	9.0917402149	5.0992646788	3.3086126935
H	10.5168518313	6.1671879105	3.2287422007
C	10.1338380381	5.1255554704	0.7262485132
H	10.4484113568	4.6283942273	-0.2046682062
H	10.4810449827	6.1701418535	0.700632411
H	9.0343932116	5.1431689816	0.7375005649

WB97XD/SDD preoptimized with acetone pcm solvent model:

Charge = 1 Multiplicity = 1

Ru	13.0596598965	2.4155378372	4.6724594435
P	15.2099039857	3.2685807661	3.9990955962
N	14.3122671792	4.719657038	1.5363681603
N	12.9019463824	3.7809846094	2.9546140656
C	12.314545436	2.4525060083	6.645871663
C	11.2362963162	1.9739245065	5.7994124963
C	11.6963404038	0.7956804309	5.151857963
C	13.0443795117	0.5108992396	5.6134406613
C	13.4026253595	1.5092180441	6.5746877677
C	12.2406931281	3.6460966735	7.5447341604
H	11.702399004	3.3940572095	8.4728993347
H	11.7068494963	4.4766789103	7.0615142581
H	13.2421510849	4.0000046929	7.8232546684
C	9.8560409665	2.5504161759	5.7437594939
H	9.2102994894	2.0425173718	6.4782171576
H	9.3967337044	2.4324653142	4.7540280843
H	9.856690035	3.6200182021	5.9905735978
C	10.9331506063	-0.0667456389	4.1961637782
H	10.6742103865	-1.0237858503	4.6762692251
H	11.5295883677	-0.2956034289	3.3008350345
H	10.0001009406	0.4114378075	3.8729749534
C	13.8415411412	-0.6964104206	5.2312408733
H	13.552607293	-1.559064869	5.8532937145
H	14.917789478	-0.5284495474	5.3688430095
H	13.6711417388	-0.9702285868	4.1806892625
C	14.6602279035	1.5636938439	7.3862727474
H	14.5001765676	1.0950266752	8.3701733329
H	14.9828093329	2.6002132125	7.5565641991
H	15.4840650323	1.0317710622	6.8927349943
C	15.9002084129	1.226035608	2.2590015289
H	16.6860434357	0.6087970901	1.7988738147

H	15.3381480363	1.7183010064	1.4512722994
H	15.2101106983	0.5576806319	2.7981805877
C	16.5347728463	2.2375129022	3.2145561851
H	17.1945156276	2.9121335801	2.6462256748
C	17.3517182098	1.5547460763	4.3145532325
H	18.1542498562	0.9534518438	3.8624448275
H	16.7177284032	0.8782377787	4.9082782527
H	17.8198220287	2.2770445649	4.9995588289
C	17.2120927455	5.2975888417	4.2560926389
H	17.6580574913	6.0488654781	4.9254671522
H	16.9044935018	5.8196508288	3.3375124014
H	18.0004004007	4.5753590732	3.9997640875
C	16.017673924	4.6452153292	4.9501641329
H	16.3668109611	4.1315152363	5.8628445005
C	14.9545635929	5.6716435821	5.3499070878
H	15.3902586604	6.4052856488	6.0438265905
H	14.0926888653	5.1972974589	5.8419808997
H	14.5846715818	6.2187657077	4.4679785451
C	14.1962878761	4.012535228	2.674770025
C	12.1574409693	4.3811375452	1.9623778406
C	13.0351200179	4.9595752262	1.0790610009
H	12.8644648096	5.5161873531	0.1633360679
C	15.5352711175	5.163951299	0.8876923454
H	16.3916262124	4.6720530247	1.3601700486
H	15.6394359746	6.2523997136	0.9823913336
H	15.5059837491	4.8868264822	-0.1728196919
C	10.6494154317	4.3688773721	1.9561638958
C	10.1661593116	2.9102271335	1.9566572472
H	10.4745951894	2.3953144902	1.0334386186
H	9.067936041	2.8699820725	2.0256268052
H	10.5901570511	2.3625373358	2.8093362615
C	10.162246128	5.0942806216	3.2220314032

H	10.5957731709	4.638256324	4.1227416148
H	9.0651182484	5.0413197914	3.29875307
H	10.4574230827	6.1549166656	3.1998399634
C	10.119915282	5.0894432011	0.7117418694
H	10.4552924186	4.595827037	-0.2136887891
H	10.4483433425	6.140038919	0.6840047508
H	9.019735128	5.0825876075	0.7176473534

Cp‡Ru(iPr2PIm')+ (3.15)

B3LYP/LANL2DZ:

Charge = 1 Multiplicity = 1

Ru	15.5590477497	3.6774696473	12.6479767057
P	13.2563627881	3.8495130183	13.4418439267
F	16.489218422	7.9415869757	13.0286092692
F	14.524678597	7.0198392719	12.9527637151
F	15.706139648	6.9112927054	14.774675805
N	12.4226825114	1.0061361771	12.948816351
N	14.4226293455	1.7699967226	12.3482874416
C	17.1951612661	4.6330298427	13.6867945664
C	13.1078225302	-0.0309019452	12.345910134
H	12.6551796897	-1.0113969683	12.2410476345
C	17.8256536033	3.7328954993	12.7249527395
C	13.2419076796	2.086010382	12.9294373823
C	16.5179899129	5.2473519461	11.5295526777
C	17.4171036872	4.1055623678	11.4190683118
C	14.3483404464	0.4362938839	11.9673550964
C	11.9754655272	4.7960944249	12.4327591311
H	12.2665713519	5.8400362591	12.6426952613
C	16.4399306178	5.6006242781	12.9281782581
C	12.1792144064	4.5308133198	10.9347743901
H	13.2166691566	4.7130169924	10.6177421287

165

H	11.5243355523	5.1964392772	10.3502298933
H	11.9187346933	3.4925363461	10.6705154393
C	12.7350879936	3.9337190086	15.2480459886
H	11.7028297355	3.5454294167	15.2925641245
C	15.4506954302	-0.3240032521	11.2563355056
C	12.7332476268	5.3914916481	15.7334029479
H	13.73363136	5.8420391579	15.6587911014
H	12.4252841271	5.4236745049	16.7906854774
H	12.0332414856	6.0251776584	15.1680833116
C	11.0768207976	0.8986491736	13.5030994156
H	10.347285498	0.7135942992	12.7011583377
H	10.8181966177	1.8312579711	14.015114791
H	11.0376671284	0.0707716457	14.2252061383
C	15.7527560388	0.3702230688	9.9109889815
H	14.8721708065	0.3489125643	9.249250628
H	16.5787522159	-0.1431586481	9.3935354397
H	16.0393826351	1.4202591961	10.0610482657
C	18.808402376	2.6648389285	13.0955374059
H	18.469008969	2.073360626	13.9584123765
H	19.7713554106	3.1263850685	13.376307833
H	19.0022753338	1.9752980339	12.2642237611
C	15.7936368926	6.8581146304	13.4256069142
C	17.8837408676	3.5179721003	10.1231802324
H	18.2502461116	2.4902189829	10.2416791655
H	18.7132504864	4.1232313658	9.7167417744
H	17.0867132436	3.5107887697	9.3662046242
C	15.9782158831	6.0316867432	10.3726575103
H	15.6987188549	5.3754097321	9.536114112
H	16.7507860903	6.7291519667	10.0029027465
H	15.1029404961	6.627769763	10.6564285981
C	13.6385038148	3.043723707	16.1109106864
H	13.6258718309	1.9911928883	15.7871240471

H	13.2967545427	3.0759278412	17.1578992021
H	14.6828185194	3.3939019789	16.0877935242
C	16.7107684282	-0.3424845131	12.1462229956
H	17.0382085137	0.6773223604	12.3891963523
H	17.5358717697	-0.8580823629	11.6294425406
H	16.5185432432	-0.8729409345	13.0926802537
C	17.4849679616	4.6142241922	15.1574731263
H	16.6795118669	5.0641801774	15.7468467284
H	18.4064294495	5.1875357087	15.3649084773
H	17.6520086299	3.58715475	15.511568493
C	15.0012744415	-1.772103071	10.987912018
H	14.7821202226	-2.3117438503	11.9231182791
H	15.8033634837	-2.320869311	10.4716372234
H	14.1081721789	-1.8101598603	10.343973591
C	10.5122045936	4.59537079	12.8468902073
H	10.1575884809	3.5783315379	12.6150213445
H	9.8761848059	5.2925474448	12.2773663892
H	10.3332535275	4.793865978	13.9136207531

B3LYP/SDD:

Charge = 1 Multiplicity = 1

Ru	15.5522136425	3.6740138309	12.6545947663
P	13.2674081438	3.8543713003	13.4664764667
F	16.5228369653	7.9328562129	12.9849840212
F	14.5456739435	7.0519543888	12.8011119745
F	15.6170116618	6.9323156143	14.6892276325
N	12.4451811565	1.0030942423	12.9786038382
N	14.4245980247	1.7923129648	12.3424016782
C	17.1591670501	4.645603082	13.7054058805
C	13.1271668735	-0.0207534603	12.3492325232
H	12.6816433403	-1.0042853686	12.2428609634
C	17.7981010284	3.7072359729	12.7887197784

C	13.2521960946	2.0907303584	12.9523657592
C	16.5378050796	5.1943396412	11.5114048856
C	17.4261562814	4.040684073	11.4595404845
C	14.3535020062	0.461470063	11.9457419412
C	11.9752519158	4.7945171341	12.464702065
H	12.2395329761	5.8408523807	12.6982183824
C	16.4289823905	5.5927246899	12.8974533728
C	12.198217513	4.5650741106	10.9636034581
H	13.2336942801	4.7792008711	10.6613269335
H	11.5321940936	5.2257970551	10.3865584895
H	11.9667903726	3.5259910813	10.6764673628
C	12.7494930733	3.9366677527	15.2744488166
H	11.7263530952	3.5252226185	15.3203689501
C	15.4345449376	-0.2775629564	11.1819762851
C	12.7122234336	5.3952389142	15.7568256092
H	13.6972362398	5.876805217	15.6697087405
H	12.4160109293	5.4204696587	16.8176498242
H	11.9860300542	6.0061467078	15.1994937616
C	11.1145175879	0.873911121	13.564726124
H	10.3757105515	0.6460919014	12.7827538089
H	10.8392128591	1.8135325728	14.0545383581
H	11.1126151434	0.0658863357	14.3101745075
C	15.6491936148	0.4222389159	9.8220617808
H	14.7367007059	0.3754159456	9.2065135747
H	16.4614855799	-0.0691007923	9.2631847257
H	15.9139202805	1.4801020235	9.9571282984
C	18.7625569893	2.6440653221	13.2196021735
H	18.3802205463	2.0579070364	14.0683185811
H	19.7076728003	3.111415477	13.5463985888
H	19.0024230236	1.9489665542	12.405374061
C	15.7816444304	6.8669356994	13.3468691436
C	17.930956133	3.411282663	10.19709889

H	18.246488294	2.3707772935	10.3488489992
H	18.8048349987	3.973694121	9.8237954638
H	17.1737441625	3.4243954578	9.4006794218
C	16.0327535275	5.9407878626	10.3138279407
H	15.7576617077	5.2545770973	9.4999642075
H	16.8249424256	6.6077734724	9.9300032331
H	15.1634142189	6.5636715329	10.5550959236
C	13.6715311568	3.0679840491	16.1397064871
H	13.6902663924	2.0171390581	15.8106421879
H	13.3218104986	3.0858018475	17.1842108187
H	14.7057547917	3.4460754533	16.1250286675
C	16.7391910077	-0.2686922855	12.0037368607
H	17.0572772723	0.7581832683	12.226038167
H	17.5456078496	-0.7697174173	11.4451081889
H	16.6080200899	-0.7991935371	12.9605185483
C	17.4285191784	4.6772796564	15.1804052307
H	16.6130356178	5.1396988235	15.7457989874
H	18.3432195614	5.2632855736	15.3811167704
H	17.5979232818	3.663310708	15.5691800923
C	15.0022502153	-1.7350772714	10.936985306
H	14.8390103995	-2.2768754391	11.8823265357
H	15.7901339018	-2.2678904741	10.3835369635
H	14.0809270388	-1.7933884724	10.3357996819
C	10.5138130029	4.5507374462	12.8619944108
H	10.1845655358	3.5324287968	12.6000808165
H	9.8662769781	5.2482270664	12.3060996225
H	10.3225800516	4.7166673856	13.9321532054

CAM-B3LYP/LANL2DZ:

Charge = 1 Multiplicity = 1

Ru	15.5613716335	3.6646312317	12.664559152
P	13.2705583762	3.8467479833	13.4691816588

F	16.4281157104	7.9164829447	12.9285056149
F	14.4991778823	6.9515166567	12.8377476824
F	15.6345655819	6.9253995113	14.6781540668
N	12.4464154198	1.0143612614	12.9786111417
N	14.4153237339	1.793739016	12.3425626366
C	17.1606174611	4.6464910106	13.7058098445
C	13.119910761	-0.0084267418	12.3485571777
H	12.6726481232	-0.9909323304	12.2427714962
C	17.7975539127	3.7111849702	12.7964463337
C	13.2533496552	2.0923630888	12.9508154461
C	16.5390285264	5.1829997519	11.5239670318
C	17.4242962143	4.0370110223	11.4736338348
C	14.3398894822	0.4709406939	11.9461997557
C	12.0056312087	4.7811244605	12.4697360262
H	12.2625127559	5.8269659435	12.7057429814
C	16.4333095985	5.5829126786	12.9001421652
C	12.2461030931	4.5559776227	10.9768879171
H	13.2829291539	4.7788820953	10.6889520088
H	11.5826999255	5.2103809555	10.3923351546
H	12.0268278712	3.516238304	10.6867581678
C	12.7582297364	3.9317277132	15.25609829
H	11.7320979709	3.5341933174	15.3157625503
C	15.422673918	-0.2550329264	11.1839210918
C	12.7451792635	5.3884124844	15.7267411609
H	13.7336564831	5.8561742007	15.6167598494
H	12.4689249879	5.4274589009	16.7908091752
H	12.0177459315	6.0018448648	15.1758383479
C	11.1189951601	0.8968055684	13.561035058
H	10.3709664606	0.7274196268	12.7747292601
H	10.8731123868	1.8188912422	14.0960797585
H	11.097594835	0.0571065586	14.2679038626
C	15.6224687936	0.4415410181	9.829189438

H	14.7090279641	0.3831260586	9.2182855835
H	16.4375876168	-0.0402332142	9.2683749746
H	15.8753913705	1.5017310033	9.9624969783
C	18.753245626	2.6465242814	13.2295405143
H	18.3584935824	2.0551682682	14.0671610301
H	19.6937363551	3.109224228	13.5693534787
H	18.9987664066	1.9582054193	12.4128355698
C	15.7530022917	6.837239774	13.3409603679
C	17.9172573207	3.3976593365	10.2161190149
H	18.2133226784	2.3532622616	10.3721085333
H	18.7984493582	3.9434079051	9.8411155856
H	17.158517212	3.4201607826	9.4231732151
C	16.0168691263	5.9222341717	10.3343391786
H	15.7359214503	5.2329078643	9.5269668162
H	16.7970680341	6.5947580873	9.9420953605
H	15.1454744629	6.5355878676	10.5886463824
C	13.6765011105	3.0630969497	16.1148817355
H	13.6764908842	2.0099261489	15.7962474186
H	13.3439490122	3.0954951323	17.1630805342
H	14.7141633099	3.4280484541	16.0805468922
C	16.7236731441	-0.2231938767	11.9961382949
H	17.0285059375	0.8090645034	12.2087783062
H	17.5334922558	-0.7168675377	11.4380794013
H	16.6037627524	-0.7477190533	12.9563123687
C	17.4135531775	4.6751952933	15.1796536084
H	16.5879605581	5.1319309739	15.732773082
H	18.3212463112	5.2635928734	15.3929297662
H	17.5807456963	3.6611859324	15.5656634218
C	15.0078753696	-1.710849526	10.9480812581
H	14.8542712646	-2.248348867	11.8960647125
H	15.7976766444	-2.2373850838	10.3936749011
H	14.0852339243	-1.7801506062	10.3522895505

C	10.5477113422	4.5283639016	12.8488910083
H	10.233702188	3.5060091213	12.5888611243
H	9.899639991	5.2151087051	12.2836888196
H	10.3448322618	4.6963977664	13.9157460745

CAM-B3LYP/SDD:

Charge = 1 Multiplicity = 1

Ru	15.551739215	3.6637835348	12.6578142908
P	13.2807571171	3.8534659015	13.4802837007
F	16.442935918	7.9089578864	12.9079990631
F	14.5053153309	6.9702738635	12.7374914426
F	15.5655656894	6.9243873157	14.6214089315
N	12.4575146811	1.0178808919	12.9869584441
N	14.4184663472	1.809253813	12.339865593
C	17.1309984212	4.6495258578	13.7052828779
C	13.1318142315	0.0011237252	12.347161446
H	12.6885016047	-0.9828920023	12.2392124843
C	17.7697305125	3.6936433446	12.820581073
C	13.257907387	2.0994897258	12.9578908124
C	16.5403326336	5.1520951075	11.5040187557
C	17.4177725611	3.9997608932	11.4853929696
C	14.3462253654	0.4866696651	11.9372168812
C	12.0050607581	4.7903812846	12.4967241628
H	12.2402654466	5.8348032468	12.760499074
C	16.4173787793	5.575246879	12.8729384435
C	12.2582581312	4.6082609501	11.0001314159
H	13.2914036103	4.8617148502	10.7256192423
H	11.5834918232	5.2617059808	10.4280682105
H	12.0649026942	3.5712145098	10.6830817848
C	12.7775598588	3.9267345779	15.2712993862
H	11.7607843839	3.5061813448	15.3326283026
C	15.421512848	-0.232720478	11.1587365851

172

C	12.7314751775	5.3802929913	15.7496027515
H	13.7050709678	5.8766083139	15.6323475916
H	12.4654745252	5.4058938839	16.8167047103
H	11.9811100561	5.9760683437	15.2103102641
C	11.1361113731	0.8884029128	13.5810196025
H	10.3859402429	0.6974120427	12.8018747759
H	10.8797537087	1.8139220194	14.104858231
H	11.132233744	0.0577910081	14.298919708
C	15.6020289395	0.4730215421	9.8059646659
H	14.6822624418	0.4115156725	9.2049489513
H	16.4143543958	0.0004793344	9.2334974198
H	15.8484020182	1.533993665	9.943397039
C	18.713545208	2.6313084949	13.2857485749
H	18.2970266715	2.0465735984	14.1175118496
H	19.6450222092	3.0962882586	13.6460237787
H	18.9797937264	1.9370750996	12.4807229619
C	15.737071583	6.8374067366	13.2890816806
C	17.9337025633	3.3430553163	10.2455520768
H	18.2135477517	2.2966475576	10.4169109538
H	18.8302327451	3.8751846924	9.8882141862
H	17.195493	3.3680606111	9.4336844054
C	16.0411063198	5.869618243	10.2905401486
H	15.7443652952	5.1631566382	9.5036555267
H	16.8410344715	6.5070287118	9.8801166997
H	15.1861512672	6.5147700931	10.5205224274
C	13.7167846886	3.0732885874	16.1229480971
H	13.7418423371	2.0232305733	15.7950658292
H	13.383823977	3.0889956869	17.1711958663
H	14.745225236	3.4625989327	16.0905965999
C	16.7312078637	-0.203148267	11.9565076519
H	17.0301058227	0.8280283396	12.1801699869
H	17.5380176053	-0.6836101719	11.3829372392

H	16.6252457218	-0.7414630969	12.9106432728
C	17.3776895143	4.7072495491	15.1801394562
H	16.5568477192	5.1861601874	15.7214725142
H	18.2923438446	5.2879536714	15.3838176373
H	17.5304778935	3.6997675988	15.5888338362
C	15.0074061675	-1.6880842948	10.9186695859
H	14.8654835964	-2.2317695876	11.8649256334
H	15.793030077	-2.2087767195	10.3529759695
H	14.0789672345	-1.7564303934	10.3319007739
C	10.5502390842	4.5006114988	12.861384845
H	10.2557271741	3.4818056249	12.5670279136
H	9.8923975007	5.1935864576	12.3155030415
H	10.3402311899	4.630887372	13.9321478949

WB97XD/LANL2DZ:

Charge = 1 Multiplicity = 1

Ru	15.535907114	3.6712124036	12.6489411284
P	13.280704905	3.8468633104	13.5085014576
F	16.3966359381	7.9098193457	12.6126867222
F	14.4694106919	6.9380827968	12.6339907811
F	15.617297334	7.1006140747	14.4581926118
N	12.4772415441	0.9989241519	13.0655844341
N	14.3819560166	1.8295845254	12.3155856571
C	17.0645147533	4.6854257357	13.7284624554
C	13.130186244	-0.0007414654	12.3760215662
H	12.700642647	-0.9930592677	12.2838626482
C	17.721883309	3.6746696882	12.9179455821
C	13.2565695222	2.0949592099	12.9993765143
C	16.5914575952	5.0949181885	11.4797094979
C	17.4466391806	3.927840758	11.550558168
C	14.3107364654	0.5158062961	11.9030780905
C	11.9912738012	4.7390629268	12.5155126275

H	12.1563700872	5.7916581746	12.8001827367
C	16.4118398509	5.5858091359	12.8214503486
C	12.3079270304	4.5881683542	11.0258844218
H	13.3334878378	4.9123945876	10.7975312734
H	11.6132366074	5.2017826597	10.4337426014
H	12.1977679168	3.542278099	10.6966092996
C	12.8229113763	3.947338371	15.300677153
H	11.7852391771	3.5891206585	15.4027886521
C	15.373573551	-0.1369031336	11.0559039122
C	12.8840896484	5.4099764546	15.7510176933
H	13.8835848838	5.8376876327	15.5847936054
H	12.6580175778	5.4772100177	16.8253443012
H	12.1544746783	6.038652401	15.2195580956
C	11.2031157193	0.8549490239	13.7496444705
H	10.3997163857	0.6694353701	13.0245476637
H	10.985724299	1.776793516	14.2990835246
H	11.2564454425	0.0197450965	14.459756998
C	15.4967488629	0.660135505	9.7459658476
H	14.5597724258	0.614727387	9.1700296433
H	16.303231502	0.2476952956	9.1206008607
H	15.7203349416	1.7169794568	9.9495204837
C	18.5953998039	2.5972996691	13.4779773707
H	18.0832008735	2.0309745507	14.2690566404
H	19.4980578744	3.0462391802	13.9211752838
H	18.9178044772	1.8898939704	12.7049918707
C	15.7247478986	6.8784373958	13.1379138423
C	18.0196456012	3.2083800222	10.370899506
H	18.1638802717	2.138813157	10.5675823519
H	18.9997668886	3.6413656862	10.1150089826
H	17.3763339145	3.3051059664	9.4868080382
C	16.1215932149	5.7451855759	10.217677819
H	15.8165913589	4.9922795455	9.4779913529

H	16.9392689062	6.3395515307	9.7798802335
H	15.2758329484	6.4180552941	10.3988782781
C	13.7493018282	3.0449195557	16.1170934111
H	13.6731981156	1.9891304897	15.8149832451
H	13.4888426948	3.1100720838	17.1838714651
H	14.7997486627	3.3546050259	16.0034745778
C	16.7029466784	-0.1082417734	11.8247617162
H	16.9661672129	0.9220305334	12.098576425
H	17.5127844806	-0.5256059783	11.2067366636
H	16.6376834516	-0.7006024809	12.7503963568
C	17.2171317562	4.7969078399	15.213263463
H	16.3440489161	5.2606642821	15.6829168033
H	18.0955110327	5.4167057103	15.454333926
H	17.3735267803	3.8063478566	15.6604945275
C	14.983285058	-1.58623511	10.7463523199
H	14.888191508	-2.1854438164	11.6653890864
H	15.7563415646	-2.057386955	10.1220803476
H	14.0325613993	-1.6395859379	10.1935289943
C	10.5521135946	4.3446591209	12.8416763487
H	10.3465047254	3.307389094	12.5342528095
H	9.8562791403	4.9911387472	12.2861437503
H	10.3126405044	4.4507334259	13.9100886639

WB97XD/SDD:

Charge = 1 Multiplicity = 1

Ru	15.5320455344	3.667676314	12.6501916939
P	13.290179821	3.8522900137	13.5099543929
F	16.4064851619	7.901857036	12.6116149095
F	14.4694308009	6.948321833	12.6037627424
F	15.5926626823	7.0955882173	14.4438901224
N	12.4857851273	1.0027374454	13.0621811672
N	14.3914218556	1.838231601	12.3187581249

C	17.0513415778	4.6829117351	13.7283071758
C	13.1413966634	0.0065082924	12.3693819263
H	12.7128562004	-0.9856299802	12.2713224396
C	17.7041703516	3.6647403876	12.9245011036
C	13.263098921	2.0993265636	13.0017851837
C	16.5787621779	5.0782066065	11.4744271028
C	17.4334971844	3.9114959283	11.5536276177
C	14.3220510592	0.5248758307	11.9000458333
C	11.9967766861	4.7438185915	12.5202040114
H	12.170967836	5.7978911928	12.7940992552
C	16.398742027	5.5778606728	12.8141344216
C	12.2984440318	4.5776236951	11.0288921342
H	13.3250879621	4.8886694121	10.7875485833
H	11.6043956602	5.1927782702	10.4380831321
H	12.1755502725	3.5298983505	10.7099160011
C	12.8334695276	3.9492813135	15.302990702
H	11.7983162862	3.5829256255	15.4015805407
C	15.3830625025	-0.1264537189	11.0500493328
C	12.8814265214	5.4110362696	15.7574210237
H	13.8782988944	5.8471797291	15.5985931323
H	12.6487505515	5.4731805503	16.8306432789
H	12.1499920858	6.0357624045	15.2237849744
C	11.2094615088	0.8546252262	13.7414273135
H	10.4083699253	0.6747827846	13.0123886824
H	10.990894308	1.7723930016	14.2972132848
H	11.2603618196	0.0140830939	14.4453315806
C	15.5085473678	0.6786351588	9.7453728346
H	14.5728246308	0.6350212809	9.1672524312
H	16.3170997964	0.2712869416	9.1194079965
H	15.7294482923	1.734391611	9.955998058
C	18.5752088972	2.5890803236	13.4932841221
H	18.0541301083	2.018457839	14.2755068736

H	19.4701518617	3.0396368833	13.9498382855
H	18.9108162607	1.8852830287	12.7226026168
C	15.7177370882	6.8748375063	13.1246357598
C	18.0161583635	3.1904006432	10.3792221818
H	18.1635381863	2.121987728	10.5789908743
H	18.9960873128	3.6267816602	10.1289528282
H	17.3787712889	3.2832577549	9.4905126256
C	16.1128665233	5.7204563753	10.2060437958
H	15.8114577425	4.9622070397	9.4701823996
H	16.9311978155	6.3127370301	9.7668524852
H	15.2652525612	6.3933560441	10.378752768
C	13.7636177462	3.0508253289	16.11968339
H	13.698586218	1.996077565	15.8113942147
H	13.4966427011	3.1082241606	17.1851317693
H	14.8117543961	3.3697298789	16.0130648716
C	16.7106235769	-0.109133128	11.8219633297
H	16.9729289315	0.9165478094	12.1118725792
H	17.5218934178	-0.5181072734	11.2003209387
H	16.6423118989	-0.7149009206	12.7386766225
C	17.2082730139	4.8037604344	15.2124803162
H	16.341865782	5.2798520968	15.6819057273
H	18.0941315312	5.4151481999	15.4469268266
H	17.355059648	3.8145940223	15.6661855682
C	14.9877152075	-1.5723167066	10.7304309035
H	14.8891743535	-2.1774429428	11.6452135721
H	15.7606987415	-2.0416008171	10.1046869004
H	14.0380225383	-1.618978632	10.1752663893
C	10.5578453613	4.3625507028	12.8634253538
H	10.3407381087	3.3241474561	12.568081131
H	9.8621553383	5.0092719125	12.3080450223
H	10.3287138659	4.4808617149	13.9326827162

<u>WB97XD/SDD with THF pcm solvent model: (also used this optimized geometry for CEP-121G calc)</u>

Charge = 1 Multiplicity = 1

Ru	15.5317340664	3.678300008	12.6506363177
P	13.2817845886	3.8563257283	13.5088971992
F	16.4699251658	7.909606585	12.6257964531
F	14.5131246764	7.0009841505	12.566881798
F	15.596924811	7.1096194327	14.4325460706
N	12.4933311922	1.0045937906	13.0820161127
N	14.3890657278	1.8454427791	12.3185471259
C	17.0509242779	4.6869809528	13.731324024
C	13.1444066578	0.0097458145	12.3858015028
H	12.7149224391	-0.9824512001	12.2948188009
C	17.7008147515	3.6638239587	12.9333538427
C	13.2650439635	2.1027691311	13.0105075216
C	16.5869802247	5.075527868	11.4720832347
C	17.436049794	3.9061754026	11.560212967
C	14.3185422432	0.5317441227	11.903493076
C	11.9812073942	4.7315253833	12.5144055551
H	12.1241443143	5.7869491703	12.8008345738
C	16.4051746081	5.5820468138	12.8105187618
C	12.2990086471	4.5846390878	11.0244503038
H	13.3170257243	4.9265348349	10.7891866388
H	11.5887829292	5.182863381	10.435269221
H	12.2060812531	3.5354329991	10.7008984469
C	12.8335992711	3.955553983	15.3034147357
H	11.7985045453	3.5927573152	15.4068581335
C	15.3736918794	-0.1135768962	11.0417542962
C	12.8901547241	5.414668611	15.7632523511
H	13.8911063667	5.8431063078	15.6091888266
H	12.6558515513	5.4705460845	16.8365114679
H	12.1632018968	6.0449886445	15.2303161331

179

C	11.2276381097	0.8512468265	13.7818444773
H	10.4263550534	0.6301467269	13.0659935376
H	10.9951285589	1.7813475468	14.3094627587
H	11.3082694024	0.0367032325	14.5117793768
C	15.4977717586	0.7049641238	9.7453662305
H	14.5614707704	0.6623736946	9.1676937895
H	16.3102507872	0.3084587913	9.1172219045
H	15.7126246668	1.759666206	9.9666823702
C	18.559827446	2.5827854526	13.5102335604
H	18.0253500898	2.0143516527	14.2849598149
H	19.4505686323	3.0289639649	13.9789360437
H	18.9005177294	1.8797670304	12.7409990711
C	15.743839246	6.8864840548	13.1149422368
C	18.0178821045	3.1768177552	10.3905953413
H	18.1569188633	2.1081773188	10.5947016631
H	19.001816187	3.6059414892	10.1436179209
H	17.38358654	3.2720300359	9.5000066008
C	16.1272431221	5.7098801321	10.1975745299
H	15.8245362439	4.9449203688	9.4695679349
H	16.9491398524	6.2938297555	9.75394976
H	15.279641815	6.384589506	10.3625826255
C	13.7650190636	3.0517515899	16.1127744332
H	13.6863771925	1.9976455613	15.80681542
H	13.5045041754	3.1147687022	17.1795217728
H	14.8147222862	3.3626943527	15.997387294
C	16.7048292614	-0.1105745638	11.807476107
H	16.9693898804	0.9098221861	12.1130540435
H	17.5141224785	-0.5086400382	11.1760673445
H	16.6370889171	-0.7299942352	12.7152695414
C	17.2005050953	4.8125111499	15.2156962126
H	16.3223455259	5.2714693146	15.681012589
H	18.0758090874	5.4379991101	15.4527022453

H	17.3606857017	3.8256785734	15.6694292419
C	14.9714127379	-1.5537694328	10.7065250115
H	14.8754504814	-2.1683522191	11.6151987458
H	15.7392119731	-2.0160482017	10.0685910195
H	14.0156045193	-1.5878571321	10.1610740397
C	10.5484844178	4.3093451712	12.8351171057
H	10.3621615812	3.2729547076	12.5139370765
H	9.8460265663	4.9531350256	12.2847387581
H	10.3063623935	4.3981904686	13.904024957

Ru-P and Ru-X bond distances

Table 3.9. Calculated Ru-P and Ru-Cl bond distances for complex **3.10**

3.10		Ru-P bond distance (Å)	Ru-Cl bond distance (Å)	Sum of Diff
Crystal structure		2.370/2.358	2.358/2.371	
Functional	**Basis set for Ru**			
B3LYP	LANL2DZ	2.455	2.411	0.133
CAM-B3LYP	LANL2DZ	2.440	2.396	0.098
CAM-B3LYP	SDD	2.419	2.371	0.052
WB97XD	LANL2DZ	2.408	2.403	0.073
WB97XD	**SDD**	**2.394**	**2.378**	**0.034**

Table 3.10. Calculated Ru-P and Ru-N bond distances for complex **3.15**

3.15		Ru-P bond distance (Å)	Ru-N bond distance (Å)	Sum of Diff
Crystal structure		2.390	2.150	
Functional	**Basis set for Ru**			
B3LYP	LANL2DZ	2.442	2.241	0.142
B3LYP	SDD	2.432	2.216	0.107
CAM-B3LYP	LANL2DZ	2.435	2.218	0.112
CAM-B3LYP	SDD	2.423	2.197	0.079
WB97XD	LANL2DZ	2.420	2.199	0.078
WB97XD*	LANL2DZ	2.426	2.204	0.090
WB97XD	**SDD**	**2.408**	**2.181**	**0.049**

Table 3.11. Calculated Ru-P and Ru-N bond distances for complex **3.14**

3.14		Ru-P bond distance (Å)	Ru-N bond distance (Å)	Sum of Diff
Crystal structure		2.386	2.242	
Functional	**Basis set for Ru**			
B3LYP	LANL2DZ	2.465	2.261	0.098
B3LYP	SDD	2.437	2.230	0.063
B3LYP	CEP-121G	2.473	2.266	0.111
CAM-B3LYP	**LANL2DZ**	**2.444**	**2.238**	**0.062**
CAM-B3LYP	SDD	2.425	2.216	0.065
WB97XD	LANL2DZ	2.433	2.212	0.077
WB97XD	SDD	2.404	2.195	0.065
WB97XD**	SDD	2.409	2.200	0.065

**Optimized with solvent model – acetone

NMR

Table 3.12. Calculated ^{1}H and ^{15}N NMR chemical shifts for complex **3.15**

3.15		Im-CH$_3$	N-CH$_3$	iPr-H	Cp-CH$_3$	iPr-CH$_3$	tBu	Sum of Diff	^{15}N-B	^{15}N-NB	Sum of Diff
Actual		7.40	3.71	2.98	1.78	1.20	1.62	N/A	-155.8	-204.2	N/A
Funct	**Basis set Ru**										
CAM-B3LYP	LANL2DZ	7.37	3.94	3.13	2.44	1.73	2.18	2.16	-135.7	-205.7	21.6
CAM-B3LYP	SDD	7.37	3.97	3.18	2.41	1.77	2.20	2.27	-135.7	-206.5	22.4
WB97XD	**LANL2DZ**	**7.37**	**3.82**	**2.94**	**2.35**	**1.61**	**2.17**	**1.71**	-138.4	-208.0	21.2
WB97XD	SDD	7.37	3.86	3.00	2.32	1.67	2.18	1.85	-138.2	-208.8	22.2
WB97XD*	**SDD**	7.50	3.91	3.08	2.32	1.61	2.17	2.04	**-140.9**	**-204.2**	**14.9**

*With solvent model – THF
**Preoptimized with solvent model – THF

Table 3.13. Calculated ^1H and ^{15}N NMR chemical shifts for complex **3.14**

3.14		Im-CH$_3$	N-CH$_3$	iPr-H	Cp-CH$_3$	iPr-CH$_3$	tBu	Sum of Diff	^{15}N-B	^{15}N-NB	Sum of Diff
Actual		7.29	3.77	3.01	1.73	1.23	1.59	N/A	-147.0	-203.1	N/A
Funct	**Basis set Ru**										
CAM-B3LYP	LANL2DZ	7.34	3.92	3.01	2.39	1.73	2.23	2.00	-133.1	-207.2	18.0
CAM-B3LYP	SDD	7.34	3.98	3.10	2.34	1.77	2.24	2.15	-132.9	-207.8	18.8
WB97XD	**LANL2DZ**	**7.30**	**3.82**	**2.89**	**2.29**	**1.62**	**2.22**	**1.76**	-135.4	-208.9	17.4
WB97XD	**SDD**	**7.33**	**3.85**	**2.90**	**2.29**	**1.57**	**2.22**	**1.76**	-135.9	-210.1	18.1
WB97XD*	**SDD**	7.47	3.93	3.09	2.29	1.62	2.20	1.98	**-139.6**	**-205.5**	**9.8**
WB97XD**	SDD	7.47	3.91	3.07	2.30	1.61	2.20	1.94	-138.7	-205.6	10.8

*With solvent model – acetone
**Preoptimized with solvent model – acetone

Table 3.14. Calculated ^1H and ^{15}N NMR chemical shifts for complex **3.10**

3.10		Im-CH$_3$	N-CH$_3$	iPr-H	Cp-CH$_3$	iPr-CH$_3$	tBu	Sum of Diff	^{15}N-B	^{15}N-NB	Sum of Diff
Actual		6.67	3.22	3.03	1.52	1.16	1.23	N/A	-100.6	-213.1	N/A
Funct	**Basis set Ru**										
CAM-B3LYP	LANL2DZ	6.90	3.45	3.43	2.28	1.64	1.76	2.63	-99.1	-208.1	6.5
CAM-B3LYP	SDD	6.93	3.46	3.46	2.18	1.62	1.77	2.59	-99.5	-208.8	5.4
WB97XD	**LANL2DZ**	**6.86**	**3.30**	**3.24**	**2.20**	**1.52**	**1.69**	**1.98**	**-102.9**	**-210.1**	**5.3**
WB97XD	**SDD**	**6.87**	**3.27**	**3.27**	**2.21**	**1.49**	**1.70**	**1.98**	-103.1	-210.1	5.5

UV-Vis (TDDFT)

Table 3.15. Calculated UV-vis spectra from TDDFT calculations for complex **3.15**

3.15	Abs 1		Abs 2		Abs 3		λ_{max} (nm)
Crystal structure							**572**
Functional	**Basis set for Ru**						
CAM-B3LYP	LANL2DZ	662.9	0.0061	640.6	0.0057	536.6	0.0015	643
CAM-B3LYP	SDD	671.2	0.0062	639.0	0.0066	546.1	0.0016	649
WB97XD	LANL2DZ	653.6	0.0064	596.1	0.0070	532.9	0.0013	624
WB97XD	SDD	656.9	0.0068	598.2	0.0074	541.8	0.0013	624
WB97XD*	SDD	663.5	0.0091	598.2	0.0096	532.8	0.0013	624
WB97XD*#	SDD	663.5	0.0091	598.2	0.0096	532.8	0.0013	624
WB97XD*#	**CEP121G**	662.9	0.0100	**591.2**	0.0091	530.9	0.0010	**623**

Note: the row columns are: Functional | Basis set for Ru | Abs1-λ | Abs1-f | Abs2-λ | Abs2-f | Abs3-λ | Abs3-f | λmax

**With solvent model – THF
#With # of states = 20 (Default is 3)

Table 3.16. Calculated UV-vis spectra from TDDFT calculations for complex **3.14**

3.14	Abs 1		Abs 2		Abs 3		λ_{max} (nm)
Crystal structure							**580**
Functional	**Basis set for Ru**						
CAM-B3LYP	LANL2DZ						
CAM-B3LYP	SDD	690.8	0.0059	645.6	0.0064	556.3	0.0023	655
WB97XD	**LANL2DZ**	675.6	0.0060	**607.3**	0.0062	552.5	0.0022	628
WB97XD	**SDD**	664.3	0.0067	610.0	0.0070	557.7	0.0021	**625**
WB97XD*	SDD	676.1	0.0089	610.8	0.0088	551.2	0.0023	633
WB97XD*#	SDD	676.1	0.0089	610.7	0.0087	551.2	0.0023	633
WB97XD**	SDD	675.7	0.0092	611.9	0.0091	552.9	0.0024	634

*With solvent model – acetone
**With solvent model – THF
#With # of states = 20 (Default is 3)

Table 3.17. Calculated UV-vis spectra from TDDFT calculations for complex **3.10**

3.10		Abs 1		Abs 2		Abs 3		λ_{max} (nm)
Crystal structure								
Functional	**Basis set for Ru**							
CAM-B3LYP	LANL2DZ	688.3	0.0041	634.8	0.0072	592.2	0.0028	639
CAM-B3LYP	SDD	684.1	0.0041	632.6	0.0086	599.6	0.0032	637
WB97XD	LANL2DZ	657.4	0.0044	603.5	0.0079	586.7	0.0036	612
WB97XD	SDD	657.4	0.0041	604.2	0.0086	594.2	0.0049	612
WB97XD*[#]	SDD	676.1	0.0089	610.8	0.0087	551.2	0.0023	634

Molecular orbital and electronic transition analysis

Optimized input geometries
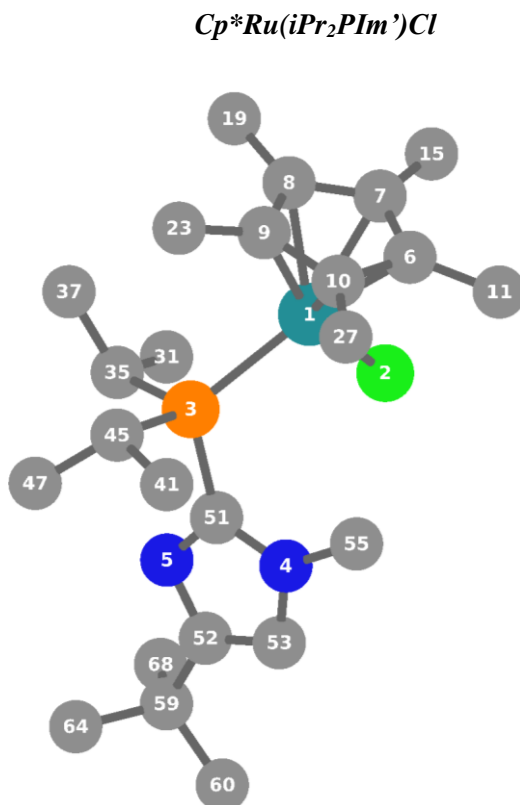
Cp*Ru(iPr₂PIm')Cl

Figure 3.60. Optimized Input Geometry Cp*Ru(iPr₂PIm')Cl

```
-------------------------------------------------
#p wb97xd/genecp td(NStates=150) gfinput pop=full
-------------------------------------------------
            -----------------------------------
            CpstarCl with acetone solvent model
            -----------------------------------
                  Symbolic Z-matrix:
            Charge = 0 Multiplicity = 1
    Ru            1.66236  -0.35044  -0.18173
    Cl            0.53646  -2.09012  -1.34876
    P            -0.36743   0.90326   0.01295
    N            -2.03908  -1.19737   1.0006
    N            -3.07151   0.31149  -0.25503
```

C	3.4155	-1.33104	0.57274
C	3.69035	-0.83316	-0.72957
C	3.48866	0.60348	-0.70198
C	3.15597	0.99263	0.64184
C	3.06121	-0.20734	1.42388
C	3.46696	-2.76007	1.01375
H	2.70626	-2.96228	1.7809
H	4.4535	-2.99932	1.44316
H	3.27714	-3.44099	0.17428
C	4.08559	-1.63068	-1.9322
H	3.68086	-2.64968	-1.88036
H	5.18251	-1.69155	-2.01977
H	3.69285	-1.17397	-2.85093
C	3.76246	1.52335	-1.8512
H	3.31068	1.15004	-2.78124
H	4.84877	1.61334	-2.01647
H	3.36995	2.53123	-1.6639
C	3.05036	2.39982	1.14364
H	2.55787	3.05515	0.4109
H	4.05171	2.81494	1.34393
H	2.47666	2.45268	2.07908
C	2.85214	-0.30249	2.90413
H	2.43643	0.62575	3.31696
H	3.8118	-0.49209	3.41252
H	2.16961	-1.12396	3.16608
C	-0.86652	0.92641	-2.75135
H	0.11853	0.48726	-2.97127
H	-1.1947	1.5049	-3.62982
H	-1.57442	0.10125	-2.5978
C	-0.8078	1.84884	-1.53386
H	-1.81647	2.24804	-1.35192
C	0.18742	2.98891	-1.74934
H	0.21276	3.70244	-0.91136

187

H	-0.08292	3.55358	-2.65553
H	1.20265	2.59004	-1.89348
C	-0.49015	1.4529	2.7409
H	-1.42209	0.88852	2.90674
H	-0.39653	2.18566	3.55805
H	0.35152	0.75027	2.81115
C	-0.52352	2.16686	1.38803
H	0.38966	2.77462	1.29495
C	-1.74978	3.07439	1.28112
H	-1.72042	3.71464	0.38803
H	-1.79969	3.73576	2.16107
H	-2.67769	2.48375	1.23943
C	-1.90987	-0.05816	0.25873
C	-3.98857	-0.62429	0.14836
C	-3.36053	-1.56479	0.92915
H	-3.72345	-2.45572	1.43165
C	-1.02393	-1.95242	1.70901
H	-0.83582	-2.90674	1.1991
H	-1.34819	-2.12474	2.74515
H	-0.08205	-1.39034	1.71438
C	-5.43696	-0.5289	-0.27148
C	-6.23809	-1.69635	0.31478
H	-5.85141	-2.66463	-0.04084
H	-7.29444	-1.62481	0.01256
H	-6.2033	-1.69389	1.41602
C	-6.01311	0.80364	0.23529
H	-5.97943	0.85287	1.33528
H	-7.0615	0.92084	-0.08349
H	-5.43165	1.64891	-0.1611
C	-5.50914	-0.56765	-1.80705
H	-4.91443	0.24983	-2.23996
H	-6.55145	-0.46323	-2.14951
H	-5.10976	-1.51794	-2.19453
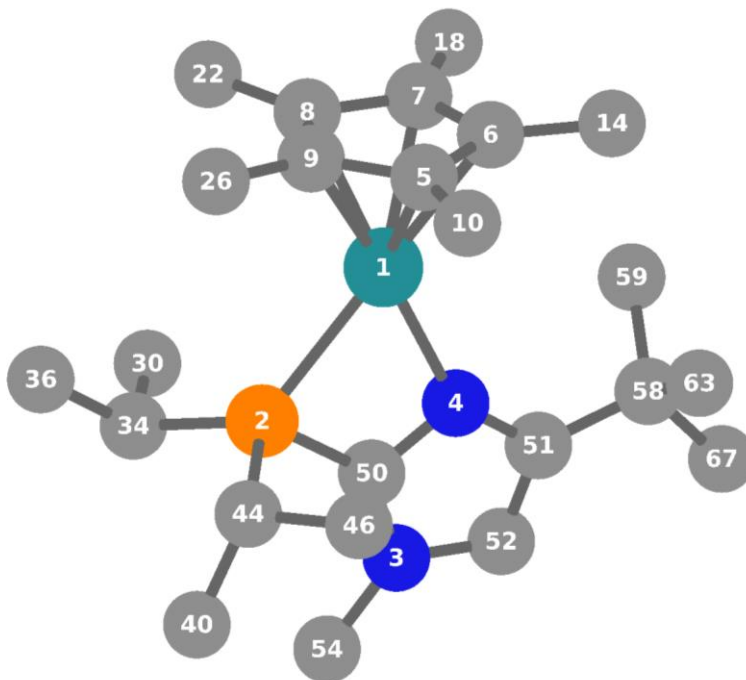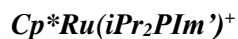
Cp*Ru(iPr₂PIm')⁺

Figure 3.61. Optimized Input Geometry Cp*Ru(iPr₂PIm')⁺

#p wb97xd/genecp scrf=(pcm,solvent=acetone) td(NStates=150) gfinput pop=full
----
wb97xd SDD from CpstarCation CS

Symbolic Z-matrix:
Charge = 1 Multiplicity = 1

Ru	0	-0.152	-0.8496	-0.001
P	0	1.77948	0.58098	0.05566
N	0	0.35341	3.18738	-0.3484
N	0	-0.7081	1.27371	-0.0428
C	0	-0.5416	-2.5003	1.2639
C	0	-1.7168	-2.3241	0.43118

C	0	-1.2994	-2.4511	-0.9214
C	0	0.12505	-2.7354	-0.94
C	0	0.57908	-2.8135	0.41559
C	0	-0.5429	-2.4846	2.75957
H	0	-0.926	-3.4413	3.1501
H	0	-1.1858	-1.6833	3.15062
H	0	0.46732	-2.3402	3.1646
C	0	-3.1204	-2.183	0.9312
H	0	-3.583	-3.1782	1.02768
H	0	-3.7442	-1.5864	0.25363
H	0	-3.1518	-1.7089	1.92077
C	0	-2.1594	-2.378	-2.1436
H	0	-2.2503	-3.3768	-2.5989
H	0	-1.7276	-1.7057	-2.8994
H	0	-3.1707	-2.0229	-1.9108
C	0	0.91932	-3.0384	-2.1713
H	0	0.81046	-4.1003	-2.4443
H	0	1.98921	-2.841	-2.0222
H	0	0.57716	-2.4386	-3.0262
C	0	1.95393	-3.187	0.87754
H	0	2.01399	-4.2698	1.06886
H	0	2.22019	-2.6682	1.80884
H	0	2.71345	-2.9392	0.1243
C	0	2.29805	0.72655	-2.6644
H	0	3.02754	0.84317	-3.4795
H	0	1.54743	1.52527	-2.7644
H	0	1.78505	-0.2384	-2.7996
C	0	3.0147	0.77562	-1.3141
H	0	3.49727	1.75923	-1.1929
C	0	4.08216	-0.3147	-1.1876
H	0	4.82334	-0.2095	-1.9935
H	0	3.63127	-1.3153	-1.2763

H	0	4.62334	-0.2646	-0.2311
C	0	3.58402	2.1038	1.68062
H	0	4.11378	2.15399	2.64388
H	0	3.01989	3.04336	1.57372
H	0	4.34721	2.06073	0.89007
C	0	2.64958	0.89524	1.66915
H	0	3.2476	-0.0242	1.79963
C	0	1.61336	0.95949	2.79425
H	0	2.12054	1.00218	3.76912
H	0	0.94846	0.08307	2.78574
H	0	0.98396	1.85932	2.70268
C	0	0.49489	1.86325	-0.1465
C	0	-1.6614	2.26276	-0.1626
C	0	-1.0008	3.44985	-0.3586
H	0	-1.377	4.45698	-0.5068
C	0	1.40127	4.17316	-0.5503
H	0	2.37109	3.66557	-0.5807
H	0	1.4016	4.90231	0.27072
H	0	1.2416	4.69511	-1.5026
C	0	-3.1406	1.99248	-0.0525
C	0	-3.5435	0.99691	-1.1513
H	0	-3.3871	1.42908	-2.1517
H	0	-4.6076	0.73196	-1.0547
H	0	-2.9453	0.07837	-1.0797
C	0	-3.4128	1.39531	1.33863
H	0	-2.8103	0.4906	1.49963
H	0	-4.4758	1.12868	1.44056
H	0	-3.1633	2.1183	2.13033
C	0	-3.9281	3.29666	-0.2193
H	0	-3.757	3.75051	-1.208
H	0	-3.6614	4.03238	0.55526
H	0	-5.0056	3.09702	-0.1281
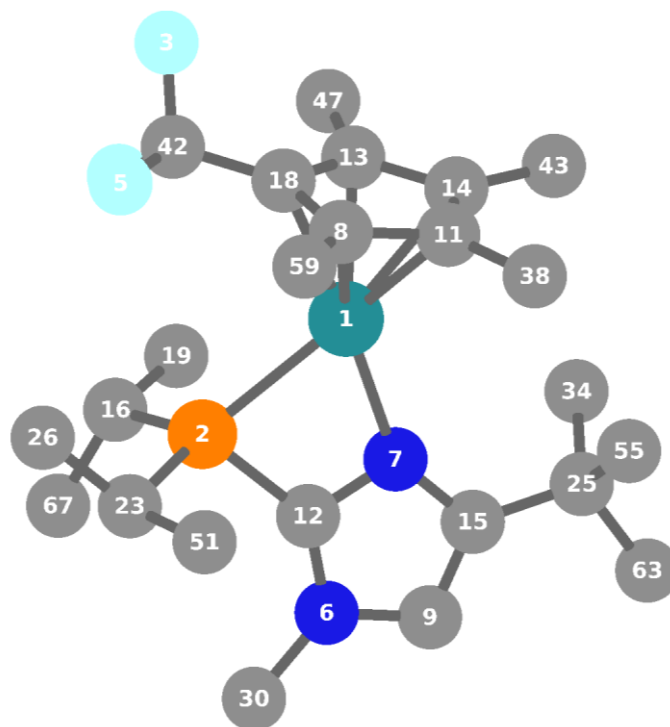
$Cp^{\ddagger}Ru(iPr_2PIm')^+$

Figure 3.62. Optimized Input Geometry $Cp^{\ddagger}Ru(iPr_2PIm')^+$

#p wb97xd/genecp td(NStates=150)gfinput pop=full scrf=(pcm,solvent=thf) guess=read geom=checkpoint

----

WB97XD with SDD basis set using CpDD crystal structure

Structure from the checkpoint file:
"CpDDRuiPr2PImPrimeCation_wb97xd_SDD_scmTHF_tddft_150pop.chk"
Charge = 1 Multiplicity = 1
Redundant internal coordinates found in file.

		x	y	z
Ru	0	15.5317	3.6783	12.6506

192

P	0	13.2818	3.85633	13.5089
F	0	16.4699	7.90961	12.6258
F	0	14.5131	7.00098	12.5669
F	0	15.5969	7.10962	14.4325
N	0	12.4933	1.00459	13.082
N	0	14.3891	1.84544	12.3185
C	0	17.0509	4.68698	13.7313
C	0	13.1444	0.00975	12.3858
H	0	12.7149	-0.9825	12.2948
C	0	17.7008	3.66382	12.9334
C	0	13.265	2.10277	13.0105
C	0	16.587	5.07553	11.4721
C	0	17.436	3.90618	11.5602
C	0	14.3185	0.53174	11.9035
C	0	11.9812	4.73153	12.5144
H	0	12.1241	5.78695	12.8008
C	0	16.4052	5.58205	12.8105
C	0	12.299	4.58464	11.0245
H	0	13.317	4.92653	10.7892
H	0	11.5888	5.18286	10.4353
H	0	12.2061	3.53543	10.7009
C	0	12.8336	3.95555	15.3034
H	0	11.7985	3.59276	15.4069
C	0	15.3737	-0.1136	11.0418
C	0	12.8902	5.41467	15.7633
H	0	13.8911	5.84311	15.6092
H	0	12.6559	5.47055	16.8365

H	0	12.1632	6.04499	15.2303
C	0	11.2276	0.85125	13.7818
H	0	10.4264	0.63015	13.066
H	0	10.9951	1.78135	14.3095
H	0	11.3083	0.0367	14.5118
C	0	15.4978	0.70496	9.74537
H	0	14.5615	0.66237	9.16769
H	0	16.3103	0.30846	9.11722
H	0	15.7126	1.75967	9.96668
C	0	18.5598	2.58279	13.5102
H	0	18.0254	2.01435	14.285
H	0	19.4506	3.02896	13.9789
H	0	18.9005	1.87977	12.741
C	0	15.7438	6.88648	13.1149
C	0	18.0179	3.17682	10.3906
H	0	18.1569	2.10818	10.5947
H	0	19.0018	3.60594	10.1436
H	0	17.3836	3.27203	9.50001
C	0	16.1272	5.70988	10.1976
H	0	15.8245	4.94492	9.46957
H	0	16.9491	6.29383	9.75395
H	0	15.2796	6.38459	10.3626
C	0	13.765	3.05175	16.1128
H	0	13.6864	1.99765	15.8068
H	0	13.5045	3.11477	17.1795
H	0	14.8147	3.36269	15.9974
C	0	16.7048	-0.1106	11.8075

194

H	0	16.9694	0.90982	12.1131
H	0	17.5141	-0.5086	11.1761
H	0	16.6371	-0.73	12.7153
C	0	17.2005	4.81251	15.2157
H	0	16.3223	5.27147	15.681
H	0	18.0758	5.438	15.4527
H	0	17.3607	3.82568	15.6694
C	0	14.9714	-1.5538	10.7065
H	0	14.8755	-2.1684	11.6152
H	0	15.7392	-2.016	10.0686
H	0	14.0156	-1.5879	10.1611
C	0	10.5485	4.30935	12.8351
H	0	10.3622	3.27295	12.5139
H	0	9.84603	4.95314	12.2847
H	0	10.3064	4.39819	13.904

Cp*Ru(iPr₃P)Cl
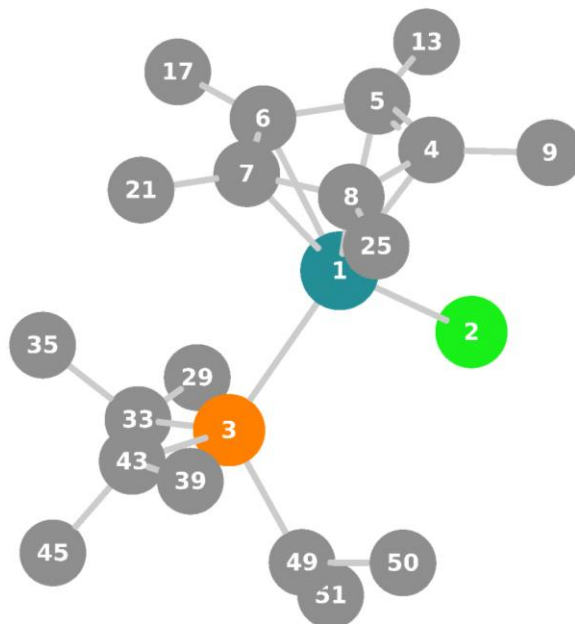
Figure 3.63. Optimized Input Geometry Cp*Ru(iPr₃P)Cl

```
-----------------------------------------------------------------------
#p wb97xd/genecp scrf=(pcm,solvent=acetone) td(NStates=150) gfinput po
                    p=full guess=read geom=checkpoint
-----------------------------------------------------------------------

               -----------------------------------
               CpstarCl with acetone solvent model
               -----------------------------------
                  Charge =  0 Multiplicity = 1
```

Ru	0	1.626474236	-0.402505758	-0.218069657
Cl	0	0.5685063228	-2.2363930775	-1.4249480936
P	0	-0.4222675613	0.8786325878	-0.0453158648
C	0	3.4106372098	-1.3752469694	0.5014947925
C	0	3.6729658272	-0.8079581771	-0.7740848023
C	0	3.4282984582	0.6184471514	-0.6843103785
C	0	3.0769597978	0.9345204729	0.674438407
C	0	3.0132195504	-0.3048928126	1.3979479679
C	0	3.5267972539	-2.8142745015	0.8946490128

H	0	2.7311772511	-3.0959956674	1.5990672283
H	0	4.493592569	-3.0008974597	1.3895169823
H	0	3.4564641183	-3.4764394514	0.0221596051
C	0	4.1249291782	-1.5212007033	-2.0090352061
H	0	3.8583848408	-2.5855229393	-1.9794346898
H	0	5.2185829574	-1.4432486387	-2.1197819713
H	0	3.6656189094	-1.083959949	-2.9070296121
C	0	3.6994198623	1.5913678413	-1.7898505228
H	0	3.2322367526	1.2716431712	-2.7322536661
H	0	4.784902406	1.6716434766	-1.9646706981
H	0	3.3288933516	2.5954200186	-1.5475213966
C	0	2.978754128	2.311690305	1.2530840411
H	0	2.5663319516	3.0289249878	0.5299874297
H	0	3.9811631402	2.6689478896	1.5400817611
H	0	2.348913439	2.3345396909	2.1517628423
C	0	2.7840187071	-0.4845114776	2.8674870277
H	0	2.413273409	0.4347253424	3.3375796948
H	0	3.7287851255	-0.755436554	3.3663854774
H	0	2.0594050894	-1.2869364058	3.0678760806
C	0	-0.515082232	0.990495817	-2.8762909763
H	0	0.5533454185	0.7414473443	-2.977343031
H	0	-0.8176982305	1.5601629539	-3.7693774843
H	0	-1.0709318605	0.0459745351	-2.8650838744
C	0	-0.74492553	1.844344198	-1.6249531107
H	0	-1.7999812458	2.1646566544	-1.5931856259
C	0	0.1538719404	3.0831867726	-1.7008850931
H	0	-0.0474684145	3.8220800173	-0.9138901858
H	0	0.0075424909	3.584415781	-2.6705520046
H	0	1.2129638658	2.7921446103	-1.6362328611
C	0	-0.3661208507	1.637677316	2.67323379
H	0	-1.2998718648	1.1569122553	3.0040197884
H	0	-0.1382857609	2.4404514408	3.3921944889

H	0	0.4372657058	0.8906218872	2.7243959405
C	0	-0.5116220159	2.2178870403	1.2649081025
H	0	0.3806939598	2.8257303993	1.0583117431
C	0	-1.7394906749	3.1309105884	1.1904779644
H	0	-1.8639689725	3.6067665896	0.2080607833
H	0	-1.6405885304	3.9344457099	1.937628261
H	0	-2.668391587	2.5874792547	1.4221484349
C	0	-1.9979427313	-0.0926310564	0.3135638304
C	0	-1.7033951683	-1.2430371342	1.2845137773
C	0	-2.7375808081	-0.6166502332	-0.9187794683
H	0	-2.6645379612	0.6248328764	0.8185548029
H	0	-1.1724906131	-0.9108245374	2.1873034709
H	0	-2.6484327885	-1.7115491327	1.6033163517
H	0	-1.0860461086	-2.0084951175	0.7921407392
H	0	-3.0433965168	0.1900731287	-1.6002173427
H	0	-2.1172306825	-1.335094596	-1.4742851295
H	0	-3.6529215239	-1.137824966	-0.5943918431

Results

Cp*Ru(iPr₂PIm')Cl

Table 3.18. Relevant pi-bonding molecular orbitals for complex **3.10**
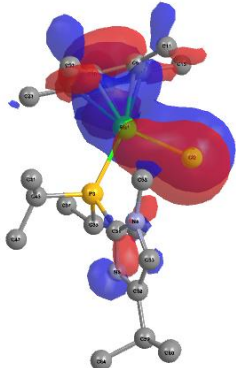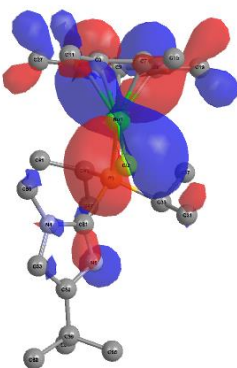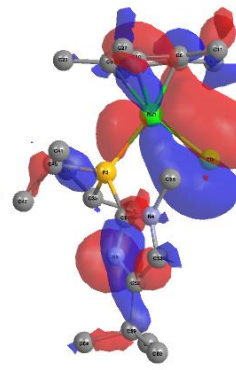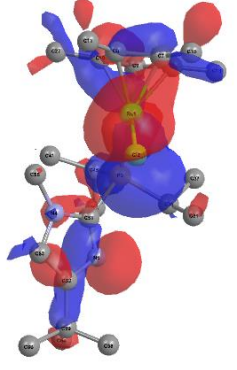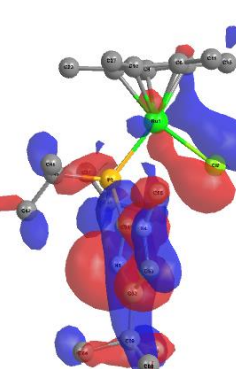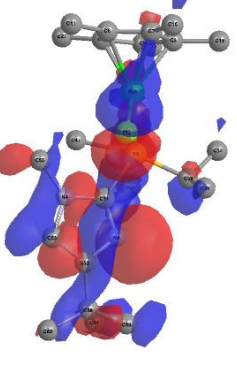
Molecular Orbital	Face View	Side View	Bonding or Antibonding?[a]
115 (HOMO – 9)			*Bonding*
116 (HOMO – 8)			*Bonding*
117 (HOMO – 7)			*Bonding*

Table 3.18 cont.

119

(HOMO – 5)

Bonding

122

(HOMO – 2)

Antibonding

123

(HOMO – 1)
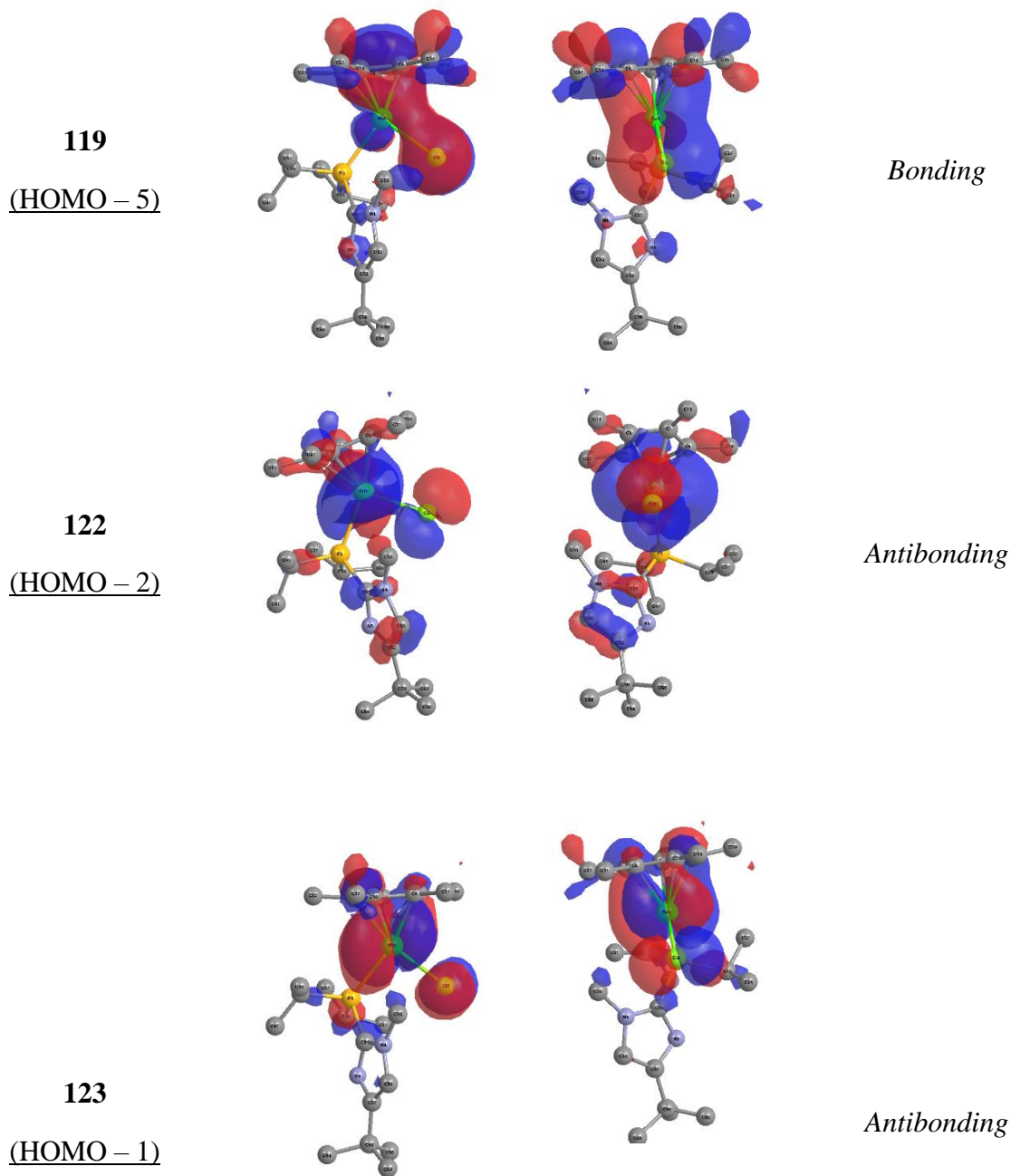
Antibonding

Table 3.18 cont.
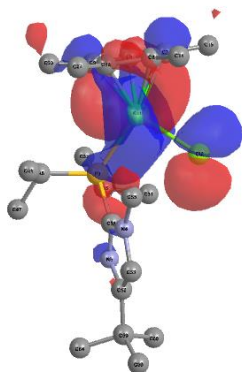
124 (HOMO)		*Antibonding*
125 (LUMO)		*Antibonding*
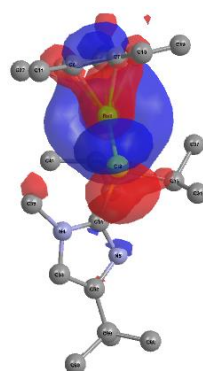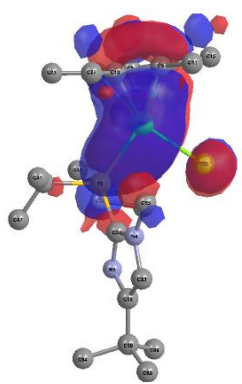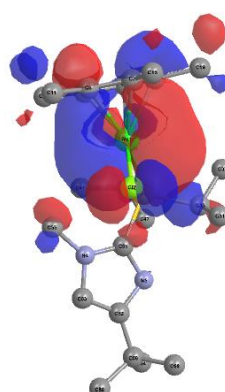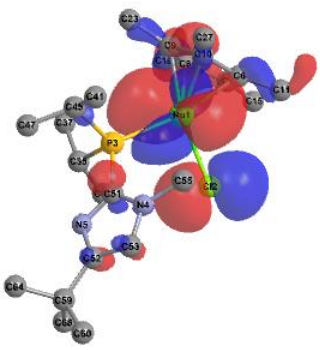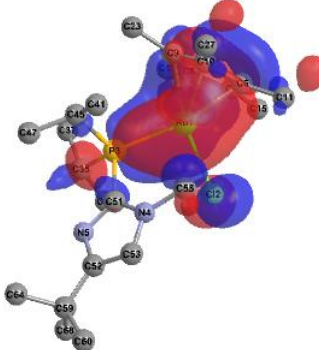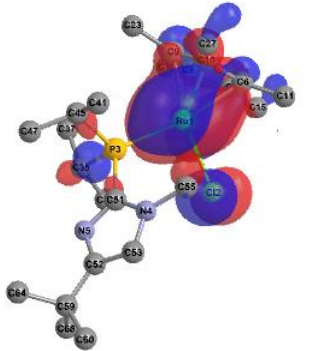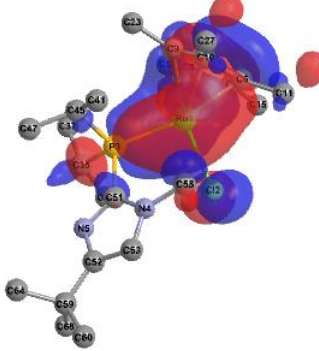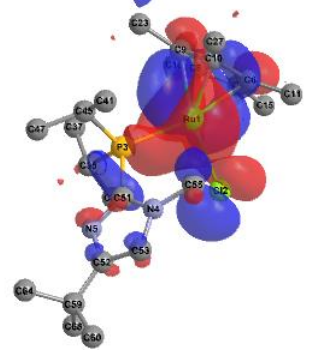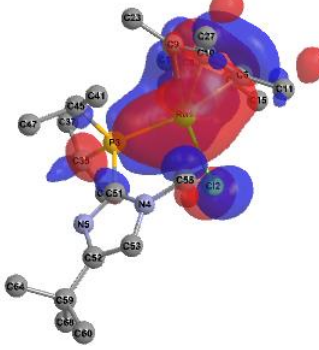
[a]'Bonding' and 'antibonding' refer to π-orbitals that appear either bonding or antibonding with respect to Ru and Cl

Table 3.19. Visible excited state transitions for complex **3.10**

Wavelength (nm) & (Intensity)	Ground State	Excited State	Contributing Orbitals
594 (0.005)			*122 -> 125* *0.83* *123 -> 125* *0.37* *124 -> 125* *-0.27*
604 (0.009)			*123 -> 125* *0.89* *122 -> 125* *-0.33* *121 -> 125* *0.15* *119 -> 125* *-0.15*
657 (0.004)			*124 -> 125* *0.93* *122 -> 125* *0.29*
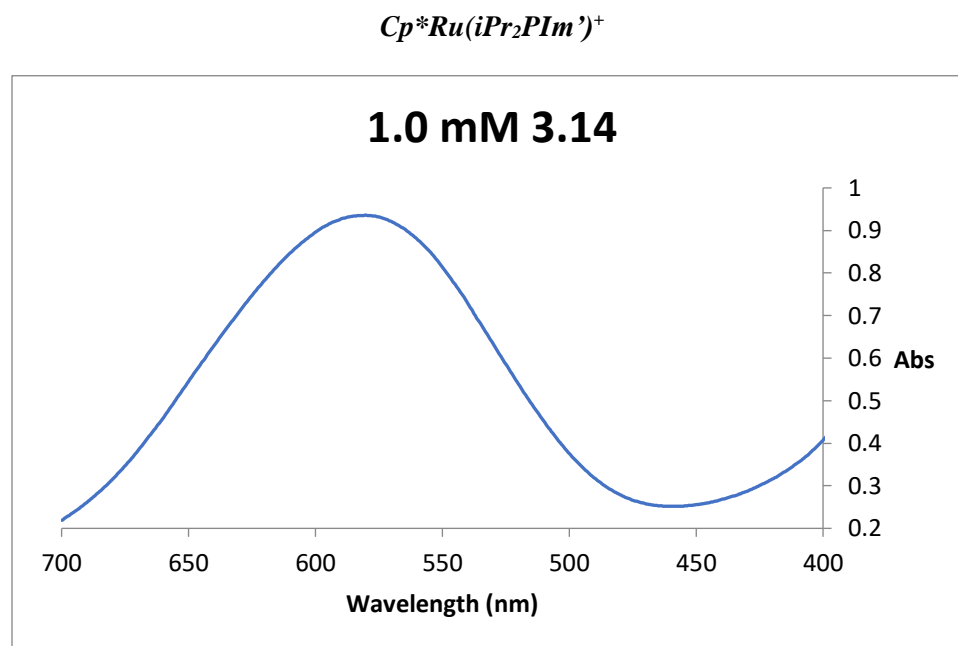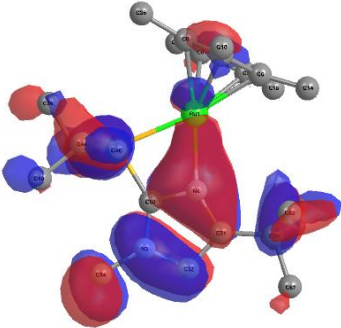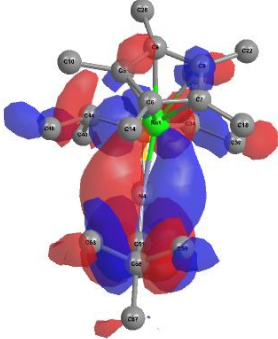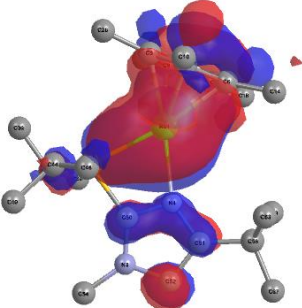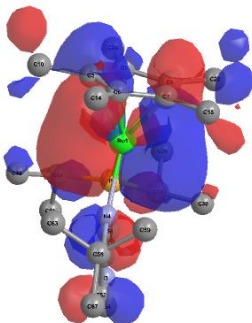
Cp*Ru(iPr₂PIm')⁺

Figure 3.64. UV-vis spectrum of Cp*Ru(iPr$_2$PIm')PF$_6$ (Complex **3.14**)
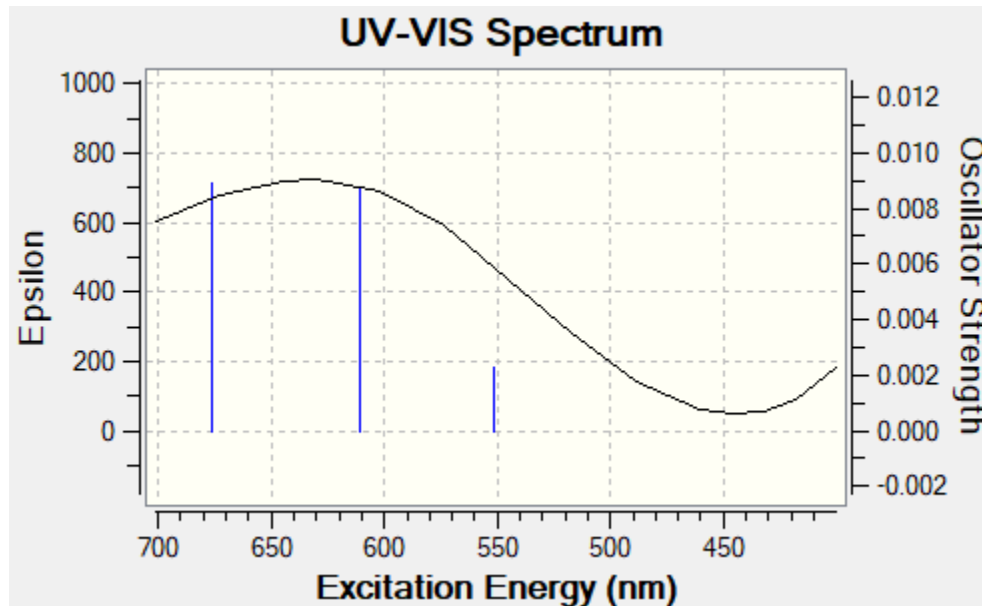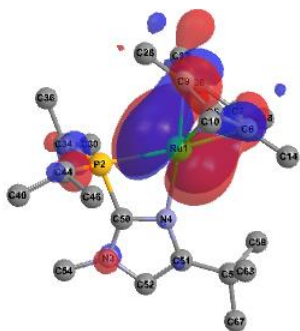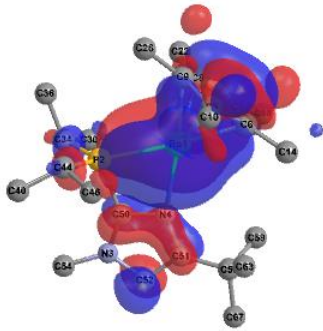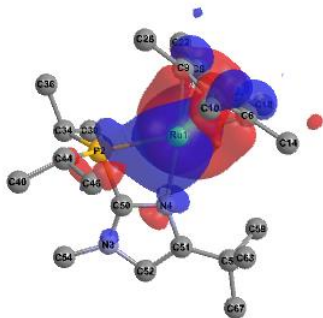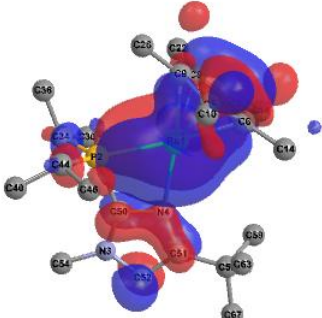
Figure 3.65. Simulated UV-vis spectrum - TDDFT - Cp*Ru(iPr$_2$PIm')PF$_6$ (Complex **3.14**)

Table 3.20. Relevant pi-bonding molecular orbitals for complex **3.14**

Molecular Orbital	Face View	Side View	Bonding or Antibonding?[a]
108 (HOMO – 8)			*Bonding*
116 (LUMO)			*Antibonding*
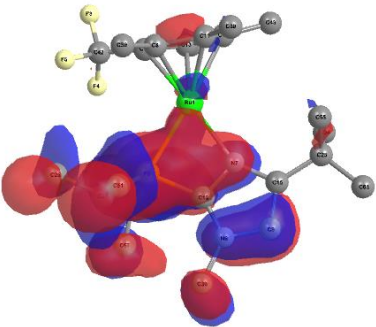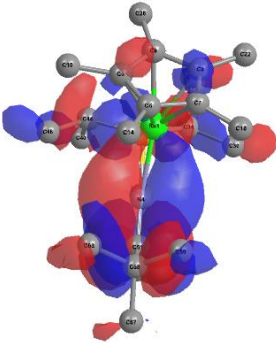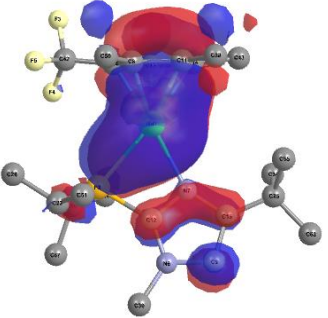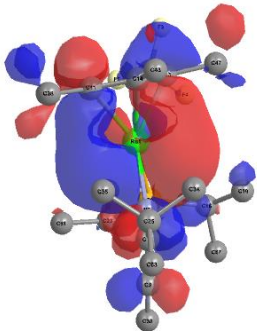
[a]'Bonding' and 'antibonding' refer to π-orbitals that appear either bonding or antibonding with respect to Ru and N

Table 3.21. Major Computed Transitions – Visible Region for complex **3.14**

Wavelength (nm) & (Intensity)	Ground State	Excited State	Contributing Orbitals
610 (0.009)			*114 -> 116* ***0.97***
676 (0.009)			*115 -> 116* ***0.95*** *113 -> 116* ***0.25***

Cp‡Ru(iPr₂PIm')⁺
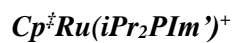
Table 3.22. Relevant pi-bonding molecular orbitals for complex **3.14**

Molecular Orbital	Face View	Side View	Bonding or Antibonding?[a]
119 (HOMO – 9)			*Bonding*
128 (LUMO)			*Antibonding*

[a]'Bonding' and 'antibonding' refer to π-orbitals that appear either bonding or antibonding with respect to Ru and N
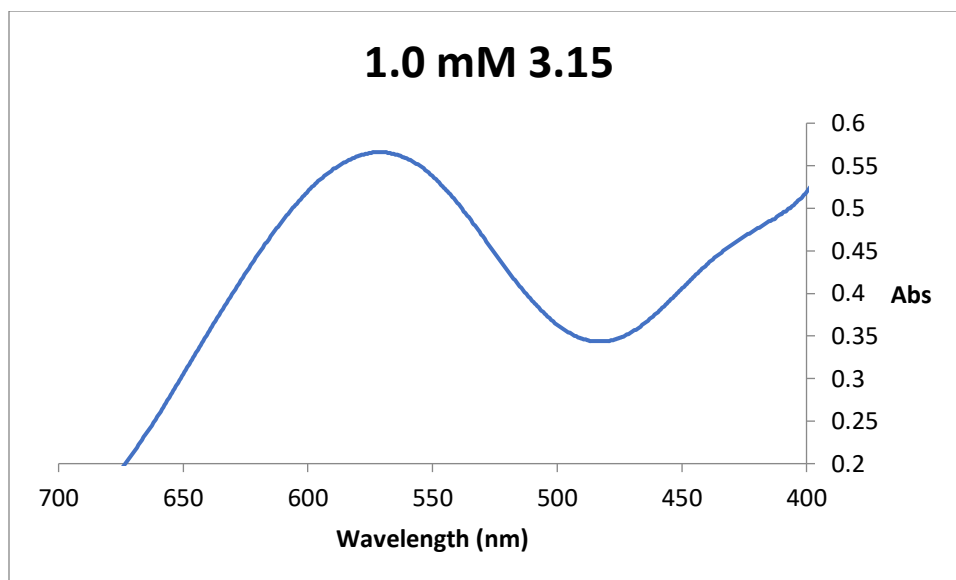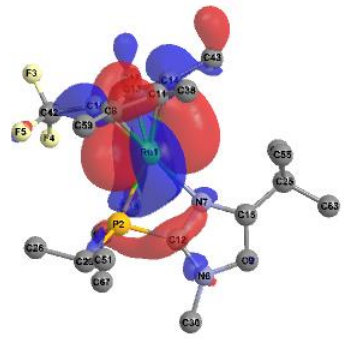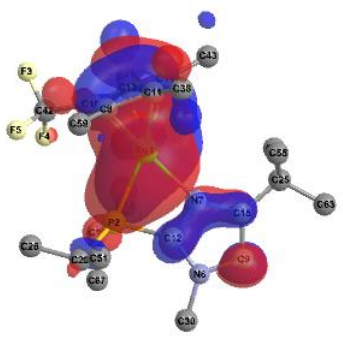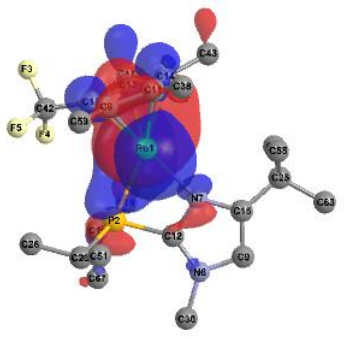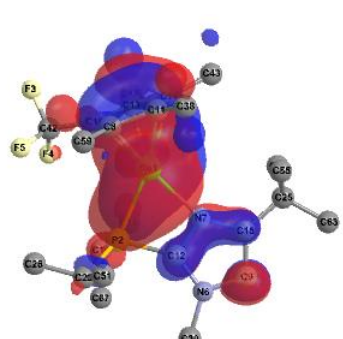
Figure 3.66. UV-vis spectrum of Cp‡Ru(iPr$_2$PIm')PF$_6$ (Complex **3.15**)
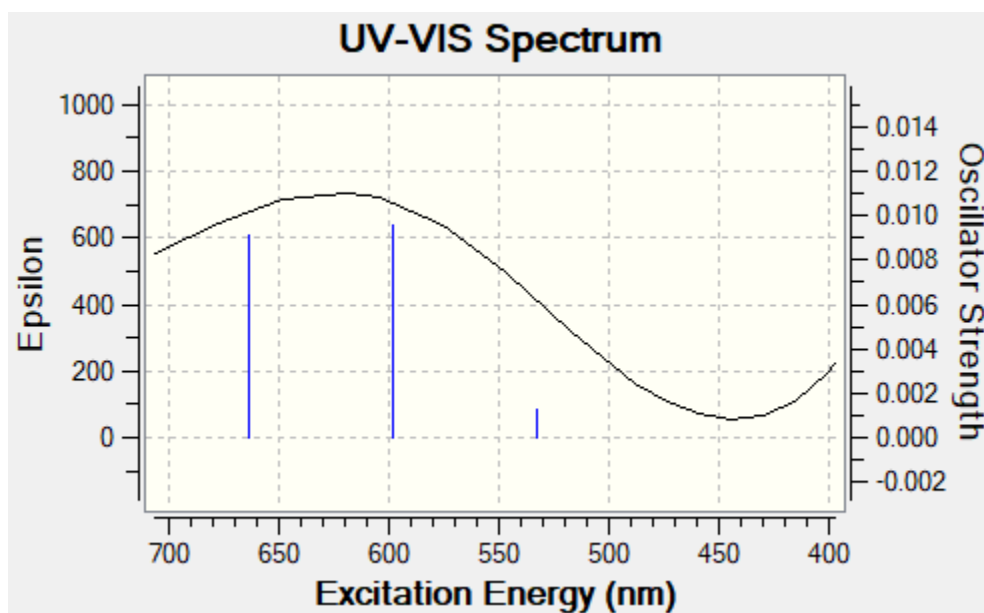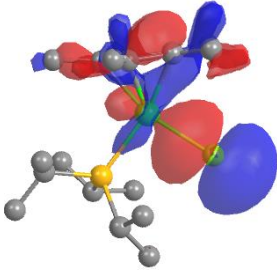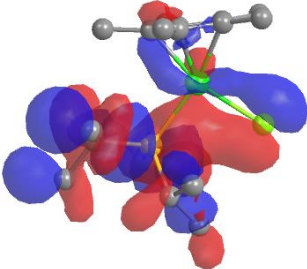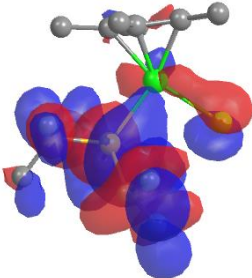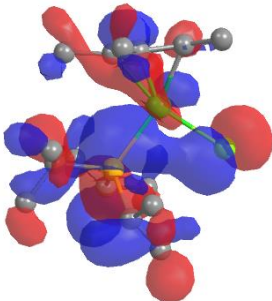
Figure 3.67. Simulated UV-vis spectrum – TDDFT – Cp‡Ru(iPr$_2$PIm')PF$_6$ (Complex **3.15**)

Table 3.23. Major Computed Transitions – Visible Region for complex **3.15**

Wavelength (nm) & (Intensity)	Ground State	Excited State	Contributing Orbitals
598 (0.010)			*126 -> 128* **0.95** *125 -> 128* **0.20**
663 (0.009)			*127 -> 128* **0.94** *125 -> 128* **0.25** *126 -> 128* **-0.15**

Cp*Ru(iPr₃P)Cl

Table 3.24. Relevant pi-bonding molecular orbitals for Cp*Ru(iPr₃P)Cl

Molecular Orbital	Face View	Bonding or Antibonding?[a]
89 (HOMO – 10)		*Bonding* *(sigma)*
90 (HOMO – 9)		*Bonding*
91 (HOMO – 8)		*Bonding*
92 (HOMO – 7)		*Bonding*

209

Table 3.24 cont.

93

(HOMO – 6)
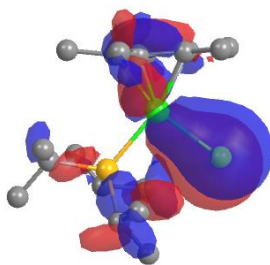
Bonding

94

(HOMO – 5)
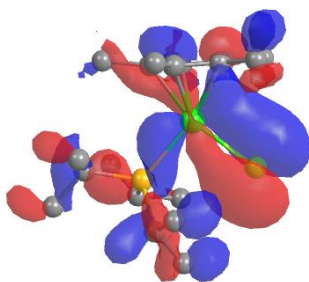
Bonding

95

(HOMO-4)
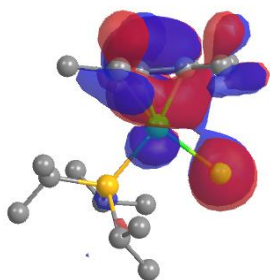
Weakly antibonding?
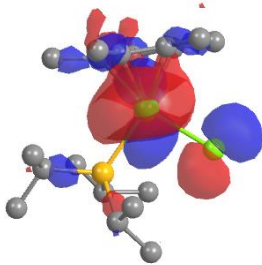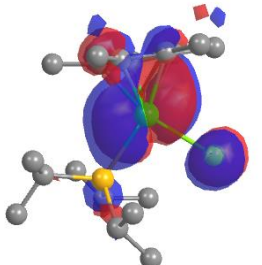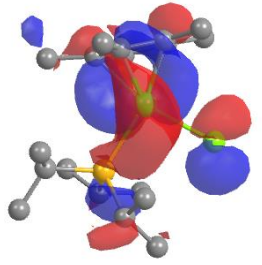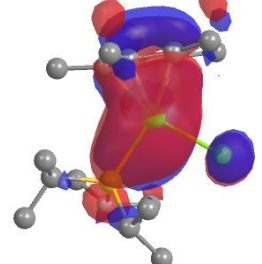
96

(HOMO-3)
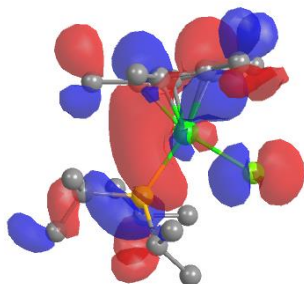
Antibonding

Table 3.24 cont.

97 (HOMO-2)		*Antibonding*
98 (HOMO-1)		*Antibonding*
99 (HOMO)		*Antibonding*
100 (LUMO)		*Antibonding*

[a]'Bonding' and 'antibonding' refer to π-orbitals that appear either bonding or antibonding with respect to Ru and Cl

The contents of Chapter 3 are similar to a portion of the material submitted for publication in the following manuscript: Paulson, E.R., Moore, C.E., Rheingold, A.L., Grotjahn, D.B. "Dynamic π-Bonding of Imidazolyl Substituent in a Formally 16-electron Cp*Ru(κ^2P,N) Catalyst Allows Dramatic Rate Increases in (E)-Selective Monoisomerization of Alkenes" *ACS Catalysis*, In Review.

3.6. References

1.   Bouziane, A.; Carboni, B.; Bruneau, C.; Carreaux, F.; Renaud, J.-L., Pentamethylcyclopentadienyl ruthenium: an efficient catalyst for the redox isomerization of functionalized allylic alcohols into carbonyl compounds. *Tetrahedron* **2008**, *64*, 11745.

2.   Uma, R.; Crevisy, C.; Gree, R., Transposition of Allylic Alcohols into Carbonyl Compounds Mediated by Transition Metal Complexes. *Chem. Rev.* **2003**, *103*, 27.

3.   Kuznik, N.; Krompiec, S., Transition metal complexes as catalysts of double-bond migration in O-allyl systems. *Coord. Chem. Rev.* **2007**, *251*, 222.

4.   Krompiec, S.; Krompiec, M.; Penczek, R.; Ignasiak, H., Double bond migration in N-allylic systems catalyzed by transition metal complexes. *Coord. Chem. Rev.* **2008**, *252*, 1819.

5.   for an overview of positionally selective isomerization catalysts, see ref. 5 from our JACS 2014 publication (ref. 9).

6.   Chen, C.; Dugan, T. R.; Brennessel, W. W.; Weix, D. J.; Holland, P. L., Z-Selective Alkene Isomerization by High-Spin Cobalt(II) Complexes. *J. Am. Chem. Soc.* **2014**, *136*, 945.

7.   Weber, F.; Schmidt, A.; Rose, P.; Fischer, M.; Burghaus, O.; Hilt, G., Double-Bond Isomerization: Highly Reactive Nickel Catalyst Applied in the Synthesis of the Pheromone (9Z, 12Z)-Tetradeca-9-12-dienyl Acetate. *Org. Lett.* **2015**, *17*, 2952.

8.   Schmidt, A.; Nodling, A. R.; Hilt, G., An Alternative Mechanism for the Cobalt-Catalyzed Isomerization of Terminal Alkenes to (Z)-2-Alkenes. *Angew. Chem. Int. Ed.* **2015**, *54*, 801.

9.   Larsen, C. R.; Erdogan, G.; Grotjahn, D. B., General Catalyst Control of the Monoisomerization of 1-Alkenes to *trans*-2-Alkenes. *J. Am. Chem. Soc.* **2014**, *136*, 1226.

10.   Wang, Y.; Qin, C.; Jia, X.; Leng, X.; Huang, Z., An agostic iridium pincer complex as a highly efficient and selective catalyst for monoisomerization of 1-alkenes to *trans*-2-alkenes. *Angew. Chem. Int. Ed.* **2017**, *56*, 1614.

11.   Grotjahn, D. B.; Larsen, C. R.; Gustafson, J. L.; Nair, R.; Sharma, A., Extensive Isomerization of Alkenes Using a Bifunctional Catalyst: An Alkene Zipper. *J. Am. Chem. Soc.* **2007**, *129*, 9592.

12.   Morrill, T. C.; D'Souza, C. A., Efficient Hydride-Assisted Isomerization of Alkenes via Rhodium Catalysis. *Organometallics* **2003**, *22*, 1626.

13.   Grotjahn, D. B.; Larsen, C. R.; Erdogan, G., Bifunctional Catalyst Control of Alkene Isomerization. *Top. Catal.* **2014**, *57*, 1483.

14.   Campion, B. K.; Heyn, R. H.; Tilley, T. D., Preparation and Reactivity of 16-Electron 'Half-Sandwich' Ruthenium Complexes; X-Ray Crystal Structure of $(h^5-C_5Me_5)Ru(iPr_3P)Cl$. *J. Chem. Soc., Chem. Comm.* **1988**, 278.

15.   Arliguie, T., Border, C., Chaudret, B., Devillers, J. Pollblanc, R., Chloro- and Hydrido(pentamethylcyclopentadienyl)ruthenium Complexes: Anomalous NMR Behavior of $C_5Me_5RuH_3PR_3$ (R=CHMe$_2$, Cy). *Organometallics* **1989**, *8*, 1308.

16.   Johnson, T. J.; Folting, K. S., W.E.; Martin, J. D.; Huffman, J. C.; Jackson, S. A.; Eisenstein, O.; Caulton, K. G., p-Stabilized, yet Reactive, Half-Sandwich Cp*Ru(PR$_3$)X Compounds: Synthesis, Structure, and Bonding. *Inorg. Chem.* **1995**, *34*, 488.

17.   Johnson, T. J.; Coan, P. S.; Caulton, K. C., Spectroscopic Investigation of the Reactivity of Cp*Ru(PiPr$_2$Ph)X toward H$_2$ and Silanes: Formation in Solution of Cp*Ru(PiPr$_z$Ph)(H)$_3$ and Cp*Ru(PiPr$_2$Ph)(H)$_2$Y (Y = Halide, OR, and SiR'$_3$). *Inorg. Chem.* **1993**, *32*, 4594.

18.   Streib, W. E.; Alota, A. A.; Caulton, K. G., Molecular Structure of Cp*RuCl(PtBu$_2$Me). *Bull. Pol. Acad. Sci. Chem.* **1994**, *42*, 197.

19.   Jimenez-Tenorio, M.; Puerta, M. C.; Valerga, P., Synthesis and properties of the 16-electron complex $(C_5Me_5)RuCl(PMeiPr_2)$] and of half-sandwich ruthenium hydrido complexes containing bulky monodentate phosphine ligands. *J. Organometal. Chem.* **2000**, *609*, 161.

20.   Rankin, M. A.; Hesp, K. D.; Schatte, G.; McDonald, R.; Stradiotto, M., Reactivity of a coordinatively unsaturated Cp*Ru(k^2-P,O) complex. *Chem. Commun.* **2008**, 250.

21.   Fasulo, M. E.; Glaser, P. B.; Tilley, T. D., Cp*(PiPr$_3$)RuOTf: A Reagent for Access to Ruthenium Silylene Complexes. *Organometallics* **2011**, *30*, 5524.

22.   Gassman, P. G.; Macomber, D. W.; Herschberger, J. W., Evaluation by ESCA of the Electronic Effect of Methyl Substitution on the Cyclopentadienyl Ligand. A Study of Titanocenes, Zirconocenes. *Organometallics* **1983**, *2*, 1470.

23.   Sowa, J. R.; Angelici, R. J., Calorometric Determination of the Heats of Protonation of the Metal in (Methyl-Substituted Cyclopentadienyl)Iridium Complexes, Cp'Ir(1,5-COD). *J. Am. Chem. Soc.* **1991**, *113*, 2537.

24.   Lenges, C. P.; Brookhart, M., Isomerization of Aldehydes Catalyzed by Rhodium (I) Olefin Complexes. *Angew. Chem. Int. Ed.* **1999**, *38*, 3530.

25.   Zhang, H.-J.; Demerseman, B.; Xi, Z.; Bruneau, C., Ruthenium Complexes Bearing Bulky Pentasubstituted Cyclopentadienyl Ligands and Evaluation of [Ru(η^5-C$_5$Me$_4$R)(MeCN)$_3$][PF$_6$] Precatalysts in Nucleophilic Allylic Substitution Reactions. *Eur. J. Inorg. Chem.* **2008**, 3212.

26.   Mercier, A.; Yeo, W. C.; Chou, J.; Chaudhuri, P. D.; Bernardinelli, G.; Kundig, E. P., Synthesis of highly enantiomerically enriched planar chiral ruthenium complexes via Pd-catalysed asymmetric hydrogenolysis. *Chem. Commun.* **2009**, 5227.

27.   Mercier, A.; Urbaneja, X.; Yeo, W. C.; Chaudhuri, P. D.; Cumming, G. R.; House, D.; Bernardinelli, G.; Kundig, E. P., Asymmetric Catalytic Hydrogenolysis of Aryl Halide Bonds in Fused Arene Chromium and Ruthenium Complexes. *Chem. Eur. J.* **2010**, *16*, 6285.

28.   Wodrich, M. D.; Ye, B.; Gonthier, J. F.; Corminboeuf, C.; Cramer, N., Ligand-Controlled Regiodivergent Pathways of Rhodium(III)-Catalyzed Dihydroisoquinolone Synthesis: Experimental and Computational Studies of Different Cyclopentadienyl Ligands. *Chem. Eur. J.* **2014**, *20*, 15409.

29.   Hyster, T. K.; Dalton, D. M.; Rovis, T., Ligand design for Rh(III)-catalyzed C–H activation: an unsymmetrical cyclopentadienyl group enables a regioselective synthesis of dihydroisoquinolones. *Chem. Sci.* **2015**, *6*, 254.

30.   Oakdale, J. S.; Sit, R. K.; Fokin, V. V., Ruthenium-Catalyzed Cycloadditions of 1-Haloalkynes with Nitrile Oxides and Organic Azides: Synthesis of 4-Haloisoxazoles and 5-Halotriazoles. *Chem. Eur. J.* **2014**, *20*, 11101.

31.   Gassman, P. G.; Mickelson, J. W.; John R. Sowa, J., 1,2,3,4-Tetramethyl-5-(trifluoromethyl)cyclopentadienide: A Unique Ligand with the Steric Properties of Pentamethylcyclopentadienide and the Electronic Properties of Cyclopentadienide. *J. Am. Chem. Soc.* **1992**, *114*, 6942.

32.   Barthel-Rosa, L. P.; John R. Sowa, J.; Gassman, P. G.; Fischer, J.; McCarty, B. M.; Goldsmith, S. L.; Gibson, M. T.; Nelson, J. H., Syntheses, Properties, and X-ray Crystal Structures of Iron and Ruthenium Compounds with the η^5-C$_5$Me$_4$CF$_3$ Ligand. Compounds of the Type [(η^5-C$_5$Me$_4$CF$_3$)M(μ-CO)(CO)]$_2$ (M) Fe, Ru). *Organometallics* **1997**, *16*, 1595.

33.   Nataro, C.; Thomas, L. M.; Angelici, R. J., Cyclopentadienyl Ligand Effects on Enthalpies of Protonation of the Ru-Ru Bond in Cp'$_2$Ru$_2$(CO)$_4$ Complexes. *Inorg. Chem.* **1997**, *36*, 6000.

34.   Evju, J. K.; Mann, K. R., A Facile Route to 1-Trifluoromethyl-2,3,4,5-tetramethylcyclopentadienyl Ruthenium Half- and Mixed-Sandwich Compounds. *Organometallics* **2002**, *21*, 993.

35.   Fagan, P. J.; Mahoney, W. S.; Calabrese, J. C.; Williams, I. D., Structure and Chemistry of the Complex Tetrakis(pentamethylcyclopentadienyl)tetrakis(η^3-chloro)-tetraruthenium(II): A Useful Precursor to (Pentamethylcyclopentadienyl ruthenium(0), -(II), and -(IV) Complexes. *Organometallics* **1990**, *9*, 1843.

36.   Grotjahn, D. B., Bifunctional catalysts and related complexes: structures and properties. *Dalton Trans.* **2008**, 6497.

37.   Rankin, M. A.; McDonald, R.; Ferguson, M. J.; Stradiotto, M., Exploring the Influence of Ancillary Ligand Charge and Geometry on the Properties of New Coordinatively Unsaturated Cp*(κ^2-P,N)Ru$^+$ Complexes: Linkage Isomerism, Double C-H Bond Activation, and Reversible b-Hydride Elimination. *Organometallics* **2005**, *24*, 4981.

38.   Mauthner, K.; Slugovc, C.; Mereiter, K.; Schmid, R.; Kirchner, K., Synthesis and Reactivity of RuCp*(κ^2(*P*,*N*)-Ph$_2$PCH$_2$CH$_2$NMe$_2$)Cl. Chelate-Assisted Methyl C-H Activation and Formation of the Novel Complex [RuCp*(κ^3(*P*,*N*,*C*)- Ph$_2$PCH$_2$CH$_2$N(CH$_2$)Me)Cl]BPh$_4$. *Organometallics* **1997**, *16*, 1956.

39.   Ito, M.; Hirakawa, M.; Osaku, A.; Ikariya, T., Highly Efficient Chemoselective Hydrogenolysis of Epoxides Catalyzed by a (η^5-C$_5$(CH$_3$)$_5$)Ru Complex Bearing a 2-(Diphenylphosphino)ethylamine Ligand. *Organometallics* **2003**, *22*, 4190.

40.   Ito, M.; Kitahara, S.; Ikariya, T., Cp*Ru(PN) Complex-Catalyzed Isomerization of Allylic Alcohols and Its Application to the Asymmetric Synthesis of Muscone. *J. Am. Chem. Soc.* **2005**, *127*, 6172.

41.   Ito, M.; Osaku, A.; Shiibashi, A.; Ikariya, T., An Efficient Oxidative Lactonization of 1,4-Diols Catalyzed by Cp*Ru(PN) Complexes. *Org. Lett.* **2007**, *9*, 1821.

42.   Nagashima, H.; Kondo, H.; Hayashida, T. Y., Y.; Gondo, M.; Masuda, S.; Miyazaki, K.; Matsubara, K.; Kirchner, K., Chemistry of coordinatively unsaturated organoruthenium amidinates as entry to homogeneous catalysis. *Coord. Chem. Rev.* **2003**, *245*, 177.

43.   Yamaguchi, Y.; Nagashima, H., C$_5$Me$_5$Ru(amidinate) Highly Reactive Ruthenium Complexes Formally Bearing 16 Valence Electrons Showing Signs of Coordinative Unsaturation. *Organometallics* **2000**, *19*, 725.

44.   Gemel, C.; Sapunov, V. N.; Mereiter, K.; Ferencic, M.; Schmid, R.; Kirchner, K., Cationic 16-electron half-sandwich ruthenium complexes containing asymmetric diamines: understanding the stability and reactivity of coordinatively unsaturated two-legged piano stool complexes. *Inorg. Chim. Acta* **1999**, *286*, 114.

45.   Phillips, A. D.; Thommes, K.; Scopelliti, R.; Gandolfi, C.; Albrecht, M.; Severin, K.; Schreiber, D. F.; Dyson, P. J., Modulating the Steric, Electronic, and Catalytic Properties of Cp*Ruthenium Half-Sandwich Complexes with β-Diketiminato Ligands. *Organometallics* **2011**, *30*, 6119.

46.   Palacios, M. D.; Puerta, M. C.; Valerga, P.; Lledos, A.; Veilly, E., Coordinatively Unsaturated Semisandwich Complexes of Ruthenium with Phosphinoamine Ligands and Related Species: A Complex Containing (R,R)-1,2-Bis((diisopropylphosphino)amino)cyclohexane in a New Coordination Form κ^3P,P',N-η^2-*P*,*N*. *Inorg. Chem.* **2007**, *46*, 6958.

47.   Rankin, M. A.; MacLean, D. F.; Schatte, G.; McDonald, R.; Stradiotto, M., Silylene Extrusion from Organosilanes via Double Geminal Si-H Bond Activation by a Cp*Ru(κ^2-*P*,*N*)$^+$ Complex: Observation of a Key Stoichiometric Step in the Glaser-Tilley Alkene Hydrosilylation Mechanism. *J. Am. Chem. Soc.* **2007**, *129*, 15855.

48.   Larsen, C. R.; Grotjahn, D. B., Stereoselective Alkene Isomerization over One Position. *J. Am. Chem. Soc.* **2012**, *134*, 10357.

49.   Erdogan, G.; Grotjahn, D. B., Mild and Selective Deuteration and Isomerization of Alkenes by a Bifunctional Catalyst and Deuterium Oxide. *J. Am. Chem. Soc.* **2009**, *131*, 10354.

50.   Ito, M.; Sakaguchi, A.; Kobayashi, C.; Ikariya, T., Chemoselective Hydrogenation of Imides Catalyzed by Cp*Ru(PN) Complexes and Its Application to the Asymmetric Synthesis of Paroxetine. *J. Am. Chem. Soc.* **2007**, *129*, 290.

51.   Ito, M.; Ootsuka, T.; Watari, R.; Shiibashi, A.; Himizu, A.; Ikariya, T., Catalytic Hydrogenation of Carboxamides and Esters by Well-Defined Cp*Ru Complexes Bearing a Protic Amine Ligand. *J. Am. Chem. Soc.* **2011**, *133*, 4240.

52.   Lundgren, R. J.; Rankin, M. A.; McDonald, R.; Stradiotto, M., Neutral, Cationic, and Zwitterionic Ruthenium(II) Atom Transfer Radical Addition Catalysts Supported by P,N-Substituted Indene or Indenide Ligands. *Organometallics* **2008**, *27*, 254.

53.   Kelly, C. M.; Ruddy, A. J.; Wheaton, C. A.; Sydora, O. L.; Small, B. L.; Stradiotto, M.; Turculet, L., Synthesis, structural characterization, and reactivity of Cp*Ru(N-phosphinoamidinate) complexes. *Can. J. Chem.* **2014**, *92*, 194.

54.   Arliguie, T.; Chaudret, B.; Jalon, F. A.; Otero, A.; Lopez, J. A.; Lahoz, F. J., Reactivity of Ruthenium Trihydrides with Brernsted and Lewis Acids. X-ray Crystal Structures of (Cp*RuH[C$_6$H$_9$P(C$_6$H$_{11}$)$_2$]]BF$_4$ and {{Cp*RuH[P(C$_6$H$_{11}$)$_3$]}(µ-H)$_2$Cu(µ-Cl)}$_2$ Evidence for Exchange Coupling between Two Hydrogen Atoms. *Organometallics* **1991**, *10*.

55.   Lindner, E.; Pautz, S.; Haustein, M., Reactivity of the Ru-O bond in η^2(O,P)-chelated mono(ether-phospine)(pentamethylcyclopentadienyl) ruthenium(II) complexes. *J. Organometal. Chem.* **1996**, *509*, 215.

56.   Jimenez-Tenorio, M., Mereiter, K., Puerta, M. C., Valerga, P., Structural Characterization of Cationic 16-Electron Half-Sandwich Ruthenium Phosphine Complexes with and without Agostic Interaction. *J. Am. Chem. Soc.* **2000**, *122*, 11230.

57.   Aneetha, H.; Jimenez-Tenorio, M.; Puerta, M. C.; Valerga, P.; Sapunov, V. N.; Schmid, R.; Kirchner, K.; Mereiter, K., Coordinatively Unsaturated Ruthenium Phosphine Half-Sandwich Complexes: Correlations to Structure and Reactivity. *Organometallics* **2002**, *21*, 5334.

58.   Mayer, M.; Welther, A.; von Wangelin, A. J., Iron-Catalyzed Isomerizations of Olefins. *ChemCatChem* **2011**, *3*, 1567.

59.   Siddappa, R. K. G.; Chang, C.-W.; Chein, R.-J., From precursor to catalyst: the involvement of [Ru(η^5-Cp*)Cl$_2$]$_2$ in highly branch selective allylic etherification of cinnamyl chlorides. *Tetrahedron Letters* **2014**, *55*, 1031.

60.   Fagan, P. J.; Ward, M. D.; Caspar, J. V.; Calabrese, J. C., Synthesis and unusual properties of a helically twisted multiply metalated rubrene derivative. *J. Am. Chem. Soc.* **1988**, *110*, 2981.

Chapter 4

The Activity and Behavior of (*E*)-Selective Monoisomerization Catalyst 3.14

4.1. Introduction

This Chapter starts with a short discussion on previous alkene isomerization catalysts developed in the Grotjahn group. Then, testing of the activity and selectivity of **3.14** in the isomerization of a broad scope of alkenes is discussed. A side-by-side comparison of catalysts **1.1** and **3.14** is outlined to highlight the differences in positional selectivity between the two catalysts. The Chapter ends with an analysis of the binding of alkenes to **3.14**, providing insight into bonding characteristics, selectivity, and includes the first direct spectroscopic evidence of the pendent base participating in proton transfer during alkene isomerization.

As discussed in Chapter 1, a major challenge of subjecting a substrate of interest to catalytic alkene isomerization is the possibility of forming several isomers. In the example of the isomerization of 1-heptene discussed on page 27, a non-selective isomerization would provide what is essentially the thermodynamic ratio of the five possible isomers: 1-heptene: 0.43%, (*Z*)-2-heptene: 11.7%, (*E*)-2-heptene: 48.5%, (*Z*)-3-heptene: 6.94%, and (*E*)-3-heptene: 32.4%.[1] With heptene and other linear alkene substrates, there is a considerable challenge in controlling the formation of a particular isomer over another. In terms of limiting the number of geometric isomers, catalyst **1.1** has shown a notable proclivity to favor the (*E*)-isomers across a large variety of substrates as discussed in Chapter 2.[2-10] When **1.1** encounters substrates that contain multiple positional isomers of similar stability, as in the case of linear alkenes like hexene (**4.1**)

and heptene (**4.4**), a mixture of (*E*)-isomers is quickly formed (see Table 4.1 for results with substrate **4.1**). The search for a catalyst that maintains (*E*)-selectivity but is more *positionally* selective led to the development of **1.2 + 1.2a**, discussed at the beginning of Chapter 3.

Although **1.2 + 1.2a** was an essential development in the search for simultaneous geometric <u>and</u> positionally selective isomerization catalysts, a major shortcoming of the catalyst has been its efficiency: with reasonable catalyst loading (1 mol%), a typical isomerization from 1- to (*E*)-2-alkene would require 48 h at 40 °C to complete.[11] As discussed in Chapter 3, the development of **3.14** (Figure 4.1) stemmed from an attempt to increase that efficiency. The hypothesis was that the removal or replacement of a relatively strong acetonitrile ligand would help facilitate binding of alkenes. When the chloride-containing precursor **3.10** was ionized with TlPF$_6$ in acetone, there was an expectation that the basic imidazole nitrogen would bind, but an additional ligand (likely solvent – acetone or water) would also coordinate to form an 18-electron complex. An acetone or water complex would still likely still be an improvement compared to the nitrile complexes, as both are much more labile ligands.
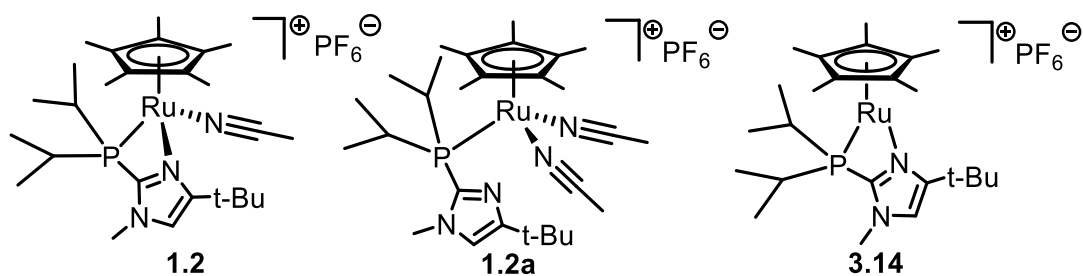
Figure 4.1. Catalysts **1.2 + 1.2a** and **3.14** for (*E*)-selective monoisomerization of alkenes

However, as discussed in Chapter 3, the imidazole appears to be a competent enough π-donor, and the presence of the *tert*-butyl group on the imidazole also inhibits other ligands from coordinating. As a result, **3.14** remains coordinatively unsaturated both in solution and in the solid state. The advantage of the coordinative unsaturation with respect to alkene isomerization catalysis is that an alkene does not need to wait for dissociation of any other ligands to occur

before binding to the catalyst. This could result in dramatic rate increase if the ligand dissociation rate is slow, as was evidenced in **1.2** + **1.2a**.
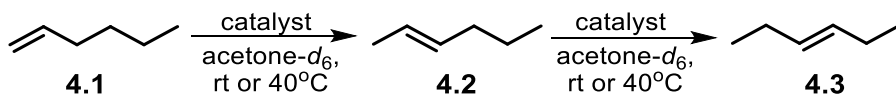
Figure 4.2. Isomerization of **4.1** to **4.2** and **4.3**

4.2. Results of Isomerization with 3.14

In an initial experiment, 1-hexene (**4.1**, figure 4.2) was subjected to catalyst **3.14** (0.1 mol%) in order to study its activity and selectivity in the production of **4.2** and **4.3**. The reaction was allowed to proceed until <3% of the terminal alkene (1-hexene) remained, which is generally considered to be the completion of the reaction (1-alkene amount typically does not drop much below 2% with any substrate). In order to consider the selectivity of **3.14** in the production of (*E*)-2-hexene (**4.2**) to be comparable to the selectivity of **1.2** + **1.2a**, the maximum production of **4.2** must exceed 95%. The results and comparison with catalysts **1.1**, **1.2** + **1.2a,** and **3.15** are summarized in Table 4.1 below. Two time points are listed for catalyst **1.1** to illustrate its rapid overisomerization in a short time frame.

Table 4.1. Isomerization of **4.1** with catalysts **1.1**, **1.2** + **1.2a**, **3.14**, and **3.15**[a]

Catalyst	Mol %	Time	1-hexene	(*E*)-2-hexene	(*E*)-3-hexene
1.1	0.1	15 min	2.3	86.3	10.9
		20 min	2.0	78.6	20.1
1.2+1.2a[b,c]	1	48 h	2.3	95.5	2.1
3.14	0.1	4 h	1.9	96.1	2.6
3.15	0.1	32 h	2.1	95.0	0.7

[a]Reactions run at 0.50 M in acetone-d_6 with internal standard. [b]Reaction run at 40˚C. [c]From ref. [11]

As expected, **3.14** proved to be an exceedingly efficient catalyst relative to its nitrile-containing counterpart. Isomerization reactions of linear 1-alkenes to (*E*)-2-alkenes using catalyst **3.14** can be performed at room temperature in acetone-d_6, using as little as 0.1 mol%

catalyst, and reach full conversion within 3 to 4 h at this low loading. In several cases, alkene samples could be used as received once deoxygenation was performed by bubbling nitrogen gas through the alkene substrates prior to use. However, we suspect that trace impurities of allylic peroxides in some of the alkene substrates lead to significant deactivation of the catalyst at 0.1 mol% loadings, that can be resolved by pretreatment of the substrate by passing it through a small plug of basic alumina. At catalyst loadings of 0.5 mol%, pretreatment was not necessary, and all unfunctionalized as well as some functionalized substrates underwent complete isomerization within 15 min to 1 h. In addition to the alkenol and alkenol silyl ether substrates reported for **1.2** + **1.2a**[11], we show that protected amide (**4.14**) and ester (**4.15**) substrates are tolerated and isomerize efficiently at 1.0 mol% loading. In almost all cases, with conversions of starting 1-alkene at 95% or greater, yields of (*Z*)-alkenes were less than 0.5%, and 3-alkenes less than 3%, showing remarkable general selectivity for the formation of (*E*)-2-alkene products.

To investigate the relative efficiency of **3.14** to the mixture of **1.2** + **1.2a**, we compared the half-life of conversion of 1-hexene to (*E*)-2-hexene at room temperature using 0.25 mol% of each catalyst. We found that while catalyst **1.2** + **1.2a** reached ~50% conversion after 40 h, catalyst **3.14** reached 50% conversion in only 5.6 minutes, making it *>400 times more efficient.*

A major advantage that catalyst **3.14** has over **1.2** + **1.2a** is its ability to isomerize substrates that contain potentially strongly binding or chelating functional groups, which can slow down catalysis. **1.2** + **1.2a** (1 mol%, 40 °C, 48 h) was able to isomerize the *tert*-butyldiphenylsilylether of pent-4-en-1-ol (**4.12**) to provide >90% yield of the (*E*)-2-isomer, but required 6 mol% extra phosphine ligand to prevent catalyst deactivation from formation of an arene complex.[11] With the same substrate, catalyst **3.14** still suffered from arene complex formation, but due to its greater efficiency, 1 mol% **3.14** can achieve >95% yield of the (*E*)-2-

isomer within 10 min with no added ligand. This result opened the door to testing other substrates containing phenyl groups; 9-phenyl-1-decene (**4.13**) was isomerized smoothly with 1 mol% **3.14**, as was the phenyl butene (**4.17**) discussed below.

Terminal alkene substrates containing unsaturated moieties in the 5-position present an interesting thermodynamic challenge for catalyst **3.14**. In these substrates, if a double bond is isomerized once, the resulting product is not conjugated, but if a second isomerization occurs, the result is a conjugated pi system that generally provides significant extra stability over the unconjugated isomer. For example, an equilibrium mixture of phenyl butenes, established between 25-55°C, gave ratios of conjugated 1-phenyl-(*E*)-2-butene to unconjugated 1-phenyl-(*E*)-3-butene that ranged from 92:6 to 94:3[12-14]. Similarly, an equilibrium mixture of hexenones was reported to contain ~16% unconjugated hex-(*E*)-4-en-2-one, ~7% conjugated hex-(*Z*)-3-en-2-one, and ~77% conjugated hex-(*E*)-3-en-2-one[15]. If the ratios are recalculated excluding the (*Z*)-isomer, the ratio becomes 83:17 in favor of the conjugated (*E*) isomer.
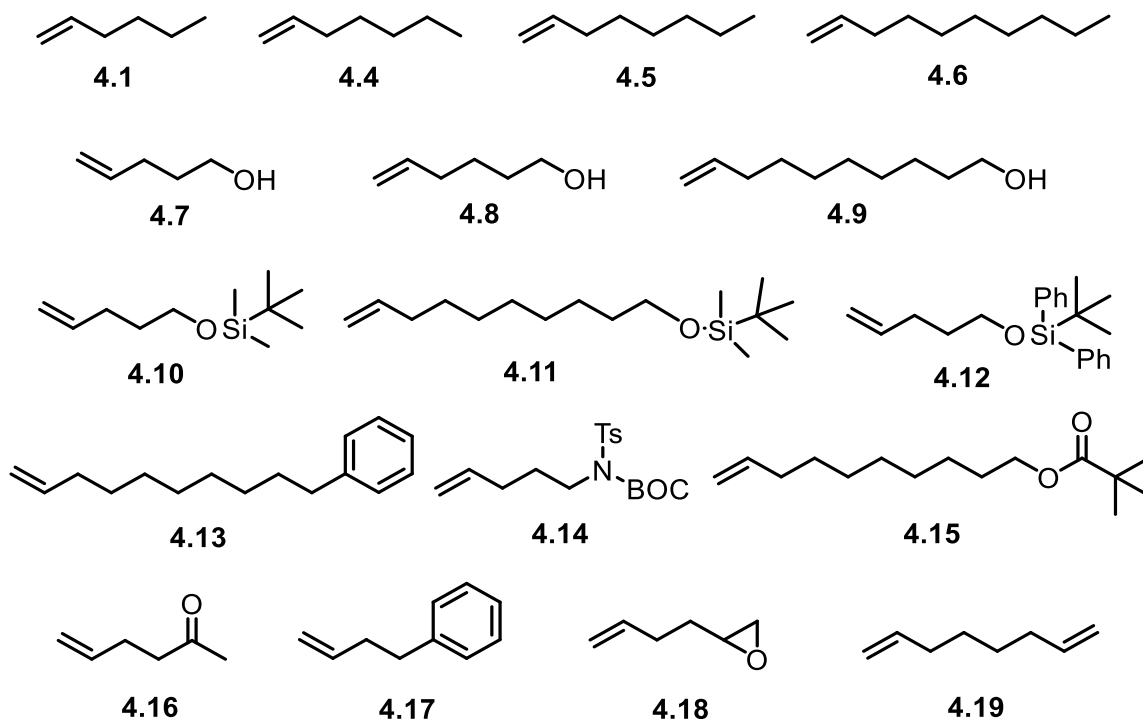
Figure 4.3. Terminal alkene substrates **4.1, 4.4 – 4.19**

222

Table 4.2. Isomerization Results with Complex **3.14**[a]

Entry	Substrate[a]	Mol % **3.14**	Time	1-alkene (%)	(E)-2-alkene (%)	(E)-2/ (Z)-2 ratio[b]	(E)-3-alkene (%)
1	**4.1**	0.1	4 h	1.9	95.7	>400:1	2.6
2		0.5	15 min	1.9	96.3	>400:1	2.6
3	**4.4**	0.5	30 min	2.0	95.5	>200:1	2.4
4	**4.5**	0.1	4 h	2.5	96.4	>400:1	1.6
5		0.5	30 min	2.0	94.0	>400:1	2.9
6	**4.6**	0.1	4 h	1.8	96.8	>400:1	1.8
7		0.5	1 h	2.2	95.9	>400:1	1.8
8	**4.7**	0.5	45 min	3.3	96.6	>400:1	0.5
9	**4.8**	0.5	15 min	2.3	95.4	>200:1	2.0
10	**4.9**	0.5	15 min	3.3	96.8	N/D	<0.5
11	**4.10**	0.5	15 min	3.3	96.8	N/O	-
12	**4.11**	0.5	15 min	2.2	97.5	>89:1	0.9
13	**4.12**	1.0	10 min	4.5	95.1	>400:1	0.8
14	**4.13**	1.0	15 min	2.7	95.7	>50:1	1.0
15	**4.14**	1.0	40 min	4.4	95.3	N/O	0.3
16	**4.15**	1.0	30 min	2.7	95.3	>400:1	1.8
17	**4.16**	1.0	4 h	11.9	65.8	>400:1	22.1
18	**4.17**	1.0	30 min	3.5	91.9	>400:1	4.3
19	**4.18**	0.5	2 h	2.4	92.9	>100:1	2.1
20	**4.19**	2.0	10 min	<2.5	>94	N/D	0.4

[a]Reactions run at room temperature with 0.50 M substrate in acetone-d^6. [b] Conservative estimates based on detailed NMR analysis (see Experimental Section – Figures 4.27 – 4.48 and Table 4.7).

Given the strong thermodynamic preference for the conjugated internal isomer, a true challenge for catalyst **3.14** is the isomerization of the terminal alkene substrates **4.16** and **4.17**. Other substrates, such as 1,7-octadiene (**4.19**) and 1,2-epoxy-5-hexene (**4.18**), are also prone to overisomerization, in the former case, an internal conjugated diene would result, and we have observed ring opening and conjugated enal formation in the latter case when subjected to catalyst **1.1**.[16]

Higher catalyst loadings are ultimately required for the diene, enone, and phenyl substrates; the first two results are likely due to chelation, whereas the latter is probably due to

deactivation of the catalyst via arene complex formation. The results for phenyl butene are striking: In 30 minutes with 1.0 mol% loading, catalyst **3.14** can achieve the complete opposite of the thermodynamic ratio of conjugated to unconjugated isomers reported above, with the mixture favoring the unconjugated isomer 92:4. Overisomerization was quite slow likely due to deactivation of the complex. Selective monoisomerization was also seen with 1,2-epoxy-5-hexene, with very little enal formation, due to the deactivation of catalyst by decarbonylation of the aldehyde.[16] 5-hexen-2-one suffers from more rapid overisomerization, with a maximum yield of monoisomerized product at 66% at 4 hours with 1.0 mol% **3.14**, but monoisomerization is still favored over conjugation by around 3:1 at this point. The conversion of **4.19** to (2*E*, 6*E*)-2,6-octadiene requires the migration of two separate double bonds; the first migration appeared to be facile, as the starting octadiene was consumed within 1 hour, but the singly monoisomerized product persisted at >10% levels even after 24 h. Interestingly, the conjugated diene amount does not increase in the same time period.

4.3. Sterics or Electronics?
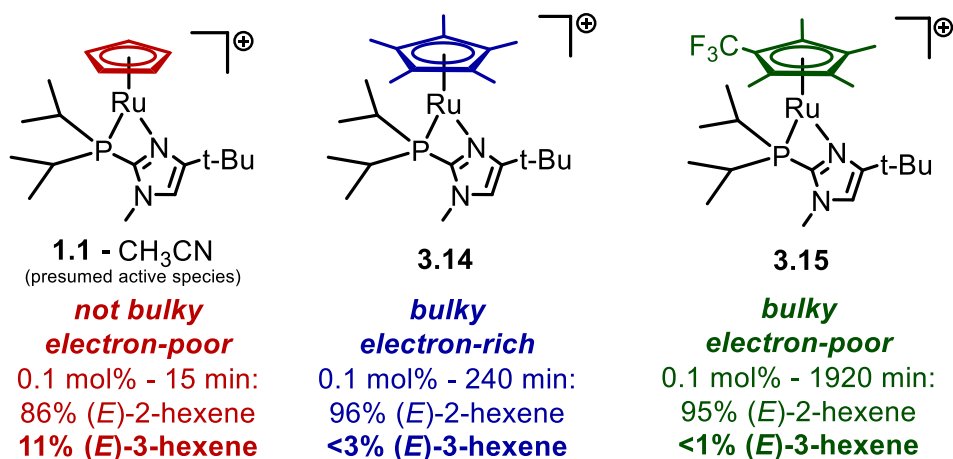
Figure 4.4. Steric and electronic influences on selectivity

Albeit slower than **3.14**, complex **3.15** is also able to cleanly isomerize 1-hexene to >95% (*E*)-2-hexene using 0.1 mol% catalyst after 32 h. Since the alkene isomerization positional

selectivity shown by **3.15** more closely aligns with those of catalysts **1.2** + **1.2a** and **3.14** rather than that of **1.1**, it can be inferred that the selectivity for monoisomerization for catalysts **1.2** + **1.2a** and **3.14** is a result of increased steric bulk of the Cp* ligand rather than its increased electron-donating ability.

4.4. Positional Selectivity Comparision – 1.1 and 3.14

When catalysts are touted for their selectivity (or maligned for their lack of selectivity), a single yield is frequently reported. Sometimes the reported yield is the maximum yield produced by the catalyst after monitoring reactions at several timepoints, but the reported yield can also simply be a single number obtained after a set period of time. However, in a kinetically-controlled isomerization process, the ratios of isomers are in constant flux. From a practical point of view, it would be useful to observe the isomerization process over time to better understand catalyst behavior. More rigorous observation and analysis can allow us to more accurately determine not only the maximum yields of various isomers, but also their persistence. A chemist can then decide which catalyst best suits their purpose. Our work below describes the monitoring and analysis of a number of substrates subjected to isomerization with catalysts **1.1** and **3.14**, in an effort to provide a practical, quantitative comparison of selectivity for the user.

Substrates **4.1**, **4.5**, **4.7**, **4.9**, **4.10,** and **4.16** (Figure 4.5) represent a sample of functionalized and unfunctionalized, linear and branched alkenes, which were chosen to provide a variety of steric and electronic environments. The unfunctionalized substrates **4.1** and **4.5** have different numbers of possible isomers (five for **4.1**, and seven for **4.5**), but both exhibit no branching or other increased steric constraints that would lead to a strong kinetic bias. *It could be argued that unfunctionalized linear alkenes **4.1** and **4.5** are the most challenging substrates to selectively isomerize because all selectivity must derive from the catalyst.* The other four

substrates **4.7**, **4.9**, **4.10,** and **4.16** contain functional groups capable of conjugating with the alkene, which presents a challenge of its own, as the increased stability of the conjugated isomers should, in theory, lower the kinetic barrier to further isomerization.
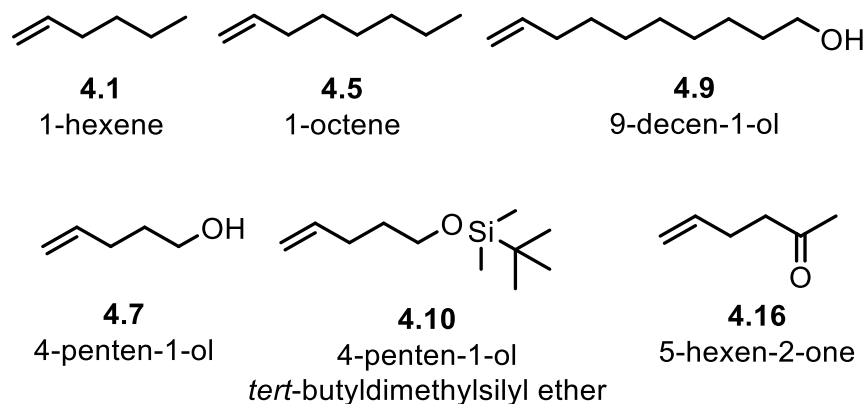
Figure 4.5. Substrates **4.1**, **4.5**, **4.7**, **4.9**, **4.10**, and **4.16** used for selectivity comparison between catalysts **1.1** and **3.14**.

Isomerizations were carried out for the six substrates with each catalyst (**1.1** and **3.14**), for a total of 12 runs, all at room temperature. Each isomerization was designed, by choice of an appropriate catalyst loading, to full conversion of 1-alkene within 30 min. For substrates **4.1**, **4.5**, **4.7**, **4.9**, and **4.10**, 8 to 9 NMR spectra were obtained within the first 30 min, in order to reliably capture the maximum yield of monoisomerized product and provide sufficient information about the rate of initial isomerization. An effort was made to gather spectra at further times in order to allow isomeric mixtures to reach equilibrium, in some cases as many as 200 h (8 d) later, but was not practically feasible for all reactions. Notably, despite high catalyst loading of **3.14** (2.0 mol%) for the isomerization of **4.16**, the reaction still required >200 min for full conversion of starting alkene. The catalyst loadings and maximum yields of the (*E*)-monoisomerized isomers are indicated in Table 4.3, and reaction profiles for all 12 runs are shown in Figures 4.6 – 4.17.

Table 4.3. Time points of reactions of **4.1**, **4.5**, **4.7**, **4.9**, **4.10**, and **4.16** with catalysts **1.1** and **3.14** where percentage of monoisomerized alkene is highest (maximum).

Substrate	Catalyst	Catalyst Loading (mol %)	Time (min)	1-alkene[a] (%)	(E)-2 alkene[a] (maximum)	(E)-3 alkene[a]
4.1	**1.1**	0.1	15	1.7	90.5	7.5
	3.14	0.3	40	2.0	96.1	2.0
4.5	**1.1**	0.1	12	3.3	91.3	3.9
	3.14	0.3	30	2.2	96.1	1.6
4.9	**1.1**	0.1	12	5.6	91.3	3.6
	3.14	0.3	12	2.9	97.1	0.0
4.7	**1.1**	0.2	90	2.4	92.1	4.0
	3.14	0.3	180	2.1	96.8	0.6
4.10	**1.1**	0.1	30	2.6	97.1	3.4
	3.14	0.3	40	4.7	95.7	0.5
4.16	**1.1**	0.1	120	5.2	85.2	9.1
	3.14	2.0	120	11.5	67.9	21.0

[a] For clarity of comparison, all terminal alkenes are called 1-alkenes even though some, such as 5-hexen-2-one, are numbered differently in the IUPAC system.
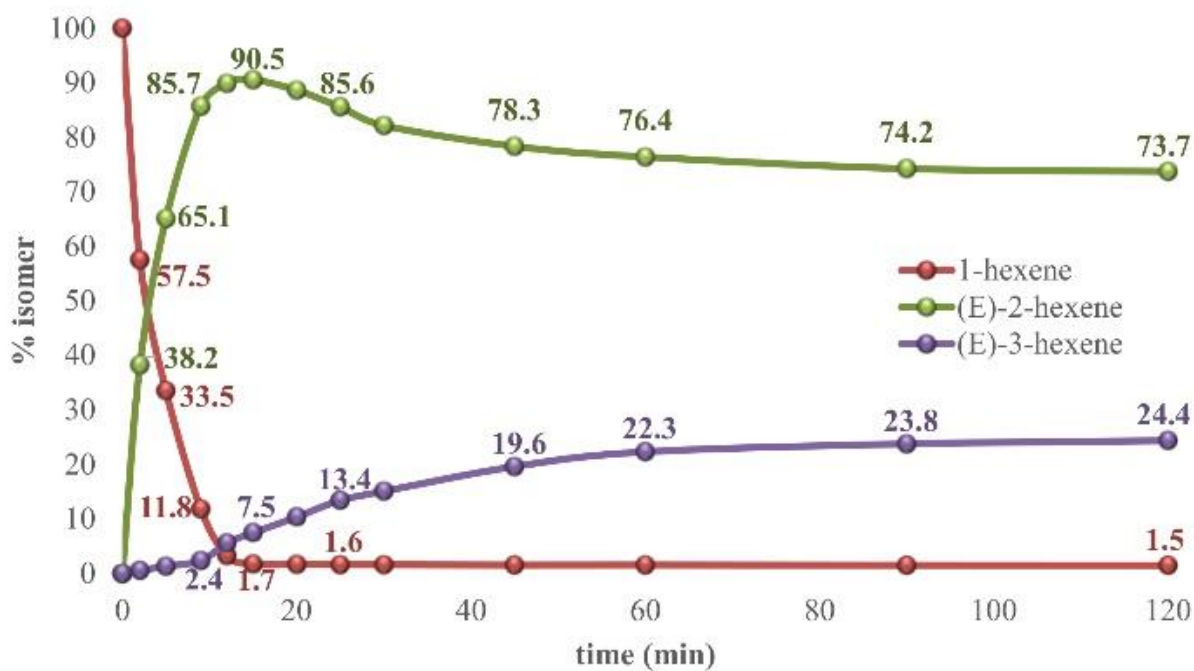
Figure 4.6. Isomerization of **4.1** with catalyst **1.1**
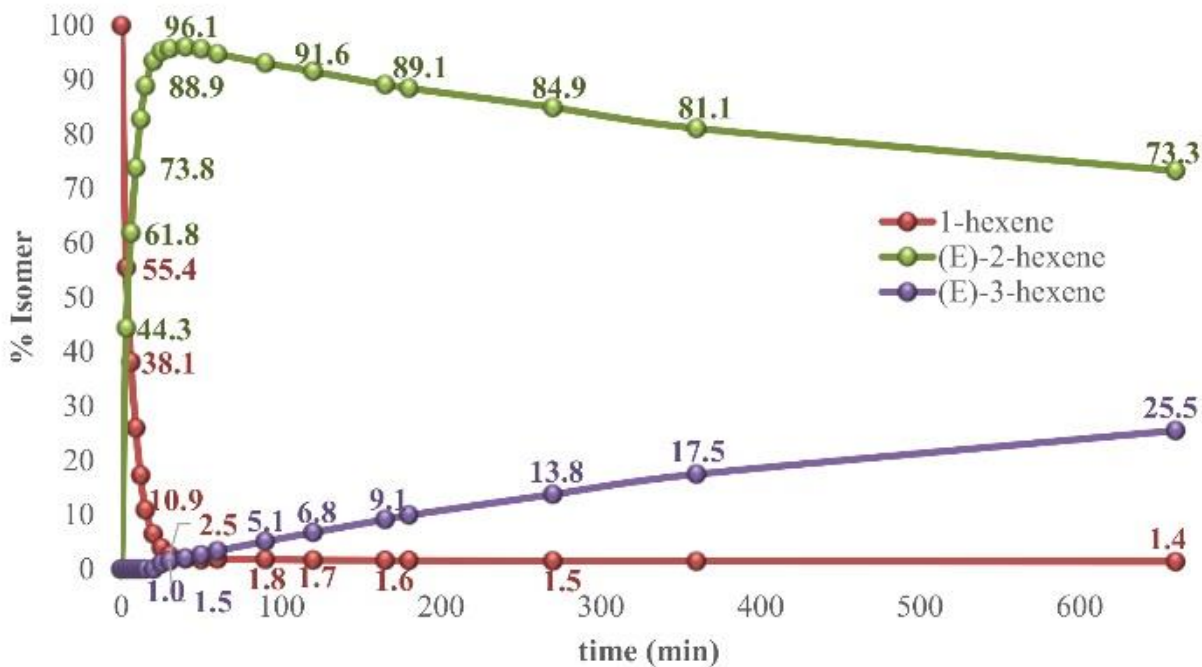
Figure 4.7. Isomerization of **4.1** with catalyst **3.14**

228
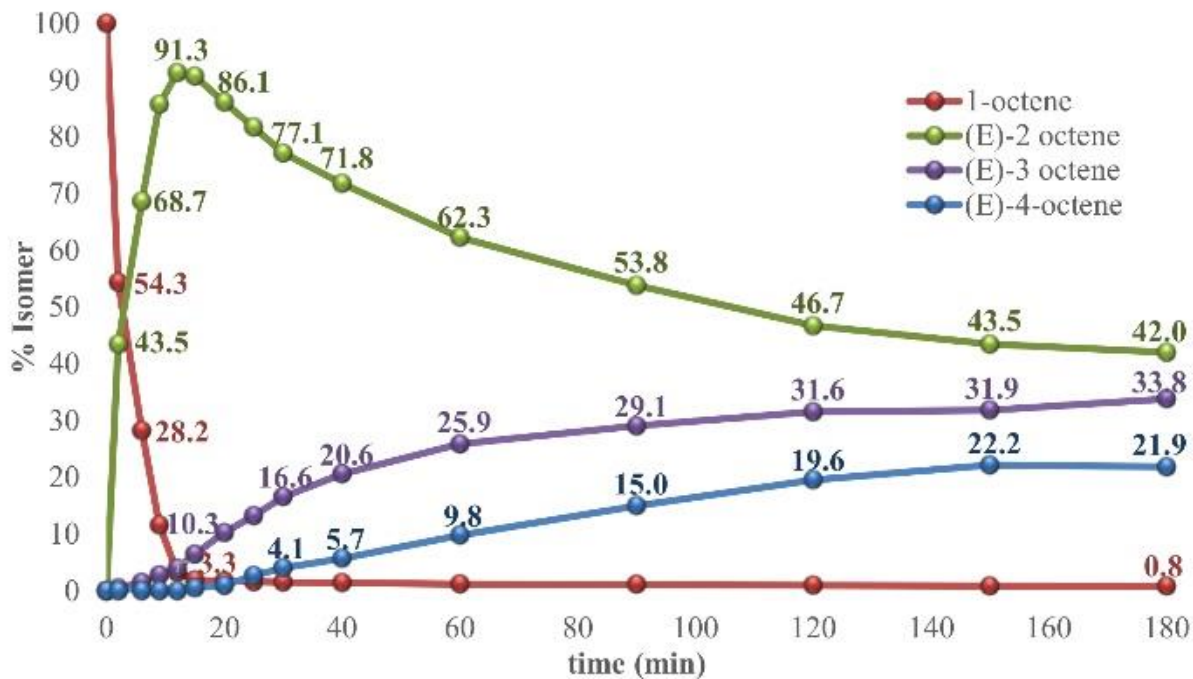
Figure 4.8. Isomerization of **4.5** with catalyst **1.1**
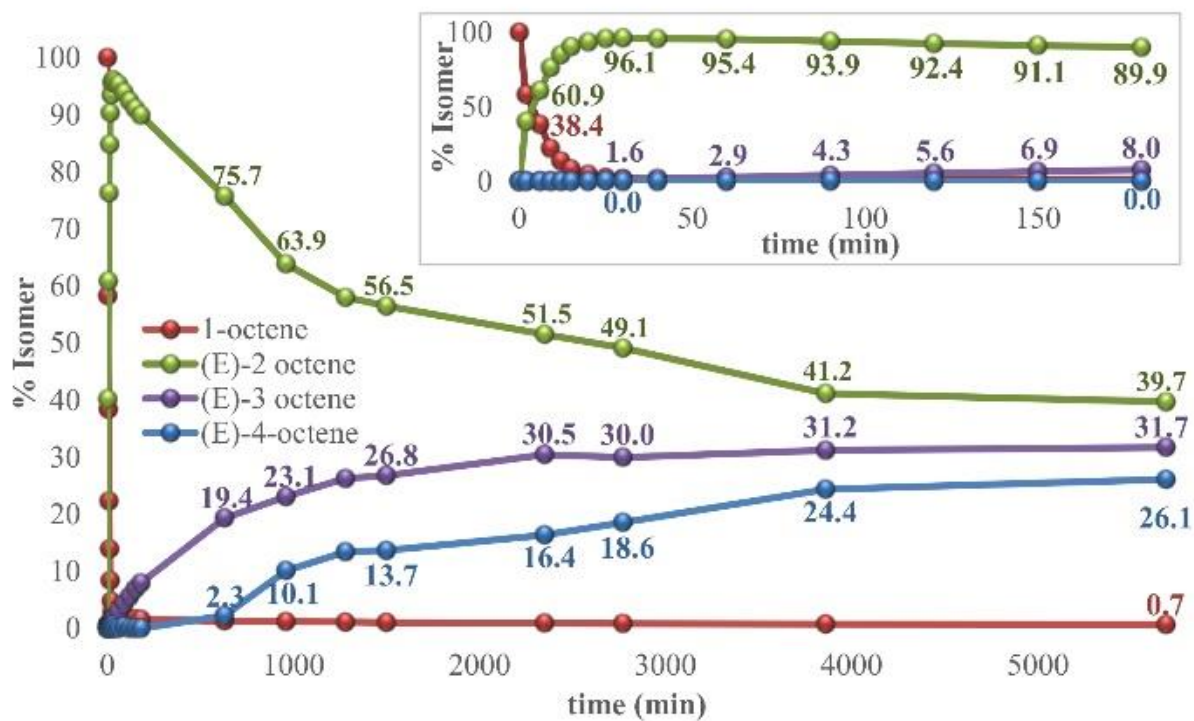
Figure 4.9. Isomerization of **4.5** with catalyst **3.14**. Inset: first 180 min of reaction.
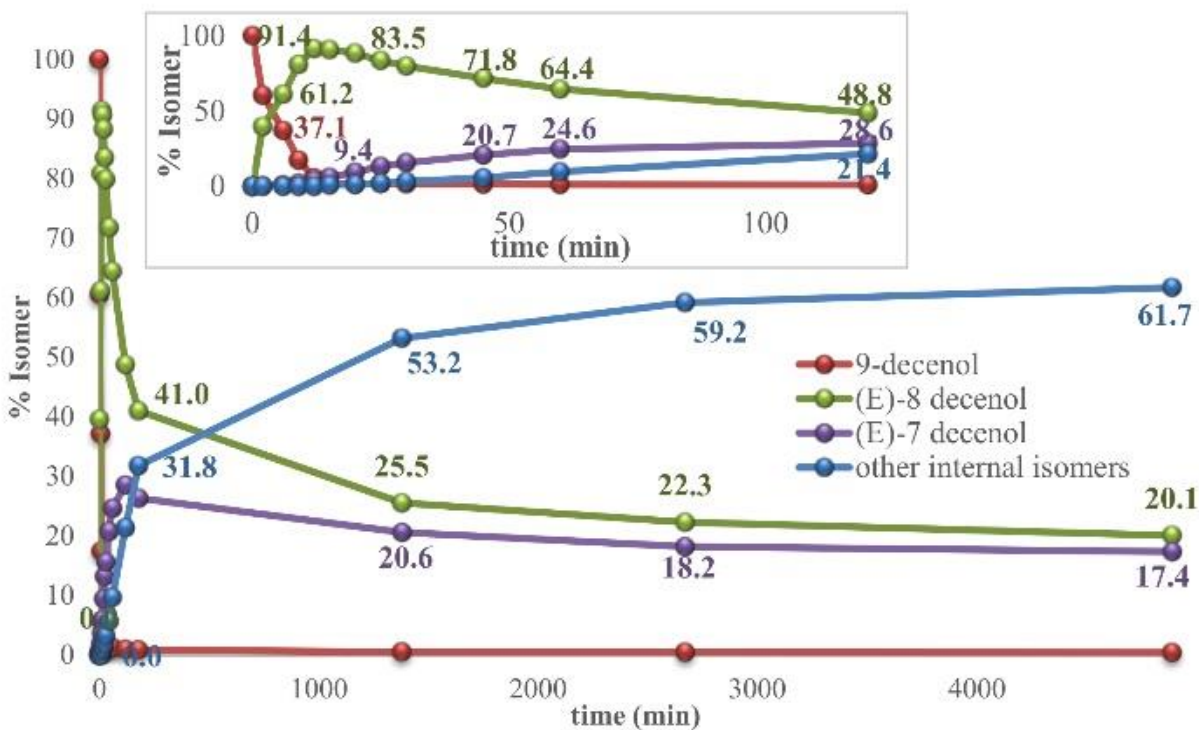
Figure 4.10. Isomerization of **4.9** with catalyst **1.1**. Inset: first 180 min of reaction.
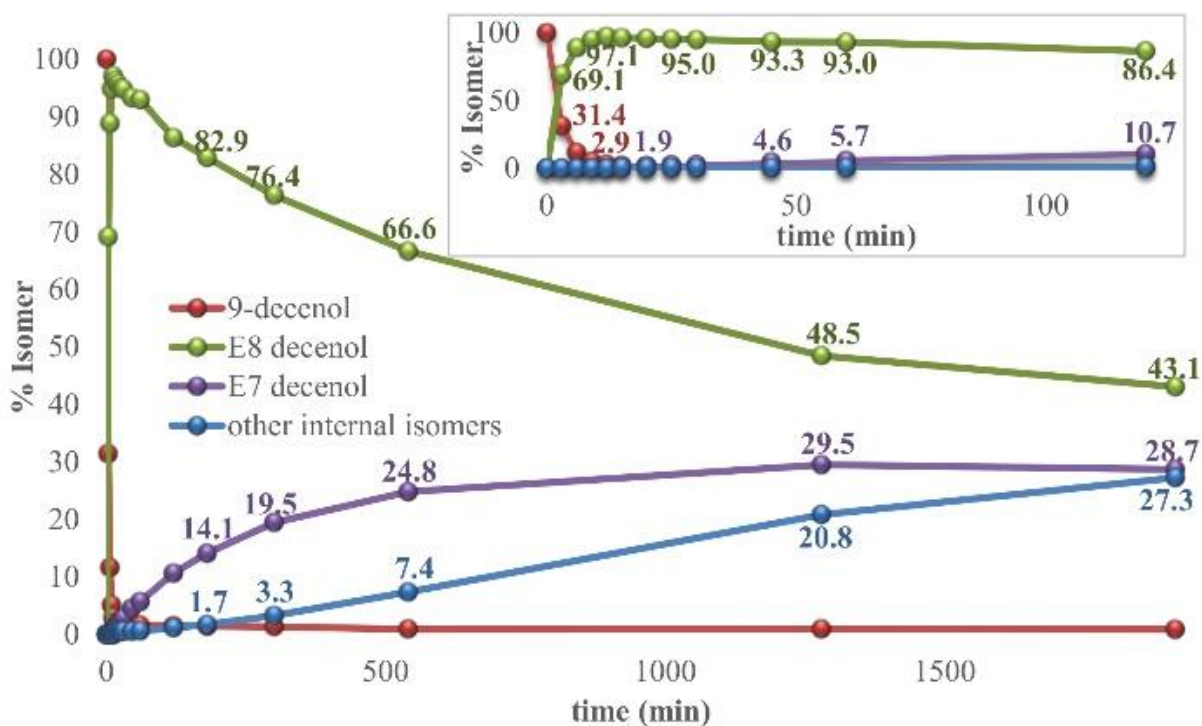
Figure 4.11. Isomerization of **4.9** with catalyst **3.14**. Inset: first 120 min of reaction.
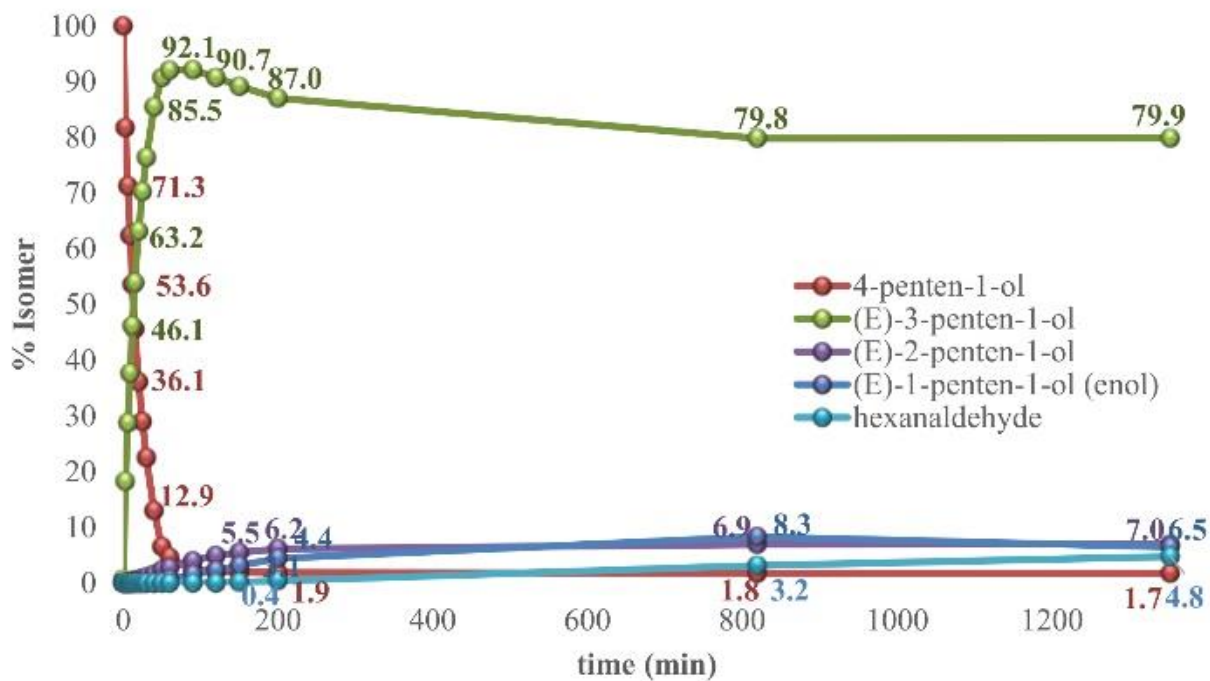
Figure 4.12. Isomerization of **4.7** with catalyst **1.1**
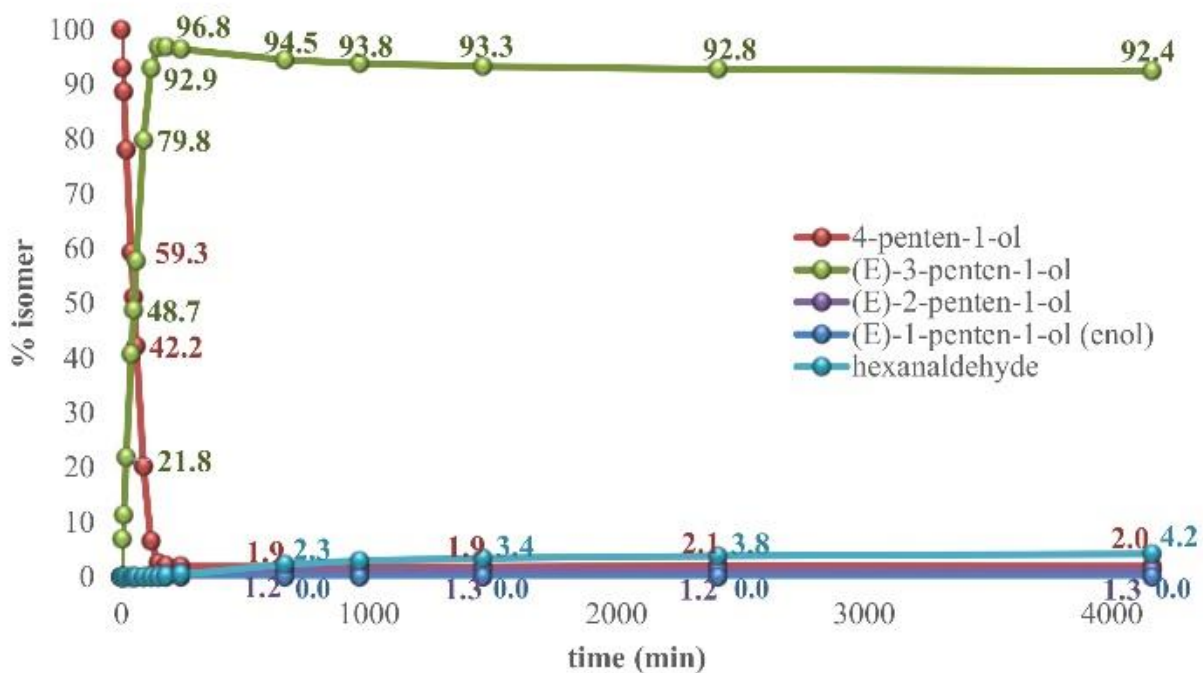
Figure 4.13. Isomerization of **4.7** with catalyst **3.14**
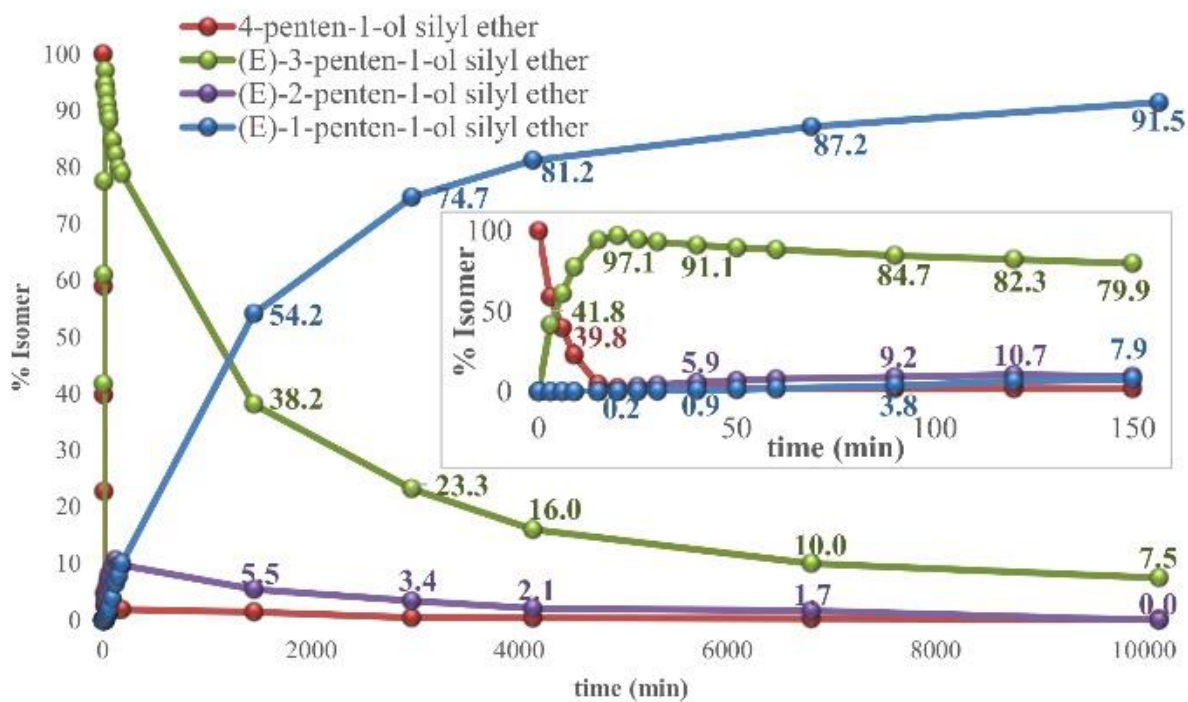
Figure 4.14. Isomerization of **4.10** with catalyst **1.1**. Inset: first 150 min of reaction.
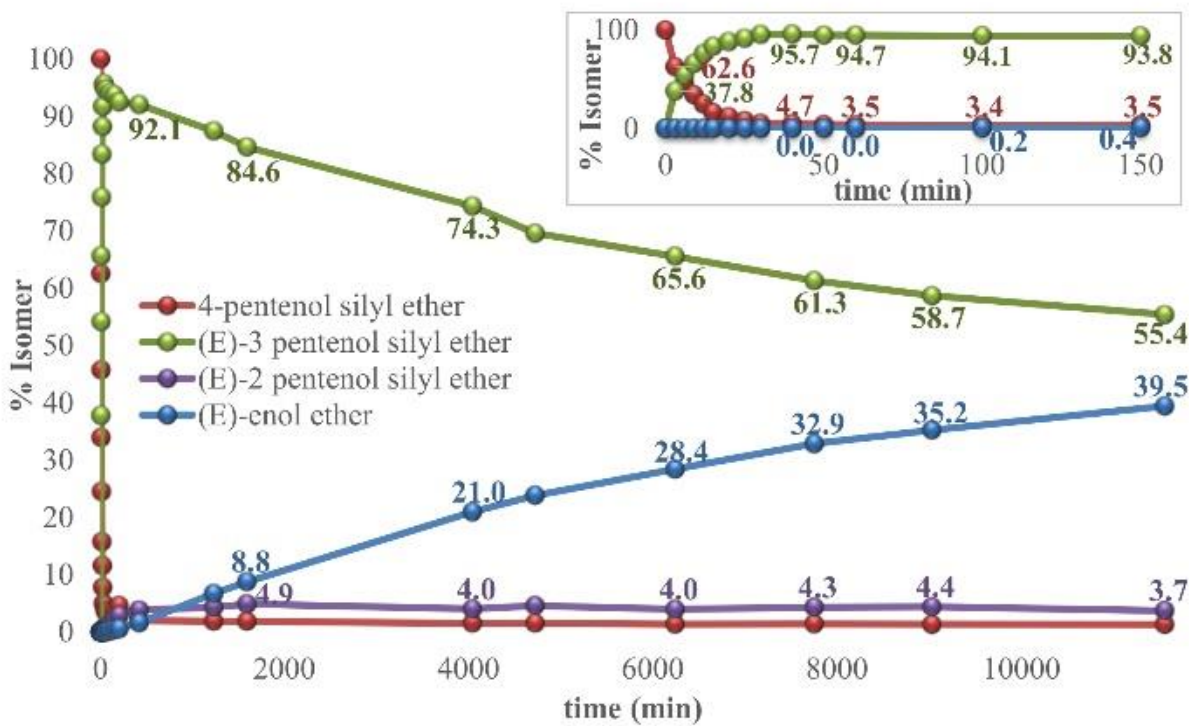
Figure 4.15. Isomerization of **4.10** with catalyst **1.1**. Inset: first 150 min of reaction.
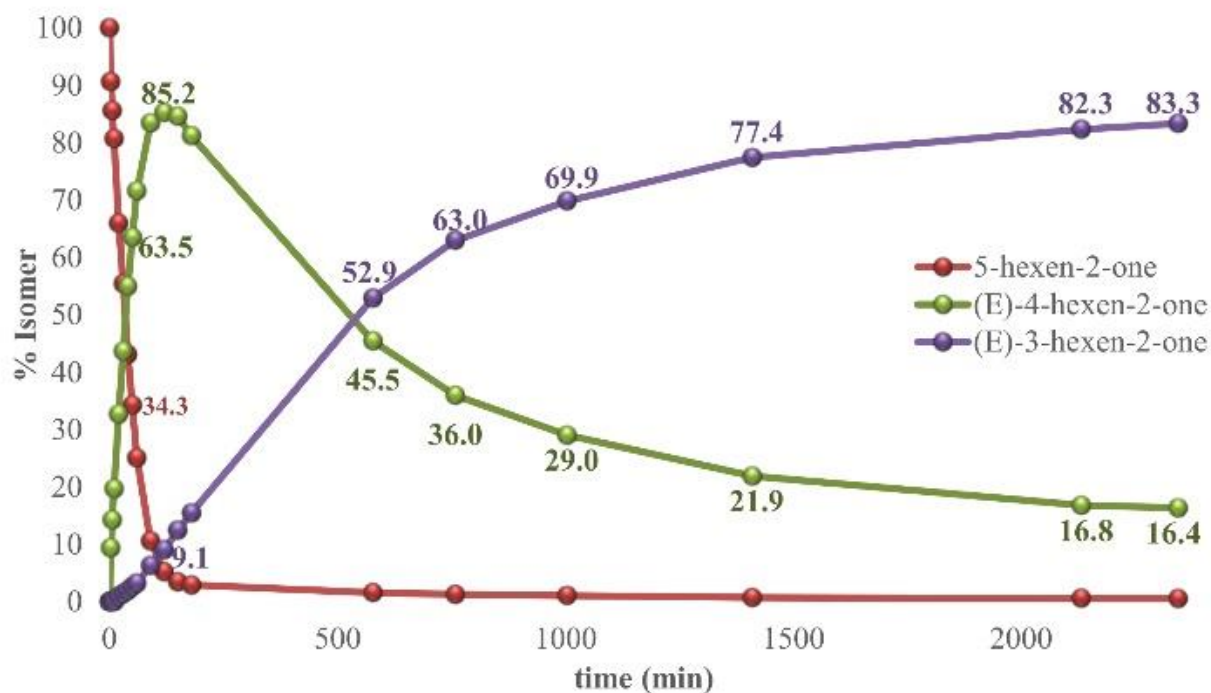
Figure 4.16. Isomerization of **4.16** with catalyst **1.1**
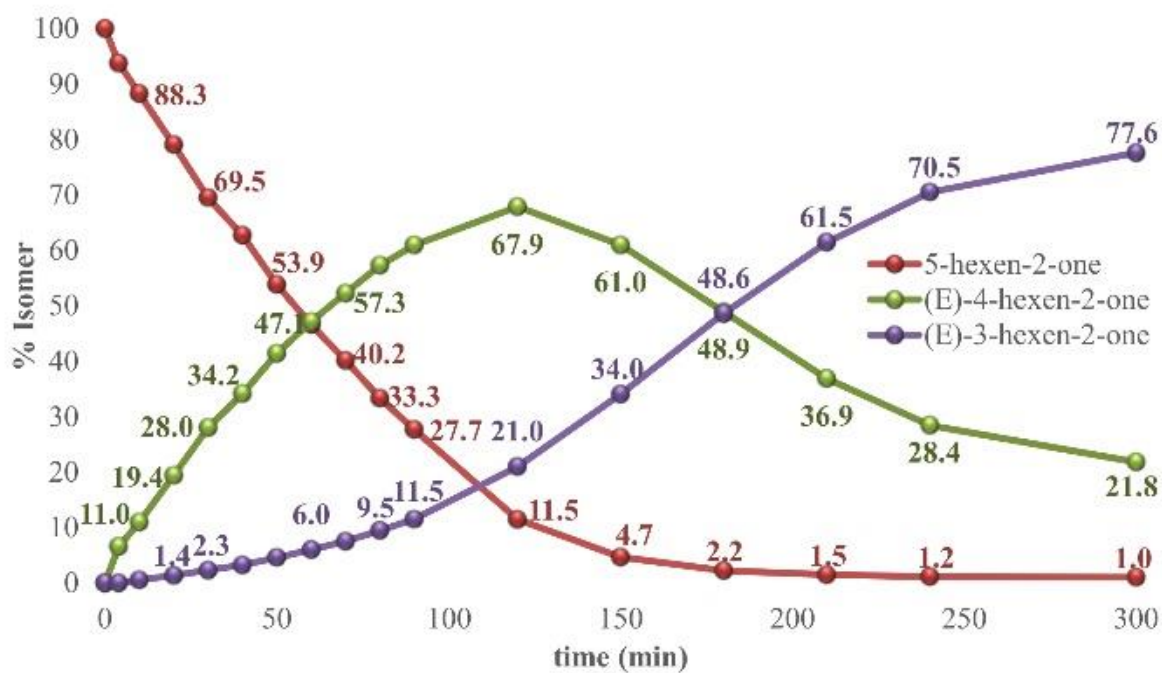
Figure 4.17. Isomerization of **4.16** with catalyst **3.14**

233

One significant finding shown in Table 4.3 is that reactions with every substrate except **4.16** reach >90% of monoisomerized product at their maximum with both catalysts. Similar yields to those shown in Table 4.3 have been reported for catalyst **3.14** (and related complexes **1.2** + **2a**), but yields >90% have not been reported thus far with catalyst **1.1** for substrates that do not contain significant branching or functionality near the isomerization site.[4, 11, 17] The higher yields encountered here are likely due to low catalyst loading and higher frequency of data collection early in the reaction.

What is clear from Table 4.3 is that the level of positional selectivity achievable with catalyst **1.1** can be higher than what has been reported, but that very careful reaction monitoring would be necessary to know when to stop each reaction. For the practical chemist, the variability in product distribution is precisely why a single reported measurement fails to capture the likelihood of isolating the product with similar yield. Of similar importance to high maximum yield is the *duration* with which that isomer remains at high yield, both of which arise from the relative reaction rates of 1- to 2-alkene versus 2- to 3-alkene. With that in mind, our first attempt at comparison in selectivity between catalysts **1.1** and **3.14** focuses on two parameters: the first is a comparison of time to reach 50% conversion of the terminal and monoisomerized alkenes, as a way of measuring half-life. The second parameter is the ratio of the time it takes for the yield to reach 90% to the duration of time that the monoisomerized product remains >90% of the mixture, as both a practical measure and a quantifiable determination of selectivity. Since the ratio is a relative comparison of the two measurements, and both measurements scale with catalyst loading, the ratios should remain constant regardless of catalyst loading. The results are shown in Table 4.4.

Table 4.4. Selectivity ratios with substrates from Figure 4.5: 50% conversion and 90% duration. All times are in minutes.

Substrate	Cat.	Time of 50% conv of 1-alkene	Time of 50% conv of (E)-2-alkene	50% ratio (E)-2:1	Time to reach >90% (E)-2	Duration at >90% (E)-2	>90% Ratio
4.1	**1.1**	~2.5	N/A	-	12	5	0.42
	3.14	~3	N/A	-	~16	134	8.4
Selectivity	**3.14:1.1**			-			**20**
4.5	**1.1**	~2.5	~105	42	>9	<11	1.2
	3.14	~3	~2500	830	~15	~165	11
Selectivity	**3.14:1.1**			**20**			**9.1**
4.9	**1.1**	~4	~110	28	<12	<11	0.91
	3.14	~2	~1200	600	~7	~90	13
Selectivity	**3.14:1.1**			**21**			**14**
4.7	**1.1**	~14	N/A	**-**	~48	~90	1.9
	3.14	~52	N/A	**-**	~110	>4100	>>37
Selectivity	**3.14:1.1**			**-**			**>>20**
4.10	**1.1**	4.5	1000	220	~12	~38	3.2
	3.14	~6.5	~15000 (?)[a]	2300	~23	~470	20
Selectivity	**3.14:1.1**			**10**			**6.3**
4.16	**1.1**	~33	~500	15	N/A	N/A	-
	3.14	~55	~170	3.1	N/A	N/A	-
Selectivity	**3.14:1.1**			**0.21**			-

[a] See Figure 4.15: Very slow reaction.

Ratios comparing relative 50% conversion times for the first and second isomerizations were calculated for substrates **4.5**, **4.9**, **4.10** and **4.16**. Values for 50% conversion times were not determined for substrates **4.1** (because of equilibrium position) and **4.7** (because of likely catalyst deactivation),[16] where deactivation can generally be overcome to complete reactions using higher catalyst loadings. Duration at >90% was not determined for substrate **4.16** because neither catalyst was selective enough to reach 90%. According to the ratios presented above, selectivity ratios ranged from 6 to 20 in favor of catalyst **3.14** for all substrates except **4.16**. Substrates **4.5**, **4.9** and **4.10** were compared using both ratios, and a significant disparity is seen between the two for all three substrates, indicating one of the several shortcomings of using these two particular parameters for selectivity analysis. Another challenge lies in the fact that none of

the time points measured for all 12 reactions pinpoints precisely when the reactions reach 50% 1- or 2-alkene, or 90% 2-alkene, so estimations must be made that introduce large sources of error. The error could be mitigated by collection of a larger number of time points, but the long duration of the experiments prohibited that option. Most importantly, both measures are rather arbitrary; half-life can only legitimately relate to the rate if the kinetics of the reaction are first-order, as is often not the case in catalysis by **1.1** and **3.14** (see below), and the 90% threshold is only useful if the isomer in question reaches that value in the course of both isomerizations. Therefore, a more sophisticated analysis is required: a direct comparison of rate constants, generated from modeling the kinetics of the reaction.

Prof. Andrew Cooksy then fit the experimental data to curves generated by adjustment of relative rate constants, to provide an initial fit for each of the reactions except those with substrate **4.7** (because of the significant deactivation). This fit was then improved on by systematic modifications to each isomerization, including determining the reversibility of the isomerization as well as the order of the reaction. His results are included because they are essential to the discussion, and the details of the modeling are included in the experimental section. An example of the fits are included below in Figure 4.18. It should be noted that the time axis on the graphs are in log format, so the change in concentrations appear more dramatic than normal.
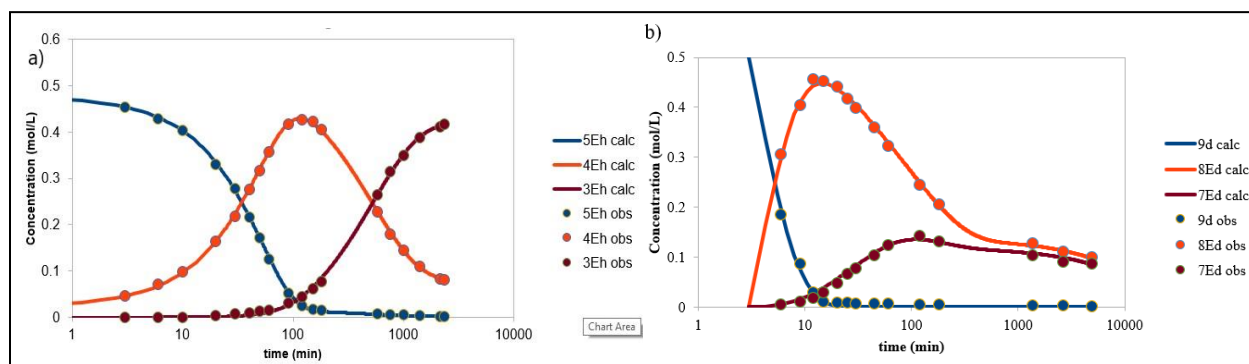
Figure 4.18. Observed time-dependent concentrations and fitted profiles for (a) the **4.16/1.1** and (b) **4.9/1.1** systems. The horizontal time axis is in log format to more clearly display the evolution of the concentrations in different time regimes. The compound names in each legend are shorthand; for example, 3Eh – (*E*)-3-hexen-2-one, and 7Ed – (*E*)-7-decen-1-ol.

To provide uniform rate constants for comparison, 2nd-order rate constants were multiplied by the catalyst concentration (rate constants calculated from 2nd-order reaction steps are indicated with * in Table 4.5). k_1 refers to conversion of 1-alkene to (*E*)-(2)-alkene, k_2 refers to conversion of (*E*)-(2)-alkene to (*E*)-(3)-alkene, and so on. Selectivity ratios were then generated by dividing k_1 by k_2 to indicate relative selectivity between catalysts for the 1- to 2-alkene versus 2- to 3-alkene transformations, for what could be called the 'terminal/internal ratio'. An 'internal/internal' ratio was also calculated by dividing k_2 by k_3. Results are shown in Table 4.5.

Table 4.5. Selectivity ratios comparing relative rate constants for substrates **4.1**, **4.5**, **4.9**, **4.10**, and **4.16** with catalysts **1.1** and **3.14**.

Substrate	Cat.	k_1	k_2	k_1:k_2	k_3	k_2:k_3
4.1	**1.1**	0.326	0.01126	28.95	N/A	-
	3.14	0.1292	0.000674	191.69	N/A	-
Selectivity	**3.14:1.1**			**6.62**		-
4.5	**1.1**	0.407	0.01046	38.91	0.0194	0.54
	3.14	0.1676	5.54E-4	302.53	7.71E-4	0.72
Selectivity	**3.14:1.1**			**7.78**		**1.33**
4.9	**1.1**	0.3166	0.00985	32.14	0.0116	0.85
	3.14	0.3951	0.001015	389.26	5.94E-4	1.71
Selectivity	**3.14:1.1**			**12.11**		**2.01**
4.10	**1.1**	0.1701	5.22E-3*	32.59	0.0168*	0.31
	3.14	0.1249	8.7E-5	1435.63	1.53E-3	0.06
Selectivity	**3.14:1.1**			**44.06**		**0.18**
4.16	**1.1**	0.0991*	1.533E-3	64.64	N/A	-
	3.14	0.1042*	0.02208	4.72	N/A	-
Selectivity	**3.14:1.1**			**0.07**		-

*indicates 2nd order rate constant multiplied by catalyst concentration – for pseudo-1st order rate constant

Ratios for k_1/k_2 for catalyst **1.1** were relatively similar across all four substrates, ranging from 28 to 65. The range of ratios for catalyst **3.14** was much larger, ranging from 4.8 to 1400. When comparing k_1/k_2 ratios between catalysts **1.1** and **3.14**, linear unfunctionalized alkenes **4.1** and **4.5** show a modest 6 – 8 fold larger ratio; in other words, catalyst **3.14** is 6 – 8 times more selective for monoisomerization of shorter-chain linear alkenes than catalyst **1.1**. Longer-chain functionalized alkene **4.9** provides slightly higher selectivity for both terminal/internal ratio and internal/internal ratios, at 12.11. The largest difference in terminal/internal selectivity, however, is seen with substrate **4.10**, which is the *tert*-butyl(dimethyl)silyl-protected ether of pentenol. **4.10** shows a *44-fold increase* in selectivity with catalyst **3.14** over catalyst **1.1**. While this cannot be compared to the unprotected pentenol **4.7** because of loss of catalyst through some form of deactivation, we have seen previously with **1.1** that the presence of a silyl protecting group can slow isomerization. It seems likely that the bulk of the protecting group is responsible for the slower (*E*)-3- to (*E*)-2-pentenol silyl ether isomerization with catalyst **3.14**.

While substitution at the 5-position (relative to the alkene) with a bulky protecting group likely contributed to the increased terminal/internal selectivity in the case of substrate **4.10**, the presence of a carbonyl oxygen in the 5-position (in the case of substrate **4.16**) leads to a *decrease* in selectivity for catalyst **3.14**. The initial isomerization with catalyst **3.14** appears to proceed with a similar rate constant (k_1) to catalyst **1.1**, which is the case with the other three substrates. The second isomerization with **3.14** proceeds at a rate that is faster than catalyst **1.1**, leading to a selectivity ratio that is 4:1 *in favor* of catalyst **1.1**.

The change in selectivity of **3.14** in the case of **4.16** is accompanied by qualitative and quantitative changes in the NMR spectra during isomerization. Catalyst **3.14** itself possesses a brilliant blue color, and most isomerization reactions using **3.14** (including substrates **4.1**, **4.5**, **4.9**, and **4.10**) maintain the blue color during the course of the reaction. By contrast, the reaction of **4.16** with **3.14** exhibits an orange color, suggesting a stronger interaction of **4.16** and **3.14** (recall discussion in Chapter 3 regarding color and Cp*Ru species). Taken together, the orange color is consistent with **4.16** being the only substrate which, in combination with **3.14**, requires the reaction complex to be invoked in order to fit the rate constants reported in Table 4.5. Likewise, an examination of the ^{1}H chemical shift of the imidazolyl C-H of **3.14** reveals larger chemical shift changes with **4.16** than is seen with substrates **4.1** and **4.9** (Figure 4.19). An initial chemical shift of 7.27 ppm without substrate is shifted upfield by 0.03-0.05 ppm by the addition of **4.1** and **4.9**. In contrast, the early course of the reaction with **4.16**, the imidazoyl C-H shift is 0.2 ppm upfield, and later when approaching equilibrium, the imidazolyl C-H has shifted downfield relative to catalyst by ~0.45 ppm.
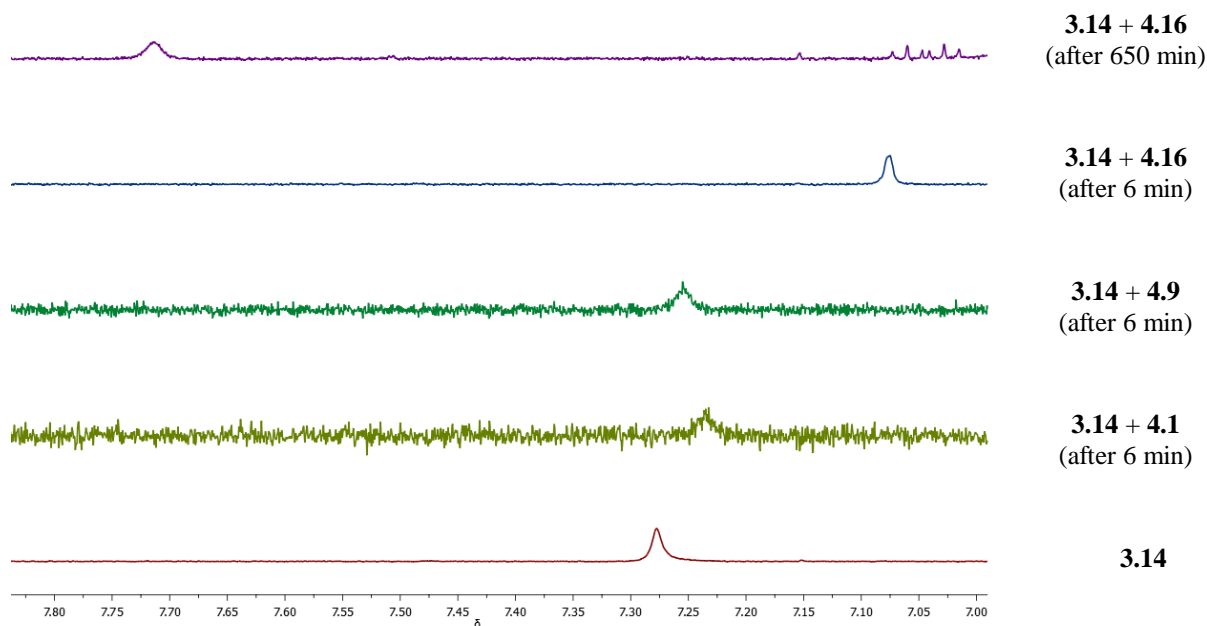
Figure 4.19. Stacked ^{1}H NMR spectra of catalyst **3.14** (7.0 to 7.8 ppm) in the presence of substrates **4.1** (0.3 mol% catalyst loading), **4.9** (0.3 mol% catalyst loading), and **4.16** (2.0 mol% catalyst loading).

Upon closer inspection of the isomerization of **4.16** with catalyst **3.14**, (Figure 4.20) the upfield peak remains until complete consumption of **4.16** has taken place; the disappearance of the upfield peak (assigned to intermediate **4.20**) is concurrent with the disappearance of **4.16**. As the upfield peak disappears, the downfield peak (assigned to intermediate **4.21**) increases in intensity.

240
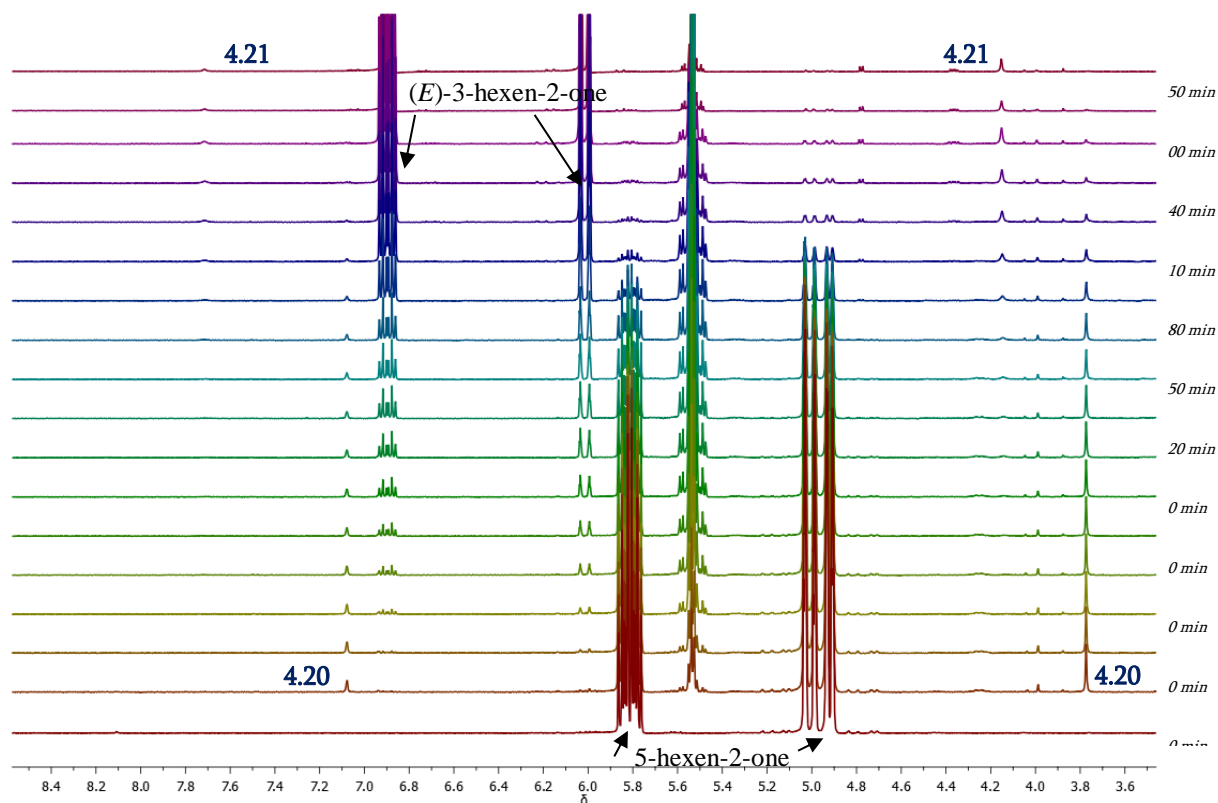
Figure 4.20. Stacked ^{1}H NMR plot (3.6 to 6.4 ppm) for the conversion of **4.16** to a mixture of (*E*)-4-hexen-2-one and (*E*)-3-hexen-2-one over 650 min with catalyst **3.14**.
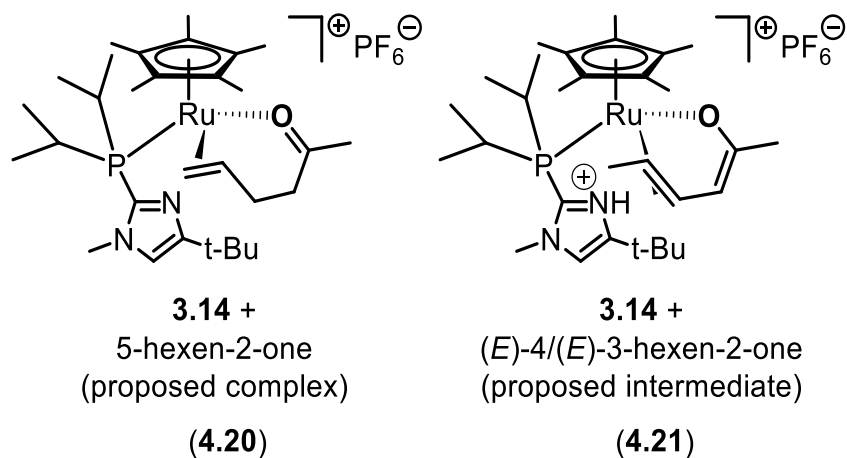
Figure 4.21. Proposed intermediates **4.20** and **4.21** from isomerization of **4.16** with catalyst **3.14**

The upfield shift of the imidazolyl C-H in **3.14** when exposed to **4.1**, **4.9**, and **4.16** is consistent with reversible binding of alkene to catalyst, which may or may not involve opening of the P,N-chelate.[18] The shift is greater with substrate **4.16**, which could be due to chelation of

241

the carbonyl oxygen (see structure of intermediate **4.20** in Figure 4.21), increasing the stability of alkene binding. The downfield shift that appears later in the reaction is consistent with protonated imidazole,[18] which could come from conjugated enolate **4.21** (Figure 4.21), a possible intermediate between (*E*)-4- and (*E*)-3-hexen-2-one isomers. Intermediate **4.21** appears to be long-lived enough to show vinyl peaks consistent with bound alkene; a partial assignment of peaks is shown in Figure 4.22. The presence of strongly-bound alkene species during catalysis is in agreement with fitted second-order kinetics for both conversion of 5- to (*E*)-4-hexen-2-one and (*E*)-3-hexen-2-one.
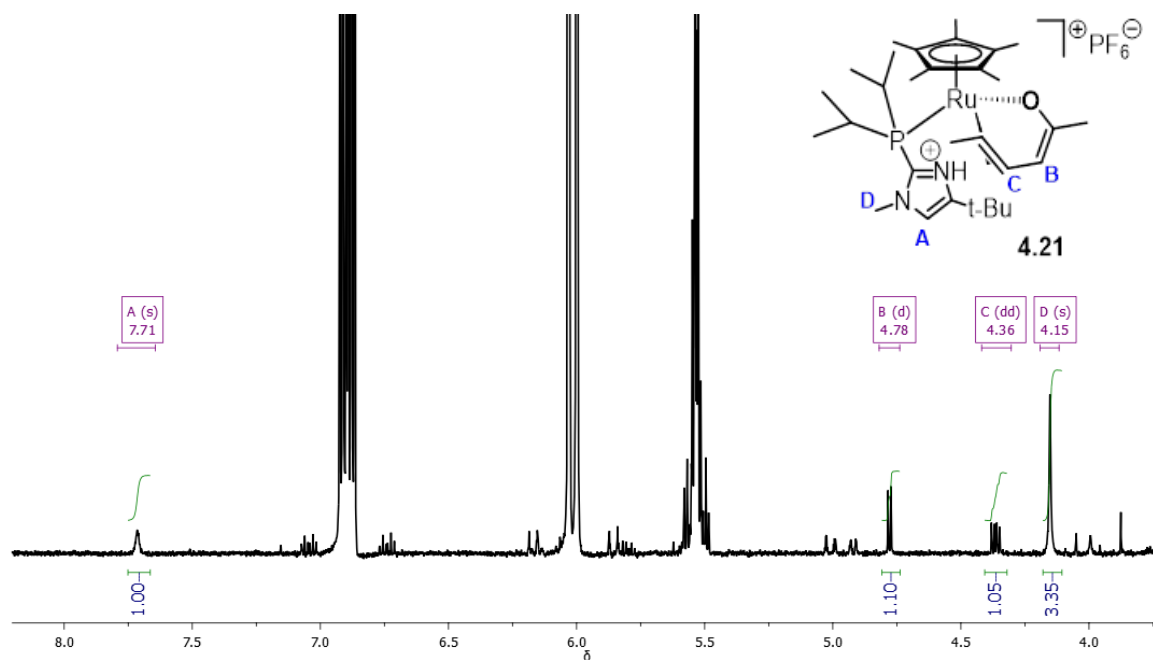
Figure 4.22. Partial ¹H NMR of **4.16** with **3.14** after 650 min. Signals A – D are believed to originate from complex **4.21**; partial assignments are included in the Figure.

Binding and chelation of the carbonyl oxygen acidifies the α-protons of the carbonyl, which would make the formation of intermediate **4.21** easier, thus facilitating the (*E*)-4- to (*E*)-3-hexen-2-one isomerization. The chelation of alkene substrates to Cp^{R}Ru systems have been shown to influence product formation and selectivity by Trost (R = H)[19] and Vidovic (R = Me)[20] In contrast to catalyst **3.14**, catalyst **1.1** shows no enhanced rate with respect to the (*E*)-4-/(*E*)-3-

conversion, perhaps due to the presence of the nitrile as a competitive ligand preventing the binding of the carbonyl oxygen.

In summary, catalyst **3.14** provides a 6- to 12-fold enhancement in selectivity for monoisomerization as compared to highly optimized and carefully monitored reactions using **1.1** for a number of linear substrates, rendering it a superior alternative to catalyst **1.1** when a single positional isomerism is required, but high amounts of (*E*)-isomers are desired. However, functionality or branching near the alkene can provide a significant positive or negative influence on the relative selectivity depending on the nature of the interaction of the functional group with catalyst **3.14**, making catalysis with **3.14** much more substrate-dependent than previously expected. Future work will focus on expansion of the substrate scope to further understand how position, size and composition of functional groups and/or branching can affect the relative positional selectivity of **3.14** compared with **1.1** and other isomerization catalysts.

4.5. Further studies of alkene binding

In an effort to understand the general modes of binding of alkenes to **3.14** and how they influence selectivity, we extended the examination of the interaction of **3.14** to substrates that can only contain a single alkene ligand. The most prominent feature of a UV-visible spectrum of catalyst **3.14** is a broad, intense absorbance with a maximum of 582 nm, which is responsible for its deep blue color. TDDFT calculations of the complex ascribe this absorbance to two major transitions: HOMO→LUMO and HOMO-1→LUMO, which are both metal-to-π^* transitions. When 1-hexene is introduced, a significant drop in the absorbance at 582 nm occurs, and then throughout the course of the next 30 min, the peak begins to return towards its original intensity. We attribute the initial decrease in intensity to binding of 1-hexene to the complex, which populates the LUMO and quenches the metal-to-LUMO transition and therefore the absorbance

at 582 nm. As the 1-hexene is consumed, the absorbance partially returns, indicating an increase in amount of free complex. Qualitatively, the rate of increase in absorbance roughly correlates with the rate of isomerization of 1-hexene to (*E*)-2-hexene, which leads to the hypothesis that the (*E*)-2-hexene that is formed does not bind as favorably to the complex. Further evidence for the hypothesis is that in a separate experiment, addition of (*E*)-2-hexene to a solution of **3.14** produces a much smaller drop in absorbance. A possible explanation is that of the alkenes under discussion, 1-hexene binds more readily to **3.14** than does (*E*)-2-hexene; the relative binding affinities may help favor isomerization of 1 to (*E*)-2-hexene over isomerization of (*E*)-2 to (*E*)-3-hexene.
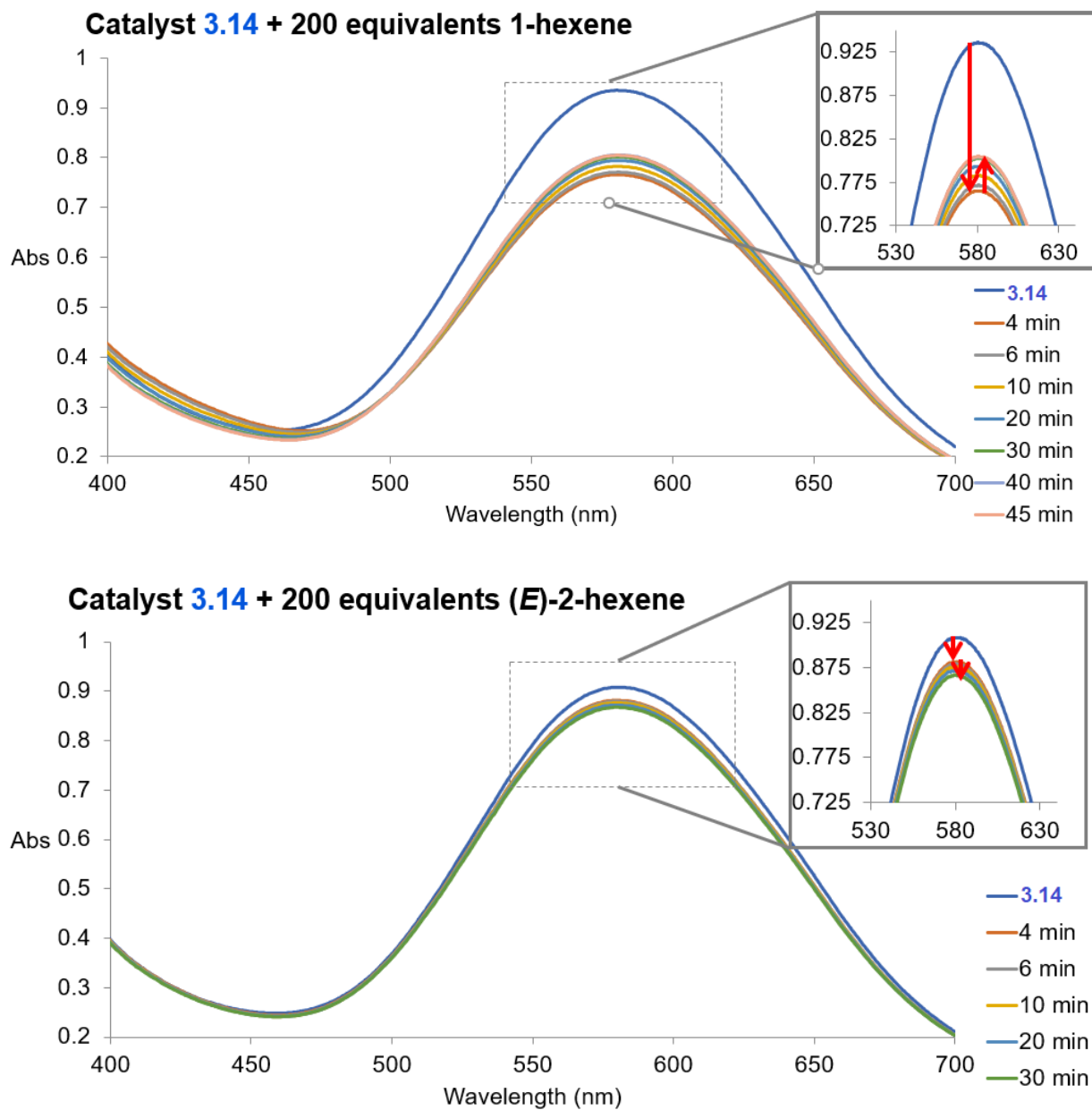
Figure 4.23. UV-visible spectra of **3.14** before and after addition of hexenes. Top: **3.14** with 200 equiv of added 1-hexene, monitored every 2-10 min. Bottom: **3.14** with 200 equiv of added (*E*)-2-hexene, monitored every 2-10 min.

More direct evidence of alkene binding is seen when NMR spectroscopy is used with smaller alkenes at low temperatures. When ethylene was bubbled through an acetone solution containing **3.14**, an immediate change in color from deep blue to light orange-brown was

observed, which persisted when kept under an atmosphere of ethylene. NMR data of **3.14** with ethylene are consistent with structure **4.22** (Figure 4.25), which is an 18-electron complex containing a single bound ethylene. In the ^{1}H NMR spectrum, the ethylene signal was visible as a broad signal centered at 2.45 ppm. When cooled to -30 °C, four separate ethylene C-H signals were visible, ranging from 2.1 to 3.5 ppm, which became sharper upon further cooling. Two isopropyl C-H and four isopropyl-CH$_3$ peaks were also resolved, consistent with diasterotopic methyls as **4.22** features bound ethylene and chelated imidazole.

Minor species: consistent with allyl intermediate **4.24**

major species: consistent with bound propylene **4.23**
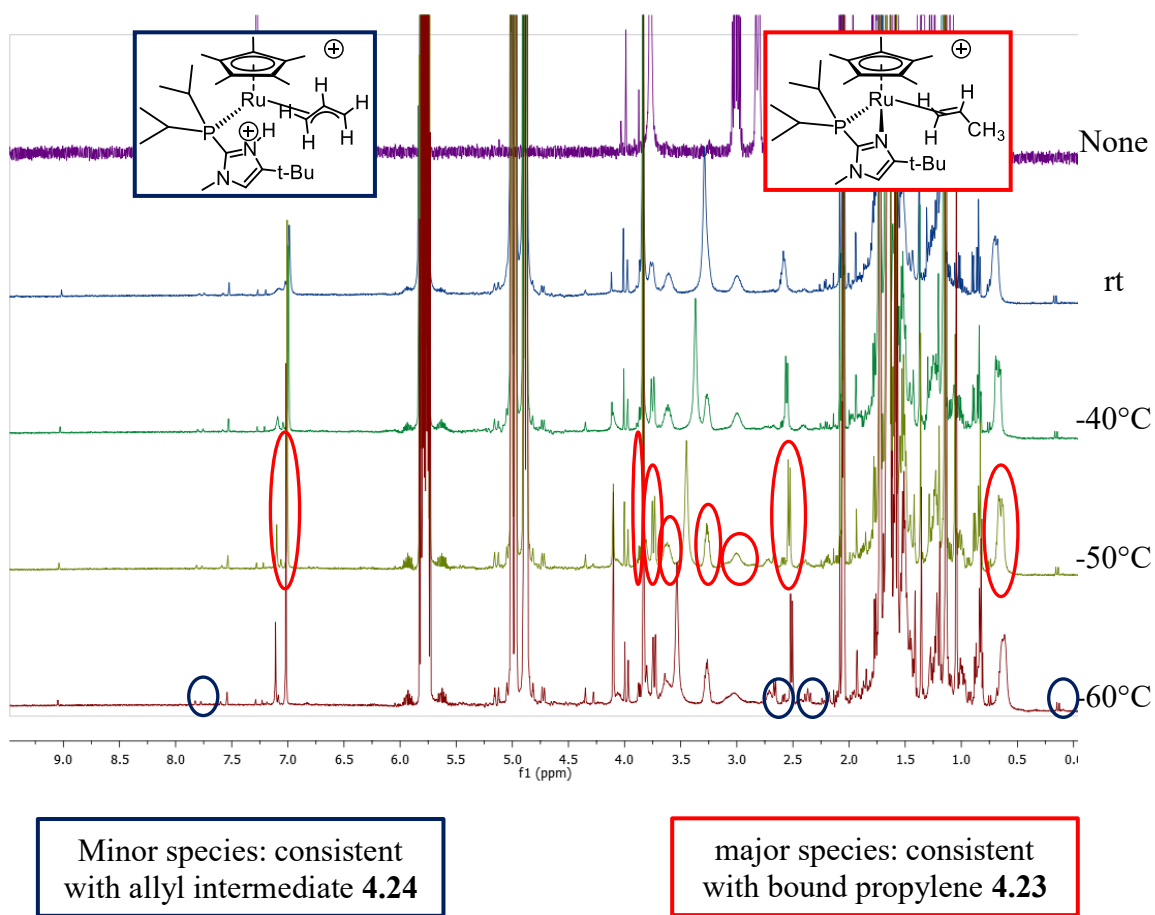
Figure 4.24. VT NMR spectra at 500 MHz of **3.14** + propylene in acetone-d_6

When propylene was introduced to a solution of **3.14**, the blue color lightened considerably, and NMR data at low temperatures (≤-30 ˚C) were consistent with **4.23** (Figure 4.25) as the major species. At all temperatures, the imidazole C-H signal in the ^{1}H NMR spectra as well as the phosphorus signal corresponding to the complex in ^{31}P NMR shifted upfield relative to that of complex **3.14**, accompanied by the splitting of the isopropyl C-H protons into two distinct signals, signifying a desymmetrization of the complex consistent with binding of the propylene. In addition, between -40 and -60 °C, three additional signals in ^{1}H NMR began to resolve (one broad, and two doublets) between 2.5 and 3.8 ppm that integrate to one proton each for the major species. These new signals could represent the alkene C-H peaks for bound propylene, although no crosspeaks were observed between these signals in an 2D COSY NMR spectrum.

3.14

4.22: R=H
4.23: R=Me
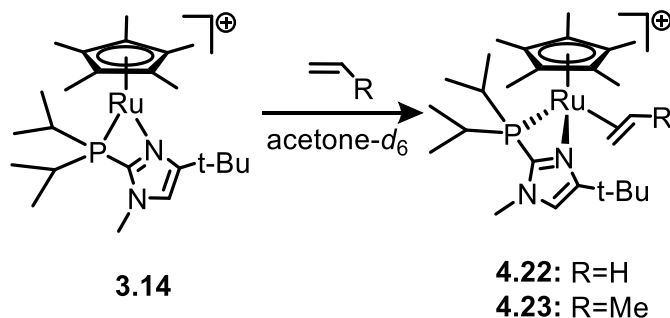
Figure 4.25. Reactions of ethylene and propylene with **3.14**, generating **4.22** and **4.23** respectively

In addition to the major signals that are assigned to **4.23**, a number of small ^{1}H signals corresponding to other minor species were present and were more noticeable at the reduced temperatures. We aimed to probe whether one or more of these species corresponds to another intermediate in the catalytic cycle, in particular, an intermediate that is consistent with the bifunctional mechanism proposed by ourselves[2-3] and Fang[21] in which the phosphino-imidazole ligand acts as a pendant base, shuttling an allylic proton between carbons in the key step. In the

proposed intermediate (see structure **4.24** in Figure 4.26), the imidazole is protonated by the propene, generating an allylic anion stabilized by the metal. One indication of **4.24** would be the presence of a downfield signal in the ¹H NMR spectrum corresponding to the N-H peak of the protonated imidazole, as well as downfield shift of the imidazole CH proton. At low temperatures (-30 to -60 °C, Figures 4.59-4.68), both a downfield shifted CH singlet at 7.75 ppm and a very downfield singlet assigned to the N-H proton were present at 12.4 ppm, which split into a doublet (J = 100 Hz) when an ¹⁵N-labeled ligand was used. The 12.4 ppm doublet is ascribed to the NH of an unchelated and protonated imidazole.[22] Further analysis of the mixture by 2D NMR leads to identification of most of the signals ascribable to **4.24** (Table 4.68 and Figure 4.70). Assigned ¹H NMR signals for the bound allyl ligand range from 0.69 ppm to 2.62 ppm, while ¹³C NMR signals for the terminal carbons of the allyl group are at 41.0 and 44.7 ppm, with the central carbon (C2) of the allyl at 87.8 ppm. The presence of five distinct ¹H NMR signals and three distinct ¹³C NMR signals for the allyl ligand would suggest asymmetry in complex **4.24**, which would not be expected from the nature of the ligands on the complex (non-chelated phosphine ligand, symmetrical allyl ligand). The asymmetry could be induced by the imidazole moiety being positioned to one side of the allyl group, with restricted rotation at low temperatures limiting the interconversion of the two atropisomers.
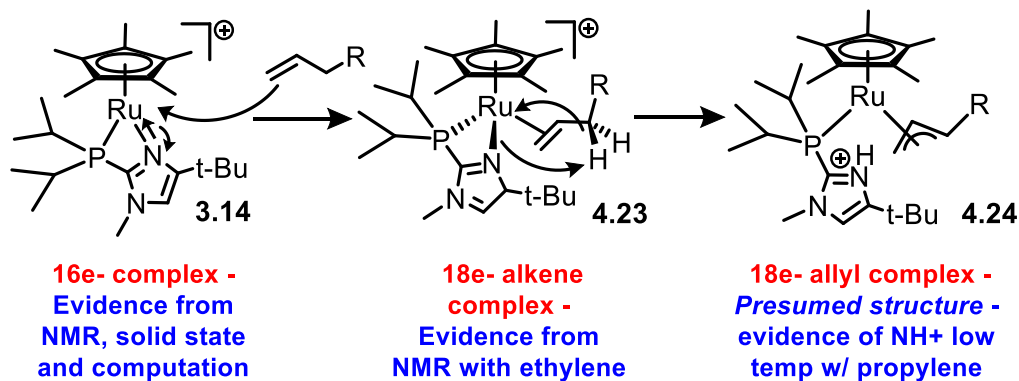
Figure 4.26. Binding modes of imidazolyl moiety and alkene/allyl ligand

4.6. Conclusion

In summary, the coordinatively unsaturated Cp*Ru catalyst **3.14** provides the same exceptionally high selectivity for (*E*)-2-alkenes as catalyst **1.2**+**1.2a**, with yields usually exceeding 95%, but with a dramatic increase in reaction efficiency (>400 times faster). Expeditious isomerization occurs at room temperature, with practical loadings of 0.1 to 0.5 mol % for most substrates, and commercial-grade substrates can be used after a simple deoxygenation. The binding and reactivity studies of **3.14** with alkenes, combined with computational modeling, depict the imidazole moiety on the diisopropyl(2-methyl-4-tert-butylimidazolyl)phosphine ligand as a hemilabile 4-electron donor. Binding modes can range from 4-electron donation, like in its resting state (both the lone pair from the basic nitrogen and the π-system of the imidazole donate to the ruthenium - see **3.14**), to two-electron donation in **4.22** and **4.23**, to no donation (imidazole completely unchelated and protonated – see **4.24**), a range that is unique in Cp*Ru(L)X chemistry, where L= P or N, and X= P, N or halide. In **3.14**, breaking the Ru-N bond of the κ^2-*P,N* ligand provides two coordination sites for the allyl intermediate that is formed during catalysis, and characterized here for the first time. UV-vis spectral data, as well as electronic modifications to **3.14** (in the form of **3.15**),have provided some initial insights into the selectivity for monoisomerization. The increased steric bulk of the pentamethylcyclopentadienyl (Cp*) ligand in complex **3.14** compared to the smaller cyclopentadienyl (Cp) ligand in **1.1** appears to inhibit binding of internal alkenes, which prevents further migration after the initial isomerization. Bulky groups near the double bond on the substrate appear to enhance the preference of binding terminal alkenes over internal ones, considering that the isomerization of 5-methyl-1-hexene is dramatically more selective for

catalyst **3.14** than the isomerization of 1-hexene (470-fold difference in selectivity for 5-methyl-1-hexene, six-fold for 1-hexene, as compared to catalyst **1.1**). This result further supports the conclusion that the increased steric bulk of Cp* is responsible for the increase in selectivity for monoisomerization. Further studies to fully elucidate the isomerization mechanism are ongoing and will be reported in due course.

Future work will include a full kinetic and computational analysis of the isomerization of alkenes with **3.14** to explore the mechanism and to verify the origin of selectivity. An additional area of exploration is in further increasing the selectivity of **3.14** for monoisomerization by increasing the bulkiness of the Cp* ligand. While it is clear that increasing the bulk of the Cp* ligand enhances selectivity, it is possible that too much bulk could inhibit binding of the terminal alkene as well, which would lead to decreased rates of isomerization; moreover, there is the danger that added bulk will aid in dissociation of the phosphine ligand. A series of complexes with small, systematic changes, such as exchanging a methyl group on the Cp* for an ethyl group, would be informative. If increasing the bulk further does indeed make the catalyst more selective, a comparison of rates for the series could allow for the determination of the ideal catalyst, one that is a compromise that allows for the most selectivity without too large of a decrease in efficiency.

4.7. Experimental

Preparation of catalyst stock solutions for isomerization reactions
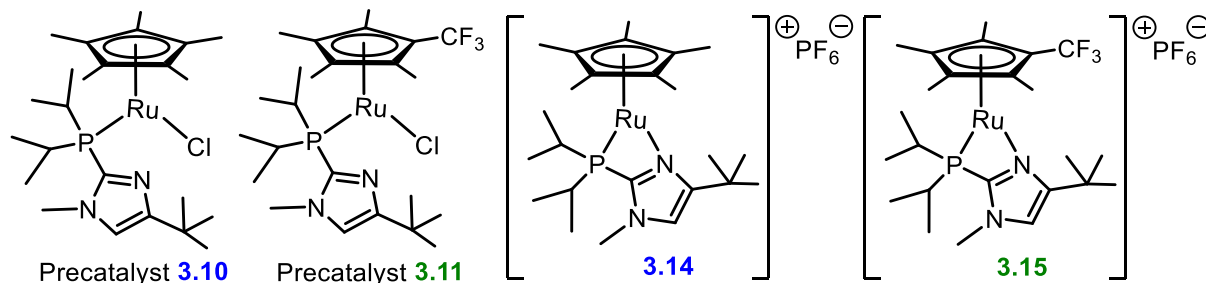
Figure 4.27. Precatalysts **3.10** and **3.11** and catalysts **3.14** and **3.15** used for isomerization reactions

Preparation of Precatalyst Solution A

In a scintillation vial with a Teflon-lined cap, precatalyst **3.10** (19.0 mg, 0.0360 mmol) was weighed out and acetone-d_6 (500 μL) was added, forming a solution with a molarity of **0.072 M**, which was kept in the glovebox, under inert atmosphere. Aliquots of precatalyst solution A were measured from this vial and added to the reaction. NMR data have shown that the complex **3.10** contained in this solution transforms to the ionized complex (catalyst **3.14**) immediately upon addition to reaction mixtures containing a sufficient amount of TlPF$_6$ ($\geq$ 1:1 TlPF$_6$: complex **3.14**) to achieve ionization.

Preparation of Precatalyst Solution B

In a scintillation vial with a Teflon-lined cap, precatalyst **3.10** (13.2 mg, 0.0251 mmol) was weighed and acetone-d_6 (1.00 mL) was added, forming a solution with a molarity of **0.0251 M**, which was kept in the glovebox, under inert atmosphere. Aliquots of precatalyst solution B were measured from this vial and added to the reaction. NMR data have shown that the complex **3.10** contained in this solution transforms to the ionized complex (catalyst **3.14**) immediately

upon addition to reaction mixtures containing a sufficient amount of TlPF$_6$ ($\geq$ 1:1 TlPF$_6$: complex **3.10**) to achieve ionization.

Preparation of Catalyst Solution C

In a small scintillation vial with a Teflon-lined cap, catalyst **3.14** (3.2 mg, 0.0050 mmol) was weighed and acetone-d_6 (1.00 mL) was added, forming a deep blue solution with a molarity of **0.0050 M**, which was kept in the glovebox under inert atmosphere. Aliquots of catalyst solution C were measured from this vial and added to the reaction.

Preparation of Catalyst Solution D

In a small scintillation vial with a Teflon-lined cap, catalyst **3.15** (15.9 mg, 0.0250 mmol) was weighed and acetone-d_6 (1.00 mL) was added, forming a deep blue solution with a molarity of **0.025 M**, which was kept in the glovebox under inert atmosphere. Aliquots of catalyst solution D were measured from this vial and added to the reaction.

Treatment to Remove Peroxides from Alkene Samples

In a scintillation vial outside the glovebox, the weighed alkene (~2-5 g) was pipetted into a plug containing activated neutral alumina (~100 mg), and the filtrate was collected in a resealable scintillation vial. If filtration was performed outside of the glovebox, N$_2$ was bubbled through the sample for 1 min, after which the vial was sealed and brought into the glovebox. Alkene samples already in the glovebox had been deoxygenated prior to this work. After treatment, treated alkenes were isomerized following the same procedure as untreated alkene samples. The following text refers to 'treated' alkenes as alkene samples that have been filtered through an alumina plug as described above. 'Untreated' alkenes did not go through the filtering process.

Isomerization data for Table 4.1

General note: In tables of isomerization data detailed below, (*Z*)-2- and (*Z*)-3-alkenes are not listed. Figure 4.29 is a typical NMR spectrum for an isomerization reaction (the one shown in Table 4.1, entry 3), taken at the 4 h time point of the isomerization described in Table 4.7 below, generally considered the 'end' of the isomerization, as the amount of 1-hexene (~1.9%) does not decrease past this point for linear alkenes. The inset for Figure 4.29 shows the region from 1.45 to 1.75 ppm which includes the signal for the terminal allylic CH_3 for *E*-2 and *Z*-2 hexene. According to Figure 4.28, the signal for *E*-2-hexene is the large signal centered at 1.60 ppm, and the *Z*-2-hexene signal appears at 1.57 ppm (0.03 ppm upfield), which overlaps with the upfield spinning sideband peak from the CH_3 for *E*-2-hexene, representing ~0.5 to 1% of the *E*-2 signal. Assuming the sidebands are symmetrical, a comparison of the downfield and upfield sideband signal should indicate the magnitude of the *Z*-2 signal. If the difference between the two peaks represents the *Z*-2 signal relative to 100 integral units assigned to the *E*-2 signal, $1.24 - 1.11 = 0.13$. The ratio can then be found by dividing the *E*-2 signal by the *Z*-2 signal: $100/0.13 = 770:1$. Also visible are the ^{13}C satellite peaks for the *E*-2 CH_3 signal. Since the ^{13}C abundance is ~1.1%, each ^{13}C peak is roughly 0.55% of the main *E*-2 peak. The integrations for the two ^{13}C peaks for hexene are 0.54 and 0.56, which suggest the integrations can be accurate at this magnitude of signal. For an additional verification of the viability of the analysis, in a separate experiment, we subjected 1-hexene to isomerization using 0.3 mol% catalyst **3.14**, but otherwise following the same conditions as for Table 4.1, entry 3 outlined below. After >90% isomerization to (*E*)-2-hexene, the sample was spiked with 1% (0.62 µL) of authentic (*Z*)-2-hexene. Before addition, the integration value assigned to the (Z)-2 signal was 0.08; after addition, the value increased to

1.02, a difference of 0.94%, which is close to the actual amount added. The results are fully outlined in Table 4.6.

Heptene and octene (Figures 4.30 and 4.32) show the same trend as hexene, namely, the C-1 methyl protons of the (Z)-isomer are 0.03 ppm upfield of those of the (E)-isomer. Following a similar analysis as in the previous paragraph, the difference of the two sideband peaks for 2-heptene shown in Figure 4.31 is 1.39-0.91 =0.48. 100/0.48 = 210:1, and the difference of the two sideband peaks for 2-octene shown in Figure 4.32 is 0.80-0.66=0.14. 100/0.14 = 710:1.

The analysis for hexene, heptene and octene isomers was made possible by the fact that we had samples of authentic (Z)-2 isomers for each of the three substrates. For the remaining 13 substrates, we do not have access to the authentic (Z)-2 isomers. We suspect for the longer-chain functionalized and unfunctionalized substrates, the relative positions of the (E)-2- and (Z)-2-alkene signals (the (Z)-2 signal slightly upfield from the (E)-2 signal) remain the same, and thus should be visible around the (E)-2 signal. Figure 4.33 shows the stacked full spectra for all 16 substrates, scaled to a similar intensity for the allylic CH_3 signal for (E)-2-alkene (~1.60 to 1.67 ppm), while Figures 4.35 and 4.36 show the terminal allylic region of the spectrum (1.55 to 1.70 ppm). Figures 4.37 to 4.49 are the allylic CH_3 regions for the remaining 13 substrates. The same analysis used for determinations of the E/Z ratios for hexene, heptene and octene are applied to the other 13 substrates, and the results are displayed in Table 4.7. A few substrates are not amenable to the current analysis, such as entries 10, 11, 15 and 20, due to either broadness of the E-2 signal or overlap of the Z-2 signal with another signal in the spectrum. We indicate N/O (not observed) if no signal can be seen, or N/D (not determined) if other signals are obscuring the signal.

Despite the rigorous analysis, we accept that the close proximities of the *E*-2 and *Z*-2 signals can introduce uncertainties into the integrations, so we have chosen to report more conservative ratios, none exceeding 400:1.
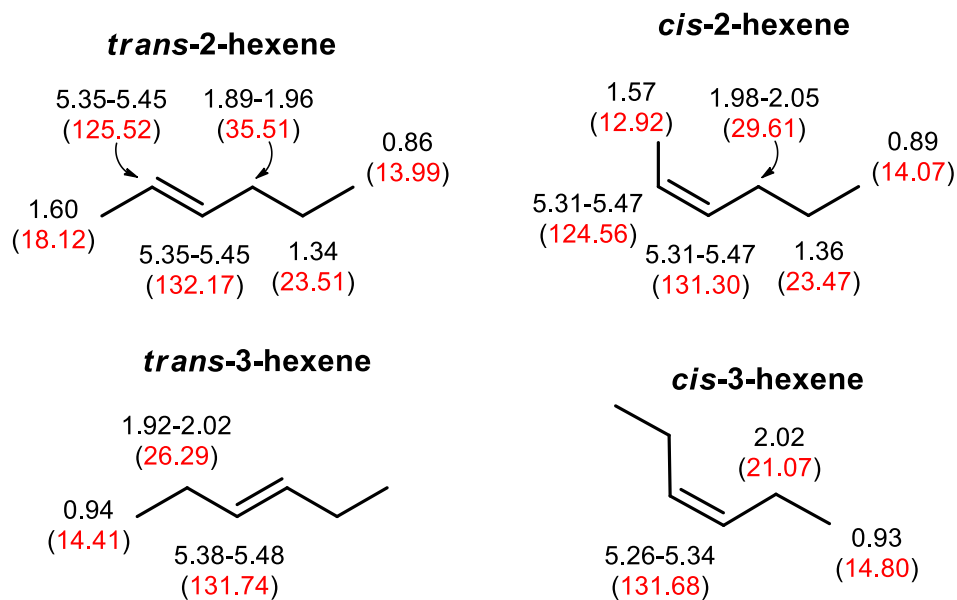
Figure 4.28. ^{1}H and ^{13}C NMR data for authentic hexene isomers in acetone-*d*$_6$[11]
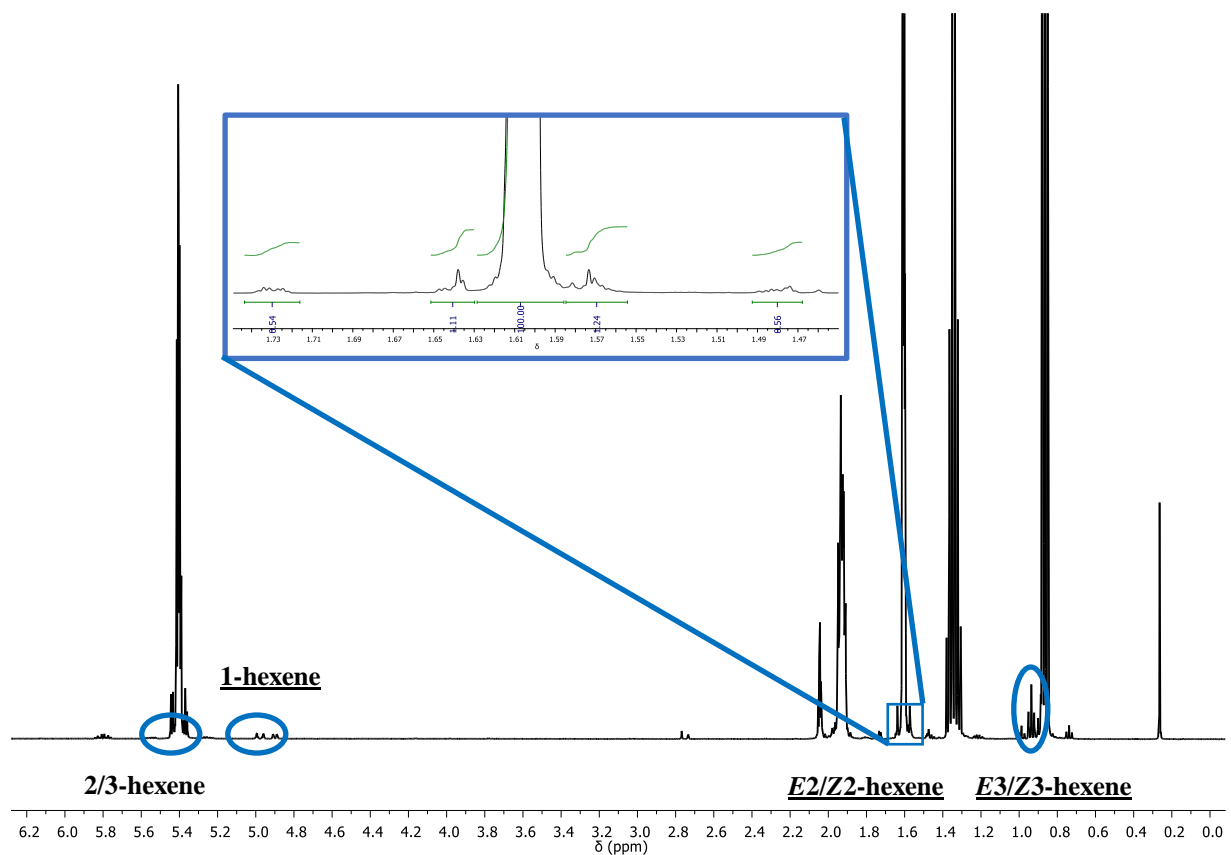
Figure 4.29. ^{1}H NMR spectrum for Table 4.1, Entry 3 after 240 min. Inset: Region from 1.45 – 1.75 ppm

Table 4.6. ^{1}H NMR experiment: addition of authentic (Z)-2-hexene (1%) to isomerized 1-hexene

	1-hexene signal int	1-hexene (%)	(E)-2-hexene int	(E)-2-hexene (%)	Downfield Sideband	Upfield Sideband	(UFSB – DFSB)/3 ((Z)-2-hexene int)	(Z)-2-hexene (%)
0 min	142.65	100	0	**0**	0	0	0	**0**
40 min	5.97	4.2	132.02	**92.5**	4.95	5.33	0.127	**0.08**
55 min (5 min after 1% (Z)-2 addition)	4.21	3.0	134.71	**94.4**	4.67	9.06	1.46	**1.02**

256
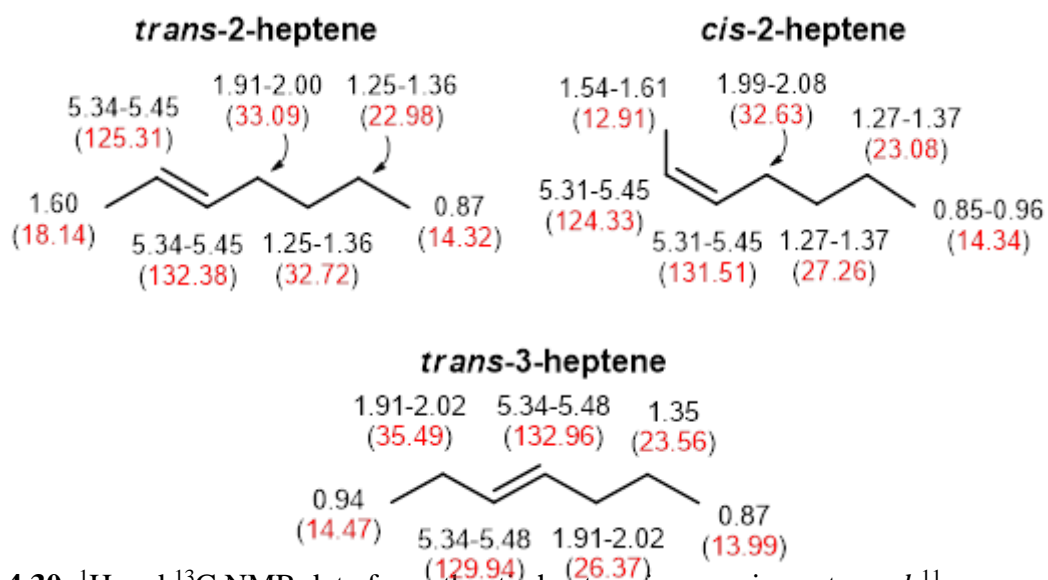
Figure 4.30. ^{1}H and ^{13}C NMR data for authentic heptene isomers in acetone-d_6[11]
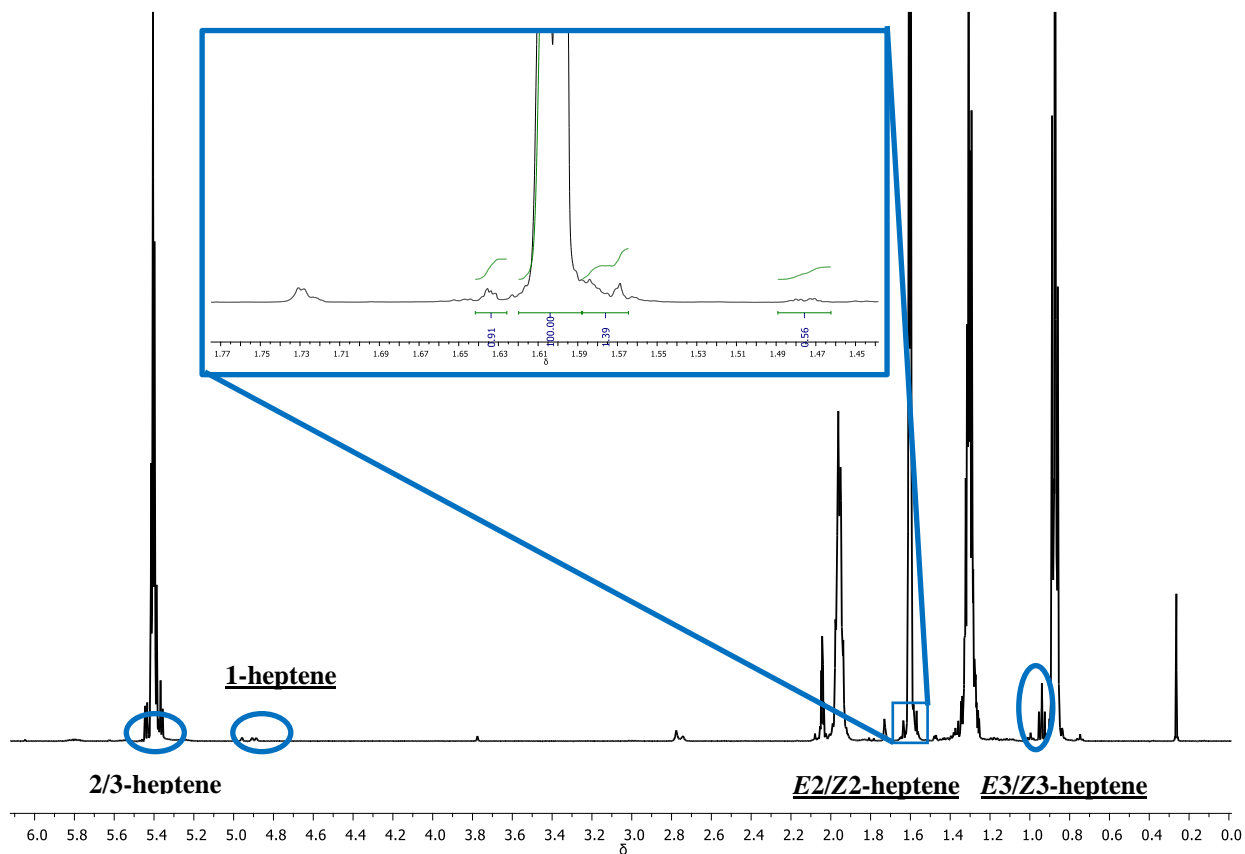
Figure 4.31. ^{1}H NMR spectrum for Table 4.2, Entry 3 after 30 min Inset: Region from 1.54 – 1.67 ppm
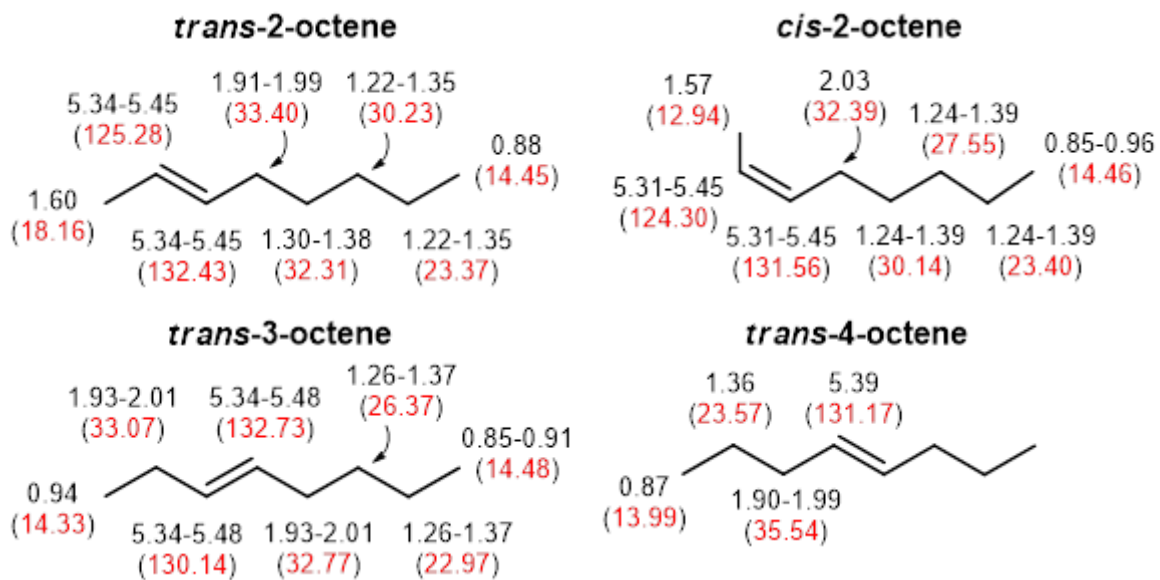
Figure 4.32. NMR data for authentic octene isomers[11]
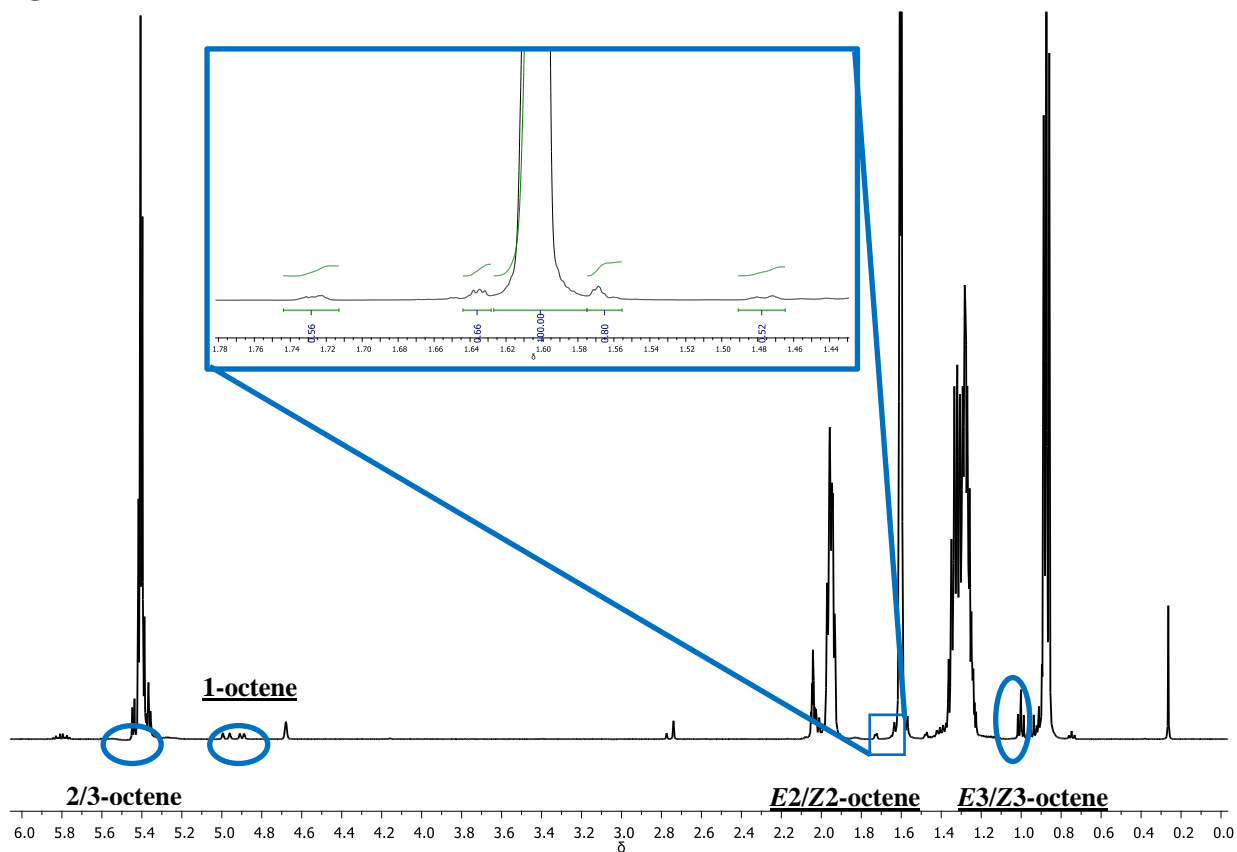
Figure 4.33. ^{1}H NMR spectrum from Table 4.2, Entry 4 after 240 min. Inset: Region from 1.44 – 1.78 ppm
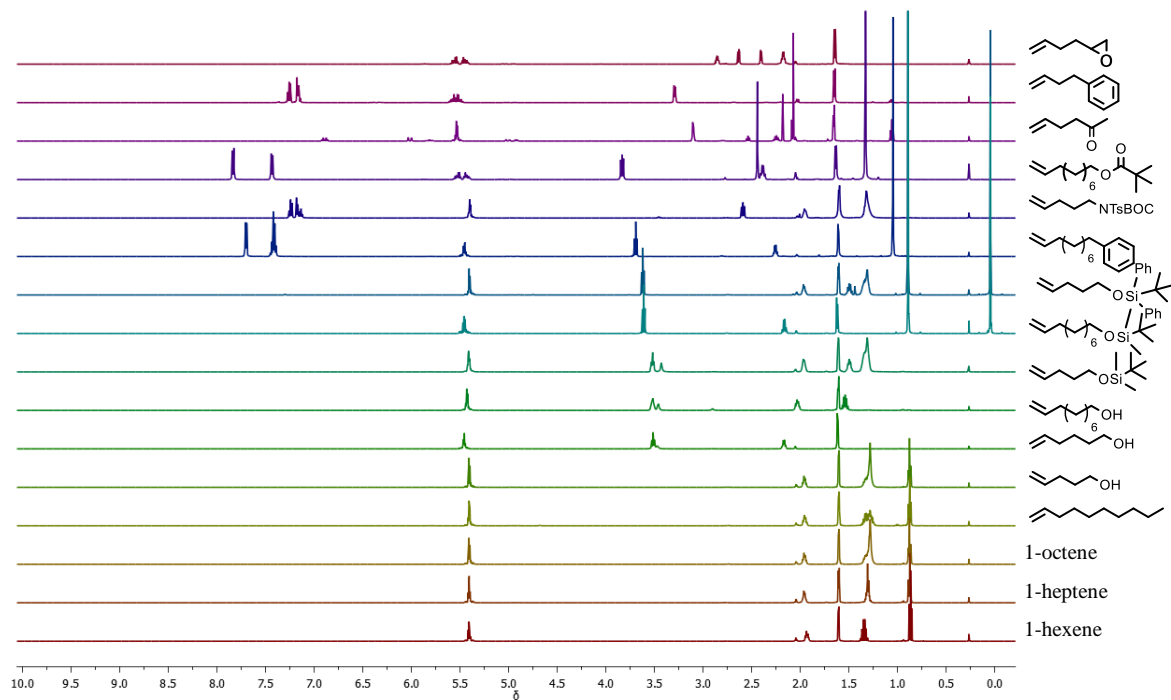
Figure 4.34. ^{1}H NMR for all substrates in Table 4.2 after 'full' conversion
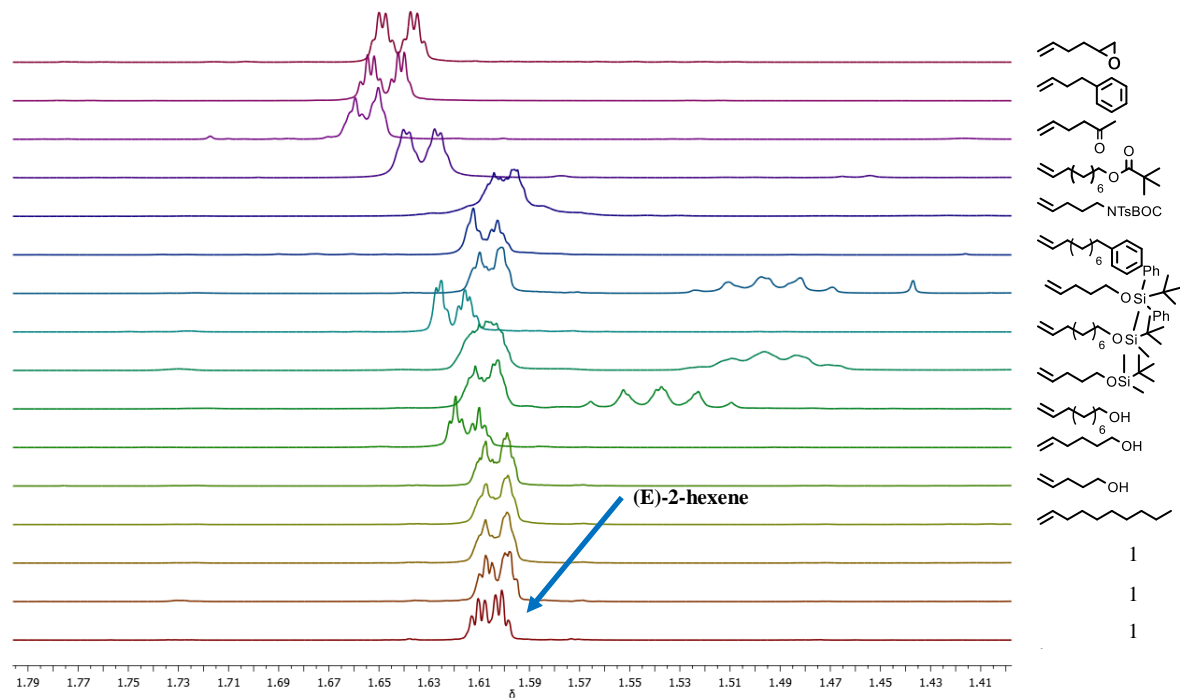
Figure 4.35. ^{1}H NMR spectra for all substrates in Table 4.2 after 'full' conversion – 1.80 to 1.40 ppm (allylic CH$_3$ region (*E*)-2- and (*Z*)-2-alkenes)
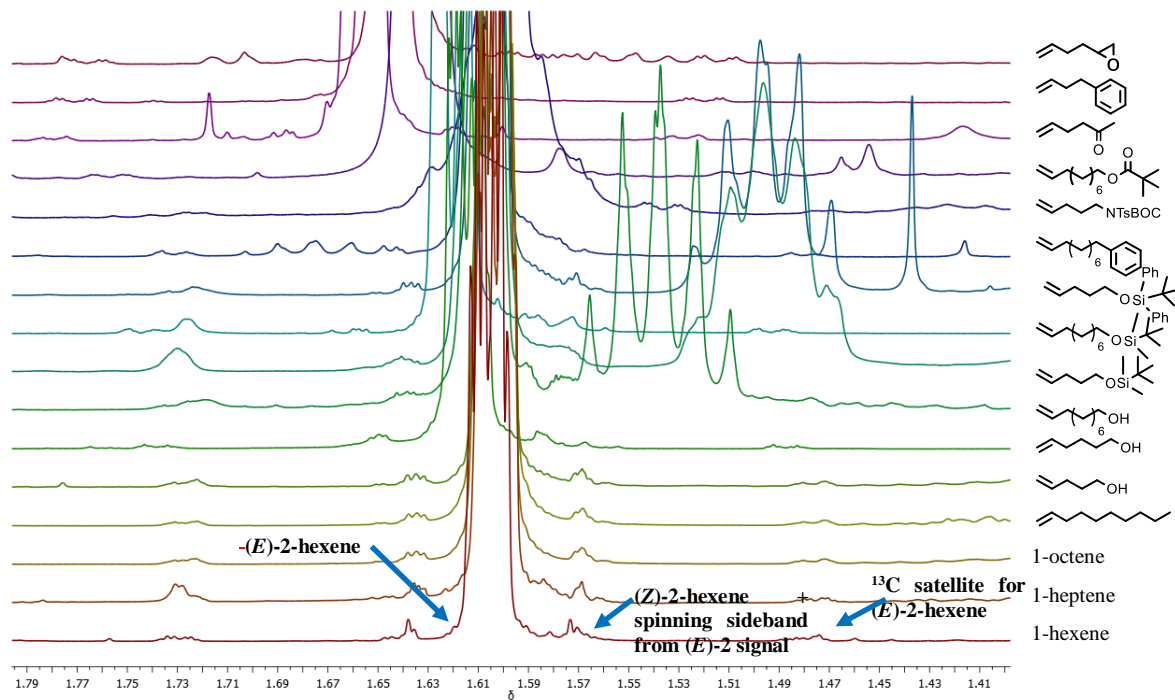
Figure 4.36. ^{1}H NMR spectra for all substrates in Table 4.2 after 'full' conversion – 1.80 to 1.40 ppm (allylic CH$_3$ region (*E*)-2- and (*Z*)-2-alkenes) – higher intensity
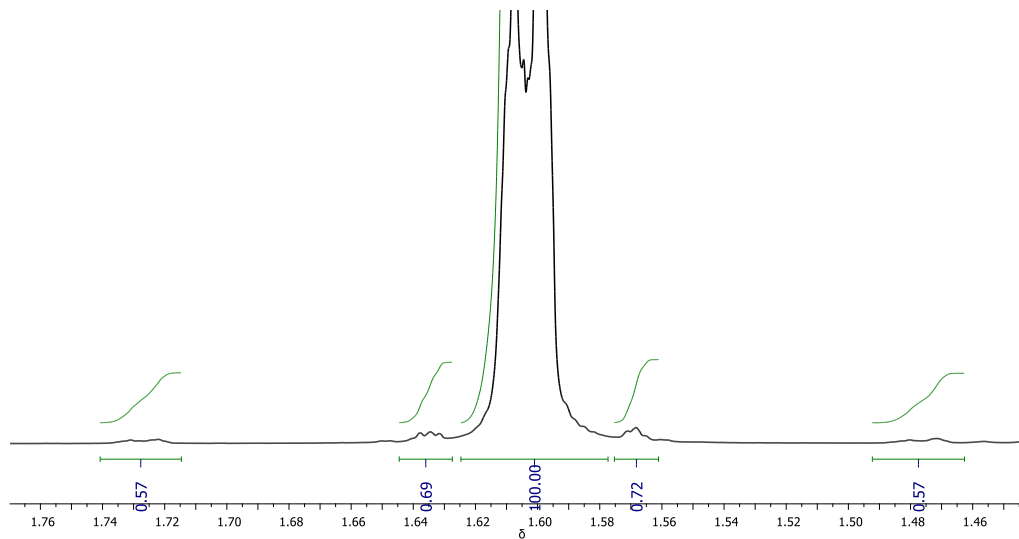
Figure 4.37. ^{1}H NMR spectrum from Table 4.2, Entry 4 after 240 min (region from 1.40 – 1.80 ppm)
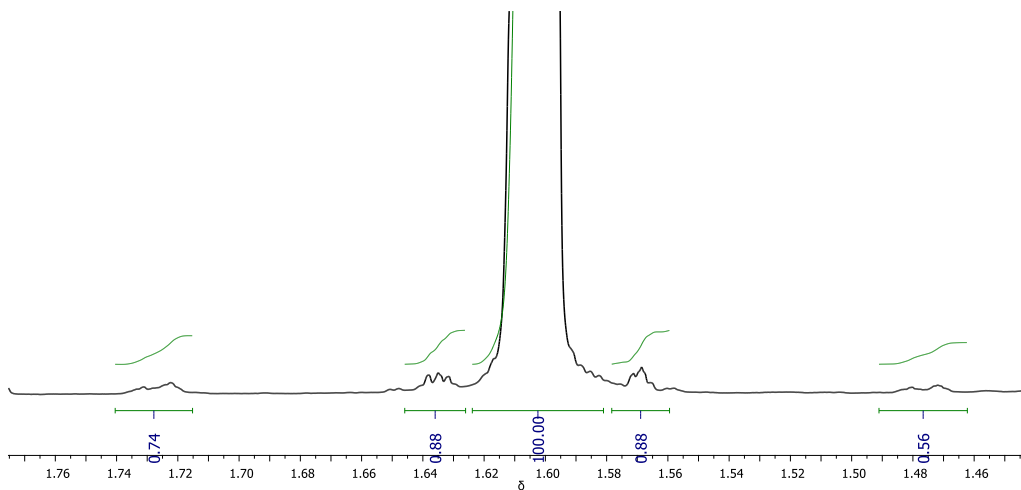
Figure 4.38. ^{1}H NMR spectrum from Table 4.2, Entry 8 after 45 min (region from 1.45 – 1.77 ppm)
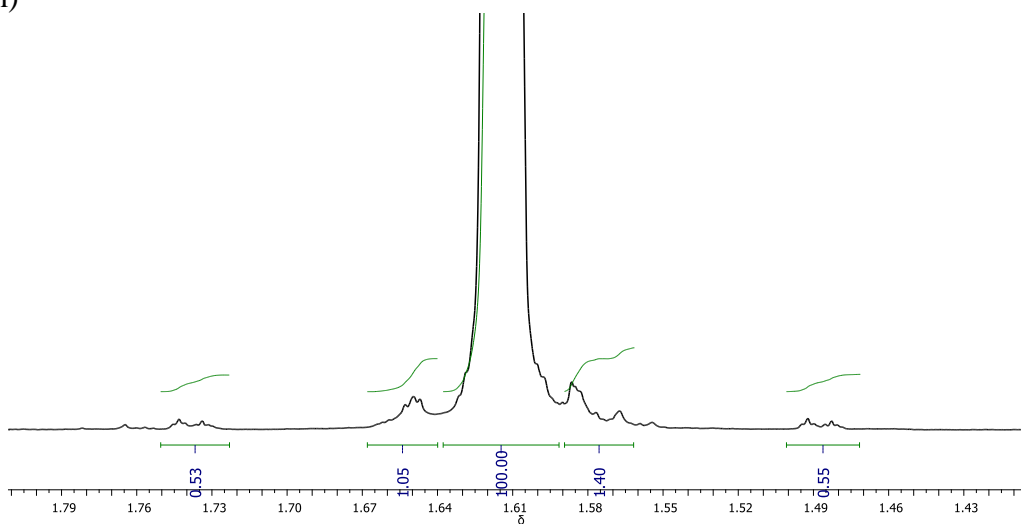
Figure 4.39. ^{1}H NMR spectrum from Table 4.2, Entry 9 after 15 min (region from 1.42 – 1.80 ppm)
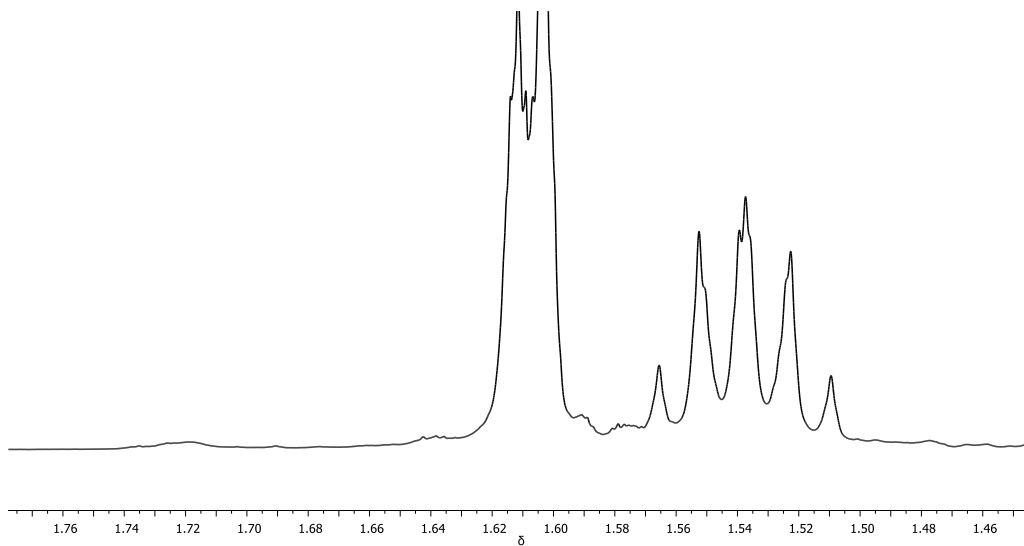
Figure 4.40. ^{1}H NMR spectrum from Table 4.2, Entry 10 after 15 min (region from 1.45 – 1.77 ppm)
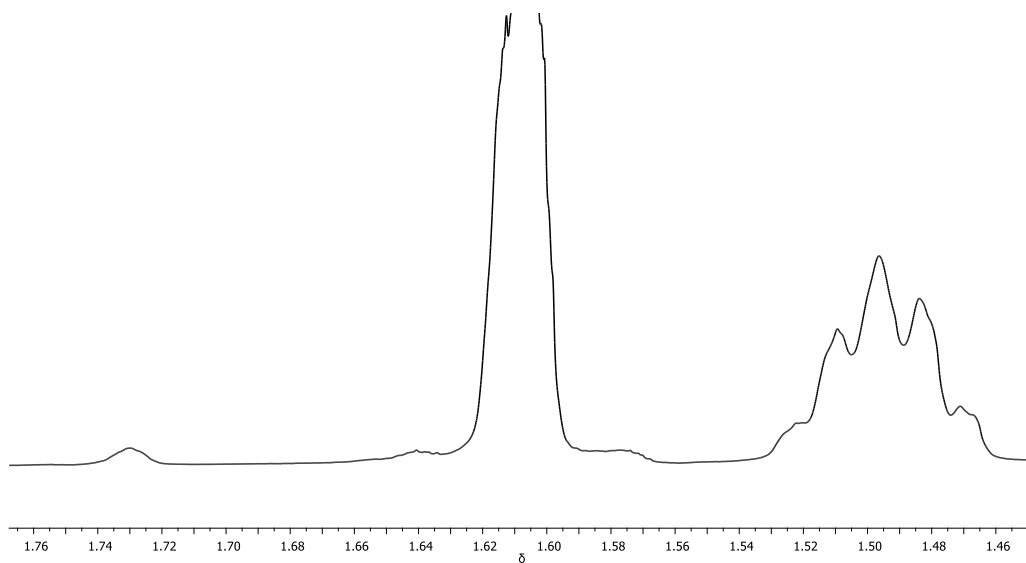
Figure 4.41. ^{1}H NMR spectrum from Table 4.2, Entry 11 after 15 min (region from 1.45 – 1.77 ppm)
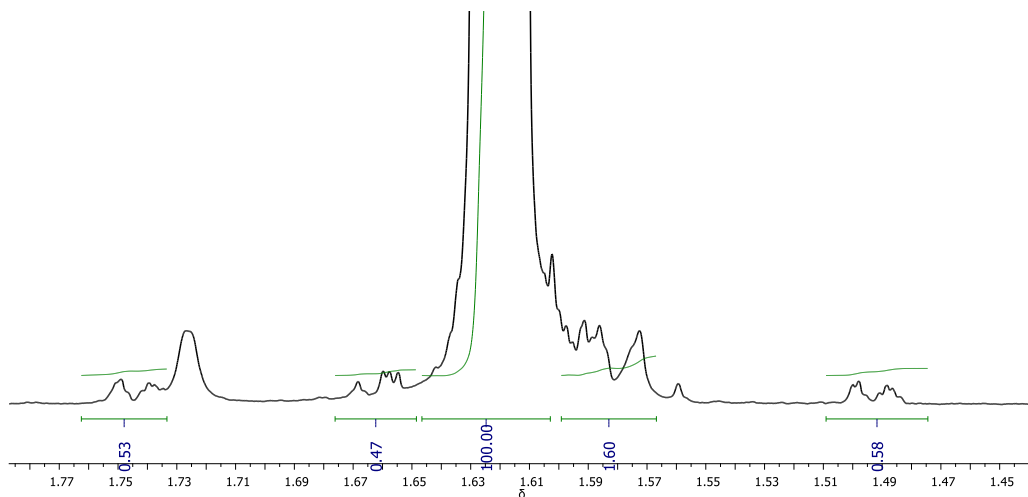
Figure 4.42. ^{1}H NMR spectrum from Table 4.2, Entry 12 after 15 min (region from 1.45 – 1.78 ppm)
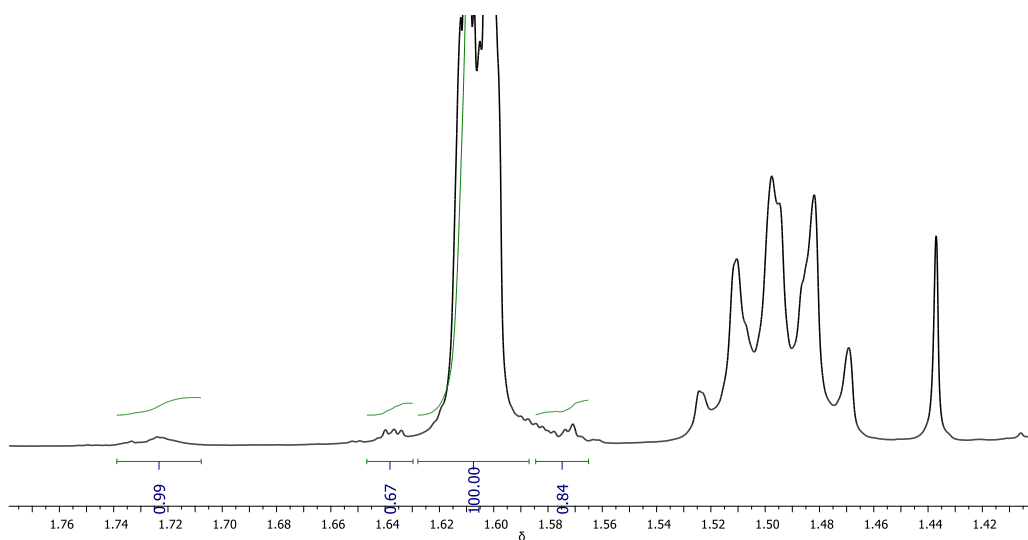
Figure 4.43. ^{1}H NMR spectrum from Table 4.2, Entry 13 after 10 min (region from 1.45 – 1.78 ppm)
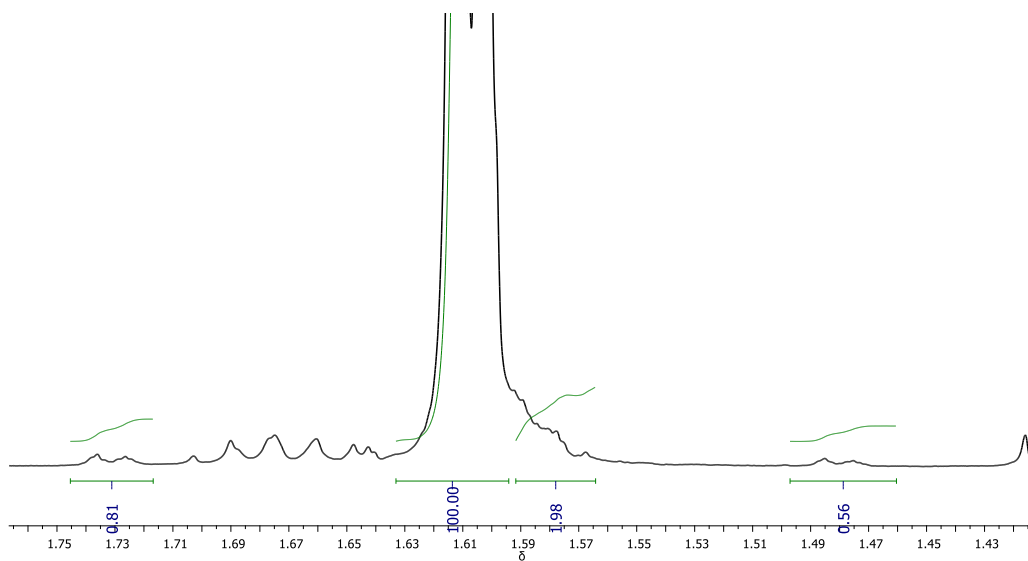
Figure 4.44. ^{1}H NMR spectrum from Table 4.2, Entry 14 after 15 min (region from 1.45 – 1.78 ppm)
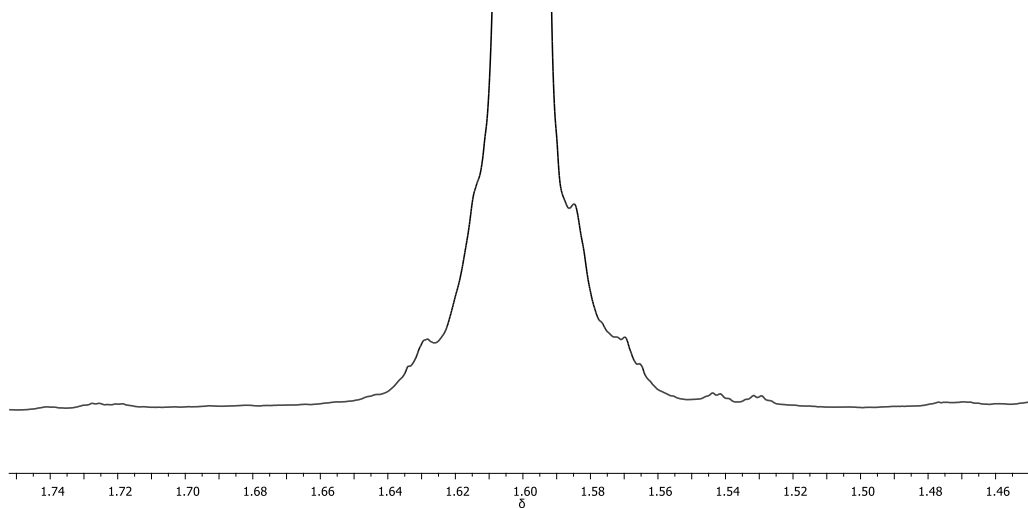
Figure 4.45. ^{1}H NMR spectrum from Table 4.2, Entry 15 after 40 min (region from 1.45 – 1.78 ppm)
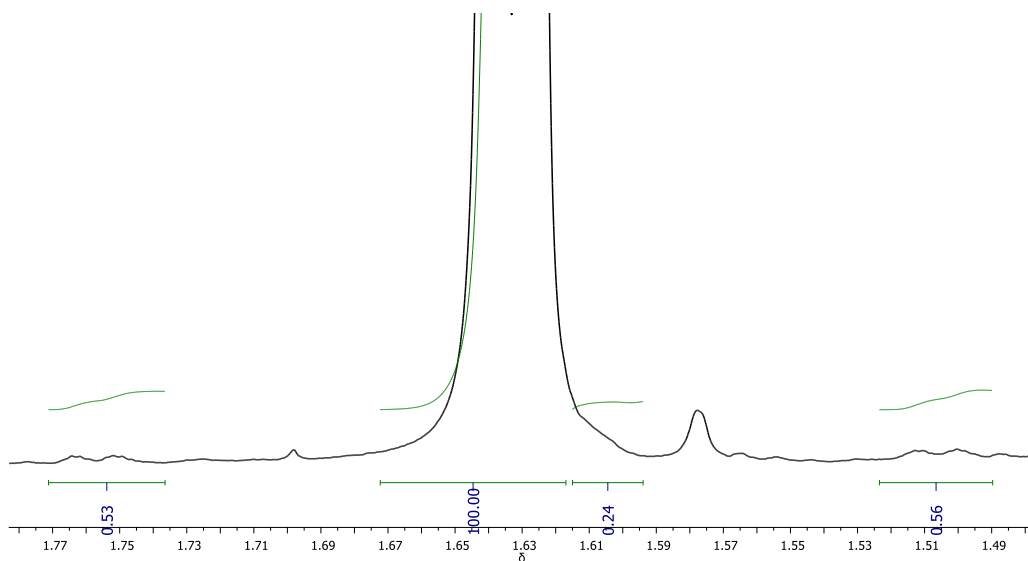
Figure 4.46. ^{1}H NMR spectrum from Table 4.2, Entry 16 after 30 min (region from 1.48 – 1.78 ppm)
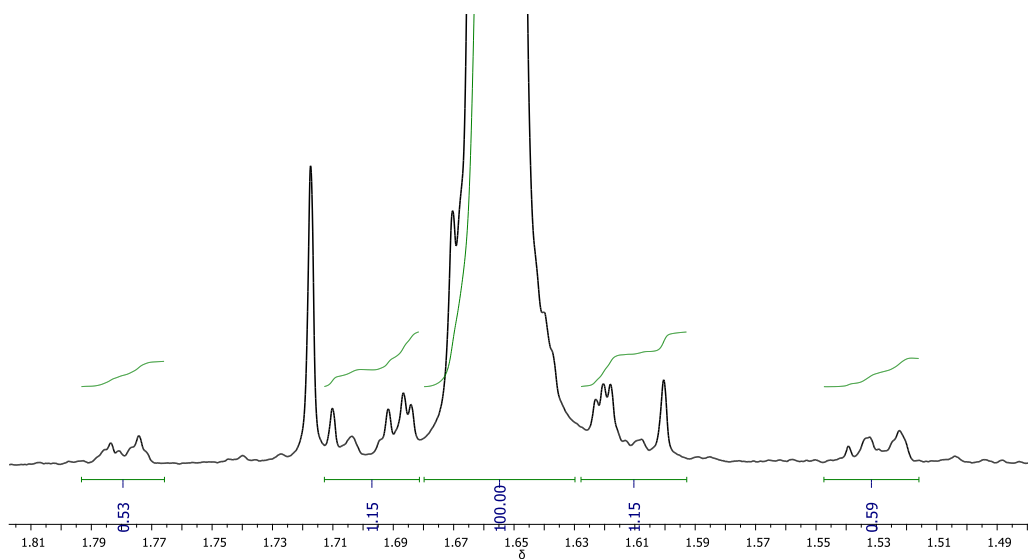
Figure 4.47. ^{1}H NMR spectrum from Table 4.2, Entry 17 after 240 min (region from 1.48 – 1.82 ppm)
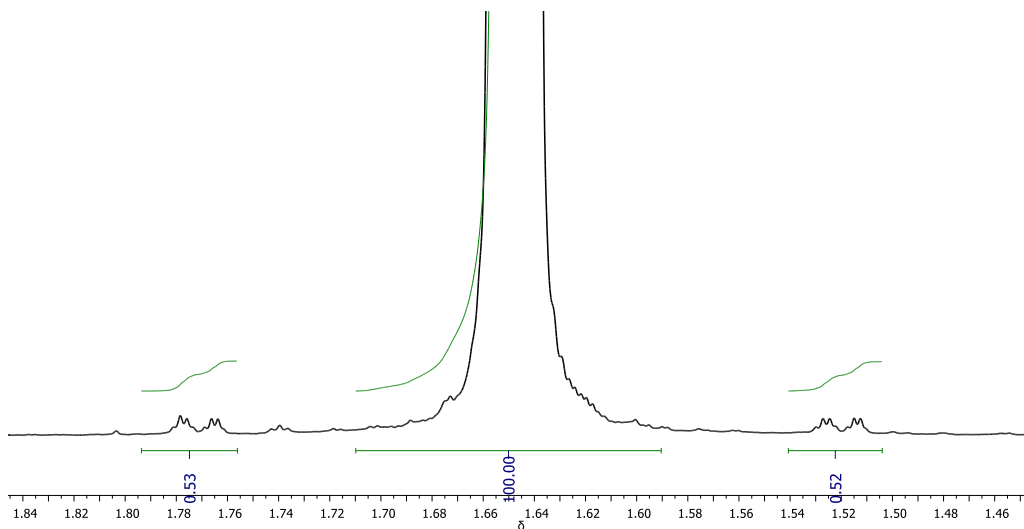
Figure 4.48. ^{1}H NMR spectrum from Table 4.2, Entry 18 after 30 min (region from 1.45 – 1.85 ppm)
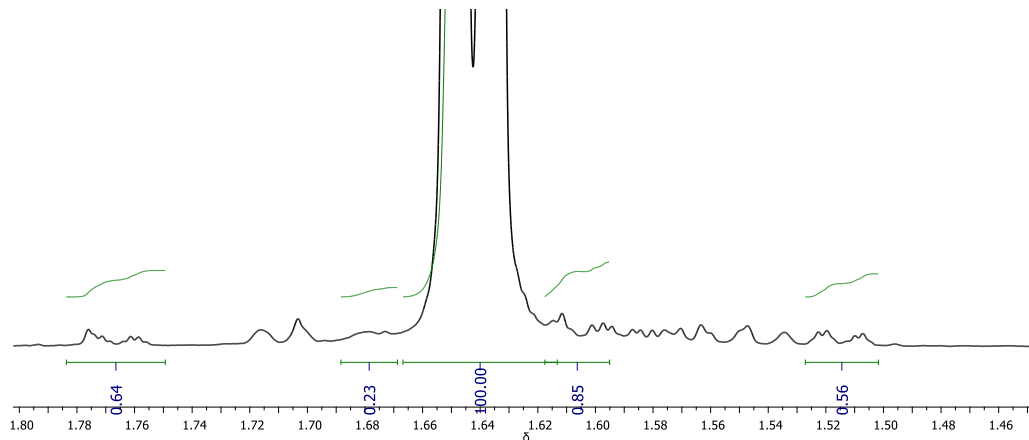
Figure 4.49. ^{1}H NMR spectrum from Table 4, Entry 19 after 120 min (region from 1.45 – 1.80 ppm)

Table 4.7. Integrations of (*E*)-2- and (*Z*)-2-alkene substrates and determination of *E/Z* ratio for Table 4.2

Entry from Table 4.2	Alkene	^{13}C sat down-field	^{13}C sat up-field	Sideband downfield (DF)	Sideband upfield (UF)	SB UF – SB DF	(*E*)-2/diff[a]	*E:Z* ratio[b]
1	**4.1**	0.54	0.56	1.11	1.24	0.13	**770:1**	**>400:1**
3	**4.4**	-	0.57	0.91	1.39	0.48	**210:1**	**>200:1**
4	**4.5**	0.56	0.52	0.66	0.80	0.14	**710:1**	**>400:1**
6	**4.6**	0.57	0.57	0.69	0.72	0.03	**3300:1**	**>400:1**
8	**4.7**	0.74	0.56	0.88	0.88	0.00	**>10000:1**	**>400:1**
9	**4.8**	0.53	0.50	1.05	1.40	0.35	**290:1**	**>200:1**
10	**4.9**	-	-	-	-	-	**-**	**N/D**
11	**4.10**	-	-	-	-	-	**-**	**N/O**
12	**4.11**	0.53	0.58	0.47	1.60	1.13	**89:1**	**89:1**
13	**4.12**	0.99	obs	0.67	0.84	0.17	**590:1**	**>400:1**
14	**4.13**	0.81	0.53	obs	1.98	1.98	**51:1**	**>50:1**
15	**4.14**	ND	Too	Broad				**N/O**
16	**4.15**	0.53	0.56	None	0.24	0.24	**420:1**	**>400:1**
17	**4.16**	0.53	0.59	1.15	1.15	0.00	**>10000:1**	**>400:1**
18	**4.17**	0.53	0.52	None	None	0.00	**>10000:1**	**>400:1**
19	**4.18**	0.64	0.56	0.23	0.85	0.62	**160:1**	**>100:1**
20	**4.19**	-	-	-	-	-	**-**	**N/D**
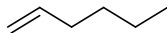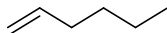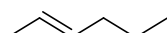
[a]Determined by dividing (E)-2 signal by the difference of the upfield and downfield sideband signals, which represents the signal from the (Z)-2-alkene; essentially, the calculated (E):(Z) ratio. [b]A more conservative estimate for E/Z ratio, rounded down for most substrates, in some cases significantly, so that no listed ratio is above 400:1.

Isomerization data for Table 4.1:

Data for Table 4.1, Entry 1: Procedure for isomerization of untreated 1-hexene to E-2 and E-3-hexenes using 0.1 mol% catalyst 1.1 at room temperature in acetone-d_6.

To a resealable J. Young NMR tube in a glovebox, internal standard (Me$_3$Si)$_4$C (~0.2 mg), and 1-hexene (42.7 mg, 0.507 mmol) were combined with a mixture of deoxygenated acetone-d_6 (700 µL), and an initial NMR spectrum was acquired. Back in the glovebox, to this mixture was added an aliquot of catalyst solution C (101 µL, 0.000504 mmol) and enough acetone-d_6 to reach a total volume of 1.0 mL. The reaction was kept at room temperature and monitored at the times given below.

Table 4.8. Yields determined by NMR in isomerization of **4.1** using 0.1 mol% catalyst **1.1** at room temperature in acetone-d_6.
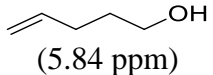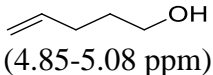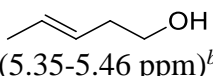
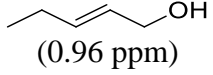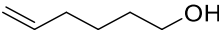| Time	0 min	5 min	15 min	20 min	30 min	1 hr
Measured integrals in arbitrary units relative to internal standard = 10.0 units and (in bold) derived per cent yields of products and amount of starting 1-alkene.						
(5.79 ppm)	85.7	20.6	2.01	1.65	1.44	1.69
(4.85-5.01 ppm)	173.3	41.9	4.05	3.44	3.33	2.65
units per proton[a]	86.2	20.8	2.02	1.69	1.55	1.51
% starting material remaining	**100**	**24.1**	**2.3**	**2.0**	**1.8**	**1.7**
(5.35-5.46 ppm)[b]	-	129.8	167.6	170.1	169.8	168.7
units per proton[c]	-	63.2	76.9	67.8	62.0	52.0
% of E-2	**0**	**72.2**	**86.3**	**78.6**	**71.9**	**60.2**
(0.94 ppm)	-	7.94	28.3	52.0	68.8	97.1
units per proton	-	2.65	9.43	17.3	22.9	32.4
% of E-3	**0**	**3.1**	**10.9**	**20.1**	**26.6**	**37.5**

[a]Units calculated by taking the average of the integrations of the two resonances. [b]Signal is a mixture of vinylic C-H from E-2 and E-3 hexene isomers. [c] Vinylic proton units for E-2 hexene determined by subtracting proton units of E-3 hexene from total proton units of E-2/E-3 signal.

Data for Table 4.1, Entry 2: Procedure for isomerization of untreated 1-hexene to E-2 and E-3 hexenes using 1 mol% catalyst 1.2+1.2a at 40°C in acetone-d_6.
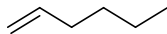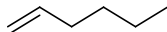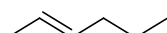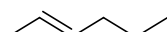
See reference 3 – supporting info for more details

Data for Table 4.1, Entry 3: Procedure for isomerization of untreated 1-hexene to E-2 and E-3 hexenes using 0.1 mol% catalyst 3.14 at room temperature in acetone-d_6.

To a resealable J. Young NMR tube in a glovebox, internal standard (Me$_3$Si)$_4$C (~0.2 mg), and 1-hexene (42.5 mg, 0.505 mmol) were combined with a mixture of deoxygenated acetone-d_6 (700 μL), and an initial NMR spectrum was acquired. Back in the glovebox, to this mixture was added an aliquot of catalyst solution C (101 μL, 0.000504 mmol) and enough

acetone-d_6 to reach a total volume of 1.0 mL. The reaction was kept at room temperature and

monitored at the times given below.

Table 4.9. Yields determined by NMR in isomerization of **4.1** using 0.1 mol% catalyst **3.14** at room temperature in acetone-d_6.
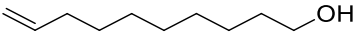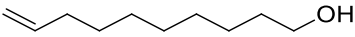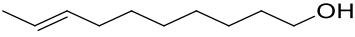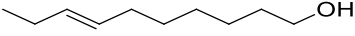
Time	0 min	15 min	1 hr	2 hr	3 hr	4 hr
Measured integrals in arbitrary units relative to internal standard = 10.0 units and (in bold) derived per cent yields of products and amount of starting 1-alkene.						
(5.79 ppm)	71.3	36.2	8.56	2.67	1.53	1.40
(4.85-5.01 ppm)	147.7	74.5	17.6	5.26	3.30	2.78
units per proton[a]	72.6	36.7	8.68	2.65	1.59	1.40
% starting material remaining	**100**	**50.6**	**12.0**	**3.7**	**2.2**	**1.9**
(5.35-5.46 ppm)[b]	-	72.5	128.9	141.0	142.5	139.5
(1.60 ppm)	-	112.0	198.2	215.0	217.9	214.2
units per proton[c]	-	36.6	65.3	70.3	70.9	69.5
% of *E*-2	**0**	**50.4**	**89.2**	**96.9**	**97.7**	**95.7**
(0.94 ppm)	-	-	1.53	3.44	5.01	5.57
units per proton	-	-	0.51	1.15	1.67	1.86
% of *E*-3	**0**	**0**	**0.7**	**1.6**	**2.3**	**2.6**

[a]Units calculated by taking the average of the integrations of the two resonances. [b]Signal is a mixture of vinylic C-H from E-2 and E-3 hexene isomers. [c] Vinylic proton units for E-2 hexene determined by subtracting proton units of E-3 hexene + catalyst Cp*CH_3 from total proton units of E-2/E-3 signal.

Isomerization data for Table 4.2:
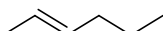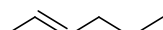
Data for Table 4.2, Entry 1: Procedure for isomerization of untreated 1-hexene to E-2 and E-3 hexenes using 0.1 mol% catalyst 5 at room temperature in acetone-d_6.

See above – table 1, entry 3

Data for Table 4.2, Entry 2: Procedure for isomerization of untreated 1-hexene to E-2 and E-3 hexenes using 0.5 mol% catalyst 3.14 at room temperature in acetone-d_6.

To a resealable J. Young NMR tube in a glovebox, internal standard (Me$_3$Si)$_4$C (~0.2 mg), and 1-hexene (42.5 mg, 0.505 mmol) were combined with a mixture of deoxygenated acetone-d_6 (700 μL), and an initial NMR spectrum was acquired. Back in the glovebox, to this mixture was added an aliquot of catalyst solution D (101 μL, 0.00253 mmol) and enough acetone-d_6 to reach a total volume of 1.0 mL. The reaction was kept at room temperature and monitored at the times given below.

Table 4.10. Yields determined by NMR in isomerization of **4.1** using 0.5 mol% catalyst **3.14** at room temperature in acetone-d_6.
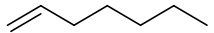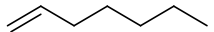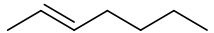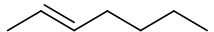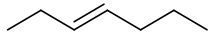
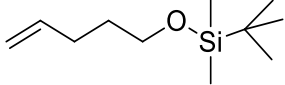| Measured integrals in arbitrary units relative to internal standard = 10.0 units and (in bold) derived per cent yields of products and amount of starting 1-alkene.			
Time	0 min	15 min	30 min
(5.79 ppm)	80.9	1.32	1.58
(4.85-5.01 ppm)	166.6	3.23	3.10
units per proton[a]	82.1	1.47	1.57
% starting material remaining	**100**	**1.8**	**1.9**
(5.35-5.46 ppm)[b]	-	160.1	160.2
(1.60 ppm)	-	243.9	240.7
units per proton[c]	-	79.1	78.3
% of E-2	**0**	**96.3**	**95.3**
(0.94 ppm)	-	5.33	12.6
units per proton	-	0.89	2.10
% of E-3	**0**	**1.1**	**2.6**

[a]Units calculated by taking the average of the integrations of the two resonances. [b]Signal is a mixture of vinylic C-H from E-2 and E-3 hexene isomers. [c]Vinylic proton units for E-2 hexene determined by subtracting proton units of E-3 hexene + catalyst Cp*CH_3 from total proton units of E-2/E-3 signal.

Data for Table 2, Entry 3: Procedure for isomerization of untreated 1-heptene to E-2 and E-3 heptenes using 0.5 mol% catalyst 3.14 at room temperature in acetone-d_6.

To a resealable J. Young tube in a glovebox, internal standard $(Me_3Si)_4C$ (~0.2 mg), and 1-heptene (49.0 mg, 0.499 mmol) were combined with a mixture of deoxygenated acetone-d_6 (700 µL), and an initial NMR spectrum was acquired. Back in the glovebox, to this mixture was added an aliquot of catalyst solution D (100 µL, 0.00250 mmol) and enough acetone-d_6 to reach a total volume of 1.0 mL. The reaction was kept at room temperature and monitored at the times given below.

Table 4.11. Yields determined by NMR in isomerization of **4.4** using 0.5 mol% catalyst **3.14** at room temperature in acetone-d_6.
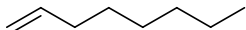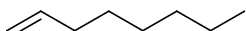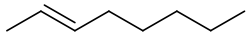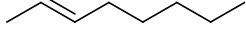
Measured integrals in arbitrary units relative to internal standard = 10.0 units and (in bold) derived per cent yields of products and amount of starting 1-alkene.			
Time	0 min	15 min	30 min
(5.80 ppm)	110.2	3.02	2.48
(4.90-4.97 ppm)	229.2	5.62	3.99
units per proton[a]	112.4	2.92	2.24
% starting material remaining	**100**	**2.6**	**2.0**
(5.34-5.46 ppm)[b]	-	218.1	218.8
(1.60 ppm)	-	333.7	332.6
units per proton[c]	-	107.9	107.4
% of E-2	**0**	**96.0**	**95.5**
(0.94 ppm)	-	4.82	8.07
units per proton	-	1.61	2.69
% of E-3	**0**	**1.4**	**2.4**

[a]Units calculated by taking the average of the integrations of the two resonances. [b] Signal is a mixture of vinylic C-H from E-2 and E-3 heptene isome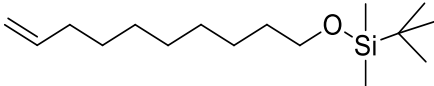rs. [b] Vinylic C-H proton units for E-2 heptene determined by subtracting proton units of E-3 heptene from total proton units of E-2/E-3 signal.

Data for Table 4.2, Entry 4: Procedure for isomerization of untreated 1-octene to E-2, E-3, and E-4 octenes using 0.1 mol% catalyst 3.14 at room temperature in acetone-d_6.

To a resealable J. Young tube in a glovebox, internal standard $(Me_3Si)_4C$ (~0.2 mg), and 1-octene (57.0 mg, 0.508 mmol) were combined with a mixture of deoxygenated acetone-d_6 (700 µL), and an initial NMR spectrum was acquired. Back in the glovebox, to this mixture was added an aliquot of catalyst solution C (102 µL, 0.000508 mmol) and enough acetone-d_6 to reach a total volume of 1.0 mL. The reaction was kept at room temperature and monitored at the times given below.

Table 4.12. Yields determined by NMR in isomerization of **4.5** using 0.1 mol% catalyst **3.14** at room temperature in acetone-d_6.
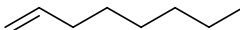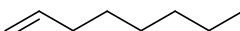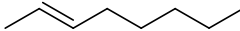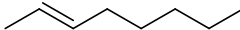
Measured integrals in arbitrary units relative to internal standard = 10.0 units and (in bold) derived per cent yields of products and amount of starting 1-alkene.							
Time	0 min	15 min	30 min	1 hr	2 hr	3 hr	4 hr
(5.80 ppm)	98.7	42.0	26.2	13.3	5.13	3.01	2.50
(4.89-4.97 ppm)	204.2	85.6	53.7	27.0	11.1	6.43	5.20
units per proton[a]	100.4	42.4	26.5	13.4	5.34	3.11	2.55
% starting material remaining	**100**	**42.2**	**26.4**	**13.3**	**5.3**	**3.1**	**2.5**
(5.42 ppm)[b]	-	113.4	147.9	175.5	188.1	189.9	194.4
(1.60 ppm)	-	170.3	222.8	264.9	287.1	286.3	295.4
units per proton[c]	-	56.5	73.7	87.6	94.2	94.9	96.8
% of E-2	**0**	**56.2**	**73.4**	**87.2**	**93.8**	**94.5**	**96.4**
(0.94 ppm)	-	-	0.74	1.17	2.42	2.69	4.70
units per proton	-	-	0.25	0.39	0.81	0.90	1.57
% of E-3	**0**	**0**	**0.2**	**0.4**	**0.8**	**0.9**	**1.6**

[a]Units calculated by taking the average of the integrations of the two resonances. [b]Signal is a mixture of vinylic C-H protons from internal isomers, although none are present in the above reaction. [c]Vinylic C-H proton units for E-2 octene determined by subtracting proton units of E-3 octene from total proton units of E-2/E-3 signal.
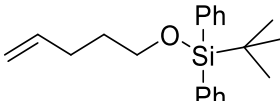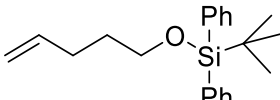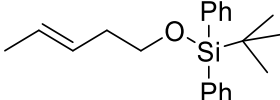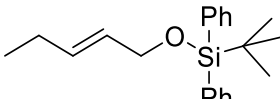
Data for Table 4.2, Entry 5: **Procedure for isomerization of untreated 1-octene to E-2, E-3, and E-4 octenes using 0.5 mol% catalyst 3.14 at room temperature in acetone-d_6.**

To a resealable J. Young tube in a glovebox, internal standard (Me$_3$Si)$_4$C (~0.2 mg), and 1-octene (56.4 mg, 0.502 mmol) were combined with a mixture of deoxygenated acetone-d_6 (700 µL), and an initial NMR spectrum was acquired. Back in the glovebox, to this mixture was added an aliquot of catalyst solution D (100 µL, 0.00250 mmol) and enough acetone-d_6 to reach a total volume of 1.0 mL. The reaction was kept at room temperature and monitored at the times given below.

Table 4.13. Yields determined by NMR in isomerization of **4.5** using 0.5 mol% catalyst **3.14** at room temperature in acetone-d_6.
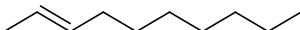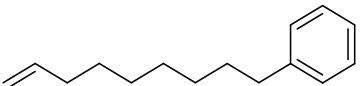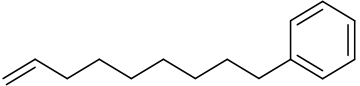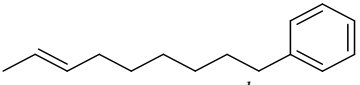
Measured integrals in arbitrary units relative to internal standard = 10.0 units and (in bold) derived per cent yields of products and amount of starting 1-alkene.

Time	0 min	15 min	30 min
(5.80 ppm)	67.2	8.53	1.36
(4.89-4.97 ppm)	139.2	17.9	2.74
units per proton[a]	68.4	8.74	1.37
% starting material remaining	**100**	**12.8**	**2.0**
(5.42 ppm)[b]	-	116.2	132.9
(1.60 ppm)	-	176.2	197.6
units per proton[c]	-	57.2	64.2
% of E-2	**0**	**83.6**	**94.0**
(0.94 ppm)	-	2.08	6.05
units per proton	-	0.69	2.02
% of E-3	**0**	**1.0**	**2.9**

[a]Units calculated by taking the average of the integrations of the two resonances. [b]Signal is a mixture of vinylic C-H protons from internal isomers, although none are present in the above reaction. [c]Vinylic C-H proton units for E-2 octene determined by subtracting proton units of E-3 octene from total proton units of E-2/E-3 signal.

To a resealable J. Young tube in a glovebox, internal standard $(Me_3Si)_4C$ (~0.2 mg), and 1-decene (70.4 mg, 0.502 mmol) were combined with a mixture of deoxygenated acetone-d_6 (700 µL), and an initial NMR spectrum was acquired. Back in the glovebox, to this mixture was added an aliquot of catalyst solution C (100 µL, 0.00050 mmol) and enough acetone-d_6 to reach a total volume of 1.0 mL. The reaction was kept at room temperature and monitored at the times given below.

Table 4.14. Yields determined by NMR in isomerization of **4.6** using 0.1 mol% catalyst **3.14** at room temperature in acetone-d_6.
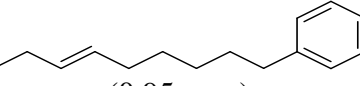
Measured integrals in arbitrary units relative to internal standard = 10.0 units and (in bold) derived per cent yields of products and amount of starting 1-alkene.							
Time	0 min	15 min	30 min	1 hr	2 hr	3 hr	4 hr
(5.80 ppm)	97.8	46.6	25.6	10.3	2.91	2.00	1.73
(4.91 ppm)	199.1	94.8	52.1	20.9	5.91	3.98	3.56
units per proton[a]	98.7	47.0	25.8	10.4	2.93	2.00	1.76
% starting material remaining	**100**	**47.6**	**26.1**	**10.5**	**3.0**	**2.0**	**1.8**
(5.41 ppm)[b]	-	101.0	142.2	174.0	186.7	191.6	191.0
(1.60 ppm)	-	151.2	213.9	261.8	280.7	287.3	285.9
units per proton[c]	-	50.5	70.4	86.4	92.5	94.6	93.8
% of E-2	**0**	**51.2**	**71.3**	**87.5**	**93.7**	**95.9**	**95.1**
(0.95 ppm)	-	-	2.08	1.92	2.66	3.73	5.09
units per proton	-	-	0.69	0.64	0.89	1.24	1.70
% of E-3	**0**	**0**	**0.7**	**0.6**	**0.9**	**1.3**	**1.7**
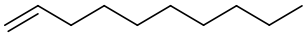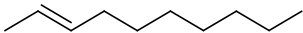
[a]Units calculated by taking the average of the integrations of the two resonances. [b]Signal is a mixture of vinylic C-H internal decene isomers.. [c]Proton units for E-2 decene determined by subtracting proton units of E-3 decene from total proton units of E-2/E-3 signal.

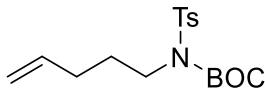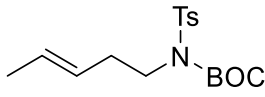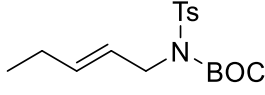**Data for Table 4.2, Entry 7: Procedure for isomerization of untreated 1-decene to E-2 and E-3 decenes using 0.5 mol% catalyst 3.14 at room temperature in acetone-d_6.**

To a resealable J. Young tube in a glovebox, internal standard $(Me_3Si)_4C$ (~0.2 mg), and 1-decene (70.4 mg, 0.502 mmol) were combined with a mixture of deoxygenated acetone-d_6 (700 μL), and an initial NMR spectrum was acquired. Back in the glovebox, to this mixture was added an aliquot of catalyst solution D (100 μL, 0.00250 mmol) and enough acetone-d_6 to reach a total volume of 1.0 mL. The reaction was kept at room temperature and monitored at the times given below.

Table 4.15. Yields determined by NMR in isomerization of **4.6** using 0.5 mol% catalyst **3.14** at room temperature in acetone-d_6.
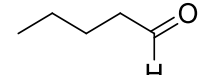
Measured integrals in arbitrary units relative to internal standard = 10.0 units and (in bold) derived per cent yields of products and amount of starting 1-alkene.			
Time	0 min	15 min	1 h
(5.80 ppm)	116.2	11.9	2.56
(4.91 ppm)	236.6	24.1	5.27
units per proton[a]	117.3	12.0	2.60
% starting material remaining	**100**	**10.2**	**2.2**
(5.41 ppm)[b]	-	210.9	229.4
(1.60 ppm)	-	322.2	346.4
units per proton[c]	-	104.4	112.6
% of E-2	**0**	**89.0**	**95.9**
(0.95 ppm)	-	3.56	6.27
units per proton	-	1.19	2.09
% of E-3	**0**	**1.0**	**1.8**

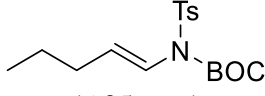[a]Units calculated by taking the average of the integrations of the two resonances. [b]Signal is a mixture of vinylic C-H internal decene isomers, although these are not present in any detectable quantity within the time points listed above. [c]Proton units for E-2 decene determined by subtracting proton units of E-3 decene from total proton units of E-2/E-3 signal.

Data for Table 4.2, Entry 8: **Procedure for isomerization of untreated 4-penten-1-ol to E-3 and E-2 penten-1-ols using 0.5 mol% catalyst 3.14 at room temperature in acetone-d_6.**

To a resealable J. Young tube in a glovebox, internal standard $(Me_3Si)_4C$ (~0.2 mg), and 4-penten-1-ol (44.5 mg, 0.516 mmol) were combined with a mixture of deoxygenated acetone-d_6 (700 μL), and an initial NMR spectrum was acquired. Back in the glovebox, to this mixture was added an aliquot of precatalyst solution D (103 μL, 0.00258 mmol) and enough acetone-d_6 to reach a total volume of 1.0 mL. The reaction was kept at room temperature and monitored at the times given below.

Table 4.16. Yields determined by NMR in isomerization of **4.7** using 0.5 mol% catalyst **3.14** at room temperature in acetone-d_6.

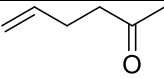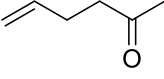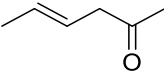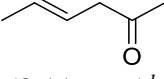| Measured integrals in arbitrary units relative to internal standard = 10.0 units and (in bold) derived per cent yields of products and amount of starting 1-alkene.				
Time	0 min	15 min	30 min	45 min
∕∕∕∕OH (5.84 ppm)	154.7	78.3	27.3	5.15
∕∕∕∕OH (4.85-5.08 ppm)	321.3	163.4	55.8	10.67
units per proton[a]	157.7	80.0	27.6	5.24
% starting material remaining	**100**	**50.7**	**17.5**	**3.3**
∕∕∕∕OH (5.35-5.46 ppm)[b]	-	156.5	259.1	306.2
units per proton[c]	-	78.3	129.5	152.3
% yield product	**0**	**49.7**	**82.1**	**96.6**
∕∕∕∕OH (0.96 ppm)	-	-	-	2.32
units per proton	-	-	-	0.77
% of isomer	**0**	**-**	**-**	**0.5**
∕∕∕∕CHO (9.72 ppm)	-	-	-	-
units per proton	-	-	-	-
% of aldehyde	**0**	**-**	**-**	**-**
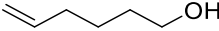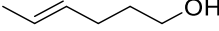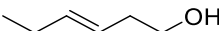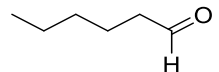
[a]Units calculated by taking the average of the integrations of the two resonances. [b]Signal is a mixture of E-3- and E-2-penten-1-ol isomers. [c]Vinylic C-H proton units for E-3-penten-1-ol determined by subtracting proton units of E-2-penten-1-ol from total proton units of E-3/E-2 signal.

Data for Table 4.2, Entry 9: Procedure for isomerization of untreated 5-hexen-1-ol to E-4 and E-3 hexen-1-ols using 0.5 mol% catalyst 3.14 at room temperature in acetone-d_6.

To a resealable J. Young tube in a glovebox, internal standard (Me$_3$Si)$_4$C (~0.2 mg), and 4-penten-1-ol (50.2 mg, 0.501 mmol) were combined with a mixture of deoxygenated acetone-d_6 (700 μL), and an initial NMR spectrum was acquired. Back in the glovebox, to this mixture was added an aliquot of precatalyst solution D (100 μL, 0.00250 mmol) and enough acetone-d_6 to

reach a total volume of 1.0 mL. The reaction was kept at room temperature and monitored at the

times given below.

Table 4.17. Yields determined by NMR in isomerization of **4.8** using 0.5 mol% catalyst **3.14** at room temperature in acetone-d_6.
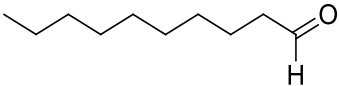
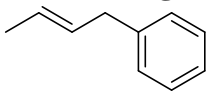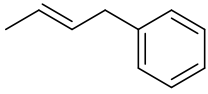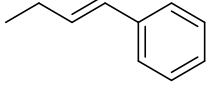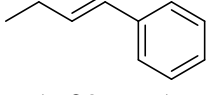| Measured integrals in arbitrary units relative to internal standard = 10.0 units and (in bold) derived per cent yields of products and amount of starting 1-alkene.			
Time	0 min	15 min	75 min
⌇⌇OH (5.84 ppm)	106.8	2.83	1.86
⌇⌇OH (4.89-5.01 ppm)	216.2	5.05	4.14
units per proton[a]	107.8	2.68	1.97
% starting material remaining	**100**	**2.5**	**1.8**
⌇⌇OH (5.38-5.44 ppm)[b]	-	210.0	211.7
units per proton[c]	-	102.7	98.5
% yield product	**0**	**95.3**	**91.4**
⌇⌇OH (0.94 ppm)	-	6.73	22.0
units per proton	-	2.24	7.33
% of isomer	**0**	**2.1**	**6.8**
⌇⌇O H (9.72 ppm)	-	-	0.28
units per proton	-	-	0.28
% of aldehyde	**0**	**-**	**0.3**

[a]Units calculated by taking the average of the integrations of the two resonances. [b]Signal is a mixture of E-4- and E-3-hexen-1-ol isomers. [c] Vinylic C-H proton units for E-4-hexen-1-ol determined by subtracting proton units of E-3-hexen-1-ol from total proton units of E-4/E-3 signal.

To a resealable J. Young tube in a glovebox, internal standard $(Me_3Si)_4C$ (~0.2 mg) and 9-decen-1-ol (74.1 mg, 0.474 mmol) were combined with a mixture of deoxygenated acetone-d_6 (700 µL), and an initial NMR spectrum was acquired. Back in the glovebox, to this mixture was added an aliquot of cat solution D (95 µL, 0.00238 mmol) and enough acetone-d_6 to reach a total volume of 1.0 mL. The reaction was kept at room temp and monitored at the times given below.

Table 4.18. Yields determined by NMR in isomerization of **4.9** using 0.5 mol% catalyst **3.14** at room temperature in acetone-d_6.

Measured integrals in arbitrary units relative to internal standard = 10.0 units and (in bold) derived per cent yields of products and amount of starting 1-alkene.				
Time	0 min	15 min	30 min	45 min
[structure] OH (5.76-5.84 ppm)	57.4	1.08	1.29	1.06
[structure] OH (4.85-5.02 ppm)	116.9	2.42	1.98	1.81
units per proton[a]	57.9	1.28	1.14	0.98
% starting material remaining	**100**	**2.0**	**2.0**	**1.7**
[structure] OH (5.23 – 5.54 ppm)	-	113.4	114.0	114.4
units per proton	-	55.6	55.2	53.5
% yield product	**0**	**96.0**	**95.3**	**92.4**
[structure] OH (0.94 ppm)	-	3.29	5.51	11.1
units per proton	-	1.10	1.84	3.70
% of isomer	**0**	**1.9**	**3.2**	**6.4**
[structure] O H (9.72 ppm)	-	-	-	-
units per proton	-	-	-	-
% of aldehyde	**0**	**-**	**-**	**-**
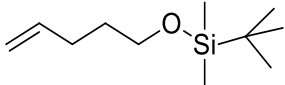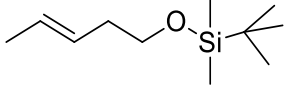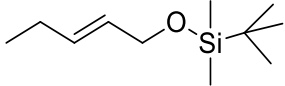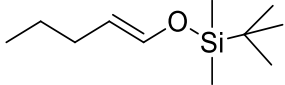
[a]Units calculated by taking the average of the integrations of the two resonances.

Data for Table 4.2, Entry 11: **Procedure for isomerization of 4-pentenol t-butyldime silyl ether to E-3 and E-2 silyl ethers using 0.5 mol% catalyst 3.14 at room temp. in acetone-d_6.**
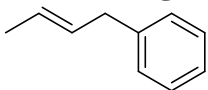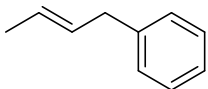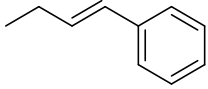
To a resealable J. Young tube in a glovebox, internal standard $(Me_3Si)_4C$ (~0.2 mg) and 4-penten-1-ol t-butyldimethylsilylether (101.3 mg, 0.505 mmol) were combined with a mixture of deoxygenated acetone-d_6 (700 µL), and an initial NMR spectrum was acquired. Back in the glovebox, to this mixture was added an aliquot of catalyst solution D (101 µL, 0.00253 mmol) and enough acetone-d_6 to reach a total volume of 1.0 mL. The reaction was kept at room temperature and monitored at the times given below.

Table 4.19. Yields determined by NMR in isomerization of **4.10** using 0.5 mol% catalyst **3.14** at room temperature in acetone-d_6.

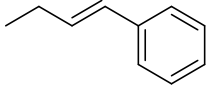| Measured integrals in arbitrary units relative to internal standard = 10.0 units and (in bold) derived per cent yields of products and amount of starting 1-alkene.				
Time	0 min	15 min	30 min	1 h
(5.82 ppm)	42.0	1.62	1.14	1.19
(4.82-5.10 ppm)	85.9	2.37	2.14	1.97
units per proton[a]	42.5	1.40	1.11	1.09
% starting material remaining	**100**	**3.3**	**2.6**	**2.6**
(5.38-5.52 ppm)	-	82.3	81.2	79.8
units per proton[b]	-	41.2	40.5	39.9
% yield product	**0**	**96.8**	**95.2**	**93.8**
(4.12 ppm)	-	-	1.52	2.30
units per proton	-	-	0.76	1.15
% of isomer	**0**	**-**	**3.6**	**2.7**
(6.23 ppm)	-	-	-	0.34
units per proton	-	-	-	0.34
% of enol ether	**0**	**-**	**-**	**0.8**
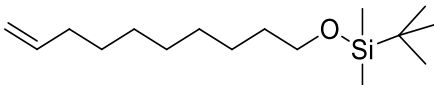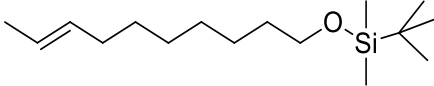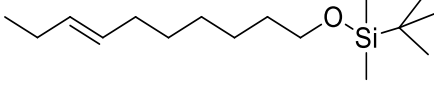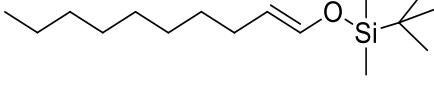
[a]Units calculated by taking the average of the integrations of the two resonances.

Data for Table 4.2, Entry 12: Procedure for isomerization of 9-decenol t-butyldime silyl ether to E-8 and E-7 silyl ethers using 0.5 mol% catalyst 3.14 at room temp in acetone-d_6.

To a resealable J. Young tube in a glovebox, internal standard $(Me_3Si)_4C$ (~0.2 mg) and 1-9-decen-1-ol tert-butyldimethylsilylether (135.3 mg, 0.500 mmol) were combined with a mixture of deoxygenated acetone-d_6 (700 μL), and an initial NMR spectrum was acquired. Back in the glovebox, to this mixture was added an aliquot of catalyst solution D (100 μL, 0.00250

mmol) and enough acetone-d_6 to reach a total volume of 1.0 mL. The reaction was kept at room

temperature and monitored at the times given below.

Table 4.20. Yields determined by NMR in isomerization of **4.11** using 0.5 mol% catalyst **3.14** at room temperature in acetone-d_6.

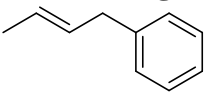| Measured integrals in arbitrary units relative to internal standard = 10.0 units and (in bold) derived per cent yields of products and amount of starting 1-alkene.				
Time	0 min	15 min	30 min	1 h
(structure) (5.75-5.83 ppm)	104.1	2.02	1.75	1.54
(structure) (4.88-4.99 ppm)	212.5	5.01	3.87	3.55
units per proton[a]	105.2	2.26	1.84	1.66
% starting material remaining	**100**	**2.2**	**1.8**	**1.6**
(structure) (5.25-5.43 ppm)[b]	-	207.3	208.9	207.7
units per proton[c]	-	102.7	102.3	100.9
% yield product	**0**	**97.5**	**97.3**	**95.9**
(structure) (0.94 ppm)	-	2.95	6.26	8.98
units per proton	-	0.98	2.09	2.99
% of isomer	**0**	**0.9**	**2.0**	**2.8**
(structure) (6.23 ppm)	-	-	-	-
units per proton	-	-	-	-
% of enol ether	**0**	**-**	**-**	**-**

[a]Units calculated by taking the average of the integrations of the two resonances. . [b]Signal is a mixture of E-8- and E-7-decen-1-ol silyl ether isomers. [c] Vinylic C-H proton units for E-8-product determined by subtracting proton units of E-7 product from total proton units of E-8/E-7 signal.
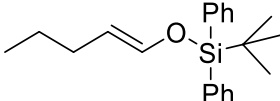
Data for Table 4.2, Entry 13: Procedure for isomerization of 4-penten-ol t-butyldiph silyl ether to E-3 and E-2 silyl ethers using 1.0 mol% catalyst 3.14 at room temp in acetone-d_6.

To a resealable J. Young tube in a glovebox, internal standard (Me$_3$Si)$_4$C (~0.2 mg) and

4-penten-1-ol tertbutyldiphenylsilylether (162.5 mg, 0.501 mmol) were combined with a mixture

of deoxygenated acetone-d_6 (700 µL), and an initial NMR spectrum was acquired. Back in the glovebox, to this mixture was added an aliquot of catalyst solution D (100 µL, 0.00250 mmol) and enough acetone-d_6 to reach a total volume of 1.0 mL. The reaction was kept at room temperature and monitored at the times given below.

Table 4.21. Yields determined by NMR in isomerization of **4.12** using 1.0 mol% catalyst **3.14** at room temperature in acetone-d_6.

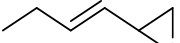| Measured integrals in arbitrary units relative to internal standard = 10.0 units and (in bold) derived per cent yields of products and amount of starting 1-alkene.			
Time	0 min	10 min	20 min
[1-butenyl silyl ether structure] (5.80 ppm)	88.7	4.05	2.26
[1-butenyl silyl ether structure] (4.87-5.03 ppm)	187.8	8.15	4.66
units per proton[a]	91.3	4.07	2.30
% starting material remaining	**100**	**4.5**	**2.5**
[E-3-pentenol silyl ether structure] (5.12-5.25 ppm)	-	175.2	175.1
units per proton	-	86.9	86.5
% yield product	**0**	**95.1**	**94.7**
[allylic silyl ether structure] (3.92 ppm)	-	1.49	2.17
units per proton	-	0.75	1.09
% of isomer	**0**	**0.8**	**1.2**
[enol ether structure] (5.85 ppm)	-	-	1.77
units per proton	-	-	0.89
% of enol ether	**0**	**-**	**0.9**

[a]Units calculated by taking the average of the integrations of the two resonances. . [b] Signal is a mixture of E-3- and E-2-penten-1-ol silyl ether isomers. [c] Vinylic C-H proton units for E-3-pentenol silyl ether determined by subtracting proton units of E-2-pentenol silyl ether from total proton units of E-3/E-2 signal.

Data for Table 4.2, Entry 14: Procedure for isomerization of untreated 9-phenyl-1-decene to E-2 and E-3 decenes using 1.0 mol% catalyst 3.14 at room temperature in acetone-d_6.

To a resealable J. Young tube in a glovebox, internal standard ($Me_3Si)_4C$ (~0.2 mg), and 9-phenyl-1-decene (111.1 mg, 0.513 mmol) were combined with a mixture of deoxygenated acetone-d_6 (700 µL), and an initial NMR spectrum was acquired. Back in the glovebox, to this mixture was added an aliquot of catalyst solution C (205 µL, 0.00513 mmol) and enough acetone-d_6 to reach a total volume of 1.0 mL. The reaction was kept at room temperature and monitored at the times given below.

Table 4.22. Yields determined by NMR in isomerization of **4.13** using 1.0 mol% catalyst **3.14** at room temperature in acetone-d_6.

Measured integrals in arbitrary units relative to internal standard = 10.0 units and (in bold) derived per cent yields of products and amount of starting 1-alkene.			
Time	0 min	15 min	75 min
(5.80 ppm)	82.9	2.19	1.59
(4.91 ppm)	168.2	4.61	4.11
units per proton[a]	83.5	2.25	1.82
% starting material remaining	**100**	**2.7**	**2.2**
(5.41 ppm)[b]	-	161.5	162.4
units per proton[c]	-	79.9	79.7
% of *E*-2	**0**	**95.7**	**95.4**
(0.95 ppm)	-	2.42	4.52
units per proton	-	0.81	1.51
% of *E*-3	**0**	**1.0**	**1.8**
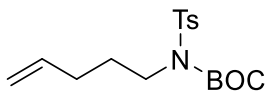
[a]Units calculated by taking the average of the integrations of the two resonances. [b]Signal is a mixture of vinylic C-H internal phenyl decene isomers, although these are no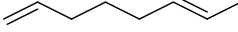t present in any detectable quantity within the time points listed above. [c]Proton units for E-2 phenyldecene determined by subtracting proton units of E-3 phenyl decene from total proton units of E-2/E-3 signal.

Data for Table 4.2, Entry 15: Procedure for isomerization of 4-penten-1-(tosyl)-1-Boc-amide to E-3 and E-2 pentenyl amides using 0.5 mol% catalyst 3.14 at room temp in acetone-*d*₆.

To a resealable J. Young tube in a glovebox, internal standard (Me₃Si)₄C (~0.2 mg) and amide (75.7 mg, 0.226 mmol) were combined with a mixture of deoxygenated acetone-*d*₆ (700 µL), and an initial NMR spectrum was acquired. Back in the glovebox, to this mixture was added an aliquot of solution D (101 µL, 0.00253 mmol) and enough acetone-*d*₆ to reach a total volume of 1.0 mL. The reaction was kept at room temp and monitored at the times given below.

Table 4.23. NMR yields in isomerization of **4.14** with 1.0 mol% **3.14** room temp in acetone-*d*₆.
Measured integrals in arbitrary units relative to internal standard = 10.0 units and (in bold) derived per cent yields of products and amount of starting 1-alkene.
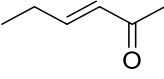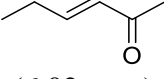
Time	0 min	10 min	20 min	30 min	40 min
Ts–N–BOC structure (5.80-5.95 ppm)	31.54	2.58	1.59	1.47	1.34
Ts–N–BOC structure (4.92-5.15 ppm)	63.87	5.11	3.67	3.28	2.86
units per proton[a]	31.7	2.70	1.90	1.56	1.39
% starting material remaining	**100**	**8.5**	**6.0**	**4.9**	**4.4**
Ts–N–BOC structure (5.38-5.52 ppm)	-	58.00	58.29	60.42	60.68
units per proton	-	28.9	29.7	30.1	30.2
% yield product	**0**	**91.1**	**93.7**	**95.0**	**95.3**
Ts–N–BOC structure (4.38 ppm)	-	0.13	0.14	0.20	0.21
units per proton	-	0.07	0.07	0.10	0.11
% of isomer	**0**	**0.2**	**0.2**	**0.3**	**0.3**
Ts–N–BOC structure (6.25 ppm)	-	0.15	0.15	0.19	0.19
units per proton	-	0.15	0.15	0.19	0.19
% of enamide	**0**	**0.5**	**0.5**	**0.6**	**0.6**

[a]Units calculated by taking the average of the integrations of the two resonances.

Data for Table 4.2, Entry 16: Procedure for isomerization of 5-hexen-2-one to (E)-4- and (E)-3-hexen-2-ones using 1.0 mol% catalyst 3.14 at room temperature in acetone-d_6.

To a resealable J. Young tube in a glovebox, internal standard (Me$_3$Si)$_4$C (~0.2 mg), and 5-hexen-2-one (49.9 mg, 0.508 mmol) were combined with a mixture of deoxygenated acetone-d_6 750 µL), and an initial NMR spectrum was acquired. Back in the glovebox, to this mixture was added an aliquot of catalyst solution C (203 µL, 0.00508 mmol) and enough acetone-d_6 to reach a total volume of 1.0 mL. The reaction was kept at room temp and monitored at times given below.

Table 4.24. Yields determined by NMR in isomerization of **4.15** using 1.0 mol% catalyst **3.14** at room temperature in acetone-d_6.

Measured integrals in arbitrary units relative to internal standard = 10.0 units and (in bold) derived per cent yields of products and amount of starting 1-alkene.								
Time	0 min	15 min	1 h	2 h	3 h	4 h	5 h	6 h
structure (5.80 ppm)	138.9	119.3	86.1	54.1	29.7	16.8	8.50	5.70
structure (4.90-5.03 ppm)	291.1	249.6	179.9	112.7	61.4	34.1	17.0	10.6
units per proton[a]	142.2	122.0	88.0	55.2	30.2	16.9	8.5	5.5
% starting material remaining	**100**	**85.8**	**61.9**	**38.8**	**21.2**	**11.9**	**6.0**	**3.9**
structure (5.54 ppm)[b]	-	36.7	95.9	145.4	170.8	181.5	168.6	155.0
structure (3.11 ppm)[b]		38.9	101.8	154.6	181.1	192.6	177.9	162.7
units per proton[c]	-	18.9	49.4	75.0	88.0	93.5	86.6	79.4
% E-4		**13.3**	**34.7**	**52.7**	**61.9**	**65.8**	**60.9**	**55.9**
structure (6.89 ppm)	-	0.96	5.13	11.6	21.0	31.9	44.7	58.8
structure (6.02 ppm)		0.94	4.80	11.5	20.3	31.1	43.4	57.2
units per proton	-	0.95	4.98	11.6	20.7	31.5	44.1	58.0
% of *E*-3 (conj)	**0**	**0.7**	**3.5**	**8.1**	**14.5**	**22.1**	**31.0**	**40.8**
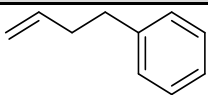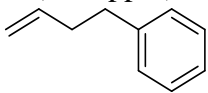
[a]Units calculated by taking the average of the integrations of the two resonances. [b] Signal is a mixture of vinylic C-H from E-2 and E-3 heptene isomers. [b] Vinylic C-H proton units for E-2 heptene determined by subtracting proton units of E-3 heptene from total proton units of E-2/E-3 signal.

Data for Table 4.2, Entry 18a: Procedure for isomerization of treated 4-phenyl-1-butene to 4-phenyl-E-2 and 4-phenyl-E-3 butenes using 0.5 mol% 3.14 at room temp in acetone-d_6.

To a resealable J. Young NMR tube in a glovebox, internal standard (Me$_3$Si)$_4$C (~0.2

mg), and 4-phenyl-1-butene (69.1 mg, 0.523 mmol) were combined with a mixture of

deoxygenated acetone-d_6 (700 µL), and an initial NMR spectrum was acquired. Back in the

glovebox, to this mixture was added an aliquot of precatalyst solution D (104 µL, 0.00260

mmol) and enough acetone-d_6 to reach a total volume of 1.0 mL. The reaction was kept at room

temperature and monitored at the times given below.

Table 4.25. Yields determined by NMR in isomerization of **4.17** using 0.5 mol% catalyst **3.14** at room temperature in acetone-d_6.

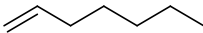| Measured integrals in arbitrary units relative to internal standard = 10.0 units and (in bold) derived per cent yields of products and amount of starting 1-alkene.					
Time	0 min	15 min	35 min	1 h	2 h
(5.85 ppm)	73.4	27.5	22.0	19.0	17.4
(4.92-5.04 ppm)	152.1	56.8	45.2	39.6	35.9
units per proton[a]	74.7	27.9	22.3	19.4	17.7
% starting material remaining	**100**	**37.4**	**30.0**	**26.0**	**23.7**
(5.47-5.61 ppm)	-	87.9	100.1	105.1	107.8
(1.65 ppm)	-	133.4	152.4	161.2	165.6
units per proton[a]	-	44.2	50.4	53.1	54.6
% of *E*-2	**0**	**59.1**	**67.5**	**71.1**	**73.0**
(6.39 ppm)	-	-	0.88	0.91	0.97
(6.29 ppm)	-	-	0.87	0.96	1.02
units per proton	-	-	0.88	0.94	1.0
% of *E*-3	**0**	**0**	**1.2**	**1.3**	**1.3**
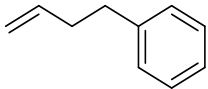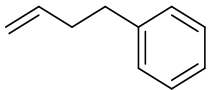
[a]Units calculated by taking the average of the integrations of the two resonances.

Data for Table 4.2, Entry 18b: Procedure for isomerization of treated 4-phenyl-1-butene to 4-phenyl-E-2 and 4-phenyl-E-3 butenes using 0.5 mol% 3.14 + 10 mol% iPr₂PIm' at room temperature in acetone-*d₆*.

To a resealable J. Young NMR tube in a glovebox, internal standard $(Me_3Si)_4C$ (~0.2 mg), 4-phenyl-1-butene (66.1 mg, 0.500 mmol) and the phosphine (12.8 mg, 0.0503 mmol) were combined with a mixture of deoxygenated acetone-d_6 (700 µL), and an initial NMR spectrum was acquired. Back in the glovebox, to this mixture was added an aliquot of precatalyst solution D (100 µL, 0.00250 mmol) and enough acetone-d_6 to reach a total volume of 1.0 mL. The reaction was kept at room temperature and monitored at the times given below.

Table 4.26. Yields determined by NMR in isomerization of **4.17** using 0.5 mol% **3.14** and 10 mol% phosphine at room temperature in acetone-d_6.

Measured integrals in arbitrary units relative to internal standard = 10.0 units and (in bold) derived per cent yields of products and amount of starting 1-alkene.					
Time	0 min	15 min	35 min	1 h	2 h
(5.85 ppm)	127.9	48.0	12.5	3.22	2.86
(4.92-5.04 ppm)	263.1	98.8	24.9	6.37	5.25
units per proton[a]	129.7	48.7	12.5	3.20	2.7
% starting material remaining	**100**	**37.5**	**9.6**	**2.5**	**2.1**
(5.47-5.61 ppm)	-	159.2	230.1	236.6	232.3
(1.65 ppm)	-	241.2	352.3	362.3	361.9
units per proton[a]	-	80.0	116.2	119.5	118.4
% of E-2	**0**	**61.6**	**89.6**	**92.1**	**91.3**
(6.39 ppm)	-	1.00	2.91	6.90	9.30
(6.29 ppm)	-	1.06	2.97	6.92	9.39
units per proton	-	1.03	2.94	6.91	9.35
% of E-3	**0**	**0.8**	**2.3**	**5.3**	**7.2**
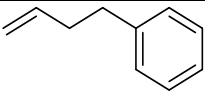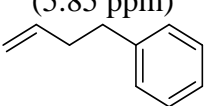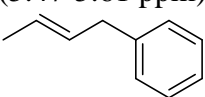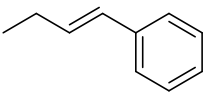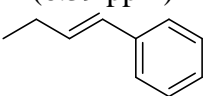
[a]Units calculated by taking the average of the integrations of the two resonances.
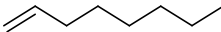
Data for Table 2, Entry 18c: Procedure for isomerization of treated 4-phenyl-1-butene to 4-phenyl-E-2 and 4-phenyl-E-3 butenes using 1.0 mol% catalyst 3.14 at room temperature in acetone-d_6.

To a resealable J. Young NMR tube in a glovebox, internal standard (Me$_3$Si)$_4$C (~0.2 mg), and 4-phenyl-1-butene (66.0 mg, 0.499 mmol) were combined with a mixture of deoxygenated acetone-d_6 (600 µL), and an initial NMR spectrum was acquired. Back in the glovebox, to this mixture was added an aliquot of precatalyst solution C (200 µL, 0.00500 mmol) and enough acetone-d_6 to reach a total volume of 1.0 mL. The reaction was kept at room temperature and monitored at the times given below.

Table 4.27. Yields determined by NMR in isomerization of **4.17** using 1.0 mol% catalyst **3.14** at room temperature in acetone-d_6.

	0 min	10 min	20 min	30 min	40 min	50 min
Measured integrals in arbitrary units relative to internal standard = 10.0 units and (in bold) derived per cent yields of products and amount of starting 1-alkene.						
Time	0 min	10 min	20 min	30 min	40 min	50 min
(5.85 ppm)	91.3	7.03	4.34	3.23	2.80	2.98
(4.92-5.04 ppm)	188.8	13.86	8.82	6.59	5.57	5.76
units per proton[a]	92.9	6.98	4.38	3.26	2.79	2.93
% starting material remaining	**100**	**7.5**	**4.7**	**3.5**	**3.0**	**3.1**
(5.47-5.61 ppm)	-	162.9	167.4	168.6	167.9	166.7
(1.65 ppm)	-	255.1	258.8	259.6	258.7	256.5
units per proton[a]	-	83.2	85.0	85.4	85.1	84.4
% of E-2	**0**	**89.6**	**91.5**	**91.9**	**91.6**	**90.9**
(6.39 ppm)	-	2.48	3.54	3.99	4.07	4.60
(6.29 ppm)	-	2.53	3.55	4.07	4.10	4.74
units per proton	-	2.51	3.55	4.03	4.09	4.67
% of E-3	**0**	**2.7**	**3.8**	**4.3**	**4.4**	**5.0**
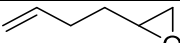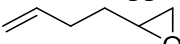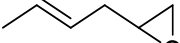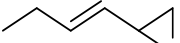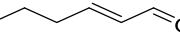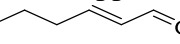
[a]Units calculated by taking the average of the integrations of the two resonances.

Data for Table 4.2, Entry 19: Procedure for isomerization of untreated 1,2-epoxy-5-hexene to E-4 and E-3-hexenes using 0.5 mol% catalyst 3.14 at room temperature in acetone-d_6.

To a resealable J. Young tube in a glovebox, internal standard (Me$_3$Si)$_4$C (~0.2 mg) and

1,2-epoxy-5-hexene (49.3 mg, 0.502 mmol) were combined with a mixture of deoxygenated

acetone-d_6 (850 µL), and an initial NMR spectrum was acquired. Back in the glovebox, to this mixture was added an aliquot of cat. solution D (100 µL, 0.00250 mmol) and enough acetone-d_6 to reach total of 1.0 mL. Reaction was kept at room temp and monitored at the times given below.

Table 4.28. Yields determined by NMR in isomerization of **4.18** using 0.5 mol% catalyst **3.14** at room temperature in acetone-d_6.

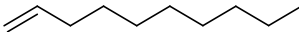| Measured integrals in arbitrary units relative to internal standard = 10.0 units and (in bold) derived per cent yields of products and amount of starting 1-alkene.						
Time	0 min	15 min	30 min	1 h	2 h	16 h
(5.82-5.91 ppm)	113.3	12.96	8.20	5.35	2.69	2.49
(4.93-5.06 ppm)	236.1	27.92	18.49	11.8	6.02	5.67
units per proton[a]	115.7	13.46	8.72	5.63	2.85	2.66
% starting material remaining	**100**	**11.6**	**7.5**	**4.9**	**2.5**	**2.3**
(5.37-5.58 ppm)	-	200.6	210.2	214.7	222.0	224.5
units per proton[b]	-	99.0	103.2	106.2	106.6	107.6
% yield product	**0**	**85.6**	**89.2**	**91.8**	**92.1**	**93.0**
(4.05 ppm)	-	0.96	1.92	3.27	4.48	4.85
(5.62 ppm)	-	1.57	1.81	2.22	4.40	4.47
units per proton[a]	-	1.27	1.87	2.75	4.44	4.66
% of isomer	**0**	**1.1**	**1.6**	**2.4**	**3.8**	**4.0**
(6.17 ppm)	-	0.44		1.03	2.14	2.16
(6.03 ppm)	-	0.55		1.29	2.83	2.86
units per proton[a]	-	0.50		1.16	2.49	2.51
% of enal	**0**	**0.4**		**1.0**	**2.1**	**2.2**
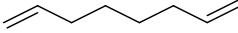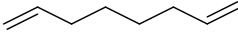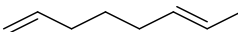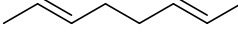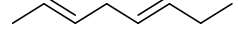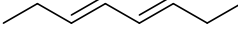
[a]Units calculated by taking the average of the integrations of the two resonances. [b]Signal is a mixture of E-3- and E-2-penten-1-ol isomers.

293

Data for Table 4.2, Entry 20: Procedure for isomerization of 1,7-octadiene to (2E,6E)-2,6- and (2E,5E)-2,5-octadiene using 2.0 mol% catalyst 3.14 at room temperature in acetone-d_6.

       To a resealable J. Young tube in a glovebox, internal standard (Me$_3$Si)$_4$C (~0.2 mg), and 1,7-octadiene (54.9 mg, 0.498 mmol) were combined with a mixture of deoxygenated acetone-d_6 (700 μL), and an initial NMR spectrum was acquired. Back in the glovebox, to this mixture was added an aliquot of catalyst solution C (398 μL, 0.00995 mmol) and enough acetone-d_6 to reach a total volume of 1.0 mL. The reaction was kept at room temp and monitored at the times given below.

Measured integrals in arbitrary units relative to internal standard = 10.0 units and (in bold) derived per cent yields of products and amount of starting 1-alkene.					
Time	0 min	10 min	30 min	1 h	24 h
(5.81ppm)	59.94	1.48	1.22	1.19	0.98
(4.95 ppm)	123.85	3.15	2.63	2.48	2.24
units per proton[a]	30.47	UL[b]: 0.76	UL[b]: 0.63	UL[b]: 0.61	UL[b]: 0.53
% starting material remaining	**100**	**UL[b]: 2.5**	**UL[b]: 2.1**	**UL[b]: 2.0**	**UL[b]: 1.7**
(5.81ppm)	59.94	1.48	1.22	1.19	0.98
(4.95 ppm)	123.85	3.15	2.63	2.48	2.24
units per proton[d]	N/A	UL[b]: 1.53	UL[b]: 1.26	UL[b]: 1.22	UL[b]: 1.06
% 1,6	N/A	**UL[b]: 5.0**	**UL[b]: 4.2**	**UL[b]: 4.0**	**UL[b]: 3.4**
(1.60 ppm)[e]	-	176.5	174.2	172.5	152.9
units per proton[d,e]	-	UL[b]: 29.4 LL[c]: 28.6	UL[b]: 29.0 LL[c]: 28.4	UL[b]: 28.7 LL[c]: 28.1	UL[b]: 25.4 LL[c]:24.8
% 2,6	**-**	**UL[b]: 96.5 LL[c]: 93.9**	**UL[b]: 95.2 LL[c]: 93.1**	**UL[b]: 94.2 LL[c]: 92.2**	**UL[b]: 83.3 LL[c]: 81.4**
(2.62 ppm)	-	0.14	0.19	0.21	0.57
units per proton	-	0.07	0.10	0.11	0.29
% of 2,5	**0**	**0.2**	**0.3**	**0.4**	**1.0**
(5.99 ppm)	-	0.09	0.45	0.76	6.07
units per proton	-	0.05	0.22	0.38	3.04
% of conj isomer	**0**	**0.2**	**0.7**	**1.2**	**10.0**
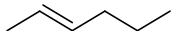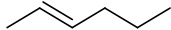
[a]Units calculated by taking the average of the integrations of the two resonances, assuming 100% of signal is from 1,7-octadiene. [b]"UL" refers to 'upper limit.' [c]"LL" refers to 'lower limit.' [d]Units calculated by taking the average of the integrations of the two resonances, assuming 100% of signal is from 1,(E)-6-octadiene. [e]Signal is a mixture of terminal allylic -CH$_3$ from 2,7- and 2,6-octadiene isomers. [f]"Upper limit" (UL) units calculated by assuming 100% of signal is from 2, 6-octadiene. "Lower limit (LL) units calculated by subtracting UL values for other (E)-2 isomers. Note: calculations assume minimum to no presence of 2,4-, 1,4-, or 1,3-octadiene isomers, and no distinction is made between (E) and (Z) isomers because of complicated spectra.

Additional isomerization data – in situ ionization of complex 3.10 with TlPF$_6$

Procedure for isomerization of untreated 1-hexene to E-2 and E-3 hexenes using 0.1 mol% precatalyst 3.10 and 0.15 mol% TlPF$_6$ at room temperature in acetone-d_6.
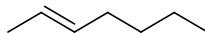
To a resealable J. Young NMR tube in a glovebox, internal standard (Me$_3$Si)$_4$C (~0.2 mg), TlPF$_6$ (0.3 mg, 0.000859 mmol) and 1-hexene (42.1 mg, 0.500 mmol) were combined with a mixture of deoxygenated acetone-d_6 (700 μL), and an initial NMR spectrum was acquired. Back in the glovebox, to this mixture was added an aliquot of precatalyst solution B (20 μL, 0.000500 mmol) and enough acetone-d_6 to reach a total volume of 1.0 mL. The reaction was kept at room temperature and monitored at the times given below.

Table 4.30. Yields determined by NMR in isomerization of **4.1** using 0.1 mol% catalyst mixture **3.10** and 0.1 mol% TlPF$_6$ at room temperature in acetone-d_6.
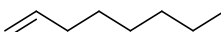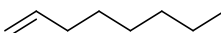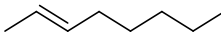
Measured integrals in arbitrary units relative to internal standard = 10.0 units and (in bold) derived per cent yields of products and amount of starting 1-alkene.						
Time	0 min	15 min	1 h	2 h	4 h	24 h
(5.79 ppm)	65.8	36.5	6.88	1.60	1.32	1.07
(4.85-5.01 ppm)	135.3	73.9	14.0	3.45	2.56	2.13
units per proton[a]	66.7	36.7	6.94	1.66	1.30	1.07
% starting material remaining	**100**	**55.1**	**10.4**	**2.5**	**1.9**	**1.6**
(5.35-5.46 ppm)[b]	-	60.5	120.0	131.7	135.1	130.8
(1.60 ppm)	-	90.9	180.1	195.1	193.4	181.4
units per proton[c]	-	30.3	59.6	64.6	64.5	57.7
% of E-2	**0**	**45.3**	**89.3**	**96.9**	**96.6**	**86.5**
(0.94 ppm)	-	-	2.62	4.80	9.29	31.5
units per proton	-	-	0.44	0.80	1.55	5.25
% of E-3	**0**	**0**	**0.6**	**1.2**	**2.3**	**7.9**
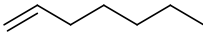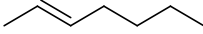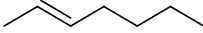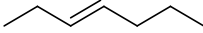
[a]Units calculated by taking the average of the integrations of the two resonances. [b]Signal is a mixture of vinylic C-H from E-2 and E-3 hexene isomers. [c]Vinylic proton units for E-2 hexene determined by subtracting proton units of E-3 hexene from total proton units of E-2/E-3 signal.

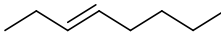**Procedure for isomerization of untreated 1-heptene to E-2 and E-3 heptenes using 0.1 mol% catalyst 3.10 and 0.15 mol% TlPF$_6$ at room temperature in acetone-d_6.**

To a resealable J. Young tube in a glovebox, internal standard (Me$_3$Si)$_4$C (~0.2 mg), TlPF$_6$ (0.3 mg, 0.000859 mmol) and 1-heptene (49.9 mg, 0.510 mmol) were combined with a mixture of deoxygenated acetone-d_6 (700 µL), and an initial NMR spectrum was acquired. Back in the glovebox, to this mixture was added an aliquot of precatalyst solution A (6.9 µL, 0.00050 mmol) and enough acetone-d_6 to reach a total volume of 1.0 mL. The reaction was kept at room temperature and monitored at the times given below.

Table 4.31. Yields determined by NMR in isomerization of **4.4** using 0.1 mol% catalyst mixture **3.10** and 0.1 mol% TlPF$_6$ at room temperature in acetone-d_6.

Measured integrals in arbitrary units relative to internal standard = 10.0 units and (in bold) derived per cent yields of products and amount of starting 1-alkene.								
Time	**0 min**	**15 min**	**1 h**	**2 h**	**3 h**	**4 h**	**6 h**	**31 h**
(5.80 ppm)	54.8	26.9	6.84	2.08	1.39	1.03	1.00	1.04
(4.90-4.97 ppm)	111.2	54.6	13.9	4.36	2.36	2.09	2.04	2.06
units per proton[a]	55.2	27.1	6.90	2.10	1.44	1.04	1.01	1.04
% starting material remaining	**100**	**49.1**	**12.5**	**3.8**	**2.6**	**1.9**	**1.8**	**1.9**
(5.34-5.46 ppm)[b]	-	51.0	97.2	107.1	108.4	106.4	105.4	103.0
(1.60 ppm)	-	82.1	145.2	159.6	162.0	158.7	156.9	153.4
units per proton[c]	-	27.6	48.5	53.4	54.1	53.1	52.5	51.3
% of E-2	**0**	**49.9**	**87.9**	**96.7**	**98.0**	**96.1**	**95.1**	**93.0**
(0.94 ppm)	-	-	1.07	1.51	2.18	2.70	4.22	9.33
units per proton	-	-	0.35	0.50	0.73	0.90	1.41	3.11
% of E-3	**0**	**0**	**0.6**	**0.9**	**1.3**	**1.9**	**2.5**	**5.6**
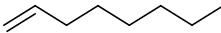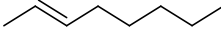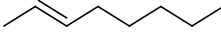
[a] Units calculated by taking the average of the integrations of the two resonances. [b] Signal is a mixture of vinylic C-H from E-2 and E-3 heptene isomers. [b] Vinylic C-H proton units for E-2 heptene determined by subtracting proton units of E-3 heptene from total proton units of E-2/E-3 signal.

Procedure for isomerization of untreated 1-octene to E-2, E-3, and E-4 octenes using 0.1 mol% catalyst 3.10 and 0.15 mol% TlPF₆ at room temperature in acetone-d₆.

To a resealable J. Young tube in a glovebox, internal standard $(Me_3Si)_4C$ (~0.2 mg), TlPF₆ (0.3 mg, 0.000859 mmol) and 1-octene (59.9 mg, 0.534 mmol) were combined with a mixture of deoxygenated acetone-d_6 (700 μL), and an initial NMR spectrum was acquired. Back in the glovebox, to this mixture was added an aliquot of precatalyst solution A (6.9 μL, 0.000500 mmol) and enough acetone-d_6 to reach a total volume of 1.0 mL. The reaction was kept at room temperature and monitored at the times given below.

Table 4.32. Yields determined by NMR in isomerization of **4.5** using 0.1 mol% catalyst mixture **3.10** and 0.15 mol% TlPF₆ at room temperature in acetone-d_6.
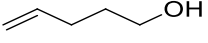
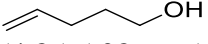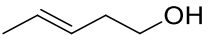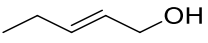| Time	0 min	15 min	1 h	2 h	6 h	24 h	124 h
Measured integrals in arbitrary units relative to internal standard = 10.0 units and (in bold) derived per cent yields of products and amount of starting 1-alkene.							
(5.80 ppm)	47.6	39.0	33.0	28.9	26.9	20.1	14.2
(4.89-4.97 ppm)	96.3	78.9	66.7	58.3	54.1	40.9	28.6
units per proton[a]	47.9	39.2	33.2	29.0	27.0	20.3	14.2
% starting material remaining	**100**	**81.9**	**69.3**	**60.6**	**56.3**	**42.3**	**29.6**
(5.42 ppm)[b]	-	17.4	30.5	37.4	41.9	56.4	68.7
(1.60 ppm)	-	25.7	45.0	55.2	61.5	84.0	100.4
units per proton[c]	-	8.61	15.1	18.6	20.7	28.1	33.9
% of E-2	**0**	**18.0**	**31.6**	**38.7**	**43.2**	**58.7**	**70.8**
(0.94 ppm)	-	-	-	-	-	-	-
units per proton	-	-	-	-	-	-	-
% of E-3	**0**	**0**	**0**	**0**	**0**	**0**	**0**

[a]Units calculated by taking the average of the integrations of the two resonances. [b]Signal is a mixture of vinylic C-H protons from internal isomers, although none are present in the above reaction. [c]Vinylic C-H proton units for E-2 octene determined by subtracting proton units of E-3 octene from total proton units of E-2/E-3 signal.

Procedure for isomerization of untreated 1-decene to E-2 and E-3 decenes using 0.1 mol% precatalyst 3.10 and 0.15 mol% TlPF$_6$ at room temperature in acetone-d_6.

To a resealable J. Young tube in a glovebox, internal standard (Me$_3$Si)$_4$C (~0.2 mg), TlPF$_6$ (0.3 mg, 0.000859 mmol) and 1-decene (70.8 mg, 0.505 mmol) were combined with a mixture of deoxygenated acetone-d_6 (700 µL), and an initial NMR spectrum was acquired. Back in the glovebox, to this mixture was added an aliquot of precatalyst solution A (6.9 µL, 0.000500 mmol) and enough acetone-d_6 to reach a total volume of 1.0 mL. The reaction was kept at room temperature and monitored at the times given below.

Table 4.33. Yields determined by NMR in isomerization of **4.6** using 0.1 mol% catalyst mixture **3.10** and 0.1 mol% TlPF$_6$ at room temperature in acetone-d_6.
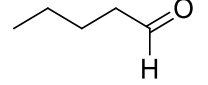
Measured integrals in arbitrary units relative to internal standard = 10.0 units and (in bold) derived per cent yields of products and amount of starting 1-alkene.

Time	0 min	15 min	1 h	2 h	4 h	6 h	24 h
(5.80 ppm)	42.4	36.6	33.0	31.6	30.0	29.5	26.7
(4.91 ppm)	85.5	73.9	66.5	63.4	60.7	59.2	53.5
units per proton[a]	42.6	36.8	33.1	31.7	30.2	29.6	26.7
% starting material remaining	**100**	**86.3**	**77.8**	**74.2**	**70.8**	**61.7**	**55.8**
(5.41 ppm)[b]	-	10.7	18.4	21.3	23.6	25.1	31.9
(1.60 ppm)	-	16.9	26.7	31.5	35.2	37.2	46.2
units per proton[c]	-	5.48	9.04	10.6	11.8	12.5	15.7
% of E-2	**0**	**12.9**	**21.2**	**22.1**	**24.5**	**26.0**	**32.7**
(0.95 ppm)	-	-	-	-	-	-	-
units per proton	-	-	-	-	-	-	-
% of E-3	**0**	**0**	**0**	**0**	**0**	**0**	**0**

[a]Units calculated by taking the average of the integrations of the two resonances. [b]Signal is a mixture of vinylic C-H internal decene isomers, although these are not present in any detectable quantity within the time points listed above. [c]Proton units for E-2 decene determined by subtracting proton units of E-3 decene from total proton units of E-2/E-3 signal.

Procedure for isomerization of treated 1-hexene to E-2 and E-3 hexenes using 0.1 mol% precatalyst 3.10 and 0.15 mol% TlPF$_6$ at room temperature in acetone-d_6.

To a resealable J. Young tube in a glovebox, internal standard (Me$_3$Si)$_4$C (~0.2 mg), TlPF$_6$ (0.3 mg, 0.000859 mmol) and alumina-fltered 1-hexene (44.2 mg, 0.525 mmol) were combined with a mixture of deoxygenated acetone-d_6 (700 µL), and an initial NMR spectrum was acquired. Back in the glovebox, to this mixture was added an aliquot of precatalyst solution B (20 µL, 0.00050 mmol) and enough acetone-d_6 to reach a total volume of 1.0 mL. The reaction was kept at room temperature and monitored at the times given below.

Table 4.34. Yields determined by NMR in isomerization of **4.4** using 0.1 mol% catalyst mixture **3.10** and 0.1 mol% TlPF$_6$ at room temperature in acetone-d_6.
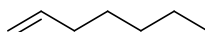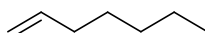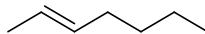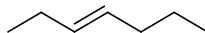
Measured integrals in arbitrary units relative to internal standard = 10.0 units and (in bold) derived per cent yields of products and amount of starting 1-alkene.							
Time	0 min	15 min	30 min	1 h	2 h	5 h	7 h
(5.79 ppm)	84.6	44.2	27.5	11.8	2.89	1.45	1.68
(4.85-5.01 ppm)	172.9	89.9	55.8	24.0	5.71	2.86	3.04
units per proton[a]	85.5	44.6	27.7	11.9	2.87	1.44	1.60
% starting material remaining	**100.0**	**52.1**	**32.4**	**13.9**	**3.4**	**1.7**	**1.9**
(5.35-5.46 ppm)[b]	-	79.3	112.5	144.0	162.3	164.5	165.5
(1.60 ppm)	-	118.5	168.8	216.0	243.1	244.2	243.2
units per proton[c]	-	39.6	56.3	71.7	80.3	80.2	79.6
% of E-2	**-**	**46.3**	**65.8**	**83.9**	**93.9**	**93.8**	**93.1**
(0.94 ppm)	-	-	-	1.97	5.01	9.52	13.9
units per proton	-	-	-	0.33	0.84	1.59	2.32
% of E-3	**0**	**0**	**0**	**0.4**	**1.0**	**1.9**	**2.7**

[a]Units calculated by taking the average of the integrations of the two resonances [b]Signal is a mixture of E-2 and E-3 vinylic C-Hs. [c]Proton units for E-2 hexene determined by subtracting proton units of E-3 hexene from total proton units of E-2/E-3 signal.

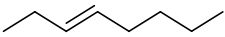**Procedure for isomerization of treated 1-heptene to E-2 and E-3 heptenes using 0.1 mol% precatalyst 3.10 and 0.15 mol% TlPF₆ at room temperature in acetone-*d₆*.**

To a resealable J. Young tube in a glovebox, internal standard (Me₃Si)₄C (~0.2 mg), TlPF₆ (0.3 mg, 0.00086 mmol) and alumina-filtered 1-heptene (49.1 mg, 0.500 mmol) were combined with a mixture of deoxygenated acetone-*d₆* (700 µL), and an initial NMR spectrum was acquired. Back in the glovebox, to this mixture was added an aliquot of precatalyst solution B (20 µL, 0.00050 mmol) and enough acetone-*d₆* to reach a total volume of 1.0 mL. The reaction was kept at room temperature and monitored at the times given below.

Table 4.35. Yields determined by NMR in isomerization of **4.4** using 0.1 mol% catalyst mixture **3.10** and 0.1 mol% TlPF₆ at room temperature in acetone-*d₆*.

Measured integrals in arbitrary units relative to internal standard = 10.0 units and (in bold) derived per cent yields of products and amount of starting 1-alkene.								
Time	0 min	15 min	30 min	1 h	2 h	4 h	8.5 h	52 h
(5.80 ppm)	34.7	29.8	26.5	22.2	19.3	16.8	15.3	13.2
(4.90-4.97 ppm)	71.2	60.5	54.0	45.2	39.3	34.2	30.8	26.9
units per proton[a]	35.2	30.0	26.8	22.4	19.5	17.0	15.4	13.3
% starting material remaining	**100**	**85.2**	**76.1**	**63.6**	**55.4**	**48.2**	**43.8**	**37.8**
(5.34-5.46 ppm)[b]	-	12.0	19.5	27.2	33.8	38.3	42.6	45.1
(1.60 ppm)	-	18.1	29.2	40.7	50.3	57.2	63.0	67.2
units per proton[c]	-	6.03	9.74	13.6	16.8	19.1	21.2	22.5
% of E-2	**0**	**17.1**	**27.7**	**38.6**	**47.7**	**54.2**	**60.2**	**63.9**
(0.94 ppm)	-	-	-	-	-	-	-	-
units per proton	-	-	-	-	-	-	-	-
% of E-3	**0**	**0**	**0**	**0**	**0**	**0**	**0**	**0**

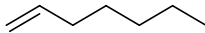[a]Units calculated by taking the average of the integrations of the two resonances [b]Signal is a mixture of E-2 and E-3 heptene isomers. [c]Vinylic C-H proton units for E-2 heptene determined by subtracting proton units of E-3 heptene from total proton units of E-2/E-3 signal.

Procedure for isomerization of treated 1-octene to E-2, E-3, and E-4- octenes using 0.1 mol% precatalyst 3.10 and 0.1 mol% TlPF$_6$ at room temperature in acetone-d_6.

To a resealable J. Young tube in a glovebox, internal standard (Me$_3$Si)$_4$C (~0.2 mg), TlPF$_6$ (0.3 mg, 0.00143 mmol) and alumina-filtered 1-octene (57.8 mg, 0.515 mmol) were combined with a mixture of deoxygenated acetone-d_6 (700 µL), and an initial NMR spectrum was acquired. Back in the glovebox, to this mixture was added an aliquot of precatalyst solution A (6.9 µL, 0.00050 mmol) and enough acetone-d_6 to reach a total volume of 1.0 mL. The reaction was kept at room temperature and monitored at the times given below.

Table 4.36. Yields determined by NMR in isomerization of **4.5** using 0.1 mol% catalyst mixture **3.10** and 0.1 mol% TlPF$_6$ at room temperature in acetone-d_6.
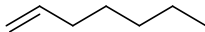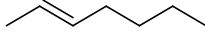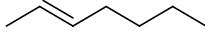
Measured integrals in arbitrary units relative to internal standard = 10.0 units and (in bold) derived per cent yields of products and amount of starting 1-alkene.

Time	0 min	15 min	30 min	1 h	2 h	4 h	24 h	72 h
(5.80 ppm)	59.0	10.4	2.28	1.13	1.07	1.09	0.84	0.71
(4.89-4.97 ppm)	118.3	21.3	4.82	2.51	2.38	2.23	1.71	1.38
units per proton^a	59.1	10.5	2.35	1.19	1.13	1.10	0.85	0.70
% starting material remaining	**100**	**17.8**	**4.0**	**2.0**	**1.9**	**1.9**	**1.4**	**1.2**
(1.60 ppm)	-	144.4	167.6	168.1	164.9	160.8	136.5	112.2
units per proton		48.1	55.9	56.0	55.0	53.3	45.5	37.4
% of E-2	**-**	**81.4**	**94.6**	**94.8**	**93.0**	**90.3**	**77.0**	**63.3**
(0.94 ppm)	-	-	3.38	3.91	8.13	11.2	33.3	46.6
units per proton	-	-	1.13	1.30	2.71	3.74	11.1	15.5
% of E-3	**-**	**-**	**1.9**	**2.2**	**4.6**	**6.3**	**18.8**	**26.3**

^{a}Units calculated by taking the average of the integrations of the two resonances.

Procedure for isomerization of treated 1-decene to E-2 and E-3 decenes using 0.1 mol% precatalyst 3 and 0.15 mol% TlPF₆ at room temperature in acetone-*d₆*.

To a resealable J. Young tube in a glovebox, internal standard (Me₃Si)₄C (~0.2 mg), TlPF₆ (0.3 mg, 0.000859 mmol) and alumina-filtered 1-decene (70.1 mg, 0.500 mmol) were combined with a mixture of deoxygenated acetone-*d₆* (700 μL), and an initial NMR spectrum was acquired. Back in the glovebox, to this mixture was added an aliquot of precatalyst solution B (20 μL, 0.000500 mmol) and enough acetone-*d₆* to reach a total volume of 1.0 mL. The reaction was kept at room temperature and monitored at the times given below.

Table 4.37. Yields determined by NMR in isomerization of **4.6** using 0.1 mol% catalyst mixture **3.10** and 0.1 mol% TlPF₆ at room temperature in acetone-*d₆*.
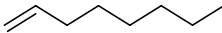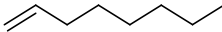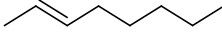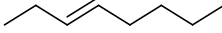
Measured integrals in arbitrary units relative to internal standard = 10.0 units and (in bold) derived per cent yields of products and amount of starting 1-alkene.							
Time	0 min	15 min	30 min	1 h	2 h	4 h	8.5 h
(5.80 ppm)	69.8	46.8	31.3	15.1	4.65	1.49	1.28
(4.91 ppm)	142.7	94.2	63.3	30.6	9.24	3.19	2.57
units per proton[a]	70.6	47.0	31.5	15.2	4.64	1.54	1.28
% starting material remaining	**100**	**66.5**	**44.6**	**21.5**	**6.6**	**2.2**	**1.8**
(1.60 ppm)	-	75.2	118.8	164.8	198.8	206.6	204.2
units per proton	-	25.1	39.6	54.9	66.3	68.9	68.1
% of *E*-2	**0**	**35.5**	**56.1**	**77.8**	**93.8**	**97.5**	**96.4**
(0.95 ppm)	-	-	-	1.22	2.52	4.11	7.14
units per proton	-	-	-	0.41	0.84	1.37	2.38
% of *E*-3	**0**	**0**	**0**	**0.6**	**1.2**	**1.9**	**3.4**

[a]Units calculated by taking the average of the integrations of the two resonances.

Procedure for isomerization of treated 4-penten-1-ol to E-3 and E-2 penten-1-ols using 0.5 mol% precatalyst 3.10 and 0.5 mol% TlPF$_6$ at room temperature in acetone-d_6.

To a resealable J. Young tube in a glovebox, internal standard (Me$_3$Si)$_4$C (~0.2 mg), TlPF$_6$ (1.0 mg, 0.0029 mmol) and 4-penten-1-ol (43.5 mg, 0.505 mmol) were combined with a mixture of deoxygenated acetone-d_6 (700 µL), and an initial NMR spectrum was acquired. Back in the glovebox, to this mixture was added an aliquot of precatalyst solution B (100 µL, 0.00250 mmol) and enough acetone-d_6 to reach a total volume of 1.0 mL. The reaction was kept at room temperature and monitored at the times given below.

Table 4.38. Yields determined by NMR in isomerization of **4.7** using 0.5 mol% catalyst mixture **3.10** and 0.5 mol% TlPF₆ at room temperature in acetone-d_6.

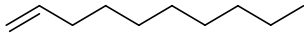|	Measured integrals in arbitrary units relative to internal standard = 10.0 units and (in bold) derived per cent yields of products and amount of starting 1-alkene.							
Time	0 min	15 min	30 min	1 h	5 h	7 h	24 h	48 h
(5.84 ppm)	144.4	89.8	47.0	4.67	3.27	2.97	3.05	3.27
(4.85-5.08 ppm)	295.4	183.1	96.2	9.22	6.32	6.42	6.23	6.06
units per proton[a]	146.1	90.7	47.6	4.64	3.22	3.09	3.08	3.15
% starting material remaining	**100**	**62.1**	**32.5**	**3.2**	**2.2**	**2.1**	**2.1**	**2.2**
(5.35-5.46 ppm)[b]	-	113.3	198.1	284.6	274.8	266.1	265.9	265.7
units per proton[c]	-	56.7	99.0	141.9	137.4	133.0	133.0	132.9
% yield product	**0**	**38.8**	**67.8**	**97.1**	**94.0**	**91.1**	**91.0**	**90.9**
(0.96 ppm)	-	-	-	2.19	6.49	5.83	6.18	6.02
units per proton	-	-	-	0.73	2.16	1.94	2.06	2.01
% of isomer	**0**	**0**	**0**	**0.5**	**1.5**	**1.3**	**1.4**	**1.4**
(9.72 ppm)	-	-	-	-	4.85	6.04	7.53	7.61
units per proton	-	-	-	-	4.85	6.04	7.53	7.61
% of aldehyde	**0**	**0**	**0**	**0**	**3.3**	**4.1**	**5.2**	**5.2**

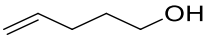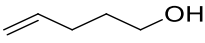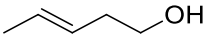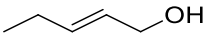[a]Units calculated by taking the average of the integrations of the two resonances. [b]Signal is a mixture of E-3- and E-2-penten-1-ol isomers. [c]Vinylic C-H proton units for E-3-penten-1-ol determined by subtracting proton units of E-2-penten-1-ol from total proton units of E-3/E-2 signal.
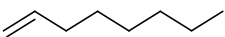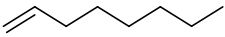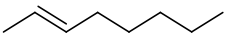
Procedure for isomerization of treated 1-octene + 1 mol % H₂O to E-2, E-3, and E-4-octenes using 0.1 mol% precatalyst 3.10 and 0.1 mol% TlPF₆ at room temperature in acetone-d_6.

To a resealable J. Young tube in a glovebox, internal standard Me₃Si)₄C (~0.2 mg), TlPF₆

(0.3 mg, 0.00143 mmol) and alumina-filtered 1-octene (57.8 mg, 0.515 mmol) were combined

with a mixture of deoxygenated acetone-d_6 (700 μL), and an initial NMR spectrum was acquired.

Back in the glovebox, to this mixture was added an aliquot of precatalyst solution A (6.9 µL, 0.00050 mmol) and enough acetone-d_6 to reach a total volume of 1.0 mL. The reaction was kept at room temperature and monitored at the times given below.

Table 4.39. Yields determined by NMR in isomerization of **4.5 + 1 mol% H$_2$O** using 0.1 mol% catalyst mixture **3.10** and 0.1 mol% TlPF$_6$ at room temperature in acetone-d_6.

Measured integrals in arbitrary units relative to internal standard = 10.0 units and (in bold) derived per cent yields of products and amount of starting 1-alkene.								
Time	0 min	15 min	1 h	2 h	4 h	7.5 h	29 h	57.5 h
(5.80 ppm)	47.9	35.3	20.4	11.9	4.36	1.59	1.13	0.93
(4.89-4.97 ppm)	96.9	71.8	41.2	23.8	8.93	2.99	1.86	1.43
units per proton[a]	48.2	35.6	20.5	11.9	4.41	1.54	1.03	0.82
% starting material remaining	**100**	**73.9**	**42.5**	**24.7**	**9.2**	**3.2**	**2.1**	**1.7**
(1.60 ppm)	-	39.9	55.6	109.8	130.9	139.8	137.3	136.4
units per proton		13.3	18.5	36.6	43.6	46.6	45.8	45.5
% of _E_-2	**-**	**27.6**	**38.5**	**75.9**	**90.5**	**96.6**	**94.9**	**94.3**
(0.94 ppm)	-	-	-	-	1.32	2.14	3.05	4.02
units per proton	-	-	-	-	0.44	0.71	1.02	1.34
% of _E_-3	**0**	**0**	**0**	**0**	**0.9**	**1.5**	**2.1**	**2.8**

[a]Units calculated by taking the average of the integrations of the two resonances

Procedure for isomerization of treated 1-hexene to E-2 and E-3 hexenes using 0.5 mol% precatalyst 3.10 and 0.5 mol% TlPF$_6$ at room temperature in acetone-d_6.

To a resealable J. Young tube in a glovebox, internal standard (Me$_3$Si)$_4$C (~0.2 mg), TlPF$_6$ (1 mg, 0.0029 mmol) and alumina-filtered 1-hexene (42.1 mg, 0.500 mmol) were combined with a mixture of deoxygenated acetone-d_6 (700 µL), and an initial NMR spectrum was acquired. Back in the glovebox, to this mixture was added an aliquot of catalyst solution B (100 µL, 0.00250 mmol) and enou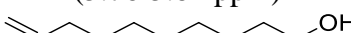gh acetone-d_6 to reach a total volume of 1.0 mL. The reaction was kept at room temperature and monitored at the times given below.

Table 4.40. Yields determined by NMR in isomerization of **4.1** using 0.5 mol% catalyst mixture **3.10** and 0.5 mol% TlPF$_6$ at room temperature in acetone-d_6.
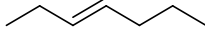
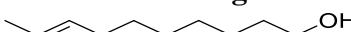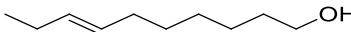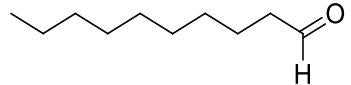| Measured integrals in arbitrary units relative to internal standard = 10.0 units and (in bold) derived per cent yields of products and amount of starting 1-alkene.				
Time	0 min	15 min	30 min	1 h
(5.79 ppm)	66.0	2.14	1.43	1.36
(4.85-5.01 ppm)	135.4	4.17	2.46	2.60
units per proton[a]	66.9	2.11	1.33	1.33
% starting material remaining	**100**	**3.2**	**2.0**	**2.0**
(5.35-5.46 ppm)[b]	-	131.8	131.8	131.8
(1.60 ppm)	-	197.7	194.5	189.2
units per proton[c]	-	64.7	64.2	62.1
% of E-2	**0**	**97.6**	**95.9**	**92.7**
(0.94 ppm)	-	3.61	7.27	14.4
units per proton	-	0.60	1.21	2.40
% of E-3	**0**	**0.9**	**1.8**	**3.6**

[a]Units calculated by taking the average of the integrations of the two resonances. [b]Signal is a mixture of E-2 and E-3 hexene isomers. [c] Vinylic C-H proton units for E-2 hexene determined by subtracting proton units of E-3 hexene from total proton units of E-2/E-3 signal

Procedure for isomerization of untreated 1-heptene to E-2 and E-3 heptenes using 0.5 mol% precatalyst 3.10 and 0.5 mol% TlPF$_6$ at room temperature in acetone-d_6.

To a resealable J. Young tube in a glovebox, internal standard (Me$_3$Si)$_4$C (~0.2 mg), TlPF$_6$ (1 mg, 0.0029 mmol) and 1-heptene (49.1 mg, 0.500 mmol) were combined with a mixture of deoxygenated acetone-d_6 (700 µL), and an initial NMR spectrum was acquired. Back in the glovebox, to this mixture was added an aliquot of precatalyst solution B (100 µL, 0.00250 mmol) and enough acetone-d6 to reach a total volume of 1.0 mL. The reaction was kept at room temperature and monitored at the times given below.

Table 4.41. Yields determined by NMR in isomerization of **4.4** using 0.1 mol% catalyst mixture **3.10** and 0.1 mol% TlPF$_6$ at room temperature in acetone-d_6.
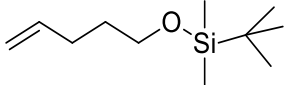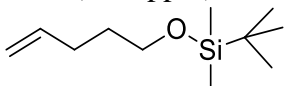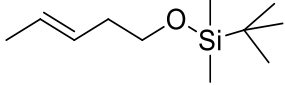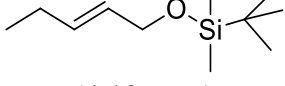
Measured integrals in arbitrary units relative to internal standard = 10.0 units and (in bold) derived per cent yields of products and amount of starting 1-alkene.					
Time	0 min	15 min	30 min	1 h	2 h
(5.80 ppm)	40.0	1.21	0.83	0.75	0.81
(4.90-4.97 ppm)	80.9	2.31	1.55	1.55	1.55
units per proton[a]	40.2	1.18	0.80	0.76	0.79
% starting material remaining	**100**	**2.9**	**2.0**	**1.9**	**2.0**
(5.34-5.46 ppm)[b]	-	78.0	79.1	79.7	80.6
(1.60 ppm)	-	NA	117.3	115.5	112.1
units per proton[c]	-	38.4	38.8	38.0	37.2
% of E-2	**0**	**95.5**	**96.5**	**94.6**	**92.6**
(0.94 ppm)	-	1.80	3.18	6.82	9.70
units per proton	-	0.60	1.06	2.27	3.23
% of E-3	**0**	**1.5**	**2.6**	**5.6**	**8.0**

[a]Units calculated by taking the average of the integrations of the two resonances. [b]Signal is a mixture of E-2 and E-3 heptene isomers. [c]Vinylic C-H proton units for E-2 heptene determined by subtracting proton units of E-3 heptene from total proton units of E-2/E-3 signal.

Procedure for isomerization of untreated 1-octene to E-2, E-3, and E-4 octenes using 0.5 mol% precatalyst 3.10 and 0.5 mol% TlPF$_6$ at room temperature in acetone-d_6.

To a resealable J. Young tube in a glovebox, internal standard (Me$_3$Si)$_4$C (~0.2 mg), TlPF$_6$ (0.9 mg, 0.0026 mmol) and 1-octene (56.1 mg, 0.500 mmol) were combined with a mixture of deoxygenated acetone-d_6 (700 µL), and an initial NMR spectrum was acquired. Back in the glovebox, to this mixture was added an aliquot of precatalyst solution B (100 µL, 0.00250 mmol) and enough acetone-d_6 to reach a total volume of 1.0 mL. The reaction was kept at room temperature and monitored at the times given below.

Table 4.42. Yields determined by NMR in isomerization of **4.5** using 0.5 mol% catalyst mixture **3.10** and 0.5 mol% TlPF$_6$ at room temperature in acetone-d_6.

Measured integrals in arbitrary units relative to internal standard = 10.0 units and (in bold) derived per cent yields of products and amount of starting 1-alkene.						
Time	0 min	15 min	30 min	1 h	2 h	5 h
(structure) (5.80 ppm)	74.0	5.68	2.36	1.37	1.51	1.67
(structure) (4.89-4.97 ppm)	150.0	11.9	4.72	2.95	2.77	2.93
units per proton^a	74.5	5.82	2.36	1.42	1.45	1.57
% starting material remaining	**100**	**7.8**	**3.2**	**1.9**	**1.9**	**2.1**
(structure) (1.60 ppm)	-	211.4	223.2	217.7	215.6	208.4
units per proton	-	70.5	73.7	72.6	71.9	69.5
% of E-2	**0**	**94.6**	**99.8**	**97.4**	**96.5**	**93.3**
(structure) (0.94 ppm)	-	-	4.01	5.41	9.79	15.4
units per proton	-	-	1.34	1.80	3.26	5.1
% of E-3	**0**	**0**	**1.8**	**2.4**	**4.4**	**6.9**
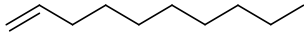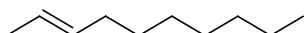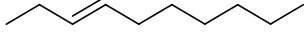
^{a}Units calculated by taking the average of the integrations of the two resonances

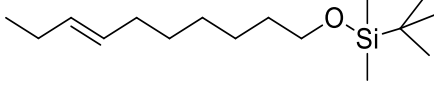**Procedure for isomerization of untreated 1-decene to E-2 and E-3 decenes using 0.5 mol% precatalyst 3.10 and 0.5 mol% TlPF$_6$ at room temperature in acetone-d_6.**

To a resealable J. Young tube in a glovebox, internal standard (Me$_3$Si)$_4$C (~0.2 mg), TlPF$_6$ (1.0 mg, 0.0029 mmol) and 1-decene (70.2 mg, 0.501 mmol) were combined with a mixture of deoxygenated acetone-d_6 (700 µL), and an initial NMR spectrum was acquired. Back in the glovebox, to this mixture was added an aliquot of precatalyst solution B (100 µL, 0.00250 mmol) and enough acetone-d_6 to reach a total volume of 1.0 mL. The reaction was kept at room temperature and monitored at the times given below.

Table 4.43. Yields determined by NMR in isomerization of **4.6** using 0.5 mol% catalyst mixture **3.10** and 0.5 mol% TlPF$_6$ at room temperature in acetone-d_6.
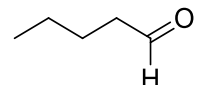
Measured integrals in arbitrary units relative to internal standard = 10.0 units and (in bold) derived per cent yields of products and amount of starting 1-alkene.					
Time	**0 min**	**15 min**	**30 min**	**1 h**	**2 h**
(5.80 ppm)	44.3	5.36	1.58	0.94	0.92
(4.91 ppm)	89.2	10.4	3.02	1.72	1.69
units per proton	44.5	5.29	1.55	0.90	0.88
% starting material remaining	**100**	**11.8**	**3.5**	**2.0**	**2.0**
(1.60 ppm)	-	118.5	128.3	130.0	129.5
units per proton	-	39.5	42.8	43.3	43.2
% of E-2	**0**	**88.8**	**96.1**	**97.4**	**97.0**
(0.95 ppm)	-	0.54	2.26	2.80	4.38
units per proton	-	0.18	0.75	0.93	1.46
% of E-3	**0**	**0.4**	**1.7**	**2.1**	**3.3**

[a]Units calculated by taking the average of the integrations of the two resonances

Procedure for isomerization of untreated 4-penten-1-ol to E-3 and E-2 penten-1-ols using 0.5 mol% precatalyst 3.10 and 0.5 mol% TlPF$_6$ at room temperature in acetone-d_6.

To a resealable J. Young tube in a glovebox, internal standard (Me$_3$Si)$_4$C (~0.2 mg), TlPF$_6$ (1.0 mg, 0.0029 mmol) and 4-penten-1-ol (43.5 mg, 0.505 mmol) were combined with a mixture of deoxygenated acetone-d_6 (700 µL), and an initial NMR spectrum was acquired. Back in the glovebox, to this mixture was added an aliquot of precatalyst solution B (100 µL, 0.00250 mmol) and enough acetone-d_6 to reach a total volume of 1.0 mL. The reaction was kept at room temp and monitored at the times given below.

Table 4.44. Yields determined by NMR in isomerization of **4.7** using 0.5 mol% catalyst mixture **3.10** and 0.5 mol% TlPF$_6$ at room temperature in acetone-d_6.
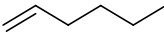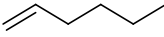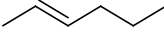
Time	0 min	15 min	30 min	45 min	1 h	2 h	7 h	24 h
(structure) OH (5.84 ppm)	60.5	26.7	7.91	1.62	1.51	2.18	1.47	1.22
(structure) OH (4.85-5.08 ppm)	124.1	54.6	16.3	3.37	2.99	3.26	2.64	2.63
units per proton[a]	61.3	27.0	8.03	1.65	1.50	1.90	1.40	1.27
% starting material remaining	**100**	**44.0**	**13.1**	**2.7**	**2.5**	**3.1**	**2.3**	**2.1**
(structure) OH (5.35-5.46 ppm)[b]	-	70.9	107.3	119.4	118.2	117.1	111.9	111.3
units per proton[c]	-	35.5	53.5	59.7	59.1	58.6	56.0	55.7
% yield product	**0**	**57.8**	**87.3**	**97.4**	**96.4**	**95.6**	**91.3**	**90.8**
(structure) OH (0.96 ppm)	-	-	0.43	1.35	1.81	2.68	3.21	2.63
units per proton	-	-	0.14	0.45	0.60	0.89	1.07	0.88
% of isomer	**0**	**0**	**0.2**	**0.7**	**0.9**	**1.5**	**1.7**	**1.4**
(structure) O, H (9.72 ppm)	-	-	-	0.09	0.29	1.19	3.05	3.78
units per proton	-	-	-	0.09	0.29	1.19	3.05	3.78
% of aldehyde	**0**	**0**	**0**	**0.1**	**0.5**	**1.9**	**5.0**	**6.2**

Measured integrals in arbitrary units relative to internal standard = 10.0 units and (in bold) derived per cent yields of products and amount of starting 1-alkene.

[a]Units calculated by taking the average of the integrations of the two resonances. [b]Signal is a mixture of E-3- and E-2-penten-1-ol isomers. [c]Vinylic C-H proton units for E-3-penten-1-ol determined by subtracting proton units of E-2-penten-1-ol from total proton units of E-3/E-2 signal.

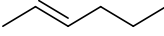**Procedure for isomerization of untreated 9-decen-1-ol to E-8 and E-7 decen-1-ols using 0.5 mol% precatalyst 3.10 and 0.5 mol% TlPF$_6$ at room temperature in acetone-d_6.**

To a resealable J. Young tube in a glovebox, internal standard (Me$_3$Si)$_4$C (~0.2 mg), TlPF$_6$ (1.0 mg, 0.0029 mmol) and 9-decen-1-ol (78.3 mg, 0.501 mmol) were combined with a mixture of deoxygenated acetone-d_6 (700 μL), and an initial NMR spectrum was acquired. Back

in the glovebox, to this mixture was added an aliquot of precatalyst solution B (100 µL, 0.00250 mmol) and enough acetone-d_6 to reach a total volume of 1.0 mL. The reaction was kept at room temperature and monitored at the times given below.

Table 4.45. Yields determined by NMR in isomerization of **4.9** using 0.5 mol% catalyst mixture **3.10** and 0.5 mol% TlPF$_6$ at room temperature in acetone-d6.
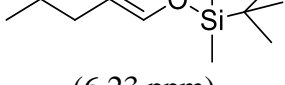
Measured integrals in arbitrary units relative to internal standard = 10.0 units and (in bold) derived per cent yields of products and amount of starting 1-alkene.							
Time	0 min	15 min	30 min	1 h	2 h	5 h	7 h
(structure, OH) (5.76-5.84 ppm)	42.4	21.0	14.7	9.04	4.26	1.48	1.12
(structure, OH) (4.85-5.02 ppm)	85.7	42.5	29.7	18.2	8.68	2.91	2.13
units per proton[a]	42.6	21.1	14.8	9.07	4.30	1.47	1.09
% starting material remaining	**100**	**49.6**	**34.7**	**21.3**	**10.1**	**3.4**	**2.6**
(structure, OH) (1.60 ppm)	-	44.4	59.4	67.9	79.3	83.6	84.2
units per proton	-	22.2	29.6	33.8	39.4	41.8	42.1
% yield product	**0**	**52.1**	**69.4**	**79.4**	**92.4**	**98.1**	**98.8**
(structure, OH) (0.94 ppm)	-	-	0.33	0.35	0.87	1.41	1.55
units per proton	-	-	0.11	.12	0.29	0.47	0.52
% of isomer	**0**	**0**	**0.3**	**0.3**	**0.6**	**1.1**	**1.2**
(structure, aldehyde) (9.72 ppm)	-	-	-	-	-	-	-
units per proton	-	-	-	-	-	-	-
% of aldehyde	**0**	**0**	**0**	**0**	**0**	**0**	**0**

[a]Units calculated by taking the average of the integrations of the two resonances.

Procedure for isomerization of 4-penten-1-ol t-butyldimethyl silyl ether to E-3 and E-2 silyl ethers using 0.5 mol% precatalyst 3.10 and 0.5 mol% TlPF$_6$ at room temp in acetone-d_6.

To a resealable J. Young tube in a glovebox, internal standard $(Me_3Si)_4C$ (~0.2 mg), TlPF$_6$ (0.9 mg, 0.0026 mmol) and 4-penten-1-ol tertbutyldimethylsilylether (100.2 mg, 0.500 mmol) were combined with a mixture of deoxygenated acetone-d_6 (700 µL), and an initial NMR spectrum was acquired. Back in the glovebox, to this mixture was added an aliquot of precatalyst solution B (100 µL, 0.00250 mmol) and enough acetone-d_6 to reach a total volume of 1.0 mL. The reaction was kept at room temperature and monitored at the times given below.

Table 4.46. Yields determined by NMR in isomerization of **4.10** using 0.5 mol% **3.10** and 0.5 mol% TlPF$_6$ at room temp in acetone-d_6.

Measured integrals in arbitrary units relative to internal standard = 10.0 units and (in bold) derived per cent yields of products and amount of starting 1-alkene.				
Time	0 min	15 min	30 min	1 h
(5.82 ppm)	82.5	2.35	2.23	2.61
(4.82-5.10 ppm)	166.7	5.39	4.52	2.99
units per proton[a]	82.9	2.52	2.25	1.50
% starting material remaining	**100**	**3.0**	**2.7**	**2.5**
(5.38-5.52 ppm)	-	155.1	163.6	158.8
units per proton	-	77.6	81.8	79.4
% yield product	**0**	**93.6**	**98.7**	**95.8**
(4.12 ppm)	-	2.38	3.28	5.31
units per proton	-	1.19	1.64	2.66
% of isomer	**0**	**1.4**	**2.0**	**3.2**
(6.23 ppm)	-	-	-	-
units per proton	-	-	-	-
% of enol ether	**0**	**0**	**0**	**-**

[a]Units calculated by taking the average of the integrations of the two resonances.
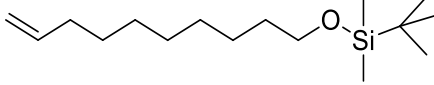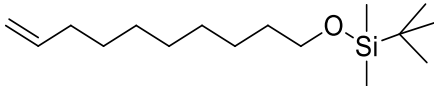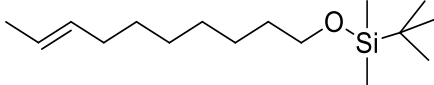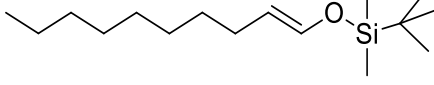
Procedure for isomerization of 9-decen-1-ol t-butyldimethyl silyl ether to E-8 and E-7 silyl ethers using 0.5 mol% precatalyst 3.10 and 0.5 mol% TlPF$_6$ at room temp in acetone-d_6.

To a resealable J. Young tube in a glovebox, internal standard (Me$_3$Si)$_4$C (~0.2 mg), TlPF$_6$ (0.3 mg, 0.000859 mmol) and 1-9-decen-1-ol tert-butyldimethylsilylether (135.3 mg, 0.500 mmol) were combined with a mixture of deoxygenated acetone-d_6 (700 µL), and an initial NMR spectrum was acquired. Back in the glovebox, to this mixture was added an aliquot of precatalyst solution B (100 µL, 0.00250 mmol) and enough acetone-d_6 to reach a total volume of 1.0 mL. The reaction was kept at room temperature and monitored at the times given below.

Table 4.47. Yields determined by NMR in isomerization of **4.11** using 0.5 mol% **3.10** and 0.5 mol% TlPF$_6$ at room temp in acetone-d_6.
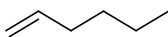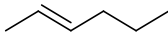
Measured integrals in arbitrary units relative to internal standard = 10.0 units and (in bold) derived per cent yields of products and amount of starting 1-alkene.				
Time	0 min	15 min	30 min	1 h
(structure) (5.75-5.83 ppm)	60.7	1.84	2.38	1.60
(structure) (4.88-4.99 ppm)	122.3	2.80	2.71	2.46
units per proton[a]	60.9	1.62	1.86	1.42
% starting material remaining	**100**	**2.7**	**3.0**	**2.3**
(structure) (1.61 ppm)	-	169.8	164.3	157.1
units per proton	-	56.6	54.8	52.4
% yield product	**0**	**92.9**	**90.0**	**86.0**
(structure) (0.94 ppm)	-	9.20	12.6	18.2
units per proton	-	3.07	4.20	6.07
% of isomer	**0**	**5.0**	**6.9**	**10.0**
(structure) (6.23 ppm)	-	-	-	-
units per proton	-	-	-	-
% of enol ether	**0**	**0**	**0**	**0**

[a]Units calculated by taking the average of the integrations of the two resonances.

Rate comparisons with nitrile catalyst

Procedure for isomerization of treated 1-hexene to E-2 and E-3 hexenes using 0.5 mol% precatalyst 3 and 0.5 mol% TlPF₆ at room temperature in acetone-d_6.

To a resealable J. Young tube in a glovebox, internal standard $(Me_3Si)_4C$ (~0.2 mg), TlPF₆ (1 mg, 0.0029 mmol) and alumina-filtered 1-hexene (42.1 mg, 0.500 mmol) were combined with a mixture of deoxygenated acetone-d_6 (700 µL), and an initial NMR spectrum was acquired. Back in the glovebox, to this mixture was added an aliquot of precatalyst solution B (100 µL, 0.00250 mmol) and enough acetone-d_6 to reach a total volume of 1.0 mL. The reaction was kept at room temperature and monitored at the times given below.

Table 4.48. Yields determined by NMR in isomerization of **4.1** using 0.5 mol% catalyst mixture **3.10** and 0.5 mol% TlPF₆ at room temperature in acetone-d_6.
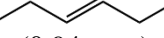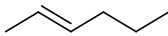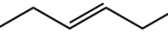
Measured integrals in arbitrary units relative to internal standard = 10.0 units and (in bold) derived per cent yields of products and amount of starting 1-alkene.				
Time	0 min	15 min	30 min	1 h
(5.79 ppm)	66.0	2.14	1.43	1.36
(4.85-5.01 ppm)	135.4	4.17	2.46	2.60
units per proton[a]	66.9	2.11	1.33	1.33
% starting material remaining	**100**	**3.2**	**2.0**	**2.0**
(5.35-5.46 ppm)[b]	-	131.8	131.8	131.8
(1.60 ppm)	-	197.7	194.5	189.2
units per proton[c]	-	64.7	64.1	62.1
% of E-2	**0**	**96.7**	**95.9**	**92.7**
(0.94 ppm)	-	3.61	7.27	14.4
units per proton	-	1.20	2.42	4.82
% of E-3	**0**	**1.8**	**3.6**	**7.2**

[a]Units calculated by taking the average of the integrations of the two resonances. [b]Signal is a mixture of E-2 and E-3 hexene isomers. [c] Vinylic C-H proton units for E-2 hexene determined by subtracting proton units of E-3 hexene from total proton units of E-2/E-3 signal

Procedure for isomerization of treated 1-hexene to E-2 and E-3 hexenes using 0.5 mol% 1.2 + 1.2a at room temperature in acetone-d_6.

To a resealable J. Young tube in a glovebox, internal standard $(Me_3Si)_4C$ (~0.2 mg) and treated 1-hexene (42.1 mg, 0.500 mmol) were combined with a mixture of deoxygenated acetone-d_6 (700 µL), and an initial NMR spectrum was acquired. Back in the glovebox, to this mixture was added an aliquot of precatalyst solution B (100 µL, 0.00250 mmol) and enough acetone-d_6 to reach a total volume of 1.0 mL. The reaction was kept at room temp and monitored at the times given below.

Table 4.49. Yields determined by NMR in isomerization of **4.1** using 0.5 mol% **1.2** + **1.2a** at room temperature in acetone-d_6.
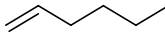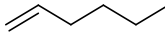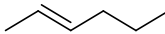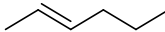
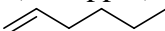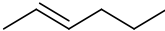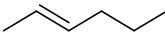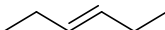| Measured integrals in arbitrary units relative to internal standard = 10.0 units and (in bold) derived per cent yields of products and amount of starting 1-alkene.									
Time	0 min	15 min	1 h	5 h	21 h*	24 h*	48 h	72 h	96 h
(5.79 ppm)	42.2	40.5	38.8	32.7	17.1	16.5	9.64	5.94	4.28
(4.85-5.01 ppm)	86.9	82.9	79.4	67.1	35.6	33.5	19.7	11.9	8.48
units per proton[a]	42.8	41.0	39.2	33.1	17.5	16.6	9.75	5.95	4.26
% starting material remaining	**100**	**95.7**	**91.7**	**77.4**	**40.8**	**38.8**	**22.8**	**13.9**	**10.0**
(5.35-5.46 ppm)[b]	-	2.78	5.89	18.1	39.6	44.1	64.7	71.9	75.8
(1.60 ppm)	-	4.15	8.99	27.6	61.7	66.9	97.5	107.6	112.4
units per proton[c]	-	1.39	2.97	9.05	20.1	22.0	32.2	35.6	37.4
% of E-2	**0**	**3.2**	**6.9**	**21.1**	**46.9**	**51.4**	**75.2**	**83.2**	**87.3**
(0.94 ppm)	-	-	-	-	0.61	0.82	1.40	1.71	1.92
units per proton	-	-	-	-	0.20	0.27	0.47	0.57	0.64
% of E-3	**0**	**0**	**0**	**0**	**0.5**	**0.6**	**1.1**	**1.3**	**1.5**

[a]Units calculated by taking the average of the integrations of the two resonances. [b]Signal is a mixture of E-2 and E-3 hexene isomers. [c] Vinylic C-H proton units for E-2 hexene determined by subtracting proton units of E-3 hexene from total proton units of E-2/E-3 signal.

318

Procedure for isomerization of treated 1-hexene to E-2 and E-3 hexenes using 0.5 mol% 1.2 + 1.2a at room temperature in acetone-d_6.

To a resealable J. Young tube in a glovebox, internal standard (Me$_3$Si)$_4$C (~0.2 mg) and treated 1-hexene (42.1 mg, 0.500 mmol) were combined with a mixture of deoxygenated acetone-d_6 (700 μL), and an initial NMR spectrum was acquired. Back in the glovebox, to this mixture was added an aliquot of precatalyst solution B (100 μL, 0.00250 mmol) and enough acetone-d_6 to reach a total volume of 1.0 mL. The reaction was kept at room temp and monitored at the times given below.

Table 4.50. Yields determined by NMR in isomerization of **4.1** using 0.5 mol% **1.2+1.2a** at room temperature in acetone-d_6.
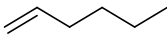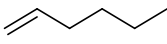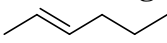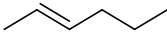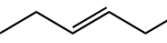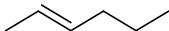
Measured integrals in arbitrary units relative to internal standard = 10.0 units and (in bold) derived per cent yields of products and amount of starting 1-alkene.								
Time	0 min	72 h	96 h	120 h	144 h	191 h	216 h	240 h
(5.79 ppm)	56.6	16.8	11.3	7.82	5.40	3.06	2.36	1.96
(4.85-5.01 ppm)	117.1	33.9	22.8	15.7	10.9	6.12	4.85	3.96
units per proton[a]	57.6	16.9	11.4	7.84	5.43	3.06	2.39	1.97
% starting material remaining	**100**	**29.4**	**19.7**	**13.6**	**9.4**	**5.3**	**4.2**	**3.4**
(5.35-5.46 ppm)[b]	-	81.8	93.2	101.1	104.5	111.7	111.0	112.9
(1.60 ppm)	-	121.5	138.6	150.7	155.8	165.5	164.4	167.2
units per proton[c]	-	40.5	45.7	49.6	51.5	54.8	54.4	55.3
% of E-2	**0**	**70.3**	**79.3**	**86.2**	**89.5**	**95.1**	**94.5**	**96.0**
(0.94 ppm)	-	2.42	2.67	2.77	3.35	4.07	4.44	4.92
units per proton	-	0.81	0.89	0.92	1.12	1.36	1.48	1.64
% of E-3	**0**	**1.4**	**1.5**	**1.6**	**1.9**	**2.4**	**2.6**	**2.8**

[a]Units calculated by taking the average of the integrations of the two resonances. [b]Signal is a mixture of E-2 and E-3 hexene isomers. [c] Vinylic C-H proton units for E-2 hexene determined by subtracting proton units of E-3 hexene from total proton units of E-2/E-3 signal.

Procedure for isomerization of treated 1-hexene to E-2 and E-3 hexenes using 0.1 mol% precatalyst 3.10 and 0.15 mol% TlPF$_6$ at 40$^\text{o}$C in acetone-d_6.

To a resealable J. Young tube in a glovebox, internal standard (Me$_3$Si)$_4$C (~0.2 mg), TlPF$_6$ (1 mg, 0.0029 mmol) and treated 1-hexene (42.1 mg, 0.500 mmol) were combined with a mixture of deoxygenated acetone-d_6 (700 µL), and an initial NMR spectrum was acquired. Back in the glovebox, to this mixture was added an aliquot of catalyst solution B (100 µL, 0.00250 mmol) and enough acetone-d_6 to reach a total volume of 1.0 mL. The reaction was kept at 40 $^\text{o}$C in the NMR probe for the first 2 h. After 2 h, the tube was kept in a 40 $^\text{o}$C bath except for NMR acquisitions.

Table 4.51. Yields determined by NMR in isomerization of **4.1** using 0.1 mol% catalyst mixture **3.10** and 0.15 mol% TlPF$_6$ at 40°C in acetone-d_6.
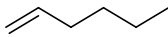
	Measured integrals in arbitrary units relative to internal standard = 10.0 units and (in bold) derived per cent yields of products and amount of starting 1-alkene.								
Time	0 min	15 min	30 min	45 min	1 h	1.5 h	2 h	4 h	6 h
(5.79 ppm)	61.2	30.7	14.2	7.26	4.20	2.09	1.66	1.35	1.41
(4.85-5.01 ppm)	125.4	62.2	28.6	14.7	8.54	4.12	3.32	2.77	2.85
units per proton[a]	62.0	30.9	14.3	7.31	4.23	2.08	1.66	1.36	1.42
% starting material remaining	**100**	**49.8**	**23.0**	**11.8**	**6.8**	**3.3**	**2.7**	**2.2**	**2.3**
(5.35-5.46 ppm)[b]	-	65.3	95.6	109.8	115.4	121.9	122.3	120.6	122.1
(1.60 ppm)	-	98.3	143.5	164.1	171.5	181.2	180.7	177.7	178.4
units per proton[c]	-	32.7	47.5	54.	57.0	59.9	59.3	58.3	58.3
% of E-2	**0**	**52.7**	**76.6**	**87.8**	**91.8**	**96.6**	**95.7**	**94.0**	**94.0**
(0.94 ppm)	-	-	1.77	2.34	2.92	4.78	5.50	8.78	11.6
units per proton	-	-	0.59	0.78	0.97	1.59	1.83	2.93	3.87
% of E-3	**0**	**0**	**0.9**	**1.3**	**1.6**	**2.6**	**3.0**	**4.7**	**6.2**

[a]Units calculated by taking the average of the integrations of the two resonances. [b]Signal is a mixture of E-2 and E-3 hexene isomers. [c] Vinylic C-H proton units for E-2 hexene determined by subtracting proton units of E-3 hexene from total proton units of E-2/E-3 signal

Procedure for isomerization of treated 1-hexene to E-2 and E-3 hexenes using 0.1 mol% 1.2 + 1.2a at room temperature in acetone-d_6.

To a resealable J. Young tube in a glovebox, internal standard (Me$_3$Si)$_4$C (~0.2 mg) and alumina-filtered 1-hexene (42.1 mg, 0.500 mmol) were combined with a mixture of deoxygenated acetone-d_6 (700 µL), and an initial NMR spectrum was acquired. Back in the glovebox, to this mixture was added an aliquot of precatalyst solution B (20 µL, 0.00250 mmol) and enough acetone-d_6 to reach a total volume of 1.0 mL. The reaction was kept at room temperature and monitored at the times given below.

Table 4.52. Yields determined by NMR in isomerization of **4.1** using 0.1 mol% **1.2** + **1.2a** at 40°C in acetone-d_6.

Measured integrals in arbitrary units relative to internal standard = 10.0 units and (in bold) derived per cent yields of products and amount of starting 1-alkene.					
Time	0 min	5 h	24 h	48 h	72 h
(5.79 ppm)	91.4	83.3	83.0	81.2	80.0
(4.85-5.01 ppm)	187.8	170.2	169.9	165.7	166.8
units per proton[a]	92.7	84.2	85.0	82.0	81.7
% starting material remaining	**100**	**90.8**	**91.6**	**88.5**	**88.1**
(5.35-5.46 ppm)[b]	-	12.6	14.6	16.6	19.0
(1.60 ppm)	-	18.6	21.0	23.8	26.7
units per proton[c]	-	6.25	7.12	8.10	9.20
% of E-2	**0**	**6.8**	**7.7**	**8.8**	**9.9**
(0.94 ppm)	-	-	-	-	-
units per proton	-	-	-	-	-
% of E-3	**0**	**0**	**0**	**0**	**0**

[a]Units calculated by taking the average of the integrations of the two resonances. [b]Signal is a mixture of E-2 and E-3 hexene isomers. [c] Vinylic C-H proton units for E-2 hexene determined by subtracting proton units of E-3 hexene from total proton units of E-2/E-3 signal.

Procedure for isomerization of treated 1-hexene to E-2 and E-3 hexenes using 0.25 mol% precatalyst 3.10 and 0.25 mol% TlPF$_6$ at room temperature (24 ^{o}C) in acetone-d_6.

To a resealable J. Young tube in a glovebox, internal standard (Me$_3$Si)$_4$C (~0.2 mg), TlPF$_6$ (0.5 mg, 0.0014 mmol) and treated 1-hexene (42.1 mg, 0.500 mmol) were combined with a mixture of deoxygenated acetone-d_6 (700 µL), and an initial NMR spectrum was acquired. Back in the glovebox, to this mixture was added an aliquot of catalyst solution B (50 µL, 0.00125 mmol) and enough acetone-d_6 to reach a total volume of 1.0 mL. The reaction was kept at room temp for about 2 min and then inserted in the NMR probe set at 24 ^{o}C and monitored at times given below.

Table 4.53. Yields determined by NMR in isomerization of **4.1** using 0.25 mol% catalyst mixture **3.10** and 0.25 mol% TlPF$_6$ at 24 ^{o}C in acetone-d_6.

Time	0 min	3 min	6 min	8 min	11 min	14 min	16 min	19 min	21 min	24 min	27 min	29 min	32 min
(5.79 ppm)	73.2	43.5	34.8	25.4	18.8	13.2	9.11	6.16	4.71	3.51	2.73	2.38	1.92
(4.85-5.01 ppm)	149.3	97.7	71.3	52.1	38.1	26.6	18.5	12.7	9.69	7.09	5.41	4.45	3.97
units per proton[a]	73.9	46.0	35.2	25.7	18.9	13.3	9.18	6.26	4.78	3.53	2.72	2.30	1.95
% starting material remaining	**100**	**62.2**	**47.6**	**34.8**	**25.6**	**17.9**	**12.4**	**8.5**	**6.5**	**4.8**	**3.7**	**3.1**	**2.6**
(5.35-5.46 ppm)[b]	-	44.6	75.4	94.7	109.2	119.8	127.6	131.5	137.4	138.4	139.5	140.8	142.6
(1.60 ppm)	-	72.0	113.9	143.3	163.7	180.6	191.8	199.8	207.5	208.5	210.5	212.3	215.0
units per proton[c]	-	23.2	37.8	47.6	54.6	59.7	63.4	64.3	68.4	68.6	69.3	69.9	70.7
% of *E*-2	**0**	**31.3**	**51.2**	**64.4**	**73.9**	**80.7**	**85.8**	**87.1**	**92.5**	**92.8**	**93.8**	**94.5**	**95.6**
(0.94 ppm)	-	-	-	-	-	2.31	2.65	2.96	3.40	3.72	4.01	4.42	4.95
units per proton	-	-	-	-	-	0.77	0.88	0.99	1.13	1.24	1.34	1.47	1.65
% of *E*-3	**0**	**0**	**0**	**0**	**0**	**1.0**	**1.2**	**1.3**	**1.5**	**1.7**	**1.8**	**2.0**	**2.2**

[a]Units calculated by taking the average of the integrations of the two resonances. [b]Signal is a mixture of E-2 and E-3 hexene isomers. [c] Vinylic C-H proton units for E-2 hexene determined by subtracting proton units of E-3 hexene from total proton units of E-2/E-3 signal.

Procedure for isomerization of treated 1-hexene to E-2 and E-3 hexenes using 0.25 mol% 1.2 + 1.2a at room temperature in acetone-*d*₆.
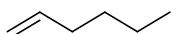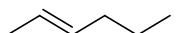
To a resealable J. Young tube in a glovebox, internal standard (Me₃Si)₄C (~0.2 mg) and treated 1-hexene (42.1 mg, 0.500 mmol) were combined with a mixture of deoxygenated acetone-*d*₆ (700 µL), and an initial NMR spectrum was acquired. Back in the glovebox, to this mixture was added an aliquot of precatalyst solution B (50 µL, 0.00125 mmol) and enough acetone-*d*₆ to reach a total volume of 1.0 mL. The reaction was kept at room temp and monitored at the times given below.

Table 4.54. Yields determined by NMR in isomerization of **4.1** using 0.25 mol% **1.2 + 1.2a** at room temperature in acetone-*d*₆.

Measured integrals in arbitrary units relative to internal standard = 10.0 units and (in bold) derived per cent yields of products and amount of starting 1-alkene.					
Time	0 min	30 min	24 h	48 h	72 h
(5.79 ppm)	43.3	42.0	27.2	19.7	15.5
(4.85-5.01 ppm)	89.1	86.4	55.3	39.8	31.2
units per proton[a]	43.9	42.6	27.4	19.8	15.6
% starting material remaining	**100**	**97.0**	**62.5**	**45.1**	**35.5**
(5.35-5.46 ppm)[b]	-	1.81	33.1	47.1	56.5
(1.60 ppm)	-	2.74	49.4	69.9	83.6
units per proton[c]	-	0.91	16.5	23.4	27.8
% of E-2	**0**	**2.1**	**37.6**	**53.3**	**63.3**
(0.94 ppm)	-	-	-	-	1.46
units per proton	-	-	-	-	0.49
% of E-3	**0**	**0**	**0**	**0**	**1.1**

[a]Units calculated by taking the average of the integrations of the two resonances. [b]Signal is a mixture of E-2 and E-3 hexene isomers. [c] Vinylic C-H proton units for E-2 hexene determined by subtracting proton units of E-3 hexene from total proton units of E-2/E-3 signal.
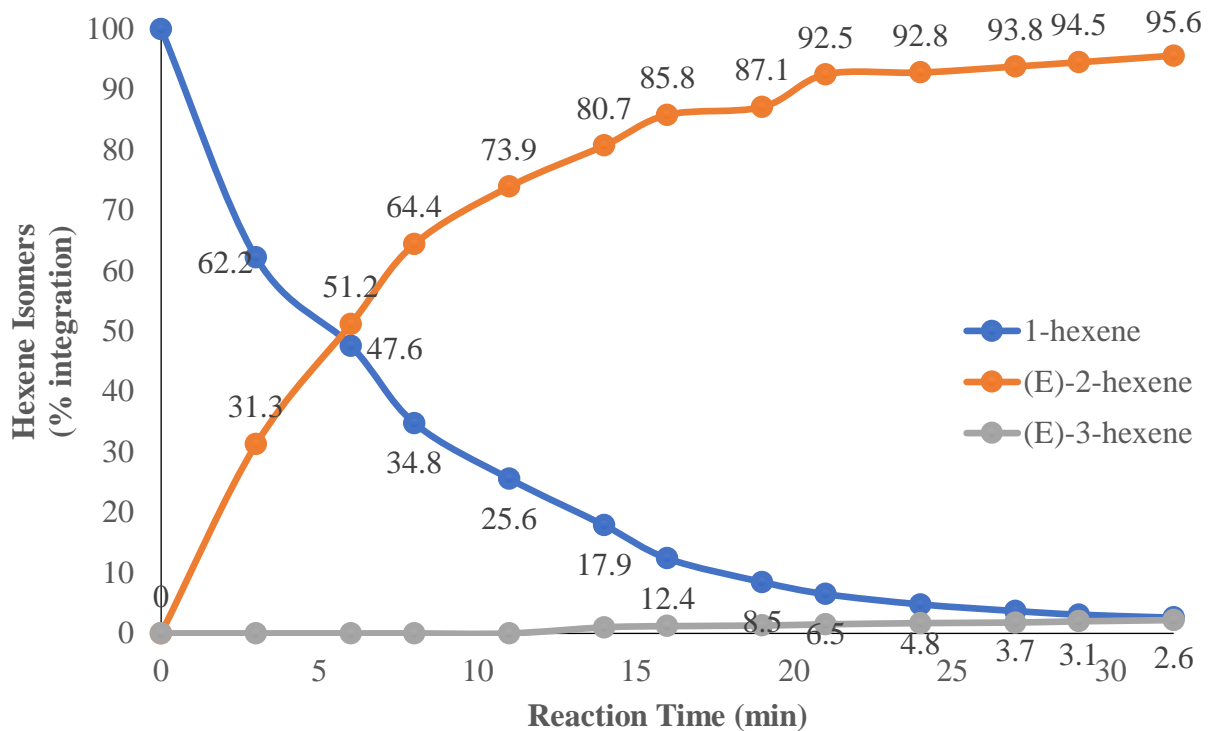
Figure 4.50. Isomerization of **4.1** with 0.25 mol% **3.14** at room temperature
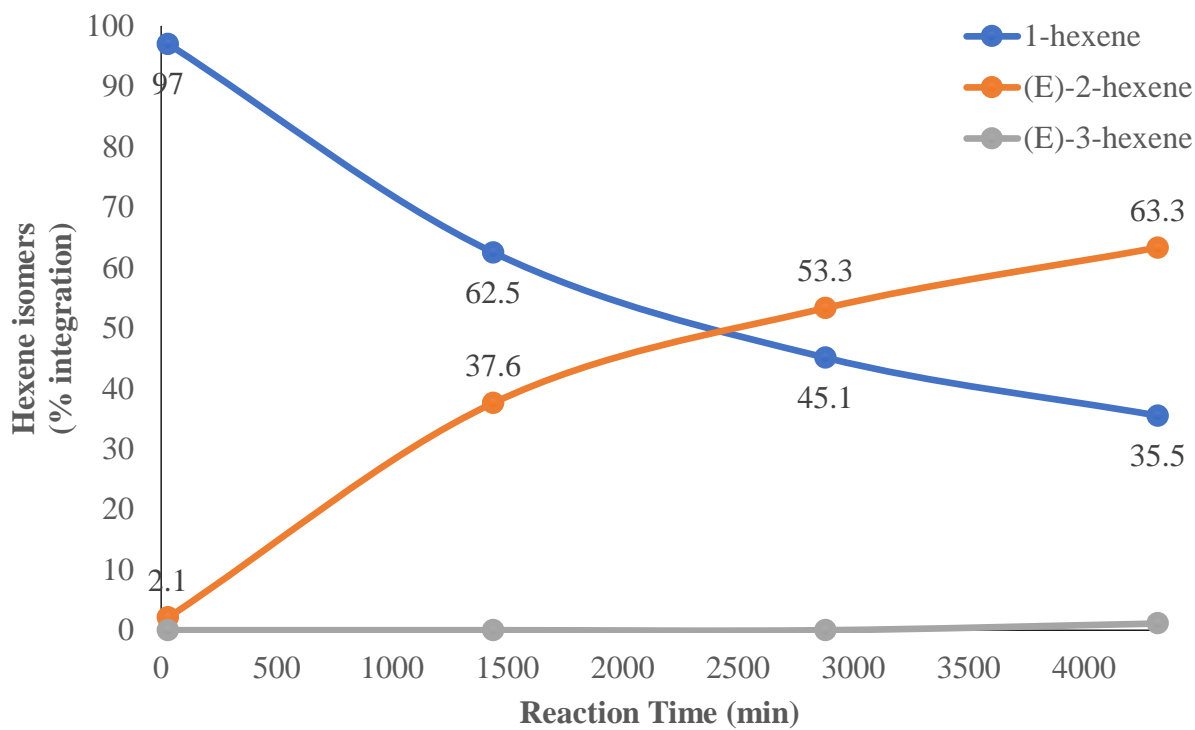
Figure 4.51. Isomerization of **4.1** with 0.25 mol% **1.2** + **1.2a** at room temperature

Procedure and details for catalyst comparison studies.

NMR tube reactions were performed in resealable J. Young NMR tubes. All NMR data were measured at room temperature (22 - 25 ˚C). Varian spectrometers were used: a 500 MHz INOVA (500 MHz listed below for 1 H = 499.940 MHz), and a 400 MHz Varian NMR-S (400 MHz listed below for 1 H = 399.763 MHz). For all reactions, a 2.048 s acquisition time, 10 second relaxation delay, and 15˚ pulse width were used. ^{1}H chemical shifts are referenced to the tetrakis- (trimethylsilyl)methane internal standard (0.264 ppm). All isomerization reactions were carried out with 0.500 M substrate concentration. Catalyst loadings relative to substrate were chosen to keep the conversion of terminal alkene over time to be relatively consistent between catalysts. For a typical isomerization reaction, 10 – 11 spectra were acquired at time points spread out over the initial 60 min, followed a gradual increase in time between spectra to reflect the lower reaction rates after consumption of terminal alkene substrate. The spectra were then processed using the MestreNova processing software. The spectra were manually integrated after an automatic global and metabonomics phase correction and a Whittaker-Smoother baseline correction. Integrations were referenced to the internal standard (tetrakis(trimethylsilyl)methane), which was set to 10.0 integral units. One or two signals were chosen to represent each isomer, and their integrations were compared to the initial integration values for terminal alkene (set to 100%) in order to calculate the percentages of each isomer in the mixture at each time point. The integrated and scaled values for each isomer are given in the tables below.

Preparation of stock catalyst solution 1A

In a 1-dram glass vial fitted with a Teflon-lined cap, **1** (3.0 mg, 0.0050 mmol) was weighed out and enough acetone-d_6 was added to bring the solution to a total volume of 1.0 mL, forming a 0.0050 M solution of catalyst **1.1**.

Preparation of stock catalyst solution 1B

In a 1-dram glass vial fitted with a Teflon-lined cap, **1** (6.1 mg, 0.010 mmol) was weighed out and enough acetone-d_6 was added to bring the solution to a total volume of 1.0 mL, forming a 0.010 M solution of catalyst **1.1**.

Preparation of stock catalyst solution 3A
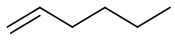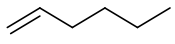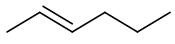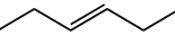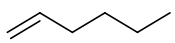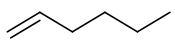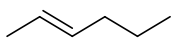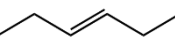
In a 1-dram glass vial fitted with a Teflon-lined cap, **3** (9.5 mg, 0.015 mmol) was weighed out and enough acetone-d_6 was added to bring the solution to a total volume of 1.0 mL, forming a 0.015 M solution of catalyst **3.14**.

NMR Isomerization Data

Data for Figure 4.6. Procedure for isomerization of 1-hexene to E-2 and E-3 hexenes using 0.1 mol% 1.1 at room temperature in acetone-d_6.

To a resealable J. Young tube in a glovebox, internal standard $(Me_3Si)_4C$ (~0.2 mg) and 1-hexene (42.3 mg, 0.503 mmol) were combined in a mixture with deoxygenated with enough acetone-d_6 for a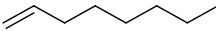 total volume of 900 µL, and an initial NMR spectrum was acquired. Back in the glovebox, to this mixture was added an aliquot of catalyst solution 1A (100 µL, 0.000500 mmol). The reaction was kept at room temperature and monitored at the times given below.

Table 4.55. Yields determined by NMR in isomerization of **4.1** using 0.1 mol% **1.1** at room temperature in acetone-d_6.
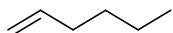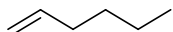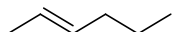
Measured integrals in arbitrary units relative to internal standard = 10.0 units and (in bold) derived per cent yields of products and amount of starting 1-alkene.							
Time (min)	0	2	5	9	12	15	20
(5.79 ppm)	72.8	40.2	24.4	8.6	2.4	1.1	1.2
(4.85-5.01 ppm)	147.4	88.0	49.4	17.4	4.7	2.9	2.6
units per proton[a]	73.2	42.1	24.6	8.6	2.4	1.3	1.2
% SM remaining	**100**	**57.5**	**33.5**	**11.8**	**3.3**	**1.7**	**1.7**
(1.60 ppm)	0.4	84.4	143.4	188.6	197.9	199.3	195.1
units per proton	0.1	28.1	47.8	62.9	66.0	66.4	65.0
% of E-2	**0.2**	**38.4**	**65.3**	**85.9**	**90.1**	**90.7**	**88.8**
(0.94 ppm)	2.6	2.4	5.8	10.4	24.5	32.8	45.5
units per proton	0.4	0.4	1.0	1.7	4.1	5.5	7.6
% of E-3	**0.6**	**0.5**	**1.3**	**2.4**	**5.6**	**7.5**	**10.4**
Time (min) cont.	25	30	45	60	90	120	
(5.79 ppm)	1.2	1.2	1.1	1.2	1.0	1.0	
(4.85-5.01 ppm)	2.4	2.4	2.3	2.3	2.3	2.3	
units per proton[a]	1.2	1.2	1.1	1.1	1.1	1.1	
% SM remaining	**1.6**	**1.6**	**1.5**	**1.6**	**1.5**	**1.5**	
(1.60 ppm)	188.3	180.9	172.5	168.2	163.5	162.4	
units per proton	62.8	60.3	57.5	56.1	54.5	54.1	
% of E-2	**85.8**	**82.3**	**78.5**	**76.6**	**74.4**	**73.9**	
(0.94 ppm)	59.0	66.2	86.2	98	104.4	107.1	
units per proton	9.8	11.0	14.4	16.3	17.4	17.8	
% of E-3	**13.4**	**15.1**	**19.6**	**22.3**	**23.8**	**24.4**	

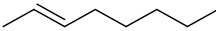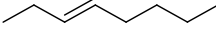[a]Units calculated by taking the average of the integrations of the two resonances.

329

Data for Figure 4.7. Procedure for isomerization of 1-hexene to E-2 and E-3 hexenes using 0.3 mol% 3.14 at room temperature in acetone-d_6.
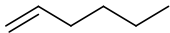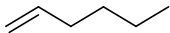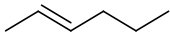
To a resealable J. Young tube in a glovebox, internal standard $(Me_3Si)_4C$ (~0.2 mg) and 1-hexene (42.1 mg, 0.503 mmol) were combined in a mixture with deoxygenated with enough acetone-d_6 for a total volume of 900 µL, and an initial NMR spectrum was acquired. Back in the glovebox, to this mixture was added an aliquot of catalyst solution 3A (100 µL, 0.000500 mmol). The reaction was kept at room temperature and monitored at the times given below.

Table 4.56. Yields determined by NMR in isomerization of **4.1** using 0.1 mol% **3.14** at room temperature in acetone-d_6.

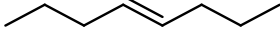| Measured integrals in arbitrary units relative to internal standard = 10.0 units and (in bold) derived per cent yields of products and amount of starting 1-alkene.							
Time (min)	0	3	6	9	12	15	20
(5.79 ppm)	236.2	127.9	90.3	61.9	42.2	25.7	15.6
(4.85-5.01 ppm)	481.5	272.8	182.9	123.9	80.1	52.6	30.3
units per proton[a]	238.5	132.1	90.9	61.9	41.1	26.0	15.4
% SM remaining	**100**	**55.4**	**38.1**	**26.0**	**17.2**	**10.9**	**6.5**
(1.60 ppm)	0	317.2	442.5	528.3	592.3	636.1	668.7
units per proton	0	105.7	147.5	176.1	197.4	212.0	222.9
% of E-2	**0**	**44.3**	**61.8**	**73.8**	**82.8**	**88.9**	**93.5**
(0.94 ppm)	0	0	0	0	0	0	0
units per proton	0	0	0	0	0	0	0
% of E-3	**0**	**0**	**0**	**0**	**0**	**0**	**0**

Table 4.56 cont.
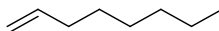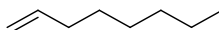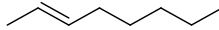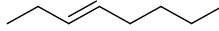
Time (min) cont.	25	30	40	50	60	90
(5.79 ppm)	9.7	6.0	4.7	4.4	4.8	4.5
(4.85-5.01 ppm)	18.2	12.3	8.9	7.9	7.8	8.1
units per proton[a]	9.4	6.1	4.6	4.1	4.3	4.3
% SM remaining	**3.9**	**2.5**	**1.9**	**1.7**	**1.8**	**1.8**
(1.60 ppm)	681.6	684.9	687.3	684.2	678.2	665.9
units per proton	227.2	228.3	229.1	228.1	226.1	222.0
% of _E_-2	**95.3**	**95.7**	**96.1**	**95.6**	**94.8**	**93.1**
(0.94 ppm)	7.4	10.6	14.4	19.0	24.3	36.5
units per proton	2.5	3.5	4.8	6.3	8.1	12.2
% of _E_-3	**1.0**	**1.5**	**2.0**	**2.7**	**3.4**	**5.1**
Time (min)	120	165	180	270	360	660
(5.79 ppm)	4.2	3.7	3.7	3.3	3.3	3.1
(4.85-5.01 ppm)	7.7	8.1	7.8	7.5	7.3	7.2
units per proton[a]	4.0	3.9	3.8	3.5	3.4	3.3
% SM remaining	**1.7**	**1.6**	**1.6**	**1.5**	**1.4**	**1.4**
(1.60 ppm)	655.1	637.4	632.9	607.7	580.1	524.4
units per proton	218.4	212.5	211.0	202.6	193.4	174.8
% of _E_-2	**91.6**	**89.1**	**88.5**	**84.9**	**81.1**	**73.3**
(0.94 ppm)	48.5	65.4	71.2	98.5	125.1	182.5
units per proton	16.2	21.8	23.7	32.8	41.7	60.8
% of _E_-3	**6.8**	**9.1**	**9.9**	**13.8**	**17.5**	**25.5**

[a]Units calculated by taking the average of the integrations of the two resonances
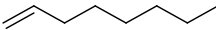
Data for Figure 4.8. Procedure for isomerization of 1-octene to E-2, E-3, and E-4 octenes using 0.1 mol% 1.1 at room temperature in acetone-d_6.
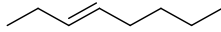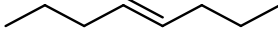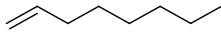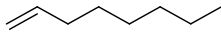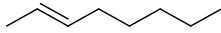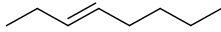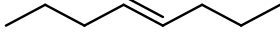
To a resealable J. Young tube in a glovebox, internal standard $(Me_3Si)_4C$ (~0.2 mg) and 1-octene (56.1 mg, 0.500 mmol) were combined in a mixture with deoxygenated with enough acetone-d_6 for a total volume of 900 µL, and an initial NMR spectrum was acquired. Back in the glovebox, to this mixture was added an aliquot of catalyst solution 1A (100 µL, 0.000500 mmol). The reaction was kept at room temperature and monitored at the times given below.

Table 4.57. Yields determined by NMR in isomerization of **4.5** using 0.1 mol% **1.1** at room temperature in acetone-d_6.

Measured integrals in arbitrary units relative to internal standard = 10.0 units and (in bold) derived per cent yields of products and amount of starting 1-alkene.								
Time (min)	0	2	6	9	12	15	20	25
(5.80 ppm)	171.5	93.1	49.0	20.0	6.0	3.4	3.0	2.9
(4.89-4.97 ppm)	349.2	192.8	98.8	40.7	11.5	6.6	6.1	5.6
units per proton[a]	174.4	94.8	49.2	20.2	5.7	3.3	3.0	2.8
% starting material remaining	**100**	**54.3**	**28.2**	**11.6**	**3.3**	**1.9**	**1.7**	**1.6**
(1.60 ppm)	0	227.3	359.1	448.4	477.6	474.4	450.5	427.4
units per proton	0	75.8	119.7	149.5	159.2	158.1	150.2	142.5
% of E-2	**0**	**43.5**	**68.7**	**85.7**	**91.3**	**90.7**	**86.1**	**81.7**
(0.94 ppm)	0	2.5	7.9	14.60	20.6	33.8	53.6	69.1
units per proton	0	0.8	2.6	4.9	6.9	11.3	17.9	23.0
% of E-3	**0**	**0.5**	**1.5**	**2.8**	**3.9**	**6.5**	**10.3**	**13.2**
(5.42 ppm)[b]	0	150.8	244.0	309.8	330.3	340.6	339.4	340.3
Units per proton[b]	0	0	0	0.6	-0.9	0.9	1.6	4.7
% of E-4	**0**	**0**	**0**	**0**	**0**	**0.5**	**0.9**	**2.7**

Table 4.57 cont.

Time (min)	30	40	60	90	120	150	180
(5.80 ppm)	2.4	2.3	2.1	1.8	1.7	1.4	1.5
(4.89-4.97 ppm)	5.8	5.3	4.2	4.3	3.5	3.0	2.8
units per proton[a]	2.7	2.5	2.1	2.0	1.7	1.5	1.4
% starting material remaining	**1.5**	**1.4**	**1.2**	**1.1**	**1.0**	**0.8**	**0.8**
(1.60 ppm)	403.5	375.4	325.9	281.6	244.4	227.4	219.9
units per proton	134.5	125.1	108.6	93.9	81.5	75.8	73.3
% of E-2	**77.1**	**71.8**	**62.3**	**53.8**	**46.7**	**43.5**	**42.0**
(0.94 ppm)	86.7	107.8	135.3	152.1	165.1	166.7	176.9
units per proton	28.9	35.9	45.1	50.7	55.0	55.6	59.0
% of E-3	**16.6**	**20.6**	**25.9**	**29.1**	**31.6**	**31.9**	**33.8**
(5.42 ppm)	341	342.0	341.6	341.3	341.2	340.0	340.7
Units per proton[b]	7.1	9.9	17.1	26.1	34.1	38.7	38.1
% of E-4	4.1	5.7	9.8	15.0	19.6	22.2	21.9
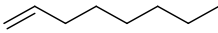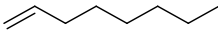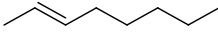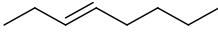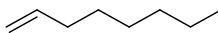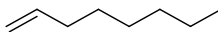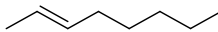
[a]Units calculated by taking the average of the integrations of the two resonances. [b]Units calculated by subtracting E-2 + E-3 units from 5.42 ppm resonance.

Data for Figure 4.9. Procedure for isomerization of 1-octene to E-2, E-3, and E-4 octenes using 0.3 mol% 3.14 at room temperature in acetone-d_6.

To a resealable J. Young tube in a glovebox, internal standard $(Me_3Si)_4C$ (~0.2 mg) and 1-octene (56.2 mg, 0.501 mmol) were combined in a mixture with deoxygenated with enough acetone-d_6 for a total volume of 900 µL, and an initial NMR spectrum was acquired. Back in the glovebox, to this mixture was added an aliquot of catalyst solution 3A (100 µL, 0.001500 mmol). The reaction was kept at room temperature and monitored at the times given below.

Table 4.58. Yields determined by NMR in isomerization of **4.5** using 0.3 mol% **3.14** at room temperature in acetone-d_6.

Measured integrals in arbitrary units relative to internal standard = 10.0 units and (in bold) derived per cent yields of products and amount of starting 1-alkene.								
Time (min)	0	2	6	9	12	15	20	25
(5.80 ppm)	92.2	52.6	35.1	20.4	12.7	7.6	4.3	2.6
(4.89-4.97 ppm)	188.6	112.4	73.2	42.6	26.5	16.0	9.3	5.4
units per proton[a]	93.3	54.4	35.8	20.8	13.0	7.8	4.5	2.6
% SM remaining	**100**	**58.3**	**38.4**	**22.3**	**13.9**	**8.4**	**4.8**	**2.8**
(1.60 ppm)	0.5	112.6	170.4	213.5	237.3	252.9	261.6	267.7
units per proton	0.2	37.5	56.8	71.2	79.1	84.3	87.2	89.2
% of *E*-2	**0**	**40.2**	**60.9**	**76.3**	**84.8**	**90.4**	**93.5**	**95.6**
(0.94 ppm)	1.7	1.8	1.7	1.7	1.9	2.0	2.7	3.5
units per proton	0.6	0.6	0.6	0.6	0.6	0.7	0.9	1.2
% of *E*-3	**0.6**	**0.6**	**0.6**	**0.6**	**0.7**	**0.7**	**1.0**	**1.3**
(5.42 ppm)	0.4	74.0	114.2	143.0	157.9	169.6	174.7	181.6
Units per proton[b]	0	0	0	-0.2	-0.8	-0.2	-0.7	0.4
% of *E*-4	**0**	**0**	**0**	**0**	**0**	**0**	**0**	**0.4**
Time (min) cont	30	40	60	90	120	150	180	630
(5.80 ppm)	2.0	1.6	1.5	1.5	1.4	1.5	1.4	1.2
(4.89-4.97 ppm)	4.3	3.5	3.3	3.4	3.2	3.2	3.2	2.6
units per proton[a]	2.1	1.7	1.6	1.6	1.5	1.5	1.5	1.2
% SM remaining	**2.2**	**1.8**	**1.7**	**1.7**	**1.6**	**1.6**	**1.6**	**1.3**
(1.60 ppm)	268.9	267.8	266.8	262.9	258.6	254.8	251.6	211.9
units per proton	89.6	89.3	88.9	87.6	86.2	84.9	83.9	70.6
% of *E*-2	**96.1**	**95.7**	**95.4**	**93.9**	**92.4**	**91.1**	**89.9**	**75.7**

334

Table 4.58 cont.
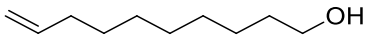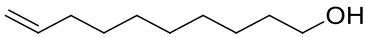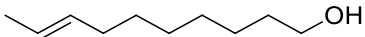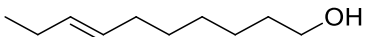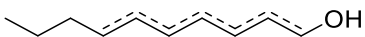
[structure] (0.94 ppm)	4.4	6.1	8.1	12.0	15.7	19.3	22.3	54.2
units per proton	1.5	2.0	2.7	4.0	5.2	6.4	7.4	18.1
% of E-3	**1.6**	**2.2**	**2.9**	**4.3**	**5.6**	**6.9**	**8.0**	**19.4**
[structure] (5.42 ppm)	181.1	182.6	182.9	184.0	181.6	181.9	181.9	181.7
Units per proton[b]	-0.6	0	-0.2	0.3	-0.6	-0.4	-0.3	2.1
% of E-4	**0**	**0**	**0**	**0.4**	**0**	**0**	**0**	**2.3**

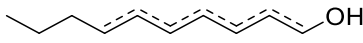| Time (min) cont	960	1280	1500	2350	2770	3860	5690
[structure] (5.80 ppm)	1.1	1.0	0.9	0.9	0.8	0.7	0.6
[structure] (4.89-4.97 ppm)	2.4	2.2	2.1	1.9	1.8	1.6	1.5
units per proton[a]	1.2	1.1	1.0	0.9	0.8	0.7	0.7
% SM remaining	**1.2**	**1.1**	**1.1**	**1.0**	**0.9**	**0.8**	**0.7**
[structure] (1.60 ppm)	178.8	162.4	158.1	144.2	137.5	115.2	111.1
units per proton	59.6	54.1	52.7	48.1	45.8	38.4	37.0
% of E-2	**63.9**	**58.0**	**56.5**	**51.5**	**49.1**	**41.2**	**39.7**
[structure] (0.94 ppm)	64.6	73.6	75.1	85.3	83.9	87.4	88.8
units per proton	21.5	24.5	25.0	28.4	28.0	29.1	29.6
% of E-3	**23.1**	**26.3**	**26.8**	**30.4**	**30.0**	**31.2**	**31.7**
[structure] 5.42ppm	182.6	184.0	183.3	186.4	185.5	183.6	184.4
Units per proton[b]	9.5	12.5	12.8	15.3	17.3	22.7	24.4
% of E-4	**10.1**	**13.4**	**13.7**	**16.4**	**18.6**	**24.4**	**26.1**

[a]Units calculated by taking the average of the integrations of the two resonances. [b]Units calculated by subtracting E-2 + E-3 units from 5.42 ppm resonance.
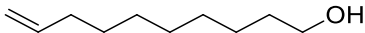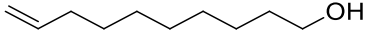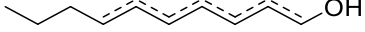
Data for Figure 4.10. Procedure for isomerization of 9-decen-1-ol to E-8 and E-7 decen-1-ols using 0.1 mol% catalyst 1.1 at room temperature in acetone-d_6.

To a resealable J. Young tube in a glovebox, internal standard $(Me_3Si)_4C$ (~0.2 mg) and 9-decen-1-ol (70.7 mg, 0.504 mmol) were combined in a mixture with deoxygenated with enough acetone-d_6 for a total volume of 900 µL, and an initial NMR spectrum was acquired. Back in the glovebox, to this mixture was added an aliquot of catalyst solution 1A (101 µL, 0.000504 mmol). The reaction was kept at room temp and monitored at the times given below.
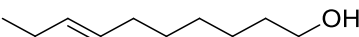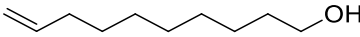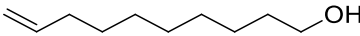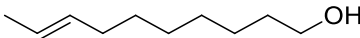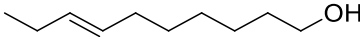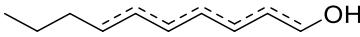
Table 4.59. Yields determined by NMR in isomerization of **4.9** using 0.1 mol% catalyst **1.1** at room temperature in acetone-d6.

Measured integrals in arbitrary units relative to internal standard = 10.0 units and (in bold) derived per cent yields of products and amount of starting 1-alkene.								
Time (min)	0	2	6	9	12	15	20	25
⌇⌇⌇⌇ OH (5.76-5.84 ppm)	136.0	82.1	50.6	23.9	7.7	3.1	2.3	2.4
⌇⌇⌇⌇ OH (4.85-5.02 ppm)	276.4	167.9	102.5	47.8	15.4	6.0	4.6	4.5
units per proton[a]	137.1	83.0	50.9	23.9	7.7	3.0	2.3	2.3
% starting material remaining	**100**	**60.5**	**37.1**	**17.4**	**5.6**	**2.2**	**1.7**	**1.7**
⌇⌇⌇⌇ OH (1.6 ppm)	0	162.6	251.5	332.7	375.8	372.7	363.2	343.4
units per proton	0	54.2	83.8	110.9	125.3	124.2	121.1	114.5
% yield product	**0**	**39.5**	**61.2**	**80.9**	**91.4**	**90.6**	**88.3**	**83.5**
⌇⌇⌇⌇ OH (0.94 ppm)	0	1.7	3.9	8.0	14.7	24.4	38.8	54.2
units per proton	0	0.6	1.3	2.7	4.9	8.1	12.9	18.1
% of isomer	**0**	**0.4**	**1.0**	**2.0**	**3.6**	**5.9**	**9.4**	**13.2**
⌇⌇⌇⌇ OH (0.85 ppm)	0	0	0	0	0	3.2	4.6	8.1
units per proton	0	0	0	0	0	1.1	1.5	2.7
% of other internal isomers	**0**	**0**	**0**	**0**	**0**	**0.8**	**1.1**	**2.0**

Table 4.59 cont.

Time (min) cont	30	45	60	120	180	1380	2670	4890
⌇⌇⌇OH (5.76-5.84 ppm)	2.1	2.0	1.7	1.3	1.2	0.6	0.7	0.6
⌇⌇⌇OH (4.85-5.02 ppm)	4.2	3.9	3.4	2.5	2.2	1.4	1.3	1.2
units per proton[a]	2.1	2.0	1.7	1.3	1.1	0.7	0.7	0.6
% starting material remaining	**1.5**	**1.4**	**1.2**	**0.9**	**0.8**	**0.5**	**0.5**	**0.4**
⌇⌇⌇OH (1.6 ppm)	328.5	295.2	265.0	200.6	168.6	104.9	91.6	82.6
units per proton	109.5	98.4	88.3	66.9	56.2	35.0	30.5	27.5
% yield product	**79.9**	**71.8**	**64.4**	**48.8**	**41.0**	**25.5**	**22.3**	**20.1**
⌇⌇⌇OH (0.94 ppm)	64.0	85.3	101.2	117.5	108.2	84.6	74.8	71.4
units per proton	21.3	28.4	33.7	39.2	36.1	28.2	24.9	23.8
% of isomer	**15.6**	**20.7**	**24.6**	**28.6**	**26.3**	**20.6**	**18.2**	**17.4**
⌇⌇⌇OH (0.85 ppm)[b]	13.2	23.2	39.7	87.8	130.8	218.8	243.4	253.8
units per proton	4.4	7.7	13.2	29.3	43.6	72.9	81.1	84.6
% of other internal isomers	**3.2**	**5.6**	**9.7**	**21.4**	**31.8**	**53.2**	**59.2**	**61.7**
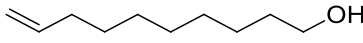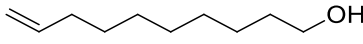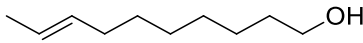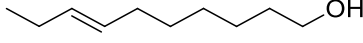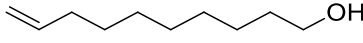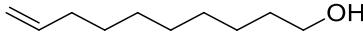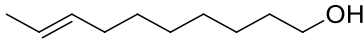
[a]Units calculated by taking the average of the integrations of the two resonances. [b]Signal includes E-6 through decanal isomers.

Data for Figure 4.11. Procedure for isomerization of 9-decen-1-ol to E-8 and E-7 decen-1-ols using 0.3 mol% catalyst 3.14 at room temperature in acetone-d_6.

To a resealable J. Young tube in a glovebox, internal standard $(Me_3Si)_4C$ (~0.2 mg) and 9-decen-1-ol (70.3 mg, 0.501 mmol) were combined in a mixture with enough deoxygenated acetone-d_6 for a total volume of 900 μL, and an initial NMR spectrum was acquired. Back in the glovebox, to this mixture was added an aliquot of catalyst solution 3A (100 μL, 0.001500 mmol). The reaction was kept at room temperature and monitored at the times given below.

Table 4.60. Yields determined by NMR in isomerization of **4.9** using 0.3 mol% catalyst **3** at room temperature in acetone-d_6.

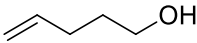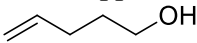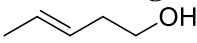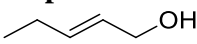| Measured integrals in arbitrary units relative to internal standard = 10.0 units and (in bold) derived per cent yields of products and amount of starting 1-alkene.						
Time (min)	0	3	6	9	12	15
⌇⌇⌇⌇OH (5.76-5.84 ppm)	289.5	90.9	34.1	14.3	8.4	6.2
⌇⌇⌇⌇OH (4.85-5.02 ppm)	579.3	182.1	66.3	30.6	16.9	11.5
units per proton[a]	289.6	91.0	33.6	14.8	8.4	6.0
% starting material remaining	**100**	**31.4**	**11.6**	**5.1**	**2.9**	**2.1**
⌇⌇⌇⌇OH (1.6 ppm)	0	600.6	772.2	824.1	843.4	836.0
units per proton	0	200.2	257.4	274.7	281.1	278.7
% yield product	**0**	**69.1**	**88.9**	**94.9**	**97.1**	**96.2**
⌇⌇⌇⌇OH (0.94 ppm)	0	0	0	0	0	11.7
units per proton	0	0	0	0	0	3.9
% of isomer	**0**	**0**	**0**	**0**	**0**	**1.3**
⌇⌇⌇⌇OH (0.85 ppm)	0	0	0	0	0	3.7
units per proton	0	0	0	0	0	1.2
% of other internal isomers	**0**	**0**	**0**	**0**	**0**	**0.4**
Time (min)	20	25	30	45	60	120
⌇⌇⌇⌇OH (5.76-5.84 ppm)	5.4	5.0	4.9	4.8	4.8	4.4
⌇⌇⌇⌇OH (4.85-5.02 ppm)	10.1	10.0	9.9	9.6	8.9	8.7
units per proton[a]	5.2	5.0	4.9	4.8	4.6	4.4
% starting material remaining	**1.8**	**1.7**	**1.7**	**1.7**	**1.6**	**1.5**
⌇⌇⌇⌇OH (1.6 ppm)	831.3	825.3	824.1	810.6	808.0	750.4
units per proton	277.1	275.1	274.7	270.2	269.3	250.1
% yield product	**95.7**	**95.0**	**94.9**	**93.3**	**93.0**	**86.4**

Table 4.60 cont.

(structure) E-alkenol (0.94 ppm)						
(0.94 ppm)	16.6	21.6	24.5	39.7	49.5	92.6
units per proton	5.5	7.2	8.2	13.2	16.5	30.9
% of isomer	**1.9**	**2.5**	**2.8**	**4.6**	**5.7**	**10.7**
other internal isomers (0.85 ppm)	4.3	4.6	4.9	4.9	5.2	10.0
units per proton	1.4	1.5	1.6	1.6	1.7	3.3
% of other internal isomers	**0.5**	**0.5**	**0.6**	**0.6**	**0.6**	**1.1**

Time (min)	180	300	540	1280	1913
(structure) (5.76-5.84 ppm)	4.1	3.8	2.1	2.7	2.9
(structure) (4.85-5.02 ppm)	8.6	8.2	6.8	5.7	4.7
units per proton[a]	4.2	4.0	2.7	2.8	2.6
% starting material remaining	**1.5**	**1.4**	**0.9**	**0.9**	**0.9**
(structure) (1.6 ppm)	720.3	663.4	578.9	421.1	374.1
units per proton	240.1	221.1	193.0	140.4	124.7
% yield product	**82.9**	**76.4**	**66.6**	**48.5**	**43.1**
(structure) (0.94 ppm)	122.7	169.1	215.4	256.3	249.5
units per proton	40.9	56.4	71.8	85.4	83.2
% of isomer	**14.1**	**19.5**	**24.8**	**29.5**	**28.7**
(structure) (0.85 ppm)[b]	15.1	28.6	64.1	181.1	236.8
units per proton	5.0	9.5	21.4	60.4	78.9
% of other internal isomers	**1.7**	**3.3**	**7.4**	**20.8**	**27.3**

[a]Units calculated by taking the average of the integrations of the two resonances. [b]Signal includes E-6 through decanal isomers.

Data for Figure 4.12. Procedure for isomerization of 4-penten-1-ol to E-3, E-2, and E-1 penten-1-ol and pentenal using 0.2 mol% catalyst 1.1 at room temperature in acetone-*d6*.

To a resealable J. Young tube in a glovebox, internal standard $(Me_3Si)_4C$ (~0.2 mg) and 4-penten-1-ol (43.3 mg, 0.502 mmol) were combined in a mixture with deoxygenated with enough acetone-d_6 for a total volume of 900 µL, and an initial NMR spectrum was acquired. Back in the glovebox, to this mixture was added an aliquot of catalyst solution 1B (100 µL, 0.00200 mmol). The reaction was kept at room temperature and monitored at the times given below.

Table 4.61. Yields determined by NMR in isomerization of **4.7** using 0.2 mol% catalyst **1.1** at room temperature in acetone-d_6.
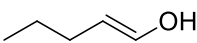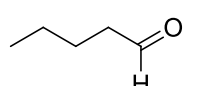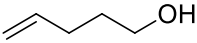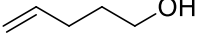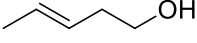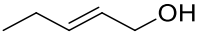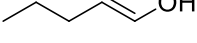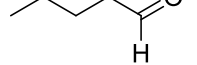
Measured integrals in arbitrary units relative to internal standard = 10.0 units and (in bold) derived per cent yields of products and amount of starting 1-alkene.								
Time (min)	0	3	6	9	12	15	20	25
(5.84 ppm)	127.1	103.4	90.6	80.1	68.4	58.4	46.2	37.4
(4.85-5.08 ppm)	259.3	212.8	184.6	160.1	138.2	117.3	93.1	73.9
units per proton[a]	128.4	104.9	91.5	80.1	68.8	58.5	46.4	37.2
% starting material remaining	**100**	**81.7**	**71.3**	**62.4**	**53.6**	**45.6**	**36.1**	**29.0**
(5.35-5.46 ppm)[b]	1.7	46.9	73.8	96.6	119.2	138.5	162.2	180.4
units per proton[c]	0.85	23.4	36.9	48.3	59.2	68.6	80.3	89.2
% yield product	**0.7**	**18.3**	**28.8**	**37.6**	**46.1**	**53.9**	**63.2**	**70.3**
(0.96 ppm)	0	0	0	0	1.2	1.8	2.5	3.0
units per proton	0	0	0	0	0.4	0.6	0.8	1.0
% of isomer	**0**	**0**	**0**	**0**	**0.3**	**0.5**	**0.6**	**0.8**
(6.3 ppm)	0	0	0	0	0	0	0	0
units per proton	0	0	0	0	0	0	0	0
% of isomer	**0**	**0**	**0**	**0**	**0**	**0**	**0**	**0**
(2.4 ppm)	0	0	0	0	0	0	0	0
units per proton	0	0	0	0	0	0	0	0
% of aldehyde	**0**	**0**	**0**	**0**	**0**	**0**	**0**	**0**

Table 4.61 cont.
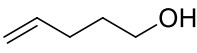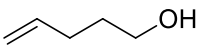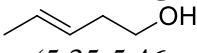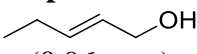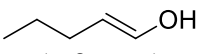
Time (min)	30	40	50	60	90	120	150	200
(pent-4-en-1-ol structure) (5.84 ppm)	28.8	16.9	8.4	6.2	3.4	2.7	2.5	2.5
(pent-4-en-1-ol structure) (4.85-5.08 ppm)	57.8	32.7	16.8	11.4	5.6	5.1	4.9	4.9
units per proton[a]	28.9	16.6	8.4	5.9	3.1	2.6	2.5	2.4
% starting material remaining	**22.5**	**12.9**	**6.5**	**4.6**	**2.4**	**2.1**	**1.9**	**1.9**
(E-penten-1-ol structure) (5.35-5.46 ppm)[b]	198.8	223.6	240.0	244.9	250.6	251.5	251.1	250.7
units per proton[c]	98.0	109.7	116.4	118.2	118.2	116.5	114.5	111.7
% yield product	**76.4**	**85.5**	**90.7**	**92.1**	**92.1**	**90.7**	**89.2**	**87.0**
(structure) (0.96 ppm)	4.1	6.2	8.9	10.3	15.3	19.0	21.1	23.7
units per proton	1.4	2.0	3.0	3.4	5.1	6.3	7.0	7.9
% of isomer	**1.1**	**1.6**	**2.3**	**2.7**	**4.0**	**4.9**	**5.5**	**6.2**
(structure) (6.3 ppm)	0	0	0.6	0.8	2.0	2.9	4.0	5.7
units per proton	0	0	0.6	0.8	2.0	2.9	4.0	5.7
% of isomer	**0**	**0**	**0.5**	**0.6**	**1.6**	**2.3**	**3.1**	**4.4**
(aldehyde structure) (2.4 ppm)	0	0	0	0	0	0	0.4	1.1
units per proton	0	0	0	0	0	0	0.2	0.5
% of aldehyde	**0**	**0**	**0**	**0**	**0**	**0**	**0.1**	**0.4**

[a]Units calculated by taking the average of the integrations of the two resonances. [b]Signal is a mixture of E-3- and E-2 penten-1-ol isomers. [c]Vinylic C-H proton units for E-3-penten-1-ol determined by subtracting proton units of E-3-penten-1-ol from total proton units of E-2/E-3 signal.
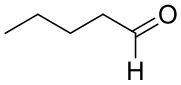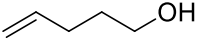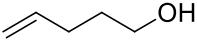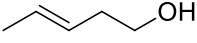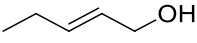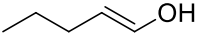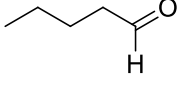
Data for Figure 4.13. Procedure for isomerization of 4-penten-1-ol to E-3, E-2, E-1 penten-1-ols and pentenal using 0.3 mol% catalyst 3.14 at room temperature in acetone-d_6.

To a resealable J. Young tube in a glovebox, internal standard $(Me_3Si)_4C$ (~0.2 mg) and 4-penten-1-ol (45.0 mg, 0.522 mmol) were combined in a mixture with deoxygenated with enough acetone-d_6 for a total volume of 900 μL, and an initial NMR spectrum was acquired. Back in the glovebox, to this mixture was added an aliquot of catalyst solution 3A (104 μL, 0.00156 mmol). The reaction was kept at room temperature and monitored at the times given below.

Table 4.62. Yields determined by NMR in isomerization of **4.7** using 0.3 mol% catalyst **3.14** at room temperature in acetone-d_6.

Measured integrals in arbitrary units relative to internal standard = 10.0 units and (in bold) derived per cent yields of products and amount of starting 1-alkene.								
Time (min)	0	3	9	20	40	50	60	90
OH (5.84 ppm)	125.0	115.2	111.1	97.5	74.1	64.1	52.8	25.6
OH (4.85-5.08 ppm)	254.7	239.0	225.5	198.8	151.1	130.0	107.4	50.6
units per proton[a]	126.2	117.3	111.9	98.4	74.8	64.5	53.2	25.5
% SM remaining	**100**	**93.0**	**88.7**	**78.0**	**59.3**	**51.1**	**42.2**	**20.2**
OH (5.35-5.46 ppm)[b]	0	17.43	28.6	55.1	102.6	123.0	145.8	201.4
units per proton[c]	0	8.7	14.3	27.6	51.3	61.5	72.9	100.7
% yield product	**0**	**6.9**	**11.3**	**21.8**	**40.7**	**48.7**	**57.8**	**79.8**
OH (0.96 ppm)	0	0	0	0	0	0	0	0
units per proton	0	0	0	0	0	0	0	0
% of isomer	**0**	**0**	**0**	**0**	**0**	**0**	**0**	**0**
OH (6.3 ppm)	0	0	0	0	0	0	0	0
units per proton	0	0	0	0	0	0	0	0
% of isomer	**0**	**0**	**0**	**0**	**0**	**0**	**0**	**0**

Table 4.62 cont.

(2.4 ppm)	0	0	0	0	0	0	0	0
units per proton	0	0	0	0	0	0	0	0
% of aldehyde	**0**	**0**	**0**	**0**	**0**	**0**	**0**	**0**
Time (min) cont	120	150	180	240	660	962	1460	2410
(5.84 ppm)	8.4	3.4	2.6	2.6	2.5	2.4	2.4	2.8
(4.85-5.08 ppm)	16.17	6.2	5.6	4.9	4.7	4.7	4.6	4.9
units per proton[a]	8.3	3.2	2.7	2.5	2.4	2.4	2.3	2.6
% SM remaining	**6.5**	**2.6**	**2.1**	**2.0**	**1.9**	**1.9**	**1.9**	**2.1**
(5.35-5.46 ppm)[b]	235.2	245.5	246.03	245.48	241.4	239.9	238.7	237.2
units per proton[c]	117.6	122.8	123.0	122.7	120.7	120.0	119.3	118.6
% yield product	**92.9**	**96.8**	**96.8**	**96.4**	**94.5**	**93.8**	**93.3**	**92.8**
(0.96 ppm)	1.0	1.8	2.4	3.2	4.5	4.6	4.8	4.6
units per proton	0.3	0.6	0.8	1.1	1.5	1.5	1.6	1.5
% of isomer	**0.3**	**0.5**	**0.6**	**0.8**	**1.2**	**1.2**	**1.3**	**1.2**
(6.3 ppm)	0	0	0	0	0	0	0	0
units per proton	0	0	0	0	0	0	0	0
% of isomer	**0**	**0**	**0**	**0**	**0**	**0**	**0**	**0**
(2.4 ppm)	0	0	0.5	1.23	5.8	7.46	8.58	9.57
units per proton	0	0	0.2	0.6	2.9	3.7	4.3	4.8
% of aldehyde	**0**	**0**	**0.2**	**0.5**	**2.3**	**3.0**	**3.4**	**3.8**

[a]Units calculated by taking the average of the integrations of the two resonances. [b]Signal is a mixture of E-3- and E-2-penten-1-ol isomers. [c]Vinylic C-H proton units for E-3-penten-1-ol determined by subtracting proton units of E-2-penten-1-ol from total proton units of E-3/E-2 signal.

Data for Figure 4.14. Procedure for isomerization of 4-penten-1-ol t-butyldimethyl silyl ether to E-3, E-2, and E-1 silyl ethers using 0.1 mol% catalyst 1.1 at room temp in acetone-d_6.

To a resealable J. Young tube in a glovebox, internal standard $(Me_3Si)_4C$ (~0.2 mg) and 4-penten-1-ol t-butyldimethylsilylether (101.5 mg, 0.506 mmol) were combined with enough deoxygenated acetone-d_6 for a total volume of 900 µL, and an initial NMR spectrum was acquired. Back in the glovebox, to this mixture was added an aliquot of catalyst solution 1A (101 µL, 0.000505 mmol). The reaction was kept at room temp and monitored at times below.

Table 4.63. Yields determined by NMR in isomerization of **4.10** using 0.1 mol% catalyst **1.1** at room temperature in acetone-d_6.
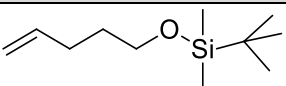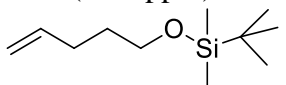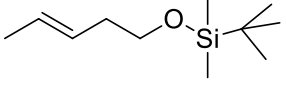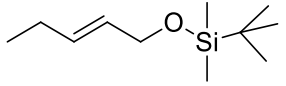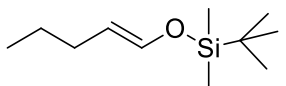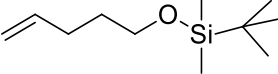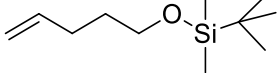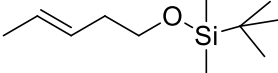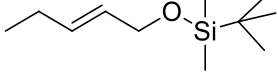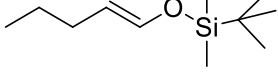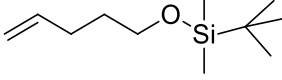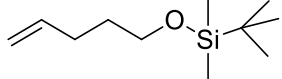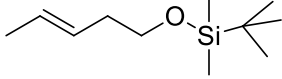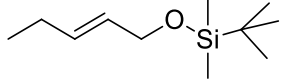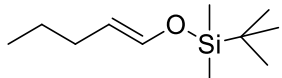
Measured integrals in arbitrary units relative to internal standard = 10.0 units and (in bold) derived per cent yields of products and amount of starting 1-alkene.							
Time (min)	0	3	6	9	15	20	25
(structure) (5.82 ppm)	175.4	103.1	69.7	40.1	7.9	4.5	4.1
(structure) (4.82-5.10 ppm)	364.7	215.8	145.4	82.8	18.5	9.9	9.5
units per proton[a]	178.9	105.5	71.2	40.7	8.6	4.7	4.4
% starting material remaining	**100**	**59.0**	**39.8**	**22.8**	**4.8**	**2.6**	**2.5**
(structure) (1.60 ppm)	0	224.3	327.6	416.3	506.6	509.6	507.7
units per proton	0	74.8	109.2	138.8	168.9	169.9	169.2
% yield product	**0**	**41.8**	**61.0**	**77.6**	**94.4**	**95.0**	**94.6**
(structure) (0.94 ppm)	0	0	0	0	8.0	12.6	18.2
units per proton	0	0	0	0	2.7	4.2	6.1
% of isomer	**0**	**0**	**0**	**0**	**1.5**	**2.3**	**3.4**
(structure) (6.23 ppm)	0	0	0	0	0	0.3	0.6
units per proton	0	0	0	0	0	0.3	0.6
% of enol ether	**0**	**0**	**0**	**0**	**0**	**0.2**	**0.3**

Table 4.63 cont.

Time (min)	30	40	50	60	90	120	150
(structure) (5.82 ppm)	4.0	3.7	3.7	3.6	3.4	3.4	3.5
(structure) (4.82-5.10 ppm)	9.4	8.4	8.0	7.7	7.4	7.4	7.4
units per proton[a]	4.3	4.0	3.9	3.7	3.6	3.6	3.6
% starting material remaining	**2.4**	**2.2**	**2.2**	**2.1**	**2.0**	**2.0**	**2.0**
(structure) (1.60 ppm)	500.1	489.0	480.7	474.6	454.6	441.8	428.8
units per proton	166.7	163.0	160.2	158.2	151.5	147.3	142.9
% yield product	**93.2**	**91.1**	**89.6**	**88.4**	**84.7**	**82.3**	**79.9**
(structure) (0.94 ppm)	23.3	31.5	37.8	43.2	49.6	57.4	51.8
units per proton	7.8	10.5	12.6	14.4	16.5	19.1	17.3
% of isomer	**4.3**	**5.9**	**7.0**	**8.0**	**9.2**	**10.7**	**9.7**
(structure) (6.23 ppm)	0.9	1.6	2.4	3.6	6.9	11.6	14.1
units per proton	0.9	1.6	2.4	3.6	6.9	11.6	14.1
% of enol ether	**0.5**	**0.9**	**1.3**	**2.0**	**3.8**	**6.5**	**7.9**

Table 4.63 cont.

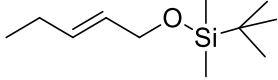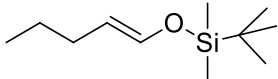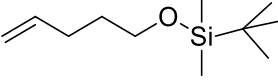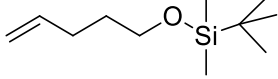| Time (min)	180	1450	2965	4310	6805	10145
[structure] (5.82 ppm)	3.3	2.0	0.8	1.0	0.4	0.3
[structure] (4.82-5.10 ppm)	7.1	6.7	1.8	1.5	1.4	1.1
units per proton[a]	3.4	2.6	0.9	0.9	0.6	0.4
% starting material remaining	**2.0**	**1.5**	**0.5**	**0.5**	**0.3**	**0.2**
[structure] (1.60 ppm)	423.5	204.8	110.7	76.7	53.9	40.4
units per proton	141.2	68.3	37.0	25.6	18.0	13.5
% yield product	**78.9**	**38.2**	**20.6**	**14.3**	**10.0**	**7.5**
[structure] (0.94 ppm)	52.2	29.3	18.2	10.94	9.12	0
units per proton	17.4	9.8	6.1	3.6	3.0	0
% of isomer	**9.7**	**5.5**	**3.4**	**2.0**	**1.7**	**0**
[structure] (6.23 ppm)	18.0	96.9	135.3	150.0	156.0	163.6
units per proton	18.0	96.9	135.3	150.0	156.0	163.6
% of enol ether	**10.1**	**54.2**	**75.6**	**83.8**	**87.2**	**91.5**
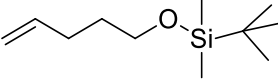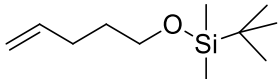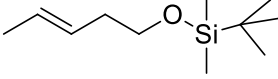
[a]Units calculated by taking the average of the integrations of the two resonances.

Data for Figure 4.15. Procedure for isomerization of 4-penten-1-ol t-butyldimethyl silyl ether to E-3, E-2, and E-1 silyl ethers using 0.3 mol% catalyst 3.14 at room temp in acetone-d_6.
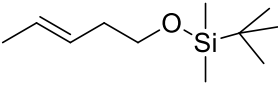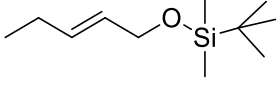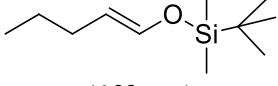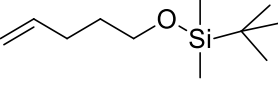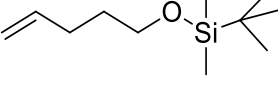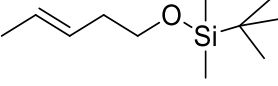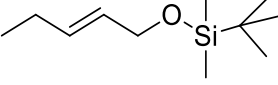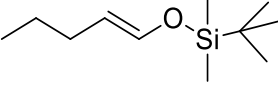
To a resealable J. Young tube in a glovebox, internal standard (Me$_3$Si)$_4$C (~0.2 mg) and 4-penten-1-ol t-butyldimethylsilylether (100.2 mg, 0.500 mmol) were combined with enough deoxygenated acetone-d_6 for a total volume of 900 μL, and an initial NMR spectrum was acquired. Back in the glovebox, to this mixture was added an aliquot of cat solution 3A (100 μL, 0.001500 mmol). The reaction was kept at room temp and monitored at the times given below.

Table 4.64. Yields determined by NMR in isomerization of **4.10** using 0.3 mol% catalyst **3.14** at room temperature in acetone-d_6.

Measured integrals in arbitrary units relative to internal standard = 10.0 units and (in bold) derived per cent yields of products and amount of starting 1-alkene.								
Time (min)	0	3	6	9	12	15	20	25
[structure] (5.82 ppm)	89.2	55.8	41.2	30.7	22.1	14.1	10.4	7.1
[structure] (4.82-5.10 ppm)	185.0	115.9	84.1	62.0	45.0	29.1	21.3	14.2
units per proton[a]	90.8	56.9	41.5	30.9	22.3	14.3	10.5	7.1
% starting material remaining	**100**	**62.6**	**45.7**	**34.0**	**24.5**	**15.7**	**11.6**	**7.8**
[structure] (1.60 ppm)	0	103.0	147.7	179.0	206.9	227.3	240.4	250.0
units per proton	0	34.3	49.2	59.7	69.0	75.8	80.1	83.3
% yield product	**0**	**37.8**	**54.2**	**65.7**	**75.9**	**83.4**	**88.2**	**91.7**
[structure] (0.94 ppm)	0	0	0	0	0	0	0	0
units per proton	0	0	0	0	0	0	0	0
% of isomer	**0**	**0**	**0**	**0**	**0**	**0**	**0**	**0**
[structure] (6.23 ppm)	0	0	0	0	0	0	0	0
units per proton	0	0	0	0	0	0	0	0
% of enol ether	**0**	**0**	**0**	**0**	**0**	**0**	**0**	**0**
Time (min) cont.	30	40	50	60	100	150	200	420
[structure] (5.82 ppm)	4.6	2.8	2.1	2.2	2.1	2.0	2.0	1.7
[structure] (4.82-5.10 ppm)	9.0	11.4	9.8	8.4	8.1	8.8	9.0	4.0
units per proton[a]	4.5	4.3	3.5	3.2	3.1	3.2	3.2	1.9
% SM remaining	**5.0**	**4.7**	**3.8**	**3.5**	**3.4**	**3.5**	**3.5**	**2.0**

Table 4.64 cont.
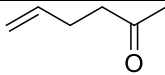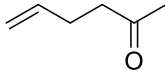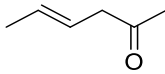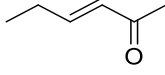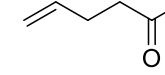
(1.60 ppm)	260.1	260.8	258.1	258.1	256.4	255.6	252.1	250.9
units per proton	86.7	86.9	86.0	86.0	85.5	85.2	84.0	83.6
% yield product	**95.4**	**95.7**	**94.7**	**94.7**	**94.1**	**93.8**	**92.5**	**92.1**
(0.94 ppm)	0	1.5	2.1	2.5	3.3	6.0	7.8	10.5
units per proton	0	0.5	0.7	0.8	1.1	2.0	2.6	3.5
% of isomer	**0**	**0.5**	**0.8**	**0.9**	**1.2**	**2.2**	**2.9**	**3.9**
(6.23 ppm)	0	0	0	0	0.2	0.4	0.5	1.5
units per proton	0	0	0	0	0.2	0.4	0.5	1.5
% of enol ether	**0**	**0**	**0**	**0**	**0.2**	**0.4**	**0.6**	**1.6**

Time (min) cont.	1230	1590	4040	4720	6240	7750	9030	11560
(5.82 ppm)	1.7	1.7	1.4	1.5	1.2	1.3	1.3	1.2
(4.82-5.10 ppm)	3.5	3.3	2.9	2.8	2.5	2.5	2.4	2.4
units per proton[a]	1.7	1.7	1.4	1.4	1.3	1.3	1.2	1.2
% SM remaining	**1.9**	**1.9**	**1.5**	**1.6**	**1.4**	**1.4**	**1.4**	**1.3**
(1.60 ppm)	238.3	230.7	202.6	190.0	178.7	167.2	160.0	151.0
units per proton	79.4	76.9	67.5	63.2	60.0	55.7	53.3	50.3
% yield product	**87.5**	**84.6**	**74.3**	**69.6**	**65.6**	**61.3**	**58.7**	**55.4**
(0.94 ppm)	11.8	13.4	11.0	12.6	10.8	11.8	12.07	10.2
units per proton	3.9	4.5	3.7	4.2	3.6	3.9	4.0	3.4
% of isomer	**4.3**	**4.9**	**4.0**	**4.6**	**4.0**	**4.3**	**4.4**	**3.7**
(6.23 ppm)	6.1	8.0	19.1	21.7	25.8	29.9	32.0	35.8
units per proton	6.1	8.0	19.1	21.7	25.8	29.9	32.0	35.8
% of enol ether	**6.7**	**8.8**	**21.0**	**23.9**	**28.4**	**32.9**	**35.2**	**39.5**

[a]Units calculated by taking the average of the integrations of the two resonances.
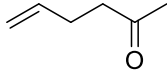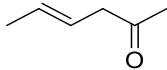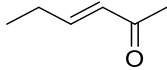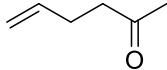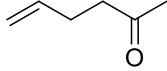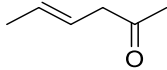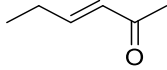
Data for Figure 4.16. Procedure for isomerization of 5-hexen-2-one to (E)-4-hexen-2-one and (E)-3-hexen-2-one using 0.1 mol% catalyst 1.1 at room temperature in acetone-d_6.

To a resealable J. Young tube in a glovebox, internal standard $(Me_3Si)_4C$ (~0.2 mg), and 5-hexen-2-one (48.9 mg, 0.498 mmol) were combined in a mixture with deoxygenated with enough acetone-d_6 for a total volume of 900 µL, and an initial NMR spectrum was acquired. Back in the glovebox, to this mixture was added an aliquot of catalyst solution 1A (100 µL, 0.000500 mmol). The reaction was kept at room temp and monitored at the times given below.

Table 4.65. Yields determined by NMR in isomerization of **5-hexen-2one** using 0.1 mol% catalyst **1.1** at room temperature in acetone-d_6.

Measured integrals in arbitrary units relative to internal standard = 10.0 units and (in bold) derived per cent yields of products and amount of starting 1-alkene.

Time (min)	0	3	6	10	20	30	40
(5.80 ppm)	272.4	241.7	233.7	220.3	179.6	151.3	117.0
(4.90-5.03 ppm)	558.8	516.6	477.2	449.9	369.1	309.4	241.5
units per proton[a]	275.9	250.0	236.1	222.6	182.1	153.0	118.9
% starting material remaining	**100**	**90.6**	**85.6**	**80.7**	**66.0**	**55.5**	**43.1**
(1.6 ppm)	0	77.8	118.0	163.0	270.7	361.4	455.4
units per proton	0	25.9	39.3	54.3	90.2	120.5	151.8
% E-2	**0**	**9.4**	**14.3**	**19.7**	**32.7**	**43.7**	**55.0**
(0.94 ppm)	0	0	0	0	7.8	11.7	16.1
units per proton	0	0	0	0	2.6	3.9	5.4
% of E-3 (conj)	**0**	**0**	**0**	**0**	**0.9**	**1.4**	**2.0**

Time (min) cont	50	60	90	120	150	180
(5.80 ppm)	93.9	68.9	28.4	14.6	9.5	8.2

Table 4.65 cont.

(structure, 4.90-5.03 ppm)	190.6	138.7	60.0	28.4	19.2	16.2
units per proton[a]	94.6	69.1	29.2	14.4	9.5	8.1
% starting material remaining	**34.3**	**25.1**	**10.6**	**5.2**	**3.5**	**2.9**
(structure, 1.6 ppm)	525.5	592.5	690.5	705.5	700.4	672.0
units per proton	175.2	197.5	230.2	235.2	233.5	224.0
% E-2	**63.5**	**71.6**	**83.4**	**85.2**	**84.6**	**81.2**
(structure, 0.94 ppm)	21.8	27.0	52.5	75.1	103.2	128.2
units per proton	7.2	9.0	17.5	25.0	34.4	42.7
% of E-3 (conj)	**2.6**	**3.3**	**6.3**	**9.1**	**12.5**	**15.5**

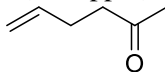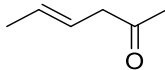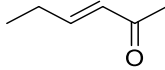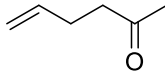| Time (min) cont	578	759	1004	1410	2132	2344
(structure, 5.80 ppm)	4.6	3.5	3.1	2.3	1.6	1.8
(structure, 4.90-5.03 ppm)	8.5	7.1	6.0	3.7	3.4	2.9
units per proton[a]	4.4	3.5	3.0	2.0	1.6	1.6
% starting material remaining	**1.6**	**1.3**	**1.1**	**0.7**	**0.6**	**0.6**
(structure, 1.6 ppm)	376.3	297.6	240.3	181.4	139.2	135.4
units per proton	125.4	99.2	80.1	60.5	46.4	45.1
% E-2	**45.5**	**36.0**	**29.0**	**21.9**	**16.8**	**16.4**
(structure, 0.94 ppm)	438.0	521.4	578.1	640.9	681.4	689.7
units per proton	146.0	173.8	192.7	213.6	227.1	229.9
% of E-3 (conj)	**52.9**	**63.0**	**69.9**	**77.4**	**82.3**	**83.3**
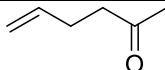
[a]Units calculated by taking the average of the integrations of the two resonances.

Data for Figure 4.17. Procedure for isomerization of 5-hexen-2-one to (E)-4-hexen-2-one and (E)-3-hexen-2-one using 2.0 mol% catalyst 3.14 at room temperature in acetone-d_6.
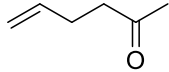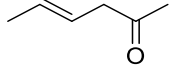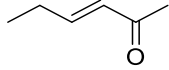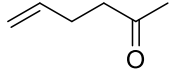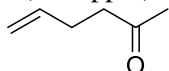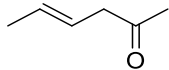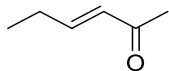
To a resealable J. Young tube in a glovebox, internal standard $(Me_3Si)_4C$ (~0.2 mg), and 5-hexen-2-one (49.3 mg, 0.502 mmol) were combined in a mixture with deoxygenated with enough acetone-d_6 for a total volume of 900 μL, and an initial NMR spectrum was acquired. Back in the glovebox, to this mixture was added preweighed solid catalyst 3.14 (6.4 mg, 0.010 mmol) and more acetone-d_6 (100 μL) to rinse down the sides of the tube. The reaction was kept at room temperature and monitored at the times given below.

Table 4.66. Yields determined by NMR in isomerization of **4.16** using 2.0 mol% catalyst **3.14** at room temperature in acetone-d_6.

Measured integrals in arbitrary units relative to internal standard = 10.0 units and (in bold) derived per cent yields of products and amount of starting 1-alkene.						
Time (min)	0	4	10	20	30	40
(5.80 ppm)	162.1	151.6	141.5	127.2	112.3	101.7
(4.90-5.03 ppm)	331.0	310.9	295.3	263.5	230.7	207.5
units per proton[a]	163.8	153.5	144.6	129.5	113.8	102.7
% starting material remaining	**100**	**93.7**	**88.3**	**79.1**	**69.5**	**62.7**
(1.6 ppm)	0	32.29	53.9	95.4	137.6	167.9
units per proton	0	10.8	18.0	31.8	45.9	56.0
% E-2	**0**	**6.6**	**11.0**	**194**	**28.0**	**34.2**
(0.94 ppm)	0	0	2.9	6.7	11.4	16.1
units per proton	0	0	1.0	2.2	3.8	5.4
% of E-3 (conj)	**0**	**0**	**0.6**	**1.4**	**2.3**	**3.3**
Time (min)	50	60	70	80	90	120
(5.80 ppm)	87.2	75.0	64.1	53.3	45.0	18.6

Table 4.66 cont.

(allyl acetone structure) (4.90-5.03 ppm)	178.5	155.4	134.9	111.8	91.3	38.2
units per proton[a]	88.2	76.3	65.8	54.6	45.3	18.8
% starting material remaining	**53.9**	**46.6**	**40.2**	**33.3**	**27.7**	**11.5**
(E-2 structure) (1.6 ppm)	203.5	231.6	256.9	281.6	299.6	333.5
units per proton	67.8	77.2	85.6	93.9	99.9	111.2
% E-2	**41.4**	**47.1**	**52.3**	**57.3**	**61.0**	**67.9**
(E-3 structure) (0.94 ppm)	22.6	29.7	37.0	46.7	56.7	103.2
units per proton	7.5	9.9	12.3	15.6	18.9	34.4
% of *E*-3 (conj)	**4.6**	**6.0**	**7.5**	**9.5**	**11.5**	**21.0**
Time (min)	**150**	**180**	**210**	**240**	**300**	**650**
(allyl acetone structure) (5.80 ppm)	7.7	3.8	2.7	1.9	1.7	1.3
(allyl acetone structure) (4.90-5.03 ppm)	15.3	7.0	4.4	3.8	3.4	1.7
units per proton[a]	7.7	3.7	2.5	1.9	1.7	1.1
% starting material remaining	**4.7**	**2.2**	**1.5**	**1.2**	**1.0**	**0.6**
(E-2 structure) (1.6 ppm)	299.7	240.4	181.2	139.8	107.2	69.8
units per proton	99.9	80.1	60.4	46.6	35.7	23.3
% E-2	**61.0**	**48.9**	**36.9**	**28.4**	**21.8**	**14.2**
(E-3 structure) (0.94 ppm)	167.2	238.8	301.9	346.4	381.3	418.9
units per proton	55.7	79.6	100.6	115.5	127.1	139.6
% of *E*-3 (conj)	**34.0**	**48.6**	**61.5**	**70.5**	**77.6**	**85.3**

[a]Units calculated by taking the average of the integrations of the two resonances.

Kinetic Modeling – Isomerization of substrates 4.1, 4.5, 4.9, 4.10, 4.17 (Performed by Prof. Andrew Cooksy)

Rate constants were least squares fit to the time-dependent NMR datausing a 4th order Runge-Kutta numerical integration program developed in-house. In some cases, the effective start time of the reaction was also optimized to allow for differences in mixing times.

For each system, the data may be sensitive to different functional forms of the reaction rate law, determining which rate constants can be resolved and whether a given step is better modeled as a unimolecular or bimolecular process. Each isomerization step is presumed to take place through a two-step process: first, the substrate combines with the catalyst (a bimolecular step) to form a reaction complex; subsequently the reaction complex dissociates into the catalyst and the product alkene (a unimolecular step). Typically, however, the first of these steps is rate-limiting over the entire observable duration of the process, and only that rate constant can be extracted from the data. The catalyst concentration is usually sufficiently consistent over the course of the process that the rate law is pseudo-first-order in substrate concentration, and the catalyst concentration is effectively factored into the fitted rate constant. Furthermore, in many cases a reverse reaction rate can be resolved because the substrate concentration for that isomerization step approaches a detectable equilibrium value.

Therefore, in fitting the rate constants several mechanisms were tried for each system, always beginning with the simplest model of a series of irreversible, first-order reaction steps. Reversible steps, catalyst concentration, and reaction complex concentration have been included in any given mechanism only if they reduce the overall standard deviation of the fit and result in well-determined rate constants. Results for the best fits are given in Table 4.66, and graphed for two representative cases in Figure 4.18. We emphasize that more than one mechanism may

354

result in fits of similar quality, and therefore the uncertainties attached to the values only indicate the quality of the fit for the given mechanism.

The final fits to the data from substrates **5** and **6** are the most straightforward, being adequately modeled by first-order steps (some reversible) throughout. The (*E*)-7-decenol is the last identified alkene in the progression of the reaction, but it continues to react to form several isomers. With catalyst **1**, it was necessary to model those subsequent reactions in two steps: formation of one intermediate (presumed to be (*E*)-6-decenol in Table 1), followed by further reaction of that intermediate. This observed decay of the (*E*)-7-decenol concentration could not be well fit otherwise, because there are two distinct time scales for the equilibration of these isomers. The separation of these time scales in **6/1** is apparent from the orders of magnitude of the rate constants k_3 (0.0116 min^{-1} for (*E*)-7 → (*E*)-6) and the much slower k_4 (1.25×10^{-4} min^{-1} for (*E*)-6 → other), and results in the late drop in concentrations for the (*E*)-7 and (*E*)-8 isomers in the last few measurements shown in Figure 4.18.

We were also able to model the reaction of substrate **4.10** with catalyst **3.14** using only first-order steps. However, significant concentrations of both the (*E*)-1 and (*E*)-3 forms are observed at long times, requiring the addition of reverse steps coupling the two isomers. We do not resolve individual contributions from (*E*)-1 → (*E*)-2 and (*E*)-2 → (*E*)-3, so a single rate constant for the combine reverse reaction (*E*)-1 → (*E*)-3 is fit instead. Substrate **4.7** was not subjected to analysis due to failure of the reaction to proceed towards equilibrium; indications of catalyst deactivation were present in both catalyst runs.

Table 4.67. Rate constants (min^{-1} and L·mol^{-1} min^{-1}) for best-fit mechanisms.[a]

4.1 + 0.1 mol% **1.1**: $1h \underset{k_{-1}}{\overset{k_1}{\rightleftharpoons}} 2Eh \underset{k_{-2}}{\overset{k_2}{\rightleftharpoons}} 3Eh$

k₁	k₋₁	k₂	k₋₂	k₃	k₋₃	k₄	k₋₄	σ
0.326(21)	3.1(1.3)E-3	0.01126(52)	0.0326(22)					0.0053

4.1 + 0.3 mol% **3.14**: $1h \underset{k_{-1}}{\overset{k_1}{\rightleftharpoons}} 2Eh \underset{k_{-2}}{\overset{k_2}{\rightleftharpoons}} 3Eh$

k₁	k₋₁	k₂	k₋₂	k₃	k₋₃	k₄	k₋₄	σ
0.1292(10)	1.83(23)E-3	6.74(22)E-4	1.11(14)E-3					0.0033

4.5 + 0.1 mol% **1.1**: $1o \underset{k_{-1}}{\overset{k_1}{\rightleftharpoons}} 2Eo \underset{k_{-2}}{\overset{k_2}{\rightleftharpoons}} 3Eo \underset{k_{-3}}{\overset{k_3}{\rightleftharpoons}} 4Eo$

k₁	k₋₁	k₂	k₋₂	k₃	k₋₃	k₄	k₋₄	σ
0.407(26)	0.0075(18)	0.01046 (25)	0.01065(60)	0.0194(21)	0.0268(38)			0.0047

4.5 + 0.3 mol % **3.14**: $1o \underset{k_{-1}}{\overset{k_1}{\rightleftharpoons}} 2Eo \underset{k_{-2}}{\overset{k_2}{\rightleftharpoons}} 3Eo \underset{k_{-3}}{\overset{k_3}{\rightleftharpoons}} 4Eo$, $1Eo \overset{k_4}{\rightarrow} 2Zo$

k₁	k₋₁	k₂	k₋₂	k₃	k₋₃	k₄	k₋₄	σ
0.1676(16)	3.02(38)E-3	5.54(12)E-4	6.91(28)E-4	7.71(56)E-4	9.54(92)E-4	3.48(86)E-3		0.0054

4.9 + 0.1 mol% **1.1**: $9d \underset{k_{-1}}{\overset{k_1}{\rightleftharpoons}} 8Ed \underset{k_{-2}}{\overset{k_2}{\rightleftharpoons}} 7Ed \underset{k_{-3}}{\overset{k_3}{\rightleftharpoons}} [6Ed] \overset{k_4}{\rightarrow} [\text{other isomers}]$

k₁	k₋₁	k₂	k₋₂	k₃	k₋₃	k₄	k₋₄	σ
0.3166(62)	3.5(1.5)E-3	9.85(29)E-3	0.01107 (66)	0.0116(11)	5.28(83)E-3	1.25(38)E-4		0.0060

4.9 + 0.3 mol% **3**: $9d \underset{k_{-1}}{\overset{k_1}{\rightleftharpoons}} 8Ed \underset{k_{-2}}{\overset{k_2}{\rightleftharpoons}} 7Ed \overset{k_3}{\rightarrow} [\text{other isomers}]$

k₁	k₋₁	k₂	k₋₂	k₃	k₋₃	k₄	k₋₄	σ
0.3951(49)	8.62(74)E-3	1.015(23) E-3	1.186(58) E-3	5.94(22)E-4				0.0035

4.10 + 0.1 mol% **1.1**: $4p \overset{k_1}{\rightarrow} 3Ep$, $3Ep + cat \underset{k_{-2}}{\overset{k_2}{\rightleftharpoons}} 2Ep + cat \underset{k_{-2}'}{\overset{k_2'}{\rightleftharpoons}} 2Ep\text{-}cx \underset{k_{-3}}{\overset{k_3}{\rightleftharpoons}} 1Ep + cat$

k₁	k₋₁	k₂	k₋₂	k₃	k₋₃	k₄	k₋₄	σ
0.1701(28)		5.22(52)	22.4(6.1)	78(15)	339(42)	$k_2' = 16.8(2.2)$	$k_{-2}' = 0.061(18)$	0.0037

4.10 + 0.3 mol% **3.14**: $4p \underset{k_{-1}}{\overset{k_1}{\rightleftharpoons}} 3Ep \overset{k_2}{\rightarrow} 2Ep \overset{k_3}{\rightarrow} 1Ep$, $3Ep \underset{k_{-4}}{\leftarrow} 1Ep$

k₁	k₋₁	k₂	k₋₂	k₃	k₋₃	k₄	k₋₄	σ
0.1249(13)	4.84(31)E-3	8.70(27)E-5		1.53(12)E-3			9.81(83)E-5	0.0051

4.16 + 0.1 mol% **1.1**: $5hn + cat \overset{k_1}{\rightarrow} 5hn\text{-}cx \overset{k_1'}{\rightarrow} 4Ehn + cat \underset{k_{-2}}{\overset{k_2}{\rightarrow}} 3Ehn + cat$, $5hn \underset{k_{-1}}{\leftarrow} 4Ehn$

k₁	k₋₁	k₂	k₋₂	k₃	k₋₃	k₄	k₋₄	σ
93.1(6.2)	1.04(38)E-3	1.533(24) E-3	2.58(15)E-4			$k_1' = 23.6(1.1)$		0.0052

4.16 + 2.0 mol% **3.14**: $5hn + cat \overset{k_1}{\rightarrow} 5hn\text{-}cx \overset{k_2}{\rightarrow} 4Ehn + cat \underset{k_{-3}}{\overset{k_3}{\rightleftharpoons}} 3Ehn + cat$

k₁	k₋₁	k₂	k₋₂	k₃	k₋₃	k₄	k₋₄	σ
5.21(29)		0.527(16)		1.104(44)	0.162(32)			0.0054

[a] Uncertainties in parentheses are 1σ; σ values given in the last column are the standard deviations of the fit in mol L^{-1}; cx indicates a catalyst complex; d = decenol; h = hexane; hn = hexen-2-one; o = octene; p = penten-1-ol silyl ether.
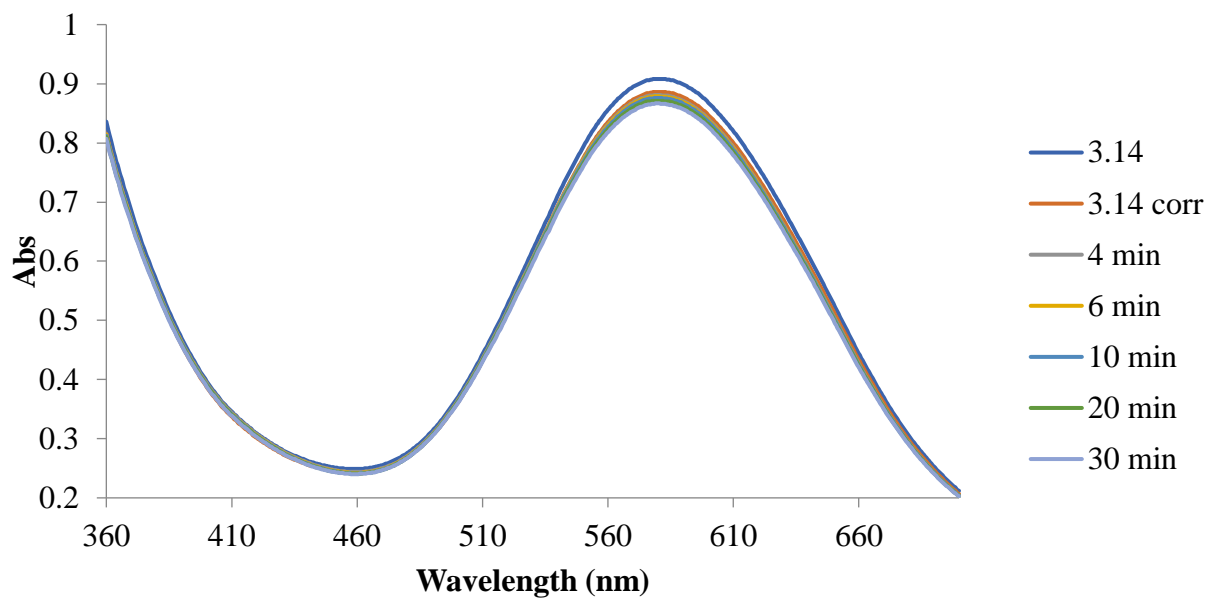
UV-vis studies

Solutions for UV-visible spectroscopy were prepared in an air-free glovebox and placed in quartz cuvettes (1 cm x 1 cm width) with resealable screw caps prior to the measurement. A typical solution was prepared by weighing out **3.14** (3.2 mg, 5.0 mmol) and adding dry, deoxygenated, alumina-filtered THF to reach a volume of 5.0 mL inside the glovebox. 2.5 mL of the solution is then transferred to the cuvette, sealed and wrapped in parafilm. An additional blank cuvette containing the same volume of solvent is then prepared in the same fashion, and cuvettes were immediately removed from the glovebox and all measurements were performed on a Shimadzu UV-Vis spectrophotometer. For the reactions with hexene, an initial reading was acquired with the catalyst, then both the catalyst and blank solution were brought into the glovebox and hexene (for 0.5 mol% loading – 200 equivalents: 0.5 mmol hexene = 42.1 mg / 0.763 mg/µL = 63 µL) was added to both catalyst and blank solutions. All data were plotted in Excel.
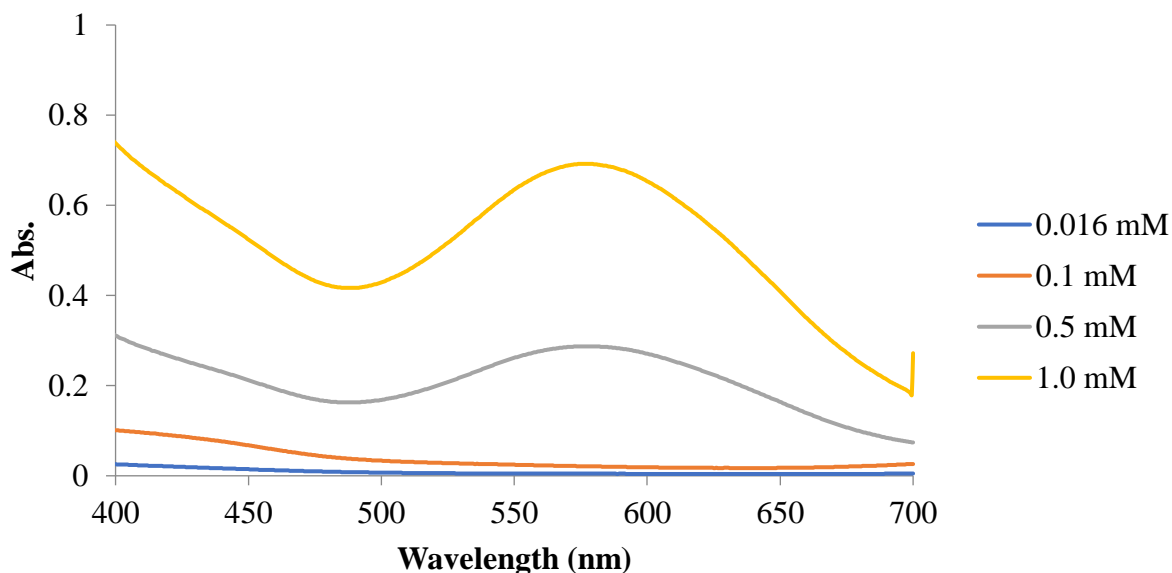
Figure 4.52. Determination of optimal concentration of **3.14** for analysis
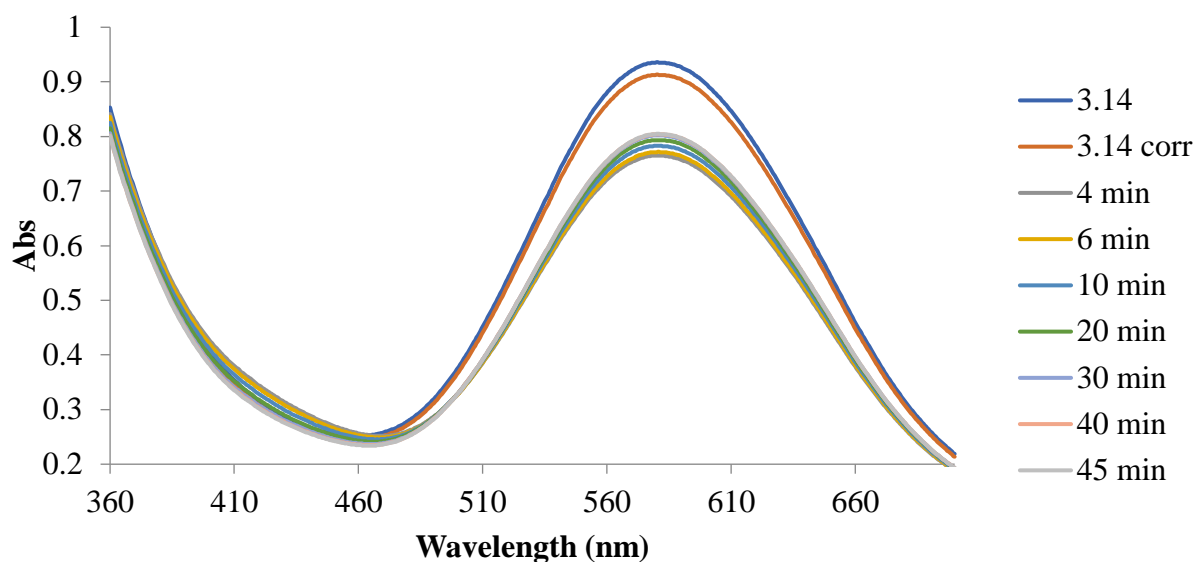
Figure 4.53. UV-visible spectra of isomerization of 200 equivalents 1-hexene with 1.0mM **3.14**


Figure 4.54. UV-visible spectra of isomerization of 200 equivalents (*E*)-2-hexene with 1.0 mM **3.14**
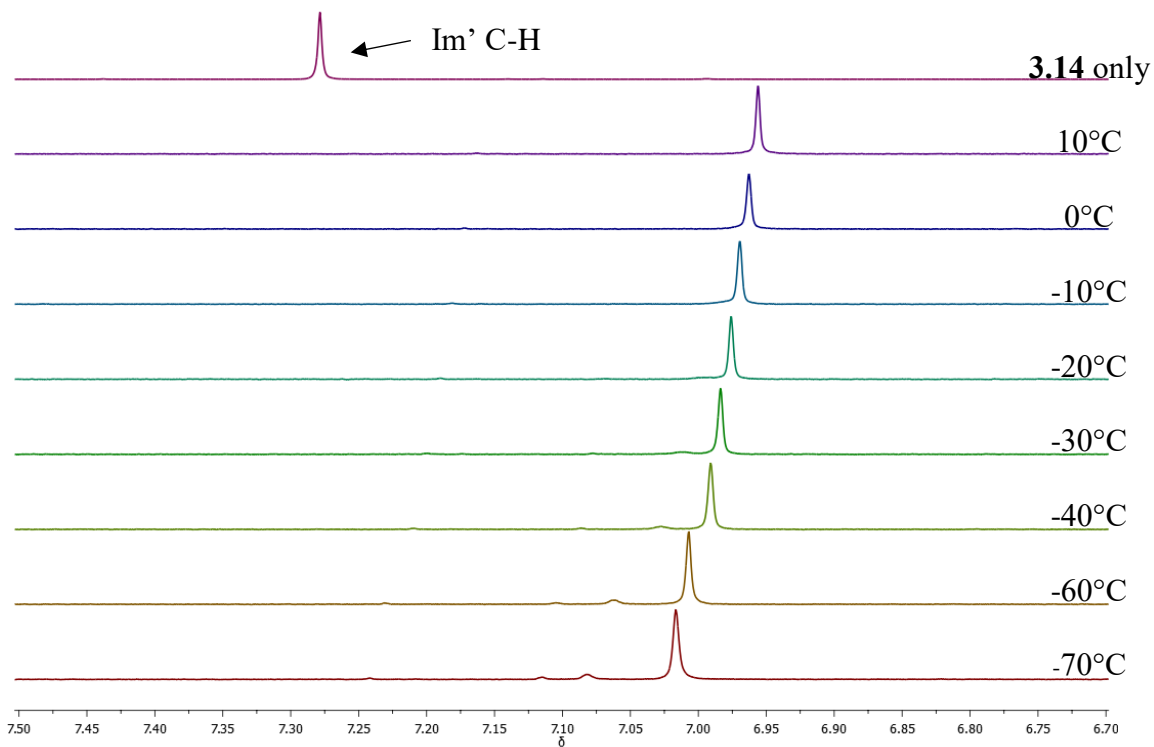
NMR studies of ethylene and propylene with catalyst 3.14

Ethylene

Binding studies of small alkenes with catalyst **3.14** were performed in resealable J. Young NMR tubes. In a typical ethylene experiment, ~5 mg catalyst was added to the J. Young NMR tube in the glovebox and deoxygenated acetone-d_6 (0.7 mL) was added, forming a blue solution. Ethylene gas was then bubbled through the solution for ~1 min, during which time the solution turned orange. NMR analysis of the resulting complex was performed on the 500-MHz Varian INOVA spectrometer. Initial ^{1}H (16 scans) and ^{31}P (64 scans) NMR spectra were obtained at 25˚C, then the temperature was lowered in the probe to 10˚C, 0˚C, -10˚C, -20˚C, -30˚C, -40˚C, -60˚C and -70˚C, with ^{1}H and ^{31}P spectra acquired at each temperature. Each ^{1}H spectra were referenced to the acetone-d_5 solvent peak (2.05 ppm), and the plots were stacked and shown below.
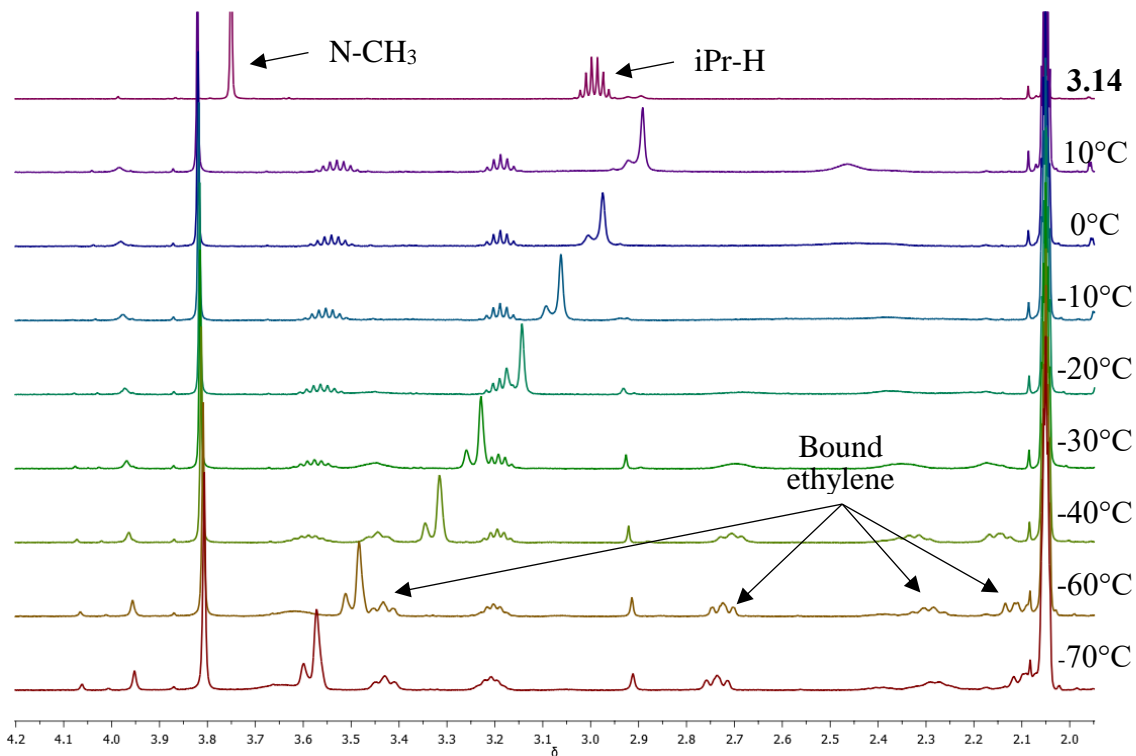
Variable temperature ^{1}H and ^{31}P NMR spectra of catalyst 5 with ethylene:
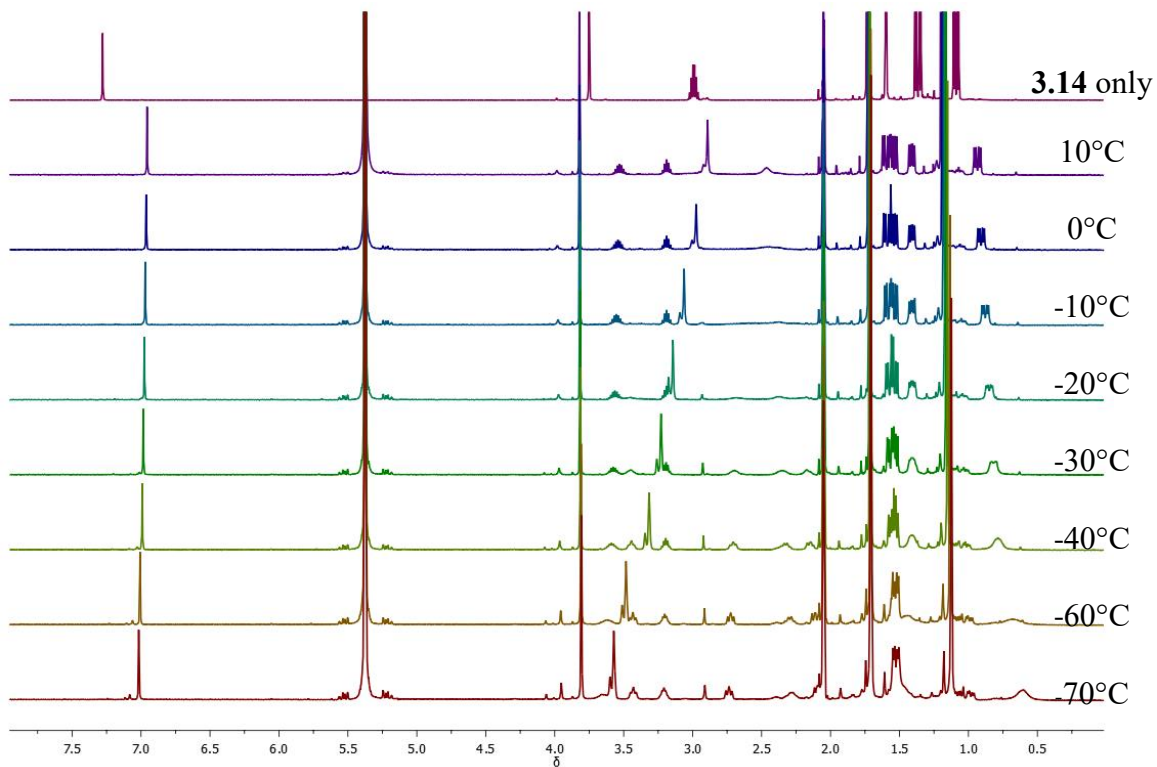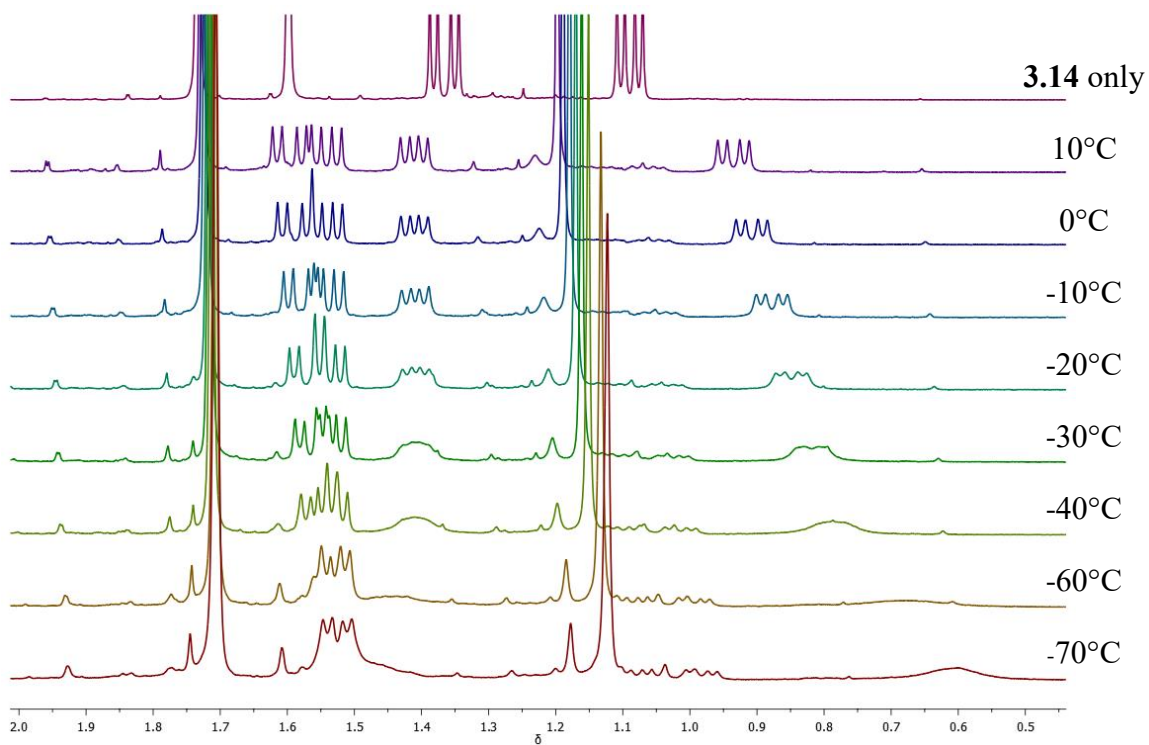
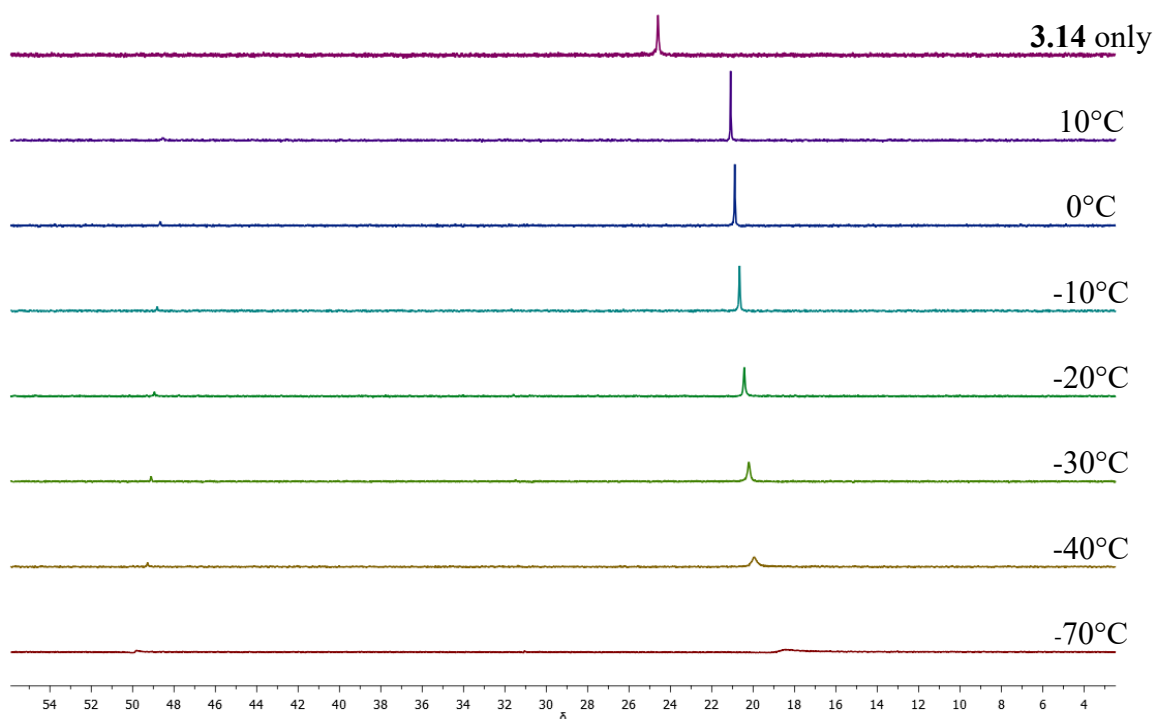**Figure 4.55**. VT NMR spectra at 500 MHz of catalyst **3.14** + ethylene

Figure 4.56. VT NMR spectra at 500 MHz of **3.14** + ethylene – 6.70 to 7.50 ppm

Figure 4.57. VT NMR spectra at 500 MHz of **3.14** + ethylene - 2.0 to 4.2 ppm

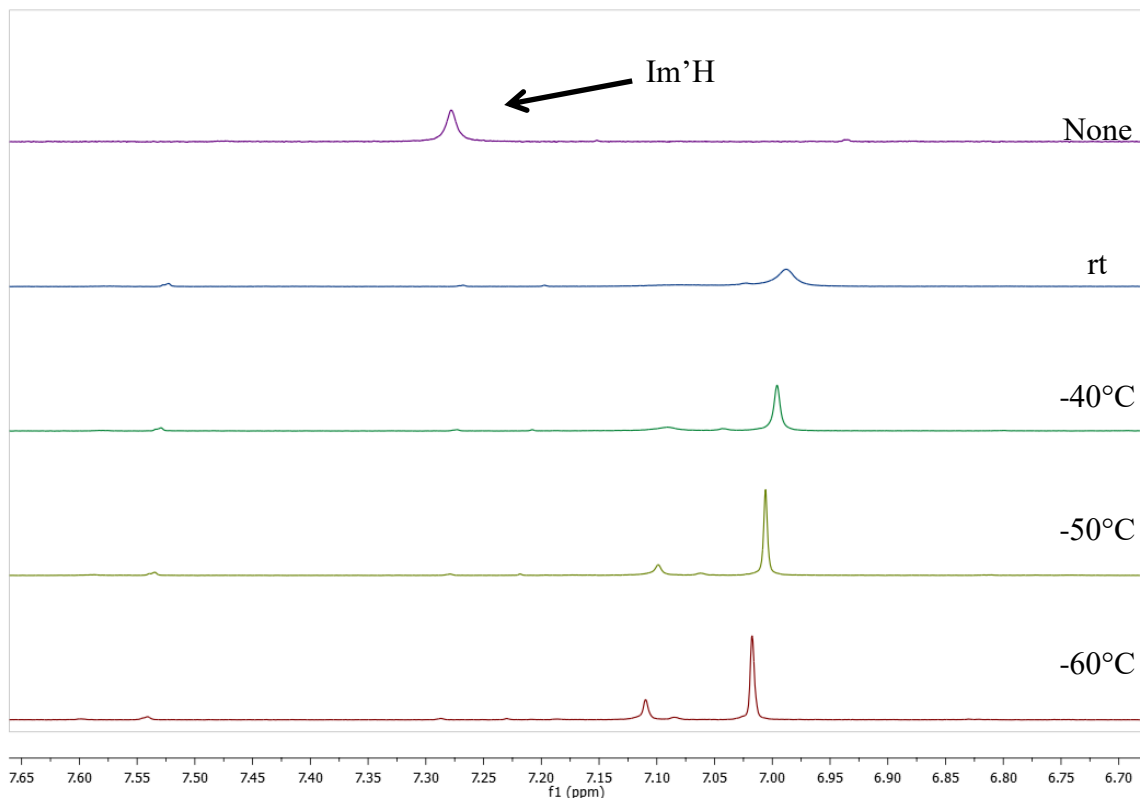**Figure 4.58**. VT NMR spectra at 500 MHz of **3.14** + ethylene - 0.5 to 2.0 ppm

**Figure 4.59**. VT ^{31}P NMR spectra at 202 MHz of **3.14** + ethylene – 3 to 55 ppm

Propylene

Binding studies of small alkenes with catalyst **5** were performed in resealable J. Young NMR tubes. In a typical propylene experiment, ~5 mg catalyst was added to the J. Young NMR tube in the glovebox and deoxygenated acetone-d_6 (0.7 mL) was added, forming a blue solution. Propylene gas was then bubbled through the solution for ~1 min, during which time the solution turned light bluish-green. NMR analysis of the resulting complex was performed on the 500-MHz Varian INOVA and 600 MHz Bruker Avance III spectrometers. Initial ^{1}H (16 scans) and ^{31}P (64 scans) NMR spectra were obtained at 25˚C, then the temperature was lowered in the probe to -40˚C, -50˚C and -60˚C, with ^{1}H and ^{31}P spectra acquired at each temperature. Each ^{1}H spectrum was referenced to the acetone-d_5 solvent peak (2.05 ppm), and the plots were stacked and shown below.

362

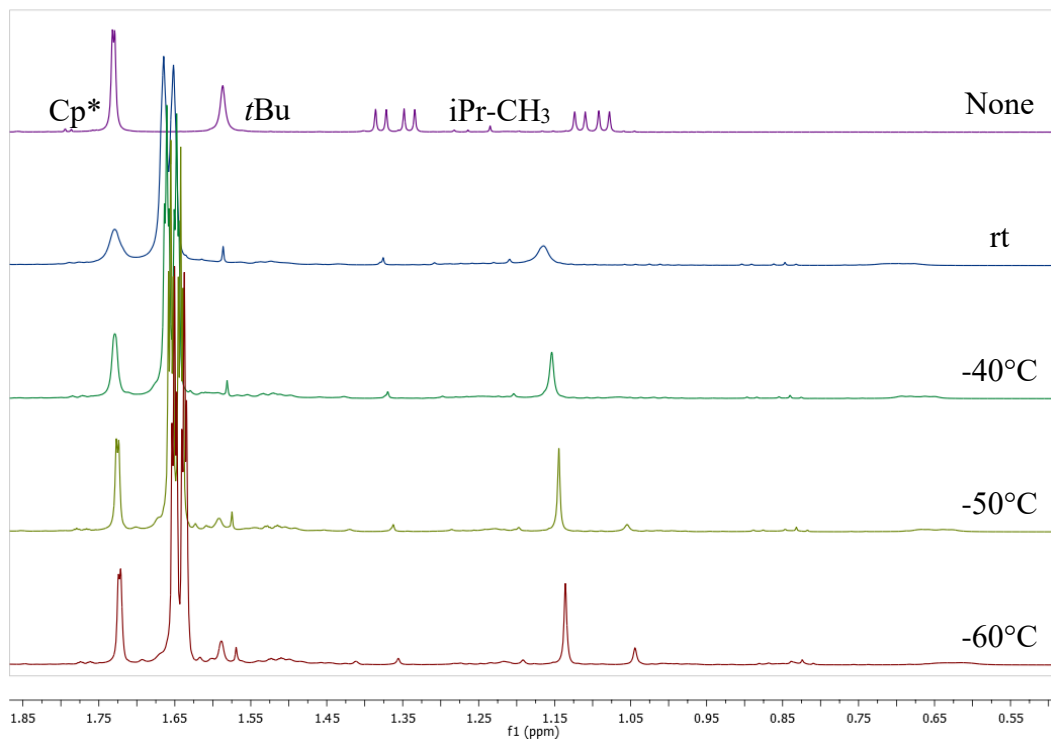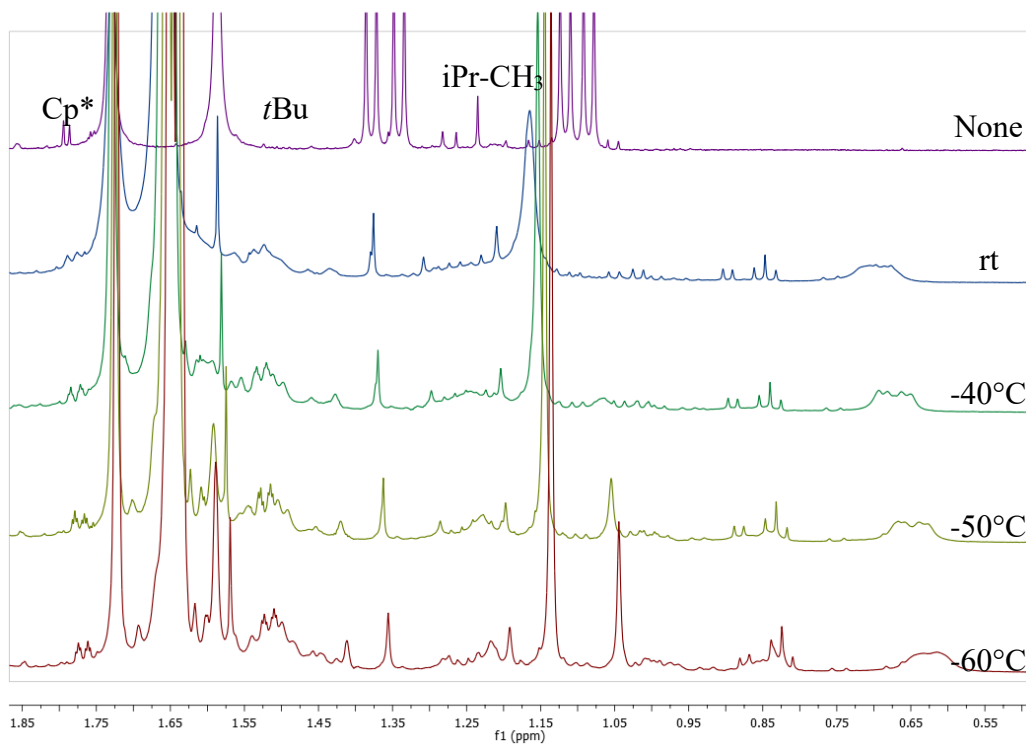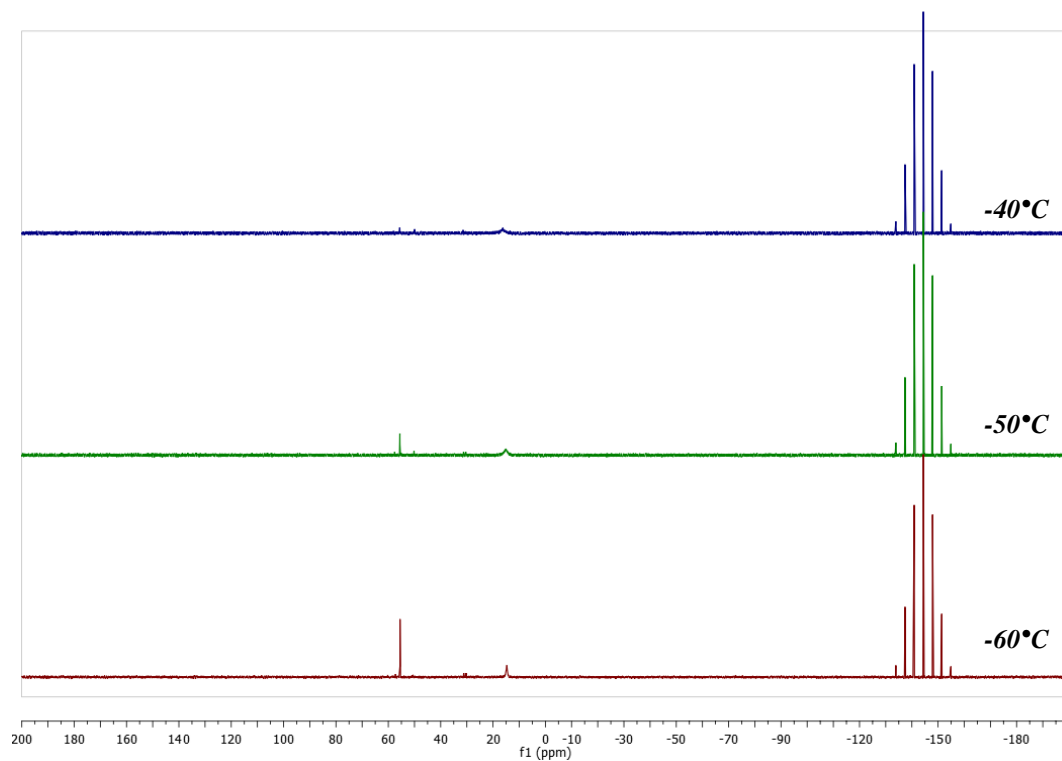**Figure 4.60**. VT ^{1}H NMR spectra at 500 MHz of **3.14** + propylene - 6.70 to 7.65 ppm
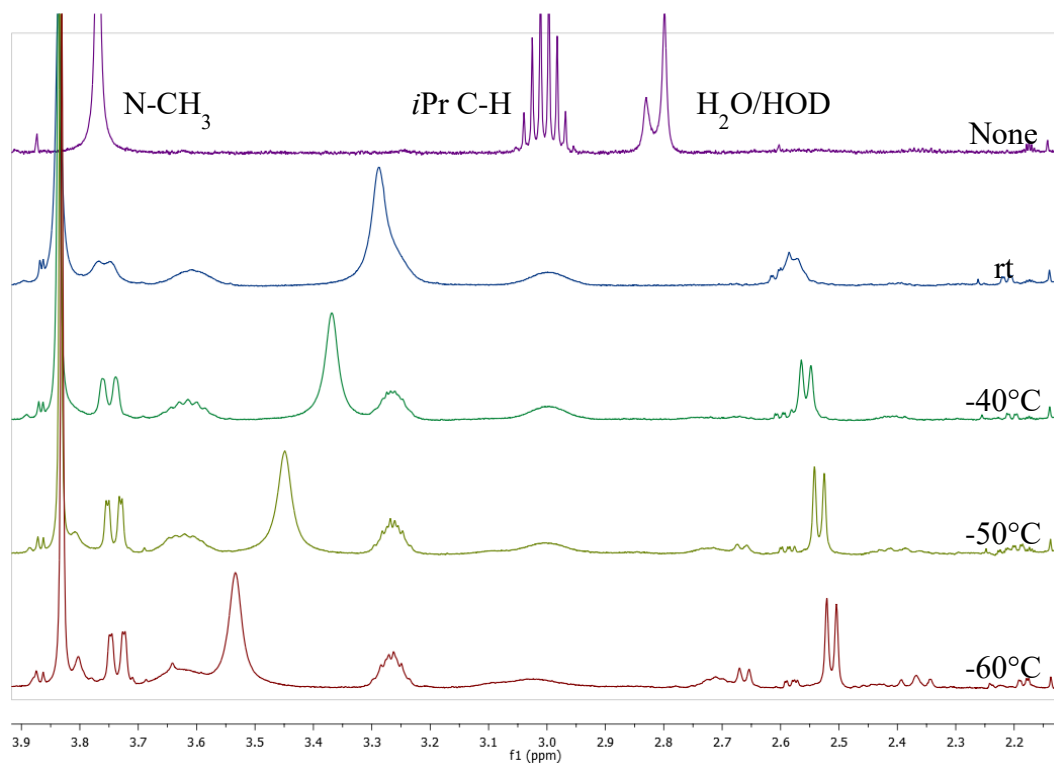
Figure 4.61. VT ^{1}H NMR spectra at 500 MHz of **3.14** + propylene - 2.1 to 3.0 ppm

Figure 4.62. VT ^{1}H NMR spectra at 500 MHz of **3.14** + propylene - 0.50 to 1.85 ppm

Figure 4.63. VT ^{1}H NMR spectra at 500 MHz of **3.14** + propylene - 0.50 to 1.85 ppm (increased intensity)

Figure 4.64. VT ^{31}P NMR spectra at 202 MHz of **3.14** + propylene

^{15}N Studies – Catalyst 3.14 with ^{15}N-labeled ligand

Catalyst **3.14** was synthesized using ligand with an ^{15}N-labeled nitrogen at the basic position. Reactions with propylene were carried out using the same procedure detailed above
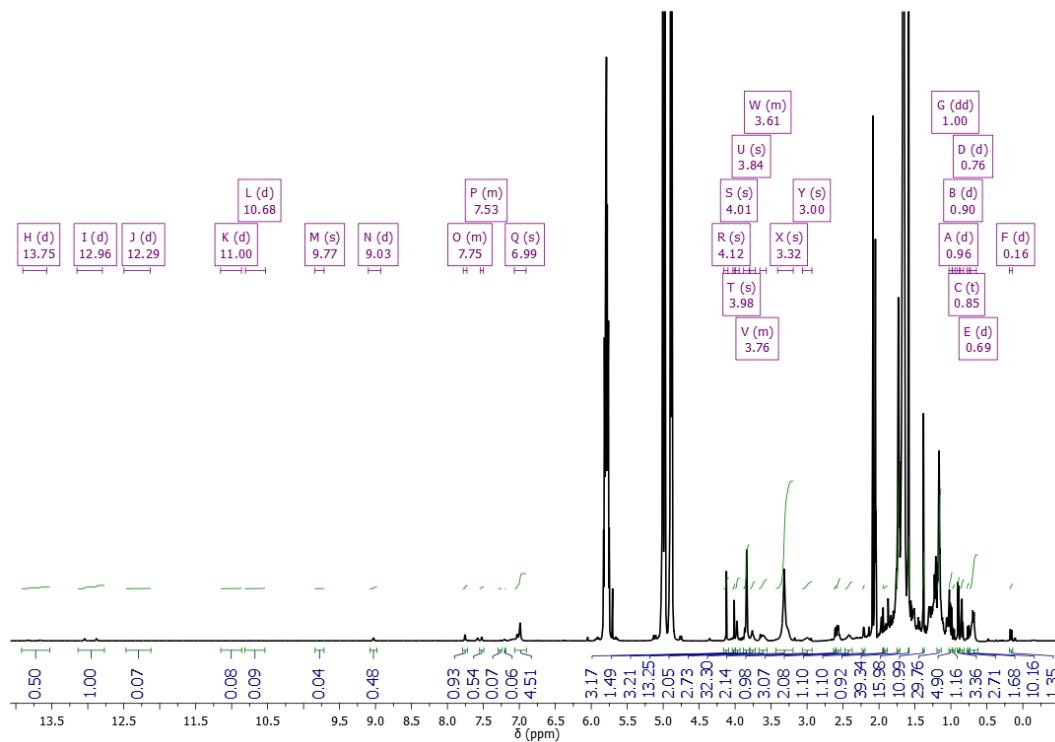
Figure 4.65. ¹H NMR spectrum at 600 MHz of ¹⁵N-labeled **3.14** with propylene at -30˚C
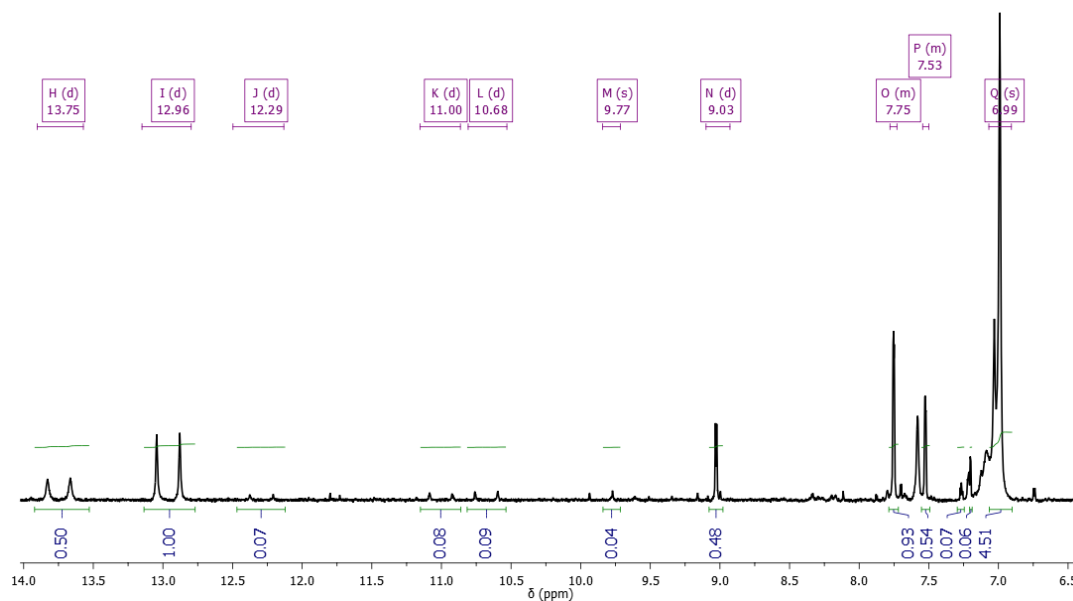
Figure 4.66. ¹H NMR spectrum at 600 MHz of ¹⁵N-labeled **3.14** with propylene -30˚C in the region from 6.5 to 14 ppm
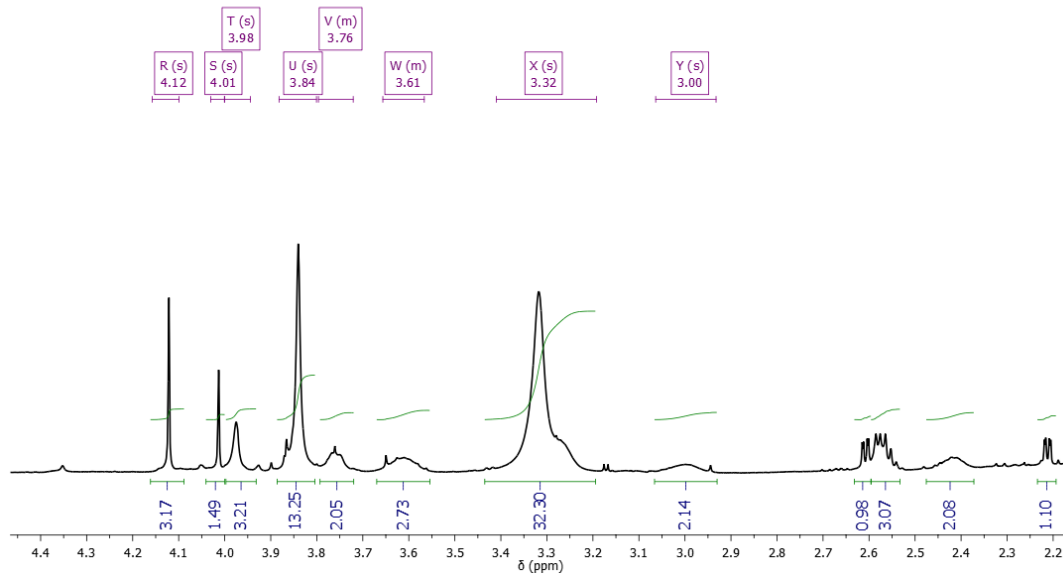
Figure 4.67. ^{1}H NMR spectrum at 600 MHz of ^{15}N-labeled **3.14** with propylene -30˚C in the region from 2.2 to 4.4 ppm
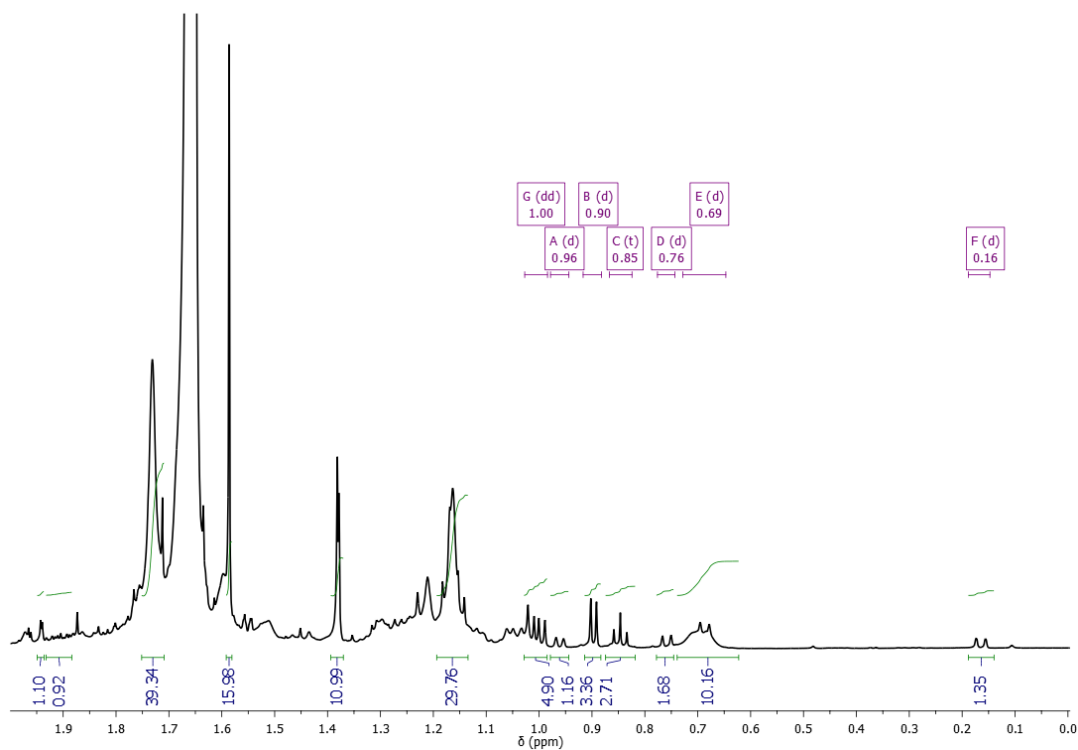
Figure 4.68. ^{1}H NMR spectrum at 600 MHz of ^{15}N-labeled **3.14** with propylene -30˚C in the region from 0.0 to 2.0 ppm

Table 4.68. ¹H NMR spectral data at 600 MHz for reaction of ^{15}N-labeled 5 with propylene at -30˚C. See below (*) for explanation of color coding and ^{15}N conversion.

| ¹H shift (ppm)	mult	J (Hz)	Int (rel to acetone peak =10)	¹⁵N HSQC cross peak	¹⁵N HMBC cross peak	HSQC N15 (ref to CH₃NO₂)	HMBC N15 (ref to CH₃NO₂)	HSQC ¹³C	HMB C ¹³C	HMB C ¹³C #2	COSY
13.75	d	97.5	0.50	169.1	N/A	-205.9	N/A	N/A	N/A	N/A	N/A
12.96	d	98.8	1.00	176	150.5	-199	-224.5	N/A	N/A	N/A	N/A
12.29	d	100.8	0.07	170.3	N/A	-204.7	N/A	N/A	N/A	N/A	N/A
11.00	d	114.5	0.08	189.3	N/A	-185.7	N/A	N/A	N/A	N/A	N/A
10.68	d	63.6	0.09	188.1	N/A	-186.9	N/A	N/A	N/A	N/A	N/A
9.83	s	N/A	0.04	188.4	N/A	-186.6	N/A	N/A	N/A	N/A	N/A
9.03	d	5.1	0.48	N/A	169.1	N/A	-205.9	N/A	N/A	N/A	N/A
7.75	m	N/A	0.93	N/A	176.1	N/A	-198.9	121.3	145.57	N/A	N/A
7.52	bs	N/A	0.54	N/A	169.2	N/A	-205.8	117.54	N/A	N/A	N/A
7.20	d	2.5	0.06	N/A	182.1	N/A	-192.9	N/A	146.01	N/A	N/A
6.99	s	N/A	4.51	N/A	201.1	N/A	-173.9	120.21	146.11	151.83	N/A
4.13	s	N/A	3.17	N/A	N/A	N/A	N/A	35.87	145.6	121.34	N/A
4.01	s	N/A	1.49	N/A	N/A	N/A	N/A	35.17	135.59	117.69	N/A
3.97	bs	N/A	3.21	N/A	N/A	N/A	N/A	33.32	N/A	N/A	N/A
3.84	bs	N/A	13.25	N/A	N/A	N/A	N/A	34.19	146.18	120.27	1.8
3.76	m	N/A	2.05	N/A	N/A	N/A	N/A	N/A	N/A	N/A	3.0
3.61	m	N/A	2.73	N/A	N/A	N/A	N/A	24.32	N/A	N/A	1.63
3.32	bs/m	N/A	32.3	N/A	N/A	N/A	N/A	23.86	N/A	N/A	1.54, 0.69
3.00	bm	N/A	2.14	N/A	N/A	N/A	N/A	N/A	N/A	N/A	N/A
2.61	dd	6.4, 1.5	0.98	N/A	N/A	N/A	N/A	41.13	44.74	N/A	1.91
2.59	dd	N/A	3.07 (comb)	N/A	N/A	N/A	N/A	N/A	28.74	68.8	N/A
2.58	m	N/A		N/A	N/A	N/A	N/A	23.00	18.99	N/A	1.16
2.42	bm	N/A	2.08	N/A	N/A	N/A	N/A	26.17	N/A	N/A	1.00
2.21	dd	6.3, 1.4	1.10	N/A	N/A	N/A	N/A	29.32	40.9	N/A	1.91
1.94	d	1.7	1.10	181.97	182	N/A	-193	10.14	94.93	N/A	N/A
1.91	m	N/A	0.92	N/A	N/A	N/A	N/A	87.78	91.6	N/A	2.61, 2.22, 1.91
1.74	s	N/A	39.34	N/A	201.1	N/A	-173.9	10.24	89.67	N/A	N/A
1.59	s	N/A	15.98	N/A	N/A	N/A	N/A	8.81	71.79	N/A	N/A
1.38	d	1.8	10.99	N/A	176.1	N/A	-198.9	28.14	N/A	N/A	N/A
1.16	dd overlaps	N/A	29.76	N/A	N/A	N/A	N/A	19.10	151.79	68.78	2.58
1.00	dd	12.3, 6.9	4.90	N/A	N/A	N/A	N/A	18.76	19.09	22.98	2.41
0.96	d	8.5	1.16	N/A	N/A	N/A	N/A	40.05	14.89	N/A	2.59

Table 4.68 cont.

0.90	d	6.4	3.36	N/A	N/A	N/A	N/A	15.00	40.80	44.77	1.29
0.85	t	7.3	2.71	N/A	N/A	N/A	N/A	15.78	15.87	N/A	N/A
0.76	**d**	**9.7**	**1.68**	**N/A**	**N/A**	**N/A**	**N/A**	**41.10**	**44.86**	**N/A**	**1.91**
0.69	**d**	**10.2**	**10.16**	**N/A**	**N/A**	**N/A**	**N/A**	**44.63**	**40.80**	**N/A**	**1.91**
0.16	d	10.5	1.35	N/A	N/A	N/A	N/A	40.44	14.98	N/A	1.25

N/A – no signal found. Colored, bolded rows are peaks that are tentatively assigned to a particular species: red – protonated imidazole, purple – complex with bound propylene, blue – allyl species. ^{15}N values were obtained on Bruker instrument, which is referenced to NH_3(l). Values were converted to CH_3NO_2 standard reference by subtracting 380.6 ppm from obtained value (380.6 ppm – measured chemical shift of CH_3NO_2 in a 10%CH_3NO_2/90%CD_3NO_2 solution on Bruker instrument – see figures 3.19 and 3.20).

NMR Assignments – 4.23 (propylene complex) and 4.24 (putative allyl intermediate)
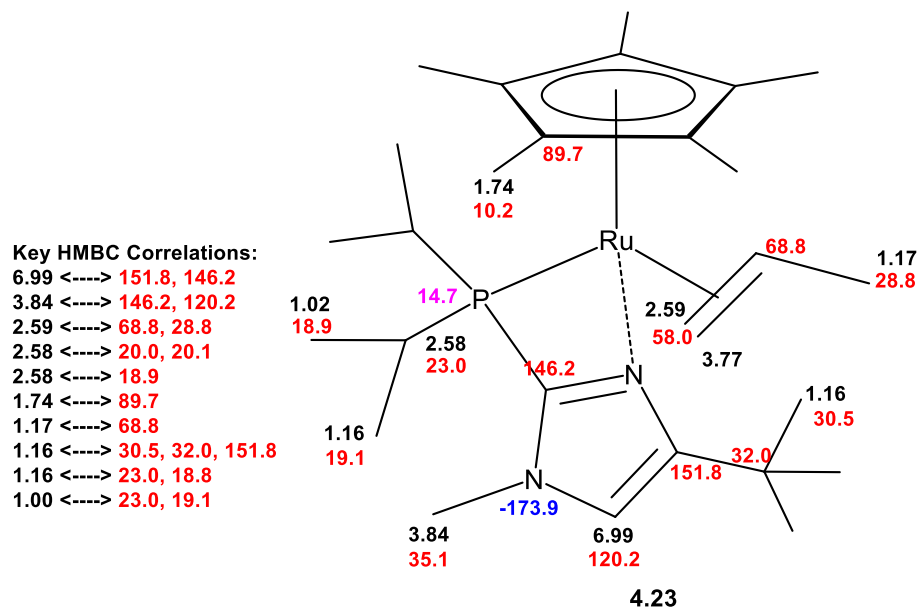
Figure 4.69. Selected NMR data for complex **4.23**

369
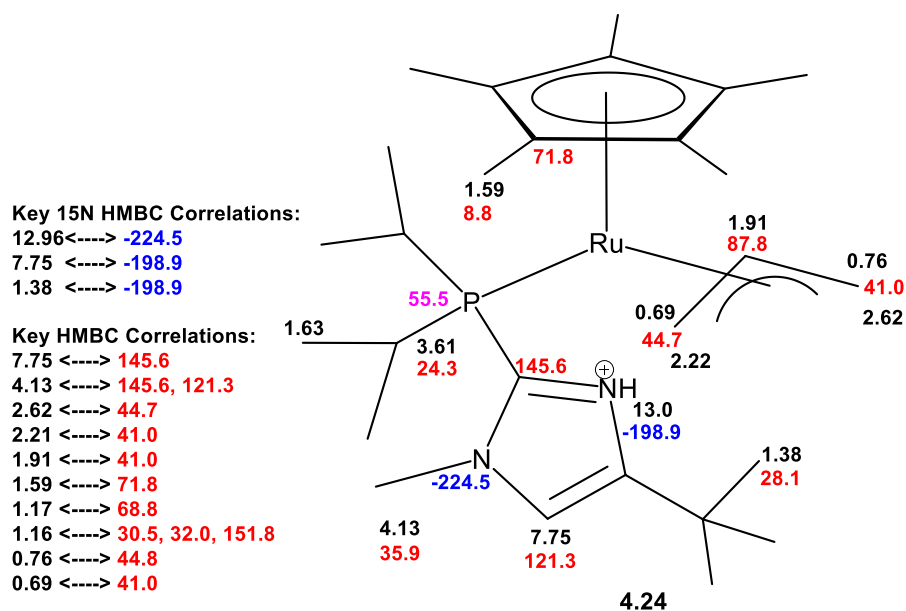
Figure 4.70. Selected NMR data for complex **4.24**

The contents of Chapter 4 contain material from the following two publications: 1) Paulson, E.R., Moore, C.E., Rheingold, A.L., Grotjahn, D.B. "Dynamic π-Bonding of Imidazolyl Substituent in a Formally 16-electron Cp*Ru(κ^2P,N) Catalyst Allows Dramatic Rate Increases in (E)-Selective Monoisomerization of Alkenes" *ACS Catalysis*, Under Review. 2) Paulson, E.R., Delgado III, E., Cooksy, A.L., Grotjahn, D.B. "Catalyst vs. Substrate Control of Monoselectivity in Bifunctional Ruthenium Alkene Isomerization", *Organic Process Research and Development* **2018**, Accepted.

4.8. References

1.   Morrill, T. C.; D'Souza, C. A., Efficient Hydride-Assisted Isomerization of Alkenes via Rhodium Catalysis. *Organometallics* **2003**, *22*, 1626.

2.   Grotjahn, D. B.; Larsen, C. R.; Gustafson, J. L.; Nair, R.; Sharma, A., Extensive Isomerization of Alkenes Using a Bifunctional Catalyst: An Alkene Zipper. *J. Am. Chem. Soc.* **2007**, *129*, 9592.

3.   Erdogan, G.; Grotjahn, D. B., Mild and Selective Deuteration and Isomerization of Alkenes by a Bifunctional Catalyst and Deuterium Oxide. *J. Am. Chem. Soc.* **2009**, *131*, 10354.

4.   Larsen, C. R.; Grotjahn, D. B., Stereoselective Alkene Isomerization over One Position. *J. Am. Chem. Soc.* **2012**, *134*, 10357.

5.   Dobereiner, G. E.; Erdogan, G.; Larsen, C. R.; Grotjahn, D. B.; Schrock, R. R., A One-Pot Tandem Olefin Isomerization/Metathesis-Coupling (ISOMET) Reaction. *ACS Catal.* **2014**, *4*, 3069.

6.   Higman, C. S.; Araujo, M. P. d.; Fogg, D. E., Tandem catalysis versus one-pot catalysis: ensuring process orthogonality in the transformation of essential-oil phenylpropenoids into high-value products via olefin isomerization– metathesis. *Catal. Sci. Technol.* **2016**, *6*, 2077.

7.   Liniger, M.; Liu, Y.; Stoltz, B. M., Sequential Ruthenium Catalysis for Olefin Isomerization and Oxidation: Application to the Synthesis of Unusual Amino Acids. *J. Am. Chem. Soc.* **2017**, *139*, 13944.

8.   Miura, T.; Nakahashi, J.; Zhou, W.; Shiratori, Y.; Stewart, S. G.; Murakami, M., Enantioselective Synthesis of *anti*-1,2-Oxaborinan-3-enes from Aldehydes and 1,1-Di(boryl)alk-3-enes Using Ruthenium and Chiral Phosphoric Acid Catalysts. *J. Am. Chem. Soc.* **2017**, *139*, 10903.

9.   Larsen, C. R., Paulson, E.R., Erdogan, G., Grotjahn, D.B., A Facile, Convenient, and Green Route to (E)-Propenylbenzene Flavors and Fragrances by Alkene Isomerization. *Synlett* **2015**, *26*, 2462.

10.   Sytniczuk, A.; Forcher, G.; Grotjahn, D. B.; Grela, K., Sequential Alkene Isomerization and Ring-Closing Metathesis in Production of Macrocyclic Musks from Biomass. *Chem. Eur. J.* **2018**, *24*, 10403.

11.   Larsen, C. R.; Erdogan, G.; Grotjahn, D. B., General Catalyst Control of the Monoisomerization of 1-Alkenes to *trans*-2-Alkenes. *J. Am. Chem. Soc.* **2014**, *136*, 1226.

12.   Doering, W.E.; Bragole, R., The carbon analog of the Claisen rearrangement of phenyl allyl ether. Equilibration of butenylbenzenes and o-propenyltoluenes. *Tetrahedron* **1966**, *22*, 385.

13.   Carleton, P. S., Conjugative Interaction of Benzene Rings and Double Bonds (Ph.D. Thesis). *Diss. Abstr. Intern. B* **1967**, *27*, 4265.

14.   Doering, W. v. E.; Benkoff, J.; Carleton, P. S.; Pagnotta, M., Conjugative Interaction in Styrenes. *J. Am. Chem. Soc.* **1997**, *119*, 10947.

15.   Hine, J.; Linden, S.-M.; Wang, A.; Thiagarajan, V., Double-Bond-Stabilizing Abilities of Dimethylamino, Alkylsulfonyl, and Acetyl Substituents. *J. Org. Chem.* **1980**, *45*, 2821.

16.   Larsen, C. R., Ph.D. Thesis, UCSD and SDSU. **2012**.

17.   Grotjahn, D. B.; Larsen, C. R.; Erdogan, G., Bifunctional Catalyst Control of Alkene Isomerization. *Top. Catal.* **2014**, *57*, 1483.

18.   Paulson, E. R.; Moore, C. E.; Rheingold, A. L.; Grotjahn, D. B., Dynamic π-Bonding of Imidazolyl Substituent in a Formally 16-electron Cp*Ru(κ^2-P,N)$^+$ Catalyst Allows Dramatic Rate Increases in (*E*)-Selective Monoisomerization of Alkenes. *ACS Catal.* **2018**, *Under Review*.

19.   Trost, B. M.; Toste, F. D.; Shen, H., Ruthenium-Catalyzed Intramolecular [5 + 2] Cycloadditions. *J. Am. Chem. Soc.* **2000**, *122*, 2379.

20.   Smarun, A. V.; Petkovic, M.; Shchepinov, M. S.; Vidovic, D., Site-Specific Deuteration of Polyunsaturated Alkenes. *J. Org. Chem.* **2017**, *82*, 13115.

21.   Tao, J.; Sun, F.; Fang, T., Mechanism of alkene isomerization by bifunctional ruthenium catalyst: A theoretical study. *J. Organometal. Chem.* **2012**, *698*, 1.

22.   Alei, M.; Morgan, L. O.; Wageman, W. E.; Whaley, T. W., pH Dependence of ^{15}N NMR Shifts and Coupling Constants in Aqueous Imidazole and 1-Methylimidazole. Comments on Estimation of Tautomeric Equilibrium Constants for Aqueous Histidine. *J. Am. Chem. Soc.* **1980**, *102*, 2881.